

ACTA PHYSIOLOGICA SCANDINAVICA

Editorial Board

F Buchthal
Copenhagen

K Hartola
Turku

Y Zotterman
Stockholm

U S von Euler
(Editor) Stockholm

Vol 91 INDEX

Fasc 1 (May 1974)

- Regional Cerebral Blood Flow in the Rat Measured by the Tissue Sampling Technique
a Critical Evaluation Using Four Indicators C^{14} Antipyrine C^{14} Ethanol H^3 Water
and Xenon¹³³ By B EKLOF N A LASSEN L NILSSON K NORBERG B A SIESJO and
P TORLOF
- Local Anesthetics Effects on Permeability Properties of Nodal Membrane in Myelinated
Nerve Fibres from *Xenopus* Potential Clamp Experiments By P ARHEM and B
FRANKENHAEUSER
- Distribution of Renal Cortical Blood Flow during Hemorrhagic Hypotension in Conscious
Dogs By A HIRKEBO and I TISSEBOM
- Arterial Hypo- and Hypertension By J JARHULT and S MELLANDER
- The Effect of Glucagon on Hepatosplanchnic Hemodynamics Functional Capacity and
Metabolism of the Liver in Cats By A KRARUP and J A LARSEN
- The Effect of Barbiturate on Retinal Functions I Effects on the Conventional Electro-
retinogram of the Sheep Eye By B KNAVE and H E PERSSON
- Effect of Lowered CSF Sodium Concentration on the Central Control of Fluid Balance
By L ERIKSSON
- Utilization of Energy Reserves by Cells Isolated from Newborn Rat Brain By K HEM-
MINKI and M HARKOVEN
- The Effect of Glycerol on the Postexercise Lactate Clearance By CHR OLSEN and E S
PETERSEN
- Effects of Ethanol tert Butanol and Clomethiazole on Net Movements of Sodium and
Potassium in Electrically Stimulated Cerebral Tissue By H WALLGREN P NIKANDER
P VON BOGUSLAWSKY and J LINQOLA

- Plasma Hyperosmolality and Pulmonary Capacitance Vessels By H PIENE P AARSETH and G BO
- Rate and Extent of Adaptive Cardiovascular Changes in Rats during Experimental Renal Hypertension By Y LUNDGREN M HALLBACK L WEISS and B FOLKOW
- The Effect of Extracellular Calcium on Thermal Excitability of the Sensory Units in the Tooth of the Cat By L OLGART C HÄGERSTAM and L EDWALL
- Effect of Changes in Plasma Na^+ and Ca^{++} Ion Concentration on Body Temperature during Exercise By B NIELSEN

- DDT and Related Substances on Myelinated Nerve Effects on Permeability Properties By P ARHEM B FRANKENHAEUSER R GÖTHE and P O BRYAN
- Hypoxia Causes Prostaglandin Release from Perfused Rabbit Hearts By A WENNEMALM PHAM HUY CHANH and M JUNSTAD
- Blood Flow and Oxygen Consumption in the Rat Brain in Dilutional Anemia By H JOHANSSON and B K-SIESJO
- Failure of Adrenalectomy to Influence the Acute Effect of FSH on Ovarian Metabolism By L NILSSON
- Measurement of Colloid Osmotic Pressure of Interstitial Fluid By H M JOHENSEN

Fasc 2 (June 1974)

- Morphology and Storage Properties of Rat Mast Cell Granules Isolated by Different Methods By P ANDERSON P ROHLICH S A SLORACH and B UYNAS
- Quantitative Measurement of Blood Flow and Oxygen Consumption in the Rat Brain By K NORBERG and B K-SIESJO
- High Energy Phosphate Compound in Adipose Tissue The Effect of Hemorrhage By B B FRIEDHOLM and A FROVEX
- Disappearance of ^{133}Xe and ^{125}I and Extraction of ^{86}Rb in Subcutaneous Adipose Tissue during Sympathetic Nerve Stimulation By B LYNDE and J L GARNER
- The Effect of Barbiturate on Retinal Functions II Effects on the C-wave of the Electroretinogram and the Standing Potential of the Sheep Eye By B KNAVE H E PERSSON and S E G NILSSON
- The Effect of Barbiturate on Retinal Functions III Effects on the Isolated Receptor Responses and the Inner Nuclear Layer Components in the Low intensity Electroretinogram of the Sheep Eye By B KNAVE and H E PERSSON
- The Action Potential in End Plate and Extrajunctional Regions of Rat Skeletal Muscle By S THESLEFF F VYSKOCIL and M R WARD
- Effects of 3,5-Cyclic Adenine Monophosphate 5-Hydroxytryptamine Noradrenaline and Theophylline on the Simultaneous Release of Peroxidase and Amylase from the Guinea Pig Submandibular Gland By B CARLSÖO A DANIELSSON S MARKLUND and T STIGBRAND
- Method for Gravimetric Registration of Changes in Tissue Volume By P O GRANDE J JARHULT and S MELLANDER
- Histochemical Studies on Adenosine Triphosphatase Activity in the Rat Cornea By T TERVO and A PALKAMA
- Parallel Activation of Dynamic Fusimotor Neurons and a Climbing Fibre System from the Cat Brain Stem. I Effects from the Rubral Region By T JENESKÖG
- Titrateable Acid PCO_2 Bicarbonate and Ammonium Ions along the Rat Proximal Tubule By B KARLMARK and H G DANIELSON

- The Immediate Effects of Ligation of the Hepatic Artery on Liver Hemodynamics and Liver Function in the Cat By N KRARUP and J A LARSEN
- Effects of Prolonged Treatment with Adrenergic β Receptor Antagonists on Blood Pressure Cardiovascular Design and Reactivity in Spontaneously Hypertensive Rats (SHR) By L WEISS Y LUNDGREN and B FOLKOW
- Electrical Activity and Isometric Tension in Motor Units of the Cat's Inferior Oblique Muscle By G LÖNNERSTRAND
- Glycogen Utilization in Leg Muscles of Men during Level and Uphill Running By D L COSTILL E JANSSON P D GOLLNICK and B SALTIN
- Middle Ear Muscle Effects on Cochlear Responses to Bone-conducted Sound By D R F IRVINE and K G WESTER
- Transcapillary Passage of Plasma Proteins in Experimental Burns By K GANROT S JACOBSSON and U ROTHMAN
- DDT and Related Substances Effects on Permeability Properties of Myelinated Xenopus Nerve Fibre By P ÅRHEM and B FRANKENHAEUSER
- Afterhyperpolarization Conductance Time Course in Lumbar Motoneurons of the Cat By F BALDISSERA and B GUSTAFSSON
- Firing Behaviour of a Neurone Model Based on the Afterhyperpolarization Conductance Time Course First Interval Firing By F BALDISSERA and B GUSTAFSSON
- Maximal Work Performance at Raised Air and Helium Oxygen Pressures By L FAGRAEUS
- Transport and Oxidation of Amino Acids and Glucose in the Isolated Exocrine Mouse Pancreas Effects of Insulin and Pancreozymin By Å DANIELSSON and J SEHLIN

Short Communications

- Effects of Piperazine on Sleep and Waking in the Rat Evidence for Increased Waking by Blocking Inhibitory Adrenaline Receptors on the Locus Coeruleus By K FUXE P LIDBRINK T HOKFELT P BOLME and M GOLDSTEIN
- Myosin ATPase in Skeletal Muscle of Healthy Men By A W TAYLOR B ESSÉN and B SALTIN
- Reinnervation of the Rat Diaphragm during Perfusion with α Bungarotoxin By D VAN ESSEN and J K S JANSEN
- The Temperature Dependence of Action Potentials in Rat Skeletal Muscle Fibres By M R WARD and S THIELEFF

Supplements

- Supplementum 404 A Spectrophotometric Method for Analysis of Oxygen Consumption *in vivo* on the Microscale By R HOLMBOE
- Supplementum 405 The Effect of Quantitated Training on the Capacity for Short and Prolonged Work By L O NORDESJO
- Supplementum 406 Studies on Fibre Size in Developing Sciatic Nerve and Spinal Roots Normal Undernourished and Rehabilitated Rats By A SIMA
- Supplementum 407 Physiology of Swimming Man By I HOLMÉR

INDEX AUCTORUM

- AARSETH P see PIENE H
- ANDERSON P P ROHLICH S A SLORACH and B UNAS Properties of Mast Cell Granules
- AGND A Distribution of OXITOCIN
- ARIEN P and B FRANKENHAELSER Local Anesthetics on Nerve
- ARIEN P and B FRANKENHAELSER DDT and Related Substances on Myelinated Nerve
- ARIEN P B FRANKENHAELSER R GOTHE and P O BRYAN DDT and Related Substances on Myelinated Nerve
- ASMUSSEN E and F BONDE PETERSEN Elastic Energy in Muscles
- AUKLAND K and H M JOHNSON Skeletal Muscle Interstitial Protein and COP
- BALDISSERA F and B GLASTOFFSON AHP Conductance in Motoneurons
- BALDISSERA F and B GLASTOFFSON Repetitive Firing of a Neurone Model First Interval
- BO G see PIENE H
- BOGUSLAWSKI P von see WALLGREN H.
- BOLME P see FUXE KJ
- BONDE PETERSEN F see ASMUSSEN E
- BRADLEY G W Pulmonary Receptor Recording in *Uro*
- CARLSSON B A DANIELSSON S MARKLUND and T STIGBRAND Peroxidase Release from Salivary Gland
- CHAKRABARTY N and H J SØRENSEN Metabolic Stimulation during Histamine Release
- COSTILL D L E JANSSON P D GOLLNICK and B SALTIN Muscle Glycogen Depletion during Running
- DANIELSSON A see CARLSSON B
- DANIELSON B G see KARLMARK B
- DANIELSSON A and J SEHLIN Metabolism in Exocrine Pancreas
- DOVING K B and K HOLMBERG A Note on the Function of the Olfactory Organ
- EDSTROM A and H LARSSON Barbiturates Synthesis and Fast Axonal Transport of Proteins
- EDWALL L see OLLGART L
- EKLOF B N A LASSEN L NILSSON K NORBERG B K SIESJO and P TORLOF Regions Cerebral Blood Flow
- ELMER M Drugs on Urinary Bladder
- ERIKSSON L CSF Na and Water Balance
- ESSEN B see TAYLOR A W
- FAGRAELS L Exercise in Hyperbaric Environment
- FAGRAELS L C M HESSER and D LINNARSSON Exercise at Increased Air Pressure
- FOLKOW B see LUNDGREN Y
- FOLKOW B see WEISS L
- FRANKENHAELSER B see ARIEN P
- FRANKENHAELSER B see ARIEN P
- VAN-NEUMELDER Z see JACOBSEN T
- FREDHOLM B B and A FRONEK Phosphagens in Fat Following Bleeding
- FRONEK A see FREDHOLM B B
- FR T C and E D SCHOMBERG Spinal Projection of Secondary Spindle Afferents
- FR T C M SANTINI and E D SCHOMBERG Spinal Group II Focal Synaptic Potentials
- FUNE KJ P LIDBRINK T HOKFELY P BOLME and M GOLDSTEIN Piperhexane on Sleep and Waking
- GARNER J L see LINDE B
- GARNOT K S JACOBSSON and L ROTHMANN Proteins in Lymph in Burns

- GOLDSTEIN M see FUXE KJ
 GOLLNICK P D see COSTILL D L
 GOTHE R see ARIEN P
 GRANDE P O J JARHULT and S MELLANDER Measurement of Tissue Volume Changes
 GUSTAFSSON B see BALDISSERA F
 GUSTAFSSON B see BALDISSERA F
 HAEGERSTAM G see OLGART L
 HALLBACK M see LUNDGREN Y
 HALLBACK M see WEISS L
 HANNERZ J Discharge Properties in Motor Units
 HARKONEN M see HEMMINKI K
 HEMMINKI K and M HARKONEN Energy Reserves in Isolated Brain Cells
 HESSER C M see FAGRAEUS L
 HOKFELT T see FUXE KJ
 HOLMBERG K see DOVING K B
 IRVINE D R F and K G WESTER Middle Ear Muscles and Bone Conduction
 JACOBSSON S see GANROT K
 JANSEN J K S see VAN ESSEN D
 JANSSON E see COSTILL D L
 JARHULT J and S MELLANDER Autoregulation of Capillary Pressure
 JARHULT J see GRANDE P O
 JENSEKOG T Parallel Fusimotor and Climbing Fibre Activation
 JOHANSSON H and B K SIESJO CBF and CMRO₂ in Anemia
 JOHNSEN H M Colloid Osmotic Pressure of Interstitial Fluid
 JOHNSEN H M see ALKLAND K
 JONSTAD M see WENNVALM A
 KARLMARK B and B G DANIELSON Acid Base Analysis of Rat Proximal Urine
 KIRKEBO A and I TYSEBOM Renal Cortical Blood Flow
 KNAVE B and H E PERSSON Barbiturate on Retinal Functions I
 KNAVE B and H E PERSSON Barbiturate on Retinal Functions III
 KNAVE B H E PERSSON and S E G NILSSON Barbiturate on Retinal Functions II
 KOLMODIN R see OLSSON K
 KRARUP N and J A LARSEN Glucagon Liver Function and Hemodynamics
 KRARUP N and J A LARSEN Liver Hemodynamics and Function
 LARSEN J A see KRARUP N
 LARSEN J A see KRARUP N
 LARSSON H see EDSTROM A
 LASSEN N A see EKLOF B
 LENNERSTRAND G Extraocular Motor Units
 LIDBRINK P see FUXE KJ
 LINDE B and J L GAFNER Disappearance of ¹³³Xenon during Sympathetic Stimulation
 LINKOLA J see WALLGREN H
 LINNARSSON D see FAGRAEUS L
 LUNDGREN Y Regression of Hypertrophic Cardiovascular Changes
 LUNDGREN Y Propranolol Treatment in Renal Hypertension
 LUNDGREN Y M HALLBACK L WEISS and B FOLKOW Cardiovascular Changes in Hypertension
 LUNDGREN Y see WEISS L
 MARKLUND S see CARLSSON B
 MELLANDER S see GRANDE P O
 MELLANDER S see JARHULT J
 NIELSEN B Plasma Ions and Body Temperature

- NIKANDER P see WALLGREN H
 NILSSON L. Adrenalectomy and FSH Effects on the Ovary
 NILSSON L. see EKLOF B
 NILSSON S E G see KNAVE B
 NORBERG K. and B. K. SIESJO CBF and CMRO₂ in Rat Brain
 NORBERG K. see EKLOF B
 NORMELL, L. A. and B. G. WALLIN Sympathetic Skin Nerve Activity
 O'BRYAN P. see ARHEM P
 OLGART L. G. HÄGERSTAM and L. EDWALL, Extracellular Calcium and Excitability
 OLSEN CHR. and E. S. PETERSEN Glycerol and Lactate Elimination
 OLSSON K. and R. HOLMÖDIN Antidiuretic Hormone and CSF Na⁺
 PALKAMA A. see TERVO T
 PERSSON H. E. see KNAVE B
 PERSSON H. E. see KNAVE B
 PERSSON H. E. see KNAVE B
 PETERSEN E. S. see OLSEN CHR.
 PHAM HUI-CHANH see WENMÄLM A
 PIEVE H. P. AARSETH and G. BO Plasma Hyperosmolality and Lung Vessels
 ROHLICH P. see ANDERSON P
 ROTHMAN L. see GAMMOT K.
 SALTIN B. see COSTILL, D. L.
 SALTIN B. see TAYLOR, A. W.
 SANTINI M. see FL. T. C.
 SCHONBURG E. D. see FL. T. C.
 SCHONBURG E. D. see FL. T. C.
 SEHLEN J. see DANIELSSON A.
 SIESJO B. K. see EKLOF B
 SIESJO B. K. see JÖHANNESSON H.
 SIESJO B. K. see NORBERG K.
 SLORACH S. A. see ANDERSON P
 SØRENSEN H. J. see CHAKRABARTY A.
 STIGBRAND T. see CARLSSON B.
 TAYLOR, A. W. B. ESEN and B. SALTIN ATPase in Skeletal Muscle
 TERVO T. and A. PALKAMA ATPase in Rat Cornea
 THIESLEFF S. see WARD M. R.
 THIESLEFF S. F. VYSKOCIL and M. R. WARD Regenerative Responses in Muscle
 TORLOF P. see EKLOF B
 TYSSERÖT I. see HIRKEBO A.
 LUNAS B. see ANDERSON P
 WALLGREN H. P. NIKANDER P. von BOGUSLAWSKY and J. LINCOLN Drugs and Movements
 WALLIN B. G. see NORMELL L. A.
 VAN ESEN D. and J. K. S. JANSEN Reinnervation of Rat Diaphragm
 WARD M. R. see THIESLEFF S.
 WARD M. R. and S. THIESLEFF Temperature Dependent Action Potentials
 WEISS L. Hypotensive Drugs in Hypertensive Rats
 WEISS L. and M. HALLBACK Vascular Adaptation to Hypotension in SHR
 WEISS L. A. LUNDGREN and B. FOLKOW β Receptor Blockade in Spontaneously Hypertensive Rats
 WEISS L. see LUNDGREN A.
 WENMÄLM A. PHAM HUI-CHANH and M. JONSTAD Prostaglandin Release from H
 WESTER K. G. see IRVINE D. R. F.
 WIKSTRÖM E. see THIESLEFF S.

Regional Cerebral Blood Flow in the Rat Measured by the Tissue Sampling Technique, a Critical Evaluation Using Four Indicators C^{14} -Antipyrine, C^{14} -Ethanol H^3 -Water and Xenon¹³³

By

B EKLOF N A LASSEN¹ L NILSSON K NORBERG B K SJESJO and P TORLOF

Received 11 October 1973

Abstract

Eklof B N A Lassen L Nilsson K Norberg B K Sjesjo and P Torlof

Regional cerebral blood flow in the rat measured by the tissue sampling technique: a critical evaluation using four indicators C^{14} antipyrine C^{14} -ethanol H^3 water and xenon¹³³

Acta physiol scand 1974 91 1-10

The validity of the assumptions inherent in the tissue sampling technique for measuring cerebral blood flow was tested in the rat using the 4 indicators C^{14} antipyrine C^{14} ethanol H^3 water and Xenon. Each one of the indicators was infused i.v. during either 30 60 or 120 s and the blood flow was calculated from the integrated arterial curve and from the tracer concentration in the tissue. The calculated flows varied with the time of infusion and at high perfusion rates all tracers gave flow values that were lower than those obtained with the Kety and Schmidt technique. For C^{14} antipyrine the method gives an error already at normal perfusion rates. It is concluded that the cerebral uptake of the tracers is diffusion limited and that the tissue sampling technique cannot be used for quantitative measurement of cerebral blood flow in high flow situations. However the error of the method is considerably reduced if C^{14} -ethanol is used and if the time of infusion is limited to 30 s.

In order to gain more information on cerebral metabolism in pathological states it seems essential to combine measurements of the cerebral metabolic state as obtained after freezing the tissue *in situ* with determinations of the rate of tissue blood flow. Since measurements of the cerebral energy state are greatly facilitated if small animals can be used the problem has been to find blood flow methods applicable to small animals like rats. Ideally such a method should neither require exposure of the tissue by means of a craniectomy nor should it disturb the local circulation of the tissue. In 1969 Reivich *et al* described a method for regional measurements of

¹Permanent address: Department of Clinical Physiology Bpebjerg Hospital Copenhagen Denmark

the cerebral blood flow generally applicable to small animals. This method is based on an equation derived by Kety (1951, 1960) and represents a modification of an earlier method based on the radioactive gas tritfluoriodo methane (Landau *et al* 1955) using instead C^{14} labelled antipyrine. The C^{14} antipyrine is infused intravenously over a one minute period with repeated sampling of arterial blood and subsequent autoradiographic determination of brain tissue activity.

We recently applied the antipyrine method to the rat cerebral cortex in situations with normal and decreased cerebral blood flow (Eklof and Siesjö 1973). Since the cerebral blood flow (CBF) values obtained agreed with those expected from arteriovenous differences for oxygen and carbon dioxide we tried to apply it also to situations with increased CBF (hypercapnia and hypoxia). However the results showed large variations from those expected from arteriovenous oxygen differences suggesting that the antipyrine method grossly underestimated the cortical blood flow. A comparison of the antipyrine results with those obtained using the Kety and Schmidt (1948) technique in rats (Eklof *et al* 1973) corroborated the discrepancy.

The present work represents an evaluation of the method of Reivich *et al* (1969) as applied to C^{14} antipyrine, C^{14} ethanol, H^3 water and Xenon¹³³. It will be shown that neither of these isotopes give CBF values approaching those obtained with the Kety and Schmidt technique in high flow situations and that the calculated CBF values vary with the time of infusion. As applied to antipyrine the method gives grossly erroneous values in situations with high cerebral blood flow. In such situations the other isotopes give values that are not quantitatively correct but if C^{14} ethanol is used with an infusion time of 30 s the method may be used for a semiquantitative assessment of the regional CBF.

The equation derived by Kety (1951, 1960) for calculating local blood flow is based on mass balance at the capillary level

$$\frac{dC_t}{dt} = f(C_a - C_v) \quad (1)$$

where C_t is the tissue concentration, f the blood flow per gram of tissue and C_a and C_v the arterial and local venous concentrations of tracer respectively. Provided instantaneous diffusion equilibrium between blood and tissue occurs the tissue and blood concentrations of the tracer are related through the partition coefficient (λ) i.e.

$$C_v = C_t/\lambda \quad (2)$$

Inserting this into equation (1) gives a first order differential equation that Kety solved for the boundary condition of $C_t(0) = 0$ to get

$$C_t(T) = \lambda \cdot k \cdot \int_0^T e^{-kx} \cdot C_a(t) e^{-kx} dt \quad (3)$$

with $k = f/\lambda$.

The validity of this local CBF method depends on the assumption inherent in equation (2). Two factors may contribute to render this assumption invalid

- 1) The tissue is inhomogeneous with respect to blood flow
- 2) The tracer fails to equilibrate momentarily at the level of the single capillary

The influence of these errors was discussed by Kety in 1960 and experimentally tested by Fieschi *et al* (1968). These authors varied the time of infusion (T) because it is fundamental that this time should not influence the result. We have followed the same approach using several other indicators and an experimental situation (high flow) that more critically exposes the limitations of the method.

Methods

Experimental protocol

The experiments were performed on 300–400 g male Wistar rats which were anesthetized with divinyl ether, tracheotomized and maintained on artificial respiration with 70% N_2O and 30% O_2 . The body temperature was adjusted to 37°C. Both femoral arteries and femoral veins were cannulated. One of the arterial catheters was used for continuous recording of arterial blood pressure and for anaerobic sampling of blood. The other arterial catheter was cut to a length of 15–20 mm and was employed for sampling of radioactive blood. One of the femoral veins was used for infusion of the radioactive tracer and the other for injection of saturated potassium chloride at the end of the experiment.

The animals were either maintained normocapnic (Paco 35–40 mm Hg) or were rendered hypocapnic (Paco 10–15 mm Hg) or hypercapnic (Paco 80–90 mm Hg). Hypocapnia was induced by increasing the tidal volume 3 times compared to normocapnia and hypercapnia was achieved by adding 7–8% CO_2 to the inspired gas; the ventilation being kept constant. CBF determinations were not performed until the Paco had been constant for at least 30 min.

Regional blood flow was determined according to Reivich *et al* (1969) with the slight modifications previously described (Eklof and Siesjö 1973). Thus the radioactive tracer in the tissue was determined with liquid scintillation counting instead of autoradiography and since the sampling catheter was less than 20 mm in length no correction was applied for catheter smearing. The radioactive tracers ^3H -antipyrine, ^{14}C -ethanol, ^3H -water and ^{86}Kr were dissolved in physiological saline (about 1 mCi of Xenon and about 20 μCi of the others) and infused for 30, 60 or 120 s. Arterial blood was sampled in glass capillaries every 3–10 s during the infusion. Immediately after the last sample had been taken 1 ml of a saturated KCl solution was rapidly injected and the rat was decapitated and the head as frozen in liquid nitrogen. The brain was then flushed out in the frozen state under intermittent irrigation with liquid nitrogen.

When Xenon was used about 25 μl of blood from the capillaries were delivered to the bottoms of 3 ml test tubes filled with water and the tubes were stoppered. When using the other isotopes blood was added directly to vials containing the proper scintillation fluids.

For counting of the activity of the β -emitting isotopes the brains were dissected in a refrigerated glove box at -22°C . Cortical tissue from the frontal and parietal regions were dissected, weighed and added to scintillation vials and subsequently counted together with the blood samples in a Nuclea Chicago liquid scintillation counter. For counting of the Xenon activity pieces of tissue containing predominantly cortical grey matter were chilled off under liquid nitrogen, placed in water-filled 3 ml test tubes and counted together with the appropriate blood samples in a Wallac gamma counting equipment.

Alcohol dehydrogenase which oxidizes ethanol to acetaldehyde has been found in the brain (Rakic and Sokoloff 1970). From the K_m and V_{max} values reported in their paper it can be calculated that at an activity of 2000 cps in the brain only 9% is oxidized per hour. We therefore assume that oxidation of ethanol can be neglected during the short periods of infusion used presently (maximally 2 min).

The partition coefficient λ for antipyrine and Xenon has been determined by Reivich *et al* (1969) and Veall and Mallet (1965) respectively. The value for H_2O was calculated from the relation

$$\lambda = \frac{\text{solubility coefficient in tissue}}{\text{solubility coefficient in blood}}$$

to 1.04. To determine λ for ethanol we occluded bilaterally the arterial supply to the kidneys and the liver and made a portacaval anastomosis. Ethanol was injected intravenously and after 30 min repeated blood samples were taken from the femoral artery and the superior sagittal sinus.

the cerebral blood flow generally applicable to small animals. This method is based on an equation derived by Kety (1951, 1960) and represents a modification of an earlier method based on the radioactive gas trifluoriodo-methane (Landau *et al.* 1955), using instead C^{14} labelled antipyrine. The C^{14} antipyrine is infused intravenously over a one minute period with repeated sampling of arterial blood and subsequent autoradiographic determination of brain tissue activity.

We recently applied the antipyrine method to the rat cerebral cortex in situations with normal and decreased cerebral blood flow (Eklöf and Siesjö 1973). Since the cerebral blood flow (CBF) values obtained agreed with those expected from arterio-venous differences for oxygen and carbon dioxide we tried to apply it also to situations with increased CBF (hypercapnia and hypoxia). However, the results showed large variations from those expected from arterio-venous oxygen differences suggesting that the antipyrine method grossly underestimated the cortical blood flow. A comparison of the antipyrine results with those obtained using the Kety and Schmidt (1948) technique in rats (Eklöf *et al.* 1973) corroborated the discrepancy.

The present work represents an evaluation of the method of Reivich *et al.* (1963) as applied to C^{14} antipyrine, C^{14} -ethanol, H^3 water and Xenon¹³³. It will be shown that neither of these isotopes give CBF values approaching those obtained with the Kety and Schmidt technique in high flow situations and that the calculated CBF values vary with the time of infusion. As applied to antipyrine, the method gives grossly erroneous values in situations with high cerebral blood flow. In such situations the other isotopes give values that are not quantitatively correct but if C^{14} -ethanol is used with an infusion time of 30 s the method may be used for a semiquantitative assessment of the regional CBF.

The equation derived by Kety (1951, 1960), for calculating local blood flow is based on mass balance at the capillary level

$$\frac{dC_t}{dt} = f(C_a - C_v) \quad (1)$$

where C_t is the tissue concentration, f the blood flow per gram of tissue and C_a and C_v the arterial and local venous concentrations of tracer respectively. Provided instantaneous diffusion equilibrium between blood and tissue occurs the tissue and blood concentrations of the tracer are related through the partition coefficient λ as

$$C_v = C_t / \lambda \quad (2)$$

Inserting this into equation (1) gives a first order differential equation that Kety solved for the boundary condition of $C_t(0) = 0$ to get

$$C_t(T) = f / k \cdot (1 - e^{-kT}) / \lambda \int_0^T C_a(t) e^{-kt} dt \quad (3)$$

with $k = f / \lambda$.

The validity of this local CBF method depends on the assumption inherent in equation (2). Two factors may contribute to render this assumption invalid

- 1) The tissue is inhomogeneous with respect to blood flow
- 2) The tracer fails to equilibrate momentarily at the level of the single capillary

The influence of these errors was discussed by Kety in 1960 and experimentally tested by Fieschi *et al* (1968). These authors varied the time of infusion (T) because it is fundamental that this time should not influence the result. We have followed the same approach using several other indicators and an experimental situation (high flow) that more critically exposes the limitations of the method.

Methods

Experimental protocol

The experiments were performed on 300–400 g male Wistar rats which were anesthetized with diethyl ether, tracheotomized and maintained on artificial respiration with 70% N_2O and 30% O_2 . The body temperature was adjusted to 37°C. Both femoral arteries and femoral veins were cannulated. One of the arterial catheters was used for continuous recording of arterial blood pressure and for anaerobic sampling of blood. The other arterial catheter was cut to a length of 15–20 mm and was employed for sampling of radioactive blood. One of the femoral veins was used for infusion of the radioactive tracer and the other for injection of saturated potassium chloride at the end of the experiment.

The animals were either maintained normocapnic (Paco 35–40 mm Hg) or were rendered hypocapnic (Paco 10–15 mm Hg) or hypercapnic (Paco 80–90 mm Hg). Hypocapnia was induced by increasing the tidal volume 3 times compared to normocapnia and hypercapnia was achieved by adding 7–8% CO_2 to the inspired gas, the ventilation being kept constant. CBF determinations were not performed until the Paco had been constant for at least 30 min.

Regional blood flow was determined according to Reivich *et al* (1969) with the slight modifications previously described (Eklöf and Sjöryd 1973). Thus the radioactivity in the tissue was determined with liquid scintillation counting instead of autoradiography and since the sampling catheter was less than 20 mm in length no correction was applied for catheter smearing. The radioactive tracers C^{14} antipyrine, C^{14} -ethanol, H^3 -water and Xe^{133} were dissolved in physiological saline (about 1 mCi of Xe non and about 20% of the others) and infused *in situ* for 30, 60 or 120 s. Arterial blood was sampled in glass capillaries every 3–10 s during the infusion. Immediately after the last sample had been taken 1 ml of a saturated KCl solution was rapidly injected *in situ*; the rat was decapitated and the head was frozen in liquid nitrogen. The brain was then chiselled out in the frozen state under intermittent irrigation with liquid nitrogen.

When Xenon was used about 25% of blood from the capillaries were delivered to the bottoms of 3 ml test tubes filled with water and the tubes were stoppered. When using the other isotopes blood was added directly to vials containing the proper scintillation fluids.

For counting of the activity of the β -emitting isotopes the brains were dissected in a refrigerated glass box at -22°C. Cortical tissue from the frontal and parietal regions were dissected, weighed and added to scintillation vials and subsequently counted together with the blood samples in a Nuclear Chicago liquid scintillation counter. For counting of the Xenon activity pieces of tissue containing predominantly cortical grey matter were chiselled off under liquid nitrogen, placed in water filled 3 ml test tubes and counted together with the appropriate blood samples in a Wallac gamma counting equipment.

Alcohol dehydrogenase which oxidizes ethanol to acetaldehyde has been found in the brain (Raskin and Sokoloff 1970). From the K_m and V_{max} values reported in their paper it can be calculated that at an activity of 2000 cps in the brain only 90% is oxidized per hour. We therefore assume that oxidation of ethanol can be neglected during the short periods of infusion used previously (maximally 2 min).

The partition coefficient λ for antipyrine and xenon has been determined by Reivich *et al* (1969) and Wall and Mallet (1965) respectively. The value for H_2O was calculated from the relation

$$\lambda = \frac{\text{solubility coefficient in tissue}}{\text{solubility coefficient in blood}}$$

to 1.04. To determine λ for ethanol we occluded by ligatures the arterial supply to the kidneys and the liver and made a portacaval anastomosis. C^{14} -ethanol was injected intravenously and after 30 min repeated blood samples were taken from the femoral artery and the superior sagittal sinus.

TABLE I Cortical blood flow using C^{14} antipyrine, C^{14} ethanol, $H_2^{18}O$ and Xe^{133} at different times of infusion compared to the CBF values determined by the Kety-Schmidt technique at the following $P_{CO_2} \pm S.E.$

Tracer	$P_{CO_2} \pm S.E.$ mm Hg	Time seconds	CBF $\pm S.E.$ ml/(min 100 g) Tissue sampling	CBF $\pm S.E.$ ml/(min 100 g) Kety-Schmidt
Antipyrine C^{14}	12.5 ± 0.3	30	63 \pm 3	64 \pm 2
		60	45 \pm 2	
		120	55 \pm 2	
Antipyrine C^{14}	36.7 ± 0.5	30	93 \pm 4	100 \pm 3
		60	90 \pm 5	
		120	86 \pm 3	
Antipyrine C^{14}	89 ± 1	30	206 \pm 12	475 \pm 25
		60	155 \pm 5	
		120	132 \pm 5	
Ethanol C^{14}	37.3 ± 0.7	30	122 \pm 10	100 \pm 3
		60	121 \pm 10	
		120	76 \pm 2	
Ethanol C^{14}	88 ± 0.9	30	370 \pm 20	465 \pm 25
		60	191 \pm 12	
		120	92 \pm 9	
Water $H_2^{18}O$	38.1 ± 0.7	30	106 \pm 14	100 \pm 3
		60	87 \pm 4	
		120	78 \pm 5	
Water $H_2^{18}O$	87 ± 2	30	290 \pm 30	465 \pm 25
		60	153 \pm 6	
		120	89 \pm 5	
Xe 133	38.0 ± 0.8	30	127 \pm 5	100 \pm 3
		60	70 \pm 2	
		120	74 \pm 4	
Xe 133	82 ± 2	30	311 \pm 18	465 \pm 25
		60	154 \pm 17	
		120	120 \pm 10	

and the animal was decapitated. The mean and S.E. of 4 determinations was 114 ± 0.07 for every matter. As a reference method for the cortical blood flow in the rat we employed the Kety-Schmidt technique using Xe 133 inhalation for 30 min calculating the cortical blood flow from the desaturation curve (Eklöf *et al.* 1973). The values given below are those presented in that publication.

The arterial P_{CO_2} was measured at 37°C with a micro CO_2 electrode with corrections for deviations in body temperature from 37°C.

Results

The blood flow of the cerebral cortex of the rat as determined by the technique involved in using equation (3) was compared to the values obtained using the Kety-Schmidt Xe 133 inhalation technique sampling from the femoral artery and the superior sagittal sinus. The cortical blood flows as determined by eq. (3) using C^{14} antipyrine, C^{14} -ethanol, $H_2^{18}O$ and Xe 133 at $T = 30, 60$ and 120 s are presented in Table I. In Fig. 1 the flow values using C^{14} antipyrine were compared to those

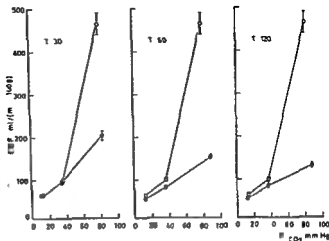


Fig 1 Comparison of CBF determined with the Kety Schmidt technique (open circles) and the method assuming instantaneous diffusion equilibrium with C^{14} antipyrine (closed circles) at $T = 30$, 60 and 120 s

obtained with the Kety Schmidt technique at 3 levels of CO_2 tensions. At high flow rate in hypercapnia all tracers gave low values for CBF compared to our reference values and these differences increased as the time of infusion was increased.

Discussion

In the present study we have chosen to compare the values obtained with the method of Reivich *et al* (1969) to those obtained with the Venon inhalation technique according to Kety and Schmidt (1948). Since the latter method does not require assumptions regarding homogeneity of flow or instantaneous diffusion of the tracer it serves as a reference method. The comparison may not be entirely valid since the regions studied with the two methods are not necessarily the same. However if other regions than the cortical ones deliver blood to the superior sagittal sinus the flow measured according to Kety and Schmidt (1948) could hardly overestimate flow in the regions sampled for C^{14} antipyrine, C^{14} ethanol, $H_2^{18}O$ or Ne^{133} . Furthermore the mere fact that the flow values calculated according to equation (3) vary with the time of infusion demonstrates that the cortical flow is inhomogeneous and/or that there is diffusion limitation for the tracers employed. We will discuss the possibilities in that order.

1. Inhomogeneous perfusion

Let it be assumed that the local tissue consists of two in parallel perfused tissues each having a homogeneous perfusion. Then

$$C_d(T) = \alpha C_1(T) + (1 - \alpha) C_2(T)$$

$$f = \alpha f_1 + (1 - \alpha) f_2$$

$$1 = \alpha + (1 - \alpha)$$

(4)

where α and $1 - \alpha$ are the fractional weights f_1 and f_2 the blood flows and C_1 and C_2 the tracer concentration in tissues 1 and 2 respectively. If f is the mean blood flow in the local region that we wish to estimate. Let us find f by the flow of the equation that we would get by equation (3) if we erroneously assumed that the region had homogeneous flow. Equation (3) gives

$$C_1(T) = \int_0^T k_1 e^{-k_1 t} \int_0^T C e^{k_1 t} dt \quad k_1 = f_1/f$$

$$C_2(T) = \int_0^T k_2 e^{-k_2 t} \int_0^T C e^{k_2 t} dt \quad k_2 = f_2/f$$

$$C_3(T) = \int_0^T k e^{-k t} \int_0^T C e^{k t} dt \quad k = f/f \quad (3)$$

Inserting (3) into eq. (4) and rearranging gives

$$k = \frac{\lambda_1 \left(\frac{\int_0^T C_1 e^{k_1 t} dt}{\int_0^T C e^{k t} dt} \right) + \lambda_2 \left(\frac{\int_0^T C_2 e^{k_2 t} dt}{\int_0^T C e^{k t} dt} \right)}{\lambda_1 + \lambda_2} \quad (6)$$

Comparing this to equation (4) for finding the correct average tissue blood flow f it appears that λ_1 and λ_2 are factors that modify the true weighing of the individual flows f_1 and f_2 . We can in the case C_3 is a step function write

$$\lambda_1 = \frac{k}{k_1} \left(\frac{1 - e^{-k_1 T}}{1 - e^{-k T}} \right)$$

$$\lambda_2 = \frac{k}{k_2} \left(\frac{1 - e^{-k_2 T}}{1 - e^{-k T}} \right) \quad (7)$$

As k can be assumed to lie between k_1 and k_2 then if $k_1 < k < k_2$

$$\left. \begin{aligned} \lambda_1 &\rightarrow \frac{k}{k_1} < 1 \\ \lambda_2 &\rightarrow \frac{k}{k_2} > 1 \end{aligned} \right\} \text{when } T \rightarrow \infty \quad (8)$$

A Taylor expansion gives $\left. \begin{aligned} \lambda_1 &\rightarrow 1 \\ \lambda_2 &\rightarrow 1 \end{aligned} \right\} \text{when } T \rightarrow 0$

This combined with the general expression for λ_1 and λ_2 as defined in equation (6) shows that λ_1 is lower than unity while λ_2 is higher than unity. Consequently the blood flow determined from k ($f = \lambda \cdot k$) will be an underestimation of the true mean blood flow f . This error only disappears as T approaches zero because then $\lambda_1 = \lambda_2 = 1$. The error increases as T increases and as flow increases.

In order to illustrate the dependence of the mean flow as obtained with the tissue sampling technique on the time of infusion (T) we have chosen an example based on the capillarity of the various cortical layers (cf. Craigie 1921). Thus if the correct mean flow is 460 ml/100g min and if the relative weights and blood flows of the layers are these given in Table II a small T dependence is obtained. However any error is small if the variations in regional flow are not larger than those given in the table.

2. The tracer is diffusion limited

The influence of incomplete equilibration between the tissue and blood at the single capillary level can be evaluated along much the same lines as for inhomogeneous perfusion. Instead of considering differently perfused areas in the tissue homogeneous perfusion is assumed but within each tissue cylinder there are regions in series with different diffusion characteristics. The result will be a decreasing flow value with the time of infusion because incomplete equilibrium underestimates the

TABLE II The dependence of mean flow for an assumed inhomogeneous tissue with the time of infusion T. The correct mean flow is assumed to be 465 ml/(min 100 g)

Region	Relative weight	Blood flow ml/(min 100 g)	Mean blood flow ml/(min 100 g)		
			T	T	T
			30	60	120
1	1/6	432	434	445	432
2	1/6	509			
3	1/6	571			
4	1/6	475			
5	2/6	391			

actual venous concentration and therefore make the relation $C_v = C_i/2$ invalid. Assuming for simplicity 2 different regions in each case the time dependence of the venous concentration is then composed of two monoexponential functions. This diffusion in series has been evaluated mathematically by Hill (1967).

As always when two rates are involved in a transport the slowest process will determine the over all rate. The rate of diffusion into and inside the tissue and the rate of flow through the capillary are here competing. This means that the higher the flow rates the assumption about infinitely fast diffusion in applying equation (3) becomes more and more critical. It should also be stressed that in pathological situations when many of the capillaries may be closed the flow/unit of weight is low but the rate of flow is large. In such cases equation (3) can hardly be applied.

The influence of incomplete equilibration in the single capillary can also be illustrated by solving equation (1) for so short times that the venous outflow $f C_v$ can be neglected. Then after integration

$$C_i(T) = f \int_0^T C_v(t) dt \quad (9)$$

In order to use this equation we need not make assumptions about flow homogeneity or infinitely fast diffusion in the whole tissue cylinder all that is necessary is complete extraction of the tracer for $t < T$. It has previously been shown that antipyrine does not freely pass the blood brain barrier (Crone 1964) and the erroneously low values obtained with this compound can thus be explained in terms of incomplete extraction. It has also been shown that H_2O is less extracted than ethanol when injected as a bolus into the carotid artery (Eklof and Gjedde unpublished results).

These data point to a certain degree of diffusion limitation of H_2O at the blood brain barrier. Raichle and coworkers (personal communication) have shown this diffusion limitation in dogs in terms of a transmitted intravascular fraction (a spike). Recent studies (Bolwig and Lassen) have confirmed this in the rat. This may explain the lower mean values obtained with H_2O than with C^{14} ethanol in hypercapnia.

3 The influence of experimental errors in C_i and T on the calculated blood flow

A typical arterial curve shown in Fig. 2 is the basis for this analysis. From assumed

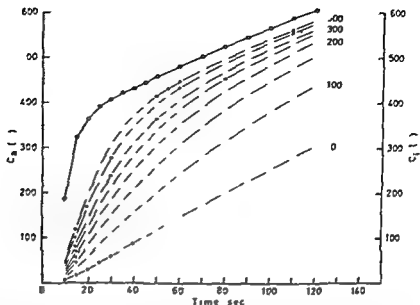


Fig. 2. Calculated values for C_1 corresponding to the flow values 50, 100, 150, 200, 250, 300, 400 and 500 ml/(min 100 g). The calculations were based on the arterial curve shown in this figure (open circles). At very high flow values the accuracy of the determination of C_1 becomes crucial, especially at long infusion times (see also Fig. 3).

hypothetical flow values indicated in this figure C_1 as a function of time was calculated from equation (3) at $\lambda = 1$. This figure has been used to answer the following questions:

a) How will the accuracy in the experimentally determined C_1 influence the accuracy in the flow determination at different times of infusion and how should T be chosen to minimize this effect? Fig. 3 shows at 5 different times of infusion the flow as a function of C_1 expressed in relation to the arterial concentration at the time of stopping the infusion. At a flow equal to 100 ml/(100 g min), the relative error in C_1 will be least when T is close to 120 seconds. At higher flows the optimal time is close to 30 seconds and nothing is gained by reducing T further. Besides other experimental errors are introduced since the arterial concentration curve will be determined with less accuracy.

b) How will the accuracy of the experimentally determined λ influence the accuracy of the blood flow determined at different values of T and f ? Flow as a function of λ at $f = 100$ and 500 ml/(min 100 g) for $T = 30, 60$ and 120 s is plotted in Fig. 4. Independent of the rate of flow a relative error in λ will have a larger influence at high than at low values of T . An erroneously too high value of λ gives a calculated flow which decays with T . On the other hand, if λ is too low the flow values will increase with T .

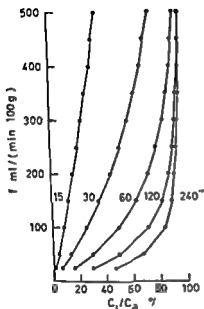


Fig 3

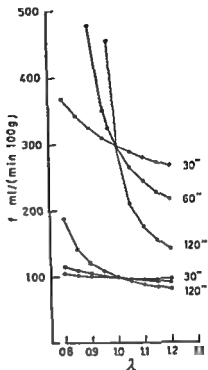


Fig 4

Fig 3 The effect of a relative error in the tissue concentration on the flow at different times of infusion. Fig 4 The influence of an error in λ at flows of 100 and 300 ml/(min 100 g) at $T = 30, 60$ and 120 s.

c) How does the rate of infusion ($\mu C/\text{time unit}$) effect the influence of the experimental errors in C_1 and λ ? For flow values greater than 200 ml/(min 100 g) the absolute deviation in C_1 from C_a is constant and it is equal to the rate of infusion divided by the flow at T greater than 120 s. This means that at constant flow an increased rate of infusion gives an increased absolute deviation which in turn diminishes the influence of an absolute error in C_1 and λ . Experimentally we have increased the rate of infusion 3 times without any significant change in the flows so evidently an absolute error in C_1 and λ cannot be a main contributing factor in the T -dependence obtained.

Inhomogeneity or diffusion limitation?

Although both inhomogeneity and diffusion limitation can explain the T dependence of the values obtained with the method of Renwick *et al* (1969) as well as the discrepancy between the values measured with this method and those obtained with the Kety and Schmidt technique, there are reasons to believe that diffusion limitation may be the predominant factor. Thus autoradiograms prepared from

normocapnic and hypercapnic rats using C^{14} antipyrine do not show an inhomogeneity of the cortical flow.

Although this apparent homogeneity does not exclude some degree of heterogeneity it is incompatible with a heterogeneity of such a degree that would explain the discrepancies obtained between the inert gas method and the method according to Reivich *et al.* Thus we conclude that the tracers used are diffusion limited when applied in the present experimental situations.

Recommendations

The present results show that C^{14} antipyrine is not suited to measure regional blood flow even at normal rates of flow. Although neither of the other tracers may quantitatively measure regional flow in high flow situations the results obtained with C^{14} ethanol suggest that this substance can be applied with reasonable accuracy provided the time of infusion is limited to 30 s. This conclusion is supported by recent (unpublished) results which show that C^{14} ethanol gives cortical blood flow in hypoxia which are close to those obtained using the Kety and Schmidt technique. As H_2O is not extracted to the same extent as ethanol, when a bolus is passing through the capillary and because of complications due to countercurrent diffusion THO cannot be regarded as suitable as C^{14} ethanol. Xenon 133 is much too volatile to be practical.

This study was supported by grants from the Swedish Medical Research Council (13 125 14X 2179 and 14X 2671) from the Swedish Bank Centenary Fund and by U.S. NIH Grant No. 5 R01 NS 078393-03 from NIH. K. Norberg is supported by grants from the Swedish Board for Technical Development.

References

- CRONE C. The permeability of brain capillaries to non-electrolytes. *Acta physiol scand* 1954 64: 407-417.
- CRATZEL F H. The vascularity of the cerebral cortex of the albino rat. *J comp Neurol* 1971 22: 193-212.
- FRICKE J and L. K. STRYÖ. Cerebral blood flow in ischemia caused by occluded artery ligature in the rat. *Staphyol scand* 1973 87: 69-77.
- EKLOF B, N. A. LAMM and L. NISSENER. K. NORBERG and L. K. STRYÖ. Blood flow and metabolic rate for oxygen in the cerebral cortex of the rat. *Acta physiol scand* 1973 88: 527-583.
- FISCH C C, C. L. HANSEN and S. S. KETY. On the question of regional blood flow in grey matter of the brain. In: *Blood Flow through Organs and Tissues* ed by W. J. Linn and A. M. Harper. Publ. F & S Livingston Ltd. 1967 226-231.
- HILL L A. Diffusion of blood perfusion in limiting the rate of uptake of inert gas by the lungs. *Am J Physiol* 1967 213: 67-73.
- KETY S S. The application of exchange of inert gas at lungs and tissues. *Pharmacol Ther* 1971 5: 41.
- KETY S S, M. J. REIVICH, S. L. FLEET and S. S. KETY. Blood flow by the exchange of an inert diffusible substance. Method. *Med Biol Res* 1968 1: 223-231.
- KETY S S, L. C. SCHMIDT. The determination of cerebral blood flow in man by the use of nitrous oxide. In: *Flow and its measurement*. *J Appl Physiol* 1957 14: 33-45.
- LANE W M, W. H. FREYMAN, JR, L. J. ROWLAND, I. SOKOLOFF and S. S. KETY. The local circulation of the brain. *Am J Physiol* 1967 213: 129.
- RASKIN N H, J. L. S. KILPATRICK. Aldehyde dehydrogenase activity in rat brain and liver. *J Neurochem* 1970 17: 11-17.
- REIVICH M J, J. FISH, L. K. STRYÖ and S. S. KETY. Measurements of regional cerebral blood flow with C^{14} antipyrine in awake cat. *J Appl Physiol* 1969 27: 231-239.
- VEALL N and J. L. MALLORY. The perfusion of trace amounts of xenon between brain and blood and brain tissue. *Am J Physiol* 1965 210: 37-39.

Local Anesthetics Effects on Permeability Properties of Nodal Membrane in Myelinated Nerve Fibres from *Xenopus* Potential Clamp Experiments

B.

PETER ARHEM and BERNHARD FRANKEHAEUSER

Received 8 October 1973

Abstract

ARHEM P and B FRANKEHAEUSER *Local anesthetic effects on permeability properties of nodal membrane in myelinated nerve fibres from Xenopus Potential clamp experiments* Acta physiol scand 1974 91 11—21

Effects of local anesthetics (procaine, lidocaine and benzocaine) on permeability parameters of single myelinated fibres were studied with potential clamp technique. These drugs decreased permeability constants P_{Na} and P_K . The decrease of P_{Na} was larger than that of P_K at corresponding concentrations. Permeability-concentration curves of the form

$$\frac{P}{P_0} = \frac{k}{k + [x]}$$

were fitted to the experimental measurements and the constant k for P_{Na} and P_K was determined for the anesthetics. Effects of procaine and lidocaine which are tertiary amines depended on $[H^+]$. The decrease of permeability was more pronounced in alkaline solutions. These tertiary amines are more ionized at low pH. The results were satisfactorily described on the basis of the assumption that both charged and uncharged forms are active but the constant k for the two forms differs slightly. Benzocaine which is uncharged in the pH range tested had a pH independent anesthetic effect. Changes in $[Ca^{2+}]$ had no effect on anesthetic activity. This excluded the idea of interaction between Ca^{2+} and local anesthetic as the base for the anesthetic action. Axoplasmic drug application was obtained through diffusion from cut ends of the fibre. Anesthetics so applied were also active. The site of action could thus be reached from outside and inside of the membrane. The empirical equations fitted to the measurements can be derived from first order reactions. It is concluded that this relationship is expected not to hold for several other types of dose response measurements on nerves.

An analysis of the action of some local anesthetics was carried out with the aim to obtain information on the permeability properties of the excitable nodal membrane. Earlier extensive studies of local anesthetics have mainly been concerned with phenomena which from the view point of the single fibre have an all or none character. Block of conduction and block of reflexes have thus been analysed. References to the vast literature on this field may be obtained from recent reviews (e.g. Ritchie and Greengard 1966, Seeman 1966, Narahashi and Frazier 1971).

Potential clamp experiments indicate that the major effect of local anesthetics is to decrease the permeability constants \bar{g}_{Na} and \bar{g}_K (or correspondingly for the myelinated fibre \bar{P}_{Na} and \bar{P}_K). This has been shown to be the case for several local anesthetics among them procaine and cocaine on the squid giant axon (Shanes *et al* 1959 Taylor 1959, Narahashi, Frazier and Moore 1972) and procaine on the lobster giant axon (Blaustein and Goldman 1966) and lidocaine on the frog nerve fibre (Hille 1966). The effect on \bar{g}_{Na} (or \bar{P}_{Na}) seems to be larger than that on \bar{g}_K (or \bar{P}_K) (Taylor 1959 Hille 1966).

Several of the common local anesthetics are tertiary amines and they appear either as the uncharged free base or as the charged substituted ammonium cation. The proportion between the two forms is determined by the pH of the solution. It has been proposed that the charged form is the dominating active form (Ritchie and Greengard 1961, Dettbarn 1962, Narahashi, Frazier and Yamada 1970).

Local anesthetics and a number of compounds including Ca^{2+} , have rather arbitrarily been classified as stabilizers with reference to their effects on the nerve although it is now known that the effects of these compounds may be principally different. Local anesthetics affect as mentioned above mainly the permeability constants while changes in calcium concentration shift the permeability potential curve along the potential axis (Frankenhaeuser 1957, Frankenhaeuser and Hodgkin 1957). It has on the other hand been proposed in a number of studies that Ca^{2+} and local anesthetics antagonize each other in their effects on the mechanism of the specific permeability changes and that this antagonism may be the basis of the local anesthetic action (Aceves and Machne 1963, Feinstein 1964, Blaustein and Goldman 1966).

In the present study the effects of three local anesthetics procaine, lidocaine and benzocaine were analysed in potential clamp experiments. The effect of the local anesthetics on the sodium and the potassium permeability systems was measured quantitatively. The influence of changes in $[H^+]$ and $[Ca^{2+}]$ on the anesthetic action was also investigated.

Methods

The experiments were carried out on single myelinated fibres dissected from the sciatic nerve of the clawed toad (*Xenopus laevis*). The recording cell and the electrode assembly were all held at a controlled temperature. The test solution surrounding the node under investigation (N_1) was changed by pipette or by a peristaltic pump. The nodal membrane potential was controlled by a feed back amplifier system as earlier described (Dodge and Frankenhaeuser 1958, Arhem, Frankenhaeuser and Moore 1973). Most fibres were polarized to -90 or -110 mV between test pulses in order to keep sodium and potassium inactivation negligibly low ($h_\infty \approx 1$ and $k \approx 1$). The peak sodium permeability (P_{Na}) and the steady state potassium permeability (P_K) were calculated by the constant field equation from the peak sodium current and the steady state potassium current associated with potential steps of required amplitudes (Frankenhaeuser *et al* 1963). The fibre was cut at the adjacent nodes N_2 and N_3 . The value used for its calibration was $14 \Omega \text{cm}^2$ (Dodge and Frankenhaeuser 1958).

Solutions: The composition of the solutions used was (mM)

(1) Ringer's solution: $NaCl$ 112, KCl 2.5, $CaCl_2$ 2.0

(2) Isotonic KCl solution: KCl 170, $CaCl_2$ 2.0. These solutions were buffered either with $\text{Tris}-(\text{hydroxymethyl})\text{aminomethane}$ (5 mM) or with $NaHCO_3$ (2.5 mM) and CO_2 to

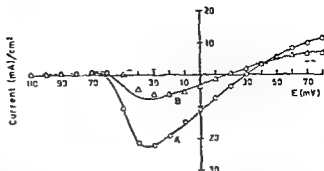


Fig 1 Plot of membrane current at the time of the peak of the initial current versus potential. Dotted line indicates leak current. A node λ_0 in Ringer's solution. B node λ_0 in Ringer's solution with 0.37 mM procaine. Smooth line in curve A drawn through the experimental points. Curve B drawn as 0.38 times I_x in A .

■ required pH. The local anesthetics (procaine HCl, lidocaine HCl, benzocaine) were added in substance to these solutions. Some experiments were carried out without any buffer; the solutions were then adjusted with NaOH or with HCl to the required pH. The nodal currents were found to be buffer independent but clearly pH dependent.

Nomenclature. Potentials are given as inside potential minus outside potential and outward current consequently as positive.

Results

The isolated nerve fibre was mounted in the recording cell; three petroleum jelly seals were applied in order to increase the external resistance at three sites on the fibre. The 4 solution pools in the recording cell were connected to the appropriate measuring and current carrying electrodes; the feed back amplifiers were balanced and turned on in the usual way (Dodge and Frankenhaeuser 1958). The membrane potential was then changed in rectangular pulse steps as required while the membrane current associated with the potential steps was measured.

Potential clamp runs were taken in which the test step for successive tests was incremented by 10 mV. The peak sodium permeability (P_N) and the steady state potassium permeability (P_K) during these potential steps were measured and calculated in the ordinary way from these families of membrane currents. Local anesthetics added to the Ringer solution were applied to the node under investigation. Potential clamp runs were made with various anesthetic concentrations. Measurements of the peak sodium current indicated that the major effect of the local anesthetic was to decrease the sodium current associated with the potential steps (Fig. 1). The sodium equilibrium potential (E_{Na}) was unaffected and the current-potential relation was affected in a simple fashion, i.e. the sodium currents at every step were decreased by approximately one and the same factor. This behaviour might be caused by 2 mechanisms. The local anesthetic might either have caused a shift of the sodium inactivation curve or it might have decreased the sodium permeability constant (P_N). Runs were therefore made to measure the inactivation-potential relation. These runs indicated that the inactivation-potential relation was unaffected by procaine. These preliminary experiments on the *Xenopus* nerve are fully consistent with Hille's (1966) measurements on fibre from *Rana pipiens* and Taylor's (1959) measurements on the squid fibre.

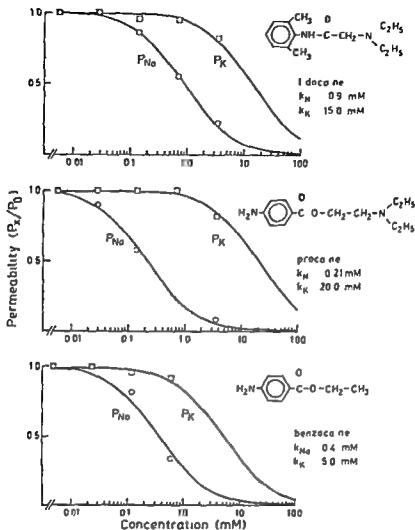


Fig. 2. Effect of three local anesthetics on max peak P_K and steady state P_K on one fibre. The curves are solutions of eqn. (1) for k values as indicated. Temperature 15°C.

Corresponding measurements were made on the delayed potassium currents. These indicated that the effect of the local anesthetics may simply be described as decreasing the permeability constant \bar{P}_K .

The next step was to do systematic measurements of the permeability concentration curves for the three local anesthetics used. The effect on the sodium system was obtained from measurements of the sodium currents associated with potential steps of a sufficient amplitude to turn on the sodium system fully. The membrane was held at a potential of -90 to -110 mV between the steps so that $h_\infty \approx 1$. The effect on the potassium system was measured on the steady state potassium current at large potential steps. In Fig. 3 are the peak sodium perme-

TABLE I Collected data of effects of local anesthetics Constant k calculated from measurements of \bar{P}_{Na} and \bar{P}_K pH 7.3

	k_{Na} (mM) mean \pm SD	k_K (mM) mean \pm SD	λ
Lidocaine	1.18 \pm 0.48	10.3 \pm 5.9	4
Procaine	0.21 \pm 0.04	9.8 \pm 7.0	5
Benzocaine	0.49 \pm 0.24	3.6 \pm 1.0	4

ability and the steady state potassium permeability associated with the test steps plotted against the concentration of the local anesthetics. The permeabilities are expressed as fractions of the permeability without any local anesthetic (i.e. P_x/P_0).

The following findings are evident from Fig. 2

1 The blocking effect on the sodium transport system as well as on the potassium system was smoothly graded with the concentration of the local anesthetics over a wide concentration range.

2 The dose response curve was satisfactorily described by the equation

$$\frac{P_x}{P_0} = \frac{k}{k + [x]}$$

where

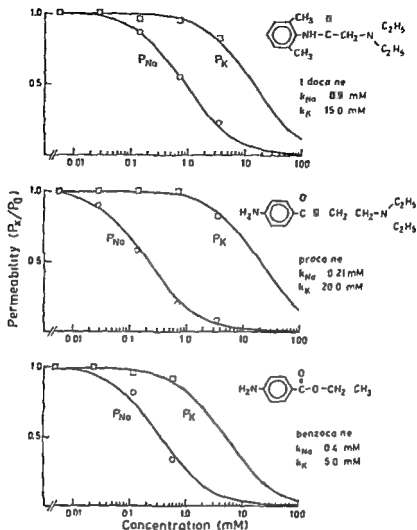
$[x]$ is concentration of local anesthetics, k is a constant with dimensions of concentration and equals the concentration at which permeability is half that when $[x] = 0$. P_0 is permeability when $[x] = 0$. P_x is permeability at concentration x .

3 The concentration constant k has different values for the different local anesthetics and different values for the sodium and for the potassium systems.

4 All these anesthetics blocked the sodium system at a lower concentration than that required to block the potassium system.

Similar measurements were made on several other fibres. Some with higher concentrations in order to check a larger part of the permeability concentration curve for the potassium system. The low water solubility of benzocaine formed an upper limit for that substance. All these measurements indicated that the effects satisfactorily were described by equation (1). The collected measurements are given in a condensed form in Table I.

Some experiments were carried out in order to obtain information about the rate with which the anesthetic effect decreased the current. The rate of decrease was compared with the rate with which the sodium current disappeared or returned at solution changes from/to ordinary Ringer solution to/from isotonic potassium chloride with 2 mM Ca^{++} . All these changes were 90% final within about 10–15 s from the beginning of the solution change if concentration of local anesthetic did not exceed that which blocks the sodium mechanism more than about 90%.



2 Effect of three local anesthetics on max peak P_{Na} and steady state P_K on one fibre. The curves are solutions of eqn (1) for f values as indicated. Temperature 15°C

Corresponding measurements were made on the delayed potassium currents. These indicated that the effect of the local anesthetics may simply be described as decreasing the permeability constant \bar{P}_K .

The next step was to do systematic measurements of the permeability concentration curves for the three local anesthetics used. The effect on the sodium system was obtained from measurements of the sodium currents associated with potential steps of a sufficient amplitude to turn on the sodium system fully. The membrane was held at a potential of -90 to -110 mV between the steps so that $h_{Na} \approx 1$. The effect on the potassium system was measured on the steady state potassium currents at large potential steps. In Fig 2 are the peak sodium perme-

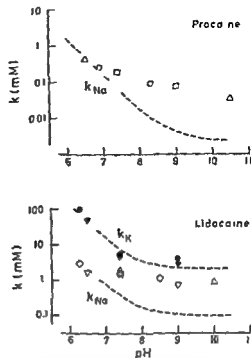


Fig. 4. pH dependence of k values for procaine and lidocaine. Smooth curves are calculated as in Fig. 3 and shifted along the y axis to get a reasonable fit with the experimental points at $\text{pH} = 7.0$. pH values used for procaine and lidocaine was 9.0 resp. 7.8. Temperature 15°C .

were more efficient in their blocking effect at high pH than at low. This holds true for the effect on the sodium system as well as on the potassium system. The pH dependence was not quantitatively predicted by the Henderson equation (see Fig. 3 legend) and the assumption that either the charged form or the uncharged form is active. The dependence was not the same for the potassium system and for the sodium system. Benzocaine had an effect that was independent of pH .

Anesthetic effect and $[\text{Ca}^{2+}]$

It has been suggested that calcium interferes with the effect of the local anesthetics (e.g. Blaustein and Goldman 1966). Measurements were therefore made of the peak P_N potential curve with external solutions with a sufficient concentration of local anesthetics to decrease the sodium permeability. Runs were made with such solutions containing a number of different calcium concentrations. Fig. 5 is a sample of such runs. Low $[\text{Ca}^{2+}]$ (0.74 mM) and high $[\text{Ca}^{2+}]$ (5.4 mM) were used here. The fibre was polarized to -110 mV between the test pulses in order to avoid the complication caused by changes in $[\text{Ca}^{2+}]$ on the sodium inactivation at the ordinary resting potential of the fibre. It is seen that the P_N at large potential steps was unaffected by the calcium concentration. The local anesthetic reduced it in both cases to approximately 70% of that in ordinary Ringer solution. The permeability curve in low $[\text{Ca}^{2+}]$ was shifted to the left. This is the common effect of changes in $[\text{Ca}^{2+}]$. This experiment and many other similar ones at a large range of [anesthetic]s and $[\text{Ca}^{2+}]$ s showed consistently that the effect of local anesthetics and of changes in $[\text{Ca}^{2+}]$ were independent of each other.

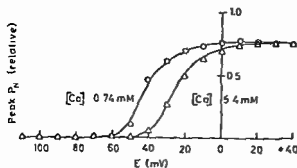


Fig. 5 Plot of peak P_{Na} and potential at 0.37 mM procaine and two different $[Ca]$ s. Ordinate given as permeability relative the permeability in ordinary Ringer solution

Corresponding measurements were made in order to resolve a possible interaction between Ca^{2+} and local anesthetics on the potassium permeability mechanism. These experiments were somewhat complicated by the effect of high $[Ca^{2+}]$ (> 25 mM) on the maximum P_K but indicated no interaction between the two substances.

Effects elicited from inside of fibre

Experiments were made in order to check whether the local anesthetics were active on the inside of the membrane. The nerve fibre was cut at the middle of internode N_1 to N_6 , i.e. the internode through which the current was forced. This was made in order to allow a substance applied to the solution pool with this end of the cut fibre, to diffuse within a reasonable time to the inside of the node under investigation (N_1). Such experiments showed that procaine applied in this way caused a slowly progressing decrease in the sodium current. The sodium currents recovered correspondingly slowly when procaine was washed away from the pool with the cut end.

Corresponding experiments were made with the aim to change pH at the inside of the node N_1 while the permeability concentration curve was measured by changing the external procaine concentration. These experiments were however inconclusive because no effect on the permeability concentration curve was detected.

Discussion

The peak sodium permeability and the steady state potassium permeability were reduced rapidly when the local anesthetics were applied. The reduction reached 90% of its final steady state value in less than 10–15 s at low concentrations. It seems likely that this time would be further reduced if the solution change at the node had a sharper border between the solution with and without the local anesthetics. The effects were well and rapidly reversed on switching to ordinary Ringer's solution provided that the fibre had been blocked less than 90%. If however higher concentrations were applied the recovery was much slower; several minutes were then required for 90% recovery. At the lower concentrations the recovery time was independent of the duration of local anesthetic application. It

therefore seems likely that the rapid and the slow recovery depend on different mechanisms

In this connection it may be pointed out that the recovery from a tetrodotoxin block of the squid giant axon is slow (Cuervo and Adelman 1970). Preliminary experiments on the node indicated that also this recovers slowly from a tetrodotoxin block.

The myelinated nerve fibre has a uniquely high ratio between axis cylinder volume and surface area of the excitable membrane. This high ratio excludes a rapid change of the axis cylinder concentration. It may therefore be concluded that these anesthetics act at a site rapidly available from the external solution, i.e. either at the external surface of the membrane or within the membrane, the blocking time is too short for a hypothetical mechanism involving a concentration change of the axis cylinder. The site of action can also be reached from the inside as indicated by the experiments where the local anesthetic was applied through an internode. This excludes that the site of action is localized exclusively at the outside surface.

It has been advocated that the local anesthetics act mainly in their charged form at the axis cylinder side of the excitable membrane but that the membrane is more permeable to the uncharged base (Narahashi, Frazier and Yamada 1970). Measurements were therefore made of the blocking effect of the local anesthetics at different pH values. These experiments indicated a minor change of the k_{∞} values with pH for lidocaine and procaine but not for benzocaine. The change was by far too small for the simple uncomplicated idea that pH at the site of action depends on external pH and that either the charged form or the uncharged base would be active while the other form would be inactive. The acid dissociation constant for lidocaine is 7.8 (Lofgren 1948) and for procaine about 9 (Eisner and Picher 1938, Lofgren 1948). The absence of a pH effect on the benzocaine action might indicate that the membrane itself is equally sensitive at these pH values to the anesthetics. Benzocaine which is undissociated at the pH range used had a blocking effect which was very similar to that of lidocaine and procaine. A charged form is therefore not *per se* required for the effect. All the present findings can be explained on the basis that the charged form and the uncharged form have somewhat different k values and these values differ between the sodium system and the potassium system. It should also be noted that the pH dependence seems to differ for the sodium and potassium system as indicated by the data on lidocaine in Fig. 4.

The experiments in which the effects of the local anesthetics were measured at a number of different calcium concentrations showed consistently that the effect of the local anesthetics was to change the permeability constants \bar{P}_{Na} and \bar{P}_{K} while that of calcium was to shift the permeability potential curve along the potential axis without affecting the permeability constants \bar{P}_{Na} and \bar{P}_{K} . These two substances thus had distinctly different effects and acted evidently independently of each other. This conclusion is contradictory to that of Blaustein and Cohen (1967) who concluded that these two substances interact on the lobster filar nerve. The explanation to the basis of this contradiction

The curve fitted to the permeability-concentration measurements are solutions of equation (1) and the curve is defined by the concentration and the constant k . Reversible first order chemical reactions and the adsorption of a gas on a surface (Langmuir adsorption isotherm) are samples of processes which follow this general type of equation (Clark 1933 Cuervo and Adelman 1970). In Fig 2 and equation (1) the solution is given for the available permeability or the fraction of unbound sites, if the equation is written for the blocked permeability or the fraction of bound sites (P_x/P_0) the equation is

$$\frac{P_x}{P_0} = \frac{[x]}{k + [x]}$$

and the solution to this is a mirror image of the solution to equation (1).

If the effect of the local anesthetic is measured on the size of the action potential an equation of the type of equation (1) is not expected to apply since the size of the action potential is not linearly related to the available permeability (Frankenhaeuser and Huxley 1964). In this case a steeper relation would be expected and has been experimentally obtained (Keynes Ritchie and Rojas 1971 Arerman 1973). The concentration constant k for the sodium system measured in the present investigation is about 10 larger than that measured for tetrodotoxine on the squid fibre (Cuervo and Adelman 1970). In the latter case it has been concluded that single tetrodotoxine molecules block single permeability sites (Moore Narahashi and Shaw 1967 Keynes *et al* 1971). For the local anesthetics this may also well be the case a difference in partition coefficient or in equilibrium and rate constants may well account for the difference in k values.

This work was supported by the Swedish Medical Research Council (Project No 14\545) and Karolinska Institutets fonder.

References

- ARCEVES J and A MACHIE The action of calcium and local anesthetics on nerve cells and their interaction during excitation *J Pharmacol exp Ther* 1963 140 138-148
- ARERMAN B Studies on the relative pharmacological effects of enantiomers of local anaesthetics with special regard to block of nervous excitation Thesis Uppsala 1973
- ARHEM P B FRANKENHAEUSER and L E MOORE Ionic currents at resting potential in nerve fibres from *Xenopus laevis* Potential clamp experiments *Acta physiol scand* 1973 88 446-454
- BLAUSTEIN T P and M E GOLDMAN Competitive action of calcium and procaine on lobster axon *J gen Physiol* 1966 49 1043-1063
- CLARK A J The Mode of Action of Drugs on Cells Williams and Wilkins Baltimore 1933
- CUERVO L A and W J ADELMAN Equilibrium and kinetic properties of the interaction between tetrodotoxin and the excitable membrane of the squid giant axon *J gen Physiol* 1970 55 309-335
- DETTBARN W H The active form of local anesthetics *Biochim biophys Acta (Amst)* 1972 57 73-16
- DOOG F A and B FRANKENHAEUSER Membrane currents in isolated frog nerve fibre under voltage clamp *Exp J Physiol Lond* 1958 143 76-90
- EISENBRAND J and H PIERER Bestimmung der Dissoziationskonstanten Löslichkeiten und Verteilungskoeffizienten von Pantikain und Novokainbase *Arch Pharm Phys* 1938 6 1-17

- FEINSTEIN M B Reaction of local anesthetics with phospholipids: a possible chemical basis for anesthesia *J gen Physiol* 1964 48 357-374
- FRANKENHAELSER B The effect of calcium on the myelinated nerve fibre *J Physiol (Lond)* 1957 137 245-260
- FRANKENHAELSER B Quantitative description of sodium currents in myelinated nerve fibres of *Xenopus laevis* *J Physiol (Lond)* 1960 151 491-501
- FRANKENHAELSER B Quantitative description of potassium currents in myelinated nerve fibres of *Xenopus laevis* *J Physiol (Lond)* 1963 169 424-430
- FRANKENHAELSER B and A L HODGKIN The action of calcium on the electrical properties of squid axons *J Physiol (Lond)* 1957 137 218-244
- FRANKENHAELSER B and A F HUXLEY The action potential in the myelinated nerve fibre of *Xenopus laevis* as computed on the basis of voltage clamp data *J Physiol (Lond)* 1964 171 307-315
- HILLE B Common mode of action of three agents that decrease the transient change in sodium permeability in nerves *Nature (Lond)* 1966 210 1220-1222
- HILLE B Charges and potentials at the nerve surface *J gen Physiol* 1968 51 291-296
- KEYNES R D J M RITCHIE and E ROJAS The binding of tetrodotoxin to nerve membranes *J Physiol (Lond)* 1971 213 235-254
- LOFGREN N *Studies on local anesthetics* Xylocaine: a new synthetic drug Thesis Stockholm 1948
- MOORE J W T NARAHASHI and T I SHAW An upper limit to the number of sodium channels in nerve membrane? *J Physiol (Lond)* 1967 188 99-103
- NARAHASHI T and D T FRAZIER Site of action and active forms of local anesthetics In *Neurosciences Research* Editors S EHRENFREIS and O C SOLNITZKY Academic Press New York & London 1971 pp 65-99
- NARAHASHI T D T FRAZIER and J W MOORE Comparison of tertiary and quaternary amine local anesthetics in their ability to depress membrane ionic conductances *J Neurobiol* 1972 3 267-276
- NARAHASHI T D T FRAZIER and M YAMADA The site of action and active forms of local anesthetics I. Theory and pH experiments with tertiary compounds *J Pharmacol exp Ther* 1970 171 32-44
- RITCHIE J M and P GREENGARD On the active structure of local anesthetics *J Pharmacol* 1961 133 241-245
- RITCHIE J M and P GREENGARD On the mode of action of local anesthetics *Ann Rev Pharmacol* 1966 6 405-430
- SEEMAN P M Membrane stabilization by drugs: tranquilizers, steroids and anesthetics *Int Rev Neurobiol* 1966 9 145-221
- SHAW A M W H FREYER, H GRUNDREIST and E AMATNEK An ester and calcium action in the voltage clamped squid giant axon *J gen Physiol* 1959 42 793-802
- TAYLOR R H Effects of procaine on electrical properties of squid axon membrane *Amer J Physiol* 1959 196 1071-1078

Distribution of Renal Cortical Blood Flow during Hemorrhagic Hypotension in Conscious Dogs

By

A KIRKEBO and I TYSSEBOTN

Received 6 November 1973

Abstract

KIRKEBO A and I TYSSEBOTN. Distribution of renal cortical blood flow during hemorrhagic hypotension in conscious dogs. *Acta physiol scand* 1974 91: 22-31.

The effect of hemorrhagic hypotension on distribution of renal cortical blood flow was investigated in 9 conscious dogs. 6 platinum electrodes were chronically implanted in inner and outer renal cortex and local cortical blood flow measured by hydrogen clearance. Urine was collected through a catheter implanted in the split bladder and total renal blood flow (RBF) determined by PAH clearance. In anesthetized dogs control blood flow averaged 3.72 ± 0.14 ml/min/g in outer cortex and 3.60 ± 0.53 ml/min/g in inner cortex. Local blood flow in conscious dogs fell to 30-60% of control in the course of 11 days after implantation of the electrodes though RBF was almost constant and filtering glomeruli were demonstrated in the small fibrotic zone (20-50 μ m) close to the electrode tip. No change in local flow was found by induction of Nembutal anesthesia. Bleeding of conscious dogs 1-3 days after implantation to mean arterial pressure 50 mm Hg reduced local blood flow to 10-30% of prebleeding control. The local blood flow in outer and inner cortex decreased near proportionately. Typically, flow at all electrode sites in outer and inner cortex showed a similar fall. A marked redistribution of cortical blood flow during hemorrhagic hypotension was never observed. Bilateral clamping of carotid arteries at normal and at low arterial pressures did not change outer or inner cortical blood flow.

Hemorrhagic hypotension (HH) causes a severe reduction in total renal blood flow (RBF). The idea of Trueta *et al* (1947) that this reduction is not general but confined to cortical zones is still controversial. By compartmental analysis of externally monitored K_r^* washout curves in anesthetized dogs, Carriere *et al* (1966) and Truniger, Rosen and Olsen (1966) found that HH reduced outer cortical blood flow to the level of the normal outer medullary flow while juxtamedullary cortical and medullary flow were well maintained for several hours. The cortical flow fraction decreased from 80-85% to about 10% of RBF.

On the other hand, a proportional fall of medullary blood flow and RBF during HH was found by Kramer and Deetjen (Kramer 1962) by measuring albumin transit time in medulla and by Aukland and Wolgast (1968) who measured local medullary clearance of H₂ and K_r and red cell transit time.

Using an improved local H desaturation technique (Loynning 1971) which allowed recording in the cortex Aukland *et al* (1973) found a proportional reduction of RBF and flow in the inner and outer cortex when dogs were bled to mean arterial pressure (\bar{AP}) of 50 mm Hg. The percentage deviation between flow at various electrode sites did not increase significantly during hypotension and thus indicated no patchy ischemia or regional redistribution of flow within cortex.

All these studies of the effect of HH on the distribution of renal blood flow were performed on dogs under barbiturate anesthesia. Since Grandchamp, Ager and Truniger (1971) have shown that α adrenergic blockade prevents a redistribution of renal blood flow during hypotension—as measured by the ^{125}I method—the depression of sympathoadrenal reflexes caused by high doses of pentobarbital (Trethewie 1953, Exley 1954) could possibly explain why no evidence for redistribution has been found by other investigators. Logan *et al* (1971) found that ligation of one carotid artery prevents redistribution of renal blood flow during shock.

The aim of the present investigation was therefore to study the effect of HH and of carotid clamping on renal cortical flow distribution by local H clearance technique in conscious dogs.

Methods

The experiments were undertaken on 9 dogs weighing 15–21 kg with free access to water and food.

Bladder splitting operation. All surgery was done with sodium pentobarbital (Nembutal) anesthesia 25 mg/kg bwt. The anesthesia was maintained by additional doses of about 50 mg Nembutal. The urinary bladder was split in 2 halves (Desautels 1957) and 2 small pouches were sewn from part of the bladder wall near the ureteral orifice. Urine flowed freely through catheters (PE 280) from each pouch to the skin surface where it could be sampled. The dogs were allowed to recover before further surgery and were trained in the meantime for experiments while awake.

Control measurements in anesthetized dogs. After 5–8 days 8 platinum electrodes were implanted in outer and inner half of renal cortex and local blood flow measured by hydrogen clearance as described previously. The coefficient of variation between consecutive control measurements was 3% between different electrode sites. However the coefficient of variation was 18% (Aukland *et al* 1973). Monoexponential desaturation curves were obtained from all electrodes used (27 of 54). RBF was determined from hematocrit and PAH clearance assuming an extraction of 80% (Aukland *et al* 1973). After control measurements in anesthetized dogs the electrode wires and the Heparin filled catheters in the renal artery and brachial vein were fixed to the skin.

Long term measurements in conscious dogs. Measurements of local cortical flow and PAH clearance were undertaken on each of the first 3–4 days later at 2–3 days intervals in the following period of 2 to 27 days. A catheter for arterial pressure measurements and blood sampling was each time inserted into a small artery usually the saphenous artery using local anesthesia (Xylocain 0.5%) not exceeding 10 ml. An infusion of PAH was given and urine collected for measurements of the RBF from each kidney. The electrodes were connected to the polarograph and hydrogen washout recorded.

At the end of the last experiment in each dog 3–27 days after electrode implantation the kidney was excised weighed and each electrode site was carefully examined macroscopically. The tissue around the electrode tip was cut out and fixed in 4% formalin and later sliced (20 μ thick) and stained with the Weigert and Gieson stain. This stained the connective tissue green and the red blood cells brilliant red.

At the end of the experiments in 7 dogs (4 and 7 days after implantation of the electrodes) 1 ml of 15% ferrocyanide solution was given into the renal artery. The kidney was clamped

by a sling, after 8–10 s and rapidly excised. Small tissue block containing the electrode sites were quickly frozen in alcoholic CO₂ ice. Na ferrocyanide was precipitated as Prussian blue by FeCl₃ and the filtered Na ferrocyanide thus made visible in the tubules (Hansen 1958 and 1963) where it could be localized by microscopic examination of 20 μ m slices.

Bleeding procedure. As shown in results, cortical H clearance fell during the first days after electrode implantation. Measurements in hemorrhagic hypotension were therefore carried out 1–3 days after implantation.

Using local anesthesia the femoral artery was cannulated with a widebore catheter for bleeding and sampling of blood to determine PAH clearance.

Control measurements of local cortical blood flow were made before and after PAH clearance measurements, the last one or two controls before bleeding being recorded after injection of 1 ml Heparin. The last H washout rate from each electrode before bleeding was used as reference for later measurements.

In 8 experiments 5 dogs were bled to $\bar{A}P$ 50 mm Hg usually in the course of 25 min. Measurement of local cortical flow was made at $\bar{A}P$ of about 70 mm Hg before further bleeding to 50 mm Hg. The pressure was maintained at this level for at least 2 hours by slight adjustment of the blood reservoir. Cortical flow measurements were made every 15–20 min. No bleeding was allowed during the hydrogen washout periods.

The conscious dogs were kept as calm as possible during the bleeding period by careful handling. One dog became excited during bleeding (2 expts) and struggled so heavily that we chose to stop the experiments.

The shed blood was retransfused in 15–20 min by elevating the blood reservoir. Cortical flow measurements were made after retransfusion and HR and $\bar{A}I$ recorded. This procedure was repeated on two consecutive days on 3 out of the 5 dogs.

Carotid artery occlusion. In 2 conscious dogs with normal arterial pressure the carotid artery on both sides was dissected free to be clamped by a sling. Cortical blood flow $\bar{A}I$ and HR were measured before and during clamping of one or both carotid arteries. The occlusion was maintained for about 2 min in 4 cases to allow recording of H washout curves. In three cases the clamp was held for more than 10 min while urine was collected for PAH clearance. Control cortical flow measurements were always made before and after the carotid artery occlusion. In 2 expts the carotid arteries were occluded for a few minutes during the hypotensive period ($\bar{A}I$ 50 mm Hg) while local flow was measured.

Results

Control measurements in anesthetized dogs. Local cortical blood flow, hematocrit, HR, $\bar{A}P$ and PAH clearance were measured after implantation of the platinum electrodes while the dogs were still anesthetized. Outer cortical blood flow (OCF) and inner cortical blood flow (ICF) in 11 expts on 9 dogs varied between 2.7–4.70 and 2.13–3.97 ml/min/g respectively, with average OCF 3.72 ± 0.74 SD ml/min/g and ICF 3.60 ± 0.53 SD ml/min/g.

RBF estimated from PAH clearance averaged 4.20 ± 1.60 SD ml/min/g and the mean hematocrit was 36%. $\bar{A}P$ varied from 120 to 135 mm Hg. HR was usually about 90 beats/min and differed little from dog to dog.

Control measurements in conscious dogs. Measurements of local cortical blood flow, $\bar{A}P$, HR and PAH clearance were repeated on 9 conscious dogs the day after implantation of the platinum electrodes. Average OCF and ICF were reduced to 86 ± 14 SD % and 81 ± 8 SD % of the control flows obtained the day before. Average PAH clearance decreased to 91 ± 13 SD % of control (Fig. 1). No change in OCF or ICF was observed by injection of Nembutal and/or Heparin. Also PAH clearance and HR were unchanged. $\bar{A}P$ increased from 95–115 mm Hg to 120–135 mm Hg with induction of anesthesia in 9 dogs.

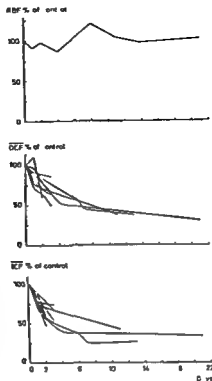


Fig 1 Average total renal blood flow (RBF) in 9 dogs (outer and inner cortical blood flow in each dog (OCF ICF mean of 3 electrodes) in per cent of initial control flow related to time after implantation of the electrodes

Long term experiments on conscious dogs OCF ICF \overline{AP} HR and PAH clearance were measured on each of the first 3–4 days and thereafter every 2nd or 3rd day until 22 days after implantation of the electrodes. The greatest fall in local blood flow was seen during the first 3 days (Fig 1). After 3 days average OCF and ICF were 72 ± 19 S.D. % and 66 ± 11 S.D. % of control values in anesthetized dogs. PAH clearance was at the same time 92 ± 9 S.D. % of control. 11 days after implantation of electrodes average OCF had fallen to 40 ± 3 S.D. % of control while average ICF fell to 36 ± 8 S.D. % of control. In contrast PAH clearance was 102 ± 24 S.D. % of control. Average \overline{AP} and HR did not vary more than 10 % from day to day.

When the kidney was removed 2–5 days after implantation macroscopic examination showed a small hematoma in 4 out of 24 electrode sites. Microscopic examination usually showed small accumulations of blood cells along the tip of the electrode surrounded by a zone with some erythrocytes in some tubular lumina and in the interstices. In kidneys excised after a week or more no macroscopic changes could be observed whereas varying degrees of degenerations of tubules and fibrosis around the tip were revealed by microscopic examination. The diameter of the hematoma and the fibrotic zone usually did not exceed 60–90 μm giving a maximum zone of diffusion of ca 45 μm .

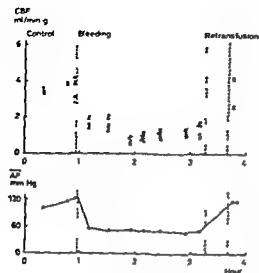


Fig 2 Effect of bleeding and retransfusion on mean arterial pressure (\overline{AP}) and local cortical blood flow (CBF) at 6 different electrode sites in one dog (Open symbols: Outer cortex. Closed symbols: Inner cortex.)

By injection of ferrocyanide filtering nephrons were demonstrated within the hemorrhagic and fibrotic zones indicating at least some filtration in these nephrons.

Hemorrhagic hypotension. 1–3 days after implantation of electrodes the conscious dogs were bled to \overline{AP} 50 mm Hg in the course of 15–20 min. As observed in Fig 2 from a typical experiment, flow fell at all electrode sites in inner and outer cortex and approximately to the same extent. In 5 of 8 expts. OCF and ICF were less reduced than \overline{AP} during the first half hour of bleeding. Usually the OCF and ICF showed a further fall to 10–30% of control values obtained shortly before bleeding (\overline{OCF} 3.16 ± 0.75 SD ml/min.g, \overline{ICF} 2.70 ± 0.69 SD ml/min.g) though the \overline{AP} was maintained at a constant level of about 50 mm Hg. Thus vascular resistance ($\overline{AP}/\overline{OCF}$ and $\overline{AP}/\overline{ICF}$) in 5 cases showed a decrease in the first period of bleeding and later on an increase exceeding the control level about 30 min after the start of hemorrhage. In 2 cases resistance remained low during the whole hypotensive period (Fig 3).

During bleeding \overline{OCF} and \overline{ICF} showed a corresponding reduction in all experiments though \overline{OCF} fell 10% more than \overline{ICF} . The ratio $\overline{OCF}/\overline{ICF}$ during HH was significantly lower than unity ($p < 0.01$).

In Fig 4 cortical blood flow has been plotted in absolute values and in Fig 5 flow is given in per cent of prebleeding control measurements.

Though some scatter was found between different animals and different electrodes essentially similar responses were seen in all experiments with no signs of patchy ischemia.

Most dogs became drowsy during the bleeding period, sometimes with obvious reduced consciousness. In the later part of HH hyperventilation was regularly observed and the dogs showed brief periods of restlessness.

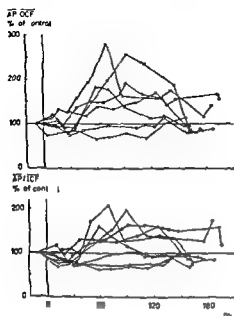


Fig 3

Fig 3 Vascular resistance in outer ($\overline{AP}/\overline{OCF}$) and in inner ($\overline{AP}/\overline{ICF}$) cortex calculated from mean arterial pressure and local blood flow in different dogs

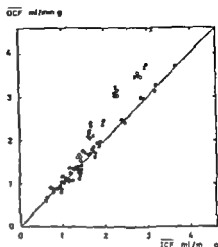


Fig 4

Fig 4 Blood flow in outer cortex (\overline{OCF}) related to flow in inner cortex (\overline{ICF}) in different experiments (Open symbols Control period Closed symbol Hypotensive period \ After retransfusion)

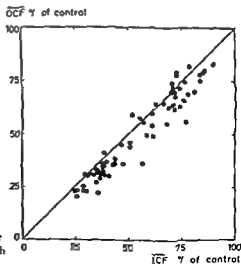


Fig 5 Outer cortical blood flow (\overline{OCF}) related to inner cortical blood flow (\overline{ICF}) both in percent of control measurements

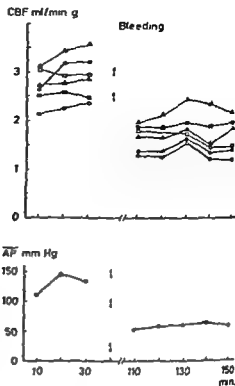


Fig 6 Effect of carotid artery occlusion and of bleeding on mean arterial pressure (\overline{AP}) and local cortical blood flow (CBF) at 6 different electrode sites in a single experiment. Hatched zone represents occlusion period (Open symbols Outer cortex. Closed symbols Inner cortex).

Retransfusion of blood restored local cortical blood flow completely in all experiments (Fig 2).

Effect of carotid artery occlusion Bilateral clamping of the carotid arteries in conscious dogs raised on the average \overline{AP} 35 mm Hg above normal pressure (Fig 6, 7). \overline{OCF} and \overline{ICF} did not change except in 2 cases showing moderate simultaneous elevation of \overline{ICF} and \overline{OCF} . Average \overline{OCF} and \overline{ICF} were 2.86 ± 0.24 and

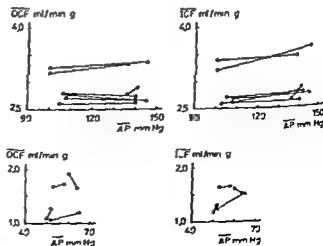


Fig 7 Effect of carotid artery occlusion at normal arterial pressure (upper panels) and in hypotensive state (lower panels). Mean outer \overline{OCF} and mean inner \overline{ICF} cortical blood flow related to mean arterial pressure \overline{AP} before (open symbols) and during occlusion (closed symbols).

2.82 ± 0.29 S.D. ml/min g before clamping and 2.88 ± 0.31 and 2.96 ± 0.38 S.D. ml/min g during the clamping period

Carotid clamping during HH induced only small and irregular variations of \overline{AP} and local blood flow (Fig. 7). No redistribution of carotid blood flow was observed as averaged \overline{OCF} and \overline{ICF} were 1.45 ± 0.42 and 1.41 ± 0.25 S.D. ml/min g before clamping and 1.46 ± 0.26 and 1.49 ± 0.14 S.D. ml/min g during occlusion.

Discussion

Control measurements The local outer and inner cortical blood flow found in the present work agrees well with the previous measurements by the same technique (Loynning 1971, Aukland *et al.* 1973). The high glomerular blood flow in outer cortex indicated by microsphere distribution (McNay and Abe 1970, Logan 1971) may be explained by the higher glomerular density in this region (Horster, Kemler and Valtin 1971).

Injection of Nembutal caused no change in OCF or ICF in the present experiments. The decrease in local flow from one day to the next therefore did not depend on anesthesia. \overline{AP} increased from 95–115 mm Hg to 120–135 mm Hg indicating higher renal vascular resistance due to autoregulation or increased sympathetic stimulation. These results agree with findings of Grangsjö and Persson (1968) and Rector *et al.* (1972) using heat clearance and microsphere techniques respectively.

Chronic implantation of electrodes During the first 3 days local cortical blood flow decreased to 65–70% of control flow. RBF measured by PAH clearance was almost constant indicating a falling blood flow mainly in the zone immediately surrounding the electrodes. The microscopic changes observed in cortical tissue had a small area of extension relative to the diffusion zone (300 μ m) calculated to supply hydrogen to the electrode and cannot satisfactorily explain the progressive fall in local flow. However all bleeding expts were performed on the second or third day after implantation of the electrodes. Within this period of time the development of fibrosis is negligible.

Bleeding of conscious dog The initial reduction and the later increase of renal peripheral resistance following start of bleeding confirmed earlier findings in anesthetized dogs (Aukland *et al.* 1973, Jurka *et al.* 1961). Bleeding to \overline{AP} 50 mm Hg diminished cortical blood flow to 10–30% of the control values. The fall in OCF was almost linearly related to the fall in ICF. Though the control OCF was slightly higher than control ICF and thus in absolute units the reduction in OCF was also slightly higher than the corresponding reduction in ICF (Fig. 4, 5) these results are in close agreement with the results obtained by the same technique during HH in anesthetized dogs (Aukland *et al.* 1973). Kramer and Deetjen (Kramer 1967) and Aukland and Wolgast (1968) found that the medullary blood flow during hemorrhage is reduced proportionately to total renal blood flow. The in

ference made from this observation, that also cortical flow is reduced proportionately to total RBF is supported by the present findings.

Results contradictory to this conclusion have been obtained by Kr^8 and Xe^{133} washout techniques. Carriere *et al* (1966), Truniger, Rosen and Oken (1966), Carriere and Daigneault (1970) and Grandchamp, Ayer and Truniger (1971) all found that HH lead to a patchy and marked reduction of perfused tissue mass and blood flow in outer cortex while blood flow in juxtamedullary cortex and outer medulla was fairly unchanged. Slotkoff *et al* (1971) and Rector *et al* (1972) demonstrated a decrease in the fraction of microspheres going to the outer cortical nephrons in hemorrhage and a concomitant relative increase in the fraction to inner cortical nephrons. The discrepancy between the present findings may possibly be related to a difference in functional flow measured by the different methods used. The hydrogen washout method probably reflects changes in peritubular capillary flow effective for gas exchange and this does not necessarily parallel glomerular perfusion rate in the same zone as measured by the microsphere method (Rector *et al* 1972). It is noteworthy that intrarenal counting of Kr^8 clearance during HH (Aukland and Wolgast 1968) provides results compatible with results obtained by H₂ clearance in the present study. It may be that the compartmental analysis which is necessary to the externally detected Kr^8 washout curves is valid only for control situation.

Carotid artery occlusion. In early stages of shock Logan *et al* (1971) found that outer cortical blood flow fell dramatically while juxtamedullary flow was well preserved. Catheterization of the carotid artery before hemorrhage however resulted in increased juxtamedullary flow in spite of lower arterial pressure. Bleeding of carotid catheterized dogs caused no further change in relative distribution of cortical blood flow though total renal blood flow fell to 35% of initial flow. Logan *et al* (1971) used these findings as an explanation for the discrepancy between results obtained by microspheres and extracorporeal counting of the Xe^{133} washout curves and results obtained by locally measured hydrogen and Xe^{133} clearance. The present observations did not confirm this explanation since occlusion of the carotid arteries had no effect on cortical blood flow distribution. This applied to both the normal and hypotensive states in conscious as well as in anesthetized dogs. Further the carotid arteries were not catheterized in our experiments.

References

- AUKLAND, K. and M. WOLGAST. Effect of hemorrhage and retransfusion on intrarenal distribution of blood flow in dogs. *J. clin. Invest.* 1968, 47: 488-501.
- AUKLAND, K., A. KIRKEBO, E. LEVING and I. TYSSEBØN. Effect of hemorrhagic hypotension on the distribution of renal cortical blood flow in anesthetized dogs. *Acta physiol. scand.* 1973, 87: 514-525.
- CARRIERE, S. and B. DAIGNEAULT. Effect of retransfusion after hemorrhagic hypotension on intrarenal distribution of blood flow in dogs. *J. clin. Invest.* 1970, 49: 2203-2217.
- CARRIERE, S., G. H. THORBLIN, C. C. C. MORCHOE and A. C. BARER. Intrarenal distribution of blood flow in dogs during hemorrhagic hypotension. *Circulat. Res.* 1968, 19: 167-179.

- DESJARDIS R E Hemisection of the bladder for the collection of separate urine samples *Surg Gynec Obstet* 1957 105 767-768
- EXLEY K A Depression of autonomic ganglia by barbiturates *Brit J Pharmacol* 1954 9 1/0-181
- GRANDCHAMP A G AYER and H TRUNIGER Pathogenesis of redistribution of intrarenal blood flow in hemorrhagic hypotension *Europ J clin Invest* 1971 1 2/1-2/6
- GRANSSJO G and H PERSSON Influence of some vaso-active substances on regional blood flow in the dog kidney *Acta anaesth scand* 1971 15 71-95
- HANSEN O H A histochemical method for evaluation of excreted sodium ferrocyanide in isolated tubules of mouse kidney *Acta path microbiol scand* 1958 44 363-371
- HANSEN O E Method for comparison of glomerular filtration in individual rat nephrons *Proc 2nd Int Nephrol Congr* 1963 577-579
- HORSTER M B J KEMLER and H VALTIN Intracortical distribution of number and volume of glomeruli during postnatal maturation in the dog *J clin Invest* 1971 50 796-800
- JIRKA J V GANZ V FENEL J H CORT and R TRUNIGER Measurement of renal blood flow in the intact kidney by local thermodilution during haemorrhagic hypotension *Lancet* 1961 2 692-693
- KRAMER H Renal failure in shock *Shock pathogenesis and therapy* Ed H D Bock Springer Verlag Berlin 1967 pp 134-144
- LOGAN A P JOSE G EISNER L LILIENTHAL and L SLOTKOFF Intracortical distribution of renal blood flow in hemorrhagic shock in dogs *Circulat Res* 1971 29 257-265
- LOYING E W Effect of reduced perfusion pressure on intrarenal distribution of blood flow in dogs *Acta physiol scand* 1971 83 191-201
- MUNAY J L and V ABE Pressure-dependent heterogeneity of renal cortical blood flow in dogs *Circulat Res* 1970 27 571-587
- RECTOR J B J H STEIN W H BAY R W O-GOOD and T F FERRIS Effect of hemorrhage and vasopressor agents on distribution of renal blood flow *Amer J Physiol* 1970 222 1125-1137
- SLOTKOFF L M A LOGAN P JOSE J DAVELLA and G M EISNER Microsphere measurement of intrarenal circulation of the dog *Circulat Res* 1971 28 158-166
- TRETHEWEY E R The influence of barbiturate on the sympathetic nervous system *Med J Austr* 1953 1 100-104
- TRUETA R J A E BARCLAY P M DANIEL K J FRANKLIN and M L PITCHARD *Studies of the renal circulation* Blackwell Scientific Publications Ltd Oxford 1947
- TRUNIGER H S M ROSEN and H E OKEN Renale Hamodynamik und hamorrhagische Hypotension *Min Wschr* 1966 44 857-867

Autoregulation of Capillary Hydrostatic Pressure in Skeletal Muscle during Regional Arterial Hypo- and Hypertension

By

JOHANNES JÄRHULT and STEFAN MELLANDER

Received 12 November 1973

Abstract

JÄRHULT J and S MELLANDER *Autoregulation of capillary hydrostatic pressure in skeletal muscle during regional arterial hypo and hypertension* Acta physiol scand 1974 91 32-41

Net transcapillary fluid movements in the sympathectomized cat skeletal muscle were observed in response to regional mean arterial pressure variations in the range from 30 to 170 mm Hg. The transcapillary Starling fluid equilibrium prevailing at normal perfusion pressure was found to be roughly maintained over the entire range of arterial hypo- and hypertension, indicating an approximate constancy of capillary hydrostatic pressure (p_c). This "autoregulation" of p_c was mainly due to active changes of vascular tone in the precapillary resistance vessels causing a resetting of the pre- to postcapillary resistance ratio (r_p/r_r) but disappeared after abolition of vascular tone by papaverine. In the lowest pressure range a passive rise of postcapillary resistance contributed to the resetting of r_p/r_r . By this autoregulation of p_c the muscle tissue is protected against undue redistributions of fluid between the intra- and extravascular spaces when arterial pressure *per se* is changed.

Most vascular beds including that of skeletal muscle exhibit an autoregulation of blood flow over a wide range of perfusion pressures. This phenomenon is conceived of as the result of an interaction of the myogenic and the metabolic control systems on the resistance vessels (for ref. see Johnson 1964). Variations of arterial pressure might also be expected to be associated with an autoregulation of capillary hydrostatic pressure, since otherwise seemingly undue shifts in the fluid distribution between the intra- and extravascular spaces would occur. This hypothesis has received some support by previous experimental observations at certain levels of arterial hypotension and at occasional transient pressure rises which indicate that the phenomenon is accomplished by adjustments of the pre- to postcapillary resistance ratio (Mellander 1960, Folkow and Öberg 1961, Lewis and Mellander 1962, Folkow *et al.* 1964, Johnson 1964, Haglund and Lundgren 1972). In the present investigation an attempt was made to analyze this problem more thoroughly over a mean arterial pressure range from about 30 to 170 mm Hg.

Methods

The study was performed on the lower leg muscles of 21 cats anesthetized iv with α -chloralose (30 mg/kg bwt) and a small single dose of pentobarbital sodium (10–20 mg). The lower leg muscles were separated from the thigh muscles and the skin the paw removed at the ankle joint and the femur cavity plugged. Small vessels between the thigh and the lower leg were ligated so that the popliteal artery and vein formed the sole vascular connections to the main part of the animal. The muscle region was sympathectomized by severing the sciatic nerve and placed in a water filled temperature controlled (38 °C) plethysmograph to permit continuous recordings of changes of tissue volume via a Grass FT 10C transducer (for details see Grande *et al* 1974). After heparinization venous outflow was diverted from the popliteal vein via a blood flow measuring unit (drop recorder) to the external jugular vein. Venous outflow pressure was monitored from a T tube close to the cannula in the popliteal vein. The arterial inflow pressure to the muscle region was monitored from a T tube in a short shunt circuit connecting the distal femoral artery to the popliteal artery and pressure could be adjusted by a screw clamp placed proximal to the T tube. Systemic arterial pressure was recorded from the right carotid artery. Statham P23AC transducers placed at the water level in the plethysmograph were used for pressure measurements. Blood flow, arterial and venous pressures and changes of tissue volume were continuously recorded on a Grass Polygraph.

In 4 of the experiments the pressures in a small artery (SAP) and a small vein (SVP) were monitored from drawn out flexible nylon tubings inserted in the sural artery and vein and recorded with Statham P23AC and P23DC transducers respectively. This technique of measuring SAP and SVP implies that the pressure in small vessels is transmitted via collaterals to the cannulated proximally occluded vessel (for details see Haddy *et al* 1954; Lundvall 1972). Free communication through the collaterals was evidenced by the rapid change in SAP and SVP occurring upon occlusion of the arterial inflow or venous outflow tubings and by blood flow drainage through the cannulas upon disconnection from the pressure transducers.

The capillary filtration coefficient (CFC) was determined by raising the venous outflow pressure a known amount and recording the concomitant change of tissue volume (Cobbold *et al* 1963). To minimize possible myogenic reactions which could influence the pre- to postcapillary resistance ratio and hence CFC the venous outflow pressure rise in these determinations was as small as 2–5 mm Hg.

Experimental procedures

A Hypotension experiments In the control period with normal mean arterial inflow pressure (≈ 100 mm Hg) the venous outflow pressure was set so as to achieve an isovolumetric state (zero net transcapillary fluid movement) in the muscle. CFC was determined and after a subsequent 5 min period of isovolumetry the arterial inflow pressure to the muscle region was lowered to different levels (range 30–80 mm Hg) by adjustments of the screw clamp on the femoral artery. The change of tissue volume occurring at each level of regional hypotension was observed for about 5 min followed by a determination of CFC. The arterial inflow pressure was then restored to the control level. After a sufficient recovery period similar observations were made but at a different level of arterial hypotension. In some other experiments arterial inflow pressure was reduced in a stepwise manner. Arterial and regional venous plasma osmolality was determined at intervals by thermistor cryoscopy (Advanced Instruments Inc.). In 3 expts papaverine (0.6–1.6 mg/min) was infused close arterially to achieve a maximal regional vasodilatation after which hypotension experiments were performed as described.

In 4 expts the arterial inflow pressure to the muscle region was maintained at 50 mm Hg for a period of 90 min. Tissue volume was recorded continuously and arterial and venous plasma osmolality followed at intervals during the period of hypotension.

B Hypertension experiments A rise of arterial inflow pressure above the normal level was accomplished by bilateral occlusion of the common carotid arteries after cervical vagotomy (3 cats). To prevent possible constrictor effects in the muscle region caused by circulating catecholamines the α -adrenergic receptors in the region were blocked in these experiments by a close arterial slow injection of phenoxylbenzamine (≈ 10 mg/kg). The venous blood from the region during the injection was discarded. The effectiveness of the blockade was checked by an injection of 5 μ g/kg of noradrenaline. B adjustments of the screw clamp mean arterial inflow pressure could be set at desired levels above normal (up to about 175 mm Hg). The experimental procedures were in other respects similar to those described for the short term hypotension experiments.

Data below are given as mean values \pm S.E.

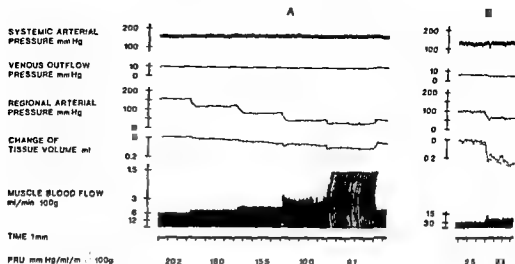


Fig. 1 Effects on net transcapillary fluid movement (change of tissue volume) and on resistance vessels during stepwise decreases of regional arterial pressure in the sympathetomized cat skeletal muscle. When vascular reactivity is preserved (panel A) the transcapillary fluid flux was small whereas when abolished by papaverine (panel B) it was pronounced.

Results

In some experiments arterial pressure was spontaneously so high as to permit observations in both the hypertensive and the hypotensive pressure range and as these show the general trend of the results they will be described first. After this follows a more detailed description of the results from the separate series of hypotension and hypertension experiments.

Fig. 1 A shows tracings of systemic pulsatile and regional mean arterial pressure, popliteal vein pressure, muscle blood flow and changes of tissue volume from a representative experiment with stepwise decreases of arterial inflow pressure from about 160 down to 30 mm Hg. Venous outflow pressure remained approximately constant but muscle blood flow decreased successively. There was however a gradual relaxation of the muscle resistance vessels as evidenced by the figures for regional resistance (PRU). Tissue volume showed only minor changes from the control isovolumetric state in response to the pressure reductions. In this sympathetomized vascular bed the initial rapid decrease of tissue volume immediately following each reduction of inflow pressure reflects a regional blood volume decrease owing to passive elastic recoil of the vessels whereas the later change of volume at each level of reduced arterial pressure represents net transcapillary fluid movements (e.g. Mellander 1960). It can thus be seen that despite large reductions of arterial inflow pressure the evoked net transcapillary fluid fluxes were small: in none of the hypotensive periods did fluid absorption occur at a rate exceeding 0.01 ml/min \times 100 g tissue. This implies that capillary hydrostatic pressure was very little influenced by the arterial pressure drop (see further below). In Fig. 1 B taken from

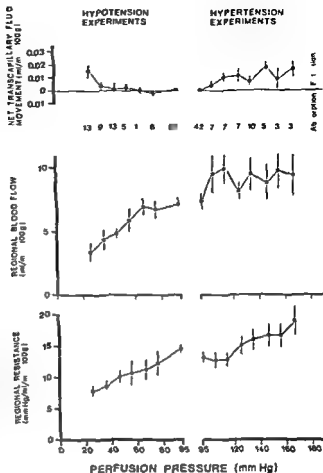


Fig. 7. Cumulated mean data \pm SE on net transcapillary fluid movement and on resistance vessel responses during short term regional arterial hypo- and hypertension in cat skeletal muscle. ■ indicates number of experimental observations.

the same experiment papaverine was infused so as to achieve a maximal vasodilatation and hence a passive vascular bed. When in this situation the regional arterial pressure was lowered from 100 to 60 mm Hg blood flow was reduced in direct relation to the decrease in perfusion pressure, further indicated by the virtually unchanged value for PRU. Tissue volume after the initial passive blood volume reduction now showed a clearcut and relatively continuous decrease in the hypotensive period, reflecting a net transcapillary fluid absorption at a rate of $0.05 \text{ ml/min} \times 100 \text{ g}$. — The abovementioned findings indicate that as long as vascular reactivity is preserved there is an approximate maintenance of a Starling equilibrium despite a wide range of arterial pressure reductions, an effect apparently caused at least in part by autoregulatory phenomena in the resistance vessels. Below follows a more detailed analysis of these events.

Hypotension experiments. In the majority of the experiments (57 observations) the vascular bed was exposed to short term ($\approx 5 \text{ min}$) regional hypotension at

intervals and in this series CFC was also determined. Mean arterial inflow pressure in the control period was here adjusted to about 100 (99 ± 0.3) mm Hg and venous outflow pressure was set so as to obtain an isovolumetric state and averaged 5.6 ± 0.6 mm Hg. Vascular tone in the control period could be considered normal for the sympathectomized muscle vascular bed as evidenced from the values for regional resistance (14.5 ± 1.3 mm Hg/ml/min $\times 100$ g) and for CFC (0.012 ± 0.002 ml/min $\times 100$ g \times mm Hg) (cf Lundvall 1972). Fig 2, left panels summarizes data from the arterial hypotension experiments. The diagrams show data on net transcapillary fluid movement, regional blood flow and peripheral resistance plotted against the perfusion pressure. (Venous outflow pressure was little affected by the arterial pressure fall and decreased in no case by more than 1.5 mm Hg). The upper panel shows that the perfusion pressure reduction did not lead to any significant net transcapillary fluid movement except at the lowest pressure (25 mm Hg) where a slight fluid filtration from the intravascular to the extravascular space took place. The resistance vessels showed trends of autoregulation most marked in the upper perfusion range (lower panels). — Arterial and regional venous plasma osmolality determined in some of the experiments was not significantly changed during the hypotension.

Hypertension experiment In this series 42 observations were made during short term regional hypertension (Fig 2 right panels). In the control period mean arterial pressure averaged 103 ± 0.8 mm Hg and venous outflow pressure 6.5 ± 0.1 mm Hg.

It can be seen from the figure (upper panel) that an increase of perfusion pressure above normal caused only slight fluid filtration from the intravascular to the extravascular space. The resistance vessels (lower panels) showed quite efficient autoregulation.

Change of capillary hydrostatic pressure The capillary filtration coefficient (CFC) tended to increase when regional arterial pressure was reduced below control and to decrease somewhat when pressure was increased (range 0.010–0.030 ml/min $\times 100$ g tissue \times mm Hg) in accordance with previous findings (Cobbold *et al* 1963; Mellander, Öberg and Odelram 1964). By dividing the observed net transcapillary fluid movement by CFC in the hypotension and hypertension experiments it was possible to calculate the net change of the mean driving forces governing transcapillary fluid exchange. Since it is unlikely, at least in short term experiments, that a sudden change of regional perfusion pressure would alter significantly the hydrostatic or oncotic pressure in the interstitium or the plasma oncotic pressure (see discussion), an observed fluid movement in these experiments can be attributed to a change of mean capillary hydrostatic pressure (p). Such calculations made it clear that p in skeletal muscle was very little influenced by regional arterial pressure changes in the range from 170 to 30 mm Hg. The data in Fig 2, upper panel, thus indicated that during hypertension p did not increase above the control value by more than 2 mm Hg and that during hypotension p was virtually unchanged ($\approx \pm 0.5$ mm Hg). This approximate maintenance of p

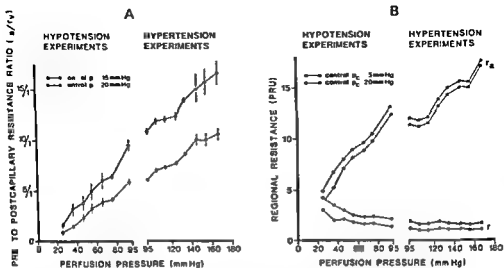


Fig 3 Panel A Calculated ratios of pre- to postcapillary resistance (mean \pm SE) during regional arterial hypo- and hypertension in skeletal muscle for assumed capillary hydrostatic pressures of 15 and 20 mm Hg respectively in the control period with normal perfusion pressure Panel B Average precapillary (r_p) and postcapillary (r_v) resistances expressed in absolute figures (mm Hg/ml/min $\times 100$ g) during regional arterial hypo- and hypertension in muscle

was further supported by the finding that small vein pressure was almost constant during arterial hypotension (range of change 0 to -3 mm Hg)

Calculation of the ratio of pre to postcapillary resistance Capillary hydrostatic pressure (p) is determined by arterial and venous pressure and by the ratio of pre to postcapillary resistance (r_p/r_v) (see Pappenheimer and Soto Rivera 1948). The findings of a roughly maintained transcapillary fluid equilibrium and virtually unchanged p during changes of arterial inflow pressure must imply a resetting of r_p/r_v . If p during normal perfusion pressure is known it is possible to calculate r_p/r_v at the different levels of arterial pressure. According to Landis (1934) p at the midpoint of the capillary in skeletal muscle is normally about 25 mm Hg but the p relevant for the present discussion should probably be less than this value let us say 20 mm Hg due to the fact that there seems to be an increased permeability towards the venous side of the capillary and that the venous microvessels may participate in the fluid exchange (for ref see Mellander 1970). In fact a recent study indicates that the isovolumetric capillary pressure in the muscle is closer to 15 mm Hg (Eliassen *et al* 1974). For the present calculations of r_p/r_v we therefore assumed isovolumetric p to be in this range and used two values 15 and 20 mm Hg for our deductions.

At normal perfusion pressure (≈ 95 mm Hg) r_p/r_v averaged about 6/1 and 10/1 for the assumed two p values of 20 and 15 mm Hg respectively (Fig 3 panel A). As can be seen r_p/r_v increased with raised and decreased with reduced arterial

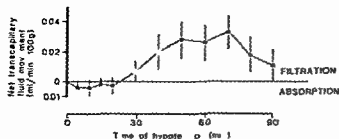


Fig 4 Net transcapillary fluid movement in muscle during prolonged regional arterial hypotension at 50 mm Hg (mean \pm S.E.)

pressure the relation being almost linear Fig 3 panel B depicts precapillary resistance (r_p) and postcapillary resistance (r_v) expressed in average absolute figures at the different levels of perfusion pressure. The precapillary resistance thus declined gradually as perfusion pressure was reduced. The postcapillary resistance tended to increase as pressure decreased but more markedly so only in the lowest pressure range.

Prolonged hypotension experiments. In 4 animals the period of regional hypotension was prolonged to 90 min and in these arterial pressure was kept at a constant level of about 50 mm Hg. Fig 4 shows that no significant net transcapillary fluid fluxes were present during the first 30 min of hypotension but that a slight filtration (0.015–0.030 ml/min \times 100 g) appeared later on corresponding to an increase of p by at most 2 mm Hg. Arterial and regional venous osmolality increased somewhat in the latest stage of hypotension but the arterio-venous osmolar difference was roughly unchanged.

Discussion

The present study has shown that the transcapillary fluid balance (Starling equilibrium) which exists at normal arterial blood pressure is surprisingly well maintained in skeletal muscle when arterial pressure is changed from 30 to 170 mm Hg. This finding noted over such a wide range of arterial hypo- and hypertension is in agreement with some previous observations in skeletal muscle during transient changes of pressure (Mellander 1960; Folkow and Öberg 1961) and during a given stable level of arterial hypotension (Levi and Mellander 1962) and with more recent similar findings in the intestine during certain levels of regional hypotension (Folkow *et al.* 1964; Johnson 1964; Haglund and Lundgren 1972).

The most reasonable explanation for the maintenance of an isovolumetric state during arterial hypo- and hypertension is that p stays roughly constant. A possible change of interstitial hydrostatic pressure for instance due to passive vascular distension and consequent changes of regional blood volume during arterial pressure alterations could have contributed to the maintenance of the Starling equilibrium. This seems refuted however by the finding that in the passive vascular bed a decrease of arterial pressure led to a clearcut transcapillary fluid absorption despite a more pronounced passive elastic recoil than in the normal vascular bed (see Fig 1). An

alteration of the transcapillary colloid osmotic gradient seems to be a fairly unlikely explanation even if it cannot be entirely excluded for instance if the colloid osmotic fluid absorption as may be the case for other osmotic processes is blood flow dependent (*cf* Lundvall 1972). Anyhow it appears that the effects of the latter mechanisms must be small.

The present data thus indicate that p_c varies by at most some 2 mm Hg from the control value during the induced arterial hypo- and hypertensions when most pronounced. This approximate maintenance of p must to a great extent depend upon active adjustments of vascular tone since in the passive vascular bed arterial pressure reduction led to a clearcut fluid absorption (see Fig 1 panel B). These active adjustments to tone seem almost exclusively confined to the precapillary vessels as evidenced by the marked decline of precapillary resistance during reduction of arterial pressure (Fig 3 B). Observed large reductions of small artery pressure when inflow pressure was only moderately decreased, in face of virtually unchanged small vein pressure support this interpretation. These adjustments of precapillary tone apparently are caused by myogenic as well as metabolic autoregulatory phenomena and seem to be the main explanation for the constancy of p in the pressure range down to about 50 mm Hg. In the lowest pressure range however postcapillary resistance rose quite significantly (Fig 3 P) which here must be an additional factor that helps to maintain p constant. It is unlikely that this increase of postcapillary resistance is due to active constriction since the vascular bed was sympathectomized and the hypotension was produced only locally in the studied region. It is instead in all probability a passive effect due to rheological factors such as increased viscosity at low shear rates and/or postcapillary aggregation of red and white cells (*cf* Eriksson and Lisander 1972, Ericson and Eriksson 1973). Passive collapse of the venous vessels might also have contributed to the phenomenon. Although r_v in absolute terms is normally a small fraction of overall regional resistance it is important indeed for the transcapillary fluid balance when r rises as during extreme hypotension it in fact approaches in absolute terms the value for precapillary resistance (Fig 3 B). A passive increase of postcapillary resistance is probably also the main explanation for the fluid filtration observed at the most pronounced short term hypotensions (Fig 2) and in late stages of prolonged hypotension (Fig 4).

It may be concluded that there is an efficient autoregulation of capillary hydrostatic pressure in skeletal muscle in response to alterations of arterial pressure in turn caused by active and to some extent passive resetting of the pre- to postcapillary resistance ratio. The functional significance of these adjustments may be evident in view of the fact that arterial blood pressure in normal daily life shows large and frequent fluctuations for instance caused by emotional stimuli, sleep etc (*cf* Bevan, Honour and Stott 1969) and these fluctuations *per se* would in most cases seem irrelevant for muscle tissue nutrition and exchange. By the autoregulation of p the muscle tissue is protected against untoward drastic redistribution of fluid between the intra- and extravascular compartments. If such adjustments

were not present implying that r_a/r_v instead remained constant at its control value p_c would be changed by as much as ± 10 mm Hg from a control level of 20 mm Hg at mean pressure fluctuations of say 70 mm Hg above or below the normal level. For the human being with a total muscle mass of 30 kg this would result in a net transcapillary plasma fluid loss of some 30 ml/min at the mentioned high pressure level and an absorption of some 75 ml/min of extravascular fluid to the blood stream at the low pressure level taking the observed different CFC values into account. The consequent large changes of plasma volume would seem irrational during such episodes of blood pressure fluctuation. In manifest arterial hypertensive disease there must be a chronic resetting of r_a/r_v to maintain the fluid homeostasis; this apparently is caused by a structural rebuild of the precapillary resistance vessels (Folkow 1971).

In certain other situations however as in hemorrhage there is a vital demand for an absorption of extravascular fluid from the muscle tissue to the blood stream to compensate for the reduced plasma volume. An autotransfusion of extravascular fluid in fact does occur during hemorrhage but is then governed by specific control systems. Thus the activation of the sympatho-adrenal system causes a reflex resetting of r_a/r_v in muscle leading to considerable fluid absorption as evidenced both for experimental animals (Öberg 1964) and man (Mellander and Öberg 1967). Another important compensation for the decreased blood volume in hemorrhage is effected by an osmolar mechanism related to arterial hyperglycemia which causes marked transcapillary osmotic absorption of extravascular fluid to the blood stream (Jarhult *et al.* 1972; Jarhult 1973). It was postulated in the latter investigations from preliminary experiments that a drop of arterial pressure *per se* would not cause any major decrease of capillary hydrostatic pressure; an assumption thus fully confirmed by the present study. In hemorrhage when the filling of the circulatory system is decreased venous pressure also can be significantly lowered which in turn can cause some passive decrease of p . Such an effect then reinforces the transcapillary fluid absorption evoked by the abovementioned control systems.

This study was supported by grants from the Swedish Medical Research Council (B 74:144, 2710 08C) and from the Faculty of Medicine, University of Lund (59423300 9). The authors thank Miss Margareta Rahm and Mrs Tora Zading Johansson for skilful technical assistance.

References

- BEVAN A. T., A. J. HONOUR and F. H. STOTT. Direct arterial pressure recording in unrestrained man. *Clin. Sci.* 1969, 36: 329-344.
- COBBOLD A., H. FOLKOW, I. KJELLMER and S. MELLANDER. Nervous and local electrical control of pre-capillary sphincter in skeletal muscle as measured by changes in filtration coefficient. *Acta physiol. scand.* 1963, 57: 180-192.
- ELIASSEN E., B. FOLKOW, H. HILTON, B. ÖBERG and B. RIPPET. Pressure-volume characteristics of the interstitial fluid space in the skeletal muscle of the cat. *Acta physiol. scand.* 1974, 90: 583-593.
- ERICSSON L. E. and E. ERIKSSON. Morphological aspects of intra- and extravascular phenomena in cat skeletal muscle at low flow states. *Advanc. Microcirc.* (Basel) 1973, 5: 6-71.
- ERIKSSON E. and S. MELLANDER. Low flow states in the microvessel of skeletal muscle in cat. *Acta physiol. scand.* 1972, 96: 20-210.

- FOLKOW B. The haemodynamic consequences of adaptive structural changes of the resistance vessels in hypertension *Clin Sci* 1971 41 1-19
- FOLKOW B and H OBERG. Autoregulation and basal tone in consecutive vascular sections of the skeletal muscle in reserpinetreated cats *Acta physiol scand* 1961 53 105-113
- FOLKOW B, D H LEWIS, O LUNDGREN, S MELLANDER and I WALLENTIN. The effect of added vasoconstrictor fibre stimulation on the intestinal resistance and capacitance vessels *Acta physiol scand* 1964 61 445-457
- GRANDE P O, J JARHULT and S MELLANDER. Method for gravimetric registration of changes in tissue volume *Acta physiol scand* 1974 In press
- HADDY F J, A G RICHARDS, J L ALDEN and M B VICKER. Small vein and artery pressures in normal and edematous extremities of dogs under local and general anaesthesia. *Amer J Physiol* 1954 176 355-360
- HAGLAND U and O LUNDGREN. Reactions within consecutive vascular sections of the small intestine of the cat during prolonged hypertension *Acta physiol scand* 1972 84 151-163
- JOHANSSON P C. Review of previous studies and current theories of autoregulation *Circulat Res* 1964 14 and 15 Suppl 1 2-9
- JOHANSSON P C. Origin, localization and homeostatic significance of autoregulation in the intestine *Circulat Res* 1964 14 and 15 Suppl 1 225-237
- JARHULT J. Osmotic fluid transfer from tissue to blood during hemorrhagic hypotension *Acta physiol scand* 1973 89 213-226
- JARHULT J, J LUNDVALL, S MELLANDER and S TISBLIN. Osmolar control of plasma volume during hemorrhagic hypotension *Acta physiol scand* 1972 83 142-144
- LANDIS E M. Capillary pressure and capillary permeability *Physiol Rev* 1934 14 401-481
- LEWIS D H and S MELLANDER. Competitive effects of sympathetic control and tissue metabolites on resistance and capacitance vessels and capillary filtration in skeletal muscle *Acta physiol scand* 1967 56 167-188
- LUNDVALL J. Tissue hyperosmolality as a mediator of vasodilatation and transcapillary fluid flux in exercising skeletal muscle *Acta physiol scand* 1972 Suppl 379 1-142
- MELLANDER S. Comparative studies on the adrenergic neuro-hormonal control of resistance and capacitance blood vessels in the cat *Acta physiol scand* 1960 50 Suppl 176 1-86
- MELLANDER S. Systemic circulation. Local control *Ann Rev Physiol* 1970 32 313-344
- MELLANDER S and B OBERG. Transcapillary fluid absorption and other vascular reactions in the human forearm during reduction of the circulating blood volume *Acta physiol scand* 1967 71 37-46
- MELLANDER S, B OBERG and H ODELMAN. Vascular adjustments to increased transmural pressure in cat and man with special reference to shifts in capillary fluid transfer *Acta physiol scand* 1964 61 34-48
- PAPPENHEIMER J R and A SOTO-RIVERA. Effects of osmotic pressure of the plasma proteins and other quantities associated with the capillary circulation in the hindlimbs of cats and

The Effect of Glucagon on Hepatosplanchnic Hemodynamics, Functional Capacity, and Metabolism of the Liver in Cats

By

NIELS KRARUP and JENS ANKER LARSEN

Received 21 November 1973

Abstract

KRARUP N and J A LARSEN *The effect of glucagon on hepatosplanchnic hemodynamics functional capacity and metabolism of the liver in cats* Acta physiol scand 1974 91 42—52

Glucagon in doses of 0.1, 0.5 and 5.0 $\mu\text{g/kg/min}$ infused i.v. caused a marked increase in portal blood flow (up to 300%) due to a dose dependent increase in conductance of gastrointestinal vessels and an increase in the conductance in the hepatic low pressure vessels (up to 30%) but only slight changes in hepatic arterial conductance and flow. Glucagon caused a decrease in the hepatic extraction of Indocyanine Green (ICG), no change in ICG clearance, an increase in bile acid secretion but only minor changes in bile flow and ICG excretion. The splanchnic glucose output and ketone production were increased by glucagon. The cytoplasmic redox level was not affected but the mitochondrial redox level was changed to a more oxidized state together with a 30% rise in hepatic oxygen consumption and a correlated increase in ethanol elimination. These last effects were not dose dependent. It is concluded that the marked changes in splanchnic hemodynamics found during glucagon infusions are not a consequence of the metabolic effects of the hormone on the liver but rather a direct effect of non physiological concentrations of glucagon on gastrointestinal vessels. The results exclude any marked influence of glucagon on the intrahepatic distribution of blood flow and functional liver mass.

Besides its metabolic effects increasing evidence for hemodynamic effects of glucagon is coming forth. Inotropic and chronotropic effects on the heart were already demonstrated by Farah and Tuttle (1960) and vasodilatation especially in the splanchnic area has been obtained repeatedly with infusion of the hormone (Koch, Tibblin and Schenk 1970; Ross 1970).

The mechanism of the glucagon effect on the hepatosplanchnic hemodynamics has not been definitely established yet but it has been suggested that the circulatory effects are secondary to the metabolic effects of glucagon on the liver especially the glucose output (Shoemaker and Van Itallie 1960).

One purpose of the present study was to investigate a possible relationship between the effects of glucagon on hepatosplanchnic hemodynamics and the metabolic effects of the hormone on the liver and on the prehepatic splanchnic area. The metabolic parameters followed were the oxygen consumption in the hepatic as well as in the gastrointestinal area, splanchnic glucose output and ketone production and

the uptake/output of pyruvate and lactate in the splanchnic area. Furthermore hepatic venous lactate/pyruvate ratio (L/P) and β hydroxybutyrate/acetoacetate ratio (HB/Ac) were calculated as a measure of possible effects of glucagon on the redox potentials in hepatic cytosol and mitochondriae respectively.

In a transillumination study it has been observed that glucagon dilates hepatic arterioles, portal venules and hepatic sinusoids (Mc Cuskey 1966). This might cause a change in the distribution of the intrahepatic blood flow and increase the number of perfused sinusoids and thereby the functional capacity of the liver.

Another purpose of the study was therefore to investigate whether glucagon increases the functional capacity of the liver as estimated by the splanchnic elimination of ethanol, the hepatic uptake and excretion of Indocyanine Green (ICG) and the secretion and composition of bile.

Methods

20 cats weighing 2.7–3.9 kg fasted overnight and anesthetized with chloralose (50 mg/kg) and Nembutal (30 mg) were used in this study. Catheterization of a liver vein was performed as previously described in detail (Kjærup 1973) and for collection of bile the choledochus was cannulated after ligation of the cystic duct. Catheters for infusions of ethanol, ICG, taurocholate and glucagon were placed in the femoral veins. The femoral arteries were cannulated for blood sampling and blood pressure measurement. Body temperature was kept at 38.5 °C by gentle heating.

In 12 of the cats the portal venous and hepatic arterial blood flow was measured by means of electromagnetic flowmeters as described earlier (Kjærup 1973). To secure contact between the flow probes and the portal vein and hepatic artery the vessels were stripped of connective tissue and surrounding nerves. In these experiments a polyethylene catheter (ID 0.40 mm) was introduced into the portal vein via a peripheral mesenteric vein for measurements of pressure and blood sampling for determination of oxygen saturation. Pressures were measured by means of condenser manometers. The outputs from the manometers and the flowmeters were recorded on a Beckman S II Dynograph.

In the remaining 8 cats only the estimated hepatic blood flow (EHBF) and the metabolic parameters were followed before and during infusion of glucagon 50 μ g/kg/min. These experiments in which the hepatic nerve supply was intact served therefore as controls.

When operation was finished the cat was left undisturbed for 90 min. During the next 60 min (control period) blood samples were drawn from the femoral artery, portal vein and hepatic venous every 15 min. Glucagon was then infused continuously into a femoral vein and blood samples drawn during the next 60 min period.

Administration of ethanol, ICG, taurocholate and glucagon. By means of a priming dose of 6.5 mmol ethanol/kg the blood ethanol concentration was elevated to about 11 mM, where it was nearly maintained by continuous infusions of 36 μ mol/kg/min ICG (Hynson, Westcott and Dunning) was given as a priming dose (300 μ g/kg) followed by continuous infusion of 11 μ g/kg/min which resulted in an almost horizontal time-concentration relationship. To compensate for the enterohepatic circulation of bile acids taurocholate (M. Cromie) 0.20 μ mol/kg/min was infused when bile was collected. Albumin was added to the ICG solution which was protected against light to increase the stability of the dye. The solutions of ethanol, ICG and taurocholate were infused at a rate of 0.1 ml/min.

The doses of glucagon used were 0.1, 0.5 and 5.0 μ g/kg/min and each dose was given to 4 of the 12 cats. The glucagon used was a commercial preparation from NOVO in half of the experiments and a chromatographically purified beef glucagon generously supplied by NOVO in the other half. No difference between the effects of the commercial and purified hormone could be detected.

Analytical procedures. Ethanol, plasma ICG and the biliary concentrations of ICG, bile acids and electrolyte were determined as previously described (Kjærup and Larsen 1972). The determination of oxygen saturation, hemoglobin and glucose has also been described elsewhere (Kjærup 1973). Lactate, pyruvate, hydroxybutyrate (HB) and acetoacetate (Ac) were measured by an enzymatic fluorometric micromethod (Olsen 1971).

Estimations of the functional capacity of the liver The elimination rate of ethanol and the bile flow were used as parameters reflecting the liver mass. At the ethanol concentrations used in the present experiments the elimination rate of ethanol is independent of changes in total hepatic blood flow and of ethanol concentration (Larsen 1963). Also bile flow may reflect the functional liver mass being independent of the total hepatic blood flow but dependent on the number of perfused sinusoids (Brauer, Leong and Holloway 1954). In contrast the hepatic uptake of dyes is dependent on hepatic plasma flow as well as dye concentration according to the model proposed by Winkler and Gram (1965). An increase in plasma flow would be expected to increase the hepatic dye clearance and decrease the extraction ratio of dyes.

Calculations By multiplying the EHBF by the arteriohepatic venous concentration gradient of ethanol, oxygen, glucose, lactate, pyruvate, HB and Δc the splanchnic uptake or output of these substances were calculated. The prehepatic splanchnic oxygen consumption was determined by multiplying the portal venous flow by the arterio-portal venous concentration gradient of oxygen and the hepatic oxygen consumption by subtraction of the prehepatic from the total splanchnic oxygen consumption. The oxygen concentrations in arterial, portal venous and hepatic venous bloods were calculated from the oxygen saturation percent and the hemoglobin concentration assuming an oxygen binding capacity of 1.34 ml/g hemoglobin. The total elimination rate of ethanol was calculated from the amount of ethanol infused per minute corrected for the amount disappeared from or retained in the solvent space (assumed as 6% of the body weight according to Larsen 1963). Once a constant ICG concentration in arterial plasma is obtained the elimination rate of ICG equals the infusion rate. The plasma clearance is then determined as infusion rate of ICG divided by the arterial equilibrium concentration and extraction ratio as the arterio-hepatic venous difference divided by the arterial concentration. The biliary excretion of ICG and bile acids were calculated as bile flow multiplied by the concentration in question.

The vascular conductances were calculated in the following manner:

$$GIC = \frac{GIF}{BP - PP} \quad \text{ml} \times \text{kg}^{-1} \times \text{min}^{-1} \times \text{mmHg}^{-1}$$

$$HAC = \frac{HAF}{BP} \quad \text{ml} \times \text{kg}^{-1} \times \text{min}^{-1} \times \text{mmHg}^{-1}$$

$$PVC = \frac{GIF}{PP} \quad \text{ml} \times \text{kg}^{-1} \times \text{min}^{-1} \times \text{mmHg}^{-1}$$

GIC, HAC, PVC conductances in the gastrointestinal area, hepatic artery and intrahepatic portal vein and sinusoids respectively. GIF gastrointestinal (= portal venous) blood flow, HAF hepatic arterial blood flow, BP mean arterial blood pressure, PP portal venous pressure. The hepatic venous pressure was set to zero.

Statistical procedures The significance of the effects of glucagon was tested by the method of paired comparisons using Student's *t*-test. Correlation was carried out according to Sjalil and Rohlf (1969).

Results

Hepatosplanchnic hemodynamics The hemodynamic parameters remained essentially constant during the control period and a typical experiment in which glucagon (0.5 $\mu\text{g/kg/min}$) was given is shown in Fig. 1. After about 1 min of infusion portal venous flow and pressure start to rise and approach steady levels in the course of 3 min. In contrast hepatic arterial blood flow is slightly decreased despite a nearly unaltered mean arterial blood pressure in the first minutes of the infusion. During the glucagon infusion a slight decrease in arterial blood pressure is seen and this is accompanied by similar changes in hepatic arterial and portal venous flows as well as a portal pressure. When the glucagon infusion is stopped the hemodynamic parameters return immediately towards their control levels.

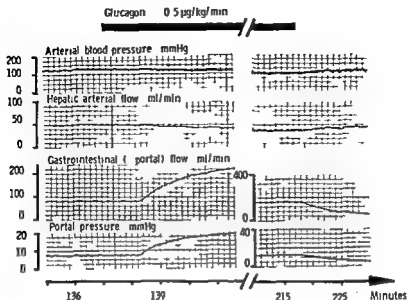


Fig 1 The effect of continuous iv infusion of glucagon 0.5 µg/kg/min on mean arterial and portal venous pressures and hepatic arterial and portal venous flows

In Table I are given the steady state levels of portal venous and hepatic arterial blood flows in the control period and during infusion of the different doses of glucagon. It appears that glucagon in all doses given causes an increase in portal venous blood flow whereas hepatic arterial flow is decreased by the larger doses of the hormone. Glucagon had only small and variable effects on the mean arterial blood pressure. The portal pressure always increased together with portal flow but the change in portal pressure was somewhat smaller than the change in portal

TABLE I The effect of continuous iv infusions of glucagon on directly measured portal venous and hepatic arterial blood flow and on total liver blood flow (EHBF) measured by means of ICC

Glucagon infusion rate µg/kg/min	Gastrointestinal blood flow ml/kg/min		Hepatic arterial blood flow ml/kg/min		EHBF ml/kg/min	
	A	B	A	B	A	B
0.1 (n = 4)	24 ± 5	30 ± 6	20 ± 5	22 ± 7	42 ± 5	52 ± 5
0.5 (n = 4)	25 ± 9	49 ± 7	14 ± 2	12 ± 2	37 ± 4	55 ± 6
5.0 (n = 4)	18 ± 2	46 ± 8	13 ± 1	9 ± 1	30 ± 2	50 ± 9
mean	22 ± 2		16 ± 4		36 ± 3	

A Mean and S.E. in the control period

B Mean and S.E. during glucagon infusions

n = number of experiments

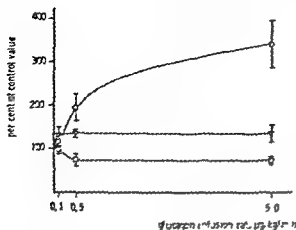


Fig. 2. Dose response curves of the glucagon effects on gastrointestinal portal venous and hepatic arterial conductances expressed as percentages of the conductances in the control period. (○) gastrointestinal conductance (△) portal venous conductance (□) hepatic arterial conductance.

flow. The changes in conductance from control level as a function of glucagon infusion rate is shown in Fig. 2. It will be noticed that there is a dose dependence of the glucagon effect on the gastrointestinal vessels whereas the observed small increase in conductance in the hepatic portal vessels seems to be an all-or-none response. The smallest dose of glucagon ($0.1 \mu\text{g/kg/min}$) is without effect on hepatic arterial conductance whereas glucagon in doses of 0.5 and $5.0 \mu\text{g/kg/min}$ cause an equal small decrease in conductance in the hepatic arterial bed. In the experiments where the hepatic blood flow was not measured electromagnetically glucagon $5.0 \mu\text{g/kg/min}$ caused a 50% increase in EHBF despite a 10% decrease in mean arterial blood pressure.

Functional capacity. From Table II it appears that glucagon increases the plasmatic and the total elimination rate of ethanol to the same extent and thus effect of glucagon is not dose dependent. There was no significant effect of glucagon

TABLE II. The effect of intravenous infusions of glucagon on splanchnic and hepatic oxygen consumption and plasmatic elimination of ethanol. The numbers in brackets in each line are the elimination of ethanol.

Glucagon infusion rate $\mu\text{g/kg/min}$	Splanchnic oxygen consumption ml/kg/min		Hepatic oxygen consumption ml/kg/min		Splanchnic elimination of ethanol mmol/kg/min	
	A	B	A	B	A	B
$0.1 (n=4)$	4-13	11 ^a 18	2-8	6 ^a 7	32-5 (39-3)	33-5 (41-1)
$0.5 (n=4)$	8-14	10 ^a 9	2-9	6 ^a 5	25-3 (33-4)	3-2 (43-3)
$5.0 (n=4)$	9-16	10 ^a 14	9-9	6 ^a 7	25-5 (31-2)	35-3 (45-4)
mean	9 ^a	11.0 ± 2	7-4	6 ^a 4	27-3 (31-2)	33-2 (43-2)
	p = 0.01		p = 0.01		p = 0.01	

A. Mean and S.E. in the control period.

B. Mean and S.E. during glucagon infusion.
n. number of experiments.

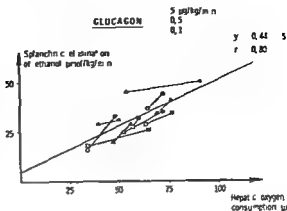


Fig 3 The correlation between the hepatic oxygen consumption and splanchnic ethanol elimination. Open symbols indicate the parameters in the control period, closed symbols the parameters during glucagon at the different doses. Symbols connected with lines belong to the same experiment.

on the hepatic clearance of ICG which was 60 ± 0.5 ml/kg/min in the control period but all doses of glucagon decreased the extraction ratio of ICG from 28 ± 3 per cent in the control period to 19 ± 2 per cent during glucagon infusion and the largest effect was seen when the highest dose of glucagon was used.

Bile flow (151 ± 17 µl/kg/min) as well as ICG recovery ($99 \pm 1\%$) was not affected by glucagon at the two lower doses but in all experiments a slight increase in the excretion of bile acids was observed (from 0.29 ± 0.04 to 0.34 ± 0.05 µmol/kg/min). When 5.0 µg/kg/min was infused bile flow as well as ICG recovery were immediately reduced but then returned towards their control level. In the control period the following biliary electrolyte concentrations were found: Na 168 ± 3 meq/l, K 3.7 ± 0.2 meq/l, Cl 113 ± 5 meq/l, HCO_3^- 33 ± 3 meq/l. Except for a slight decrease in bicarbonate concentration (3 ± 0.5 meq/l) glucagon caused no changes in the electrolyte concentrations.

In the experiments where flowmeters were not used glucagon 5.0 µg/kg/min caused a 20% increase in the splanchnic elimination rate of ethanol, a 15% decrease in hepatic clearance of ICG and a 30% decrease in the hepatic extraction of the dye.

Hepatosplanchnic metabolism As apparent from Table II the splanchnic oxygen consumption increases during the infusion of glucagon without correlation to the dose of glucagon given. Most of the extra oxygen consumed in the splanchnic area is apparently taken up by the liver whereas the gastrointestinal oxygen consumption was not significantly changed. As evident from Fig 3 there is a significant correlation between the hepatic oxygen consumption and the splanchnic elimination of ethanol before as well as during the infusion of glucagon.

Immediately after the start of the glucagon infusion arterial blood glucose concentration rose to reach a new level in the course of 10 minutes (Fig 4). The rise in arterial glucose concentration coincided with a short lasting tenfold rise in splanchnic output of glucose. No differences in the effect of the different doses were found but in two of the experiments in which 0.5 and 5.0 µg glucagon/kg/min

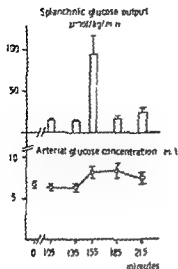
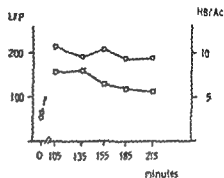


Fig 4 The effect of continuous α_1 infusions of glucagon (started at 140 min) on the arterial glucose concentration and the splanchnic output of glucose

Fig 5 The effect of continuous α_1 infusions of glucagon (started at 140 min) on hepatic venous L/P (\circ) and HB/Ac (\square) ratios



were given only a slight effect of glucagon on arterial concentration of glucose and splanchnic glucose output was seen. In contrast the hemodynamic response to glucagon as well as glucagon's effect on ethanol elimination and oxygen consumption was identical with the findings in the rest of the experiments.

Ethanol infusion caused a rise in the arterial lactate concentration (from 0.50 ± 0.04 to 1.03 ± 0.08 mM) and reversed a splanchnic uptake of lactate to an output. No further changes in lactate concentration in arterial and hepatic venous blood or in lactate output was seen during the glucagon infusions. Neither the pyruvate concentrations in arterial and hepatic venous blood were affected by ethanol nor did glucagon change the concentrations of pyruvate. However a slight increase in pyruvate uptake was seen during the hormone infusions (from 2.0 ± 0.6 to 2.7 ± 0.7 $\mu\text{mol/kg/min}$). Consequently the hepatic venous L/P ratio was greatly increased by ethanol but not further changed when glucagon is given (Fig. 5).

The hepatic venous concentration of HB increased from 275 ± 40 to 420 ± 40 μM when ethanol was administered and glucagon caused a further increase to about 510 μM . The Ac concentration in hepatic venous blood was decreased by ethanol (from 83 ± 13 to 60 ± 11 μM) but when glucagon was given the concentration of Ac rose again to about 83 μM . The hepatic venous HB/Ac ratio was therefore increased by ethanol and decreased by glucagon (Fig. 5). Glucagon caused a slight but significant increase in the splanchnic output of HB (from 5.5 ± 0.6 to 7.1 ± 0.6 $\mu\text{mol/kg/min}$) and Ac (from 1.0 ± 0.1 to 2.2 ± 0.2 $\mu\text{mol/kg/min}$). These effects of glucagon were not dose-dependent.

The splanchnic oxygen consumption glucose output and ketone production were also followed in the experiments where the flowmeters were omitted and results similar to the above mentioned were obtained

Discussion

Hepatosplanchnic hemodynamics The hemodynamic parameters measured in the control period agree well with the values given for cats by Greenway and Stark (1971) and correspond to previous findings in our laboratory (Krarup 1973)

The lag between the start of the glucagon infusion and the increase in portal flow and pressure (Fig 1) corresponds to the circulation time and points to an immediate effect of glucagon on these parameters In the course of a few minutes steady state is approached which probably reflects that a steady concentration of glucagon in arterial blood has been reached The immediate decrease in portal flow upon stopping the infusion indicates that a very fast elimination of the hormone occurs with a half life (estimated from the decrease in portal flow) of about 3 min

The observed effect on portal venous flow indicates a dose-dependent vasodilation in major parts of the gastrointestinal vessels in agreement with previous findings in cats (Ross 1970)

The decrease in hepatic arterial conductance may be overestimated as the pressure gradient is based on zero hepatic venous pressure and not sinusoidal pressure which is unknown but probably elevated during glucagon infusion However the slight decrease in hepatic arterial flow is in accordance with the experiments of Ross (1970) In contrast Madden Ludewig and Wangersteen (1972) using dogs found an increase in hepatic arterial flow reflecting a decrease in the hepatic arteriolar resistance similar findings were obtained in a microangiographic study in frogs rats and rabbits (Mc Cuskey 1966) This indicates species differences in the response to glucagon In the present experiments portal venous pressure increased a little less than portal venous flow so that a slight increase in portal venous conductance occurred In the study of Ross (1970) a much more striking increase in portal venous conductance occurred as portal pressure increased only about 2 mm Hg despite pronounced increases in superior mesenteric blood flow Absolute values of portal pressure are unfortunately not given in his study

The present experiments seem to rule out that the hemodynamic effects of glucagon are secondary to its metabolic effects on the liver as suggested by Shoemaker and Van Itallie (1960) Firstly the effect on gastrointestinal conductance was dose dependent whereas the effect of the hormone on hepatic metabolism was independent of the dose used Secondly the vascular responses were obtained also in two cats in which an effect of glucagon on glucose output was hardly detectable This is in accordance with the findings of Tibblin Kock and Schenk (1970) who demonstrated vascular responses to glucagon which were independent of effects on the arterial glucose concentration Finally changes in hepatic metabolism will only affect the hepatic arteriolar flow whereas the portal venous flow is mainly determined by the resistance in vessels lying in front of the liver

The effect of glucagon on the gastrointestinal vessels is therefore a direct effect most probably mediated via local changes in concentration of cyclic AMP. Although glucagon is known to cause accumulation of cyclic AMP in the liver (Exton *et al* 1971) the effect on liver vasculature was negligible in the present experiments. Despite the marked increase in gastrointestinal conductance the systemic blood pressure remained almost unchanged indicating that the gastrointestinal vessels are especially sensitive to glucagon.

The range of glucagon infusion rates in the *c* experiments is within the range used in other glucagon experiments referred to in this paper. However, judged from the normal levels of glucagon in humans in peripheral blood ($0.1 \mu\text{g/l}$) and blood leaving the pancreas ($3.0 \mu\text{g/l}$) (Unger 1972) the highest infusion rates of 0.5 and $5.0 \mu\text{g/kg/min}$ most likely results in unphysiological blood concentrations. This is in accordance with the findings of fully developed metabolic effects of glucagon $0.1 \mu\text{g/kg/min}$.

It must therefore be concluded that the marked effects of glucagon on splanchnic hemodynamics found in these and similar experiments are caused by blood concentrations of glucagon which exceed the normal concentration range. Denervation might have influenced the hemodynamic effects of glucagon but in the experiments where only EHBF was measured and the hepatic nerves were intact the glucagon effect on total liver blood flow was similar to the effect seen in the denervated cats. Furthermore, Ross (1970) found no difference in the glucagon response whether the nerves were intact or not.

Functional capacity. The effect of glucagon on the intrahepatic vessels in the present experiments is probably not accompanied by distribution changes in the univascular blood flow, as this would increase all parameters reflecting the functional capacity of the liver. Although glucagon increased the elimination rate of ethanol, the elimination of ICG and production of bile was either unchanged or slightly depressed.

It has previously been demonstrated that glucagon increased the ethanol disappearance rate in dogs by 11% (Clark and Owens 1966) and by 68% (Nel on and Jen en 1961). The difference from the present findings of a 30% increased ethanol elimination may be explained by the different techniques used. Due to the increased oxygen consumption in the liver during glucagon infusion the electron flux through the respiratory chain may increase as reflected in the decrease in HB/Ac ratio in hepatic venous blood which is an estimate of the mitochondrial redox potential (Scholz 1968). As I/P ratio is unchanged the conditions for transport of reducing equivalents from cytoplasm to mitochondria are improved and in this way the ethanol elimination can be accelerated. This is supported by the correlation between the splanchnic elimination of ethanol and the hepatic oxygen consumption which indicates that 44% of the oxygen consumed by the liver is used for the oxidation of ethanol before as well as during glucagon infusion. Similar findings were obtained in experiments in rats in which the splanchnic oxygen consumption was increased by infusion of amino acids (Larsen and Krarup 1973).

The observed decrease in hepatic ICG extraction may be a consequence of the increased plasma flow, according to the model proposed by Winkler and Gram (1965). However a flow dependent decrease in ICG extraction would be expected to be followed by an increase in plasma clearance of the dye in contrast to the present findings. This reflects that the mechanism of the hepatic uptake and/or excretion is depressed by glucagon. At the two smaller doses of glucagon the excretion is not affected but at a dose of $1 \mu\text{g/kg/min}$ the excretion is at least temporarily impaired.

Bile is composed of two fractions a canalicular which may depend on the secretion of bile acids and a ductular depending on an active secretion of bicarbonate (Brooks 1969). In the present experiments bile acid secretion was not decreased which indicates that glucagon does not affect the canalicular secretion. The decrease in bile flow observed only at the high infusion rate of glucagon is therefore most probably caused by a depression of the ductular secretion in accordance with the observed decrease in bicarbonate secretion.

Hepatic metabolism: The 30% increase in hepatic oxygen consumption during glucagon administration reflects an increase in the energy demands of the liver. This extra energy may be required for urea formation and for gluconeogenesis which has been shown to increase after glucagon infusion probably secondarily to a glucagon induced increase in cyclic AMP (Exton *et al* 1971, Weinstein, Klausner and Heimberg 1973).

Even if gluconeogenesis is stimulated by glucagon the pronounced and immediate effect on splanchnic glucose output is probably mainly due to glycogenolysis. The increase in ketone concentration is explained by the increase in splanchnic ketone production as also found by Exton *et al* (1971). Due to the redox shift the increase is relatively larger in Ac output than in HB output.

The metabolic effects of glucagon were not affected by the denervation as similar results were obtained in the experiments where flowprobes were not used and the hepatic nerves intact.

Conclusion

The present experiments have confirmed that infusion of glucagon is accompanied by marked hemodynamic effects in the splanchnic area which however are observed only when glucagon is infused at a rate which most likely results in blood concentrations exceeding the normal range. Glucagon appears to have a direct dilatory effect on the gastrointestinal vessels which is dose dependent and not correlated to the metabolic effects on the liver. Vasodilatation of the intrahepatic low pressure vessels occurs but apparently without major changes in the distribution of the intrahepatic blood flow whereas glucagon causes a slight constriction of the hepatic arterioles.

The glycogenolysis, ketogenesis and increased metabolic rate in the liver caused by glucagon are independent of the dose given. An increase in the splanchnic

elimination rate of ethanol may be a consequence of the increased energy demand of the liver

The technical assistance of miss S. Holm, Mrs J. Justesen and Mrs I. Nielsen is gratefully acknowledged

References

- BRAUER R. W., G. F. LEONG and R. J. HOLLOWAY: Mechanics of bile secretion. *Amer J Physiol* 1954 177 103—113.
- BROOKS F. P.: The secretion of bile. *Amer J dig Dis* 1969 14 343—49.
- CLARK W. C. and P. A. OWENS: The influence of glucocorticoid, epinephrine and glucagon on ethanol metabolism in the dog. *Arch int Pharmacodyn* 1966 162 355—63.
- EXTON J. H., S. B. LEWIS, R. J. HO, G. A. ROBINSON and C. W. PARK: The role of cyclic AMP in the interaction of glucagon and insulin in the control of liver metabolism. *Ann NY Acad Sci* 1971 185 85—100.
- FARAH A. and R. TILLYE: Studies on the pharmacology of glucagon. *J Pharmacol exp Ther* 1960 129 49—55.
- GREENWAY C. V. and R. D. STARR: Hepatic vascular bed. *Physiol Rev* 1971 51 23—65.
- KOCK N. G., S. TIBBLIN and W. G. SCHENK: Hemodynamic responses to glucagon. An experimental study of central, visceral and peripheral effects. *Ann Surg* 1970 171 373—79.
- KRARUP N.: The effect of noradrenaline and adrenaline on hepatosplanchnic hemodynamics: functional capacity of the liver and hepatic metabolism. *Acta physiol scand* 1973 87 307—19.
- KRARUP N. and J. A. LARSEN: The effect of slight hypothermia on liver function as measured by the elimination rate of ethanol, the hepatic uptake and excretion of Indocyanine Green and bile formation. *Acta physiol scand* 1972 84 396—407.
- LARSEN J. A.: Elimination of ethanol as a measure of the hepatic blood flow in the rat. *Acta physiol scand* 1963 57 209—23.
- LARSEN J. A. and N. KRARUP: Relation between the hepatic elimination rate of ethanol and mitochondrial respiration. In: *Regulation of hepatic metabolism* (F. Lundquist and L. Sestoft, ed.) In press.
- MADDEN J. J., R. M. LUDEN and S. L. WANDERSTEEN: Effects of glucagon on the splanchnic and the systemic circulation. *Res Surg* 1972 29 37—73.
- MC CLELLY R. S.: A dynamic and static study of hepatic arterioles and hepatic sphincters. *Amer J Anat* 1966 119 435—77.
- NELSON D. and C. E. JENSEN: Blood alcohol disappearance rate after the administration of iv glucagon. *Fed Proc* 1961 20 189.
- OLSEN C.: An enzymatic fluorimetric micro-method for the determination of acetylacetate, β -hydroxybutyrate, pyruvate and lactate. *Clin chim Acta* 1971 33 293—300.
- RENN G.: Regional circulatory effects of pancreatic glucagon. *Brit J Pharmacol* 1970 38 135—40.
- SCHÖLL R.: Untersuchungen zur Redoxkompartimentierung bei der Hämoglobin frei perfundierten Rattenleber. In: *Stoffwechsel der isoliert perfundierten Leber* (W. Stach and R. Scholz, ed.) p. 14—47. Springer Verlag Berlin—Heidelberg 1968.
- SHOFMAKER W. C. and T. B. VAN ITALLIE: The hepatic response to glucagon in the unanesthetized dog. *Endocrinology* 1960 66 760—68.
- SOKAL R. R. and F. J. ROHLF: *Biometry*. W. H. Freeman and Company, San Francisco 1969.
- TIBBLIN S., N. G. KOCK and W. G. SCHENK: Dislocation of the hyperglycemic and vascular effects of glucagon. *Surgery* 1970 67 816—23.
- UNDER R. H.: *Regulating pancreatic glucagon and extrapancreatic glucagon like material*. In: *Handbook of physiology*, section 7, vol. I (R. O. Greep and F. B. Atwater, ed.) p. 529—544. American Physiological Society 1971.
- WEINSTEIN I. H., A. KATZNER and M. HEIMBERG: The effect of concentration of glucagon on output of triglyceride, ketone bodies, glucose and urea by the liver. *Biochim biophys Acta (Amst)* 1973 298 300—01.
- WINKLER K. and C. CRAM: The kinetic of biliary bile acid elimination during continuous infusion in man. *Acta med scand* 1973 178 439—5.

The Effect of Barbiturate on Retinal Functions I Effects on the Conventional Electroretinogram of the Sheep Eye

By

BENGT KNAVE and HANS E PERSSON

Received 21 November 1973

Abstract

KNAVE B and H E PERSSON *The effect of barbiturate on retinal functions I Effects on the conventional electroretinogram of the sheep eye* Acta physiol scand 1974 91 53-60

The present work is the first in a series of investigations on the effect of barbiturate on retinal functions. The changes in the conventional ERG of the dark adapted intact sheep eye were studied after i.v. administration of an ultra short acting barbiturate thiopental. After injection of small and moderate doses (< 20 mg/kg) the *a* and *b* wave amplitudes were found to increase. Larger doses resulted in a further enhancement of the *a* wave amplitude whereas that of the *b* wave diminished. Transient falls in the arterial blood pressure were also recorded after barbiturate administration. Since effects on mammalian ERG of alterations in retinal blood circulation have been the subject for discussion the ERG was studied after lowering the blood pressure by electrical stimulation of the free-dissected left vagal nerve. The reduction in blood pressure obtained in this way was recorded without concomitant changes in the ERG. For this reason we exclude the possibility of a barbiturate mediated reduction in blood pressure as the mechanism behind the changes in retinal function of the intact sheep eye after administration of at least small doses of barbiturate.

It is known that barbiturates depress a wide range of cellular functions in many vital organs and influence synaptic transmission in the central nervous system (for references see e.g. Sharpless 1970). The effect of barbiturates in large doses is reflected for instance in an amplitude decrease of the *b* wave in the electroretinogram (ERG) of the intact (Noell 1958, Yonemura, Kawasaki and Tsuchida 1966) and isolated retina (Rockstroh and Hanitzsch 1966, Honda and Nagata 1971). After the administration of small doses of barbiturates however the *a* and *b* waves of the ERG have been shown to increase in amplitude in the cat (Wohlzogen 1956, Jacobson and Gestring 1958, Arden, Granit and Ponte 1960), the rat (Danis 1956), the rabbit (Noell 1958, Ponte 1960, Yonemura *et al* 1966, Bornschein, Hanitzsch and Lutzow 1966, Trimarchi 1968, Honda and Nagata 1971), the chick (Scholes and Roberts 1964) and the frog (Rockstroh and Hanitzsch 1966).

The effect of barbiturates has also been found to be reflected in an increase of the amplitude of an isolated negative component recorded in the *in vitro* perfused retinas of the rabbit (Bornschein *et al* 1966) and the cat (Wundsch and Ulrich 1971). Since this negative component has been claimed to correspond to Granitz P III (Hanitzsch and Bornschein 1965) the barbiturate effect demonstrated would imply a direct action on the cells generating the P III component of the ERG.

Several theoretical explanations have been presented as to the question of which functional processes in the retina might be influenced by barbiturates in small doses and cause the above mentioned alterations of the gross FRG. A release from tonic inhibition mediated from intraretinal neuronal structures has been proposed (Danis 1956, Wohlzogen 1956). The lack of such a barbiturate induced release is expressed in increased ERG amplitudes after section of the optic nerve (ed Jacobson and Gestring (1958), Scholes and Roberts (1964) and Trimarchi (1968) to postulate the existence of a barbiturate sensitive neural control on the retina from centrifugal fibres in the optic nerve. However, Jacobson later attributed the lack of barbiturate effect on the ERG after optic nerve section to factors other than the section (Mita *et al* 1963). On the basis of the observation that substances which influence the synaptic activity in the spinal cord did not prevent the effect of barbiturate on the ERG, Ponte (1960) suggested that synaptic transmission is unlikely to be involved. The effect on mammalian ERG of alterations in the retinal blood circulation has been the subject of much discussion (see e.g. Jacobson 1961). As a consequence the possibility has been suggested of a barbiturate mediated blood pressure reduction as the mechanism behind the changes in retinal functions with barbiturate administration. Furthermore it should be mentioned that the changes of the ERG particularly with regard to the *a* wave have been explained in terms of the algebraical interference between two potentials of opposite polarity i.e. the *a* and *b* waves (see e.g. Noell 1958, Yonemura *et al* 1966). The effects of barbiturates in large doses on the FRG have generally been explained in terms of the depressive action of the drug.

Thus available information is not unanimous as to the precise effects and mechanisms of at least small and moderate doses of barbiturates on neuroretinal functions. Hitherto no study has been made on the effects of barbiturates on the functions of the pigment epithelium of the retina. The present work constitutes a series of investigations on the effects of barbiturate on the functions of the neuroretina and the retinal pigment epithelium of the intact sheep eye. The first study deals with the changes in the conventional FRG of the dark adapted eye after intravitreal administration of an ultrashort acting barbiturate thiopental. Since thiopental was found to induce transient falls in the arterial blood pressure the FRG was also studied after lowering this by means of electrical stimulation of the left vagal nerve. The second paper describes the barbiturate (thiopental) effect on the *c* wave of the ERG and the standing potential of the eye which are known to reflect the activity of

¹ The term *neuroretina* is used in the present series of papers to denote the part of the retina which encloses the receptor and retinal neuron.

the pigment epithelial cells of the retina. In the third investigation the effect of barbiturate (thiopental) on the isolated receptor responses and the inner nuclear layer components of the intact retina was studied with the recently described low intensity electroretinographic method (Knave Moller and Persson 1972).

Methods

7 successful experiments were performed on sheep in the dark adapted state. Since the method used has been fully described recently (Knave *et al* 1972) only some of the essential steps will be taken into consideration. The sheep was anesthetized (Pentothal Sodium® 20 mg/kg i.v.) immobilized (Flaxedil® 4–8 mg/kg i.v./hr) tracheotomized and artificially ventilated. The respirator was adjusted to maintain a concentration of 4–4.5% CO₂ in the expired air. The general anesthesia was maintained throughout the surgical procedure with repeated injections (5–10 mg/kg).

A scleral contact lens with a recording electrode was applied and a reference electrode was placed subcutaneously at the upper bony margin of the orbit. The pupils were dilated with 0.5% Tropicamide 1% Homatropin and 1% Atropin eye drops. After the surgical procedure was completed the general anesthesia was discontinued. However all wound margins as well as pressure points were carefully and repeatedly infiltrated with a local anesthetic (2% Lidocaine). Cornea and conjunctiva were repeatedly anesthetized with 1% Tetracaine eye drops. Furthermore as objective criteria on pain sensation in the animal the heart frequency and blood pressure were continuously recorded. All our observations give us confidence in claiming that the animals were free from pain.

Light stimulation was provided by a xenon arc lamp (Zeus 900 W). The light flashes were led to the eye through a system of quartz fiber optics. The duration of the light flashes was 0.1 s and the intervals between these flashes were 1 min. The intensity amplitude curve of the b wave is known to have two saturation levels (see e.g. Arden *et al* 1960 Knave *et al* 1972). The stimulus intensity chosen was always well above the lower one of these levels. In the ERG records the a wave was measured from the isoelectric line and the b wave from the trough of the a wave.

The recording and reference ground electrodes were matched calomel half-cells connected to the differential inputs of a low-drift d.c. amplifier. In some experiments the ERGs were fed into a Intertechnique DIDAC 800 signal averager.

An ultra short acting barbiturate thiopental (Pentothal Sodium®) which is the thioanalogue of pentobarbital (Nembutal®) was chosen for the present study. The thiobarbiturates are characterized by high fat solubility as well as rapid onset and short duration of action. Their pharmacodynamic properties do not differ essentially from those of oxybarbiturates (Sharpless 1970). The drug was administered through a catheter placed in a foreleg vein. The first injection was made 6–8 hours after the general anesthesia was discontinued. At this time the retina was considered not to be influenced by the initially given barbiturate. This supposition is supported by the fact that control ERG responses with constant form and amplitude were recorded in each experiment during 1–2 hours before the barbiturate effects on the ERG responses were studied.

The arterial blood pressure was measured with a catheter in a femoral artery and continuously recorded on a Grass polygraph. It is well known that most barbiturates lower the arterial blood pressure (see e.g. Sharpless 1970). Such blood pressure fall *per se* could effect the ERG. In order to elucidate this question the blood pressure was lowered in some experiments by electrical stimulation (80 V, 1 ms, 100–300 Hz) of the free-dissected left vagal nerve.

Results

Because of its rapid onset and short duration of action special attention was focused on the immediate effects of thiopental. The maximal effect was generally obtained about 45 s after the i.v. injection.

Fig. 1 shows the configuration of the ERGs recorded before (A) and 45 s after administration of 10 and 20 mg thiopental per kg b.wt. (B, C and D respectively).

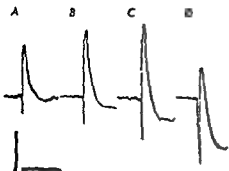


Fig 1 ERGs of the dark adapted sheep eye before (A) and 45 s after *iv* administration of 5 10 and 20 mg thiopental per kg bwt (B C and D respectively) Stimulus intensity 50 log units above *b* wave threshold Stimulus duration 0.1 s Time calibration 200 ms Amplitude calibration 500 μ V

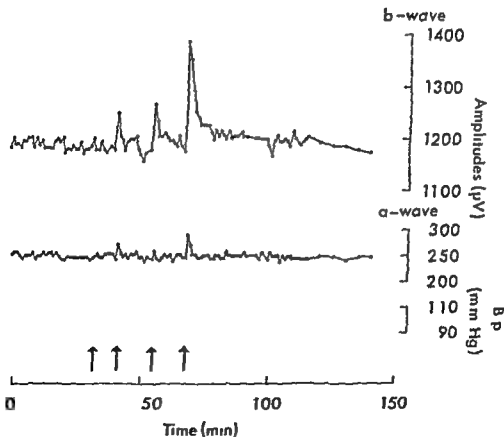


Fig 2 A Effect of thiopental on *a* (lower curve) and *b* wave amplitudes (upper curve) of the dark adapted sheep eye 4 *ix* injections of 0.3 0.6 1.2 and 2.5 mg thiopental per kg bwt respectively were given in turns (arrows) Systolic and diastolic femoral intra art rial blood pressures are represented at the upper and lower limit of the shaded area Stimulus intensity 50 log units above *b* wave threshold Stimulus duration 0.1 s

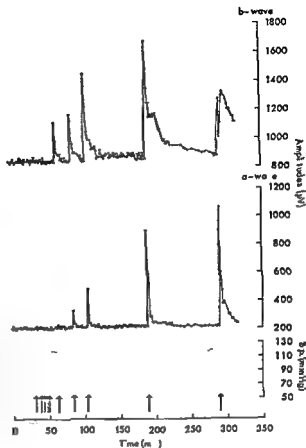


Fig 2 B Effect of thiopental on *a* (lower curve) and *b* wave amplitudes (upper curve) of the dark adapted sheep eye. 5 μ V injections of 2.5, 5, 10, 20 and 30 mg thiopental per kg bwt respectively were given in turns (solid arrows). Electrical stimulation of the left vagus nerve (dotted arrows) was performed before the injections. Systolic and diastolic femoral intra arterial blood pressures are represented at the upper and lower limit of the shaded area. Stimulus intensity 50 log units above *b* wave threshold. Stimulus duration 0.1 s.

ly) The *a* wave amplitudes were successively enhanced after each barbiturate administration. A similar successive increase was also found for the *b* wave after the first two injections (B and C). However the *b* wave amplitude decreased after administration of 20 mg thiopental (D) compared to the amplitude recorded after the immediately preceding injection (C).

In Fig 2 A the amplitudes of the *a* wave (lower curve) and the *b* wave (upper curve) as well as the systolic and diastolic intra arterial femoral blood pressures (shaded area) are illustrated from an experiment in which only low doses were given (0.3, 0.6, 1.2 and 2.5 mg thiopental per kg bwt respectively). A rapid increase of short duration of the ERG response was observed following each injection. After the 2.5 mg injection a slight fall in the blood pressure was registered simultaneously with the enhanced ERG responses.

Fig 2 B shows the effects on ERG and intra arterial blood pressure of moderate and high doses of thiopental and of electrical stimulation of π vagus. Doses of 2.5, 5, 10, 20 and 30 mg per kg bwt were injected in turns (marked by solid arrows). The injections with exception of the last one were not given until the ERG had

a-wave

b wave

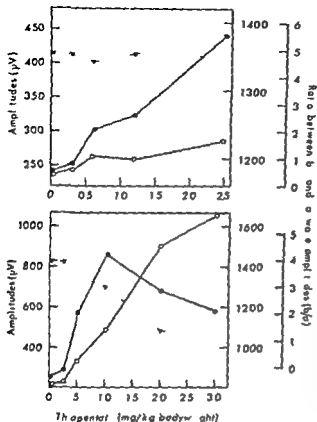


Fig. 3 Dose-amplitude diagrams of the effect of thiopental on the a- and b-wave amplitudes of the dark adapted sheep eye. The amplitude values (recorded 45 s after each injection) of the upper and lower graphs are obtained from the experiments illustrated in Fig. 2 A and B respectively. Open circles: a-wave. Filled circles: b-wave. Triangles within broken line: ratio between b and a-wave amplitudes (b/a).

regained in full its original shape and amplitude. Each injection resulted in a substantial increase of ECG amplitudes. The a-wave amplitude (lower curve) increased as a function of the increasing size of the dose of thiopental. The b-wave amplitude (upper curve) showed the same pattern of increase only to a dose of 20 mg per kg b.wt. (the amplitude recorded 1 min 45 s after the injection). An increased amplitude was still obtained after the last dose (30 mg) although its magnitude was now less than after the injection immediately before.

Also transient falls in the blood pressure were recorded during the phases of enhanced ECG amplitudes. As seen in Fig. 2 B the fall in blood pressure was related to the quantity of thiopental injected. After each of the first three injections the blood pressure was about 30–40 mm Hg below the normal level. Following the initial transient changes after the last dose there was a slow second rise in ECG amplitudes and at the same time a slow second fall in blood pressure. These slow changes were most probably due to a redistribution of the injected thiopental similar to that of alcohol after 12 injections (see Ritchie 1970; Bernhard, Knave and Persson 1973).

When the effects of falling blood pressure *per se* were studied by electrical stimulation of the free-dissected left vagal nerve (dotted arrows Fig. 2 B) the

reduction obtained was of the same order of magnitude as those obtained after injections of 5, 10 and 20 mg thiopental. The ERG amplitudes however were not affected at all. For this reason we exclude the possibility of a barbiturate mediated reduction in blood pressure as the mechanism behind the alterations observed in retinal function of the intact eye after injections of a small dose of thiopental.

The maximal effect of thiopental was generally observed about 45 s after each injection. After large doses though the maximal effect on the *b* wave was not obtained until about one min later. To quantify the immediate effects the ERG amplitudes 45 s after injection recorded in the experiments illustrated in Fig. 2 A and B are depicted in the upper and lower graphs of Fig. 3 respectively. The *a* (solid line open circles) and *b* wave amplitudes (solid line filled circles) are plotted against the injected dose of thiopental. As mentioned earlier and also seen in these two graphs there is a steady increase in the *a* wave amplitude with increasing quantities of thiopental. The *b* wave amplitude is seen to increase successively up to a dose of 10 mg per kg b.wt. Successively diminishing amplitude was then recorded after injection of 20 and 30 mg thiopental.

When comparing the *a* and *b* wave amplitudes the depressive effect on the *b* wave was detected even after doses of 5 mg per kg b.wt. This is shown in Fig. 3 in which the ratio between the *b* and *a* wave amplitude recorded 45 s after each injection was also plotted (broken line) as a function of dose. As can be seen in the graphs the amplitude ratio did not change after light doses of thiopental. After moderate and large doses (5 mg per kg b.wt. or more) however the ratio was found to decrease.

Discussion

In the present study alterations in ocular blood circulation have been excluded as a main contributory mechanism at least as regards the small dose barbiturate effects on retinal function of the intact eye. Furthermore barbiturate effects similar to those presented have been recorded from isolated mammalian retinas (Bornschein *et al.* 1966; Honda and Nagata 1971). The changes in retinal function as found in the ERG of the present study therefore seem to be due to a primary barbiturate action within the retina.

The enhancement of the *a* and *b* wave amplitudes after administration of small doses of barbiturate probably is due to an increase in retinal excitability either in the photoreceptors and/or in the neurons of the inner nuclear layer of the retina. The progressive *b* wave depression after higher doses of barbiturate may be interpreted as an expression for a presumed depressive and toxic effect on neuronal structures in the inner nuclear layer.

The results presented thus point to the necessity of further studies in order to elucidate the effects of barbiturate on retinal function. As a consequence such studies have been made on the isolated receptor cell responses and inner nuclear layer components of the low intensity ERG and on the pigment epithelial cell activity. The results of these studies will be presented in the two following papers.

This work was supported by grants from the Swedish Medical Research Council, the Magnus Bergvall Foundation for Scientific Research, the Hierta Foundation for Ophthalmological Research and Karolinska Institutet.

References

- ARDEN G. B. GRANIT and F. PONTE. Phase of suppression following each retinal *b* wave in flicker. *J. Neurophysiol.* 1960 23 305—314.
- BERNHARD C. G. B. KNAVE and H. E. PERSSON. Differential effects of ethyl alcohol on retinal functions. *Acta physiol. scand.* 1973 88 373—381.
- BORNESCHEN H. R. HANITZSCH and A. v. LUTZOW. Der Nachweis des Barbiturateffektes an der isolierten Warmbluternetzhaut. *Experientia* (Basel) 1966 22 98—99.
- DAVIS P. Modifications de l'electroretinogramme du rat produites par l'injection intra-arterielle proche de potassium de veratrine et de narcotiques. *J. Physiol. Path. gén.* 1956 48 479—483.
- HANITZSCH R. and H. BORNESCHEN. Spezielle Überlebensbedingungen für isolierte Netzhäute verschiedener Warmbluter. *Experientia* (Basel) 1965 21 484—485.
- HONDA Y. and M. NAGATA. Effect of barbiturates upon the ERG of mammalian retinas in vitro. *Vision Res.* 1971 11 1209—1210.
- JACOBSON J. H. In *Clinical Electoretinography* 1961 30—34.
- JACOBSON J. H. and G. F. GESTRINO. Centrifugal influence upon the electroretinogram. *Arch. Ophthalmol.* 1958 60 295—302.
- KNAVE B. A. MÖLLER and H. E. PERSSON. A component analysis of the electroretinogram. *Vision Res.* 1972 12 1669—1684.
- MITA T. D. YONEMURA S. A. JACOBSON and J. H. JACOBSON. Effects of pentobarbital and optic nerve section upon the electroretinogram of the cat. *Invest. Ophthalmol.* 1963 2 520.
- NOLLE W. K. Differentiation metabolic organization and viability of the visual cell. *Arch. Ophthalmol.* 1958 60 702—733.
- PONTE F. The effect of some synaptic poisons and transmitters on the increase of the electroretinogram obtained by injections of barbiturates. *Arch. ital. Biol.* 1960 98 391—401.
- RITCHIE I. M. The aliphatic alcohols. In L. Goodman and A. Gilman (Eds.) *The Pharmacological Basis of Therapeutics*. MacMillan Company New York 1970 135—150.
- ROCKSTROM W. and R. HANITZSCH. Der Einfluss von Barbituraten auf das ERG der isolierten Froschnetzhaut. *Experientia* (Basel) 1966 22 100—101.
- SCHOLES A. W. and E. ROBERTS. Pharmacological studies of the optic system of the chick. Effect of γ -aminobutyric acid and pentobarbital. *Biochem. Pharmacol.* 1964 13 1319—1329.
- SHARPLESS S. R. The barbiturates. In L. Goodman and A. Gilman (Eds.) *The Pharmacological Basis of Therapeutics*. MacMillan Company New York 1970 99—120.
- TRIMARCHI F. Effect of barbiturates on the electroretinogram. *Ann. Otol.* 1968 91 1225—1229.
- WOHLZOGEN F. A. Beeinflussung des Säugetier FRG durch zentral nervös wirksame Substanzen. *Z. Biol.* 1956 108 217—233.
- WUNDSCH L. and W. ULRICH. Der Barbiturateffekt am negativen Elektroretinogramm der Katze. *Bien. Klin. Wochschr.* 1971 83 877—878.
- YONEMURA S. K. KAWASAKI and Y. TSUCHIDA. Differential vulnerability of the ERG components to pentobarbital. *Jap. J. Ophthalmol.* 1966 10 Suppl 155—166.

Effect of Lowered CSF Sodium Concentration on the Central Control of Fluid Balance

By

LEA ERIKSSON

Received 26 November 1973

Abstract

ERIKSSON L *Effect of lowered CSF sodium concentration on the central control of fluid balance* Acta physiol scand 1974 91 61-68

Isotonic and hypertonic non-electrolyte solutions were slowly infused into the cerebral ventricular system of conscious goats in normal water balance. Infusions of all the isotonic solutions induced water diuresis. When the infusions were made into the anterior part of the lateral ventricle the response was more delayed than when the solutions were infused into the third ventricle. Also hypertonic (0.45 M or 0.6 M) solutions of d-glucose, d-fructose, glycerol and sucrose turned renal $\text{C}_{\text{H}_2\text{O}}$ positive. Hypertonic urea, instead, gave inconsistent responses. The observed increase in renal $\text{C}_{\text{H}_2\text{O}}$ obviously resulted from an inhibition of the normal release of ADH. Firstly there was no increase in renal C_{Na} and secondly intravenous injection of ADH interrupted this water diuresis. No obvious changes occurred in renal electrolyte excretion, blood pressure and heart rate during infusions. After infusions when $\text{C}_{\text{H}_2\text{O}}$ returned to the preinfusion level there was sometimes a slight increase in sodium excretion and blood pressure. Infusions of isotonic saccharides in physiologic saline did not induce water diuresis under infusions but after infusions there was (in 4 out of 8 cases) some increase in urine flow and $\text{C}_{\text{H}_2\text{O}}$ could become positive for 10 to 20 min. These results indicate that instead of osmolality the ionic composition of CSF is important for ADH release and support the concept of a Na^+ sensitive receptor system near the third ventricle.

Verney's (1947) classic investigations constitute the basis for the current theory of central osmometric regulation of the ADH release. More recent studies in the central control of fluid balance in the goat speak in favour of a possible alternative to hypothalamic osmoreceptors. There might be a receptor system near the third cerebral ventricle which is sensitive to variations in the Na^+ concentration of the CSF (Andersson 1971, Andersson *et al.* 1972, Olsson 1973). These receptors may also be of importance in the regulation of blood pressure and renal sodium excretion (Andersson *et al.* 1972). Therefore it was studied whether an artificially induced lowering of the CSF Na^+ concentration would inhibit the release of ADH normally occurring in the non-hydrated animal and whether it would influence the blood pressure and sodium excretion.

Methods

Animals and animal care Ten adult female goats (b.wt. 35 to 45 kg) were used for repeated experiments. The minimum interval between experiments on each animal was 3 days. The animals were kept in metabolism cages where the experiments were conducted. The goats had free access to hay and water. Each afternoon they received 5 g of NaCl in 300 g of crushed oats.

Brain implantations and infusion technique The goats were prepared with a permanent cannula either in the anterior part of the third cerebral ventricle (3 animals) or in the anterior part of one lateral ventricle (7 animals). The implantation and infusion techniques have been described earlier (Andersson, Olsson and Warner 1961). To ensure free communication with the CSF over long periods of time a special three cannula system (Åkerlund, Andersson and Olsson 1973) was used in 6 of the goats. In all experiments cerebrospinal fluid was observed to drain out of the permanent cannula on compression of the neck of the animal before insertion and after removal of the innermost cannula. Thus free mixing of the infused solution with the CSF of the ventricle was guaranteed.

Blood pressure recording Four of the goats had a polyvinyl catheter permanently implanted via the superficial temporal artery into the carotid artery as earlier described (Eriksson, Fernández and Olsson 1971). The catheters were flushed with isotonic saline and filled with heparin solution every second day. During the experiments the arterial catheter was connected to a "Siatham" pressure transducer. Mean and systolic/diastolic blood pressures and heart rates were recorded on a Beckman Offner Dynograph type S 11.

Urine collection and analyses The urine was collected in 10 or 20 min samples via a retention catheter. Urine Na and K were determined by use of a "Jouan" flame photometer. A "Fiske" osmometer was used for determinations of urine osmolality. Plasma osmolality 290 mosm/kg was used for calculations of the renal free water clearance (C_{H_2O}).

Planning of the experiments The infusions were started between 11 a.m. and 2 p.m. By this time of the day the goats had eaten to satisfaction from the morning refill of the hay bin and the urine flow rate was stable and low. In animals with permanent cannula in the third ventricle the duration of the infusion was 40 min and the rate of infusion 10 μ l/min or 20 μ l/min. In the animals with a cannula in the lateral ventricle the infusion duration was 60 min and the rate 20 μ l/min.

The following non-electrolytes were used: d-glucose, d-fructose, glycerol, sucrose and urea. Infusion solutions were either isotonic (0.3 M) or hypertonic (0.45 M or 0.6 M). Isotonic saccharides in physiologic saline and merely isotonic NaCl were infused as controls.

Results

Infusions of isotonic non-electrolyte solutions

All non-electrolyte infusions had the same effect on renal water excretion. Before the start of infusion the goats were in antidiuresis, i.e. the renal C_{H_2O} was negative. The infusions induced an increase in the urine flow while urine osmolality decreased. The C_{H_2O} became positive 20–30 min after start and was highest just after stopping the infusion into the third ventricle at a rate of 10 μ l/min (Fig. 1 left). When a higher rate 20 μ l/min was used in one of the goats (7 expts.) the response was more pronounced and of longer duration. The infusions into the anterior part of the lateral ventricle also induced water diuresis but the response was more delayed than during the infusions into the third ventricle (Fig. 1 right).

The infusions of isotonic non-electrolytes caused no consistent changes in renal C_{Na} or in renal sodium or potassium excretion (Fig. 1). Blood pressure was recorded in 10 expts. The mean blood pressure and heart rate did not change during the infusions. During the 4 expts. blood pressure had some tendency to decrease (2–3 mmHg). After infusion when C_{H_2O} returned to preinfusion level increases in renal sodium excretion and blood pressure were sometimes seen.

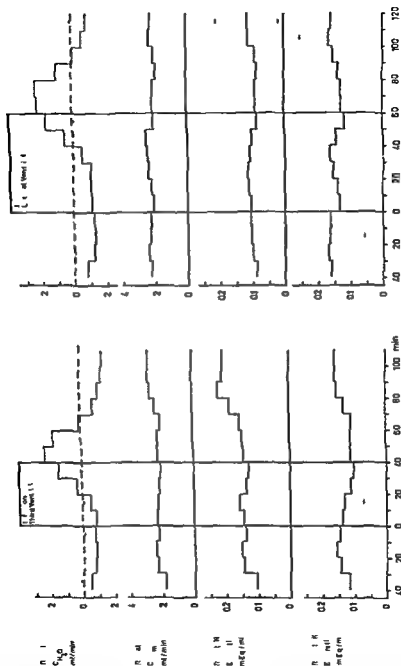


Fig. 1 Effect on renal water and electrolyte excretion of isotonic non-electrolyte solutions infused into the cerebral entricular system of goats in normal water balance. Means \pm S.D. Water diuresis developed consistently. *Left*: Infusions into the third ventricle in 3 goats (d glucose 2 expts, d fructose 1 expt, glycerol 1 expt, urea, 2 expts). Rate of infusion 10 μ l/min. *Right*: Infusions into the anterior part of lateral ventricle in 5 goats (d glucose 4 expts, d fructose 2 expts, sucrose 2 expts, glycerol 1 expt, urea 2 expts). Rate of infusion 20 μ l/min.

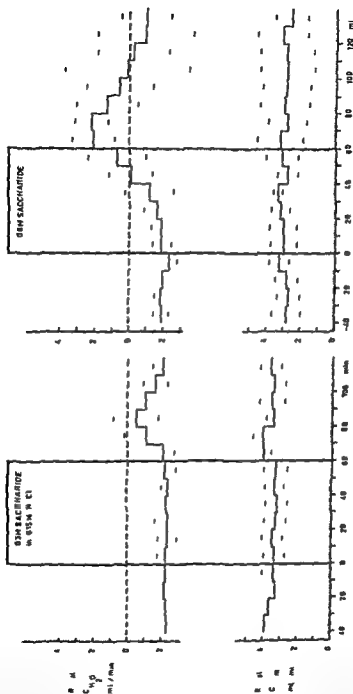


Fig. 2. A comparison between the infusions of isotonic saccharide in physiologic saline (left) and the same double isotonic 0.5 M saccharide alone (right) into the lateral ventricle of 4 goats at a rate of 0.1 ml/min. Means \pm SD. Number of experimental series: 6 (d-glucose), 2 (d-fructose), 2 (sucrose), 1 (glycerol), 1 (other). One of the infusions was d-fructose 0.5 M, which was excluded from the figure (right) because of the development of natriuresis and high osmotic diuresis before the infusion was started (left). When Na⁺ was present there was no change in water excretion during infusion, but some increase after stopping infusion. Right: The infusion of hypertonic saccharides alone induced a water diuresis.

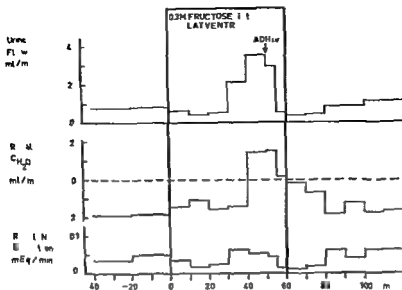


Fig 3 5 mU of ADH intravenously interrupted the water diuresis induced by infusion of isotonic fructose into the lateral ventricle. Rate of infusion 90 μ l/min

During the experiments the goats behaved normally ruminating and eating intermittently and did not seem to take notice of the infusions

Infusions of hypertonic non electrolyte solutions

Hypertonic saccharides Infusions of saccharide solutions of double isotonicity (0.6 M) into the lateral ventricle at a rate of 20 μ l/min in 5 cases of 8 expts induced a water diuresis of the same magnitude as infusions of isotonic solutions (Fig 2 right). In one experiment the goat showed a raise in renal C_{Na} and Na excretion before the start of hypertonic fructose infusion and the water diuresis failed to develop. The same infusion experiment was repeated later when renal C_{Na} was stable and the animal responded with water diuresis. In one animal 0.6 M glycerol and 0.6 M fructose were infused into the third ventricle at rate of 20 μ l/min. The infusions caused a distinct water diuresis of long duration. 0.45 M fructose and glucose infused into the lateral ventricle of one goat caused a somewhat stronger water diuresis than the infusion of isotonic fructose in the same animal.

Hypertonic urea Infusions of hypertonic urea infused into the lateral ventricle gave more inconsistent results. In one animal 0.6 M urea gave no response but 0.45 M urea induced a pronounced water diuresis of 80 min duration. In another goat 0.6 M urea induced a slightly positive C_{H_2O} 40 min after start which changed to negativity before the infusion was stopped.

The hypertonic non-electrolyte infusions (like those of 1 osmotic infusions) did not affect the renal electrolyte excretion and the C_{H_2O} (Fig 2 right). There was no change in blood pressure when recorded under the infusion of 0.45 M urea.

Infusions of isotonic saccharides in physiologic saline To find out whether the lowering of CSF Na concentration was the most important cause of the water diuresis combined infusions were used as controls. There were no obvious changes in renal C_{H_2O} during the infusions. After stopping the infusions there was in 4 out of 6 expts some increase in urine flow and C_{H_2O} became slightly positive for 10–20 min. This is illustrated in Fig 2 (left). For comparison Fig 2 (right) also shows the much more conspicuous diuretic effects of infusions of 0.6 M solutions in the same animals.

Infusion of isotonic saline did not cause any water diuresis

Intracereous injection of ADH during the water diuresis To prove that the increase in urine flow during the non-electrolyte infusions was due to lack of ADH 5 mL of vasopressin (Pitressin "Parke Davis") was injected intravenously. This interrupted the water diuresis (Fig 3).

Discussion

The osmoreceptor theory of Verney (1947) signifies that the alterations in plasma osmolality influence the ADH release by changing the volume of hypothalamic osmoreceptors. Verney found that infusions of hypertonic solutions of sodium salts or sucrose into the carotid artery induced the release of ADH in the hydrated dog. The possible interaction of brain barrier system has not been taken into consideration in these studies.

The results of more recent studies on the central control of fluid balance in the goat appear incompatible with the osmoreceptor theory. Infusions of small amounts of hypertonic NaCl into the third brain ventricle (inside the blood brain barrier) effectively elicit the release of ADH (Andersson *et al* 1967) while similar infusions of hypertonic sucrose are without effect (Olsson 1969). In similar infusion experiments a linking interaction between angiotensin and Na has been observed (Andersson *et al* 1972). Furthermore infusions of isotonic or hypertonic saccharide solutions into the lateral ventricle inhibit the antidiuretic effect of intracarotid infusions of hypertonic NaCl (Olsson 1973). All these studies support the concept that a possible alternative to hypothalamic osmoreceptors would be contained in receptors near the third ventricle which respond to changes in the CSF Na concentration (*cf* Andersson 1971). This would imply that the blood liquor barrier is of greater importance for the central control of fluid balance than the blood brain barrier.

Leusen and Lacroix (1961) produced water diuresis in chloralose anesthetized dogs by ventriculocisternal perfusion with hypotonic low sodium solution. They found a time lag of 20 min between the start of perfusion and the diuretic response. In the present study the osmolality of the infusion solutions was either isotonic or

hypertonic. Hence the increase in C_{H_2O} was not induced by reduced osmolality of CSF but more likely by dilution of the CSF Na. The observed diuresis in all probability resulted from an inhibition of the normal release of ADH. Firstly there was no increase in renal C_{Na} , or blood pressure. Secondly intravenous injection of 5 mU of vasopressin interrupted this water diuresis.

Saccharide solutions of double isotonicity (0.6 M) induced a water diuresis of the same magnitude as the corresponding isotonic (0.3 M) solutions except in one experiment. In this case the animal had a raise in C_{osm} before the start of the infusion. Zehr, Johnson and Moore (1969) found that during the course of osmotic diuresis the renal C_{H_2O} remains negative in spite of a highly significant decrease of plasma ADH.

The response to infusions of urea was inconsistent. Isotonic urea like isotonic saccharides caused water diuresis. Hypertonic solutions on the other hand were not always effective. The reason for this remains obscure. It has anyway been observed in the same species that the infusion of strongly hypertonic urea solution into the third ventricle may cause a release of ADH in the hydrated animal (Andersson *et al.* 1967).

After infusions repeated over long periods of time the responsiveness of the animals often decreased indicating some chronic damage of the periventricular tissue. Therefore after infusion of saccharides with saline it always was necessary to test the sensitivity of the goat by renewed infusion of saccharide solution alone.

Mouw and Vander (1970, 1971) found a large decrement in renal Na excretion and an increase in plasma renin activity during ventriculocisternal perfusion of artificial low sodium CSF in pentobarbital anesthetized dogs. If however the control sodium excretion was high the response was weaker. On the other hand when dogs were anesthetized with chloralose and perfused with hypotonic low sodium CSF Na excretion sometimes decreased, sometimes not (Leusen and Lacroix 1961). In the present experiments with conscious goats there was no consistent change in renal Na excretion. The divergent effect on Na excretion may in part depend on anesthesia. Species differences between herbivores and carnivores may be another factor. The negligible effect on the blood pressure and heart rate in the present study is in agreement with the results in anesthetized dogs (Mouw and Vander 1970, Leusen and Lacroix 1961).

The infusions of non electrolyte solutions into the ventricular system obviously reduces the relative concentrations of other ions in the CSF to the same degree as the Na concentration. There is however evidence that a lowering of CSF Na concentration was the most important cause for the water diuresis seen during the intraventricular infusions of pure saccharide solutions. When the Na concentration of the CSF was attempted to maintain normal by infusing isotonic NaCl alone or saccharides in physiologic saline there was no obvious inhibition of the ADH release during infusions in spite of the reduction of other ions. However after the combined infusions (saccharide + saline) some increase in C_{H_2O} was often seen (Fig. 2 left). Since these solutions in fact were hypertonic they gradually may have

drawn water into the CSF thereby reducing the Na concentration so that a post infusion reduction of the ADH release became apparent. According to the results of earlier studies in the goat (Andersson *et al* 1967) Cl does not seem to be important for the central control of fluid balance. It still remains to be settled whether K, Ca or Mg in CSF play any part in the control of ADH release.

This work was supported by grants from the Emil Aaltonen Foundation and the Finnish National Research Council for Medical Science (444 5001 3 07003/051).

References

- ÅKERLUND L. E., I. ANDERSSON and K. OLSSON. A cannula system for frequent infusions into the CSF of the cerebral ventricles of the goat. *Physiol Behav* 1973 10: 161—167.
- ANDERSSON B. Thirst—and brain control of water balance. *Amer Scientist* 1971 59: 408—415.
- ANDERSSON B., K. OLSSON and R. G. WARNER. Dissimilarities between the central control of thirst and the release of antidiuretic hormone (ADH). *Acta physiol scand* 1967 71: 57—64.
- ANDERSSON B., L. ERIKSSON, O. FERNANDEZ, C. G. HOLMÖDIN and R. ÖLTNER. Centrally mediated effects of sodium and angiotensin II on arterial blood pressure and fluid balance. *Acta physiol scand* 1972 85: 398—407.
- ERIKSSON L. O., FERNANDEZ and K. OLSSON. Differences in antidiuretic response to intra-carotid infusions of various hypertonic solutions in the conscious goat. *Acta physiol scand* 1971 83: 554—562.
- LELSEN J. and E. LACROIX. Changes in osmolality in the cerebral ventricles and diuresis. *Endocrinology* 1961 68: 719—721.
- MOLW D. R. and A. J. VANDER. Evidence for brain Na receptors controlling renal Na excretion and plasma renin activity. *Amer J Physiol* 1970 219: 872—877.
- MOLW D. R. and A. J. VANDER. Evidence for hormonal mediation of the renal response to low sodium stimulation of the brain. *Proc Soc exp Biol (NY)* 1971 137: 173—178.
- OLSSON K. Studies on central regulation of secretion of antidiuretic hormone (ADH) in the goat. *Acta physiol scand* 1969 77: 465—474.
- OLSSON K. Further evidence for the importance of CSF Na concentration in central control of fluid balance. *Acta physiol scand* 1973 88: 183—188.
- VERNEY E. B. The antidiuretic hormone and the factors which determine its release. *Proc Soc Biol* 1951 135: 25—106.
- ZAHN J. E., J. A. JOHNSON and W. W. MOORE. Left atrial pressure, plasma osmolality and ADH level in the unanesthetized ewe. *Amer J Physiol* 1969 217: 1672—1680.

Utilization of Energy Reserves by Cells Isolated from Newborn Rat Brain

II

HARI HEMMINKI and MATTI HÄRKÖNEN

Received 26 November 1973

Abstract

HEMMINKI H. and M. HÄRKÖNEN: Utilization of energy reserves by cells isolated from newborn rat brain. *Acta physiol scand* 1974 91: 69-75.

Cells were isolated from newborn rat brain cortex as previously described (Hemminki 1972a). The viability of the isolated cells was evaluated by determining the concentrations of the major energy metabolites during incubation in various conditions. In isolated cells the initial concentrations of glycogen, ATP and phosphocreatine were 2.8, 1 and 1.8 mmol/kg protein, respectively. These concentrations were lower than in newborn rat brain cortex *in situ*, while the concentrations of ADP, AMP, pyruvate and lactate were higher in the isolated cells. When the isolated cells were incubated in air without glucose the levels of ATP, phosphocreatine and glycogen decreased slowly. In a 5% saturated incubation medium the decrease was more rapid. When exogenous glucose was added and the incubations carried out in air the levels of ATP and phosphocreatine increased to 130 and 100% of the starting concentrations, respectively. These experiments indicate that the cells are metabolically active.

Several techniques have been described for the preparation of primary cell cultures (cell suspensions) from the central nervous system (Rosen 1967; Blomstrand and Hamburger 1969; Hemminki 1970; Norton and Poduslo 1970; Sellinger *et al.* 1971; Shapiro 1973; Yavin and Menkes 1973). These preparations have frequently been incubated in short term metabolic experiments and a copious literature on the differences between the various cell types has accumulated (see a review by Blomstrand 1971). Some authors have questioned whether the cells used were viable and intact (Cremer *et al.* 1968). Apart from light microscope observations few data are available to meet the criticisms raised.

Recently a technique was described for the isolation of cells from newborn rat brain cortex (Hemminki 1972a). The preparations rich in immature neurons induce active proliferation of glial cells occurs relatively late in rat brain. The cells provide a model of developing brain cells and have already been used in studies on membrane formation (Hemminki 1972b; Hemminki and Suovaniemi 1973) and on the regulation of protein and RNA synthesis by neuroactive substances (Hemminki 1973). The viability of the cell has previously been studied in long term cultures with ultrastructure, dye exclusion, amino acid uptake and organized

drawn water into the CSF, thereby reducing the Na concentration so that a post infusion reduction of the ADH release became apparent. According to the results of earlier studies in the goat (Andersson *et al* 1967), Cl does not seem to be important for the central control of fluid balance. It still remains to be settled whether K, Ca or Mg⁺⁺ in CSF play any part in the control of ADH release.

This work was supported by grants from the Emil Aaltonen Foundation and the Finnish National Research Council for Medical Science (414 5 551 3 07003705 1).

References

- AARLUND L E, I ANDERSSON and K OLSSON. A cannula system for frequent infusions into the CSF of the cerebral ventricles of the goat. *Physiol Behav* 1973 10 161—167.
- ANDERSSON B. Thirst—and brand control of water balance. *Amer Scientist* 1961 59 408—415.
- ANDERSSON B, K OLSSON and R G WARNER. Dissimilarities between the central control of thirst and the release of antidiuretic hormone (ADH). *Acta physiol scand* 1967 71 57—64.
- ANDERSSON B, L ERIKSSON, O FERNANDEZ, C G HOLMÖDIN and R OLTNER. Centrally mediated effects of sodium and angiotensin II on arterial blood pressure and fluid balance. *Acta physiol scand* 1972 80 398—407.
- ERIKSSON L, O FERNANDEZ and K OLSSON. Differences in antidiuretic response to intra carotid infusions of various hypertonic solutions in the conscious goat. *Acta physiol scand* 1971 83 554—562.
- LEUSEN I and E LACROIX. Changes in osmolality in the cerebral ventricles and diuresis. *Endocrinology* 1961 68 719—721.
- MOUW D R and A J VANDER. Evidence for brain Na receptors controlling renal Na excretion and plasma renin activity. *Amer J Physiol* 1970 219 822—832.
- MOUW D R and A J VANDER. Evidence for hormonal mediation of the renal response to low sodium stimulation of the brain. *Proc Soc exp Biol (NY)* 1971 137 179—187.
- OLSSON K. Studies on central regulation of secretion of antidiuretic hormone (ADH) in the goat. *Acta physiol scand* 1969 77 460—474.
- OLSSON K. Further evidence for the importance of CSF Na concentration in central control of fluid balance. *Acta physiol scand* 1973 88 183—188.
- VERNEY E B. The antidiuretic hormone and the factors which determine its release. *Proc roy Soc B* 1947 135 25—106.
- ZEHR J E, J A JOHNSON and W W MOORE. Left atrial pressure, plasma osmolality and ADH levels in the unanesthetized ewe. *Amer J Physiol* 1969 217 1672—1680.

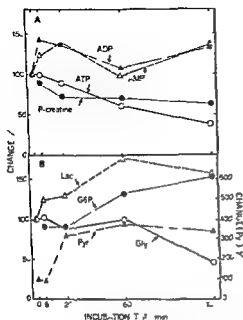
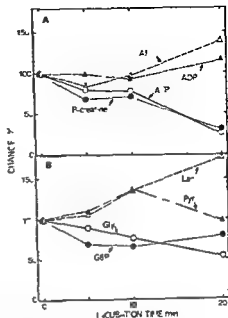


Fig 1 The concentrations of energy metabolites in immature brain cells incubated under air. Cells were isolated from newborn rat brain and incubated in Krebs-Ringer phosphate buffer pH 7.5 in open flasks. At the times indicated samples were withdrawn from the cell suspension and A) ATP, ADP, AMP and P-creatine and B) pyruvate, G6P, glycogen and lactate were analysed as described in Methods. Each point is a mean of 4 to 6 determinations with an average S.E. of about 15%.

Fig 2 Effect of anoxia on the concentrations of energy metabolites in immature brain cells. A suspension of cells was gassed with N_2 and samples were taken at the time points indicated for determination of A) ATP, ADP, AMP and P-creatine and B) pyruvate, G6P, glycogen and lactate. Each point represents the mean of 4 to 6 determinations with an average S.E. of about 15%.



glucose by centrifugation at $300 \times g$ for 10 min. The cells were resuspended in the same medium and the temperature raised to $37^\circ C$. Zero-time samples were immediately withdrawn for analysis of energy metabolites (Table I). The values were compared with those of newborn and adult rat brain cortex frozen *in situ*. The concentration of ATP, phosphocreatine, glucose-6-phosphate and glycogen were lower and those of ADP, AMP, pyruvate and lactate higher in the isolated cell than in newborn brain cortex *in situ*. This reflects consumption of energy reserves during the isolation procedure which takes altogether about 2 h. The sum of adenine nucleotides was only slightly lower in the isolated cells (26.6 mmol/kg protein) than in brain cortex (33.7 mmol/kg protein) indicating that nucleotides had not leaked out of the isolated cells. This further substantiates a previous finding of the integrity of the cellular plasma membranes (Hemminki, 1972a). The levels of ATP and phosphocreatine were relatively high, however, as compared with the values in adult rat brain (Table I) and the cells were obviously capable of utilizing their

energy reserves according to their requirements. The differences in metabolite concentrations between newborn and adult rats are related to the age-dependent protein content of (Himwich 1969) and enzyme activities (Pocchiani 1971) the brain.

Incubation under air

The concentrations of high-energy compounds and metabolic intermediates were followed during incubation for 2 h (Fig. 1 A and B). The concentration of ATP fell gradually and only 15% was present after 2 h. The concentrations of ADP and AMP rose in 5 min to 140 and 120% of the original levels respectively and fluctuated somewhat during incubation. Phosphocreatine dropped to 70% of the initial value in 20 min and showed no further change. After 2 h the molar increase in ADP and AMP was some 60% higher than the decrease in ATP and phosphocreatine. After incubation for 1 h glycogen started to fall and after 2 h about 50% of the original concentration was left. Pyruvate and lactate increased considerably during the first hour of incubation and then levelled off. The breakdown of glycogen was not sufficient to account for the increase in the concentrations of pyruvate and lactate. The extra carbon could have come from residual glucose remaining in the cells after trypsinization or from proteins. Glucose-6-phosphate increased gradually during the 2 h incubation.

Incubation under nitrogen

Brain tissue when incubated under N_2 in a closed system will continue to function for a short time by utilizing endogenous energy reserves. When isolated cells were incubated under N_2 (Fig. 2 A and B) the concentrations of ATP and phosphocreatine decreased to 70–80% of the original level during the first 10 min. After 20 min their concentration had dropped to 30% of the starting level. These changes were accompanied by a concomitant increase in the levels of AMP and ADP roughly equalling the decrease of ATP and phosphocreatine. Glycogen fell linearly during the first 20 min of incubation to 50% of the original value. This fall was again not enough to account for the rise in the concentration of lactate. Pyruvate rose only slightly during the first 10 min of incubation and then dropped to the starting level. Glucose-6-phosphate decreased in 5 min to 70% of the starting value and remained at this level.

Incubation under air with glucose

Whether ATP and phosphocreatine could be regenerated in isolated cells was studied by adding glucose to the incubation medium at 10 mM concentration (Fig. 3 A and B). After incubation for 1 h the concentration of ATP had risen by 30% and that of phosphocreatine by 70%. In absolute concentrations the level corresponds to about 1/3 of that found in immature brain cortex *in situ* (Table 1). The concentrations of ADP and AMP also increased slightly which indicates a net

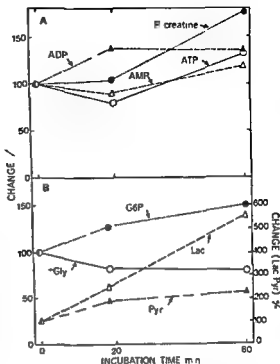


Fig 3 Effect of added glucose on the concentrations of energy metabolites in immature brain cells. Isolated cells were incubated in Krebs Ringer phosphate buffer pH 7.5 containing 10 mM glucose under air. Samples were withdrawn for determination of A) ATP, ADP, AMP and PCr, creatine and B) pyruvate, G6P, glycogen and lactate. Each point is a mean of 4 to 6 determinations. An average S.E. was about 15%.

in the total adenine nucleotides in the cells. The regeneration experiment led to increased levels of pyruvate and lactate, probably because of leakage of these compounds into the incubation medium, where they would be less accessible to cell metabolism. The exogenous glucose seems to be the major energy source, since the endogenous glycogen decreased only slightly during incubation.

Discussion

In the study reported here, the metabolic condition of cells isolated from newborn rat brain was further tested by determining the concentrations of energy metabolites. Such an evaluation was considered important because suspensions of adult neurons and glial cells had been found to contain very low levels of energy-yielding compounds (Hemminki and Harkonen, unpublished observations).

The isolation procedure is time-consuming, requiring about 2 h from the sacrifice of the animals. Although oxygen and nutrients are supplied to the cells as well as possible, some drastic metabolic changes take place during the process. These are evidenced by the low levels of ATP and phosphocreatine and the high levels of AMP, ADP, pyruvate, and lactate in the final preparations. These metabolic changes indicate some anoxia, which may be due to an inadequate supply of oxygen to the undispersed pieces of tissue at the start of isolation. However, the metabolic changes in incubation experiments under air and N_2 indicate that these cells are viable and

can utilize their energy reserves according to their requirements. In both conditions glycogen, ATP and phosphocreatine, the major energy yielding compounds in nerve tissue, were consumed slowly by the isolated cells as compared with mouse brain cortex (Lowry *et al.* 1964) or rat sympathetic ganglion (Harkonen *et al.* 1969). There are two possible reasons for this. First, glucose was included in all media used in the isolation procedure. At the end of the procedure the cells were washed twice with a glucose free medium, but despite this some glucose may still have remained in the cells and would then be used up first to support the energy production required in the incubation experiments. Secondly, the cells were from newborn rat brain, immature tissue like this is known to be resistant to anoxia (Lowry *et al.* 1964; Maenpää 1967) and differs markedly from adult tissue in which ATP and phosphocreatine drop almost instantaneously on exposure to anoxia (Lowry *et al.* 1964; Harkonen *et al.* 1969).

However, there was a definite difference in the metabolic responses of these cells under air and under N_2 , which shows that the utilization of energy stores can be varied according to need. The regeneration of ATP and phosphocreatine in the presence of glucose also shows the metabolic capacity of the isolated cells. A similar observation was made by Bradford (1969) when synaptosomes were incubated in a medium containing high concentrations of glucose, inorganic phosphate and potassium. On the other hand, Harkonen *et al.* (unpublished observation) were unable to demonstrate high-energy phosphate regeneration in their synaptosome preparation.

This study was supported by The Sigrid Juselius Foundation and The Medical Research Council in the Academy of Finland.

References

- BLOMSTRAND, C. Studies on protein metabolism in neuronal and glial cell-enriched fractions from brain tissue. *Academic Dissertation* 1971. Göteborg 1—31.
- BLOMSTRAND, C. and A. HAMBERGER. Protein turnover in cell-enriched fractions from rabbit brain. *J. Neurochem.* 1969, 16, 1401—1407.
- BRADFORD, H. F. Respiration *in vitro* of synaptosomes from mammalian cerebral cortex. *J. Neurochem.* 1969, 16, 675—684.
- CREMER, J. E., P. V. JOHNSTON, B. I. ROOTS and A. J. TREVOR. Heterogeneity of brain fractions containing neuronal and glial cells. *J. Neurochem.* 1968, 15, 1361—1370.
- HÄRKÖNEN, M. H. A. J. V. PASSONEN and O. H. LOWRY. Relationships between energy reserves and function in rat superior cervical ganglion. *J. Neurochem.* 1969, 16, 1439—1450.
- HEMMINKI, K. An improved method for preparing brain cell suspensions. *Febs Letters* 1970, 99, 290—293.
- HEMMINKI, K. Isolation of viable and morphologically intact cells from newborn rat brain. *Exp. Cell Res.* 1972a, 75, 379—384.
- HEMMINKI, K. Characterization of proteins and glycoproteins of surface membranes isolated from immature brain cells. *Life Sci.* 1972b, 11, 1173—1179.
- HEMMINKI, K. Effects of added substances on RNA and protein synthesis in immature neurons. *J. Neurochem.* 1973, 20, 373—378.
- HEMMINKI, K. and O. SLOVANIEMI. Preparation of plasma membranes from isolated cells of newborn rat brain. *Biochim. biophys. Acta* (Amst.) 1973, 298, 75—83.
- HEMICH, W. Body and brain weights and moisture content of the brain. In: *Handbook of Neurochemistry*, Vol. 2. Ed. A. LAJTHA. Plenum Press, New York—London, 1969, pp. 469—470.

- LOWRY O H J V PASSONNEAL F N HASSELBERGER and D W SCHLEITZ Effects of ischemia on known substrates and cofactors of the glycolytic pathway in brain *J Biol Chem* 1964 239 18—30
- MAENPÄÄ P High-energy phosphates the disappearance of glycogen and accumulation of lactate during anoxia in the brain heart and liver of the developing rat *Academic Dissertation* 1967 Helsinki 1—52
- NORTON W T and W E PODUSLO Neuronal soma and whole neuroglia of rat brain a new isolation technique *Science* 1970 167 1144—1146
- PASSONNEAL J V P D GATFIELD D W SCHLEITZ and O H LOWRY An enzymic method for measurement of glycogen *Analyt Biochem* 1967 19 315—326
- POCCHIALI F Some aspects of carbohydrate metabolism in the developing brain In *Chemistry and Brain Development* Ed R PAOLETTI and A N DAVISON Plenum Press New York—London 1971 pp 111—121
- ROSE S P K Preparation of enriched fractions from cerebral cortex containing isolated metabolically active neuronal and glial cells *Biochem J* 196 102 33—34
- SELLINGER O Z J M AZCURRA, D E JOHNSON W C ORLSON and Z LODIN Interdependence of protein synthesis and drug uptake in nerve cell bodies and glial cells isolated by a new technique *Nature (Lond)* 1971 230 253—256
- SIAPKO D L Morphological and biochemical alterations in foetal rat brain cells cultured in the presence of monobutyl cyclic AMP *Nature New Biol* 1973 241 203—204
- YAVIN E and J H MENKES The culture of dissociated cells from rat cerebral cortex. *J Cell Biol* 1973 57 232—237

The Effect of Glycerol on the Postexercise Lactate Clearance

By

CHRISTIAN OLSEN and EBBE STRANGE PETERSEN

Received 26 November 1973

Abstract

OLSEN CHR and E S PETERSEN *The effect of glycerol on the postexercise lactate clearance* Acta physiol scand 1974 91 76-82

The effect of increased glycerol concentrations induced by peroral intake of glycerol on the concentrations of lactate and pyruvate in blood was investigated in 7 young adults at rest and after exercise 10 min of work on a bicycle ergometer induced a small but statistically significant rise in the glycerol concentration. The concentration of lactate at rest was significantly higher after than before glycerol intake. The lactate/pyruvate ratio was significantly higher after than before glycerol intake both at rest and after 15 min of recovery and onwards. The metabolic clearance of lactate after exercise was reduced by the glycerol intake to about 70% of the control value. The effect of glycerol on the metabolic clearance of lactate was the same whether estimated at rest or after exercise. These observations are in accordance with the concept that glycerol metabolism influences the lactate/pyruvate ratio in the liver and thereby reduces the clearance of lactate.

Ethanol has been found to inhibit gluconeogenesis from glycerol by the perfused liver (Krebs 1968) also in man ethanol has been found to inhibit glycerol metabolism (Lundquist *et al* 1965). In both these conditions the hepatic content of L 3 glycerophosphate was increased probably through an increase in the extra mitochondrial NADH/NAD ratio (Krebs 1968, Robinson and Newsholme 1969).

Similarly ethanol has been found to inhibit the conversion of lactate to glucose in the perfused rat liver (Krebs *et al* 1969b) and in man following infusion of ^{14}C labelled lactate (Krebsberg, Owen and Siegel 1971) and severe exercise (Krebs *et al* 1969a). Also in these cases the underlying mechanism could be a reduction of NAD $^{+}$ to NADH driving the reaction

Lactic acid + NAD \rightleftharpoons Pyruvic acid + NADH + H $^{+}$ towards the left

Glycerol is metabolized predominantly by the liver (Larsen 1963, Borchgrevink and Havel 1963) while the small intestine (Saunders and Dawson 1962, Holt 1964), the kidney and probably other tissues as well play a minor role (Robinson and Newsholme 1969). The initial steps in the gluconeogenesis from glycerol are

Glycerol + ATP \rightarrow L 3 glycerophosphate + ADP

L-3 glycerophosphate + NAD \rightleftharpoons dihydroxyacetone phosphate + NADH

It might consequently be expected that reduced pyridinenucleotide generated by the metabolism of glycerol (*cf* Williamson *et al* 1969)—as by ethanol—might result in impairment of lactate uptake. This situation may be relevant at physiologically raised glycerol concentrations in the postexercise period. Lipolysis with increasing concentrations of free fatty acids—and glycerol—is an important energy yielding factor not only in work of long duration (Rodahl, Miller and Issekutz 1964) but also in relatively short lasting work (Keul, Doll and Kessler 1968).

In the present work we have consequently studied the clearance of lactate in the postexercise period with or without artificially raised blood glycerol concentrations. A preliminary report has been presented (Olsen and Strange Petersen 1973 a).

A study of the changes in the lactate concentration and in the ratio of lactate to pyruvate (L/P) in arterial and venous blood draining a resting limb after an injection of sodium (L+) lactate and after exercise has been reported previously (Olsen and Strange Petersen 1973 b).

Methods

The subjects were 9 healthy students: 8 men and 1 woman aged 22–28 years. The subjects came to the laboratory in the morning. They had been instructed not to take any alcohol in 24 h and not to exercise on the morning of the experiment. The experiments started at least 2 h after a light breakfast and 1 h rest on a couch.

4 types of experiments were carried out:

1. 7 subjects worked for 10 min on an electrically braked bicycle ergometer (Elema Schönan der) at a load previously determined to give a steady state heart rate of 170–180 beats per minute. When the work period had ended the subjects were placed on a couch in supine position.

2. This type of experiment was similar to the first with the one exception that the 7 subjects were given glycerol orally before work started and at intervals during the recovery period.

3. 3 subjects were given glycerol orally as above but did not exercise and spent the whole experimental period of 2 1/2 h resting on the couch.

4. 7 subjects spent the whole experimental period resting on the couch without glycerol load.

In the experiments of type 2 and 3 the subjects drank 25–50 g glycerol in 25 ml water 1/2 h before work started. 5 g glycerol in 10 ml water was subsequently given with 20 min intervals to maintain a concentration of about 8 mM.

The glycerol used was redistilled (Merck 4094)—and free from ethanol.

Venous blood was collected through a polythene catheter inserted through an antecubital vein to the axillary vein. Arterialized capillary blood was taken from the hyperemized ear lobe (in the following these samples will be referred to as arterial (*cf* Siggaard Andersen 1966)). Simultaneous samples were taken as indicated in results.

Arterial blood dripped freely into tubes with iced perchloric acid; similarly venous blood was precipitated immediately after sampling.

Lactate and pyruvate concentrations in both venous and arterial blood samples were measured by an enzymatic fluorimetric micromethod (Olsen 1971).

Glycerol concentrations (in venous plasma only) were determined according to the method of Wieland (1957) as modified by Larsen (1963).

Statistics: *F* values have been calculated from *t* tests based on paired comparison except for the L/P ratios on which Wilcoxon's signed rank test was employed (Sokal and Rohlf 1969).

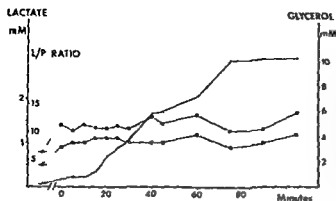


Fig 1 Results of one experiment in which glycerol was given but no work was performed. The points to the left of the break in the time axis represent samples taken before glycerol was given. Time 0 is 30 min after glycerol intake. Lactate (open circles) and L/P ratio (filled circles) were measured in arterial blood. Glycerol (dots) was measured in venous plasma.

TABLE I The effect of glycerol on the mean arterial concentrations (\pm S.E.) of Lactate, Pyruvate and L/P ratio at rest ($n = 10$)

	Control		Glycerol
Lactate (mM)	0.63 ± 0.07	$P < 0.01$	0.91 ± 0.08
Pyruvate (mM)	0.077 ± 0.011		0.084 ± 0.009
L/P ratio	8.5	$P < 0.005$	11.0

TABLE II The influence of the experimental condition on the mean arterial concentrations (\pm S.E.) of Lactate, Pyruvate and L/P ratio at rest. Sample II was taken 30 min after sample I ($n = 7$)

	I	II
Lactate (mM)	0.55 ± 0.05	0.57 ± 0.03
Pyruvate (mM)	0.079 ± 0.013	0.072 ± 0.013
L/P ratio	7.9	7.8

Results

Three resting subjects were given glycerol orally. The concentrations of glycerol and lactate and the lactate/pyruvate ratios in one of these experiments are shown in figure 1. The glycerol concentration at time 0 (that is 30 min after the intake of 50 g glycerol) was 0.46 mM compared to 0.20 mM before glycerol was taken. After this the concentration started to rise more rapidly to reach a plateau of about 10 mM in about 70 min. This pattern of changes in glycerol concentration follow

ing oral intake was also seen in the two other subjects who did not work and in the 7 subjects who were given glycerol and subsequently worked for 10 min.

The mean glycerol concentrations before and 30 min after the intake of glycerol in the 10 subjects were 0.21 mM and 2.95 mM respectively.

Fig. 1 further shows that although the glycerol concentration at time 0 had only risen moderately, both the lactate concentration and the L/P ratio had approximately doubled; these two parameters remained at this new level without further changes in spite of the further increase in glycerol concentration.

Mean values of lactate, pyruvate and the L/P ratio in arterial blood before and 30 min after oral glycerol intake in the 10 expts. are presented in Table I. Whilst the change in pyruvate concentration was not significant, both the lactate concentration and the L/P ratio were significantly higher in the glycerol than in the control experiments.

In resting conditions which were similar except that no glycerol was given, the lactate and pyruvate concentrations and the L/P ratio in two blood samples taken at 30 min interval were almost identical (Table II).

The glycerol intake did not influence significantly on the pyruvate concentrations at any time during the recovery period after exercise. The L/P ratio (like at rest) was highest in the glycerol experiments; the difference, however, was not significant during the first 15 min of recovery.

Table III shows that the maximal lactate concentrations reached in the two types of experiments were very similar. The heart rate changes too were almost the same on the two occasions, the average resting heart rate being 74 and 67 respectively and the steady state value during work 179 and 177 respectively.

The mean rate of lactate removal can be evaluated by inspection of Table III: the decline in concentration of lactate during the first 30 min after work was roughly identical in the two types of experimental situation; during the later phase of recovery, from 50 min onwards, however, the concentrations were consistently and significantly higher in the glycerol than in the control experiments.

On plotting the logarithms of the lactate concentrations against time, the points representing the last 5 samples describe a fairly well defined linear fall. Assuming this exponential decline in lactate concentration to represent the metabolic removal of lactate by conversion to glucose and by oxidation, the rates of these metabolic processes can be roughly estimated by the half times. The half time in the control experiments was about 40 min and in the glycerol experiments about 60 min.

Similar half times were obtained whether arterial or venous concentrations were used, indicating that this latter part of the curve represents metabolic changes only.

The average changes in glycerol concentration induced by work in the control experiments are shown in Fig. 2. The concentration started to increase during the work period; towards the end of work the concentrations were significantly higher ($P < 0.01$) than at rest. Maximal concentrations were seen 5–10 min after the end of work and the values were not yet normal at the end of the experiments about 1 1/2 h after work.

TABLE III The effect of glycerol on the mean arterial concentrations (\pm S.F.) of lactate (mM) in the recovery period after exercise

Minutes after exercise	0	5	10	15	20
Control n = 7	7.29 \pm 0.59	5.34 \pm 0.89	4.58 \pm 0.60	3.54 \pm 0.64	2.56 \pm 0.39
Glycerol n = 7	6.75 \pm 0.63	6.01 \pm 0.86	4.45 \pm 0.67	3.76 \pm 0.73	2.56 \pm 0.36
P	NS	NS	NS	NS	NS

Discussion

We have found the rate of removal of lactate produced during a 10 minute period of fairly heavy work significantly diminished when blood glycerol concentrations had been raised by oral intake of glycerol. This observation parallels that of Krebs *et al.* (1969 a) of the effect of alcohol on lactate clearance.

Resting arterial lactate concentrations were significantly increased following glycerol intake; this increase appeared to be caused by glycerol as the experimental condition by itself did not induce any such changes (*cf.* Table I and II).

Lactate removal is generally considered to involve at least two different mechanisms: a diffusion into body water and metabolic removal mainly by reconversion to glucose but also by direct oxidation.

Lactate removal during the first 30–40 min of recovery in our experiments was not affected by glycerol. The major cause of the fall in lactate concentration in this period being diffusion and as glycerol is not likely to affect either the distribution volume or the rate of diffusion this is not unexpected.

From 40 min onwards the decline in lactate concentration was significantly slower when glycerol concentrations were high indicating an impaired metabolism of lactate. The difference in rate of metabolism in the two experiments has been quantified by treating the latter parts of the lactate clearance curves as monoexponential and calculating the half times. Thus roughly estimated glycerol reduced the metabolic rate of conversion of lactate to 40/60 or 67% of the control value.

Assuming the production of lactate in the tissues at rest to be unaffected by glycerol and lactate concentrations to reflect a steady state between production and metabolic turn-over of lactate, the ratio of the lactate concentration at rest with or without raised glycerol concentration should similarly reflect the extent to which lactate metabolism is inhibited by glycerol. This ratio was (*cf.* Table I) 0.63/0.91 or 0.69, a closely value similar to that estimated from the half times.

The suggested mechanism underlying this finding is that an increased glycerol metabolism largely taking place in the liver causes a rise in the cytoplasmatic NADH/NAD ratio. This change again is reflected by an increased L/P ratio in the cytoplasm and in the blood leaving the liver (Schimassek 1963).

An increased lactate concentration and L/P ratio in hepatic tissue and in the blood of starved rats following injection of glycerol has been reported by William

25	30	35	50	65	80	95
2.21 ± 0.24	1.71 ± 0.15	1.41 ± 0.18	1.15 ± 0.06	0.83 ± 0.09	0.63 ± 0.07	0.67 ± 0.04
2.08 ± 0.27	1.87 ± 0.21	1.66 ± 0.15	1.33 ± 0.08	1.24 ± 0.14	0.99 ± 0.05	0.91 ± 0.05
NS	NS	NS	< 0.005	< 0.005	< 0.005	< 0.005

son *et al* (1969). Also in the perfused rat liver an initial increase of lactate output and of L/P ratio following glycerol has been observed (Olsen unpublished). In the present work both arterial lactate and L/P ratio were increased during the period of raised glycerol concentration at rest and during recovery from exercise in agreement with this concept.

Lundquist *et al* (1965) did not find the L/P ratio in hepatic venous blood significantly changed during glycerol infusion and claimed that the hepatic lactate consumption was unaffected by glycerol. In a later report (Tygstrup, Winkler and Lundquist 1971) however an increase in the hepatic venous L/P ratio from 24 to 33 was observed in 3 expts.

The level of glycerol concentration reached following oral glycerol intake in our experiments was very high. The results presented in Fig. 1 however seem to indicate that already at a glycerol concentration of slightly above twice the resting concentration—and perhaps at an even lower value—the maximum change in both lactate concentration and L/P ratio is manifest.

A question to be raised now is whether the normally occurring changes in glycerol concentration during work are sufficiently large to affect lactate removal. In our short work periods clear and significant increments in glycerol concentration were observed (Fig. 2). The mean change from rest to maximum was 0.07 mM or approximately 32% (range 7–132%).

Other workers employing longer exercise periods have reported changes of up to 600% (Havel, Pernow and Jones 1967; Johnson *et al* 1969; Keul, Doll and Haralambie 1970). Both Johnson *et al* (1969) and Keul *et al* (1970) found greater glycerol changes in trained than in untrained subjects.

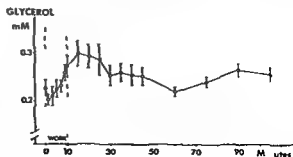


Fig. 2 Changes in glycerol concentration during and after work in the control experiments $n = 7$. Bars indicate \pm SE.

It appears therefore reasonable to believe that glycerol concentrations during work exceeding a certain intensity and duration may reach levels where lactate metabolism may be inhibited

This study was supported by the Danish Medical Research Council. We are indebted to Miss Lissi Hansen and Mrs Kirsten Klostergaard for valuable technical assistance

References

- BORCHGREVINK C F and R J HAVEL Transport of glycerol in human blood *Proc Soc exp Biol (N Y)* 1963 113 946—949
- HAVEL R J P PERROW and L J JONES Uptake and release of free fatty acids and other metabolites in the legs of exercising men *J appl Physiol* 1967 23 90—99
- HOLT P R Utilization of glycerol C¹⁴ for intestinal glyceride esterification. Studies in a patient with chyluria *J clin Invest* 1964 43 349—356
- JOHNSON R III J L WALTON H A KREBS and D H WILLIAMSON Metabolic fuels during and after severe exercise in athletes and non athletes *Lancet* 1969 2 432—435
- KELL J E DOLL and G HARALAMBIE Freie Fettsäuren Glycerin und Triglyceride im arteriellen und femoralen Blut vor und nach einem vierwöchigen körperlichen Training *Pflügers Arch ges Physiol* 1970 316 194—204
- KELL J E DOLL and D KEPPLER Zum Stoffwechsel des Skelettmuskels I Glucose Lactat Pyruvat und freie Fettsäuren im arteriellen und venösen Blut der arbeitenden Muskulatur bei Hochleistungsportlern *Pflügers Arch ges Physiol* 1968 301 198—229
- KREBS H A The effects of ethanol on the metabolic activities in the liver. In *Advances in Enzyme Regulation* Edited by G Weber Oxford Pergamon Press Ltd 1968 6 461—480
- KREBS H A D J C CUNNINGHAM M STUBBS and D J A JENKINS Effect of ethanol on postexercise lactacidemia *Israel J med Sci* 1969a 5 939—967
- KREBS H A R A FREEDLAND R HEMS and M STUBBS Inhibition of hepatic gluconeogenesis by ethanol *Biochem J* 1969b 112 117—124
- KREISBERG R A W C OWEN and A M SEIGAL Ethanolinduced hyperlactacidemia. Inhibition of lactate utilization *J clin Invest* 1971 50 166—174
- LARSEN J A Elimination of Glycerol as a Measure of the Hepatic Blood flow in the Cat *Acta physiol scand* 1963 57 224—234
- LENDQUIST F and TYGSTRUP A WINKLER and K B JENSEN Glycerol metabolism in the human liver. Inhibition by ethanol *Science* 1965 150 616—617
- OLSEN C An enzymatic fluorimetric micromethod for the determination of acetoacetate β hydroxybutyrate pyruvate and lactate *Clin chim Acta* 1971 33 293—300
- OLSEN C and E STRANGE PETERSEN Glycerol and the Postexercise Lactate Elimination *Acta physiol scand* 1973a 87 174—184
- OLSEN C and E STRANGE PETERSEN The lactate/pyruvate ratio in muscular work and following injection of lactate in man *Pflügers Arch ges Physiol* 1973b 342 359—365
- ROBINSON J and H A NEWSHOLME Some properties of hepatic glycerol kinase and their relation to the control of glycerol utilization *Biochem J* 1969 117 455—464
- RODHAHL K H I MILLER and B ISSEKLTZ JR Plasma free fatty acids in exercise *J appl Physiol* 1964 19 489—492
- SALVENDY D R and A M DAWSON Studies on the metabolism of glycerol by the small intestine in vitro and in vivo *Biochem J* 1967 82 477—483
- SCHIMASEK H Der Einfluss der Leber auf den extracellulären Redox Quotienten Lactat/Pyruvat *Biochem Z* 1963 336 468—473
- SIGGAARD-ANDERSEN O *The Acid Base Status of the Blood* Munksgaard Copenhagen 1968 p 26
- SOKAL R R and F J ROHLF *Biometry* The principles and practice of statistics in biological research San Francisco W H Freeman and Company 1969
- TYGSTRUP A WINKLER and F LENDQUIST Ethanol metabolism in man studied by liver vein catheterization. Effect of ethanol on glycerol metabolism. In *Metabolic changes induced by alcohol* Edited by Martin G A and Ch Bode Heidelberg—New York Springer Verlag 1971 pp 143—150
- WIELAND O Eine enzymatische Methode zur Bestimmung von Glycerin *Biochem Z* 1957 329 313—319
- WILLIAMSON D H D VELOSO E V ELLINGTON and H A KREBS Changes in the concentrations of hepatic metabolites on administration of dihydroxyacetone or glycerol to starved rats and their relationship to the control of ketogenesis *Biochem J* 1969 114 575—584

Effects of Ethanol, tert Butanol, and Clomethiazole on Net Movements of Sodium and Potassium in Electrically Stimulated Cerebral Tissue

By

H WALLGREN P NIKANDER P VOG BOGUSLAWSKI and J LINCOLA

Received 26 November 1973

Abstract

WALLGREN H P NIKANDER P VOG BOGUSLAWSKI and J LINCOLA *Effects of ethanol tert butanol and clomethiazole on net movements of sodium and potassium in electrically stimulated cerebral tissue* Acta physiol scand 1974 91 83-93

The sodium and potassium contents of rat brain cortex slices incubated in bicarbonate medium were measured and the intracellular quantities estimated on the basis of the inulin distribution. Ethanol (109 mM) did not affect the ion content of unstimulated tissue during passive leakage in cold medium or aerobic incubation at 37 °C.

The effects of ethanol (109 mM), tert butanol (34 mM) and clomethiazole (0.39 mM) were tested on the response to electrical stimulation (entry of sodium and loss of potassium in the non inulin space) as well as on the restoration of the ionic gradients occurring after a period of stimulation. All agents selectively inhibited the entry of sodium on stimulation with very little effect on potassium loss. The result is considered compatible with preferential action of the drugs on the activation step of the sodium channel controlling movement of sodium during the excitation cycle and presumably located on the outside of the membranes. During recovery no inhibition of sodium expulsion was observed whereas both alcohols—but not clomethiazole—slightly decreased the accumulation of potassium. Considered together with other observations it is finding suggests a special affinity of ethanol for the potassium binding site in the ion transport system.

In a review of work on the cellular basis of the depressant action of ethanol on nerve cells Wallgren and Barry (1970) concluded that ethanol molecules interfere directly with the excitable membrane structures. The action of ethanol seems to be rather widespread without clear restriction to the synaptic region or other parts of the neurons. For detailed characterization of the mechanism of this action it seems important to identify more closely that aspect of membrane function which is most sensitive to ethanol. For such an analysis we may distinguish between passive ion permeability in the resting state, changes in membrane processes governing the excitation cycle, and active transport of sodium and potassium ions.

Since ethanol is a weakly depolarizing agent it evidently alters ionic permeabilities in the resting state (Wallgren and Barry 1970) but it does not affect net potassium leakage from brain tissue subjected to anoxia or cold *in vitro* (Israel Kalant and LeBlanc 1966). Voltage clamp studies on squid giant axon (Moore Ulbricht and Takata 1964 Armstrong and Binstock 1964 Moore 1966) and experiments with frog muscle fibres (Inoue and Frank 1967) indicate a selective effect on the increase in sodium conductance constituting the rising phase of the action potential. Ethanol has been reported to inhibit active transport of sodium in frog skin (Israel and Kalant 1963) active transport of potassium into tissue slices depleted of potassium (Israel Kalant and LeBlanc 1966 Israel Jacard and Kalant 1965 Israel *et al* 1970) as well as microsomal Na^+ - K^+ activated ATPase (Israel Kalant and LeBlanc 1966 Järnefelt 1961 Israel Kalant and Laufer 1965 Israel and Salazar 1967 Sun and Samorajski 1970). Inhibition of active ion transport has been assumed to constitute an important part of the mechanism by which ethanol depresses nerve function (Israel Kalant and LeBlanc 1966 Kalant and Israel 1967 Israel 1970 Kalant 1970 Kalant 1971).

Electrical stimulation of cerebral tissue *in vitro* causes a net gain of sodium and loss of potassium which are followed by almost complete restoration of pre stimulation levels during recovery after a period of stimulation (Keesey Wallgren and McIlwain 1965). In the present experiments intended in part to be a repetition of those of Israel Jacard and Kalant (1963) and Israel Kalant and LeBlanc (1966) with brain slices electrical stimulation was used in order to find out whether the effect of ethanol was preponderantly on the response to stimulation or on the active transport observed during recovery after stimulation. Comparison in these experiments was based on the content of ions in the non multiv space of the slices in the steady state established after 30 min incubation. On this basis selective inhibition of the response to stimulation should be seen as a smaller loss of potassium and increase in sodium during stimulation whereas recovery should not be affected. Selective inhibition of the active transport process should lead to a slower recovery and possibly also to an enhanced response to stimulation. Inhibition of both processes may lead to variable effects in the stimulation phase but should of course retard recovery or make it less complete.

With electrically stimulated tissue we also studied the effects of tertiary butanol and clomethiazole. Tert butanol was selected because it is not oxidized in the organism (Williams 1959 Derache 1970). It is an interesting alternative to ethanol in experimental work on alcohol effects since its action does not involve the complications arising through the metabolism of ethanol including possible effects of acetaldehyde. Tert butanol has not been tested previously on nerve but other butyl alcohols have been studied electrophysiologically. Clomethiazole (4 methyl 5 β chloroethyl thiazole) is a sedative and hypnotic drug developed by Charonnet Lechat and Chareton (1957 1958) and used extensively in the treatment of acute withdrawal illness in alcoholic patients (Frisch 1966) being considered by some clinicians to be the drug of choice for this purpose (Amller and Bergener 1965).

Huhn and Bocker 1966 Glatt 1966) It is therefore of interest to compare its effects on nerve function with those of ethanol Clomethiazole has been tested by means of a voltage clamp technique on frog nerve (Bergman Bergman and Chareton 1967)

Preliminary reports of the results with ethanol (Nikander and Wallgren 1970) and those with tert butanol (Nikander Boguslawsky and Wallgren 1971) have been given

Methods

Preparation of tissue

Albino rats from the laboratory colony weighing 200–300 g were decapitated in a cold room (+5 °C) the brain was bared and the cerebrum transferred to a Petri dish which contained moistened filter papers the hemispheres were separated and two slices cut from each of them with a razor blade on a hand microtome The meninges were first removed and discarded The slices were weighed with a torsion balance with an accuracy of ± 1 mg and placed in separate incubation vessels The slices were about 0.35 mm thick and weighed 25–40 mg The incubation vessels were kept in ice The time from decapitation until incubation was 10–15 min

Incubation

Bicarbonate-saline (pH 7.4) with 124 mM NaCl 5 mM KCl 1.24 mM KH_2PO_4 1.30 mM MgSO_4 0.75 mM CaCl_2 26 mM NaHCO_3 10 mM glucose 1% inulin as extra cellular marker and 95% O_2 5% CO_2 as gas phase was used as an incubation medium

The flasks containing 2.5 ml of incubation medium were flushed with the gas mixture in the shaking bath for 5 min equilibrated for an additional 10 min placed in ice and transported to the cold room After receiving the slices the vessels were placed in a shaking incubator at +37 °C, flushed with gas mixture for 5 min and closed Usually an incubation period of 20 min was then allowed to ensure equilibration of the ion and inulin content of the tissue

Ethanol (Alko AaS) when used was always added to give a final concentration of 0.5 g/100 ml medium (109 mM) Tert. butanol (Merck p.a.) was similarly added to give a final concentration of 34 mM this being proportional to its thermodynamic activity in relation to that of ethanol (Lindbohm and Wallgren 1962) A final concentration of 0.39 mM was chosen for clomethiazole (Astra, Hemneveien 0.8% for infusion) on the basis of published experiments and clinical dosage

Electrodes and stimulation

Carbon electrodes (Nikander 1970) were used for the stimulation Steeply rising and exponentially falling alternating pulses from a transistor pulse generator (Teratron Co Helsinki Finland) with a frequency of 100 Hz and a time constant of 0.4 ms were used With a voltage gradient of 1.5 V/mm distance between the electrodes the current per flask was 15–30 mA

When the response to stimulation was examined alcohol or clomethiazole was added just before the electrical stimulation was started The duration of the stimulation was 2.4.7 or 10 min When the recovery after stimulation was studied stimulation was always given for 10 min after which recovery was allowed for 2.5 or 10 min Alcohol or clomethiazole was added just before the pulses were interrupted

Analytical methods

Each slice was picked up on an aluminum rider drained briefly by pulling it up along the wall of the vessel reweighed transferred to an all glass homogenizer ground in 4 ml of 6% trichloroacetic acid and left standing for 30 min before being centrifuged at 800 \times g for 10 min The supernatant was poured into a 25 ml volumetric flask The residue was recentrifuged after being suspended in 5 ml distilled water and the supernatant poured into the same flask which was then filled with distilled water The resultant solution was transferred to a 50 ml plastic vial for storage until analysis for sodium potassium and inulin was performed

The incubation medium from all the vessels was combined and 50 μ l samples were carried through the same steps as the tissue slices and diluted to 25 ml with distilled water The contents were then transferred to plastic vials From duplicate samples of these solutions the amount of inulin in the slices and the incubation medium was determined according to Varon and McIlwain (1961) For determination of potassium in the incubation medium 500 μ l samples were taken Sodium and potassium content was measured with a flame photometer (model A Evans Electroelenium Ltd Halstead Essex) directly on the plastic vials

TABLE I Ion content of cerebral cortex tissue kept 15 min after preparation in ice cold (0 °C) bicarbonate medium

Experimental condition	Na ⁺ μ eq/g fresh wt	K ⁺ μ eq/g fresh wt
Control	113.4 \pm 10.8	118.7 \pm 6.3
Ethanol	114.1 \pm 8.2	37.3 \pm 2.9

Ethanol concentration 109 mM Amounts corrected for adhering fluid Averages \pm S.D.
n = 10

All the glassware used for the sodium and potassium determinations was soaked overnight in 2 N HNO₃, rinsed with distilled water and dried at 100 °C.

Expression of results

The procedure of Keesev Wallgren and McIlwain (1963) was used. The calculation was based on the assumption that inulin marked the extracellular fluid space of the tissue and that the inulin and ions within this space equilibrated at a concentration identical with that of the medium. Non inulin space (NIS) was calculated as follows:

$$\frac{\text{final weight (mg)} - \text{slice inulin space } (\mu\text{l})}{\text{fresh weight mg}}$$

Amounts of ions corresponding to the inulin space (IS) including adhering fluid were subtracted from the total ions of the slice. The remaining quantities represented ions of the NIS.

The results have been calculated on the basis of the initial fresh weight of the tissue and are expressed as μ eq/g (ions of the NIS) or as $\mu\text{l/g}$ (IS and NIS). Averages \pm S.D. are given.

The numerical values depend on the basis of expression with the exception of estimates of concentration of ions in the NIS. Recalculations of our results on other basis can be done using the following experimentally derived values: twelve freshly cut slices had an average dry weight of 70.7 ± 0.4 mg. Twelve slices incubated for 30 min had an original fresh weight of 33.6 ± 6.3 mg, a weight after incubation of 49.7 ± 9.3 mg representing a gain of 16.1 ± 3.6 mg adhering fluid, and a dry weight of 19.9 ± 0.4 mg referred back to fresh weight. Evidently some solids (appr. 7.5%) had been lost during incubation either by solubilization or by breaking off of small fragments of the tissue.

Results

Unstimulated tissue

A test was made of the loss of potassium and gain of sodium during preparation and standing in cold medium. 10 control slices and 10 slices with ethanol (109 mM) were kept standing for 15 min in ice cold medium and analysed for sodium and potassium content. There was no difference between the two groups of slices (Table I).

Ordinary incubation: Tissue slices take up potassium and extrude sodium during incubation, reaching a steady ion concentration level after about 30 min incubation (Keesev Wallgren and McIlwain 1963). The possible inhibitory effect of ethanol on net ion transport during the initial 30 min of incubation was tested using 12 control slices and 12 with ethanol. The comparison was based on the content of sodium and potassium in the non inulin space (Table II). There was no effect of ethanol.

TABLE II Ion content of the non inulin space of unstimulated tissue

Experimental condition	Na	K ⁺
Control	35.5 ± 10.8	111.1 ± 4.9
Ethanol	36.9 ± 7.6	58.4 ± 2.8

Intracellular sodium and potassium content is expressed as $\mu\text{eq/g}$ fresh tissue \pm S.D. after subtraction of an amount of the ions corresponding to the inulin content of the tissue and assumed to be extracellular. The tissue had been incubated for ca. 100 min. Ethanol conc. 109 mM. $n = 12$.

The inulin space was $426 \pm 87 \mu\text{l/g}$ fresh tissue (46 control slices). There was no significant deviation from this value with any treatment and therefore the inulin space will not be further mentioned. Since the concentration of Na in the medium was 150 mM and that of K, 6.2 mM, average total sodium of the control slices was $99.5 \mu\text{eq/g}$ fresh wt. and of potassium $60.8 \mu\text{eq/g}$ fresh wt.

Electrically stimulated tissue

Response to stimulation. The results are summarized in Fig. 1. The control level is that of the unstimulated slices analysed after ca. 30 min incubation in connection with each stimulation experiment. Combined control values were calculated for the tert butanol and the clomethiazole series. These differed from those of the stimulated ethanol series, potassium being somewhat lower and sodium higher.

Despite this difference the net change in sodium content of the control slices after 10 min stimulation was about the same in all the experimental series, being about $20 \mu\text{eq}$. Potassium decreased by nearly $30 \mu\text{eq}$ in the controls of the ethanol series and by only about $15 \mu\text{eq}$ in the two other series.

The effects of the three agents studied were clear and rather similar. Ethanol, tert butanol and clomethiazole all markedly diminished net entry of sodium into the NIS. With ethanol the effect at 7 min was not quite significant ($P < 0.1$, Student's *t* test). Analysis of variance was therefore performed for all four time intervals combined. This showed a very significant effect of ethanol on net entry of sodium ($F = 15.1$, $P < 0.01$, d.f. 1/66).

Ethanol affected potassium loss only slightly, having a nearly significant ($0.1 > P > 0.05$) inhibitory effect at 2 min. With tert butanol the values at 4 to 10 min even showed a small increase in the potassium loss with alcohol. This reversal between the control slices and those exposed to tert butanol probably is fortuitous.

Recovery after stimulation. Recovery is summarized in Fig. 2. In all the experimental series the prestimulation level of sodium in the NIS was restored within 10 min. Despite the evidently high activity of the transport system there was no inhibitory effect on sodium extrusion of any of the agents studied. On the contrary,

RESPONSE TO STIMULATION

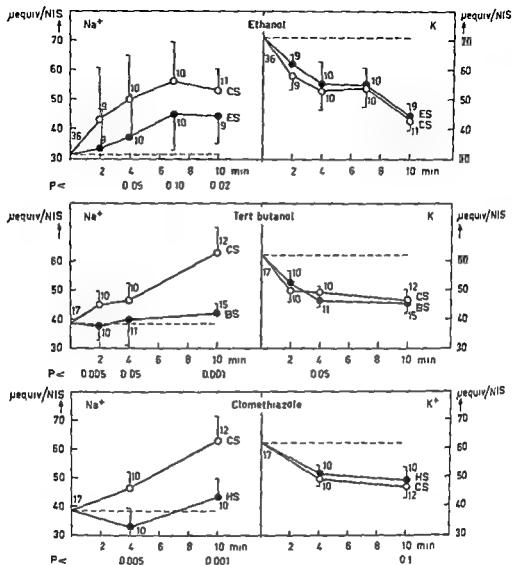


Fig 1 Effects of ethanol, tert butanol and clomethiazole on the response to electrical stimulation of cerebral cortex tissue. Intracellular sodium and potassium contents expressed as μequiv fresh tissue have been estimated using inulin as marker of the extracellular space. The pre stimulation pre-drug content of sodium and potassium in the non inulin space after 30 min incubation is indicated by the hatched line. In the tert butanol and clomethiazole series these values have been combined. Open circles controls, filled circles drug added just before start of stimulation. Vertical bars indicate SD for clarity only. + or - deviation is indicated. The figures at each point show the number of slices used. P values for differences between control and drug condition are shown at the bottom of each graph (Student's t test). Conc'n of ethanol 109 mM, of tert butanol 30 mM, of clomethiazole 0.39 mM.

RECOVERY AFTER STIMULATION

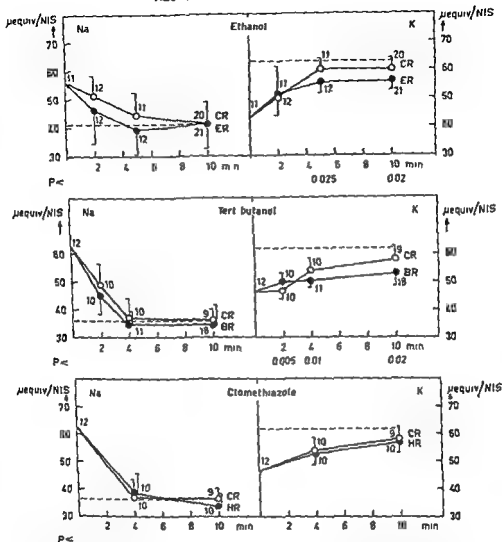


Fig. 3. Effects of ethanol, tert butanol and clomethiazole on recovery of cerebral cortex tissue after electrical stimulation. Intracellular sodium and potassium contents expressed as $\mu\text{equiv/g}$ fresh tissue have been estimated using inulin as marker of the extracellular space. Zero time control value = the ion content in the non-inulin space (NIS) after 30 min pre-incubation and 10 min stimulation. The drug was added at this time and slices taken for analysis of ion content at the time interval shown. The hatched line indicates ion content of the NIS in pre-stimulation, pre-drug condition. Open circles: controls; filled circles: drug present. Vertical bars indicate S.D. for clarity only; + or - deviation as indicated. The figures at each point show the number of slices used. P values for significant differences between control and drug condition are shown at the bottom of each graph. Concentrations: ethanol 109 mM; tert butanol 34 mM; clomethiazole 0.39 mM.

References

- AMLER G and M BERGENER Electroencephalographische Veränderungen bei der Behandlung des Delirium tremens mit Klormethiazol und ihre Interpretation *Arzneimittel-Forsch* 1965 15 837-840
- ARMSTRONG C M Interaction of tetraethylammonium ion derivatives with the potassium channels of giant axons *J gen Physiol* 1971 58 413-437
- ARMSTRONG C M and L BINSTOCK The effects of several alcohols on the properties of the squid giant axon *J gen Physiol* 1964 48 265-277
- BAKER P F M P BLAUSTEIN R D KEYNES J MANIL T I SHAW and R A STEINHARDT The ouabain sensitive fluxes of sodium and potassium in squid giant axons *J Physiol (Lond)* 1969 200 459-496
- BERGMAN C J BERGMAN and Y Y CHARETON Action d'un dérivé de la fraction thiazolique de la vitamine B₁ sur l'activité électrique et la consommation d'oxygène des fibres nerveuses myélinisées *C R Soc Biol (Paris)* 1967 161 83-87
- BOCUSLAWSKY P and P NIKANDER A difference between high and low-drinking rats in effects of ethanol on ion movements in cerebral tissue *Acta physiol scand* 1972 81 12A-13A
- CHARONNAT R P LECHAT and J Y CHARETON Sur les propriétés pharmacodynamiques d'un dérivé thiazolique *Thérapie* 1957 12 68-71
- CHARONNAT R P LECHAT and J Y CHARETON Sur les propriétés pharmacodynamiques d'un dérivé thiazolique Action sur le système nerveux central *Thérapie* 1958 13 1-16
- DERACHE R Toxicology Pharmacology and Metabolism of Higher Alcohols In *International Encyclopedia of Pharmacology and Therapeutics* section 20 Alcohols and Derivatives Edit J Tremolieres Vol 2 p 567 1970 Pergamon Press Oxford
- FRISCH E H Chlormethiazole (Heminevrin® dustraneurin®) Proceedings of a symposium arranged by ASTRA Hanks Norway July 11-13 1965 *Acta psychiat scand* 1966 42 Suppl 192
- GLATT M M Controlled trials of non barbiturate hypnotics and tranquilizers With special reference to their use in alcoholics *Psychiat et Neurol (Basel)* 1976 152 28-42
- HILLE B Ionic channels in nerve membranes *Progr Biophys molec Biol* 1970 21 3-39
- HULIN A and F BOCKER Effect of chlormethiazole upon the clinical course of alcoholic delirium *Acta psychiat scand* 1966 42 Suppl 192 145
- INOLE F and G B FRANK Effects of ethyl alcohol on excitability and on neuromuscular transmission in frog skeletal muscle *Brit J Pharmacol* 1967 30 186-193
- ISRAEL Y Cellular effects of alcohol *Quart J Stud Alcohol* 1970 31 293-361
- ISRAEL Y and H KALANT Effect of ethanol on the transport of sodium in frog skin *Nature (Lond)* 1963 200 476-478
- ISRAEL Y H KALANT and I LAUFER Effects of ethanol on Na⁺ K⁺ Mg stimulated microsomal ATPase activity *Biochem Pharmacol* 1965 14 1803-1814
- ISRAEL Y H KALANT and A H LEBLANC Effects of lower alcohols on potassium transport and microsomal adenosine triphosphatase activity of rat cerebral cortex *Biochem J* 1966 100 27-33
- ISRAEL Y H KALANT H LEBLANC J C BERNSTEIN and I SALAZAR Changes in cation transport and (Na⁺ + K⁺) activated adenosine triphosphatase produced by chronic administration of ethanol *J Pharmacol exp Ther* 1970 174 330-337
- ISRAEL Y and I SALAZAR Inhibition of brain microsomal adenosine triphosphatases by general depressants *Arch Biochem* 1967 122 310-316
- ISRAEL JACARD Y and H KALANT Effect of ethanol on electrolyte transport and electrogenesis in animal tissues *J cell comp Physiol* 1963 65 127-132
- JARNEVELT J Inhibition of the brain microsomal adenosine triphosphatase by depolarizing agents *Biochim biophys Acta (Amst)* 1961 48 111-116
- KALANT H Effects of ethanol on the nervous system In *International Encyclopedia of Pharmacology and Therapeutics* section 20 Alcohols and Derivatives Edit J Tremolieres Vol 1 pp 125-236 1970 Pergamon Press Oxford
- KALANT H Absorption distribution and elimination of ethanol Effects on biological membranes In *The Biology of Alcoholism* Edit B Kissin and H Begleiter Vol 1 pp 1-62 1971 Plenum Press New York
- KALANT H and Y ISRAEL Effects of ethanol on active transport of cations In *Biochemical Factors in Alcoholism* Edit R P Mackerell Pp 25-37 1967 Pergamon Press Oxford
- KESSEY J C H WALLER and H McILWAIN The sodium potassium and chloride of cerebral tissues Maintenance change on stimulation and subsequent recovery *Biochem J* 1965 95 289-300
- LINDBOHM R and H WALLER Changes in respiration of rat brain cortex slices induced by some aliphatic alcohols *Acta pharmacol (Kbh)* 1962 19 53-58

- MOORE J W Effects of ethanol on ionic conductance in the squid axon membrane *Psychosom Med* 1966 28 450—457
- MOORE J W and T NARAHASHI Tetrodotoxin's highly selective blockage of an ionic channel *Fed Proc* 1967 26 1655—1663
- MOORE J W W ULBRICHT and M TAKATA Effect of ethanol on the sodium and potassium conductances of the squid axon membrane *J gen Physiol* 1964 48 279—295
- NIKANDER P Carbon electrodes for stimulation of brain tissue *in vitro* *J Neurochem* 1972 19 535—537
- NIKANDER P P BOGUSLAWSKY and H WALLGREN Actions of ethanol and tertiary butanol on net movements of sodium and potassium in electrically stimulated rat brain tissue *in vitro* *Scand J clin Lab Invest* 1971 27 Suppl 116 67
- NIKANDER, P and H WALLGREN Ethanol electrical stimulation and net movements of sodium and potassium in rat brain tissue *in vitro* *Acta physiol scand* 1970 80 27A
- ROJAS E and C ARMSTRONG Sodium conductance activation without inactivation in pronase perfused axons *Nature (Lond)* *Neu Biol* 1971 229 177—178
- SEEMAN P W O KWANT M GOLDBERG and M CHAU WONG The effects of ethanol and chlorpromazine on the passive membrane permeability to Na *Biochim biophys Acta (Amst)* 1971 241 349—355
- SUN A Y and T SAMOJAJSKI Effects of ethanol on the activity of adenosine triphosphatase and acetylcholinesterase in synaptosomes isolated from guinea pig brain *J Neurochem* 1970 17 1365—1372
- VARON S and McILWAIN Fluid content and compartments in isolated cerebral tissues *J Neurochem* 1961 8 262—275
- WALLGREN H and H BARRY III *Actions of Alcohol* Elsevier Publishing Company Amsterdam 1970
- WILLIAMS R T *Detoxication Mechanisms* The metabolism and detoxication of drugs toxic substances and other organic compounds 2nd ed 1969 Chapman and Hall London

Plasma Hyperosmolarity and Pulmonary Capacitance Vessels

By

H PIENE P AARSETH and G BO

Received 3 December 1973

Abstract

PIENE H P AARSETH and G BO *Plasma hyperosmolarity and pulmonary capacitance vessels* Acta physiol scand 1974 91 94-102

Changes in pulmonary blood volume have been looked for during increased plasma osmolarity. Two different techniques, one involving freezing of whole rats and the other with removal of separate lung lobes from cats, have been used. In both cases lung blood volume was calculated from content of ^3H plasma albumin and ^{51}Cr erythrocytes. Plasma osmolarity was increased 10-23% by intravenous infusions of hyperosmolar solutions of NaCl or glucose. In the cat lung experiments vascular pressures and cardiac output were followed during iv infusions of 3 M NaCl or 3-5 M glucose solutions. The pulmonary vascular resistance decreased upon the injections, but no significant changes in pulmonary vascular volume could be detected. The extravascular lung water content decreased markedly during the hyperosmotic infusions. Also in the rat experiments the pulmonary blood volume seemed to be unchanged during hyperosmolarity.

During muscular exercise plasma osmolarity may increase by some 10%. Such changes will affect vascular smooth muscle cells. Thus increased plasma osmolarity dilate resistance vessels in skeletal muscle and osmolarity changes appear to be partly responsible for the muscular hyperemia during exercise (Lundvall 1972). Hauge and Bo (1971) have demonstrated that also pulmonary vascular resistance is reduced during increases in plasma osmolarity. Information about the effect of hyperosmolarity on capacitance vessels is more scarce. According to Mellander and Lundvall (1971) no significant active dilatation of skeletal muscle capacitance vessels takes place when plasma osmolarity is increased. In the lung Bo, Hauge and Nicolaysen (1971) found evidence for a constriction of the capacitance vessels when plasma osmolarity was raised. An explanation on the cellular levels has been provided for the vascular dilatatory response to increased osmolarity (Johansson and Johnson 1968). It appears difficult then to explain the mechanism behind the apparent constrictor response of pulmonary capacitance vessels to the same stimulus.

The intention with the present investigation was to study more closely the effect of increased plasma osmolarity on the pulmonary blood volume in animals with intact circulation. Two different methods were used involving rats and cats re-

spectively. With plasma osmolality increases within or somewhat above physiological limits no significant effect on the pulmonary vascular capacity could be detected.

Methods and preliminary experiments

Experiments on rats

Preliminary experiments Initially we wanted to increase plasma osmolality in rats by infusions of NaCl solutions. In a series of preliminary experiments 3 M NaCl was infused into a femoral vein at a rate of 0.22 ml/min for 45 s. This rate of infusion was calculated to give an osmolality increase of about 10% every 15 s.

During the infusion arterial blood samples were withdrawn each 6 s from the opposite femoral artery. ^{125}I labelled human serum albumin had previously been given i.v. to the rats. The content of ^{125}I in the arterial blood was analyzed. Hematocrit was measured by microcentrifugation and the plasma-osmolality was measured with the use of a Knauer osmometer.

It turned out that the plasma osmolality did increase markedly for the first 10–15 s of the infusion. From later samples it could be seen that the further increase in osmolality went on at a more moderate rate. The hematocrit changes and the dilution of ^{125}I did however continue indicating influx of water into the plasma compartment. A proportional fall in plasma content of ^{125}I and hematocrit showed that the plasma was predominantly diluted by influx of extravascular water and only to a small degree by erythrocyte dehydration. The increase in plasma volume therefore reflects an increased blood volume as well. This volume increase could be calculated to be about 1.1 ml. The net effects of the 45 s infusion of 3 M NaCl infusion were therefore an increased blood volume as well as an increase in plasma osmolality by some 10%.

In another series of preliminary experiments 1.1 ml of 0.15 M NaCl was infused i.v. in the course of 45 s. Again serial sampling of arterial blood was performed and the samples analyzed for ^{125}I content and hematocrit. With such an infusion we were able to mimic closely the plasma dilution and hematocrit changes found when 3 M NaCl was infused at a rate of 0.22 ml/min for 45 s.

Estimation of pulmonary blood volume Male Wistar rats weighing 200–250 g were used. In light ether anesthesia a catheter was introduced into a femoral vein. Few minutes thereafter when the animals tended to wake up pentobarbitone (Nembutal®, Abbott diluted 1:2 in saline) was given i.v. in a dose of 10 mg/kg b.w. The induced anesthesia then lasted throughout the period of the experiment.

The blood of the animals was labelled by an i.v. injection of labelled rat erythrocytes and human plasma albumin. After a mixing period of 8 min a femoral vein blood sample (0.2 ml) was withdrawn in order to measure large vessel hematocrit as well as the isotope content of plasma and erythrocytes. 2 min later the animals were suddenly immersed in liquid nitrogen. When plasma osmolality was to be changed the necessary infusion was carried out just prior to the freezing. Later the frozen lungs were removed from the animals. From the organ content of isotopes and from the isotope content in plasma and erythrocytes the pulmonary blood volume could be calculated. A muscle sample was removed from the thigh and its blood content was also evaluated from its radioactivity. The method is described in more detail elsewhere (Aarseth 1970).

Experiments on cats

Experimental design In the experiments the animals were anesthetized by an i.p. injection of pentobarbitone (Nembutal®, Abbott) 30–40 mg/kg b.wt. After tracheostomy the animals were curarized (Alloferine® Roche 1 mg/kg b.wt. i.v.) and positive pressure ventilation started. End expiratory pressure was kept at +1 cm H₂O and the tidal volume regulated so as to keep the arterial pH at 7.4 ± 0.03 . At 30 min intervals hyperinflations were performed. A midsternal incision was made and the thorax widely opened. Catheters were introduced through the right ventricle into the pulmonary artery and through the left auricle into the left atrium. Catheters were also placed in one femoral artery and vein and a large catheter was placed in the left carotid artery. Intrascular pressures were recorded from the pulmonary artery, the left atrium and the femoral artery by the use of Statham pressure transducers connected to a Grass recorder. An electromagnetic flow probe was placed on the ascending aorta and connected to a flowmeter (Nicoxon, Norway). The cardiac output could thus be measured.

Estimation of pulmonary blood volume and extravascular lung water volume A biopsy technique was used which has been extensively described previously (Aarseth and Bo 1977).

TABLE I Effects of plasma hyperosmolarity and hypervolemia on blood content in lungs and muscle and on lung extravascular water content in rats. Mean values \pm S.E.

	Iso-osmolar isovolemic rats	Hyperosmolar hypervolemic rats	Iso osmolar hypervolemic rats
NaCl infused*	0.15 M 0.22 ml/min	3.0 M 0.22 ml/min	0.15 M 1.45 ml/min
n	11	12	11
Body weight (g)	224 \pm 4	224 \pm 4	234 \pm 4
Total blood volume (ml)	13.6 \pm 0.3	13.3 \pm 0.2	13.3 \pm 0.2
Pulmonary blood volume (ml)	1.81 \pm 0.12	2.14 \pm 0.12	2.39 \pm 0.17
Lung tissue wt (mg)	705 \pm 46	786 \pm 34	808 \pm 39
Muscle blood content (l/l/g)	27 \pm 2	27 \pm 2	24 \pm 2

* Infusions for 45 s in all groups

Silk snares were loosely placed around the hilus of the 3 smaller lung lobes (the upper on each side and the right middle lobe). The erythrocytes and the plasma were labelled by isotopes (^{51}Cr and ^{131}I). One lobe after the other was then suddenly snared off and removed. A blood sample was withdrawn from the carotid artery each time a lobe was snared off. The content of the two isotopes in the lobe and in plasma and erythrocyte samples as well as wet and dry weight of the lung tissue and the blood samples were measured. From these parameters one could calculate blood content and extravascular water content in the lung lobes relative to the net dry weight of the lung tissue (Aarseth and Bo 1972).

Results

Experiments on rats

3 groups of rats were compared in the present series of experiments. The groups were equal as regards animal size and preinfusion blood volume. They were all given the same initial treatment and handling. However, NaCl solutions of different volumes and concentrations were infused during the last 45 s before the whole body freezing.

Group no. 1 (small iso-osmolar infusion: situation after infusion iso-osmolarity isovolemia) 11 rats received 0.22 ml/min of a 0.15 M NaCl solution.

Group no. 2 (small hyperosmolar infusion: situation after infusion hyperosmolarity hypervolemia) 12 rats received 0.22 ml/min of a 3 M NaCl solution.

Group no. 3 (large iso-osmolar infusion: situation after infusion iso-osmolarity hypervolemia) 11 rats received 1.45 ml/min of a 0.15 M NaCl solution.

The results from the 3 groups of rats are presented in Table I. The mean pulmonary blood volume in the control group was 1.82 ml while in the hyperosmolar group it was 2.14 ml. This difference is not significant ($p = 0.12$). In the group made hypervolemic by isotonic saline infusion the mean pulmonary blood volume was increased further to 2.39 ml. When compared with the hyperosmolar group, the difference is not significant ($p = 0.31$).

TABLE II Effects of successive lobectomies on the remaining pulmonary circulation in cats. Three small lobes are removed one by one as explained in text. For further details see text. Mean values \pm S.E.

	1 lobe	2 lobe	3 lobe
Lung blood content ml/g dry tissue wt	4.6 ± 0.5	5.0 ± 0.4	5.5 ± 0.6
Lung tissue wet weight/dry wt	4.69 ± 0.04	4.50 ± 0.07	4.69 ± 0.03
Pulmonary arterial pressure mm Hg	16 ± 1.7	18 ± 2.6	20 ± 2.8
Left atrial pressure mm Hg	4 ± 0.6	4 ± 0.4	4 ± 0.7
Cardiac output ml/min	334 ± 52	316 ± 52	318 ± 63
Pulmonary resistance $\frac{\text{mm Hg} \times \text{min}}{\text{ml}}$	0.039 ± 0.003	0.043 ± 0.004	0.052 ± 0.003

The lung tissue weight reflecting mainly extravascular water volume was calculated from the total lung weight by subtracting the lung blood content. In the control group the lung tissue weight was 690 mg. In both the hyperosmolar and the hypervolemic groups the lung weight showed some increase (to 790 and 740 mg respectively). The differences were however not significant.

The muscle blood content was almost the same in all groups $24\text{--}27 \mu\text{l/g}$ tissue.

Experiments on cats

Control experiments. In 6 cats weighing $2.5\text{--}3.5$ kg the two upper lobes and the right middle lobe were removed one by one. 30 min passed between the two first lobectomies. A further 20 min passed before the third lobe was removed. The lobes were analyzed for their blood and extravascular water content. The results are presented in Table II. Several of the moderate changes observed in the various circulatory parameters can be explained as a result of the gradual reduction of the pulmonary vascular bed. Although the cardiac output was slightly reduced the mean pulmonary arterial pressure increased by 2 mm Hg. The vascular resistance thus increased (in 5 out of 6 cats) but the increase was not significant. There was also an insignificant increase of mean lung blood content by 9% in lobe no. 2 and a further increase by 9% in lobe no. 3. A slight but significant ($p = 0.026$) reduction of the extravascular lung water content was observed in the second lobe as compared with the first one.

Hyperosmolarity in cats. Different hyperosmotic solutions were infused in 7 cats for 45 s prior to the removal of the second lobe. The plasma osmolarity was measured in the blood samples taken from the carotid artery at the point of lobe removal. We infused 18 ml of either a 3 M NaCl solution or a 6 M glucose solution or a 3 M glucose solution. The plasma osmolarity increased by about 23% and 12% respectively.

TABLE III Effects of increase in plasma hypertonicity on the pulmonary circulation of cats. Three lung lobes are removed one by one. The first and the last lobe removed during normal plasma osmolarity; the second when plasma osmolarity had been increased by infusions of concentrated glucose or NaCl solutions. For further details see text. Mean values \pm S.E.

	1 lobe	2 lobe	3 lobe
Plasma osmolarity mosm	313 \pm 2	378 \pm 9	376 \pm 3
Lung blood content ml/g dry tissue wt.	2.0 \pm 0.2	6.0 \pm 0.2	6.0 \pm 0.3
Lung tissue wet weight/dry wt.	4.48 \pm 0.08	3.95 \pm 0.06	4.44 \pm 0.08
Pulmonary arterial pressure mm Hg	15 \pm 0.8	18 \pm 0.8	17 \pm 1.3
Left atrial pressure mm Hg	5 \pm 0.6	6 \pm 0.7	5 \pm 0.7
Cardiac output, ml/min	255 \pm 15	338 \pm 15	296 \pm 15
Pulmonary vascular resistance mm Hg \times min/ml	0.040 \pm 0.003	0.033 \pm 0.004	0.043 \pm 0.004

The vascular effects of the various infusions were similar. All these cats are therefore presented as one group in Table III. The mean increase of plasma osmolarity during the infusion of the hypertonic solutions was 17.5%. By the time when the third lobe was removed 3 min later the plasma osmolarity was again nearly normalized. The greatest effect of the increased plasma osmolarity was found for the cardiac output, which increased by 32% ($p = 0.015$). The mean pulmonary vascular resistance was reduced from 0.040 (mm Hg/min/ml) to 0.033 even though the pulmonary vascular bed had been reduced by the removal of the first lobe. A few min later when the third lobe was removed the vascular resistance of the infused animals was again increased.

The lung blood content was increased by 21% in the second lobe (during plasma hypertonicity) as compared to the first lobe. The extravascular water content on the other hand was reduced by as much as 12% in the second lobe.

The net effects of plasma hypertonicity on the pulmonary vasculature were found by comparing changes from lobe 1 to lobes 2 and 3 in each animal in the control group and in the test group. In Fig. 1 is shown that percentage change in cardiac output and pulmonary vascular resistance were significantly larger in the animals receiving hypertonic infusions than could be explained by the lobectomies *per se* ($p < 0.05$). The percentage change in lung blood content and in extravascular water volume are shown in Fig. 2. In the animals receiving hypertonic infusions there was an insignificant larger increase in blood content in the second lobe. The extravascular water content was however significantly reduced during plasma hypertonicity as compared to the control group ($p = 0.04$).

Discussion

It has previously been shown that smooth muscle cells from the portal vein react to hypertonicity with shrinkage and reduction in their electrical and mechanical

Fig 1 Cardiac output and pulmonary vascular resistance in 2 groups of cats. One group received hyperosmolar infusions in order to increase the plasma osmolality (mean increase 18%) the other group served as control. The parameters are measured immediately before separate removal of 3 lung lobes. The values found when the second and third lobes were removed are given as per cent of those found at the time of the first lobectomy. Mean values \pm SE.

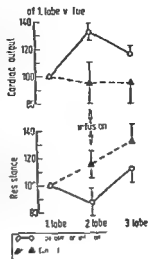


Fig 1

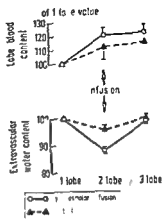


Fig 2

Fig 2 Lung blood content and extravascular lung water content in 2 groups of cats. Mean values \pm SE. Explanation see text Fig 1.

activity (Johansson and Jonsson 1968). Most of this effect was due to an inhibition of the pacemaker activity. This hyperosmolarity induced negative inotropic and chronotropic effect on smooth muscle cells may be responsible for some of the vasodilatation seen in resistance vessels of skeletal muscle during exercise (Mellander and Lundvall 1971). The same mechanism may be responsible for the reduction observed in pulmonary vascular resistance during plasma hyperosmolarity. The lack of effect of hyperosmolarity on capacitance vessels in skeletal muscle as reported by Mellander and Lundvall (1971) is perhaps not surprising since it has been claimed that there is no pacemaker activity in smooth muscle cells in this section of the vasculature. Surprisingly enough however a vasoconstrictor response to hyperosmolarity has been observed for muscle veins (Stainsby and Barclay 1971) and for pulmonary capacitance vessels (Bo Hauge and Nicolaysen 1971). Such a response must involve other and hitherto unknown mechanisms.

We were intrigued by this apparent vasoconstrictor response in capacitance vessels and we wanted to look more closely on the response to hyperosmolarity of the capacitance vessels in the lung. We attempted to observe the organ in situ with a physiological rise of plasma osmolality as the stimulus used.

As a first approach we used intact rats for the experimentation since it is known that their pulmonary blood volume may alter within relatively broad limits (Aarseth 1970, Aarseth and Pien 1972). By infusion of 3 M NaCl their plasma osmolality was increased by about 10%. Unfortunately and as a consequence of this infusion the total blood volume of the rat was also increased by about 10%. Such acute increments in blood volume in rats are to a large extent accommodated by the pulmonary vasculature (Aarseth 1971). The blood volume increase might therefore cover any effects on lung capacitance vessels by plasma hyperosmolarity *per se*. We

therefore had to make a control group of animals which developed the same degree of hypervolemia as the animals receiving hyperosmolar infusions. When comparing these two hypervolemic groups there was only a small and insignificant difference as regards pulmonary blood volume, indicating that plasma hyperosmolarity does not significantly influence the lung capacitance vessels in intact rats. Also the muscle blood content was almost the same in the three groups of animals and therefore unaffected by plasma hyperosmolarity.

There are however several uncertainties in these experiments. The pulmonary blood volume was estimated from the isotope content in the frozen lungs relative to the content in a blood sample taken about 2 min earlier. The isotope concentration in the blood changed in the short interval between the blood sampling and the freezing because plasma dilution took place to a considerable degree during the infusion. The plasma concentration of ^{51}I at the time of freezing was actually some 12% lower than the reference value found in the previously taken blood sample (as judged from the preliminary experiments). If this plasma dilution is evenly distributed throughout the circulation then the pulmonary plasma volume will be underestimated by some 12%. Furthermore if the blood content of the lung is underestimated then the net tissue weight as calculated in the present investigation will be overestimated to the same extent. The values given in Table I for these parameters should therefore probably be corrected to some extent. The pulmonary blood volume for the two hypervolemic groups could be some 0.2 ml larger than the values given in the table (the corrected values could be about 2.35 and 2.60 ml respectively). Then also net lung weight would be some 200 mg lower than the values in Table I with a corrected value of about 600 mg. This would be a tissue weight lower than that found in the normovolemic animals. This would actually be consistent with previously reported experiments on hypervolemia from this laboratory (Aarseth 1971, Aarseth and Bo 1972).

Another problem of the present experiments in rats is this: to what degree will the plasma dilution and blood volume increases taking place during the infusion of hypertonic saline really be mimicked by the infusion of isotonic saline? The rapidness with which the blood volume increase may thus be important for the pattern of vascular responses to such an increment.

Since for these reasons the results from the rat experiments are not conclusive we carried out supplementary experiments on open chested cats when a more close control with the blood changes could be achieved. In this connection we used 3 M NaCl or 3–6 M glucose solutions. The rate of infusion (relative to body size) was of the same order as in the rat experiments. In the cat experiments however there was a larger increase in plasma osmolarity (mean 18%) than in the rat experiments (mean 9%). This might conceivably be due to the more protracted circulation time for cats. Increases in total blood volume must probably also have taken place in the cats. However increases in total blood volume in this animal does not cause the same large increments in lung blood content as in rats (Aarseth and Bo 1972).

Also in the cat experiments the lung blood content was calculated from the content of isotopes in the lung tissue relative to the isotope content in the blood. However for these experiments as opposed to those in the rat the required blood sample could be withdrawn simultaneously with the closure of the lobe circulation. Any dilution of the blood in this sample therefore ought to be near identical with the dilution of the blood in the lung vasculature. For the above reasons the blood volume estimations in the cat experiments are probably more reliable than those in the rat experiments.

In order to evaluate the results from the present experiments in cats one must compare the change in relevant parameters from lobe to lobe in the control group with the same type of changes in the test group. This could be done as there were only small and insignificant ($p > 0.05$) differences between the test group and the control group as regards the values for the different parameters at the moment of the first lobectomy (Table II and III).

As previously described by Hauge and Bo (1971) the pulmonary vascular resistance was reduced by plasma hyperosmolality also in the present experiments ($p = 0.022$ Fig. 1). Plasma osmolality has previously been found to have a positive inotropic effect in the heart (Wildenthal 1969; Rowe *et al.* 1972). Also in the present experiments there was a significant increase in cardiac output upon infusion of hyperosmolar solutions ($p = 0.001$ Fig. 1). The left atrial pressure was however also increased. As a result the pulmonary arterial pressure increased even though the pulmonary vascular resistance was reduced.

The lung blood content found in the lobe exposed to the plasma hyperosmolality was increased as compared to the content in the lobe removed at normal plasma osmolality. The increase was however small and not significantly different from the changes seen in the control animals (Fig. 2, $p = 0.39$). Furthermore when lobe no. 3 was removed 5 min later there was a further increase in lobe blood content while the plasma osmolality, vascular pressures and flow had returned towards normal values (Table III).

The net weight of the lung tissue was greatly reduced during hyperosmolality. The reduction implies that 15% of lung tissue water had been removed within 45 s. As the total net dry lung tissue weight amounts to about 1 g/kg b.w. (Aarseth and Bo 1972) one can calculate that a total of about 15 ml water must have been extracted from the lung tissue.

Even with a small (but insignificant) increase in pulmonary blood volume there might have developed an increased tone in the capacitance vessels of the lung. We did observe a small increase in both pulmonary arterial and left atrial pressures upon hyperosmolar infusions (Table III), which might have masked a possible increase in vascular tone. This is not likely, however. The compliance of the vasculature in cat lungs is rather small with only some 1–2% increase in volume per mm Hg increase in left atrial pressure (Aarseth, Bo and Hauge in preparation). In the present experiments the distension pressure increased by only 1–2 mm Hg.

From the presented experiments we must conclude that we could find no

evidence for plasma hyperosmolality causing either constriction or relaxation of the capacitance vessels in the lung of intact rats or cats. This conclusion is in contrast to the one drawn by Bo, Hauge and Nicolaysen (1971) from their experiments on isolated perfused rabbit lungs. It agrees however with the findings of Mellander and Lundvall (1971) of plasma hyperosmolality reducing vascular resistance without having any effect on vascular capacitance in skeletal muscle.

H. Piené has been a Research Fellow of the Norwegian Research Council for Science and the Humanities. Financial support has also been received from the Norwegian Council on Cardiovascular Diseases. Low-dose Heparin has kindly been supplied by NOVO Norway. This support is gratefully acknowledged.

References

- AARSETH, P. Reduction in pulmonary blood volume after a blood loss. *Acta physiol scand* 1970 80 459—469.
- AARSETH, P. Pulmonary blood volume and pulmonary hematocrit during hypervolemia in rats. *Acta physiol scand* 1971 83 547—553.
- AARSETH, P. and G. BO. Content of blood and of extravascular water in cat lungs during changes in total blood volume. *Acta physiol scand* 1972 86 343—352.
- AARSETH, P. and H. PIENE. The volume responses of various vascular beds to a general blood loss. A study carried out in rats exposed to two different procedures of anesthesia. *Acta physiol scand* 1972 84 48—53.
- AARSETH, P., G. BO and A. HALGE. The effect of lung blood congestion and lung water volume on airway compliance. In preparation.
- BO, G., A. HALGE and G. NICOLAYSEN. Hyperosmolality and pulmonary vascular capacitance. *Acta physiol scand* 1971 82 375—381.
- HALGE, A. and G. BO. Blood hyperosmolality and pulmonary vascular resistance in the cat. *Circulat Res* 1971 28 371—376.
- JONSSON, H. and O. JONSSON. Cell volume as a factor influencing electrical and mechanical activity of vascular smooth muscle. *Acta physiol scand* 1968 72 456—468.
- LUNDVALL, J. Tissue hyperosmolality as a mediator of vasodilatation and transcapillary fluid flux in exercising muscle. *Acta physiol scand* 1972 Suppl. 379.
- LUNDVALL, J., S. MELLANDER, H. WESTIN and T. WHITE. Dynamics of fluid transfer between the intra- and extravascular compartments during exercise. *Acta physiol scand* 1970 70 315—325.
- MELLANDER, S. and J. LUNDVALL. Role of tissue hyperosmolality in exercise hyperemia. *Circulat Res* 1971 28—29 Suppl. 1 1—39—1—45.
- ROWE, C. C., D. H. MICHENNA, R. J. CARLSON and S. STALPR. Hemodynamic effects of hypotonic sodium chloride. *J appl Physiol* 1972 32 187—181.
- STANLEY, W. N. and J. K. BARCLAY. Effect of infusions of osmotically active substances on muscle blood flow and systemic blood pressure. *Circulat Res* 1971 28—29 Suppl. 1 1—33—1—39.
- WILSON, K. D., S. MIERZWA and J. H. MITCHELL. Acute effects of increased venous return on left ventricular performance. *Amer J Physiol* 1969 216 898—901.

Rate and Extent of Adaptive Cardiovascular Changes in Rats during Experimental Renal Hypertension

By

YEN LUNDGREN MARGARETA HALLBÄCK LILIAN WEISS and BJÖRN FOLKOW

Received 27 December 1973

Abstract

LUNDGREN Y M HALLBÄCK L WEISS and B FOLKOW *Rate and extent of adaptive cardiovascular changes in rats during experimental renal hypertension.* Acta physiol scand 1974 91 103—115

To study the extent and exact time course of cardiovascular structural adaptation to increases in pressure load renal hypertension was induced in normotensive male Wistar rats by renal artery constriction. At different intervals after operation the hemodynamic characteristics of the hypertensive rats and normotensive control rats were explored in paired hindquarter perfusions from maximal dilatation up to maximal constriction (*cf* Folkow *et al* 1970 b). At the same time intervals the extent of left ventricular hypertrophy and of water content of the aortic wall were examined. The results reveal the presence of left ventricular hypertrophy in the hypertensive rats already after one week soon followed by adaptive structural changes of the resistance vessels in the form mainly of media hypertrophy these processes being largely completed 2—3 weeks after operation. In these animals lacking genetic predisposition for hypertension the extent of the structural vascular changes seems large enough to explain a considerable part, but not all of the pressure rise. An increased water content of the hypertensive aortic wall is found first 4–5 months after operation, indicating that some water logging of arterial and maybe also arteriolar walls might occur in late phases of chronic renal hypertension.

Regional hemodynamic analyses in man with essential hypertension (Folkow 1956 Folkow Grimby and Thulesius 1958 Conway 1963 Svertsson 1970) strongly suggest that the raised flow resistance at rest can largely be ascribed to a structural change of the resistance vessels. Thus resistance is considerably increased even at maximal dilatation compared with controls and for given degrees of smooth muscle shortening luminal decreases are accentuated increasing vascular reactivity without necessitating any hypersensitivity of the contractile elements. Further comparative analyses of the entire systemic vascular bed as well as that of the hindquarters from spontaneously hypertensive rats (SHR Okamoto 1969) and normotensive control rats (NCR) show a raised flow resistance even at maximal dilatation exaggerated luminal reductions to noradrenaline (NA) without signs of smooth muscle supersensitivity and an enhanced maximal contractile strength of the resistance vessels.

in SHR (Folkow *et al* 1970 a b) These hemodynamic characteristics strongly suggest the presence of an increased wall/lumen ratio in the hypertensive resistance vessels mainly due to an increased media thickness encroaching upon the lumen even at maximal dilatation These changes in SHR seem to be pronounced enough to explain the raised pressure at rest without necessitating any raised smooth muscle activity Moreover quantitative morphological studies (Furumasa 1962 Suwa and Takahashi 1971) show that the wellknown left ventricular hypertrophy in hypertension (*cf* Pickering 1968) is accompanied by a media hypertrophy of the systemic precapillary resistance vessels that is closely balanced to the raised blood pressure level

It seems likely that such changes in vascular design represent a general adaptive phenomenon to changes in average functional load present in all mesodermal tissues Thus when cat or rat vascular bed are exposed to regional hypotension (Folkow and Sverrisson 1968 Folkow *et al* 1971 a Weiss and Hallbäck 1974) they exhibit within few weeks obvious signs of an adaptive reduction in wall/lumen ratio Further hemodynamic studies by Beilin and Ziafas (1972) and morphological and chemical studies by Wolinsky (1970 1971) on the aorta of DOCA or renal hypertensive rats indicate the development of an increased media thickness as described above for man with essential hypertension and SHR Thus these structural vascular changes seem to represent a generally occurring adjustment present not only in subjects predisposed to hypertension but also in genetically normotensive subjects Like the hypertrophy of the left heart ventricle they are evidently secondary to an increased pressure load though they become of great importance for both the development and maintenance of the hypertensive state by their hemodynamic impact on the resistance vessels (*cf* Folkow *et al* 1973 a)

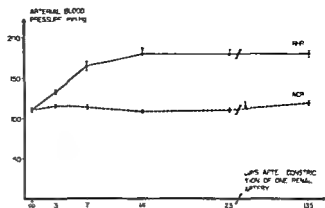
In order to study the extent and exact time course of the structural adaptation of the left heart ventricle and the resistance vessels proper in animals lacking a geneucal predisposition to hypertension renal hypertension was induced in ordinary male Wistar rats by constriction of one renal artery leaving the other kidney intact The isolated hindquarters of the renal hypertensive rats (RHR) were then perfused in parallel with NCR 3 7 14 20 and 130 days after the operation and the hemodynamics of their vascular beds were quantitatively analysed from maximal dilatation up to maximal constriction as earlier described for SHR NCR (Folkow *et al* 1970 b) At the same time intervals the left ventricular weights were compared Preliminary reports covering part of the present results have been published earlier (Hallbäck, Lundgren and Weiss 1972 Folkow *et al* 1973 b)

Methods

In order to induce renal hypertension a silver clip was placed on the left renal artery leaving the right kidney intact, in 60 6—7 weeks old male Wistar rats during ether anesthesia A group of matched male Wistar rats were sham-operated by dissecting the left renal artery without placing any silver clip on it and these sham-operated animals were later used as age and weight matched controls in the paired perfusion experiments

The development of hypertension was followed by means of intraarterial measurements in the caudal artery The tail artery was cannulated during brief ether anesthesia after which

Fig 1 Arterial blood pressure of renal hypertensive rats (RHR) and normotensive control rats (NCR) as measured in the caudal artery during awake conditions. Data after constriction of one renal artery or sham-operation on the abscissa and arterial blood pressure on the ordinate



the arterial blood pressure was measured when the animal was fully awake. The caudal artery was also used for measurement of the perfusion pressure during the experiment.

Paired perfusion experiments were performed on the hindquarters of one renal hypertensive rat (RHR) and one matched sham-operated normotensive control rat (NCR) 3, 7, 14, 25 and 135 days after the operation, each group consisting of 8–13 pairs. As perfusate was used oxygenated Tyrode solution (38°C) containing 4% Ficoll (a polymer of sucrose and epichlorohydrin, MW = 79,000, AB Pharmacia, Uppsala, Sweden) as colloid substitute. First, the pressure-flow relationships (1–40 ml/min \times 100 g) were examined during complete smooth muscle relaxation ensured by papaverine. Noradrenaline (NA) was then infused from subthreshold up to supramaximal (> 5 μ g/ml perfusate) concentrations at a constant flow of about 10 ml/min \times 100 g and to ensure definitely maximal pressor responses 10 IU of vasopressin and 150 mg of barium chloride were added as slug injections. After the experiment the weight of all parts except the hindquarters was subtracted from the total body weight in order to get an exact measurement of the perfused hindquarter preparation without edema. The experimental procedure and the construction of the resistance curves characterizing the individual vascular beds (hindquarters except tail and hindfeet) have earlier been described in detail by Folkow *et al.* (1970, 1971a).

Pressure-flow curves at maximal dilatation were constructed for each pair of hindquarters from the pressure-flow recordings and the pressure responses to NA, vasopressin and barium ions were calculated after which resistance curves were plotted for each pair of rats with log NA dose/ml perfusate on the abscissa and perfusion pressure in mm Hg on the ordinate. The characteristic key points of these resistance curves were 1) resistance at maximal dilatation, 2) threshold dose of NA, 3) steepness of the curve and 4) maximal pressor response. The mean \pm SEM of these key points were deduced for each group of rats and the difference between the group of RHR and NCR was evaluated by the paired design *t*-test.

The hearts of all animals were excised and the left heart ventricles dissected free and weighed separately. Then the mean wet ventricular weight for each group was calculated as was the percentage left heart ventricle weight/body weight. In this respect the material as in part completed with pairs of identically treated RHR/NCR that were used for other purposes.

Just before starting the perfusion the thoracic aortas of RHR 25 days and 135 days after operation and of their matched NCR were dissected free and taken out. Fat and connective tissue surrounding the vessel were removed under dissection microscope. The vessels were cut open longitudinally and divided into four equal pieces each to allow more precise measurements in each animal. The aortic pieces were then placed in oxygenated Krebs solution (37°C for 30 min) after which they were blotted and weighed (wet weight). The preparations were then dried at least 24 h in a vacuum oven at 100°C and weighed to give the dry weight. The mean \pm SEM of the percentage dry weight/wet weight was calculated for each group.

Results

Resting arterial blood pressures measured in the tail artery during awake conditions are presented in Fig 1. Already 3 days after the operation there was a highly

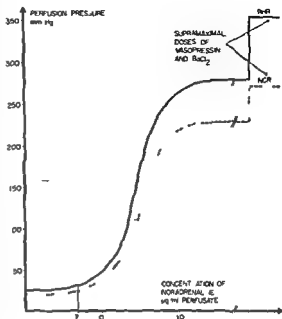
TABLE I Mean values \pm S.E.M. for renal hypertensive rats (RHR) 3 7 14 25 135 days after renal artery constriction and their matched normotensive controls (NCR) and also mean differences \pm S.E.M. with the degree of significance between RHR and their matched NCR. The following parameters are presented: 1) Blood pressure in the caudal artery during awake conditions; 2) Hindquarter flow resistance at maximal dilatation (flow = 10 and 30 ml/min \times 100 g respectively); 3) Threshold dose of noradrenaline (NA) i.e. the NA concentration producing a 25 per cent resistance increase; 4) Slope of the steep part of the NA dose-response curves (tangent of the angle); and 5) Maximal pressor response.

	Arterial blood pressure mm Hg	PRU at max dil (flow 10 ml/min)	PRU at max dil (flow 30 ml/min)	Threshold 1 g NA/ml	Tangent of the angle	Maximal pressor response mm Hg
RHR 3 days n = 8	133 \pm 3	2.07 \pm 0.007	1.27 \pm 0.04	0.047 \pm 0.007	3.3 \pm 0.4	256 \pm 12
NCR n = 8	116 \pm 2	2.14 \pm 0.003	1.32 \pm 0.04	0.030 \pm 0.007	3.3 \pm 0.3	247 \pm 11
mean difference	17 \pm 2	-0.12 \pm 0.03	-0.05 \pm 0.06	-0.003 \pm 0.009	0.0 \pm 0.3	9 \pm 19
significance	p < 0.001	n.s.	n.s.	n.s.	n.s.	n.s.
RHR 7 days n = 8	165 \pm 6	2.06 \pm 0.08	1.35 \pm 0.06	0.071 \pm 0.012	4.1 \pm 0.5	287 \pm 11
NCR n = 8	114 \pm 3	2.10 \pm 0.10	1.37 \pm 0.07	0.092 \pm 0.024	3.6 \pm 0.4	268 \pm 13
mean difference	51 \pm 6	-0.04 \pm 0.11	-0.02 \pm 0.03	-0.021 \pm 0.023	0.5 \pm 0.5	19 \pm 13
significance	p < 0.001	n.s.	n.s.	n.s.	n.s.	n.s.
RHR 14 days n = 10	180 \pm 7	2.55 \pm 0.17	1.50 \pm 0.06	0.088 \pm 0.019	3.9 \pm 0.4	380 \pm 9
NCR n = 10	109 \pm 2	2.15 \pm 0.08	1.31 \pm 0.04	0.060 \pm 0.010	3.1 \pm 0.3	297 \pm 9
mean difference	71 \pm 6	0.40 \pm 0.15	0.19 \pm 0.06	0.029 \pm 0.021	0.9 \pm 0.3	83 \pm 13
significance	p < 0.001	p < 0.05	p < 0.01	n.s.	p < 0.02	p < 0.001
RHR 25 days n = 12	180 \pm 6	2.59 \pm 0.11	1.66 \pm 0.07	0.049 \pm 0.003	5.0 \pm 0.3	352 \pm 7
NCR n = 12	111 \pm 3	2.12 \pm 0.07	1.33 \pm 0.03	0.049 \pm 0.008	3.8 \pm 0.3	271 \pm 11
mean difference	69 \pm 8	0.47 \pm 0.07	0.32 \pm 0.03	0.000 \pm 0.004	1.2 \pm 0.4	81 \pm 19
significance	p < 0.001	p < 0.001	p < 0.001	n.s.	p < 0.02	p < 0.001
RHR 135 days n = 13	180 \pm 4	3.29 \pm 0.11	2.04 \pm 0.06	0.076 \pm 0.012	5.0 \pm 0.4	357 \pm 17
NCR n = 13	119 \pm 3	2.58 \pm 0.09	1.62 \pm 0.04	0.064 \pm 0.009	3.3 \pm 0.2	268 \pm 14
mean difference	61 \pm 5	0.71 \pm 0.19	0.43 \pm 0.07	0.012 \pm 0.007	1.7 \pm 0.3	89 \pm 11
significance	p < 0.001	p < 0.001	p < 0.001	n.s.	p < 0.001	p < 0.001

significant increase in RHR blood pressure compared to that of the sham-operated NCR. Thereafter the blood pressure continued to increase until about 2 weeks after operation when it stabilized around 180 mm Hg.

In each group of rats perfusion experiments were performed on one RHR in parallel with one matched sham-operated NCR first with pressure flow recordings (1–40 ml/min \times 100 g) during maximal dilatation. Pressure flow curves were constructed and from these the peripheral resistance units per 100 g of tissue (PRU₁₀₀) at flows of 10 ml/min \times 100 g and 30 ml/min \times 100 g were deduced and are given in Table I. Of these values the flow of 30 ml/min \times 100 g is the most representative

Fig 2 Mean resistance curves based on 12 constant flow perfusions of paired hindquarter vascular beds from renal hypertensive rats (RHR) 25 days after renal artery constriction (mean arterial pressure 180 ± 6 mm Hg) and normotensive control rats (NCR) (mean arterial pressure 111 ± 3 mm Hg) showing the perfusion pressure (resistance) responses to increasing concentrations of noradrenaline (NA), from subthreshold up to supramaximal amounts. Maximal pressor responses were ensured by huge doses of vasopressin and barium chloride. Log NA concentration ($\mu\text{g}/\text{ml}$ perfusate) is plotted along the abscissa and perfusion pressure responses (mm Hg) along the ordinate. Th. denotes "threshold" i.e. the NA concentration producing 25 per cent increase of resistance above the state of maximal dilatation. Note the increased resistance already at maximal dilatation in RHR, the enhanced steepness of the resistance curve and the increased maximal pressor response while there is no difference in NA threshold dose between RHR and NCR. The thin dotted lines illustrate how resistance to flow becomes higher in RHR than in NCR for the same NA concentration i.e. the same degree of smooth muscle activation.



one for the flow condition, during maximal dilatation in striated muscle tissue *in vivo* and at these flow and pressure levels the difference in distensibility between the hypertensive and the normotensive resistance vessels becomes an increasingly important factor (Hallback, Lundgren and Weiss 1974). In order to avoid rapid edema formation during increasing vascular constriction flow was then kept constant at about $10 \text{ ml}/\text{min} \times 100 \text{ g}$, a flow more representative of the conditions at resting tone in skeletal muscle vascular bed *in vivo* and NA was now infused from subthreshold to supramaximal concentrations. To ensure that the maximal contractile strength of the hindquarter resistance vessels was finally reached 10 IU of vasopressin and 150 mg of barium chloride were added. Resistance curves were then calculated as outlined in Methods. Fig 2 shows the mean resistance curves for RHR 25 days after operation and their matched NCR.

It is seen from this Figure that rats with established renal hypertension (25 days after operation) show an increased resistance at maximal dilatation, a steeper slope of the resistance curve and an increased maximal pressor response but an unchanged sensitivity to NA. This indicates the presence of an enhanced wall/lumen ratio mainly due to an increased media thickness encroaching upon the lumen even at maximal dilatation and resulting in a vascular hyperreactivity that is not the result

of any smooth muscle supersensitivity to the constrictor fibre transmitter. Thus, for a given NA concentration which would here produce largely the same extent of smooth muscle activation there is always a bigger resistance increase in RIIR (indicated in Fig. 2).

The mean values \pm S.E.M. and the degree of significance of the different groups are illustrated in Table I. The significance is tested by using the paired design *t* test as all RIIR are perfused in parallel with matched NCR in order to avoid interference of accidental variations in e.g. temperature, viscosity, ionic NA or ion contents of the perfusate. Such unavoidable minor variations probably explain the slight differences between e.g. the NCR mean values in the different experimental groups and illustrate in fact the advantage of the paired design in experiments of this nature. The Table illustrates the rate of development of hypertension and structural vascular changes in RIIR and gives also the mean differences \pm S.E.M. between RIIR and the matched NCR. After constricting one of the renal arteries arterial pressure increases rapidly being significantly raised already after 3 days and reaching almost maximal levels in about 2 weeks after which it stabilizes around 180 mm Hg. While none of the RIIR groups displayed any significant change in NA sensitivity (threshold NA dose) there was a rapid structural adaptation of the RIIR resistance vessels subsequent to the increased pressure as judged by 1) resistance at maximal dilatation (10 ml/min and 30 ml/min), 2) steepness of the resistance curve and 3) maximal pressor response which change as follows:

1. 3 days after operation resistance at maximal dilatation is if anything slightly decreased in RIIR but it then increases gradually, differs significantly from NCR 2 weeks after operation and reaches an almost steady level after about 3 weeks. Thus with only a short latency a structural narrowing of the lumen in the RIIR resistance vessels follows upon the pressure rise. To judge from the values 135 days after operation there is a further slight increase of the RIIR resistance at maximal dilatation but this is not significant. Further, it occurs in both RIIR and NCR and may be in part associated to age and size.

2. 3 days after operation the steepness of the RIIR resistance curve is equal to that of the NCR resistance curve but then it increases gradually with the duration of the hypertension being significantly higher already 2 weeks after operation indicating a rapidly developed increase of the wall/lumen ratio in the RIIR resistance vessels. In later phases of the RIIR hypertension there may be a slow further increase in wall/lumen ratio since the steepness of the RIIR resistance curve 135 days after operation tends to be greater than that of RIIR 25 days after operation.

3. The maximal pressor response i.e. the maximal contractile strength of the RIIR resistance vessels is slightly increased already one week after operation and becomes significantly raised 2 weeks after operation compared to NCR suggesting an increased bulk of contractile media. The maximal pressor response hardly increases further in the later postoperative period suggesting that the media hypertrophy is a rapidly completed adaptive process.

TABLE II Mean values \pm S.E.M. for renal hypertensive rats (RHR) 3 7 14 25 135 days after renal artery constriction and their weight matched normotensive controls (NCR) concerning 1) body weight 2) awake arterial pressure 3) left ventricular weight and 4) percentage left ventricular weight/body weight

	Body weight g	Arterial blood pressure mm Hg	Left ventricular weight g	Percentage left ventricular weight/body weight
RHR 3 days n = 8	186 \pm 5	129 \pm 3	0.400 \pm 0.012	0.216 \pm 0.008
NCR n = 8	186 \pm 13	108 \pm 5	0.408 \pm 0.03*	0.219 \pm 0.005
significance	n.s.	p < 0.005	n.s.	n.s.
RHR 7 days n = 8	200 \pm 5	165 \pm 6	0.544 \pm 0.010	0.273 \pm 0.007
NCR n = 8	200 \pm 9	106 \pm 2	0.443 \pm 0.02	0.221 \pm 0.004
significance	n.s.	p < 0.001	p < 0.02	p < 0.001
RHR 14 days n = 9	214 \pm 8	180 \pm 7	0.649 \pm 0.023	0.308 \pm 0.012
NCR n = 9	216 \pm 8	108 \pm 2	0.471 \pm 0.017	0.218 \pm 0.003
significance	n.s.	p < 0.001	p < 0.001	p < 0.001
RHR 25 days n = 17	214 \pm 7	178 \pm 4	0.651 \pm 0.027	0.307 \pm 0.011
NCR n = 17	216 \pm 8	108 \pm 2	0.471 \pm 0.017	0.218 \pm 0.003
significance	n.s.	p < 0.001	p < 0.001	p < 0.001
RHR 135 days n = 13	340 \pm 27	176 \pm 5	0.819 \pm 0.029	0.254 \pm 0.016
NCR n = 13	344 \pm 12	116 \pm 5	0.598 \pm 0.017	0.175 \pm 0.005
significance	n.s.	p < 0.001	p < 0.001	p < 0.001

Thus the RHR vascular bed seems to be almost completely adapted in design already 2—3 weeks after operation with an increased wall/lumen ratio that seems to be mainly due to an increased media thickness with a reduced lumen even at complete smooth muscle relaxation.

When comparing left ventricular weights RHR did not differ from the matched NCR 3 days after operation but already after one week a significant increase was found in RHR (Table II). The percentage of left ventricular weight/body weight which is a good estimate of the relative increase in left heart ventricular size is thus also significantly increased after one week. The left ventricular weight increases up to 2 weeks after operation after which it seems to stabilize as was the case also with the signs of media hypertrophy in the resistance vessels. The percentage left heart ventricle weight/body weight is lower in RHR (135 days) compared to RHR (25 days) but this is evidently due to the fact that also in normotensive organisms left heart ventricle weight/body weight decreases along with increases in body weight. However the important point is the comparison between RHR and their matched NCR.

Folkow *et al* (1970 b), that the results may largely be explained by an increased media thickness leading to an enhanced wall/lumen ratio and encroaching upon the lumen even at maximal dilatation. These hemodynamic findings are supported by morphological studies by Hinke (1965), who observed a thickening of the tunica media of the tail artery in rats made hypertensive by DOCA implantation. Further, studies of the thoracic aorta on rats made hypertensive by DOCA administration and renal artery constriction reveal an increased media thickness due to smooth muscle hypertrophy as well as to increased amounts of medial elastin and collagen (Wolinsky 1970 1971).

The present experiments were designed to explore the *extent and exact time course* of left ventricular hypertrophy and of the structural adaptation of the resistance vessels in genetically normotensive Wistar rats made hypertensive by constriction of the left renal artery. By this Goldblatt procedure a marked renal hypertension developed rapidly and arterial pressure measured in the caudal artery was significantly increased 3 days after the operation and stabilized around 180 mm Hg already 2 weeks after the operation. Because of this rapid pressure rise these renal hypertensive rats (RHR) offered particularly favourable circumstances for exploring how rapidly the heart and the resistance vessels change their design once a persistent increase of pressure load is initiated. When paired hindquarter perfusions of RHR and matched NCR were performed 3 7 14 25 and 135 days after the operation the first signs of structural vascular adaptation appeared already after 7 days in RHR. After 14 days resistance at maximal dilatation steepness of the dose response curve to NA and maximal contractile strength of the resistance vessels were all considerably increased. No significant further change occurred with respect to the increase in maximal pressor response which reflects the bulk of contractile elements in relation to the lumen of the resistance vessels. There was however a slight further increase in resistance at maximal dilatation and in steepness of the RHR resistance curve during the subsequent months which will be discussed below but in general it appears as if the hypertrophic structural adaptation of the RHR resistance vessels was largely completed in 2–3 weeks. Thus 25 days after operation resting arterial pressure in RHR was increased 64 % above that in NCR while resistance at maximal dilatation (flow 10 ml/min) was increased 25 % steepness of the resistance curve was increased 39 % and the maximal pressor response 32 % — Left ventricular hypertrophy was significant already one week after operation and was fully developed 2 weeks after operation left ventricular weight/body weight being then 41 % higher in RHR than in the matched NCR.

The situation was largely the same 20 weeks after operation except for the mentioned slight further increase in resistance at maximal dilatation and in steepness of the RHR resistance curve. The establishment of a steeper resistance curve without any parallel further increase in maximal pressor response might be explained by a slight further increase in wall thickness that is not due to an increase of contractile tissue but where water logging or/and collagen invasion may be considered. In fact, a delayed increase of elastin and collagen in the rat thoracic aorta

has been reported in long term (16 months) renal hypertension while short term hypertension (25 months) was mainly characterized by an increase of the smooth muscle portion (Wolinsky 1972). An element of water logging (Tobian and Binion 1952 Tobian Olson and Chesley 1969) may also be considered. In fact the present results reveal a significantly increased water content of the aortic walls in RHR 135 days after operation compared to their matched NCR ($p < 0.001$) and compared to RHR 25 days after operation ($p < 0.001$) while no difference was found between RHR 25 days after operation and their matched NCR. It is possible that both collagen invasion and some water logging will in later phases contribute somewhat to the wall thickening of the resistance vessels though the hypertrophic change seems to be by far the most rapid and hemodynamically important structural change. In fact this hypertrophic change of the resistance vessels is evidently so rapid that its hemodynamic consequences in terms of resistance rises for a given smooth muscle activity level are likely to become intertwined in time with the functional pressor influences which act as trigger mechanisms for the structural vascular changes. Hence the latter ones may contribute also to the very creation of a raised pressure. The speed of these changes in rats is however hardly surprising considering the rapidity at which skeletal muscle hypertrophy can occur (Goldberg 1967). In man such processes are no doubt generally slower than in rats mainly because of the lower metabolic rate. However if in man it is a matter of months rather than of weeks the structural vascular changes must still be regarded as a rapid process considering the time course of hypertension development in man.

The present results also illustrate that the cardiovascular adaptation to an increased pressure load is a generally occurring process as could be expected being present not only in animals with genetically linked hypertension (SHR) but also in genetically normotensive animals in which hypertension is induced by interference with the renal blood supply (RHR). It is however, not impossible that the extent of such changes for a given functional load may vary somewhat in hypertension depending on the type of hypertension or/and on genetic predisposition. Thus if the resting blood pressure is on the whole a fair reflection of the average pressure load it appears as if the extent of structural change of the resistance vessels is somewhat more pronounced in SHR than in RHR. For example when comparing the ratio of the resting blood pressures (BP) with the ratio of e.g. the maximal pressor responses (MPR) (reflecting the bulk of contractile media tissue in relation to the lumen of the resistance vessels) in male RHR/NCR and male SHR/NCP respectively the following figures are obtained RHR/NCR BP 1.54 MPR 1.36 (present results after 20 weeks of hypertension) SHR/NCR BP 1.44 MPR 1.45 (Folkow *et al* 1970 b). Thus the increased bulk of media tissue seems to be more closely adjusted to the pressure level in SHR than in RHR.

The age of the animals was about the same in these groups. One must therefore be open to the possibility that the extent of the structural adaptation is for some reason more prominent in the primary type of rat hypertension than in the secondary renal one studied here. In fact in SHR this structural autoregulation

seems pronounced enough as to largely alone explain the raised resistance during rest but hardly so in RHR where functional excitatory influences must contribute more or less strongly to maintain the raised levels of resistance and pressure

This research has been sponsored by grants from the Swedish Medical Research Council (No B74 14X 16 10C) from Swedish National Association against Heart and Chest Diseases and from the Medical Faculty University of Göteborg

AB Hassle generously covered part of the expenses for a technician

References

- BEILIN L J and G ZIAKAS Vascular reactivity in post deoxycorticosterone hypertension in rats and its relation to irreversible hypertension in man *Clin Sci* 1972 42 579-590
- CONWAY J Vascular abnormality in hypertension Study of blood flow in the forearm *Circulation* 1963 27 510-529
- FOLKOW B *Structural myogenic lumoral and nervous factors controlling peripheral resistance Hypotensive Drugs* 163 London Pergamon Press 1956
- FOLKOW B M HALLBACK Y LUNDGREN and L WEISS Background of increased flow resistance and vascular reactivity in spontaneously hypertensive rats *Acta physiol scand* 1970 B 80 93-106
- FOLKOW B and R SIVERTSSON Adaptive changes in reactivity and wall/lumen ratio in cat blood vessels exposed to prolonged transmural pressure difference *Life Sci* 1968 7 1283-1289
- FOLKOW B G GRIMBY and O THILLESILS Adaptive structural changes of the vascular walls in hypertension and their relation to the control of the peripheral resistance *Acta physiol scand* 1958 44 255-272
- FOLKOW B M HALLBACK Y LUNDGREN and L WEISS Structurally based increase of flow resistance in spontaneously hypertensive rats *Acta physiol scand* 1970 a 79 373-378
- FOLKOW B M HALLBACK Y LUNDGREN and L WEISS Effects of intense treatment with hypotensive drugs on structural design of the resistance vessels in spontaneously hypertensive rats *Acta physiol scand* 1971 b 83 280-282
- FOLKOW B M HALLBACK Y LUNDGREN and L WEISS Effects of immunosympathectomy on blood pressure and vascular "reactivity" in normal and spontaneously hypertensive rats *Acta physiol scand* 1972 84 512-523
- FOLKOW B M HALLBACK Y LUNDGREN and L WEISS Time course and extent of structural adaptation of the resistance vessels in renal hypertensive rats (RHR) as compared with spontaneously hypertensive rats (SHR) *Acta physiol scand* 1973 b 87 10 A-11 A
- FOLKOW B M GUREVICH M HALLBACK Y LUNDGREN and L WEISS Hemodynamic consequences of regional hypotension in spontaneously hypertensive and normotensive rats *Acta physiol scand* 1971 a 83 532-541
- FOLKOW B M HALLBACK Y LUNDGREN R SIVERTSSON and L WEISS Importance of adaptive changes in vascular design for establishment of primary hypertension studied in man and in spontaneously hypertensive rats *Circulat Res* 1973 a 32-33 Suppl 1 12-13
- FURUYAMA M Histometrical investigations of arteries in reference to arterial hypertension *Tohoku J Exp Med* 1962 76 388-414
- GOLDBERG A L Work induced growth of skeletal muscle in normal and hypophysectomized rats *Amer J Physiol* 1967 213 1193-1198
- HALLBACK M Y LUNDGREN and L WEISS Adaptive structural changes of the resistance vessels in renal hypertension *Acta physiol scand* 1972 84 6 A-7 A
- HALLBACK M Y LUNDGREN and L WEISS Distensibility of the resistance vessels in spontaneously hypertensive rats as compared with normotensive control rats *Acta physiol scand* 1974 90 57-68
- HINKE J A M In vitro demonstration of vascular hyperresponsiveness in experimental hypertension *Circulat Res* 1965 17 359-371
- ORAMOTO K Spontaneous hypertension in rats *Int Rev Exp Path* 1968 7 227-240
- OVERBECK H W B T SWINDALL D F COWAN and M C FLECK Experimental renal hypertension in dogs Forelimb hemodynamics *Circulat Res* 1971 29 51-62
- PICKERING G W *High blood pressure* London J & A Churchill 1968
- SIVERTSSON R Hemodynamic importance of structural vascular changes in essential hypertension. *Acta physiol scand* 1970 suppl 343 6-36

- SUWA, N. and T. TAKAHASHI. Morphological and morphometrical analysis of circulation in hypertension and ischemic kidney. München—Berlin—Wien: Urban and Schwarzenberg, 1971.
- TOBIAN, L. and J. T. BRION. Tissue cations and water in arterial hypertension. *Circulation* 1952; 5: 754—758.
- TOBIAN, L., R. OLSON and G. CHESLEY. Water content of arteriolar wall in renovascular hypertension. *Amer J Physiol* 1969; 216: 22—24.
- WEISS, L. Long term treatment with antihypertensive drugs in spontaneously hypertensive rats (SHR). Effects on blood pressure, survival rate and cardiovascular design. *Acta physiol scand* 1974. In press.
- WEISS, L. and M. HALLBACK. Time course and extent of structural vascular adaptation to regional hypotension in adult spontaneously hypertensive rats (SHR). *Acta physiol scand* 1974. In press.
- WOLINSKY, H. Response of the rat aortic media to hypertension. *Circulat Res* 1970; 26: 507—522.
- WOLINSKY, H. Effects of hypertension and its reversal on the thoracic aorta of male and female rats. *Circulat Res* 1971; 28: 622—637.
- WOLINSKY, H. Long term effects of hypertension on the rat aortic wall and their relation to concurrent aging changes. *Circulat Res* 1972; 30: 301—309.

The Effect of Extracellular Calcium on Thermal Excitability of the Sensory Units in the Tooth of the Cat

By

LEIF OLGART GLENN HAEGERSTAM and LENNART EDWALL

Received 27 December 1973

Abstract

OLGART L G HAEGERSTAM and L EDWALL *The effect of extracellular calcium on thermal excitability of the sensory units in the tooth of the cat* Acta physiol scand 1974 91 116-122

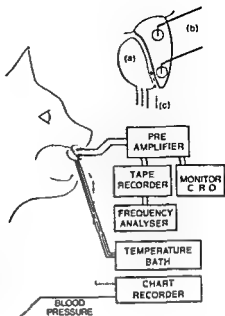
Intradermal sensory nerve impulse activity was measured from dentinal cavities in canine teeth of anesthetized cats. No spontaneous activity was usually recorded in cavities filled with isotonic saline. Heat stimulation of 15-20°C failed to give any impulse activity while other stimuli such as air blasts produced bursts of impulses. Lowering extracellular calcium ion concentration by local application of sodium citrate sodium oxalate or EDTA induced impulse activity. Under these conditions heat produced a rapid increase in discharge activity which lasted as long as the stimulus was applied. Increased extracellular calcium concentration abolished this response to heat. The present findings show that a change in the extracellular calcium ion concentration modulates the excitability of intradermal sensory units and may thus also modulate the resulting experience of pain.

It is generally accepted that the afferent neurons in the human tooth are only involved in the preception of pain (Sicher 1966). Experiments in human subjects have shown that heat is less effective in producing pain than is cold or air blasts. rapid heat stimulation of teeth (raising the temperature by 30°C) did not cause any pain (cf Brannstrom and Astrom 1972).

The neural activity recorded from exposed dentin in the cat tooth has recently been shown to originate from sensory nerves (Arwill *et al* 1973). Using a similar recording technique Edwall and Scott (1971) reported that a rapid temperature elevation of 6-8°C on the cat tooth consistently increased the intradermal nerve activity. Such responses were obtained in preparations showing spontaneous activity as well as after lowering the extracellular calcium ion concentration.

In contrast to these findings by using essentially the same technique but without lowering of the extracellular calcium ion concentration we found in preliminary experiments that heat pulses of 15-20°C did not influence the nerve activity. The present study was designed to further investigate the influence of extracellular calcium ion concentration on the response of intradermal sensory units to heat stimulation.

Fig 1 Drawing showing the experimental set up. Inset represents enlargement of tooth thermode. (a) electrodes (b) in cavities thermocouples circuit (c) located close to cavity over pulp horn in contact with enamel and thermode. For further explanation see text.



Methods

Experiments were conducted on adult cats (2–4 kg and 1–3 years old) anesthetized with sodium pentobarbital (30 mg i.v.). The experimental set up is illustrated in Fig 1. The jaws were immobilized by means of a steel rod and dental acrylic.

Based on information from X-ray pictures of canine teeth two cavities were prepared: one over the pulp horn and one within the gingival half of the crown. The enamel was removed using a diamond instrument operated at slow speed. Isotonic saline solution (20–22°C) was used to prevent drying of dentin and the cavity was deepened by means of a hand-operated end-cutting bur and observed through a binocular microscope. Both cavities were extended until the pulp was barely visible through the dentin, leaving 0.1–0.3 mm of intact dentin over the pulp. In some experiments shallower coronal cavities (0.3–0.5 mm intact dentin) were prepared and in a few cases the cavity was extended to pulp exposure. By subsequent insertion of a water-circulated thermode surrounding the major part of the tooth crown, the tooth temperature could be controlled and by using a thermocouple attached close to or within the recording cavity, the tooth temperature was continuously monitored. In control experiments a thermocouple was also placed in the pulp through a small exposure in the coronal cavity. This made it possible to measure the temperature on the tooth surface in the cavity and in the pulp tissue simultaneously. Based on previous measurements of the surface temperature on canine teeth in newly anesthetized cats, the temperature of the thermode was kept at 37°C. Heat stimulation was performed by rapidly increasing (15–20°C) of the water temperature in the thermode. The upper temperature limit chosen was beneath the level tested in control experiments to cause irreversible damage to the pulp after repetitive short applications. When the temperature of the thermode was increased to 41°C, a higher maximum temperature was recorded in the pulp (42°C) than from the dentin in the cavity (39°C). There was a consistent delay of 20 s in the temperature rise in the pulp compared to that in the dentin.

A platinum recording electrode (dia 0.20 mm) was placed in contact with the dentin in the coronal cavity, which was filled with the saline solution. The indifferent electrode was placed in the other cavity and both electrodes were connected to a PAR 113 preamplifier. Recordings and frequency analysis were made as described by Edwall and Scott (1971).

The extracellular calcium ion concentration in dentin in the recording cavity was lowered using isotonic oxalate (12 mM, 24 mM, 48 mM), isotonic sodium citrate (116 mM) or ethylene diamine tetraacetic acid (EDTA) (26 mM). A volume of 0.2 µl as applied directly to the dentin after removal of the saline solution. Within one minute the agent was usually replaced by a new application. In the same manner 0.2 µl of calcium chloride (0.86 mM, 9 mM, 18 mM, 36 mM or saturated solution) was introduced into the recording cavity.

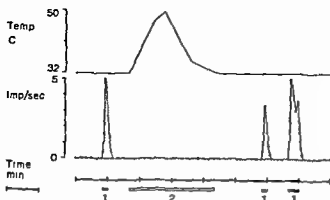


Fig 2 The effect of heat and air blasts on the sensory unit impulse frequency. Temperature recorded from contact surface between enamel and thermode. Air blasts applied to exposed dentin in the recording cavity. Cat mature 3.2 kg. Pentobarbital 1. Air blasts 1. Heat stimulation 18°C. Upper graph: Impulse frequency during activity represents the running average for 3 s interval and is given as Imp/s. Lower graph:

Results

In freshly prepared cavities filled with isotonic saline solution spontaneous activity was generally not seen. In cases where the cavities were deepened almost to a pulp exposure spontaneous activity at a relatively low frequency less than 10 Imp/s was often recorded. Application of heat ($32 \pm 18^\circ\text{C}$) to a tooth devoid of spontaneous activity did not produce any activity (Fig 2). However stimulation with air blasts on the dentin in the recording cavity before and after heat stimulation produced bursts of impulses at frequencies below 5 Imp/s (Fig 2). This figure represents the typical results obtained in 14 procedures. In spite of the absence of a response to heat in these experiments such stimulation was occasionally observed to evoke a reflex motor response involving aversive tongue and lip movements. In cases where a spontaneous activity was present a transient increase in impulse frequency was obtained at the beginning and at the end of the heat stimulation.

Low calcium concentration Lowering the extracellular calcium concentration by application of sodium citrate, sodium oxalate or EDTA to the recording cavity at the basal temperature level resulted in impulse activity after a delay of 10–60 s. In Fig 3 the effect of sodium oxalate (48 mM) is shown. The activity started after a delay of 10 s and lasted as long as the substance was present in the cavity. After removal and subsequent washing with saline (Fig 3 2) the activity was slowly reduced.

High calcium concentration Withdrawal of the calcium binding substance and application of calcium chloride resulted in a rapid decrease of the activity and a total abolition of impulses.

In Fig 3 3 calcium chloride (36 mM) is shown to rapidly abolish the activity previously produced by sodium oxalate (48 mM). This illustration represents the typical response obtained when sodium oxalate (12 mM, 24 mM, 48 mM), sodium citrate (116 mM) and EDTA (26 mM) were used in combination with calcium chloride (9 mM, 18 mM, 36 mM and saturated solution). This pattern of response could be repeated several times in the same cavity and was shown in 18 procedures in 3 cats.

Fig 3 Influence of extracellular calcium concentration on impulse frequency. Local application in the recording cavity. Cat young adult 2.6 kg. Pentobarbital 1. Sodium oxalate 4.8 mM. 2. Sodium chloride isotonic. 3. Calcium chloride 36 mM. Impulse frequency represents the running average for 10 s interval and is given as imp/s.

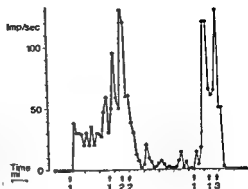


Fig 4 Influence of extracellular calcium concentration on impulse frequency. Local application in the recording cavity. Cat young adult 2.8 kg. Pentobarbital 1. Sodium oxalate 24 mM. 2. Calcium chloride 0.86 mM.

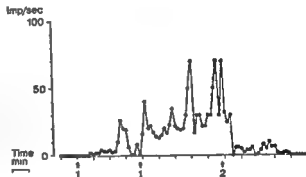


Fig 4 shows the effect of a lower concentration of calcium chloride (0.86 mM) during a period of raised impulse activity after application of sodium oxalate (24 mM). The activity was slowly reduced to zero after the introduction of calcium chloride (Fig 4 2).

Since heat stimulation failed to produce a raised discharge activity when only isotonic saline was present in the recording cavity the same heat stimulus was again applied to the tooth during a period of discharge activity obtained by lowered extracellular calcium. In Fig 5 the initial activity was produced by sodium citrate (116 mM). Increasing the tooth temperature by 16°C (Fig 5 a) resulted in a rapid increase in the discharge activity which was reduced to the initial level when the temperature was lowered again. An identical heat stimulation was repeated 5 min later (Fig 5 b) which gave a prompt rise of impulse frequency during the first 30 s of warming. Calcium chloride (36 mM) applied in the recording cavity when the temperature was still rising (Fig 5 b 1) caused a rapid abolition of the impulse activity. As long as calcium chloride was applied no activity was recorded. This pattern of response represents the typical results obtained in 4 procedures on 3 cats. The effect of calcium was consistent when concentrations above 9 mM were used. When the heat stimulation was repeated after the calcium application no nerve response was obtained. In teeth in which spontaneous activity was recorded after a deep

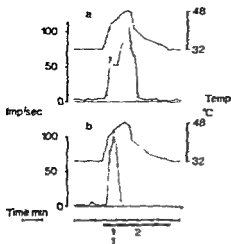


Fig 5

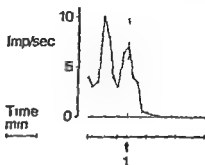


Fig 6

Fig 5 a) The effect of heat on sensory unit impulse frequency during a low extracellular calcium concentration b) The effect of calcium chloride introduced to the recording cavity during a similar response to a heat stimulation. In both procedures the excitability was raised by sodium citrate 116 mM. Upper graph temperature. Lower graph, impulse frequency. Cat mature 3.6 kg. Pentobarbital 1. Calcium chloride 36 mM. 2 Heat stimulation 16 °C.

Fig 6 Influence of increased extracellular calcium concentration on spontaneous impulse frequency. Deep cavity preparation. Cat mature 3.5 kg. Pentobarbital 1. Calcium chloride 18 mM.

cavity preparation application of calcium chloride rapidly abolished this activity. This effect of calcium chloride (18 mM) is shown in Fig 6.

Discussion

We have studied the influence of extracellular calcium on the thermal excitability of intradental sensory units. Electrical recording of impulse activity from the sensory units was made from exposed dentin in the tooth (Scott and Temple 1963; Edwall and Scott 1971; Arwall *et al.* 1973).

In contrast to the findings reported by Scott and Temple (1963) no spontaneous activity was recorded in freshly prepared cavities of standard depth. However, upon stimulation, for example with air blasts, responses were consistently observed in such preparations. This shows that the intradental neurons were accessible for recording.

Spontaneous activity often occurred when the cavities were deepened and more frequently when the preparation was extended to a small pulp exposure. This indicates that such activity is mainly due to the insult of cavity preparation (cf. Andersson 1966) which increases the excitability of sensory neurons.

Heat stimulation failed to excite these sensory units when recordings were made from a preparation of standard depth filled with isotonic saline and devoid of spontaneous activity. Under the same conditions, however, the preparation responded to

other stimuli such as air blasts. These findings are in agreement with observations from human studies showing that heat stimulation (30°C increase) on clinically healthy teeth did not give rise to pain (cf Brannstrom and Astrom 1972). It was suggested that this lack of effect was due to a slow onset of fluid displacement in dentinal tubules which was insufficient to activate nerve fibres in the pulp-dentinal border. On the other hand it has been shown that air blasts on exposed dentin cause an immediate sharp pain which was ascribed to a rapid displacement of fluid in the tubules (Brannstrom, Linden and Astrom 1967). Thus the heat stimulation used in the present study may be regarded as a subthreshold stimulus to the units from which we recorded.

In the present study, lowering the extracellular calcium concentration consistently resulted in nervous discharges. This activity as well as any spontaneous activity was rapidly abolished by adding calcium ions to the cavity. The change in excitability of peripheral nerves that is correlated with changes in the concentration of ionized extracellular calcium is well known in neurophysiology both experimental and clinical (cf Brink 1954). A lowered threshold of excitation was demonstrated in our experiments by stimulating the tooth with heat. Thus when citrate was applied to the recording cavity the sensory units responded to previously subthreshold heat stimulation. The rapid onset of this raised activity (usually within 5 s) appears to be related primarily to the thermal gradient in the dentin rather than to the absolute temperature in the vicinity of the neurons. Support for this view was found in the control experiments in which there was a latent period of about 20 s between the temperature rise in the pulp and that on the tooth surface. These findings may favour the theory of a hydrodynamic transmission to the neurons by heat stimulation. Accordingly under conditions of raised excitability a slow rate of fluid flow in tubules elicited by heat may be sufficient to induce discharges from neurons which under conditions of lower excitability only respond to stimuli (such as air blasts) which produce higher rates of fluid movement. Heat and air blasts gave pulses which could not be distinguished from each other by their appearance on the oscilloscope suggesting that sensory neurons in the same area were activated by the two stimuli.

The observation in a few experiments with deep cavities that heat produced transient activity illustrates the increased excitability due to the insult of the cavity preparation (cf Andersson 1966). These findings also corroborate the results obtained in human experiments by Brannstrom and Johnson (1971) showing that hypersensitivity to external stimuli accompanies pulp damage.

The present finding that heat stimulation occasionally evoked reflex motor responses is in agreement with observations by Scott and Tempel (1963). Since in our study these reflex responses occurred when no impulse activity was recorded it may be suggested that heat is a more adequate stimulus for nerves situated deeper in the pulp than those from which we recorded. Since heat has been shown to raise the intrapulpal pressure (Beveridge and Brown 1965, van Hassel and Brown 1969), it is possible that such raised pressure may elicit nerve impulses in the pulp which

are not recorded with the present technique. A further indication of this possibility are the observations reported by Brannstrom (1963) that heat produced pain in human teeth even when the cells in the odontoblastic zone were previously severely damaged. It is also known from clinical experience that heat may evoke severe pain in partially necrotic pulps indicating that nerves in the apical part of the pulp or in the periodontium respond to heat stimulation. Furthermore heat may act as a noxious stimulus directly on nerves in the pulp (Pfaffman 1939, Funakoshi and Zotterman 1963 cf. Andersson, Hannam and Matthews 1970).

The results of the present study show that a change in the extracellular calcium ion concentration modulates the excitability of intradental sensory units to heat stimulation. It is suggested that the excitability to other stimuli and resulting experience of pain is also modulated by this peripheral influence of calcium ions.

This investigation was supported by grants from the Swedish Medical Research Council (B74 74X 816 09), the Swedish Association of Medical Research and Karolinska Institute, Stockholm. We express our appreciation for the technical advice from Docent Aage Møller.

References

- ARWILL, T. L., EDWALL, J., LILJA, L., OLGART, S. E. and SVEINSSON, U. Ultrastructure of nerves in the dentinal pulp border zone after sensory and autonomic nerve transection in the cat. *Acta odont. scand.* 1973, 31, 273-281.
- ANDERSSON, D. J. Dental sensation. *Advances in Oral Biol.* edited by Peter H. Staple. *Acad. Press* 1966, 2, 1-30.
- ANDERSSON, D. J., A. G. HANNAM and B. MATTHEWS. Sensory mechanisms in mammalian teeth and their supporting structures. *Physiol. Rev.* 1970, 50, 171-193.
- BEVERIDGE, E. E. and A. C. BROWN. The measurement of human dental intrapulpal pressure and its response to clinical variables. *Oral Surg.* 1965, 19, 653-658.
- BRINK, F. The role of calcium ions in neural processes. *Pharmacol. Rev.* 1954, 6, 243-290.
- BRANNSTROM, M. A hydrodynamic mechanism in the transmission of pain producing stimuli through the dentine. In *Sensory mechanisms in dentin*. Ed. D. J. Andersson. Oxford: Pergamon, 1963, 50, 73-79.
- BRANNSTROM, M., L. A. LINDEN and A. ASTROM. The hydrodynamics of the dental tubule and of pulp fluid: A discussion of its significance in relation to dentinal sensitivity. *Caries Res.* 1966, 1, 310-311.
- BRANNSTROM, M. and A. ASTROM. The hydrodynamics of the dentine: its possible relationship to dental pain. *Int. dent. J.* 1972, 22, 219-227.
- EDWALL, L. and D. SCOTT, JR. Influence of changes in microcirculation on the excitability of the sensory unit in the tooth of the cat. *Acta physiol. scand.* 1971, 87, 553-566.
- FUNAKOSHI, M. and Y. ZOTTERMAN. A study in the excitation of dental pulp nerve fibres. In *Sensory Mechanisms in Dentine*. Ed. D. J. Andersson. Oxford: Pergamon, 1963, 50, 60-70.
- VAN HESSEL, H. J. and A. C. BROWN. Effect of temperature changes on intra-pulpal pressure and hydraulic permeability. *J. clin. oral Biol.* 1969, 14, 301-315.
- JOHNSON, G. and M. BRANNSTROM. Pain reaction to cold stimulus in teeth with experimental fillings. *Acta odont. scand.* 1971, 29, 632-641.
- PFÄFFMAN, C. Afferent impulses from the teeth due to pressure and noxious stimulation. *J. Physiol. (Lond.)* 1939, 97, 207-219.
- SCOTT, D. JR. and T. R. TEMPEL. Receptor potentials in response to thermal and other excitations. In *Sensory mechanisms in dentine*. Ed. D. J. Andersson. Oxford: Pergamon, 1963, 50, 27-46.
- SICHER, H. ed. *Orban's oral histology and embryology*. C. V. Mosby, St. Louis, 1966.

Effect of Changes in Plasma Na^+ and Ca^{++} Ion Concentration on Body Temperature during Exercise

By

BODIL NIELSEN

Received 10 January 1974

Abstract

NIELSEN B *Effect of changes in plasma Na and Ca^{++} ion concentration on body temperature during exercise* Acta physiol scand 1974 91 123-129

Plasma osmolality and plasma Na and Ca ion concentrations were changed in human subjects by having them drink hypertonic solutions of NaCl or CaCl_2 . Plateau values of body temperature during work were raised by increase in $[\text{Na}]$ and lowered by increase in $[\text{Ca}^{++}]$ compared to values in normal conditions. The effect on body temperature could be ascribed to a faster onset of sweating in the Ca^{++} experiments and a slower onset in the Na experiments. The effect on body temperature of increased osmotic concentrations in plasma was due to action of the specific ions rather than a general effect of change in osmolality. It was not possible to show whether the effects of Na and Ca^{++} were due to action on the central nervous system and thermoregulatory centers or to peripheral interference with the function of the sweat glands.

We have described (Nielsen *et al* 1971, Nielsen 1973) that equilibrium body temperature during work could be raised or lowered by changing the osmolality of the plasma. The plateau values of esophageal temperature were positively correlated with plasma osmolality in warm and neutral environments while the effect disappeared in cold environments when sweating was nearly absent. It could not be demonstrated conclusively whether plasma osmolality affected thermoregulatory centers in the brain or whether it acted peripherally on sweat glands.

The aim of the study presented here was to establish whether osmolality had a general effect whether on cells in the brain or on sweat glands or whether the effect was specific to the particular ion. Plasma osmolality was changed with two ions, sodium or calcium. Calcium was chosen since it has been proposed that the ratio of the concentration of Na/Ca in cerebrospinal fluid is the mechanism whereby the set point of the thermoregulatory system may be established (Feldberg, Myers and Veale 1970, Myers and Veale 1971, Myers, Veale and Yaksh 1971).

TABLE I

	height cm	weight kg	age years	T	number of experiments		
					normal	Na	Ca ⁺
KWJ	163	76	29	30 C	4	4	3
KS	180	73	25	30 C	4	4	3
MS	175	74	29	30 C	2	2	3
LJ	180	86	20	30 C	3	2	1
PR	178	76	26	30 C	3	3	3
LV	178	70	24	30 C	2	0	1
—				8 C	3	0	2

Methods

The subjects were studied during exercise in 3 conditions: normal, after drinking hypertonic NaCl solution and after drinking hypertonic CaCl₂ solution.

Methods and procedure have been described in detail (Nielsen 1973 b). The following parameters were measured: deep esophageal temperature (T_{es}), rectal temperature (T_{re}) in 3 depths (27, 22 and 17 cm), mean skin temperature (\bar{T}_a) (average of weighted measurements at 15 locations), sweat rate (Sw) and metabolic rate (M).

Blood samples (5 ml) were drawn from a cubital vein before and after 60 min of work. Care was taken to avoid stasis. Blood samples were centrifuged for 30 min at 3000 rev/min. The plasma was removed and stored in a refrigerator. The hematocrit was expressed as the average of two samples. Plasma osmolality was measured by a freezing point depression osmometer (Advanced L3) to ± 1 mOsmol/kg. Double analyses on each sample were checked against standard 100 and 500 mOsmol/kg solutions. Plasma sodium concentration [Na] and total calcium concentration [Ca_{tot}] were determined by a Zeiss Flame photometer PF5. Diluted samples (for calcium determinations after EDTA addition) were checked against known standard solutions. Repeated determinations on the sample varied less than ± 0.1 mEq/l for [Ca_{tot}] and less than ± 2 mEq/l for [Na]. Variation in sodium concentration between 100 and 200 mEq/l [Na] did not affect the determination of Ca⁺⁺ in the samples.

Exercise was performed on a Krogh bicycle ergometer suspended in the Krogh balance as described previously (Nielsen and Nielsen 1965). The experiments were performed in a climatic chamber at $30 \pm 1/4$ °C ambient temperature and at $11 \pm 1/4$ °C. In some experiments a fan blew air on the subjects' chest to promote the evaporation of sweat. Humidity was kept below 75% relative humidity.

Data on the subjects and the number of experiments in the different conditions are presented in Table I.

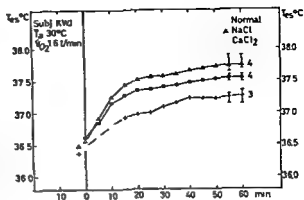
Procedure

In preliminary experiments the change in [Na] and [Ca_{tot}] and plasma osmolality was followed for 4–7 h after the subject had taken 1 l 2% NaCl or CaCl₂ solution.

Plasma osmolality was at or above normal 2–3 h after drinking 1 l 2% CaCl₂ solution and then fell to below normal values. [Ca_{tot}] increased slowly throughout the 4–7 h and was 25–30% above normal at 2–3 h. The effect on osmolality of NaCl was also maximal about 2 h after intake. Therefore work was started about 2 h after the subject had drunk the solution.

Having fasted overnight the subjects drank 1–1 1/2 l 2% NaCl or CaCl₂ solution. One hour later probes were inserted in the esophagus and in the rectum. The subjects then rested 45 min on a cot covered with a blanket in room temperature 22 °C. The body temperatures were then recorded. The first blood sample drawn and exercise was started. The work rate corresponded to about 40% of max $\dot{V}O_2$ and the heart rate recorded by ECG every 5 min was about 120 at 30 \bar{T}_a . Douglas bags to measure the metabolic rate were filled at 30 and 40 min and \bar{T}_{air} and wall temperatures were measured at 35, 45 and 55 min. A second blood sample was taken 2–3 min after work stopped.

Fig 1 Esophageal temperature during 60 min exercise in normal condition ● after drinking 1 liter hypertonic NaCl Δ and after 1 liter hypertonic CaCl_2 + Number of experiments in the different conditions are indicated on the graph Vertical bars denote range



Results

CaCl_2 lowered equilibrium body temperature whereas NaCl raised it. The effect both of NaCl (Nielsen 1973 b) and of CaCl_2 was less at low (8°C) than at high (30°C) environmental temperature. After work for 60 min at 30°C plasma osmolality was higher than normal when 1 l CaCl_2 solution had been taken 2 h previously ($+5 \text{ mOsmol/kg}$) and when the same amount of NaCl solution had been taken ($+10 \text{ mOsmol/kg}$). Nonetheless body temperature was lower than normal after CaCl_2 , higher after NaCl solution (Fig 1). The same effect was seen in all 6 subjects when the average equilibrium esophageal temperature was plotted against plasma osmolality, though plasma osmolality deviated but little from normal in most subjects (Fig 2).

The average skin temperature was higher than normal when NaCl solution had been taken ($+1/2^\circ\text{C}$) and lower when the solution taken was CaCl_2 (Fig 3 left). The change in steady state sweat rate though not so uniform was higher after CaCl_2 and lower after NaCl in most subjects (Fig 3 right). Sweating increased faster when CaCl_2 solution had been taken and slower when NaCl solution was

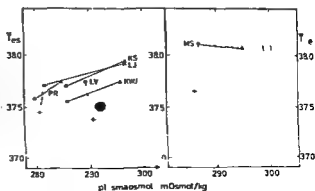


Fig 2 Plateau values of core temperature T_{es} or T_e plotted against plasma osmolality in 3 experimental conditions: Normal ● after drinking NaCl Δ after drinking CaCl_2 + Average of results from 6 subjects at 30°C \bar{T}_a . Number of experiments with the individual subjects see Table I

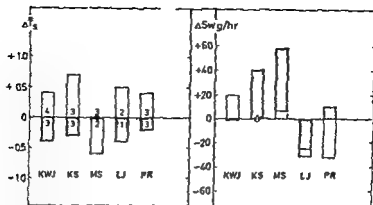


Fig 3 Left $\Delta \bar{T}_s$ difference between averages of \bar{T} during exercise in normal condition and \bar{T}_s after drinking NaCl or CaCl₂ Right $\Delta S_{wg/hr}$ difference between averages of steady state sweat rate during exercise in normal condition and steady state sweat rate after drinking NaCl or CaCl₂ 5 subjects \bar{T}_s 30 °C Na exper number of exper shown \square Ca exper number of exper shown \blacksquare

taken than normal (Fig 4). The area between heat production (Fig 4 dotted line) and evaporative heat loss (Fig 4 curved lines + CaCl₂ Δ NaCl) represents heat storage ΔS . \bar{T}_s was measured only for the last 30 min and therefore the time course for rate of (C+R) heat loss and the exact value of ΔS were not obtained.

Discussion

Where subjects drank CaCl₂ solution several hours before work the plateau of core temperature during exercise was lower than normal. By contrast intake of NaCl solution raised the plateau temperature above that during exercise in the normal

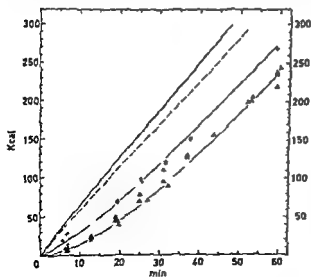


Fig 4 Total metabolic energy liberation M (full line) total heat production (MW) (dotted line) and accumulated evaporative heat loss (curved lines) as a function of time during exercise for 60 min Δ 4 expts 1 l NaCl solution taken 4 h before + 3 expts 1 l CaCl₂ solution taken 4 h before \bar{T}_s 30 °C Subj KWJ

condition (Nielsen 1973 b and this study). These findings suggest that the relation of osmolarity and plateau core temperature during exercise may be a specific effect of the ionic composition of plasma rather than a simple osmotic effect on the activity of cells in the sweat glands or temperature center (Dantas 1939 Amatruda *et al* 1953 Greenleaf *et al* 1971).

The mechanism by which differences in plateau temperature are obtained is illustrated in Fig. 4. The initial rate of increase in sweating was higher in the calcium experiments than after NaCl ingestion. This initially higher sweat rate leads to less heat accumulation and thus to lower plateau temperature during exercise.

Under normal conditions the plateau temperature during exercise is related both to the work load (Nielsen 1938) and to the relative load, i.e. the proportion of the maximal aerobic capacity of the subject (I Astrand 1960 Saltin and Hermansen 1966) but not to the heat production during work (Nielsen 1969). The reason for this apparently controlled increase in temperature is not known. It may be a prerequisite for driving the heat dissipating mechanism. The difference in plateau temperature after ingestion of NaCl and CaCl₂ solutions is not due to change in $\dot{V}O_{2\max}$ (G. Waagepetersen personal communication).

After intake of NaCl solution the initial increase in sweating was slower and \bar{T}_{re} and \bar{T}_{es} were higher than in the normal condition. The steady rate of sweating was lower or the same as normal in most subjects. When CaCl₂ solution had been taken \bar{T}_{re} and \bar{T}_{es} were lower, sweating increased faster and reached a higher level in most subjects (Fig. 3). The work load, metabolic rate and total heat production were the same in Ca, Na and control experiments. Therefore using the models for physiological thermoregulation (Hammel *et al* 1963 Hardy 1965 Stolwijk and Hardy 1966 Helstrom and Hammel 1967) the effect of the ions can be described as effecting a change in the set point, an increase with Na and a decrease with Ca⁺⁺ or as a change in the gain of the system (proportionality factors), a decrease with Na and an increase with Ca⁺⁺.

As to the possible sites of action of the ions, the concentration of Na and especially that of Ca⁺⁺ ions has a widespread effect on excitability and function of cells, neurotransmitter secretion (Richards and Sercombe 1970 Ilina *et al* 1972 Stjärne 1973) and effector organs (e.g. salivary gland Pors Nielsen and Petersen 1972 Gautvik *et al* 1972) vascular smooth muscle (Lundwall *et al* 1969 Johansson and Jonsson 1972). Their action on core temperature during work might be via the temperature centres in the central nervous system, perhaps by a mechanism like that described by Feldberg, Myers and their co-workers (Feldberg, Myers and Veale 1970 Myers, Veale and Yaksh 1971 Myers and Tytell 1972).

The rate at which divalent ions, especially Ca⁺⁺, penetrate from blood to brain and CSF (Bradbury and Wong 1972 Cooke and Robinson 1971 Levin and Patlac 1972) is low and regulated by homeostatic mechanisms. However, since blood-brain barriers are less restrictive in some areas of the central nervous system than in

others (Davson 1967) an increase in plasma Ca^{++} for 2–3 h might increase the Ca^{++} level of the brain. Correspondingly, Na^{+} ions might act directly on the temperature centres or, via specific osmoreceptors in the hypothalamus sensitive to Na^{+} in the CSF. Olsson (1972) showed in goats that Na^{+} has a greater effect than other ions on thirst and ADH secretion: the ions in equiosmotic hypertonic solutions.

A peripheral action is also a possibility. Experiments (Nielsen 1973 a) with rabbits which have no sweat glands indicated that peripheral interference with vascular tone was the most likely effect of increased plasma Na^{+} and Ca^{++} ions on body temperature. Ca^{++} produced vasodilatation and Na^{+} vasoconstriction. In the experiments reported here skin temperature and calculated peripheral tissue conductance decreased in most subjects after the intake of Ca^{++} and increased after Na^{+} solutions. If Na^{+} and Ca^{++} act by altering cutaneous vascular tone they therefore produce the opposite effect from that in rabbits: i.e. Na^{+} produces vasodilatation and Ca^{++} constriction.

Finally, the effect of the ions in humans could be a peripheral interference with the function of the sweat glands. This could be at the neuroglandular junction by interaction with neurotransmitter release or in the gland cells themselves changing their sensitivity to the central signal or by interference with the secretion/reabsorption processes in the ducts of the sweat glands.

The Advanced L 3 osmometer was obtained through a grant from the Danish Natural Science Research Council. Thanks are also due to the Institute of Biological Chemistry A, Copenhagen University, Denmark, who lent us their Zeiss photometer.

References

- AMATRIDA, T. T. J. and L. G. WELT. Secretion of electrolytes in thermal sweat. *J. appl. Physiol.* 1953, 5, 759–772.
- BRADLEY, M. W. B. and R. P. K. WONG. Entry of ^{45}Ca from blood into brain and cerebrospinal fluid of normal and adrenalectomized rats. *J. Physiol. (Lond.)* 1972, 223, 65 P.
- COOKE, W. J. and J. D. ROBINSON. Factors influencing ^{45}Ca metabolism in brain and other organs in *Adv. Soc. exp. Biol. (N.Y.)* 1971, 138, 906–913.
- DAVSON, H. *Physiology of the Cerebrospinal Fluid*. Churchill, 1967.
- DONAT, S. Über den Mechanismus der Wärmeregulation. *Pflügers Arch. ges. Physiol.* 1939, 241, 612–624.
- FELDBERG, W. R. D. MYERS and W. L. VEALE. Perfusion from cerebral ventricle to cisterna magna in the unanaesthetized cat. Effect of calcium on body temperature. *J. Physiol. (Lond.)* 1970, 207, 403–416.
- GALTVIK, K. M., M. KRIZ and K. LUND-LARSEN. Effects of alterations in Ca^{++} concentrations on secretion and protein synthesis in rat submandibular salivary gland. *Acta physiol. scand.* 1972, 85, 418–427.
- GREENLEAF, J. H. and B. L. CASTLE. Exercise temperature regulation in man during hypohydration and hyperhydration. *J. appl. Physiol.* 1971, 30, 847–853.
- HAMMEL, H. T., D. C. JACKSON, J. A. J. STOLWIJK, J. D. HARDY and S. B. STROMME. Temperature regulation by hypothalamic proportional control with an adjustable set point. *J. appl. Physiol.* 1963, 18, 1146–1165.
- HARDY, J. D. The set point concept in physiological temperature regulation. Chap. 6 in *Physiological Controls and Regulations*. Saunders, 1965. Ed. W. H. Yamamoto and J. R. Brobeck.
- HELLSTROM, B. and H. T. HAMMEL. Some characteristics of temperature regulation in the unanaesthetized dog. *Amer. J. Physiol.* 1961, 213, 547–556.

- JOHANSSON H and O JOHANSSON Cell volume as a factor influencing electrical activity of vascular smooth muscle *Acta physiol scand* 1968 72 456—468
- LEVY V and C M PATLAC A compartmental analysis of ^{22}Na kinetics in rat at cerebellum sciatic nerve and cerebrospinal fluid *J Physiol (Lond)* 1972 224 559—581
- LLINAS R, J R BLINKS and C NICHOLSON Ca²⁺ transient in presynaptic terminal of squid giant synapse Detection with Aequorin *Science* 1972 176 1122—1129
- LUNDWALL J, S MELLANDER and T WHITE Hyperosmolality and vasodilatation in human skeletal muscle *Acta physiol scand* 1969 77 224—233
- MYERS R D and W L VEALE The role of sodium and calcium ions in the hypothalamus in the control of body temperature of the unanaesthetized cat *J Physiol (Lond)* 1971 212 411—430
- MYERS R D and M TYTELL Fever Reciprocal shift in brain sodium to calcium ratio as set point temperature rises *Science* 1972 178 765—767
- MYERS R D, W L VEALE and T L YAKSH Changes in body temperature of the unanaesthetized monkey produced by sodium and calcium ions perfused through in cerebral ventricles *J Physiol (Lond)* 1971 217 381—392
- NIELSEN M Die Regulation der Körpertemperatur bei Muskelarbeit *Skand Arch Physiol* 1938 79 193—230
- NIELSEN B Thermoregulation in rest and exercise *Acta physiol scand* 1969 Suppl 323
- NIELSEN B Actions of intravenous Ca²⁺ and Na⁺ on body temperature in rabbits *Acta physiol scand* 1974 a 90 445—450
- NIELSEN B Effect of changes in plasma volume and osmolality on thermoregulation during exercise *Acta physiol scand* 1974 b 90 725—730
- NIELSEN B and M NIELSEN On the regulation of sweat secretion in exercise *Acta physiol scand* 1965 64 314—322
- NIELSEN S, PORS and O H PETERSEN Transport of calcium in the perfused submandibular gland of the cat *J Physiol (Lond)* 1972 223 685—697
- NEILSEN B, G HANSEN, S O JØRGENSEN and E NIELSEN Thermoregulation in exercising man during dehydration and hyperhydration with water and saline *Int J Biometeor* 1971 15 195—200
- OLSSON K Diuretic effects of intracarotid infusions of various hyperosmolar solutions *Acta physiol scand* 1972 85 517—522
- RICHARDS C D and R SERCOMBE Calcium, magnesium and the electrical activity of guinea pig olfactory cortex in vitro *J Physiol (Lond)* 1970 211 571—584
- SALTIN B and L HERMANSEN Esophageal rectal and muscle temperature during exercise *J appl Physiol* 1966 21 1757—1762
- STJÄRNE L Kinetics of secretion of sympathetic neurotransmitter as a function of external calcium Mechanism of inhibitory effect of prostaglandin E₂ *Acta physiol scand* 1973 87 428—430
- STOLTE J A J and J H HARDY Temperature regulation in man—a theoretical study *Pflügers Arch ges Physiol* 1966 a 291 129—262

DDT and Related Substances on Myelinated Nerve Effects on Permeability Properties

By

P. ARHEM, B. FRANKENHAUSER, R. GÖTHE and P. O'BRYEN¹

The main acute effect of the insecticide DDT on vertebrates seems to be on the central nervous system (Shankland 1964; Woolley 1970). In addition to these effects some rather specific effects on myelinated nerve fibres in the frog have been described (Hille 1968; van den Bercken 1972). The mechanism for impulse generation was affected since the dependence of sodium permeability on potential and time was altered by DDT. Hille found on fibres from *Rana pipiens* that the duration of the transient increase in sodium permeability which is associated with a positive potential step was increased in a fibre treated with DDT. DDT decreases the rate of inactivation of the sodium permeability mechanism. DDT also changed the rate of decay of the sodium currents after a short positive potential step. The rate of turn on of the sodium mechanism during a positive step was unaffected by DDT. Narahashi and Haas (1968) have described a very similar behaviour of DDT treated lobster giant nerve fibres.

The present study was undertaken in order to measure the acute effects on the myelinated nerve of DDT related substances. The tested compounds (DDT, DDE, DDD, DDMU, DDA, DDCN, bis-(p-chlorophenyl) acetamide) are or are likely metabolites of DDT and therefore are of interest in conjunction with the effects caused by DDT pollution of nature (Grummit and Marsh 1949; Grummit, Berté and Richard 1955; Albane *et al.* 1972; Jensen, Göthe and Lundstedt 1972).

The membrane currents associated with step changes of membrane potential were measured in single nodes of Ranvier in isolated myelinated nerve fibres from *Xenopus laevis*. The feed back technique used for control of membrane potential has been described earlier (Dodge and Frankenhaeuser 1958). The effects were investigated of the substances mentioned above on the membrane currents associated with step changes of membrane potential. The highly lipophilic substances tested were applied to the nerve fibre dissolved in Ringer's solution containing 1% ethanol in analogy with the procedures used by Narahashi and Haas (1968) and by Hille (1968). Saturated solutions were obtained by adding adjusted amounts of the compounds as ethanol solutions to proper volumes of Ringer's solution under stirring.

¹ Present address: Physiological Laboratory, Cambridge CB2 3 E6, England.

at room temperature. The effect of 1% ethanol *per se* was tested and found to decrease the sodium and potassium permeability less than 10%. Ethanol concentrations of 10% (i.e. about 2 M) blocked about 50% of the sodium mechanism and about 30% of the potassium mechanism. Still higher concentrations caused blocking effects which were only slowly reversible.

Experiments in which DDT was applied to fibres from *Xenopus* indicated that DDT had a marginal effect only. The striking effects described by Hille (1968) were not obtained. This discrepancy between the findings might either be explained on the basis of a difference between the two biological structures (fibres from *Xenopus* or *Rana pipiens* respectively) or a difference between possible contaminations of the substances. Measurements were therefore also made on fibres from *Rana pipiens*. The experiments fully verified Hille's findings and it is concluded that nerve fibres from these two species of frog respond in a different manner.

DDA and bis (p-chlorophenyl) acetamide affected clearly and regularly the permeability properties of the *Xenopus* nerve while no or only minor effects were obtained with the other substances (DDE, DDD, DDMU and DDCV) within an application time of about 10 min. The main effect of DDA was to decrease the rate of turn off of the potassium permeability at potentials in the range -50 to -120 mV. The potassium current is small in this potential range when the external $[K^+]$ is low since the electro-chemical driving force is small. With the fibre in solutions with high $[K^+]$ the currents are however larger and the effect is more readily measured. The potassium system of the normal fibre is described by the empirical equations given by Frankenhaeuser (1963). Fig. 1 shows the membrane currents associated with a potential step to +90 mV followed by a step to -90 mV in high $[K^+]$ solution before DDA was applied (A) and after (B). A 90% full effect appeared within 10 s. A very distinct change is seen in the time course of the current associated with the second potential step. The tail of potassium current decreased much slower than before DDA was applied. The time constant of the tail current was increased about 10 times. The time course was not always exponential when the first potential step was very large ($E \geq +80$ mV). The time course of the turn on of the potassium permeability at large potential steps did not change measurably. The curve relating potassium permeability to membrane potential was shifted about -20 mV along the potential axis. These effects were slowly but only partially reversible when the fibre was washed with high $[K^+]$ solution.

The second substance tested with a fast effect on the ionic currents of *Xenopus laevis* was bis (p-chlorophenyl) acetamide. This substance caused a decrease of the sodium permeability change and of the potassium permeability change during a potential step without affecting their time courses. The sodium permeability was decreased about 90% while the potassium permeability decreased between 5 and 50%. The full effect appeared within 30 s. It was not fully reversible when washed with Ringer's solution.

The substances tested in the present investigation are in structure very closely related to each other. DDT had a rapid and clear effect on the sodium system of

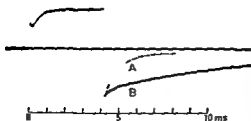


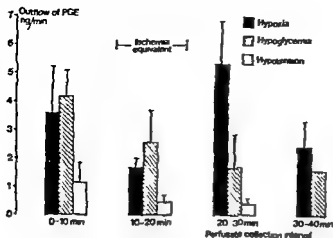
Fig. 1. Membrane current in solution with high $[K^+]$ associated with potential step to +90 mV from holding potential of -90 mV. A before B after application of DDA. (A scaled from record with different time scale. Straight line is current base line at -90 mV.)

Rana pipiens but only a negligible effect on fibres from *Xenopus*. Bis (p-chlorophenyl) acetamide blocked a fraction of the sodium mechanism and a fraction of the potassium mechanism. DDA caused a striking and very specific effect on the potassium system. A number of other related substances had no acute effects on the node of Ranvier in the *Xenopus* nerve.

This work was supported by the Swedish Medical Research Council (Project No. 14\543) Karolinska Institutets fonder and by a NIH special fellowship to P.O.B. (No. 1F11NS2575 01 NSRB).

References

- ALBONE E. S., G. EOLINTON, A. C. EVANS and M. M. RHEAD. Formation of bis-(p-chlorophenyl) acetonitrile (p,p-DDCN) from p,p-DDT in anaerobic sewage sludge. *Nature* (Lond.) 1971 240 420-421.
- BERLKEN J. VAN DEN. The effect of DDT and dieldrin on myelinated nerve fibres. *European J. Pharmacol.* 1977 205-214.
- DODGE F. A. and B. FRANKENHAELSER. Membrane currents in isolated frog nerve fibre under voltage clamp conditions. *J. Physiol. (Lond.)* 1958 143 76-90.
- FRANKENHAELSER B. A quantitative description of potassium currents in myelinated nerve fibres of *Xenopus laevis*. *J. Physiol. (Lond.)* 1963 169 424-430.
- GRUMMIT O. and D. MARSH. Derivatives of di-(p-chlorophenyl) acetic acid. *J. Amer. chem. Soc.* 1949 71 4156-4157.
- GRUMMIT O., A. BERCK and E. RICHARD. Di-(p-chlorophenyl) acetic acid. *Org. Synth. Coll.* 1955 III 70-272.
- HILLE B. Pharmacological modifications of the sodium channels of frog nerve. *J. gen. Physiol.* 1968 51 193-219.
- JENSEN S. R., R. GÖTHE and M. O. LINDSTEDT. Bis (p-chlorophenyl) acetonitrile (DDCN): a new DDT derivative formed in anaerobic digested sewage sludge and lake sediment. *Nature* (Lond.) 1972 240 421-422.
- NARAIWALLI T. and H. G. HAAS. Interaction of DDT with the components of lobster nerve membrane conductance. *J. gen. Physiol.* 1968 51 177-198.
- SEKARAKAVU D. L. Involvement of spinal cord and peripheral nerves in DDT poisoning syndrome in albino rats. *Toxicol. appl. Pharmacol.* 1964 6 197-213.
- WOOLLEY D. E. Effects of DDT on the nervous system of the rat. In *The Biological Impact of Pesticides on the Environment*. Editor J. W. Gillet. Environment Sci. Ser. No. 1. Corvallis 1970 pp. 114-124.



Perfused rabbit heart. Outflow of PGE in the perfusate during 4 consecutive periods of perfusate collection. Columns represent 3 different series where hypoxia ($n = 5$), hypoglycemia ($n = 4$) or hypotension ($n = 4$) was maintained during the second (10–20 min) period.

Thin layer chromatography (Green and Samuelsson 1964) of the lipid residue from the perfusate revealed that all the biological activity derived from its content of PGE mainly PGE₂.

During hypoglycemia a weak and reversible but definite increase in the isotonic contractile force recorded via a strain gauge transducer attached to the apex of the heart was observed. The heart rate was unaffected. The outflow of PG which was low during the initial resting period was further decreased during hypoglycemia. No increase in the outflow of PG was observed in the two post hypoglycemic periods; the PG outflow in this series decreasing exponentially through the entire experiment (Fig. 1).

In hearts perfused at a lowered pressure no change in beating rate or in contractile force was observed. The outflow of PG during the period of hypotension was low and in general there was an exponential decrease in PG release similar to that observed in the series of hypoglycemic hearts (Fig. 1).

Hypoxia caused a pronounced but almost completely reversible decrease in contractile force. During hypoxia the outflow of PG was low. In the post hypoxic state the PG synthesis and liberation of the heart was markedly increased in all experiments. The increase was limited in duration—during the last perfusate collection period the PG release had returned towards the pre-hypoxic values (Fig. 1).

The results clearly demonstrate that hypoxia but not hypoglycemia or hypotension stimulates the biosynthesis of prostaglandins in the heart. This observation is in accordance with a recent report published during the preparation of this paper showing that anoxia elicits release of prostaglandins from the heart (Kent *et al.* 1973). Since the liberation of prostaglandin E from the heart following hypoxia caused coronary vasodilatation it was suggested that prostaglandins are important in the development of reactive hyperemia (Kent *et al.* 1973). This view seems to be in contrast to the observation that the increased coronary flow caused by noradrenaline infusion attributable to some metabolic processes in the myocardium is

inhibited by prostaglandin E and enhanced by inhibition of PG synthesis by indomethacin or aspirin (Talesnik and Sunahara 1973). The discrepancy might be explained in terms of differences in species or technique.

In conclusion ischemia has earlier been shown to cause PG release from the kidney and occasionally from the heart. Since in the present study hypoxia but not hypoglycemia or hypotension caused release of PGE₂s we suggest that ischemia induces prostaglandin synthesis and liberation by restricting tissue oxygenation.

This study was supported by the Swedish Medical Research Council project 04\4341 and from Magnus Bergvalls Stiftelse.

References

- GILMORE N J R VANE and J H WYLLIE Prostaglandins released by the spleen *Nature* (Lond) 1968 218 1135-1140
- GREEN K and B SAMUELSSON Prostaglandins and related factors VII Thin layer chromatography of prostaglandins *J Lipid Res* 1964 5 117-120
- GRYGLEWSKI R and J R VANE The release of prostaglandins and rabbit aorta contracting substance (RCS) from rabbit spleen and its antagonism by anti-inflammatory drugs *Brit J Pharmacol* 1972 45 37-47
- JAFFE B M C W PARKER G R MARSHALL and P NEEDLEMAN Renal concentrations of prostaglandin E in acute and chronic renal ischemia *Biochem biophys Res Commun* 1977 49 799-803
- JUNSTAD M and A WENMÄLM On the release of prostaglandin E₂ from the rabbit heart following infusion of noradrenaline *Acta physiol scand* 1973 87 573-574
- KENT K M R W ALEXANDER J J PISANO H R KEIER and T COOPER Prostaglandin dependent coronary vasodilator responses *Physiologist* 1973 16 361
- LONGRO A J H D ISTRONITZ K CROVSHAW and J C MCGIFF Dependency of renal blood flow on prostaglandin synthesis in the dog *Circulat Res* 1973 32 712-717
- MCGIFF J C K CROVSHAW N A TERRAGIO A J LONGRO J C STRAND M A WILLIAMSON J B LEE and K K F No Prostaglandin like substances appearing in canine renal venous blood during renal ischemia *Circulat Res* 1970 27 765-787
- MINKES M S J R DOUGLAS JR and P NEEDLEMAN Prostaglandin release by the isolated perfused rabbit heart *Prostaglandins* 1973 3 439-445
- TALESNIK J and F A SUNAHARA Enhancement of metabolic coronary dilatation by aspirin like substances by suppression of prostaglandin feed back control *Nature new Biol* 1973 244 351-353
- WENMÄLM A Studies on mechanisms controlling the secretion of neurotransmitters in the rabbit heart *Acta physiol scand* 1971 87 Suppl 363
- WENMÄLM A and M JUNSTAD Endogenous prostaglandin mediated inhibition of parasympathetic neurotransmission in the rabbit heart *Acta physiol scand* 1974 90 Suppl 396

Blood Flow and Oxygen Consumption in the Rat Brain in Dilutional Anemia

By

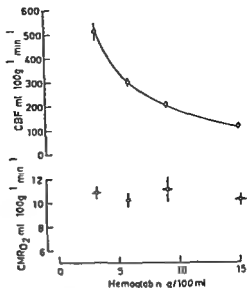
HALLDOR JOHANSSON and Bo J. SIESJO

Although it has been well established that anemia increases the cerebral blood flow (CBF) in man and experimental animals (Scheinberg 1951, Heyman *et al* 1952, Haggendal and Norback 1966 Paulson *et al* 1972) there is no agreement on the causative mechanisms. In dilutional anemia both the viscosity and the oxygen content of the blood are reduced and either of these factors may increase CBF. Haggendal and Norback (1966) noted that variations in blood hematocrit between 70 % and 30 % did not affect CBF in dog experiments and attributed the increase in CBF below a hematocrit of 30 % to tissue hypoxia. However Paulson *et al* (1972) concluded that the increase in CBF induced in man by a 20 % reduction in hematocrit was at least partly due to lowered viscosity.

In the present experiments dilutional anemia was induced in rats by bleeding and substitution with homologous plasma and measurements of CBF, CMR_{O_2} and cerebral venous P_{O_2} were carried out at steady state hemoglobin concentrations of 1.5 to 3 g (100 ml)⁻¹. The objectives of the study was to quantitate the increase in CBF induced by the anemia and to evaluate if signs of tissue hypoxia were present as evidenced by a decrease in CMR_{O_2} or cerebral venous P_{O_2} .

Materials. Wistar rats (300-400 g) were initially anesthetized with 2 % halothane tracheotomized, intubated and then maintained artificially ventilated on 70 % N_2O and 30 % O_2 . Both femoral arteries and one femoral vein were catheterized and a caudal part of the superior sagittal sinus was exposed. The body temperature was kept close to 37 °C. The arterial P_{CO_2} in the range of 34-40 mm Hg and the arterial P_{O_2} above 100 mm Hg. Dilutional anemia was induced by withdrawing blood from the carotid artery and iv substituting with amounts of homologous plasma *in vivo* sufficient to maintain mean arterial blood pressure at 120-140 mm Hg. In the control group the hemoglobin concentration remained at about 15 g (100 ml)⁻¹. In 4 other groups the Hb concentration was lowered to 12.9 g and 3 g (100 ml)⁻¹ respectively. In each animal a steady state period of 30 min was allowed before CBF, CMR_{O_2} and venous P_{O_2} were measured. The CPP was measured with a $\text{^{133}Xe}$ modification of the Kety and Schmidt principle and the CMR_{O_2} was derived from CBF and from the arteriovenous O_2 differences (see Eklof *et al* 1973). P_{O_2} was analyzed with a conventional mercuric electrode.

Fig. 1 shows CBF and CMR_{O_2} related to the blood Hb concentration. When the latter was reduced from a normal value of 15 to a minimal value of 3.1 (100 ml)⁻¹ the CBF increased progressively from 110 to 210 ml \times (100 g)⁻¹ \times min⁻¹. In the group with a Hb concentration of 3.1 g \times (100 ml)⁻¹ the total oxygen content of arterial blood was reduced to 20 % of normal. In spite of this profound anemic hypoxemia and the



Cerebral blood flow (CBF) and cerebral metabolic rate for oxygen (CMRO₂) in rat brain related to the arterial hemoglobin concentration. The values are means \pm S.E.

5 fold increase in CBF, the CMRO₂ remained unchanged. Most surprisingly, none of the anemic animals showed any significant alteration of the cerebral venous P_{O_2} , which remained in the range 40–50 mm Hg in all groups. Since these results did not reveal any hypoxic stimulus to the increase in CBF, the Hb concentration was lowered to about $6 \text{ g} \times (100 \text{ ml})^{-1}$ in 6 animals, and the brains were frozen *in situ* for subsequent metabolite analyses. In these animals the cortical lactate content was 1.99 ± 0.11 (mean \pm S.E.), a value only slightly higher than that of normoxic animals with normal Hb content (see Bachelard *et al.* 1974).

When the arterial P_{O_2} is lowered to 20–25 mm Hg there is a decrease in arterial oxygen content of the same magnitude as that observed in animals with a Hb content of $3 \text{ g} \times (100 \text{ ml})^{-1}$ (see Johansson and Siesjö 1974). With both types of hypoxia (hypoxic and anemic) there are 4 to 5 fold increases in CBF at an unchanged CMRO₂, suggesting that the oxygen supply is maintained by a homeostatic increase in CBF. However, in hypoxic hypoxia there is a decrease in venous P_{O_2} and an increased lactate content in the tissue as a possible stimulus to hyperemia (Bachelard *et al.* 1974). In contrast, the present experiments demonstrate that anemic hypoxemia induces a marked increase in CBF with no decrease in venous P_{O_2} and with an increase in the tissue lactate content which, at a comparable reduction in arterial oxygen content, is far less pronounced than in hypoxic hypoxemia. The results demonstrate a remarkable energy homeostasis in the brain in dilutional anemia and suggest that the viscosity factor may be much more important than previously realized.

This study was supported by grants from the Swedish Medical Research Council (Projects No 14\–63 and 14\–2179) from the Swedish Bankers' Society and from U.S. PHS Grant No 5 RO1 NS 07838-03 from NIH.

References

- BACHELARD H, L. LEWIS U, PONTEN and B. K. SIESJO Mechanisms activating glycolysis in the brain in arterial hypoxia *J Neurochem* In press
- EKLOF B, N. A. LASSEN, L. NILSSON, K. NORBERG and B. K. SIESJO Blood flow and metabolic rate for oxygen in the cerebral cortex of the rat. *Acta physiol scand* 1973 88 587—589
- HEYMAN A, J. L. PATTERSON and T. W. DUKE Cerebral circulation and metabolism in sickle cell and other chronic anemias with observations on the effects of oxygen inhalation *J clin Invest* 1952 31 824—828
- HAGGENDAL E and B. NORBÄCK Effect of viscosity on cerebral blood flow *Acta chir scand* 1966 Suppl. 364 13—21
- JOHANSSON H and B. K. SIESJÖ Blood flow and oxygen consumption of the rat brain in profound hypoxia. *Acta physiol scand* 1974 90 281—282
- PALLSON O, B. H. H. PARVING, J. OLESEN and E. SKINHOJ Influence of carbon monoxide and of hemodilution on cerebral blood flow and blood gases in man *J appl Physiol* 1973 35 No 1 111—116
- SCHNEINBERG F Cerebral blood flow and metabolism in pernicious anemia *Blood* 1951 6 213—227

Failure of Adrenalectomy to Influence the Acute Effect of FSH on Ovarian Metabolism

By

LARS NILSSON

It has earlier been found that intravenous (iv) injection of FSH to prepubertal rats shortly before removal of the ovaries stimulates the ovarian uptake *in vitro* of the non utilizable amino acids α -amino isobutyric acid (AIB) and L-amino-cyclopentane carboxylic acid. The same procedure also stimulates the uptake and incorporation into protein of several normal amino acids as well as ovarian glycolysis (for ref see Ahren *et al* 1969). An interesting but as yet unexplained finding is that ether anesthesia of prepubertal rats under certain conditions increased ovarian AIB uptake and that FSH did not further enhance ovarian amino acid uptake (Ahren *et al* 1967). This effect of anesthesia might be attributed to an effect on the adrenal cortex, an assumption which is favoured by many reports in the literature that adrenal cortical steroid can influence the function of the ovary both directly and indirectly via the pituitary gland (for ref see Goldzieher 1968). A project has therefore been started to investigate whether adrenal corticosteroids can influence protein and carbohydrate metabolism in the prepubertal rat ovary. As an initial part of this project the rate of AIB uptake and the lactic acid production in isolated ovaries from adrenalectomized rats were studied with the immediate question—whether the presence of corticoids is necessary for the acute effects of FSH.

24 day old rats sham operated when 20 days of age and 24, 28 and 35 day-old rats adrenalectomized through dorsal incisions when 90 days old were used. After the injection of FSH ovaries were taken out dissected free from extraneous tissues and incubated for 2 h in Krebs bicarbonate buffer containing 5.5 mM glucose, 0.1 mM AIB-1-¹⁴C (0.1 μ Ci/ml) and 0.02 mM sucrose-6-6 ³H (25 μ Ci/ml). Lactic acid accumulation in the medium was measured according to Lundholm *et al* (1963). Distribution ratios of AIB were determined as described earlier (e.g. Ahren and Rubinst in 1965). In calculating the distribution ratios sucrose space was considered to represent the extra cellular space.

Ovine FSH (NIH FSH S9) was supplied by the Endocrinology Study Section of the National Institutes of Health (NIH) USA. Statistical significances as compared to controls were calculated by Student's t test. A p-value less than 0.05 was considered significant.

It can be seen from Table I that iv injection of FSH 2 h before removal of the ovaries stimulated the rate of *in vitro* uptake of AIB and the production of lactic acid in the adrenalectomized rats as markedly as in the normal animal. In 2 other

TABLE I Effect of FSH on AIB uptake and lactic acid production in ovaries from normal and adrenalectomized rats

Injection	Sham operated rats 24 days	Adrex rats 24 days	Adrex rats 35 days
		AIB distribution ratio	
NaCl	12.1 ± 0.6 (6)	10.9 ± 0.4 (5)	11.6 ± 0.7 (10)
FSH	17.7 ± 0.7 (6)	17.3 ± 0.3 (5)	16.8 ± 0.7 (8)
		Lactic acid production	
NaCl	141 ± 12 (6)	123 ± 11 (6)	122 ± 7 (10)
FSH	353 ± 27 (6)	441 ± 19 (6)	316 ± 14 (8)

Sham operated 24 day-old rats and adrenalectomized (adrex) rats 24 or 35 days of age were injected i.v. with 500 µg NIH FSH 59 per 100 g b.wt. under light ether anesthesia. Control animals received an equal volume of solvent (0.9% NaCl 0.5 ml/100 g b.wt.). 2 h after injection rats were killed, ovaries taken out and incubated in Krebs bicarbonate buffer containing 5.5 mM glucose and 0.1 mM AIB. AIB distribution ratio is expressed as CPM per ml intracellular water/CPM per ml medium and lactate production as µg/100 mg wet tissue weight × 2 h. Means ± S.E. from a typical experiment with numbers of observations within brackets. All hormonal effects highly significant from controls with Student's *t* test.

experiments (not given in the table) FSH was also found to stimulate amino acid incorporation into ovarian protein in the adrenalectomized rats. These results show that the acute effects of FSH on ovarian amino acid transport and glycolysis are not mediated via the adrenal cortex and a permissive action of the adrenal cortical hormones for these FSH effects is therefore unlikely. It is still possible that the adrenal cortex is essential for the above mentioned effects of ether anesthesia.

The histological appearance of the ovaries from 35 day old adrenalectomized rats in this study was in agreement with that in other reports (e.g. Har et al. 1954), i.e. small ovaries with an abundance of small follicles and very scarce interstitial tissue. The effect of FSH on this type of ovary is in accordance with the theory of theca cells as target cells for FSH (e.g. Ahren et al. 1969) since the ovarian follicles of the adrenalectomized rats although small for the chronological age of the animals were as well developed as those of 24 day-old rats.

In a preliminary experiment LH was found to be markedly less effective in stimulating AIB uptake and leucine incorporation in ovaries from 35 day-old adrenalectomized rats than it was in normal rats. This observation indicates that ovaries from adrenalectomized rats might constitute another useful model for differentiating the effects of FSH and LH respectively on different compartments of the ovary.

The author wishes to thank NIH for the generous supply of FSH. For valuable advice my thanks are due to professor Kurt Ahren. Skilful technical assistance was offered by Mrs Ann Cathrine Schütt. This work was supported by grants from US Public Health (2 RO1 HD02195) from the Swedish Medical Research Council (B74-03\27) and from the Faculty of Medicine, University of Göteborg.

References

- ALLEN, A. and L. RUBINSTEIN. Effects of follicle stimulating hormone on amino acid transport and protein biosynthesis in the isolated rat ovary. *Acta physiol. scand.* 1963, 64: 463-474.

- ANDERSON, K. L. HAMBERGER and M. HARTFORD Further studies on the effect of follicle stimulating hormone on amino acid transport in the isolated rat ovary *Acta physiol scand* 1967 71 211—223
- ANDERSON, K. L. HAMBERGER and L. RUBINSTEIN Acute *in vivo* and *in vitro* effects of gonadotrophins on the metabolism of the rat ovary. In *The Gonads* Ed McEwen's K. W. Appleton Century Crofts New York 1969 pp 327—334
- GOLDSTEINER, J. W. The interplay of adrenocortical and ovarian function. In *The Ovary* Ed Mack H. C. Charles C. Thomas Springfield 1968 pp 106—129
- KAR, A. B. J. N. HARKLEY and S. K. ROY The effect of adrenocorticotrophic hormone on the genital organs of young female rats *Acta endocr (Kbh)* 1954 15 101—108
- LUNDHOLM, L. E. MOHRE LUNDHOLM and N. SÄEDHOLM Comparative investigation of methods for determination of lactic acid in blood and in tissue extracts *Scand J clin Lab Invest* 1963 15 311—316

Measurement of Colloid Osmotic Pressure of Interstitial Fluid

By

H. M. JOHNSEN

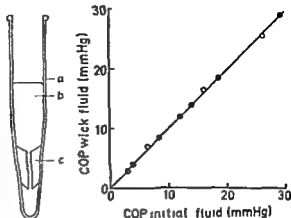
Protein concentration of interstitial fluid has recently been estimated by elution of protein from nylon wicks having been equilibrated with interstitial fluid (Aukland and Fadnes 1973)

Measurement of colloid osmotic pressure (COP) of the wick fluid would be of great interest but requires 1) isolation of undiluted fluid from the wicks and 2) an osmometer for small fluid samples. The latter requirement has been satisfied by construction of a membrane osmometer for samples down to 5 μ l (Aukland and Johnsen 1974) and the present report describes a method for isolation of native wick fluid. Recovery from plasma dilutions has been tested *in vitro* and measurements on interstitial fluid from subcutaneous tissue of rats are reported as an example. Some preliminary measurements have been reported previously (Aukland and Johnsen 1973).

Nylon wicks 0.5 mm thick and consisting of about 500 filaments are sewn into the tissue under investigation as described by Aukland and Fadnes (1973). After equilibration with the surrounding tissue fluid for about 1 h the wicks are removed. The end portions leading through the skin are cut off and the middle portion quickly transferred to a centrifuge tube filled with mineral oil. Blood stained wicks are discarded. The tube is conical and provided with a funnel shaped wick support near the bottom (Fig. 1). A central hole wide enough to fit a hematocrit capillary leads through the support. The oil has a density of 0.88 so that centrifugation forces watery fluid from the wicks towards the bottom of the tube while the wicks themselves are retained by the support. After centrifugation for about 15 min at $1300\times g$ a drop of fluid is accumulated at the pointed bottom of the tube. Evaporation is prevented by the oil. The wicks are then removed from the top of the support and the fluid at the bottom of the tube is pipetted off into a hematocrit capillary through the hole in the wick support. Inevitably some oil will be mixed up with the fluid on pipetting. This contamination is separated from the water phase by spinning the capillary tube in a hematocrit centrifuge for 5 min after previous sealing of one end of the tube. For measurement of COP the sealed end of the capillary is cut off and the fluid allowed to drain into the sample chamber of the osmometer (Aukland and Johnsen 1974). Although 5 μ l will suffice for each measurement the transfer of fluid to the osmometer membrane is easier with a fluid volume of 10 μ l.

Fig 1 Axial section through centrifuge tube (a) filled with mineral oil (b) Wick support made from acrylic plastic (c)

Fig 2 Colloid osmotic pressure (COP) of initial plasma dilutions compared to COP of the same dilutions after passage through nylon wicks and mineral oil.



or more which is usually obtained by accumulating 3—4 wicks with a total length of about 10 cm

To test the validity of the separation method COP of different dilutions of plasma with 0.9 % NaCl were measured. Nylon wicks were soaked in the same solutions for 1 h and then COP were measured in the fluid isolated from the wicks as described above. As evident from Fig 2 COP of wick fluid did not deviate by more than 0.5 mm Hg from that estimated directly on initial plasma dilutions indicating that COP of the fluid is not changed by the passage through the wicks and mineral oil.

The method has been utilized to determine COP of interstitial fluid from subcutaneous tissue of 37 rats weighing from 250 to 375 g. During implantation of the wicks the rats were anesthetized with ether and usually woke up within half an hour. The wicks were removed after 1 h. Corresponding values of plasma and interstitial fluid COP were measured on 12 of these rats. Plasma COP averaged 20.5 mm Hg (Range 18.5—22 mm Hg SD 1.2 mm Hg) and mean interstitial fluid COP of the 12 rats was 10.6 mm Hg (Range 9—12 mm Hg SD 0.8 mm Hg). No significant correlation ($r = 0.5$ $p > 0.1$) was found between plasma and interstitial fluid COP in this group of normal rats. Interstitial fluid COP of the remaining 25 rats averaged 10.8 mm Hg (Range 9—14 mm Hg SD 1.0 mm Hg).

The directly measured COP agrees well with the average of 10.2 mm Hg calculated from the average albumin and total protein concentrations of wick fluid (Aukland and Fadnes 1973) using the formula for plasma given by Landis and Pappenheimer (1963). Thus the relative composition of wick fluid globulins would not seem to be very different from that of serum globulins.

The present determinations give an average net transcapillary colloid osmotic pressure of about 10 mm Hg and permit calculation of the mean capillary pressure—provided 1) that a reasonable estimate of interstitial fluid hydrostatic pressure can be made and 2) that there is no net pressure difference across the capillary.

wall. If the interstitial pressure is 6–8 mm Hg subatmospheric as obtained by Guyton *et al* (1971) by measurement on implanted plastic capsules the present data would imply a mean capillary pressure of only 2–4 mm Hg which is not likely to be correct. On the other hand an interstitial fluid pressure in rat skin of minus 2 mm Hg as measured with Scholander's wick technique (Snashall *et al* 1971) or 0 to minus 2 mm Hg as measured with a modified Scholander method in which the wick is contained in a thin needle provided with a side hole (Fadnes 1973) gives a mean capillary pressure of 8–10 mm Hg. This is not far off from a recent estimate of the isogravimetric capillary pressure of 12 mm Hg in cat hindlimbs in which care was taken to prevent overhydration of the tissue (Eliassen *et al* 1974).

References

- ATKLAND K and H O FADNES Protein concentration of interstitial fluid collected from rat skin by a wick method *Acta physiol scand* 1973 88 350–358
- ATKLAND K and H M JOHNSON A colloid osmometer for small fluid samples *Acta physiol scand* 1974 90 485–490
- ATKLAND K and H M JOHNSON Measurement of interstitial fluid colloid osmotic pressure *Acta physiol scand* 1973 87 2A
- ELIASSEN E B FOLKOV S HILTON E ÖBERG and B RIPPÉ Pressure volume characteristics of the interstitial fluid space in the skeletal muscle of the cat *Acta physiol scand* 1974 90 583–593
- FADNES H O Interstitial fluid pressure and albumin concentration in experimental hypoproteinemia *Acta physiol scand* 1973 Suppl 396 61
- GUYTON A C H J GRANGER and A C TAYLOR Interstitial fluid pressure *Physiol Rev* 1971 51 527–563
- LANDIS E M and J R PAPPERHEIMER Exchange of substances through the capillary walls Pp 961–1034 in *Handbook of Physiology* Section 2 Circulation Vol II Eds W F Hamilton and P Dow Washington D C Amer Physiol Soc 1963
- SNASHALL D J LUCAS A GLZ and M A FLOYER Measurement of interstitial fluid pressure by means of a cotton wick in man and animals. An analysis of the origin of the pressure *Clin Sci* 1971 41 35–53

Morphology and Storage Properties of Rat Mast Cell Granules Isolated by Different Methods

By

PER ANDERSON PAL RÖHLICH¹ STUART A SLORACH and BÖRJE UVNÄS

Received 1 October 1973

Abstract

ANDERSON P P RÖHLICH S A SLORACH and B UVNÄS *Morphology and storage properties of rat mast cell granules isolated by different methods* Acta physiol scand 1974 91 145—153

Pure granule fractions were obtained from rat mast cells by sonication in sucrose for different times and at different amplitudes. Two types of mast cell granule were found. One type appeared dark blue in the light microscope when stained with toluidine blue—azur A and was homogeneous, electron dense and surrounded by a trilaminar membrane when observed in the electron microscope; thus this type had the same appearance as mast cell granules *in situ*. The second type appeared pink after staining with the above dye and had a swollen, reticular appearance with a reduced electron density and no surrounding membrane when observed in the electron microscope. With increasing sonication time and amplitude there was an increase in the proportion of the swollen, less electron dense granules with no surrounding membrane and a concomitant decrease in the amount of histamine retained (as shown by the histamine/heparin and histamine/protein ratios) after washing in isotonic sodium chloride. Granules isolated from water lysed mast cells or mast cells treated with compound 48/80 were all of the second type with no perigranular membrane; they released their histamine when suspended in isotonic sodium chloride solution.

Mast cells isolated from the peritoneal and pleural cavities of rats contain histamine and 5-hydroxytryptamine (5-HT). *In situ* these amines are stored in basophil granules surrounded by a trilaminar membrane, the perigranular membrane. On the other hand granules released from mast cells treated with compound 48/80 (Bloom and Haegermark 1965; Röhlisch, Anderson and Uvnäs 1971) or antigen *in vitro* (Anderson, Slorach and Uvnäs 1973) or granules isolated from mast cells lysed with distilled water have been reported to be membrane free.

Extensive studies in our laboratories on granules isolated by the latter procedure have established that amines bind ionically to carboxyl groups in the heparin-protein complex which forms the matrix of the granules (Uvnäs, Åberg and Bergendorff 1970; Bergendorff and Uvnäs 1972). In fact, since they lack a limiting mem-

¹ Visiting scientist from The First Central Laboratory of Electron Microscopy, Semmelweis Medical University, Budapest IX, Hungary.

brane, such granules behave like small particles of a weak cation exchange resin. They are able to retain histamine (as well as other amines) in cation free media but they release the amine on exposure to cations *e.g.* isotonic saline and take up an equivalent amount of cation. Accordingly when mast cells suspended in isotonic sucrose were challenged with compound 48/80 the discharged granules were found to contain histamine. The granules were depleted of their histamine immediately they were resuspended in isotonic saline—as were granules discharged from mast cells suspended in isotonic saline when exposed to compound 48/80. Similarly granules obtained from mast cells lysed in deionized water retain histamine provided they are suspended in a cation free medium but they release it completely in isotonic saline.

Lagunoff *et al.* (1964) reported that granules isolated from rat peritoneal mast cells sonicated in isotonic sucrose were also membrane free. Such granules were found to have retained part of their histamine but released it when resuspended in saline. The histamine release increased with increasing NaCl concentration the granule histamine stores being totally depleted at 1 M NaCl. In our hands however granules isolated from sonicated mast cells behaved rather unpredictably. It is true that they contained histamine and that release of histamine occurred when NaCl was present in the suspension fluid. However the amounts of histamine retained and released varied between experiments in some considerable amounts of histamine were retained even after suspending the granules in isotonic NaCl with no apparent correlation between NaCl concentration and the amount of histamine released.

The behaviour of the granules from sonicated cells seemed to be at variance with our observations on granules isolated from water lysed mast cells and thereby also with our hypothesis that histamine is stored in weak ionic linkage to the granule matrix. In order to explain the unpredictable behaviour of granules isolated from sonicated mast cells the present comparative study on the morphology and storage properties of granules isolated from cells sonicated under different conditions was performed.

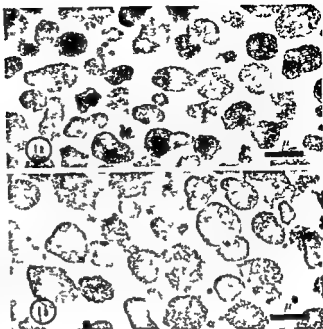
Methods

Preparation of mast cell suspension. 10–12 male Sprague Dawley rats (350–400 g) were used in each experiment. The rats were exsanguinated under light ether anaesthesia by cutting the carotids and a small incision was made along the abdominal midline. 9 ml of a buffered salt solution (NaCl 145 mM, KCl 2.7 mM, CaCl₂ 0.9 mM with 10% v/v Sorensen buffer NaH₂PO₄ + KH₂PO₄ 6.7 mM, pH = 7.0) was pipetted into the peritoneal cavity. After carefully massaging for 1–2 min the peritoneal fluid was collected and layered onto a discontinuous 30–40% Ficoll gradient. After opening the diaphragm an additional 4.5 ml of buffered salt solution was used to collect the cells from the pleural cavity. The gradients were centrifuged (350 × g, 10 min) and the mast cells were collected from the diffuse band at the interface between the 30 and 40% Ficoll layers. The mast cells were washed twice in the above buffered salt solution to which 1 mg of human serum albumin per ml had been added. The cell suspension so obtained contained more than 95% mast cells.

Isolation of granules released from compound 48/80 treated mast cells and cells lysed with water. Half of the mast cell suspension in one experiment was incubated with compound 48/80 (2 µg/ml) for 10 min at 37°C. The suspension was then centrifuged (350 × g, 10 min, 4°C).

Fig 1a A homogeneous granule fraction isolated from mast cells treated with compound 48/80 (2 $\mu\text{g}/\text{ml}$). The granules have a reticular appearance and are swollen and less electron dense compared to normal granules in untreated mast cells. No membranes surrounding the granules can be seen. Magnification 9600 \times .

Fig 1b A homogeneous granule fraction obtained from mast cells treated with distilled water. The same ultrastructural appearance as in Fig 1a. Magnification 9600 \times .



and the resulting supernatant set aside. The precipitated cells were washed twice with the albumin-containing buffered salt solution, centrifuging at 350 $\times g$ for 10 min after each wash. The granules were precipitated by centrifuging the bulked supernatants at 3000 $\times g$ for 25 min at 4 $^{\circ}\text{C}$.

The remaining half of the mast cell suspension was centrifuged (350 $\times g$, 10 min). The precipitated cells were suspended in distilled water (2 ml/rat) and the pH was adjusted to 7.1. After shaking gently for 5 min, the lysed cell suspension was centrifuged (350 $\times g$, 10 min, 4 $^{\circ}\text{C}$). The granule-containing supernatant was centrifuged (3000 $\times g$, 25 min, 4 $^{\circ}\text{C}$) to obtain a granule pellet.

Isolation of granules from sonicated mast cells. The isolated mast cells were suspended in about 25 ml of ice-cold 0.34 M sucrose. 5 ml aliquots cooled in ice were sonicated with a MSE 100 watt ultrasonic disintegrator set at 4 μm amplitude for 5, 60 or 120 s or at 8 μm for 5 or 60 s using a 10 mm probe. The sonicated suspensions were centrifuged (350 $\times g$, 15 min, 4 $^{\circ}\text{C}$) and the granule-containing supernatants were then centrifuged (3000 $\times g$, 20 min, 4 $^{\circ}\text{C}$). The sediments were suspended in 0.15 M NaCl adjusted to pH 7.0 with Sørensen phosphate buffer and half of the suspension was taken for electron microscopy and half for histamine, heparin and protein assays. The samples were centrifuged (3000 $\times g$, 20 min, 4 $^{\circ}\text{C}$) and the supernatants were discarded.

Histamine in the precipitate was assayed by the method of Shore, Burkhalter and Cohn (1959) as modified by Bergendorff and Uvnäs (1972). Heparin was measured by the amino-sugar method of Cessi and Piñero (1960) and is expressed in terms of a heparin standard. Protein was determined by the method of Lowry *et al.* (1951).

Electron microscopy. The granule pellets were fixed with cold (4 $^{\circ}\text{C}$) 5% glutaraldehyde in Millonig phosphate buffer, pH = 7.2 for 40 to 75 min at room temperature and the granule suspensions were then centrifuged (3000 $\times g$, 20 min, 20 $^{\circ}\text{C}$). The granule sediments were washed twice with Millonig phosphate buffer, pH = 7.2 and post-fixed in 1% OsO_4 in the same buffer for 40 min at 4 $^{\circ}\text{C}$. The suspensions were then centrifuged (3000 $\times g$, 20 min, 4 $^{\circ}\text{C}$), washed and recentrifuged. The pellets were dehydrated in an ethanol series transferred through styrene or propylene oxide and embedded in Vestopal W.

Thin sections for electron microscopy were cut on an LKB Ultratome III or a Reichert ultramicrotome OM U3 and stained with uranyl acetate and diluted lead citrate before examination in a Philips EM 300 electron microscope at 80 kV. Semi-thin sections for light microscopy were stained with a solution of toluidine blue and azur A containing 60% sucrose.

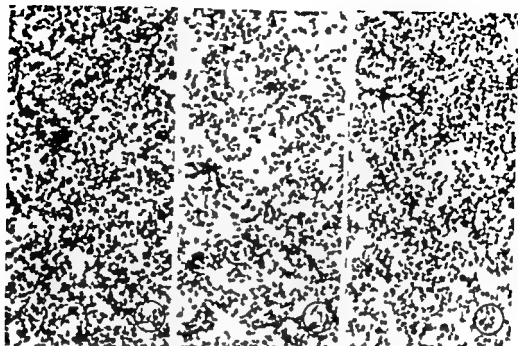


Fig. 2 Light microscopy of granules isolated from mast cells sonicated at $\frac{1}{2}$ μ m amplitude for (a) 5 s (b) 60 s (c) 120 s. Note the decrease in the proportion of dark staining granules with longer sonication times. Magnification 1300 \times .

Materials

Glutaraldehyde (25%, especially purified for electron microscopy) TAAB Laboratories Reading, England
 Heparin sodium (pig mucous) containing 92 per cent sulphur AB Vitrum Stockholm Sweden

Results

Granules from compound 48/80 treated mast cells and mast cells lysed in water

Light microscopy All granules had a swollen appearance and stained pink with toluidine blue—azur A.

Electron microscopy Granules isolated by either of the above procedures appeared almost identical in the electron microscope (Fig. 1a, 1b). The granule fractions were homogeneous and free from other cell organelles. Compared to mast cell granules *in situ* they were swollen and less electron dense. The matrix was no longer homogeneous but had a reticular appearance. No membrane surrounding the granules could be seen.

Granules from sonicated mast cells

Light microscopy In the light microscope the granules appeared either dark blue or pink after staining with toluidine blue—azur A. The pink staining granules had

Fig 3 Light microscopy of granules isolated from mast cells sonicated at 8 μ m amplitude for (a) 5 s (b) 60 s. The proportion of dark staining granules decreases with increasing sonication time and is also decreased compared to corresponding sonication times at 4 μ m setting. (See Fig 2a and 2b) Magnification 1200 \times

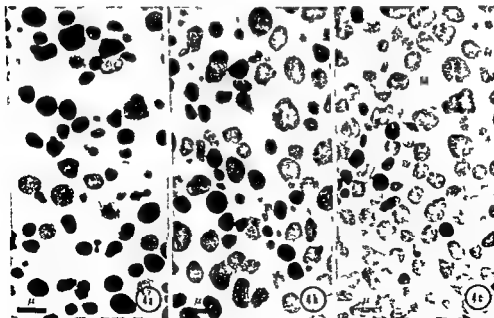
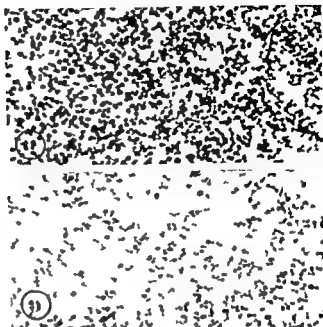


Fig 4 Electron micrographs of granules isolated from mast cells sonicated at 4 μ m amplitude for (a) 5 s (b) 120 s (c) 120 s. Two types of granule can be seen. One is homogeneous and electron dense (osmophilic) the other swollen and less electron dense. The proportion of electron dense granules decreases with increasing sonication time. Magnification 7600 \times

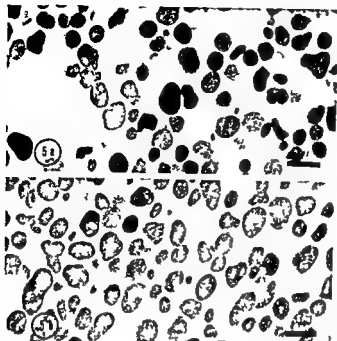


Fig 5 Electron micrographs of granules isolated from mast cells sonicated at 8 μ m amplitude for (a) 5 s (b) 60 s. The proportion of dense granules decreases with longer sonication time and also at this higher sonication amplitude compared to the corresponding times at 4 μ m. Magnification 7500 \times .

a swollen appearance. Fig 2 shows granules isolated from mast cells sonicated at 4 μ m amplitude for 5, 60 and 120 s. The proportion of dark blue staining granules (in Fig 2 seen black) was highest with the shortest sonication time and decreased progressively with increased sonication. Granules isolated from mast cells sonicated at 8 μ m for 5 and 60 s respectively can be seen in Fig 3. Again the proportion of dark blue staining granules decreased with sonication time. Sonication at 8 μ m gave fewer dark blue staining granules than sonication for the corresponding time at 4 μ m (Fig 3 a, 2 a and Fig 3 b, 2 b).

Electron microscopy. As in the light microscope two distinct types of granule could be seen at the ultrastructural level. One type had a homogeneous electron dense appearance, the other type was swollen and less electron dense. The propor-

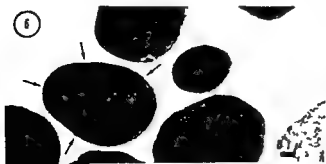


Fig 6 High power electron micrograph of granules isolated from mast cells sonicated at 4 μ m for 5 s in sucrose. Note that the homogeneous electron dense granules are surrounded by a perigranular membrane (arrows). The swollen less electron dense granule in the lower right corner has no limiting membrane. Magnification 36 000 \times .

TABLE I

Sonication conditions	Histamine	Histamine
	Heparin	Protein
4 μ m 5 s	0.12 (0.16)	0.18 (0.22)
4 μ m 60 s	0.07 (0.10)	0.07 (0.10)
4 μ m 120 s	0.06 (0.07)	0.06 (0.06)
8 μ m 5 s	0.06 (0.08)	0.13 (0.14)
8 μ m 60 s	0.01 (0.01)	0.01 (0.01)

Histamine, heparin and protein expressed in μ g/sample. Values refer to the experiment from which the electron micrographs in Figs 4–6 were taken. Values in brackets are means of 10 and 6 experiments respectively.

tion of electron dense granules decreased with increasing sonication time (Fig 4 a b c). Likewise increasing the sonication amplitude from 4 μ m to 8 μ m decreased the proportion of electron dense granules (cf Fig 4 a 5 a and Fig 4 b 5 b). At favourable planes of sectioning it could be seen that the electron dense granules were surrounded by a lamellar membrane (Fig 6). No such membrane could be seen around swollen, less electron dense granules.

Granule contents. The histamine/heparin and histamine/protein ratios in the different granule fractions after washing in isotonic sodium chloride are given in Table I. Since the matrix of the granules consists mainly of a heparin protein complex, the ratios in the table reflect fairly well the amount of histamine per unit weight of granule. Both of the ratios show that the amount of histamine per unit weight of granule decreases with increasing sonication time and also with increasing sonication amplitude. Thus fractions containing a high proportion of dark blue staining or electron dense granules, i.e. granules with a surrounding membrane, have a correspondingly higher amount of histamine. It should be noted that all granule fractions have been exposed to isotonic saline.

Discussion

The present results demonstrate the importance of well controlled sonication parameters when sonication is used for the isolation of mast cell granules. The ultrasonic vibration not only disintegrates the mast cells but can also damage the membrane surrounding the granules. Even with the lowest sonication intensity required for a reasonable yield of granules—4 μ m amplitude and 5 s duration—a mixed population of granules was obtained. A rather high proportion of the granules were electron dense and surrounded by a seemingly intact pergranular membrane. The other granules were larger, less electron dense and lacked a pergranular membrane. With increased sonication intensity the proportion of less dense, membrane free granules increased. At the highest sonication intensity used—8 μ m for 60 s—very few electron dense granules with an intact membrane were obtained.

Granules isolated from water lysed mast cells or cells exposed to compound 48/80 were all less electron dense and devoid of a limiting membrane

From previous observations (for references see Introduction) we know that granules isolated from mast cells lysed in deionized water or from cells exposed to compound 48/80 in isotonic (but salt free) sucrose retain part of their histamine but release the amine totally immediately they are resuspended in cation containing media e.g. isotonic NaCl solution. This depletion of the histamine store is the result of a simple cationic exchange between granule histamine and Na⁺ ions. This ion exchange occurs practically instantaneously, since no perigranular membrane interferes with the ion fluxes.

However if a perigranular membrane remains on the isolated granules as was often the case with sonicated mast cells, rather inconsistent and variable release of histamine can be observed. The presence of a perigranular membrane prevents or retards the passage of ions between the suspension medium and the ionic sites of the granule matrix. In other words the lower the sonication intensity the greater will be the proportion of granules with an intact perigranular membrane and the smaller will be the histamine release on suspension in NaCl solution and *vice versa*.

The choice of technique used for the isolation of granules therefore depends on the aim of the experiments. If one wants to study the storage and release properties of the granules a sonication intensity high enough to destroy all the perigranular membranes should be used or the granules should be isolated from water lysed or compound 48/80 treated mast cells. On the other hand the sonication technique might be utilized for the study of the properties of the perigranular membrane since by using appropriate techniques e.g. differential centrifugation or electrophoresis it offers the possibility of separating a satisfactorily pure intact granule suspension.

Hagen (1954) reported that a histamine containing particulate fraction obtained by differential centrifugation of dog liver homogenized in sucrose had little or no depressive effect when injected i.v. into a cat if it was suspended in isotonic sucrose or saline solution. On the other hand when the fraction was suspended in distilled water the injection was followed by a fall in blood pressure similar to that seen on injecting an equivalent amount of acidified sediment. A likely explanation of this observation is that most of the histamine storing particles (probably mast cell granules) isolated in this way are membrane bound and retain their histamine when suspended in isotonic media but release it when the membranes rupture in hypotonic media.

The occurrence of granules of different densities have been reported from electron microscopic studies on for example nerve terminals in various organs (Grillo 1966). The present results indicate that such differences in the morphological appearance in the electron microscope might be artefacts and may not always reflect functional differences.

This investigation has been supported by grants from the Swedish Medical Research Council (B71 14\ 2943-03 and B70 14\ 2938 01).

References

- ANDERSON P ■ A SLORACH and B UVVÄS Sequential exocytosis of storage granules during antigen induced histamine release from sensitized rat mast cells in vitro. An electron microscopic study *Acta physiol scand* 1973 88 359—377
- BERGENDORFF A and ■ UVVÄS Storage of 5 hydroxytryptamine in rat mast cells. Evidence for an ionic binding to carboxyl groups in a granule heparin protein complex *Acta physiol scand* 1977 84 320—331
- BLOOM G ■ and ■ HÄGERMARK A study on morphological changes and histamine release induced by compound 48/80 in rat peritoneal mast cells *Exp Cell Res* 1965 40 637—654
- CESSI, C and F PILIZOO The determination of aminosugars in the presence of amino acids and glucose *Biochem J* 1960 77 508—510
- GRILLO M A Electron microscopy of sympathetic tissues *Pharmacol Rev* 1966 18 387
- HAGEN P The intracellular distribution of histamine in dogs liver *Brit J Pharmacol* 1954 9 100—107
- LACROFF D M T PHILLIPS O A ISERI and E P BENNETT Isolation and preliminary characterization of rat mast cell granules *Lab Invest* 1964 13 1331—1344
- LOWRY O H N J ROSENBOUGH A L FARR and R J RANDALL Protein measurement with the Folin phenol reagent *J biol Chem* 1951 193 265—275
- ROULICK ■ P ANDERSON and B UVVÄS Electron microscope observations on compound 48/80 induced degranulation in rat mast cells. Evidence for sequential exocytosis of storage granules *J cell Biol* 1971 51 465—483
- SHORE P A A BURKHALTER and V ■ COHN JR. A method for the fluorometric assay of histamine in tissues *J Pharmacol exp Ther* 1959 177 182—186
- THON I L and ■ UVVÄS Mode of storage of histamine in mast cells *Acta physiol scand* 1966 67 455—470
- UVVÄS B C H ABORG and A BERGENDORFF Storage of histamine in mast cells. Evidence for an ionic binding of histamine to protein carboxyls in the granule heparin protein complex *Acta physiol scand* 1970 78 Suppl 336 1—26

Quantitative Measurement of Blood Flow and Oxygen Consumption in the Rat Brain

By

K. NORBERG and B. K. SIESJÖ

Received 19 October 1973

Abstract

NORBERG K and B. K. SIESJÖ *Quantitative measurement of blood flow and oxygen consumption in the rat brain* Acta physiol scand 1974 91 154-164

The cerebral blood flow (CBF) and oxygen consumption (CMR_{O_2}) were determined in rats under superficial (N_2O) anesthesia. The CBF was measured with a Xenon¹³³ modification of the Kety and Schmidt principle using arteriovenous sampling during the desaturation of the tissue following a 20 min saturation period. The CMR_{O_2} was calculated from the CBF and from the arteriovenous difference in total oxygen content. Since venous blood was sampled from the superior sagittal sinus the values for CBF and CMR_{O_2} are probably representative of cortical tissue. Control experiments with measurement of Xenon¹³³ activities in arterial blood and in tissue as well as in blood from different cranial veins showed that the tissue under study contained no slowly perfused masses and that significant contamination of superior sagittal sinus blood with blood from extracerebral sources did not occur. The results demonstrate that the blood flow of the rat cerebral cortex is 2-3 times higher and the oxygen consumption 3-4 times higher than the corresponding values for the human brain. These differences partly reflect a difference between cortical tissue and whole brain but an inverse relationship between body size and cerebral metabolic rate also seems involved.

There is much information on the rate of metabolism of oxygen, carbon dioxide and glucose in the human brain, but few data exist for experimental animals. Almost all studies in man have been carried out with the inert gas technique of Kety and Schmidt (1945, 1948a) with sampling of cerebral venous blood from the internal jugular bulb. With this technique the values obtained for cerebral blood flow (CBF) and cerebral metabolic rate for oxygen (CMR_{O_2}) are representative of the whole brain. The original nitrous oxide method of Kety and Schmidt (1945, 1948a) is not well suited to animal work since relatively large volumes of arterial and venous blood are required. It was nevertheless used by these authors on monkeys for calibration purposes and was later applied to dogs (Homberger *et al* 1946, Page *et al* 1951). In the latter animal cerebral venous blood was sampled from the superior sagittal sinus which makes it likely that the CBF and CMR_{O_2} values obtained mainly represent cortical grey matter. In both of these studies barbiturate anesthesia was used. In one (Page *et al* 1951) the CBF and CMR_{O_2} values were lower than those

measured in unanesthetized man (CBF about 50 ml/(100 g min) CMR_{O_2} about 3.3 ml/(100 g min), see Kety and Schmidt 1948) but in the other (Hornburger *et al* 1946) light penthotal anesthesia gave a CMR_{O_2} as high as 5.9 ml/(100 g min). A similar value was reported in unanesthetized dogs by Theye and Michenfelder (1968) who used the Kr^{83} modification of the Kety and Schmidt technique described by Lassen and Munck (1955).

There is an urgent need for quantitative studies of CBF and CMR_{O_2} in smaller animals than dogs. This is because most of the *in vivo* studies of cerebral metabolism have been carried out on brain tissue from guinea pigs or rats (see Himwich 1951, Elliott and Wolfe 1962, MacIwain and Bachelard 1971). Furthermore most of the studies of the *in vivo* levels of cerebral metabolites which have utilized freezing of the brain *in situ* have been carried out on mice or rats (see Ponten *et al* 1973). Thus a meaningful comparison between metabolic rates *in vitro* and *in vivo* as well as between metabolic state and rate of metabolism requires that metabolic flux is measured in small animals.

We recently applied a Nenon^{133} modification of the Kety and Schmidt technique to lightly anesthetized rats with sampling of venous blood from the superior sagittal sinus during the desaturation of the tissue following a 20 min period of Nenon^{133} inhalation (Eklof *et al* 1973). The present communication gives a detailed account of the technique and presents results obtained on a larger series of animals. In addition evidence will be presented that the method gives a quantitative measure of the CBF uncomplicated by the presence of slowly perfused tissue masses or significant extracerebral contamination of the cerebral venous blood sampled. The results obtained demonstrate that the CMR_{O_2} of the rat cerebral cortex is 3–4 times higher than that of the whole human brain.

Methods

In the experiments reported previously (Eklof *et al* 1973) male Wistar SPF rats weighing 375 to 375 g were initially anesthetized with diethyl ether and then maintained on 70% N_2O and 30% O_2 . Since Wistar rats could no longer be obtained the experiments reported herein were performed on male SPF rats of the Sprague Dawley strain (Anticimex Stockholm) weighing 325–425 g. The animals were anesthetized with 2.5–3% halothane in a closed jar. When unresponsive to tilting of the jar they were tracheotomized, injected with tubocurarine chloride (Nitrum) i.p. in a dose of 0.5 mg/kg and connected to a Starling type respirator that delivered 70% N_2O and 30% O_2 . In one part of the material the rats were allowed free access to tap water and commercial rat pellets (San Bolagen Malmö) until operation. In another the animals had access to water but were starved for 24–28 h prior to the experiments.

The animals were allowed a steady state period of at least 30 min after that the halothane anesthesia had been discontinued. Catheters were placed in the femoral arteries and one femoral vein. A burr hole was placed in the midline to expose the caudal part of the superior sagittal sinus. The body temperature was adjusted to 37°C and the arterial P_{CO_2} to 35–40 mm Hg. Arterial blood was drawn from a donor animal into heparinized plastic syringes and stored for later infusion into the experimental animal.

Measurements of CBF. When a respiratory steady state was at hand (P_{aCO_2} constant within 10% between two samples taken at least 10 min apart) a rubber balloon containing about 10 mCi of Nenon^{133} (obtained from Studsvik) in 70% N_2O and 30% O_2 was connected to the inlet of the respirator. About 15 min later the blood samples were collected from the artery and from the superior sagittal sinus for determination of the total oxygen content (To). The blood samples (40–50 μl) were collected in glass capillaries that were drawn to a fine tip at the ends to allow puncture of the sinus and to diminish the area open to the air.

The capillaries were filled without suction in most cases but at very low flow gentle suction sometimes had to be applied. About 20 min after the start of Xenon¹³³ inhalation arterial and venous blood were sampled for determination of the activity when the brain was saturated with Xenon. The rubber balloon was disconnected from the respirator and blood was collected simultaneously from artery and vein at 0.25, 1, 2, 3, 5, 7, 10 and 15 min. About 10 min after the start of desaturation a second set of samples were taken for determination of the arteriovenous T_{O_2} difference. During the desaturation period donor blood was infused at a speed which allowed the mean arterial blood pressure to be maintained constant.

Control experiments These had the objective of establishing the rate of equilibration of Xenon¹³³ between blood and tissue, and of studying extracerebral contamination of the venous blood sampled. Since any error due to incomplete equilibration or to extracerebral contamination should be maximal in situations of low CBF (see Discussion) all of these animals were hyperventilated to an arterial CO_2 tension of about 15 mm Hg. In one type of control experiment the Xenon¹³³ activity in arterial blood and tissue was determined after saturation periods of 15 and 30 min respectively. In order to allow determination of the tissue activity the animals were decapitated and the heads were frozen in liquid nitrogen. The brain was then chiselled out in the frozen state and pieces of tissue were split off under liquid N₂ and added to the counting tubes. The samples were taken from the hemispheres and contained predominantly cortical matter. In other experiments repeated samples for Xenon¹³³ determination were drawn from the artery superior sagittal sinus and external jugular vein during a 30 min saturation period (a single sample was also drawn from the anterior facial vein). In the third type of experiment finally the Xenon¹³³ activity in arterial and venous blood and in tissue was determined after 10 min of desaturation following a 15 min saturation period.

Analytical techniques The arterial P_{O_2} , P_{CO_2} and pH were measured with microelectrodes at 37°C (Eschweiler and Co. Hjel and Radiometer Copenhagen) with appropriate corrections for body temperature. The T_{O_2} of arterial and venous blood was measured with a potassium ferricyanide method (Fabel and Lubbers 1964) based on a commercial P_{O_2} electrode (Eschweiler and Co. Hjel). Exactly 25 μ l of blood was delivered to the electrode chamber by connecting the glass capillary to a Hamilton syringe with a fixed adaptor set to deliver that volume. A solubility factor of 0.00314 ml/(mm Hg 100 ml) was used to convert P_{O_2} to T_{O_2} . In our hands the method gives a coefficient of variation in T_{O_2} of less than 2%.

For measuring the Xenon¹³³ activity in the blood samples aliquots of blood were delivered directly from the sampling capillaries to the bottom of 3 ml water filled test tubes using the Hamilton syringe. The test tubes were then stoppered with rubber stoppers and the tubes were counted in a well type scintillation counter (Wallac). The frozen brain tissue samples with Xenon¹³³ were added to test tubes the amount of tissue was determined by weighing and the tubes were then counted together with the blood samples.

Calculations The Xenon¹³³ activity in arterial and cerebral venous blood was calculated in per cent of the venous activity at the end of the saturation period and lines were drawn as best fits to the individual points, each point representing the midtime of the period over which the sample was drawn. The CBF was then calculated by the trapezoid rule. The partition coefficient (λ) for Xenon¹³³ used was that given by Veall and Mallett (1963). In order to obtain the CMR_{O_2} the mean values of the two arteriovenous T_{O_2} differences were multiplied with the CBF value.

Statistical differences were calculated with the student *t* test.

Results

Influence of arterial CO_2 tension When the present method was first used no infusion of donor blood was given. It was then found that the arteriovenous T_{O_2} difference was larger in the second than in the first set of samples indicating a decrease in CBF with time. In view of the autoregulatory ability of the cerebral circulation it did not seem likely that this was due to the recorded decrease in mean arterial blood pressure of 10–30 mm Hg. However the decrease in blood pressure was accompanied by a fall in arterial CO_2 tension and when the arteriovenous T_{O_2} difference was plotted against P_{aCO_2} a straight line relationship was obtained for the P_{aCO_2} range of 30–40 mm Hg (Fig. 1). In view of the fact that experiments with hypercapnia and hypocapnia demonstrate a constant CMR_{O_2} within the P_{aCO_2}

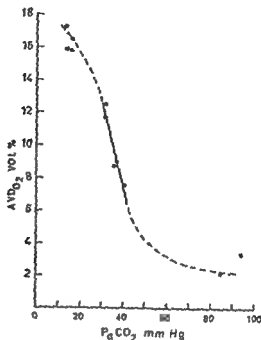


Fig 1 The relation between arteriovenous differences in oxygen content and PaCO_2 . The values given for PaCO_2 less than 20 mm Hg and higher than 70 mm Hg are those reported previously (Eklöf *et al* 1973). The regression line as determined for $30 < \text{PaCO}_2 < 40$ mm Hg is $\text{AVDO}_2 = -0.53 \text{ PaCO}_2 + 28.43$ $r=0.81$.

range 15–85 mm Hg (Eklöf *et al* 1973) it is possible to calculate from the values of Fig 1 that the CBF changes by about 5 % per mm Hg in the physiological PaCO_2 range (see Discussion). The decrease in CBF during the course of the experiments was avoided by infusion of donor blood. The CBF values reported below were all obtained in animals in which the arterial blood pressure and PaCO_2 remained constant within about 10 % during the measurements.

Validity of CBF method. The Kety and Schmidt technique gives a valid measure of the CBF provided certain requirements are fulfilled. We will list these requirements and describe the experiments that were designed to test them (see also Discussion).

1. *Equilibrium is reached between tissue and blood at the end of the saturation and desaturation periods.* Equilibrium requires that the arteriovenous Xe^{133} difference is zero. Fig 2 shows that the arteriovenous difference decreased to zero within 10 minutes after the start of the desaturation. However, since very small differences in Xe^{133} activity cannot be resolved, this result cannot exclude the possibility that there are slowly perfused tissue masses which equilibrate slowly with arterial blood. Therefore the tissue activity was measured after 15 and 30 min of saturation. As is shown by Table I, the ratio of Xe^{133} activity in tissue and arterial blood was the same at these two times and this ratio was close to that expected from the partition coefficient (see Discussion). Furthermore, in two additional experiments the tissue was saturated for 15 min, arterial and cereb- blood was sampled after 10 min of desaturation, the animals were d

The capillaries were filled without suction in most cases but at very low flow gentle suction sometimes had to be applied. About 20 min after the start of Xenon¹³³ inhalation arterial and venous blood were sampled for determination of the activity when the brain was saturated with Xenon. The rubber balloon was disconnected from the respirator and blood was collected simultaneously from artery and vein at 0.25, 1, 2, 3, 5, 7, 10 and 15 min. About 10 min after the start of desaturation a second set of samples were taken for determination of the arteriovenous T_{02} difference. During the desaturation period donor blood was infused at a speed which allowed the mean arterial blood pressure to be maintained constant.

Control experiments. These had the objective of establishing the rate of equilibration of Xenon¹³³ between blood and tissue, and of studying extracerebral contamination of the venous blood sampled. Since any error due to incomplete equilibration or to extracerebral contamination should be maximal in situations of low CBF (see Discussion) all of these animals were hyperventilated to an arterial CO_2 tension of about 15 mm Hg. In one type of control experiment the Xenon¹³³ activity in arterial blood and tissue was determined after saturation periods of 15 and 30 min respectively. In order to allow determination of the tissue activity the animals were decapitated and the heads were frozen in liquid nitrogen. The brain was then chiselled out in the frozen state and pieces of tissue were split off under liquid N_2 and added to the counting tubes. The samples were taken from the hemispheres and contained predominantly cortical matter. In other experiments repeated samples for Xenon¹³³ determination were drawn from the artery, superior sagittal sinus and external jugular vein during a 30 min saturation period (a single sample was also drawn from the anterior facial vein). In the third type of experiment finally the Xenon¹³³ activity in arterial and venous blood and in tissue was determined after 10 min of desaturation following a 15 min saturation period.

Analytical techniques. The arterial P_{O_2} , P_{CO_2} and pH were measured with microelectrodes at 37°C (Eschweiler and Co. Kiel and Radiometer Copenhagen) with appropriate corrections for body temperature. The T_{02} of arterial and venous blood was measured with a potassium ferricyanide method (Fabel and Lubbers 1964) based on a commercial P_{O_2} electrode (Eschweiler and Co. Kiel). Exactly 25 μ l of blood was delivered to the electrode chamber by connecting the glass capillary to a Hamilton syringe with a fixed adaptor set to deliver that volume. A solubility factor of 0.00314 ml/(mm Hg 100 ml) was used to convert P_{O_2} to T_{02} . In our hands the method gives a coefficient of variation in T_{02} of less than 2%.

For measuring the Xenon¹³³ activity in the blood samples aliquots of blood were delivered directly from the sampling capillaries to the bottom of 3 ml water filled test tubes using the Hamilton syringe. The test tubes were then stoppered with rubber stoppers and the tubes were counted in a well type scintillation counter (Wallac). The frozen brain tissue samples with Xenon¹³³ were added to test tubes the amount of tissue was determined by weighing and the tubes were then counted together with the blood samples.

Calculations. The Xenon¹³³ activity in arterial and cerebral venous blood was calculated in per cent of the venous activity at the end of the saturation period and lines were drawn as best fits to the individual points, each point representing the midtime of the period over which the sample was drawn. The CBF was then calculated by the trapezoid rule. The partition coefficient (λ) for Xenon¹³³ used was that given by Veall and Mallett (1965). In order to obtain the CMR_{O_2} the mean values of the two arteriovenous T_{02} differences were multiplied with the CBF value.

Statistical differences were calculated with the student *t* test.

Results

Influence of arterial CO_2 tension. When the present method was first used no infusion of donor blood was given. It was then found that the arteriovenous T_{02} difference was larger in the second than in the first set of samples indicating a decrease in CBF with time. In view of the autoregulatory ability of the cerebral circulation it did not seem likely that this was due to the recorded decrease in mean arterial blood pressure of 10–30 mm Hg. However the decrease in blood pressure was accompanied by a fall in arterial CO_2 tension and when the arteriovenous T_{02} difference was plotted against P_{aCO_2} a straight line relationship was obtained for the P_{aCO_2} range of 30–40 mm Hg (Fig. 1). In view of the fact that experiments with hypercapnia and hypocapnia demonstrate a constant CMR_{O_2} within the P_{aCO_2}

cerebral tissues which equilibrate much more slowly with nitrous oxide in arterial blood than does brain tissue. Theoretically a net arteriovenous difference at 10 min could also be due to incomplete equilibrium of brain tissue but control experiments in dogs with direct measurements of the nitrous oxide concentration in brain tissue indicated equilibration in 10 min (Kety *et al* 1948). In spite of this other workers have concluded that 10 min is too short a time to allow equilibration of the brain with Kr⁸⁵ and Lassen and Munck (1955) therefore prolonged the saturation period to 14 min and extrapolated the arteriovenous difference to infinity (*cf* also Alexander *et al* 1964, Lassen and Klee 1965). These workers concluded that failure of extrapolating the arteriovenous difference to infinity introduces a slight systematic overestimation of CBF and CMR_O and further that the error increases in situations of low flow (*e.g.* hypocapnia).

The objections which have been raised against the Kety and Schmidt technique concern the magnitude of extracerebral contamination of cerebral venous blood and the assumption of equilibration between tissue and blood. Ferris *et al* (1946) observed differences in arteriovenous oxygen content between the right and left sides during hyperventilation and concluded that extracerebral contamination of jugular venous blood invalidated the CBF method. Although later studies by Shenkin *et al* (1948) demonstrated that only about 3% of internal jugular blood was of extracerebral origin (in normocapnia) it would seem that any new application of the Kety and Schmidt principle must be preceded by an evaluation of the purity of the venous blood sampled.

It was pointed out by Sapirostein and Ogden (1956) that the Kety and Schmidt technique will seriously overestimate the CBF if the tissue contains slowly perfused tissue masses which do not equilibrate with arterial blood. The authors remarked that this error cannot be estimated from the arteriovenous curve since the venous curve can be close to the arterial even if such slowly perfused tissue masses exist. It is clear though that direct tissue measurements can reveal the presence of areas with a low perfusion rate.

In the rat the internal jugular vein is small and the external jugular vein drains blood from both cerebral and extracerebral sources. Although cerebral blood can be obtained from the transverse sinus we have chosen the superior sagittal sinus for sampling since the measurements should then reflect mainly cortical blood flow and oxygen consumption. Since veins draining into the sinus are continuous with vessels originating in subcortical brain structures (Shenkin *et al* 1948) sinus blood is not exclusively of cortical origin but there are reasons to believe that the values for CBF obtained mainly reflect cortical blood flow. In this context it is of interest to recall that different cortical structures show a relatively uniform flow in anesthetized animals (Landau *et al* 1955, Freygang and Sokoloff 1959).

The control experiments seem to exclude the presence of slowly perfused areas. Thus the ratio between Xenon¹³³ activity in tissue and arterial blood was identical after 15 and 30 min of saturation respectively indicating that the tissue was saturated already at 15 min (see Table I). The ratio obtained was slightly higher

than that expected from the partition coefficient determined for cortical tissue at the observed hemoglobin concentrations (0.82 Veal and Mallett 1965 see also Hoedt Rasmussen *et al* 1966) but this may have been due to the fact that some white matter was included in the hemispheric samples. Furthermore the tissue activity was close to that of arterial and venous blood and less than 1% of the concentration at saturation after 10 min of desaturation. These two facts together with the observed decrease to zero in the arteriovenous difference in Nenon^{133} within 10 min, strongly suggest that the present application of the Kety and Schmidt principle is not complicated by the presence of slowly perfused tissue areas. In fact less objection can be raised towards using the Kety and Schmidt method for rat cerebral cortex than for the human brain.

Three facts indicate that the superior sagittal sinus blood in the rat is not significantly contaminated by extracerebral blood. Firstly retrograd infusion of an epoxy plastic (Araldite S CIBA) into the sinus reveals only very small anatomical venous connections to surrounding bone and skin structures including the ethmoidal regions (unpublished experiments). Second simultaneous measurements of the pressure in cisterna magna and external jugular blood demonstrate that the CSF pressure exceeds the venous pressure by 3–5 mm Hg in hypocapnia, normocapnia and hypercapnia indicating that any collateral flow should be from cerebral to extracerebral veins (cf Shenkin 1948). Third the fact that the venous desaturation curves are identical after 15 and 30 min saturation in spite of evidence of a very slow extracerebral circulation (see Fig. 3) strongly indicates that significant extracerebral contamination does not occur.

The CBF obtained with the Kety and Schmidt method would not measure nutritional flow if arteriovenous shunts were present. There is no evidence that such shunts exist but it is difficult to show if they occur. However we may use the Nenon^{133} activities in arterial and venous blood and in cerebral tissue after 10 min of desaturation following a 15 min saturation period as qualitative proof. Thus if such shunts existed the arterial blood would dilute the Nenon^{133} activity in cerebral venous blood and the venous activity could be expected to be lower than the tissue activity at the end of the desaturation period. This was not the case (see Results) and we conclude that physiological arteriovenous shunts are probably not present in these experimental situations.

The final validation of the present technique would require comparisons with another method. Direct CBF measurements cannot be performed in rats. However values obtained with a tissue sampling technique using C^{14} -ethanol and 30 seconds of infusion (Ekblom *et al* 1974) indicate that cortical blood flow exceeds 100 ml/100 g/min in N_2O anesthetized rats.

Influence of $P_{a\text{CO}_2}$ on CBF The present experiments have shown that the CBF varies by more than 5% per mm Hg in $P_{a\text{CO}_2}$. This is a larger variation than that previously obtained by means of a venous outflow method in monkeys (Reinisch 1964) or by means of beta-clearance from the exposed dog cortex (Harper and Glass 1965). However our figure agrees with those reported by Kety and Schmidt

(1948 b) see also Novack *et al* 1953) in man and by Harper *et al* (1972) in monkeys. The latter results were obtained with a method that did not require exposure of the tissue. It seems possible that the venous outflow method used by Reivich (1964) does not quantitatively measure CBF and that exposure of the brain reduces the response of the blood flow to changes in P_{CO_2} .

CBF and cerebral metabolic rate for oxygen in rat cerebral cortex The present technique cannot be applied to unanesthetized animals. However, there is evidence from studies in man (Alexander *et al* 1964 see also Smith and Wollman 1972) and in the dog (Theye and Michenfelder 1968) that 70% N_2O has little influence on CBF and CMR_{O_2} , hence we can assume that the present values are representative of the unanesthetized state as well. It is therefore of interest that cortical CBF values in the unanesthetized cat using the tissue sampling technique are close to those obtained presently (Landau *et al* 1955; Fregang and Sokoloff 1959).

The present results show that the CBF in the rat is 2–3 times higher and the CMR_{O_2} 3–4 times higher than the corresponding values for the human brain. These differences cannot be entirely explained as a species difference since the values in man reflect the whole brain and thus include subcortical structures. There are few previous values on animals that can be used for comparison since most previous results have been obtained with barbiturate anesthesia which is known to depress CBF and CMR_{O_2} (Wechsler *et al* 1951; Pierce *et al* 1962). Furthermore most recent CBF values have been obtained with compartmental analysis of clearance curves for Kr^83 or Xenon¹³³. The fast component of such curves bear an uncertain relationship to the cortical flow and the CBF values obtained cannot readily be used to calculate CMR_{O_2} . However, the CMR_{O_2} values obtained in dogs under light barbiturate or nitrous oxide anesthesia using the Kety and Schmidt technique (Homburger *et al* 1946; Theye and Michenfelder 1968) are 5–6 ml/(100 g min). This would indicate that the cortical CMR_{O_2} is higher in the rat than in the dog and that it may vary inversely with the body weight.

This study was supported by grants from the Swedish Medical Research Council (Projects No 14\ 2179 and 14\ 263) from the Swedish Bank Tercentenary Fund and by US PHS Grant No 5 RO1 NS 07838-05 from NIH. K. Norberg is supported by grants from the Swedish Board for Technical Development.

References

- ALEXANDER S. C. H. WOLLMAN P. J. COHEN P. E. CHASE E. MELMAN and M. BEHAR: Krypton- and nitrous oxide uptake of the human brain during anesthesia. *Anesthesiology* 1964 22 37–47.
- ERLOF B. H. A. L. L. NILSSON K. NORBERG and H. K. SIESJO: Blood flow and metabolic rate for oxygen in the cerebral cortex of the rat. *Acta physiol scand* 1973 88 587–589.
- ERLOF B. H. A. L. L. NILSSON K. NORBERG B. K. SIESJO and P. TORLOF: Regional cerebral blood flow in the rat measured by the tissue sampling technique: a critical evaluation using four indicators: C^{14} antipyrine, C^{14} -ethanol, H^3 -water and Xenon¹³³. *Acta physiol scand* 1974 91 1–10.
- ELLIOTT K. A. C. and L. S. WOLFE: Brain tissue respiration and glycolysis. In: *Neurochemistry* Eds K. A. C. Elliott, I. H. Page and J. H. Quastel. 2nd ed. Charles C. Thomas Publisher Springfield, Ill. U.S.A. 1967 177–211.

- FABEL, H and H W LUBBERS Eine schnelle Mikromethode zur serienmassigen Bestimmung der O_2 Konzentration im Blut *Pflügers Arch ges Physiol* 1964 281 32-33
- FERRIS E B C L ENGELS C D STEVENS and M LOGAN The validity of internal jugular venous blood in studies of cerebral metabolism and blood flow in man *Amer J Physiol* 1946 147 517-521
- FREYGANG W H and L SOKOLOFF Quantitative measurements of regional circulation in central nervous system by use of radioactive inert gas In *Advances in Biol and Med Phys* Vol 6 p 263 New York Academic Press
- HARPER, A M and H I GLASS Effect of alterations in the arterial carbon dioxide tension on the blood flow through the cerebral cortex at normal and low arterial blood pressures *J Neurol Neurosurg Psychiat* 1965 28 449-452
- HARPER M A V D DEARMUCK J O ROJAN and W H JENNET The influence of sympathetic nervous activity on cerebral blood flow *Arch Neurol (Chic)* 1972 27 1-6
- HIMWICH H E *Brain metabolism and cerebral disorders* Baltimore Williams and Wilkins 1951
- HODOT RASHLESEN, E E SVEINSDOTTIR and A A LARSEN Regional cerebral blood flow in man determined by intraarterial injection of radioactive inert gas *Circulat Res* 1966 18 237-247
- HOMBELGER, E W A HIMWICH P EYSTEIN G YORK R MARESCA and H E HIMWICH Effect of pentothal anesthesia on canine cerebral cortex *Amer J Physiol* 1946 147 343-345
- KETY S S and C F SCHMIDT The determination of cerebral blood flow in man by the use of nitrous oxide in low concentrations *Amer J Physiol* 1945 143 53-66
- KETY S S and C F SCHMIDT The nitrous oxide method for the quantitative determination of cerebral blood flow in man: theory procedure and normal values *J Clin Invest* 1948 a 27 476-483
- KETY S S and C F SCHMIDT The effect of altered arterial tensions of carbon dioxide and oxygen on cerebral blood flow and cerebral oxygen consumption of normal young men *J Clin Invest* 1948 b 27 481-492
- KETY S S M H HARMEL H T BROOMEL and C B RICHIE The solubility of nitrous oxide in blood and brain *J Biol Chem* 1918 173 487-493
- LANDAU W M W H FREYGANG JR L P ROWLAND L SOKOLOFF and S S KETY The local circulation of the living brain: values in the unanesthetized and anesthetized cat. *Trans Amer Neurol Ass* 1955 80 125-129
- LARSEN N A and O MUNK The cerebral blood flow in man determined by the use of radioactive krypton *Acta physiol scand* 1955 33 30-49
- LARSEN N A and A KLER Cerebral blood flow determined by saturation and desaturation with krypton: an evaluation of the validity of the inert gas method of Kety and Schmidt. *Circulat Res* 1965 16 26-32
- McILWAIN H and H S BACHELARD *Biochemistry and the nervous system* Edinburgh and London (Churchill) Livingstone 1971
- NOVACK P H A SHENKIN L BOETTIG B GOLDBERG and A M SOFFER The effects of carbon dioxide inhalation upon the cerebral blood flow and cerebral oxygen consumption in vascular disease *J Clin Invest* 1953 32 636-702
- PAW W F W J GERMAN and L F NIMY The nitrous oxide method for measurements of cerebral blood flow and cerebral gaseous metabolism in dogs *Can J Biol Med* 1951 23 46-473
- PIERCE F C C J LAMBERTSEN S DELTCH P H CHANG H W LIFF R D DRIPPS and H I PRIE Cerebral circulation and metabolism during thiopental anesthesia and hyperventilation in man *J Clin Invest* 1964 41 1664-1671
- PONTEN L R A RATHENSON L C SALFORD and B A SIESJO Optimal freezing conditions for cerebral metabolites in rats *J Neurochem* 1973 In press
- REIVICH M A and P and cerebral hemodynamics *Amer J Physiol* 1964 206 33-35
- SAPSTEIN L A and E O DEN Thoreic limitations of the nitrous oxide method for the determination of cerebral blood flow *Circulat Res* 1955 4 245-249
- SHENKIN H A M H HARMEL and S S KETY Dynamic anatomy of the cerebral circulation. *Arch Neurol (Chic)* 1958 10 240-252
- SMITH L A and H WILKINSON Cerebral blood flow and metabolism Effects of anesthetic drugs and techniques *Anesthesiology* 1972 37 377-400
- THIEME R A and J D MICHENFELDER The effect of nitrous oxide on canine cerebral metabolism *Anesthesiology* 1969 29 1119-1124
- VFALL, N and B L MALLETT The partition of trace amounts of Xenon between human blood and brain tissues at 37 C. *Phys in Med Biol* 1965 10 373-380
- WECHSLER R L L DRIPPS and S S KETY Blood flow and oxygen consumption of the human brain during anesthesia produced by diethylpentobarbital *Anesthesiology* 1951 12 308-311

High Energy Phosphate Compounds in Adipose Tissue The Effect of Hemorrhage

By

B B FREDHOLM and A FRONEK

Received 5 November 1973

Abstract

FREDHOLM B B and A FRONEK *High energy phosphate compounds in adipose tissue the effect of hemorrhage* Acta physiol scand 1974 91 165—171

The levels of ATP and CP in gastrocnemius muscle and inguinal subcutaneous adipose tissue of cats were measured before and after withdrawal of 25—45 per cent of the calculated blood volume and after retransfusion of the shed blood. Resting values were in skeletal muscle ATP— 6.77 ± 0.49 $\mu\text{mol/g}$ tissue CP— 17.35 ± 1.31 $\mu\text{mol/g}$ tissue (mean \pm SE) and in adipose tissue ATP 86.7 ± 18.1 and CP 132.8 ± 8.5 nmol/g. Within 10 min after withdrawal of blood muscle high energy phosphate levels were unchanged whereas adipose tissue CP and ATP levels had dropped to 20 and 48 per cent of control respectively. Later during the hypotensive period skeletal muscle levels also fell. Following retransfusion of the shed blood adipose tissue levels remained low whereas skeletal muscle levels returned towards control. The results demonstrate that the high energy phosphate levels are more severely decreased in adipose tissue than in skeletal muscle following bleeding in cats and that the fall is not reversible in adipose tissue in contrast to muscle. The results are compatible with the idea that adipose tissue is one of the organs in which irreversible changes following hemorrhage are manifested.

Following severe hemorrhage in dogs blood flow is more restricted in subcutaneous adipose tissue than in several other tissues including skeletal muscle (Kovach *et al* 1970). Reinfusion of shed blood after a total period of hypotension of 3 h did not restore the blood flow in subcutaneous adipose tissue in contrast to the situation in skeletal muscle for example. These findings were taken as evidence that subcutaneous adipose tissue might be one of the organs where irreversible changes following hemorrhage are manifested. It is of interest that plasma FFA levels decreased during the bleeding period as did the rate of FFA mobilization from the tissue (Kovach *et al* 1970 Kovach *et al* 1971) although the sympathetic tone was presumably elevated when blood pressure was reduced by bleeding.

In the present study we have measured the concentrations of high energy phosphate compounds (ATP and CP) in adipose tissue and for comparison in

skeletal muscle of cat before and after bleeding. The concentration of these compounds was decreased in both tissues during bleeding, but the per cent decrease in adipose tissue was larger than in skeletal muscle. Moreover in contrast to the situation in skeletal muscle the level of these compounds was not restored following retransfusion of the shed blood.

Materials and methods

The experiments were conducted on 27 cats of either sex weighing 2.0–5.7 kg (mean 3.4) anesthetized with 30 mg/kg sodium pentobarbital *iv*. Arterial and venous loops of polyethylene tubing were inserted in the left femoral vessels. From these loops blood samples could be withdrawn, the animal bled and the shed blood retransfused. Arterial blood pressure was measured from the arterial loop by means of Statham P23AC transducers and recorded on a Beckman recorder. Heparin (100 U/kg) was administered *iv* to prevent clotting of the blood.

The experiments were started approximately two hours after the induction of anesthesia by the withdrawal of a control blood sample for the determination of hematocrit and arterial lactate followed by the injection of twice the volume of Dextran (Rheomacrodex Pharmacia) and by the extraction of two samples of the right gastrocnemius muscle (20–30 mg), one of which was immediately frozen in liquid nitrogen and then stored at -80°C for subsequent analysis of ALE and CP levels. The other sample was weighed and then placed in an oven at 105°C for 24 h and reweighed for the determination of wet and dry weights. At the same time two samples of 50–100 mg of the right inguinal subcutaneous adipose tissue for the same purposes were taken (Group I samples).

Following the extraction of these samples the animals were subjected to hemorrhage. $25\pm 45\%$ of the calculated circulating blood volume (55% of body mass, Farnsworth *et al.* 1969) was withdrawn by means of a motor driven syringe. The bleeding was completed in 10–20 min. Thereafter a new set of blood and tissue samples followed by a Dextran injection as described above was taken (Group II). The blood pressure returned towards control following bleeding. At the time of peak recovery during the hypovolemic phase a new set of samples was drawn (Group III). When the blood pressure decreased again by 20% of the peak recovered pressure samples were taken (Group IV) and the blood was retransfused by the same motor driven syringe. 20 min after retransfusion and when the pressure dropped by 20 and 40 per cent of the initial retransfusion samples were taken (Groups V and VI). There was a considerable interindividual variation between the animals for example the time elapsing from the start of the death of the animal after retransfusion ranged between 12 and 207 min.

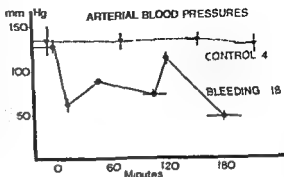
All the tissue samples were subsequently homogenized in 0.6 N perchloric acid. Adipose tissue and muscle (60 w/w adipose tissue, 3 w/w muscle) neutralized by 32 M H_2CO_3 and then extracted with diethyl ether for ALE and CP according to Lewy and Ljungerius (1972). The extract was evaporated from Löwenburg or Mannheim lactate in which was away from the extract. The residue was dried and then weighed. Statistical analysis was done by means of a Student's *t* test for paired samples.

Results

In Fig. 1 is shown the blood pressure in the group of 18 animals subjected to hemorrhage. In 10 of the animals in which no blood was withdrawn. It can be noted that in the latter case during the cats were able to maintain their blood pressure for more than 3 h longer than most of the bleeding experiments listed.

Table I and II present data from the two groups of experiments (control and bleeding). While the hematocrit was essentially unchanged in the control cats there was a progressive drop in hematocrit during the bleeding period and a recovery afterwards. The injection of dextran following each sample could contribute to the fall seen during the bleeding period. Control lactate levels were high in both groups.

Fig 1 Mean arterial blood pressure in control cats (not subjected to hemorrhage $n = 4$) and in cats subjected to withdrawal of 25–45 per cent of their calculated circulating blood volume ($n = 18$). Values given are means \pm S.E. The horizontal bars represent S.E. in the case of the bleeding experiments and range in the case of the control experiments. 0 time represents the end of the withdrawal of blood. Group I samples control were taken before bleeding. Group II after bleeding was completed. Group III at peak recovery of blood pressure during the hypotensive phase. Group IV before retransfusion. Group V 20 min after retransfusion. Group VI and VII when blood pressure had fallen by 20 and 40 per cent respectively of peak pressure following retransfusion.



Immediately following bleeding the level was almost doubled ($p < 0.01$) and the concentration of lactate continued to increase during the experiment. There were no significant changes in the water content in skeletal muscle in either group. On the other hand bleeding led to a highly significant decrease in adipose tissue water content. Following this initial fall there was a significant return towards and above control levels so that in group VII *etc* when the blood pressure had dropped by 40% from the peak value following retransfusion the tissue water content had almost doubled relative to control.

TABLE I Blood pressure, hematocrit, blood lactate as well as ATP, CP and water content of biceps of adipose tissue and skeletal muscle in control cats (female) cats (2.9 ± 0.34 kg) anaesthetized with sodium pentobarbital were subjected to surgery as in the bleeding experiments but no blood was withdrawn. The first (I) sample (or measurement) was taken approximately 2 min after the induction of anaesthesia. Sample II—60–87 min thereafter. Sample III—145–170 min and Sample IV—200–250 min after the first one. The first 3 values are mean \pm S.E. of 4 determinations while the fourth is the mean \pm S.E. of 3 determinations.

Parameter	Sample No.			
	I	II	III	IV
Hematocrit (arterial) (%)	35.3 ± 3.5	33.1 ± 2.8	34.8 ± 3.3	37.7 ± 2.4
Blood lactate (mM)	3.37 ± 0.34	3.94 ± 0.23	3.87 ± 0.22	4.74 ± 0.38
Water content (g/g w/w)				
muscle	75.3 ± 1.2	75.5 ± 1.0	77.3 ± 3.5	75.0 ± 1.0
adipose tissue	13.7 ± 1.2	15.0 ± 1.1	19.3 ± 2.2	18.6 ± 1.3
ATP content				
muscle (μ mol/g)	5.56 ± 1.08	4.10 ± 0.66	5.09 ± 1.19	4.68 ± 1.23
adipose tissue (nmol/g)	116.4 ± 29.7	154.1 ± 17.5	130.7 ± 24.9	199.7 ± 34.1
CP content				
muscle (μ mol/g)	14.49 ± 4.73	13.68 ± 3.66	13.94 ± 3.62	14.49 ± 3.47
adipose tissue (nmol/g)	159.4 ± 39.0	160.2 ± 27.0	140.4 ± 77.7	160.6 ± 76.9

PHOSPHAGENS FOLLOWING BLEEDING

A of control

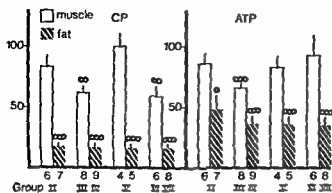


Fig. 2 Levels of creatine phosphate (CP) and ATP in muscle (unfilled bars) and adipose tissue (filled bars) in per cent of control following bleeding. Groups are explained in the text. Values given are mean and S.E. * = $p < 0.05$, ** = $p < 0.01$, *** = $p < 0.001$, **** = $p < 0.0001$. The values for CP and ATP in skeletal muscle in Group V are significantly ($p < 0.05$) higher than in Group II—IV.

The levels of high-energy phosphate compounds did not change significantly in either skeletal muscle or adipose tissue during control conditions (Table I). There were however significant alterations following bleeding. These are illustrated in Fig. 2. Control levels in these experiments were for CP 17.35 ± 1.31 $\mu\text{mol/g}$ in skeletal muscle ($n = 8$) and 132.8 ± 8.5 nmol/g in adipose tissue ($n = 10$) and for ATP 6.77 ± 0.49 $\mu\text{mol/g}$ in skeletal muscle and 86.7 ± 18.1 nmol/g in adipose tissue (same number of experiments). While there was no significant change in muscle ATP and CP levels immediately following bleeding, adipose tissue levels were decreased to 48 and 20 per cent of control respectively. Later on during the bleeding period the muscle levels did decrease significantly, but not as much on a percentage basis as in adipose tissue. Following retransfusion moreover the muscle high energy phosphate levels increased significantly in contrast to the situation in adipose tissue.

TABLE II Hematocrit, blood lactate and tissue water content in feline skeletal muscle and subcutaneous adipose tissue before and after bleeding and retransfusion. Values given are mean \pm S.E. The group numbers are as explained in the text.

Parameter	Group	I	II	III	IV	V	VI	VII
Hematocrit (%)		47.4 ± 4.2 (18)	39.0 ± 4.4 (16)	35.6 ± 2.2 (8)	33.4 ± 1.5 (12)	37.2 ± 2.1 (18)	37.3 ± 0.3 (10)	40.2 ± 2.6 (8)
Blood lactate (mM)		1.6 ± 0.9 (1)	5.68 ± 0.83 (8)	7.31 ± 0.67 (11)		9.42 ± 1.37 (9)	9.69 ± 2.14 (9)	9.79 ± 0.83 (12)
Water content (% w/w)								
skeletal muscle		75.4 ± 2.3 (18)	77.9 ± 4.3 (14)	78.6 ± 3.1 (12)	69.4 ± 4.2 (18)	75.3 ± 2.4 (10)	78.1 ± 2.1 (7)	
adipose tissue		17.9 ± 3.6 (16)	8.5 ± 2.9 (15)	14.4 ± 1.7 (11)		18.0 ± 2.6 (16)	19.8 ± 5.7 (9)	31.2 ± 6.2 (7)

During the irreversible phase of decrease of arterial pressure muscle CP levels decreased but the ATP levels were kept up

Discussion

The bleeding procedure employed is similar to that used by Haglund (1973). Moreover the changes in arterial blood pressure in the severe bleeding group (35% of blood volume) reported by this author are similar to those found by us in spite of differences in anesthetic used. The finding that control blood lactate level were high indicates that a certain preparational trauma had occurred. However the lactate values were as high in the control animals where little or no change in the parameters under investigation was noted indicating that this factor could not be of paramount importance. Haglund (1973) who did not measure lactate levels tried to correct the alterations in acid base balance following preparation by an infusion of 2 meq $\text{NaHCO}_3/\text{min}$. Following bleeding there was a marked rise in lactate concentration. The lactate level has been used as an indicator of the prognosis of shocked animals and man (Chen 1967). It can be noted that acidosis and hidden tissue acidosis was found to be more pronounced the more intense the hypotension in cats (Haglund 1973).

After bleeding adipose tissue water content fell rapidly. Since the largest part of the water in this tissue is extracellular and a substantial part of that intravascular (Fredholm 1970) it is quite probable that a large part of this fall is due to expulsion of venous blood and to a reduction in blood flow. In the intestine there is a substantial reduction in blood content within 30 s of bleeding (Haglund 1973). After this initial fall there was a progressive return of tissue water to and above the control content. Since adipose tissue blood flow is very low in dogs subjected to hemorrhage both during the hypovolemic phase and after retransfusion of blood (Kovach *et al* 1970) it is unlikely that these changes reflect a progressive increase in tissue blood content. Rather one must assume that a significant extravasation of fluid had occurred in adipose tissue as reported recently for the intestine (Haglund 1973). As a matter of fact the magnitude of this response was such that one must seriously consider the possibility that loss of fluid from blood to adipose tissue could be of significance for the overall hemodynamics. Assuming 5–10% of body weight being fat our data showing a 10–20% increase in tissue water content could mean that a 3 kg cat might loose about 30 ml of circulating volume in adipose tissue.

Following hemorrhage in rats and dogs ATP and CP levels in muscle fall only slightly (Le Page 1946; Lefer *et al* 1969) while the levels in liver and kidney are markedly reduced (Le Page 1946; Rosenbaum *et al* 1957). In our experiment in cats muscle high energy phosphate stores were also decreased only to a limited extent. On the other hand ATP and CP levels in adipose tissue which was recently implicated as another organ where irreversible changes following hemorrhage might be manifested (Kovach *et al* 1970) were markedly reduced. There seem to be a relationship between the magnitude of this fall in different organs and the irreversible damage done by bleeding.

The ATP content in adipose tissue found in the present study is similar to that in rat adipose tissue as reported in the literature (Denton *et al.* 1966 Saggerson and Greenbaum 1970 Ballard and Hansson 1969). So far there are few reports in the literature concerning *in vivo* alterations in adipose tissue ATP stores in different physiological or patho-physiological states. We are therefore left to guess as to the mechanism behind the large decrease in adipose tissue high energy stores. Following hemorrhage catecholamine stimulation in adipose tissue is increased (Kovach *et al.* 1970 1971). Adrenergic stimulation leads to decreased ATP in adipose tissue and isolated fat cells (Saggerson and Greenbaum 1969 Angel *et al.* 1971 Bihler and Jeanrenaud 1970) and there is suggestive evidence that this is at least partly due to increased intracellular concentration of free fatty acids (Angel *et al.* 1971 Bihler and Jeanrenaud 1970 Hollenberg and Patten 1970). It is of interest therefore that sympathetic nerve stimulation leads to increased free fatty acid levels in isolated canine subcutaneous adipose tissue *in situ* (Fredholm 1970). Furthermore hemorrhage leads to a greater reduction in adipose tissue blood flow than in skeletal muscle blood flow (Kovach *et al.* 1970) leading to a further reduction in the amount of oxygen delivered to the tissue. This could be expected to lead to a depressed formation of ATP since this is strongly dependent on oxidation in adipose tissue (Hepp *et al.* 1969 Hollenberg and Patten 1970).

Thus the fact that the level of high energy phosphate was more depressed in adipose tissue than in skeletal muscle could be due to several factors such as a) increased lipolysis following an increased sympathetic tone and b) a marked reduction in blood flow leading to a decreased availability of metabolic substrates including oxygen and also a trapping within the tissue of the formed fatty acids.

It is difficult to speculate about the exact role of CP in fat since there are no studies on the regulation of CP in fat cells in the literature. Our own preliminary evidence suggest that the CP is indeed localized to the fat cells and not primarily to the intravascular cells of the epididymal fat pad of the rat (Fredholm and Ahn unpublished). Both celltypes have creatine phosphokinase activity (Roberts and Fredholm unpublished) localized in the same isoenzyme (the brain type). It is reasonable to assume that CP fulfills a role in the maintenance of the level of ATP in animals with these celltypes. The ATP level is of utmost importance for the maintenance of responsiveness to lipolytic hormones (e.g. Hollenberg and Patten 1970). Fat is not contractile, presumably because ATP is required both as a substrate for adenylylation and for the activation of hormone sensitive lipase by protein kinase in fat cells (Roberts *et al.* 1970).

It is of interest to note that while muscle CP and ATP levels returned toward control upon reinfusion of shed blood this was not the case for the adipose tissue high energy phosphates. In dogs subjected to three hours of hypotension retransfusion of the shed blood led to a restitution of skeletal muscle blood flow but not to a restitution of adipose tissue blood flow (Kovach *et al.* 1970). It is not clear whether the parallelism between high-energy phosphate levels and blood flow is due to a primary defect in the adipose tissue circulation following hemorrhage or if

the failure to reconstitute blood flow is secondary to severe metabolic damage as evidenced by the low ATP and CP levels. Whichever interpretation is correct, our data do support the contention that bleeding leads to irreversible damage in adipose tissue which is not the case in muscle.

The present study was supported in part by the NIH Grant HL 12690-03 and by the Swedish Medical Research Council (40P 3898).

We want to express our gratitude to Dr Steven E. Mayer who supplied the laboratory facilities for one of us (B.F.) while being the recipient of a US Public Health International Fellowship (1F05TWO 1876-01). The skillful assistance of Mr T. Wuzel is gratefully acknowledged as is the help by Mr G. Schwab in performing some of the assays.

References

- ADEL, A. K. DE AL and M. L. HALPERIN. Free fatty acid and ATP levels in adipocytes during lipolysis. *Metabolism* 1971 119 193-219.
- BELLARD, F. J. and R. W. HANSON. Measurements of adipose tissue metabolites in vivo. *Biochem J* 1969 117 193-202.
- BONLER, I. and B. JANKOVIC. ATP content of isolated fat cells. Effects of insulin, ouabain and lipolytic agents. *Biochim Biophys Acta (Amst.)* 1970 207 496-506.
- CRILEY, S. Role of the sympathetic nervous system in hemorrhage. *Physiol Rev* 1967 47 214-288.
- DETON, R. M., R. E. YORKE and P. J. RANDLE. Measurement of concentrations of metabolites in adipose tissue and effect of insulin, alloxan, diabetes and adrenalin. *Biochem J* 1966 100 407-419.
- PARSONS, P. N. C., A. PILLINO-GONZALEZ and M. J. GREGERSEN. Fat values in the normal and splenectomized cat. Relation of F_{at} to body size. *Proc Soc exp Biol (N.Y.)* 1960 104 729-733.
- FAVIA, G., P. DOMIGO, R. BUDETTI and L. VISCO. Effect of oxidative phosphorylation on cyclic adenosine monophosphate synthesis in rat adipose tissue. *Biochem Pharmacol* 1972 21 1633-1639.
- FREDHOLM, B. B. Studies on the sympathetic regulation of circulation and metabolism in isolated canine subcutaneous adipose tissue. *Acta physiol scand* 1970 Suppl 354 1-47.
- HONORST, H. J. In *Methoden der Enzymatischen Analyse*. Verlag Chemie Weinheim 1962 266-270.
- HAGLUND, U. Vascular reaction in the small intestine of the cat during hemorrhage. *Acta physiol scand* 1973 89 129-141.
- HEPP, D. D., R. CHALLOVER and R. H. WILLIAMS. Repletion in isolated fat cells and the effects of epinephrine. *J Biol Chem* 1968 243 2321-2332.
- HOLLENBERG, C. H. and R. L. PATTEN. Relation of fat cell ATP content to lipolysis induced by dibutyryl 3',5'-cyclic AMP. *Metabolism* 1970 19 856-864.
- HUTCHESON, J. K., D. DILLIBER and S. E. MAYER. Protein kinase activation and phosphorylation of a purified hormone sensitive lipase. *Biochim Biophys Res Commun* 1970 41 1350-1356.
- KOVACH, A. G., S. ROSELL, P. SANDOR, E. KOLTAY, E. KOVACH and A. TOUKA. Blood flow, oxygen consumption and free fatty acid release in subcutaneous adipose tissue during hemorrhagic shock in control and phenoxylbenzamine treated dogs. *Circulat Res* 1970 26 733-741.
- KOVACH, A. G., S. ROSELL, P. SANDOR, E. KOLTAY, M. HAMORE and E. KOVACH. Influence of adrenergic β receptor activity on blood flow and free fatty acid release in canine subcutaneous adipose tissue during hemorrhagic shock. *Arch Pharmacol* 1971 268 140-144.
- LEPER, A. M., J. C. DIW and R. M. BERNE. Cardiac and skeletal muscle metabolic changes in hemorrhagic shock. *Am J Physiol* 1969 216 483-486.
- LEPAGE, C. A. The effects of hemorrhage on tissue metabolites. *Am J Physiol* 1946 147 446-454.
- LOWRY, O. H. and J. V. PASSONEAU. *A flexible system of enzymatic analysis*. Academic Press New York 1972 p 151-153.
- ROSENBAUM, D. K., E. D. FRANK, A. M. RUTENBERG and H. A. FRANK. High energy phosphate content of liver in experimental hemorrhagic shock. *Am J Physiol* 1957 180 86-90.
- SAGGERSON, M. D. and A. L. GREENBAUM. The regulation of triacylglyceride synthesis and free fatty acid synthesis in rat epididymal adipose tissue. *Biochem J* 1970 119 193-211.

Disappearance of $^{133}\text{Xenon}$ and $^{125}\text{Iodide}$ and Extraction of $^{86}\text{Rubidium}$ in Subcutaneous Adipose Tissue during Sympathetic Nerve Stimulation

By

BIRGITTA LINDE and JOHN L. GAINER¹

Received 15 November 1973

Abstract

LINDE, B and J L GAINER *Disappearance of $^{133}\text{Xenon}$ and $^{125}\text{Iodide}$ and extraction of $^{86}\text{Rubidium}$ in subcutaneous adipose tissue during sympathetic nerve stimulation* Acta physiol scand 1974 91 172-179

Effects of sympathetic nerve stimulation on the disappearance rates of $^{133}\text{Xenon}$ and $^{125}\text{Iodide}$ from a local depot as well as on the extraction of $^{86}\text{Rubidium}$ from blood have been studied in the subcutaneous adipose tissue of dogs during constant blood flow perfusion. Resting mean k values for $^{133}\text{Xenon}$ were 0.0040 min^{-1} ($n = 10$) and for $^{125}\text{Iodide}$ 0.0386 min^{-1} ($n = 5$) while the Pb products for $^{86}\text{Rubidium}$ had a mean value of $2.5 \text{ ml} \times \text{min}^{-1} \times 100 \text{ g}^{-1}$ ($n = 17$). During sympathetic nerve stimulation a frequency dependent decrease of disappearance rates and Pb products was found. The latter were reduced by an average of 30 % while the reductions of the disappearance rates were twice as large and similar for $^{133}\text{Xenon}$ and $^{125}\text{Iodide}$. These results suggest a decrease in the perfused capillary surface area during sympathetic nerve stimulation.

In subcutaneous adipose tissue a marked increase in the hydrodynamic conductivity, as measured by the capillary filtration coefficient (CFC) is brought about by sympathetic nerve stimulation (Öberg and Rosell 1967). The CFC is normally considered to be a measure of the surface area open for filtration and thus these data would appear to show an increase of that area during sympathetic stimulation. However, in other tissues the CFC either decreases or remains unchanged during these same circumstances (Cobbold *et al.* 1963, Folkow *et al.* 1963). Öberg 1961. This brings about the question of whether or not adipose tissue is different from other tissues in the reaction of the exchange area to sympathetic stimulation. It does the CFC increase actually reflect both area and permeability changes in this particular case?

¹ Present address: Department of Chemical Engineering, University of Virginia, Charlottesville, Virginia, U.S.A.

A preliminary report on these studies was given at the 5th European Conference on Microcirculation, Gothenburg 1968.

One of the first steps in elucidating this problem was to see if there is indeed an altered capillary surface area in adipose tissue during sympathetic stimulation and whether such an alteration could account for the CFC increases seen. Thus we decided to perform a study using different measurements of capillary exchange in order to further define the area changes occurring.

Methods

37 female mongrel dogs weighing 9–25 kg each were used for the experiments. Anesthesia was induced by 30 mg/kg b.wt sodium pentobarbital i.v. with supplements when necessary. Tracheostomies were performed on most animals. To prevent clotting heparin in a dose of 2500 IU/kg was administered.

The subcutaneous adipose tissue in the inguinal region between the pubis and the pubic mammary glands was isolated (Rosell 1966) freed from surrounding tissues and skin and all vessels except the main artery and vein were ligated. In order to avoid movements of the tissue which could disturb the disappearance measurements the tissue was placed in a plastic retainer that was attached to the table during the xenon and iodide experiments. To maintain warmth and moisture the adipose tissue was covered with saline soaked gauzes and a plastic sheet. The venous outflow was measured with a drop counter and recorded continuously. The systemic blood pressure was measured with a Statham transducer and also monitored continuously.

The nerve to the tissue was transected at the level of the external hiatus of the inguinal canal and placed on a bipolar electrode. Electrical stimuli were delivered from a Grass stimulator Model S4D 1–15 Hz 8–12 V, 2 ms pulse duration. The duration of the stimulation varied between 8 and 20 min.

Constant flow technique appeared to be of advantage for these experiments. By using this method one can eliminate changes in the total blood flow that occur during sympathetic stimulation and which would otherwise influence the measurements. We chose the constant blood perfusion technique described by Renkin and Rosell (1967) and employed it essentially as in that reference.

Blood was drawn from the animal into a reservoir and was used as the arterial supply for the adipose tissue. The perfusion pressure of the blood was adjusted to approximately 120 mmHg and the mean blood flow rate was 5.6 ml \times min \times 100 g⁻¹ of tissue.

Disappearance studies

We chose to regard capillary exchange from tissue to blood as well as that in the other direction across the capillary wall. For determining exchange from the tissue to the blood, the local clearance technique was used with Xenon (^{133}Xe) and Iodide (^{131}I) as indicators. Fifteen experiments were performed with this technique. In ten of these 10–75 μCi of ^{133}Xe (AB Atomenergi, Studsvik) were dissolved in physiological saline containing no preservatives and injected into the middle of the adipose tissue preparation. This procedure was also used in five other experiments with the exception being that the indicator was 5 μCi of ^{131}I . These amounts of radioactive substances resulted in net counting rates of 50 000–100 000 cpm. The volume of the injectate was 0.05 ml and the injection performed over a period of one minute. The needle (outer diameter of 0.4 mm) was left in place in the tissue for 30 s following the injection in order to reduce back flow and great care was taken to avoid introducing air bubbles into the tissue. In 1 experiment both the xenon and iodide indicators (in this case ^{131}I) were mixed together in the same solution and injected.

A Philips PW 4111 scintillation counter equipped with an automatic printout device was used for the counting. For the disappearance studies the crystal of the scintillation counter was placed 5–10 cm above the adipose tissue. No collimation was used. The counter flat top was held with 4 mm of lead.

All experimental data were corrected for background activity and in the double tracer experiment appropriate cross corrections were made. The counts of xenon and iodide were plotted semilogarithmically versus time and the clearance constant k value (Kety 1949) was graphically determined from the data. k values for xenon were calculated in the monoexponential part of the curve i.e. 1 min or more after the injection (Larsen *et al.* 1966).

Measurements of PS-product

PS measurements involving the use of $^{86}\text{Rubidium}$ (^{86}Rb) have been used previously in order to define the exchange area (Renkin 1959, Renkin and Rosell 1967, Renkin *et al.* 1966, Dräsi *et al.* 1966). This method was also chosen here to study diffusion exchange from the capillaries to the tissue in 17 experiments. A solution of $^{86}\text{RbCl}$ (AB Atomenergi, Studsvik) was added to the blood reservoir (2 $\mu\text{Ci/ml}$) and the perfusion was started. First the level of radioactivity in the arterial

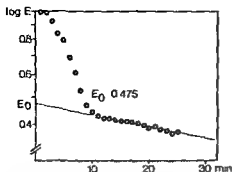


Fig 1 Extraction of ^{86}Rb determined by the continuous infusion method in subcutaneous adipose tissue. Fractional extraction is plotted semilogarithmically against time in minutes. E_0 extraction value obtained by extrapolation of the constant rate part to zero time, i.e. the time of addition of the radioactive blood.

blood was measured by diverting the perfusion directly into the measuring system, consisting of a glass coil placed in the well of the scintillation detector. The coil had a volume of about 2.5 ml and was constructed in such a manner so as to expose the largest possible amount of sample to the crystal. The counter was adequately shielded from the tissue and the perfusion apparatus. After measuring the arterial radioactivity the perfusion was switched over to the tissue and the glass coil was adapted to the venous outflow. The blood was perfused only once and no radioactive blood returned to the animal. After completion of a constant perfusion run the adipose tissue was switched to autoperfusion in order to reduce accumulation of ^{86}Rb in the extravascular space. The concentration that remained was considered to be the background for the next constant perfusion run. In this way it was possible to use the same dog for several experimental runs.

PS values were calculated from the data using the following equation, which has been derived earlier (Renkin 1959):

$$PS = -Q \ln(1 - E)$$

where Q refers to the blood flow rate and E is the extraction ratio (obtained from the differences in the arterial and venous readings on the scintillation counter). The rubidium values were corrected for loss of activity into the erythrocytes according to Renkin and Rosell (1962).

^{86}Rb has been used before in determining PS values, e.g. in skeletal muscle. In that case the problem with accumulation of indicator in the interstitial space is not as great as in adipose tissue, since the potassium pool which can dilute the rubidium is considerably larger. Thus the extraction will reach an almost constant value for perfusions of long duration. However, in the case of adipose tissue the adipocytes cannot concentrate the rubidium sufficiently in order to maintain an extracellular concentration near to zero. Consequently the extraction will decrease with time due to the diminishing diffusion gradient across the capillary wall. To correct for this phenomenon in the calculations of the extraction values, an extrapolation procedure was used as shown in Fig. 1.

Fractionation was plotted semilogarithmically versus time and a linear decrease was found after the first 10–15 min (which probably represent the washout of nonradioactive blood from the vessels and capillaries). The slope of the second part of the curve was considered to be an indication of the rate of rubidium accumulation in the interstitial space and, to correct for this, the linear part of the curve was extrapolated to zero time, i.e. the time of switching to radioactive blood. The extraction value obtained at zero time, E_0 , was then used in the calculations of the PS-products (Renkin 1959).

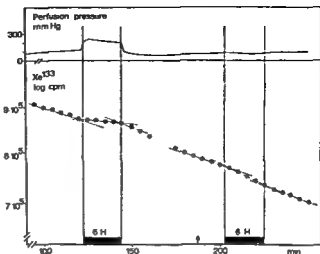
In 2 experiments the flow rate was varied over a range from $4 \text{ ml} \times \text{min}^{-1} \times 100 \text{ g}^{-1}$ to $12 \text{ ml} \times \text{min}^{-1} \times 100 \text{ g}^{-1}$ and a finite flow dependency of the PS values was found. This might be taken as an indication that the correction for back diffusion was acceptable.

Results

In the disappearance studies the blood flow rates varied from 1.9 to $12.0 \text{ ml} \times \text{min}^{-1} \times 100 \text{ g}^{-1}$ with a mean value of $4.5 \text{ ml} \times \text{min}^{-1} \times 100 \text{ g}^{-1}$. The mean k value for xenon was 0.0040 min^{-1} ($n = 10$) and for iodide 0.0386 min^{-1} ($n = 5$).

The typical response of the xenon and iodide disappearance in connection with sympathetic nerve stimulation is shown in Fig. 2. During stimulation a decrease in clearance rate was registered and after the stimulation the clearance rate exceeded

Fig 2 Perfusion pressure and disappearance rate of ^{133}Xe from subcutaneous adipose tissue in connection with sympathetic nerve stimulation before and after α receptor blockade. Constant blood flow perfusion with $2.6 \text{ ml} \times \text{min}^{-1} \times 100 \text{ g}^{-1}$. Upper graph shows perfusion pressure in mmHg. In the lower graph counts per minute of ^{133}Xe are plotted semilogarithmically against time. Sympathetic nerve stimulation was performed with 6 Hz 1° & 2 ms applied before and after $200 \mu\text{g}$ dihydroergotamine (administered at arrow)



that value noted during the resting conditions. The reduction of the elimination rate was related to the stimulus frequency up to 5 to 6 Hz, as is seen in Fig 3 and was found at impulse frequencies as low as 1 Hz. No clearcut difference in the magnitude of the reduction could be seen between the two tracers and this was further substantiated in a double tracer experiment in which the percentage reductions of the two disappearance rates did not differ by more than 3% (80% reduction for iodide and 83% for xenon). The decrease in the elimination rate could be blocked with dihydroergotamine in a dosage of $150\text{--}200 \mu\text{g}$ i.a. (Fig 2). In 15 out of 16 stimulations performed after using the α blocker an increased rate of disappearance was noted. This in turn could be blocked by the β receptor blocking agent propranolol $200 \mu\text{g}$ i.a.

For the ^{86}Rb experiments the mean blood flow was $6.5 \text{ ml} \times \text{min}^{-1} \times 100 \text{ g}^{-1}$ of tissue with a range from 2 to 13 and the average value of PS was calculated to be $2.5 \pm 0.5 \text{ ml} \times \text{min}^{-1} \times 100 \text{ g}^{-1}$ ($n = 17$). The range of the PS values was from 1.0 to $3.4 \text{ ml} \times \text{min}^{-1} \times 100 \text{ g}^{-1}$.

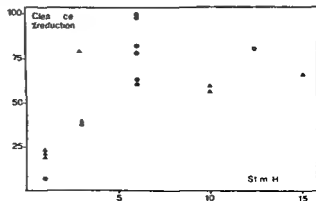


Fig 3 Percentage reduction in disappearance rate of ^{133}Xe and ^{125}I iodide during sympathetic nerve stimulation in subcutaneous adipose tissue, plotted versus stimulation frequency. Constant blood flow perfusion has been used. Δ ^{125}I iodide, \circ ^{133}Xe .

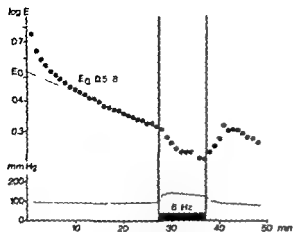


Fig. 4 Extraction of $^{86}\text{Rubidium}$ and perfusion pressure in subcutaneous adipose tissue in connection with sympathetic nerve stimulation during constant blood flow perfusion with $5.0 \text{ ml} \times \text{min}^{-1} \times 100 \text{ g}^{-1}$. Upper graph shows fractional extraction plotted semilogarithmically against time in minutes. E_0 extraction value obtained by extrapolation of constant rate part of the curve to zero time, i.e. time of addition of the radioactive blood. Sympathetic nerve stimulation was performed with 6 Hz 12V 2 ms. Lower graph shows the perfusion pressure in mmHg.

Fig. 4 represents an experiment where rubidium extraction was continuously registered before, during and after sympathetic nerve stimulation in order to demonstrate the variation in the extraction during these conditions. In most experiments, however, separate perfusion runs were made for each period of resting or stimulation in an attempt to obtain the most accurate E_0 values.

From Fig. 4 it appears that the extraction level is reduced during the stimulation period and increased above the resting level after the end of the stimulation. The decrease in extraction with stimulation in this case was only about 15%, although decreases of about 30% were usually obtained. The maximum decreases observed were 50% of the resting level.

Fig. 5 shows four experiments where different stimulation frequencies were used in the same experiment. It appears that a frequency response relationship exists with the most pronounced effects at frequencies above 2 Hz.

Discussion

The present investigation was undertaken in order to further elucidate the behaviour of the capillary section in adipose tissue during sympathetic nerve stimulation.

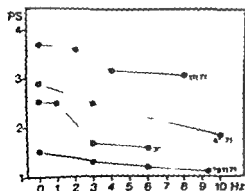


Fig. 5 Effect of sympathetic nerve stimulation on PS-products of $^{86}\text{Rubidium}$ in subcutaneous adipose tissue during constant blood flow perfusion. PS-values are plotted against stimulation frequency in four separate experiments.

Previous measurements have shown an increase of the CFC during nerve stimulation which leads to the question of whether this increase is due to a vasodilatation or whether perhaps other factors such as permeability changes may be involved.

In order to investigate this we chose to measure the disappearance of small molecules from the tissue such as xenon and iodide due to the technical simplicity of that technique. The results from these first experiments then initiated further studies of the capillary section in which we used the technique of determining the PS-values for rubidium since this technique is more commonly used for such purposes.

Xenon and iodide clearances have been used extensively for determining blood flow rates. However we used this method for a different purpose—as an indication of the variation in the number of open capillaries during sympathetic nerve stimulation. There are indications that local factors in the capillary section may be of importance for the disappearance of small compounds from a tissue (Bolme and Edwall 1971). One such local factor which has been alluded to by a number of investigators (Crone and Garlick 1969, Hills 1967) is the diffusion path lengths in the interstitial space. Our experiments were all done using constant flow perfusion of the tissue. The reason for this was to eliminate the flow effects on the disappearance rates allowing other factors in the capillary section which may change during sympathetic nerve stimulation to become more evident.

Sympathetic nerve stimulation resulted in decreases in the clearance rates of both tracers in all cases and these decreases were frequency dependent. In some cases the elimination rate even approached zero at a frequency of about 5–6 Hz.

In our opinion the most likely explanation for the reduced clearance rates during nerve stimulation is a reduction in the number of capillaries open to perfusion with the two important consequences of increasing the diffusion distances and reducing the capillary surface area. The fact that no difference was found in the magnitude of the reductions during sympathetic nerve stimulation between a lipophilic and a hydrophilic tracer implies that there were increases in diffusion distances of macroscopic dimensions (Crone and Garlick 1970). Extending this line of reasoning still further it might be assumed that the increases found in the disappearance rates after nerve stimulation as well as during nerve stimulation after an α blockade were due to an opening up of more capillaries thus shortening the diffusion distances and increasing the capillary surface area.

In order further to study the area changes occurring during sympathetic stimulation rubidium extraction was determined in another series of experiments. Certain differences exist in adipose tissue as compared to those tissues previously used with this method such as the ability of the adipocytes to concentrate rubidium and these have been discussed in the Methods section of this paper. The absolute values of the PS-products might therefore be subject to some question. However the relative changes such as the decrease of the PS values during nerve stimulation should still be valid.

Rubidium extraction has been used by various investigators to determine PS-values which have been considered to reflect changes of the capillary surface area.

However in the last few years studies have been performed which show that plateau PS values i.e. PS values calculated from extractions obtained in the equilibrium phase after the washout of the nonradioactive blood are influenced not only by the resistance in the capillary wall but also by external factors, e.g. the tissue cell membrane. Sheehan and Renkin (1972) concluded that, for skeletal muscle at rest, only one half of the resistance to rubidium transport was due to the capillary wall while the other half was located in the muscle cell membrane.

It seems possible that for adipose tissue also part of the resistance to rubidium transport is located outside the capillary wall. Perry and Hales (1970) have shown that lipolytic stimuli decrease the resistance of the fat cell membrane to the passage of substances like potassium and chloride. Therefore it appears reasonable to assume that the constant decrease in the PS products for rubidium found in this study during nerve stimulation could not be an effect of a resistance change in the fat cell membrane since that would in this case work in the opposite direction. Rather it seems quite likely that the decreases in the PS products found are due to an increased resistance in the capillary wall which might result from a decrease of the capillary surface area and also possibly from an increased resistance in the interstitial space due to prolonged diffusion distances, as is suggested by the dye appearance studies.

Thus it appears probable that the qualitative change, the decrease in the PS products with nerve stimulation is due to a decrease in the capillary surface area, a result much different from the vasodilatation suggested by the previously mentioned CFC data. This is also in accordance with the results and interpretations of the effects of sympathetic nerve stimulation in skeletal muscle (Renkin and Rosell 1962) and intestine (Dresl *et al.* 1966) using the same measuring technique. Concerning PS of rubidium as a quantitative measure of surface area changes during the present circumstances more careful conclusions should be drawn, since there are factors which tend to overestimate as well as underestimate alterations of the capillary surface area. Thus for example the increase of the flow velocity in those capillaries remaining open during stimulation will lead to an overestimation of the area changes while the existence of a resistance to the rubidium transport outside the capillary membrane will have the opposite effect.

The results from the two series of experiments performed in this study appear to indicate that a reduction of the perfused capillary surface area occurs in subcutaneous adipose tissue during sympathetic nerve stimulation. This appears reasonable considering that both the arteriolar and the capacitance sections respond to sympathetic nerve stimulation with a constriction (Öberg and Rosell 1967). Taken in connection with the results from the present study the previously mentioned CFC data indicate a flowability increase in the capillaries during nerve stimulation, an idea supported by investigations in which the CFCs were measured using vasodilating drug (Edholm *et al.* 1970). In that study it was found that the CFC increase during nerve stimulation exceeded that found during a maximal vasodilatation. In fact the CFCs measured during nerve stimulation were of the same

magnitude as those obtained using substances such as histamine and bradykinin compounds commonly considered to alter capillary permeability

In summary the results from this investigation appear to show that there is a decrease of the perfused capillary surface area during sympathetic nerve stimulation. It would thus appear that the increase in the CFC earlier found during similar conditions may indicate an increased permeability of the capillaries during nerve stimulation a possibility which should be investigated further

This investigation has been supported by the Swedish Medical Research Council (Proj. nr 40\ 3518) and from Svenska Sällskapet för Medicinsk Forskning

References

- BOLME P and L EDWALL, Dissociation of tracer disappearance rate and blood flow in isolated skeletal muscle during various vascular reactions *Acta physiol scand* 1971 87 17-27
- CORNBOLD A B FOLKOW I KJELLNER and S MELLANDER Nervous and local chemical control of pre-capillary sphincters in skeletal muscle as measured by changes in filtration coefficient *Acta physiol scand* 1963 57 180-197
- KRONZ C and D GARLICK, The penetration of inulin sucrose mannitol and tritiated water from the interstitial space in muscle into the vascular system *J Physiol (Lond.)* 1970 210 387-404
- DRESEL P B FOLKOW and I WALLENTIN Rubidium⁸⁶ clearance during neurogenic redistribution of intestinal blood flow *Acta physiol scand* 1966 67 173-184
- FOLKOW B O LUNDGREN and I WALLENTIN Studies on the relationship between flow resistance capillary filtration coefficient and regional blood volume in the intestine of the cat *Acta physiol scand* 1963 57 270-283
- FREDHOLM B II ÖBERG and S ROSELL, Effects of vasoactive drugs on circulation in canine subcutaneous adipose tissue *Acta physiol scand* 1970 79 564-574
- HILLS B A Diffusion versus blood perfusion in limiting the rate of uptake of inert non polar gases by skeletal rabbit muscle *Clin Sci* 1967 33 67-87
- KETY S S Measurement of regional circulation by the local clearance of radioactive sodium *Am Heart J* 1949 38 321-378
- LARSEN ANDREAS O N A LASSEN and F QLAAD, Blood flow through human adipose tissue determined with radioactive xenon *Acta physiol scand* 1966 66 337-345
- ÖBERG B Effects of cardiovascular reflexes on net capillary fluid transfer *Acta physiol scand* 1964 62 Suppl 229
- ÖBERG B and S ROSELL, Sympathetic control of consecutive vascular sections in canine subcutaneous adipose tissue *Acta physiol scand* 1967 71 47-56
- PERRY M C and C N HALES Factors affecting the permeability of isolated fat-cells from the rat to potassium and ³⁶Cl chloride ions *Biochem J* 1970 117 615-621
- RENKIN E M Transport of potassium 42 from blood to tissue in isolated mammalian skeletal muscles *Am J Physiol* 1959 6 1203-1210
- RENKIN E M O HUDLICKA and R M SHEEHAN Influence of metabolic vasodilatation on blood tissue diffusion in skeletal muscle *Am J Physiol* 1967 211 87-98
- RENKIN E M and S ROSELL The influence of sympathetic adrenergic vasoconstrictor nerves on transport of diffusible solutes from blood to tissues in skeletal muscle *Acta physiol scand* 1962 54 223-240
- ROSELL S Release of free fatty acids from subcutaneous adipose tissue in dogs following sympathetic nerve stimulation *Acta physiol scand* 1966 67 343-351
- SHEEHAN R M and E M RENKIN Capillary interstitial and cell membrane barriers to blood tissue transport of potassium and rubidium in mammalian skeletal muscle *Circulat Res* 1972 30 588-607

From the Department of Physiology II Karolinska Institutet Stockholm the Department of Ophthalmology University of Linköping and the National Board of Occupational Safety and Health Stockholm Sweden

The Effect of Barbiturate on Retinal Functions II Effects on the C-wave of the Electroretinogram and the Standing Potential of the Sheep Eye

By

BENGT KNAVE, HANS E PERSSON and SVEN ERIK G NILSSON

Received 21 November 1973

Abstract

KNAVE B H E PERSSON and S E G NILSSON *The effect of barbiturate on retinal functions II Effects on the c-wave of the electroretinogram and the standing potential of the sheep eye Acta physiol scand 1974 91 180-186*

The present work is the second in a series of investigations on the effect of barbiturate on retinal functions. The changes in the c-wave of the conventional ERG and in the standing potential (SP) of the intact sheep eye were studied after intravenous administration of an ultra short acting barbiturate thiopental. The c-wave was transiently decreased or abolished after a small dose (< 10 mg/kg) whereas a negative shift could be observed in the SP. Larger doses resulted in negative positive cyclic variations of the c-wave amplitude and the SP resembling damped oscillations. There was an increase of the a- and b-waves after barbiturate administration not related to the SP-changes. The effect of barbiturate on the components of the conventional ERG and the SP was also studied after selective blocking of the function of the pigment epithelial cells with sodium iodate. Hereby the barbiturate induced changes of the c-wave and the SP disappeared whereas those of the a- and b-waves remained. On the basis of these results the possibility that barbiturate has a dual site of action on the retina, namely on the inner retina and on the pigment epithelial cells cannot be excluded.

The effects of barbiturate on the functions of the neuroretina are well documented (e.g. Dainoff 1956 Wohlhagen 1956 Noell 1958 Knave and Persson 1974a, b). In short it has been found that small doses result in an increase of the a- and b-wave amplitude in the conventional electroretinogram (ERG) whereas larger doses depress them.

It has been suggested that pigment epithelial cells of the retina are specifically sensitive to certain drugs such as rifampicin (Roman 1973 Knave Persson Calissendorff and Nilsson 1973) chloroquine (Bernstein and Ginsberg 1964 Monahan and Horns 1964) and chlorpromazine (reviewed by Lindquist and Ullberg 1972).

On the basis of the aforementioned findings two questions were posed in the present study: 1. Do barbiturates also have an affinity for the pigment epithelial

cells and influence directly their function? 2 If so do barbiturates have a dual site of action on the retina namely on the neuroretina and on the pigment epithelium? To investigate these questions the *c* wave known to be generated in the pigment epithelium (Noell 1954 Brown and Wiesel 1961 Steinberg Schmidt and Brown 1970) and the standing potential (SP) which partly originates in the same cells (Noell 1954 1963 Gouras 1969) were studied before and after administration of barbiturate

Methods

The results are based on 9 successful experiments made on the intact sheep eye kept in the dark adapted state. The method used has recently been described in detail (Knave Møller and Persson 1972 see also Knave and Persson 1974a). It should be pointed out that with this method it is possible to record d.c. responses from the intact eye in long term studies during constant experimental conditions.

For the ERG recordings a stimulus intensity (i.e. about 50 log units above the *b* wave threshold) was chosen so as to provide an accurate evaluation of the *a*, *b* and *c* waves. Duration of the stimulus light was 0.1 s. Intervals between flashes were 2 min. The amplitudes of the *a* and *c* waves were measured from the isoelectric line and the amplitude of the *b* wave from the trough of the *a* wave. The amplitude values were calculated from the means of two consecutive summated responses.

The SP of the intact eye was recorded between a corneal electrode and an electrode placed subcutaneously at the upper bony margin of the orbit. These electrodes (calomel half-cells) were connected to the differential inputs of a low-drift d.c. amplifier.

An ultra short acting barbiturate thiopental (Pentothal Sodium®) which is the thioanalog of pentobarbital (Nembutal®) was used in the present study. The drug was administered through a catheter placed in a foreleg vein.

In some experiments the effect of barbiturate on the components of the conventional ERG and on the SP was registered after selective blocking of the function of the pigment epithelial cells by means of i.v. administration of sodium iodate (NaIO₃; Noell 1954).

Results

In Fig. 1A the amplitude of the *a*, *b* and *c* waves are graphically illustrated from an experiment in which low and moderate doses of thiopental were given (2.5, 5 and 10 mg thiopental per kg b.wt. arrows). A rapid dose related response increase of short duration of the *a* and *b* waves is seen following each injection. The *c* wave however immediately decreased after the injections and was even abolished after 5 and 10 mg thiopental. About 15 min after the latter injection the *c* wave amplitude reached a supernormal peak. Normal values were again obtained after another 15 min.

The i.v. injection of a large dose of thiopental (20 mg per kg b.wt.) resulted in a substantial transient increase of the *a* and *b* waves (Fig. 1B and Fig. 2 lower trace). The *c* wave decreased and was temporarily abolished. The depression of the *a* wave was followed by a slow transient increase with peak amplitudes about 16 min after injection (Fig. 1B and Fig. 2 upper trace). The *a* wave then showed amplitude variations resembling damped oscillations with a frequency of 2 per hour.

In addition to the effects described above barbiturate was found to induce changes in the standing (resting) potential (SP) of the eye. The SP is a d.c. poten-

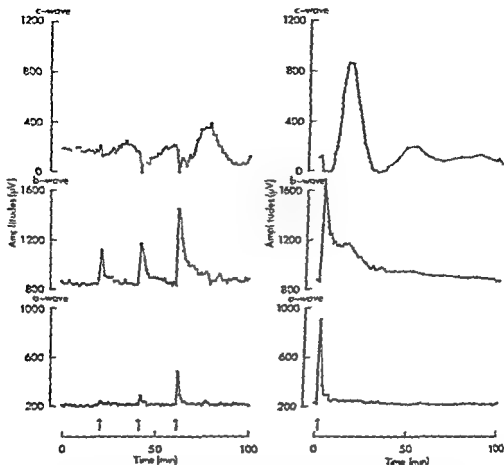


Fig. 1 A. Effect of thiopental on a, b and c wave amplitudes of the dark adapted sheep eye. Three successive injections of 2.5, 5 and 10 mg thiopental per kg b.wt., respectively, were given (arrows). Stimulus intensity: 50 log units above b-wave threshold. Stimulus duration: 0.1 s.

Fig. 1 B. Effect of thiopental on a, b and c wave amplitudes of the dark adapted sheep eye. A single injection of 20 mg per kg b.wt. was given (arrow). Stimulus intensity: 50 log units above b-wave threshold. Stimulus duration: 0.1 s.

lateral eye also is maintained across the eye making the cornea more positive than the pupil. In Fig. 3 A the SP was followed for 4 min (a: control) after 0.3, 0.6, 1.2, 2.5 and 5 mg thiopental per kg b.wt. (b, c, d, e and f, respectively). Following each injection a negative d.c. shift was recorded. An initial rapid phase was followed by a slow sustained one. As can be seen in the figure the initial phase was of the same order of magnitude after 0.3, 0.6, 1.2 and 2.5 mg thiopental as after 0.1 ml. After 5 mg thiopental this phase increased in amplitude with 0.3–0.4 mV. A dose related increase in amplitude and in duration of the slow negative shift was observed following 0.6, 1.2, 2.5 and 5 mg thiopental (cf. Sjöström in the latter recording (f)) the negative

Fig 2 ERG of the dark adapted sheep eye 18 min and 2 min after *i.v.* injection of 20 mg thiopental per kg bwt. (upper and lower recording respectively) Stimulus intensity 50 log units above the b wave threshold Stimulus duration 0.1 s Time calibration 1 s Amplitude calibration 200 μ V

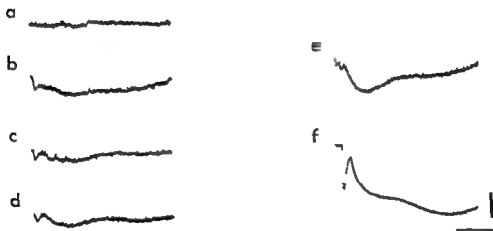
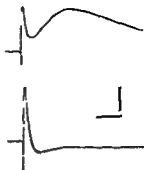


Fig 3A Effect of thiopental on the standing potential (SP) of the dark adapted sheep eye. The SP was followed 4 min (a control) after *i.v.* injections of 0.3 0.6 1.2 2.5 and 5 mg thiopental per kg bwt (b e d e and f respectively) Time calibration 1 min Amplitude calibration 0.2 mV (a-e) and 0.5 mV (f)



Fig 3B Effect of thiopental on the standing potential (SP) of the dark adapted sheep eye. The SP was followed 64 min after *i.v.* injection of 10 mg thiopental per kg bwt. Time calibration 10 min Amplitude calibration 4 mV



Fig 3C Effect of thiopental on the standing potential (SP) of the dark adapted NaIO_3 treated sheep eye. Two injections of 5 mg thiopental per kg bwt were given (arrows), 80 min after *i.v.* injection of 30 mg NaIO_3 per kg bwt. Time calibration 2 min Amplitude calibration 0.5 mV

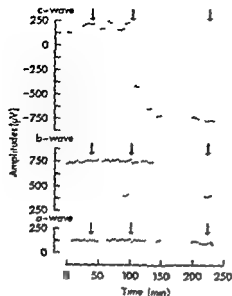


Fig 4 Effects of sodium iodate on the *a*, *b* and *c* wave amplitudes of the dark adapted sheep eye. At 40, 100 and 225 min (arrows) i.e. injections of 50 ml Ringer's solution, 30 mg NaIO_3 per kg b.wt. and 5 mg thiopental per kg b.wt. respectively were given. Stimulus intensity 5.0 log units above *b* wave threshold. Stimulus duration 0.1 s.

shift did not return to the original d.c. level, the changes in SP were studied for a much longer period of time, as illustrated in Fig 3B. In this recording the SP was followed for 64 min after an i.e. injection of 10 mg thiopental per kg b.wt. The negative d.c. shift was found to be followed by a slow, positive d.c. shift with a peak amplitude about 13 min after injection. The SP then showed smooth variations similar to the oscillations seen in the *c* wave in Fig 1B. At the end of the recording i.e. 64 min after barbiturate administration, the SP was still negative compared to the original isoelectric line.

It should be pointed out that there is a striking resemblance in the reaction pattern in terms of time course of the polarity and amplitude changes of the *c* wave and the SP in response to a single dose of thiopental. No similarities whatsoever could be demonstrated however between the SP and *a* and the *b* wave of the ERG.

The results obtained show that the changes in the *c* wave and SP after barbiturate administration have similar time characteristics differing from those of the *a* and *b* waves. This difference may be due to different sites of action in the retina: (1) the pigment epithelial cells and (2) the neuroretina. In order to further study this dual site action experiments were undertaken in which the function of the pigment epithelial cells was selectively blocked by means of administration of sodium iodate (NaIO_3 ; NaOH 19,4).

In Fig 4 the *a*, *b* and *c* waves were recorded after i.e. injection of 50 ml of Ringer's solution (arrow at 40 min) after i.e. injection of 30 mg per kg b.wt. of NaIO_3 (arrow at 100 min) and after i.e. injection of 5 mg per kg b.wt. of barbiturate (thiopental, arrow at 225 min).

The *a*, *b* and *c* waves remained unchanged after injection of Ringer's solution. After injection of NaIO_3 the *m* and *n* waves were still not changed whereas the *c* wave was abolished dramatically. This is illustrated in Fig. 4 where the *c* wave amplitude prior to the NaIO_3 injection was about 150–200 μV . After the injection the *c* wave was replaced by the so-called remnant negativity, the level of which was 750 μV below the isoelectric line. Thus the total change in amplitude amounted to about 1000 μV . Approximately 100 min after the NaIO_3 injection, the *b* wave and to a less extent the *a* wave also began to decrease in amplitude. The thiopental injection (5 mg per kg b.wt.) given 125 min after the NaIO_3 resulted in an amplitude increase of the residual *a* and *b* waves.

During the time period from 80–95 min after NaIO_3 administration the SP was followed after injections of 5 mg thiopental per kg b.wt. (Fig. 5 arrows). Insignificant negative shifts were obtained in the SP. However these changes were of a very small magnitude compared to those recorded from eyes with intact pigment epithelium (see Fig. 3A f).

Discussion

The present study shows that barbiturates have an effect on the *c* wave of the ERG and on the SP recorded from the intact eye. Furthermore there was similarity in the time course of the polarity changes of these potentials. The *c* wave is known to be generated in the pigment epithelial cells of the retina (Noell 1954; Brown and Wiesel 1961; Steinberg, Schmidt and Brown 1970) and these cells are considered at least partly to be responsible for the SP (Noell 1954, 1963; Gouras 1969). These facts give evidence that barbiturates in some way influence the pigment epithelium. This view is further supported by the observation that the barbiturate effects on the *c* wave and the SP were abolished after blocking the functions of the pigment epithelium with sodium iodate.

No similarities whatsoever could be observed between the barbiturate induced changes of the *a* and *b* waves and those of the SP. Furthermore the *a* and *b* wave alterations remained after administration of sodium iodate whereas the changes of the *c* wave and the SP were dramatically abolished. These observations may indicate that barbiturates have a dual site of action on the retina, namely on the neuroretina and on the pigment epithelium cells.

The functional mechanism behind the low dose effect on the pigment epithelial potentials is not easily explained since it is considered that large amounts of barbiturate are needed to influence the functions of non nervous tissues (*cf.* Sharpless 1970). However the results obtained may be explained by a mechanism in which the barbiturates change the conductance of ions in the pigment cell membranes. This supposition is supported by observations that barbiturates influence the sodium and potassium transmembrane conductance of voltage-clamped lobster axons (Blaustein 1968). It cannot be excluded that the normal functional relationship between receptors and pigment epithelium cells (see *eg.* Noell 1954; Steinberg *et al.* 1970) may in some way be disturbed by the barbiturates.

It should be emphasized that in the present study it was possible to analyse not only the immediate effects of the barbiturate but also to demonstrate for the first time long term effects of this drug on the *c* wave and the SP. This is even more important since the administered doses were sometimes only a few per cent of the doses used to obtain general anesthesia in the sheep. Thus, it is evident that this experiment illustrates a possibility to study the effects of other substances and drugs with neuropharmacological actions or with affinity to retinal cells (see e.g. Knave, Persson, Calusendorf and Nilsson 1973).

This work was supported by grants from the Swedish Medical Research Council, the Magnus Bergvall Foundation for Scientific Research, the Hierta Foundation for Ophthalmological Research and Karolinska Institute.

References

- BERNSTEIN H. N. and J. GINSBERG. The pathology of chloroquine retinopathy. *Arch Ophthalmol* 1964, 71: 238-245.
- BLACSTEIN M. P. Barbiturates block sodium and potassium conductance increases in voltage-clamped lobster axons. *J gen Physiol* 1968, 51: 293-307.
- BOMAN G. Melanin affinity of a new antituberculous drug rifampicin investigated by whole body autoradiography. *Acta ophthalmol (Kbh)* 1973. In press.
- BROWN K. T. and T. N. WISSEL. Localization of origins of electroretinogram components by intra retinal recording in the intact cat eye. *J Physiol (Lond)* 1961, 158: 257-280.
- DANIS P. Modifications de l'électroretinogramme du rat produites par l'injection intra artérielle proche de potassium de veratrine et de narcotiques. *J Physiol Path gen* 1956, 48: 419-483.
- GOURAS P. Clinical electro-oculography. In Straatsma, B. R. (Ed.) *The Retina*. University of California Press, Berkeley and Los Angeles 1969: 563-581.
- KNAVE B. and H. E. PERSSON. The effect of barbiturate on retinal functions. I. Effects on the conensual electroretinogram of the sheep eye. *Acta physiol scand* 1974a, 91: 53-60.
- KNAVE B. and H. E. PERSSON. The effect of barbiturate on retinal functions. III. Effects on the isolated receptor responses and the inner nuclear layer components in the low intensity electroretinogram of the sheep eye. *Acta physiol scand* 1974b, 91: 187-195.
- KNAVE B., A. R. MÖLLER and H. E. PERSSON. A component analysis of the electroretinogram. *Acta ophthalmol (Kbh)* 1972, 50: 1669-1684.
- KNAVE B., H. E. PERSSON and S. E. G. NILSSON. A comparative study on the effects of barbiturate and ethyl alcohol on retinal functions with special reference to the *c* wave of the electroretinogram and the standing potential of the sheep eye. *Acta ophthalmol (Kbh)* 1973. In press.
- KNAVE B., H. E. PERSSON, B. CALUSENDORFF and S. E. G. NILSSON. Selective effects of a new antituberculous drug rifampicin on the *c* wave of the sheep electroretinogram. *Acta ophthalmol (Kbh)* 1973, 51: 31-374.
- LUNDH G. N. C. and S. ULBERG. The melanin affinity of chloroquine and chlorpromazine studied by whole body autoradiography. *Acta pharmacol (Kbh)* 1972, 31: Suppl. II.
- MOVVAH A. and R. C. HORR. The pathology of chloroquine in the eye. *Trans Amer Acad Ophthalmol* 1954, 68: 40-44.
- NOELL W. H. Section of the electroretinogram. *Amer J Ophthalmol* 1954, 38: 18-60.
- NOELL W. H. A metabolic organization and stability of the visual cell. *Arch Ophthalmol* 1955, 53: 33.
- NOELL W. H. The structure of the retina. *J Ophthalmol Soc Amer* 1963, 53: 36-48.
- SHARPLEY S. H. Barbiturates. In L. Goodman and A. Gilman (Ed.) *The Pharmacological Basis of Therapeutics*. MacMillan Company, New York 1970: 108-120.
- STEINBERG H. H. R. SCHUMMER and K. Y. BROWN. Intracellular responses to light from cat primate epithelial origins of the electroretinogram *c* wave. *Nature (Lond)* 1970, 227: 2-730.
- WOLFGANG F. A. Beeftink. Der 5. und 6. FRC durch zentralen Nervenzusammenbruch. *Z. Pfl. 1971, 109: 21-23*.

The Effect of Barbiturate on Retinal Functions III Effects on the Isolated Receptor Responses and the Inner Nuclear Layer Components in the Low intensity Electroretinogram of the Sheep Eye

By

BERGT KNÄVE and HANS E PERSSON

Received 21 November 1973

Abstract

KNÄVE B and H E PERSSON *The effect of barbiturate on retinal functions III Effects on the isolated receptor responses and the inner nuclear layer components in the low intensity electroretinogram of the sheep eye Acta physiol scand 1974 91 187-195*

The present study is the third in a series of investigations on the effects of barbiturate on retinal functions. The changes in the isolated receptor responses and inner nuclear layer components of the low intensity electroretinogram (ERG) of the intact sheep eye were studied after iv administration of an ultra short acting barbiturate thiopental. The low intensity ERG is the electroretinographic responses below the b wave threshold have recently been shown to consist of a slow corneanegative receptor potential and two d.c. responses of opposite polarity presumably generated in the inner nuclear layer. The administration of small doses of thiopental (5 mg/kg) had no effect on the receptor response whereas larger doses (10 mg/kg) increased its amplitude. The most striking effect of thiopental was an enhancement of the positive d.c. response which could be observed already at barbiturate doses of 5 mg/kg. The results are consistent with the assumption that barbiturates primarily influence the cells of the inner nuclear layer and secondly the receptors. It is suggested that the functional mechanism behind the barbiturate effect on the inner nuclear layer (as expressed in the increase of the positive d.c. component) constitutes an intraretinally mediated disinhibition of the "on type" bipolar cells i.e. the presumed generators of the positive d.c. component.

The results of the preceding papers (Knäve and Persson 1974, Knäve, Persson and Nilsson 1974 a) support the hypothesis that barbiturates influence the functions of both the neuroretina and the pigment epithelial cells. The effect on the neuroretina of comparatively small doses was reflected in an increase of the a and b waves of the conventional electroretinogram (ERG). This observation is a confirmation of what most studies on intact and isolated mammalian eyes have shown (see e.g. Danis 1956, Wohlzogen 1956, Noell 1958, Arden, Granit and Ponte 1960, Honda and Nagata 1971). As to the studies on separated ERG components barbiturates

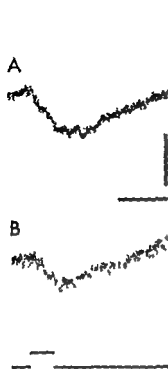


Fig. 2 Effect of thiopental on the receptor potential of the low intensity ERC (cf. lowest record Fig. 1). The summated ERGs (50 responses) are shown before (A) and after (B) the administration of 5 mg thiopental per kg b.wt. Stimulus intensity 2.5 log unit below the *b* wave threshold. Stimulus duration 1 s. Time calibration 1 s. Amplitude calibration 2 μ V.



Fig. 3 Effect of thiopental on the receptor potential. The summated ERGs (50 responses) are shown before (A) and after (B) the administration of 10 mg thiopental per kg b.wt. Note the enhancement of the receptor negativity and of the two negative notches at onset and cessation of light which occurs with this dose of barbiturate. Stimulus intensity 2.5 log units below the *b* wave threshold. Stimulus duration 1 s. Time calibration 1 s. Amplitude calibration 2 μ V.

evidence for an effect of larger doses of barbiturate (10 mg/kg) on the receptor function of the intact sheep eye as has been described for the isolated perfused rabbit retina (Bornschein *et al.* 1966). On the other hand the amplitude increase of the receptor potential may also be due to an excitability increase of the inner nuclear layer and mediated through the recently found feed back from the horizontal cells upon the receptors (Baylor and Hodgkin 1973).

In Fig. 4 A illustrates a typical record of the low intensity FRC elicited by flashes with an intensity of 1.0 log unit below the *b* wave threshold. The administration of 5 mg thiopental per kg b.wt. resulted in an increase of the amplitude of the positive dc response without a concomitant enhancement of the amplitude of the receptor negativity. A delayed return of the negativity to the isoelectric line



Fig 4 Effect of thiopental on the positive and negative dc responses of the low intensity ERG. The summed ERGs (50 responses) are shown before (A) and after (B) administration of 5 mg thiopental per kg. Note the increase of the positive dc response and the delayed return of the receptor negativity to the isoelectric line without constant enhancement of the amplitude of the receptor negativity. Stimulus intensity 10 log unit below the b-wave threshold. Stimulus duration 1 s. Time calibration 2 s. Amplitude calibration 8 μ V.

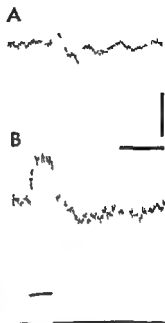


Fig 5 Effect of thiopental on the positive and negative dc responses of the low intensity ERG. At the stimulus intensity used (20 log units below threshold) the low intensity ERG has a configuration similar to the top record in Fig 1. The summed ERGs (50 responses) are shown before (A) and after (B) administration of 10 mg thiopental per kg. Note the increase of the positive dc response and the increase of the receptor response. Stimulus duration 1 s. Time calibration 2 s. Amplitude calibration 8 μ V.

(Fig 4 B) was noted however. After the administration of 10 mg thiopental per kg more pronounced alterations could be recorded in the configuration of the low intensity ERG (Fig 5 B). A positive plateau developed between the two negative notches as an indication of a substantial increase of the positive dc response. Furthermore there was an increase in amplitude of the negative receptor potential (cf Fig 3).

Discussion

The foregoing results obtained in the intact sheep eye show that small doses of barbiturates (thiopental 5 mg/kg) had no effect on the slow negative potential of the low intensity ERG whereas larger doses (10 mg/kg) increased its amplitude. Since this negativity has been claimed to be generated by the rod receptors (Knave Møller and Persson 1972) the results may be taken as evidence for an effect of larger doses of barbiturates on the receptor cells. Support for this notion is the findings from studies made on the isolated perfused retinas of the rabbit (Bornschein *et al.* 1966) and cat (Wundsch and Ulrich 1971). These authors found that a negative component identical to the P III of Granit (1933), was enhanced by the local application of larger doses of barbiturates. Furthermore, the receptor potential isolated by clamping the central retinal arteries of the cat is reported to be increased by barbiturates (Brown 1966). It is evident, however, that on the basis of the present results it is not possible to explain the nature and mode of actions of barbiturates on the receptors. For instance the possibility cannot be excluded that the barbiturate effect on receptor functions is indirectly mediated via a primary barbiturate action on the feed back from the horizontal cells (*cf.* Baylor and Hodgkin 1973).

A large number of facts favours the view that the positive d.c. component of the low intensity ERG is generated by cells located in the inner nuclear layer presumably the on type bipolar cells (see Knave Møller and Persson 1972). Since thiopental administered in small doses enhanced the positive d.c. component it is logical to suggest that barbiturates have an early precise effect on the functions of the inner nuclear layer cells. This supposition is not contradicted by the fact that the b wave which mainly originates from the same layer (see *e.g.* Brown 1968) increases in amplitude after barbiturates (see *e.g.* Danis 1956 Wohlzogen 1956 Yonemura Kawasaki and Tsuchida 1966). Further supporting the observation that the positive d.c. component is increased by barbiturates are the results obtained by Yonemura Kawasaki and Tsuchida 1966. These authors found that a slow positive potential resembling the d.c. component of Brown and Wiesel (1961 see also Brown 1968) could be unmasked in the corneal ERG after barbiturate administration.

The functional mechanisms behind the enhancement of the positive d.c. component are not easily explained since barbiturates are known to depress a wide range of cellular functions (*e.g.* Sharpless 1970) and inhibit synaptic transmission in the CNS (*e.g.* Eccles 1966 Loynning Oshima and Yokota 1966 Hongo Janikowska and Lindberg 1966 Weakly 1969). However this enhancement may be brought about by a depression of an inhibitory synaptic system in the retina which controls the functions of the cells generating the positive d.c. component. In this connection it is relevant to refer to the recently performed component analysis of the mammalian ERG in Knave Møller and Persson (1972). These authors claimed that the cells probably off type bipolar cells (see Kaneko and Hashimoto 1969) and Kaneko (1970) and horizontal cells) generating the negative d.c.

response are inhibitory in nature and exert an inhibitory influence on the cells (presumably on type bipolar cells see Kaneko and Hashimoto (1969) and Kaneko (1970)) generating the positive d.c. component. Considering the facts presented it is tempting to suggest that the primary effect of barbiturate on the retina is to selectively suppress the inhibitory cells which generate the negative d.c. component. Hereby, the inhibitory action on the cells generating the positive d.c. response is inhibited thus releasing the positive d.c. response. This hypothesis is consistent with the frequently accepted view that barbiturates in the doses used in the present study have a direct disinhibitory effect on intraretinal neuronal structure (see e.g. Danis 1956 Wohlzogen 1956 Bornschein *et al.* 1966 Yonemura *et al.* 1966 Wundsch and Ulrich 1971 Honda and Nagata 1972). The suggestion that barbiturates primarily do not have an effect on synaptic transmission (Ponte 1960) can not be excluded on the basis of the present results. However this notion is deemed unlikely.

The complementary results on the effects of thiopental on the low intensity ERG may offer an explanation of the barbiturate induced enhancement of the *a* and *b* waves of the conventional ERG as repeatedly shown. Since the *a* wave constitutes the leading edge of the receptor potential (distal P III for references see Tomita 1970 1972) the increase in amplitude of this potential may account for the increase of the *a* wave. A further enhancement of the *a* wave may be brought about by a delay in the time course of the *b* wave (Noell 1958 Yonemura *et al.* 1966). It has been shown that the *b* wave is mainly built up by the positive d.c. response (Knave *et al.* 1972). As mentioned the most striking effect of thiopental administration was the increase of the positive d.c. component which is expressed in a concomitant enhancement of the *b* wave. The increase of the positive d.c. response appears to represent a release of the activity in on type bipolar cells of the inner nuclear layer from an inhibitory influence exerted by the off type bipolar cells and/or the horizontal cells (see above). Thus the enhancement of the *b* wave is suggested to be a sign of this disinhibitory effect.

The results of the present series of investigations on the effect of thiopental on retinal functions (Knave and Persson 1974 Knave Persson and Nilsson 1974 a b) lend support to the notion that thiopental may have a dual site of action on the retina namely on the neuroretina and on the pigment epithelial cells. The thiobarbiturate thiopental has a short duration of action (Sharpless 1970 Knave and Persson 1974). The summation technique of the low intensity ERG is a time consuming process and the thiopental effects recorded with this method probably also encompass stages under which the drug action on the retina begins to decrease. Hence a direct comparison can not be made between the results obtained with this technique and those obtained with conventional ERG recording. However it should be emphasized that the aim of the present work was to compare the effects of small and moderate doses of thiopental on the low intensity ERG responses. With regard to the doses used the barbiturate primarily influenced the functions of the cells in the inner nuclear layer and secondly the functions of the receptors. These effects

- SHARPLESS E R The barbiturates In L Goodman and A Gilman (Eds) *The Pharmacological Basis of Therapeutics* MacMillan Company New York 1970 98—120
- TOMITA T Electrical activity of vertebrate photoreceptors *Quart Rev Biophys* 1970 3 179—222
- TOMITA T The electroretinogram as analysed by microelectrode studies In M G F Fuortes (Ed) *Handbook of Sensory Physiology* Springer Verlag Berlin—Heidelberg—New York 1972 Vol VII/2 635—665
- TRIMARCHI F Effect of barbiturates on the electroretinogram *Ann Ottol* 1968 94 1725—1729
- WEAKLY J N Effect of barbiturates on quantal synaptic transmission in spinal motoneurons *J Physiol (Lond)* 1969 204 63—77
- WOHLZOGEN F V Beeinflussung des Sauger ERG durch zentral nervös wirksame Substanzen *Z Biol* 1956 108 217—233
- WUNDSCH L and W D ULRICH Der Barbiturateffekt am negativen Elektroretinogramm der Katze *Klin Wochenschr* 1971 83 877—878
- YONEMLA D K KAWASAKI and Y TSUCHIDA Differential vulnerability of the ERG components to pentobarbital *Jap J Ophthalmol* 1966 10 Suppl 155—166

The Action Potential in End-Plate and Extrajunctional Regions of Rat Skeletal Muscle¹

By

S THIESLEFF, F VYSKOČIL* and M R WARD

Received 30 November 1973

Abstract

THIESLEFF, S, F VYSKOČIL and M R WARD *The action potential in end plate and extrajunctional regions of rat skeletal muscle* Acta physiol scand 1974 91 196-202

In the innervated rat diaphragm muscle, the maximum rate of rise of the action potential was approximately 20% greater in the end plate region as compared to non junctional areas. This difference in rate of rise was maintained for a period of at least 14 days after denervation. Desensitization of the post junctional membrane by carbachol or irreversible blockade of the cholinergic receptor system by use of a toxin from *Naja naja namensis* failed to reduce this difference. When TTX (10^{-6} M) was added to the bathing fluid action potentials could no longer be elicited from innervated fibres: a sodium-dependent local response remained in most fibres however but only in the end plate region. After surgical denervation the action potential becomes partially resistant to the blocking action of TTX and it was found that the action potential in the end plate region was more resistant than that in non junctional areas. The results show the presence of TTX insensitive ionophores situated in the post junctional membrane of innervated and denervated muscle fibres. It is suggested that these TTX insensitive sites contribute to the observed greater rate of rise of action potentials elicited from these areas.

Recently Nisink and Alexander (1973) reported that action potentials initiated at the end plate or transversing the junctional region of frog sartorius muscle fibres show a maximum rate of rise substantially greater ($\sim 20\%$) than that of action potential initiated or transmitted through non junctional regions. As an explanation they tentatively suggested the existence of more sodium ionophores per unit length at the junctional region.

Redfern and Thiesleff (1971 b) observed that the action potential of mammalian skeletal muscle following denervation becomes insensitive to the blocking effect of tetrodotoxin (TTX) and that this change is correlated in time and in space with the appearance of extrajunctional cholinergic receptors in the muscle membrane.

¹Footnote: The study was carried out under the auspices of The Czechoslovak Academy of Sciences and the Royal Academy of Sciences in Sweden.

*Present address: Institute of Physiology Czechoslovak Academy of Sciences Prague

Together these observations suggested the possibility that the end plate region of innervated muscle fibres in addition to normal TTX sensitive action potential ionophores also had TTX resistant ones similar to those found in denervated muscles and that these TTX resistant sodium channels were responsible for the greater rate of rise of the action potential in the end plate.

Recordings were therefore made of action potentials in junctional and non junctional regions of the isolated rat diaphragm muscle and the effects of TTX were examined.

Methods

The experiments were made on isolated hemidiaphragm muscles of adult male Wistar rats with a body weight of 180–200 g. In some experiments the hemidiaphragm muscle was denervated by intrathoracic sectioning of the phrenic nerve under ether anaesthesia.

To generate and to record the action potential two microelectrodes were inserted into the same surface fibre about 50 μm apart; one electrode was used for current passing the other to record the potential change. Constant anodal current was passed through the electrode to locally polarize the muscle fibre to -90 to -100 mV, a level previously shown to be adequate for spike generation. A cathodal shock of 3–5 ms duration was used to produce a regenerative response (for details see Redfern and Thesleff 1971 a).

Action potentials were generated and recorded in the end plate region of the fibre and in a region 2–4 mm distant from that region, i.e. about half way between the end plate and the tendon. In innervated muscles the end plate was localized by the recording of miniature end plate potentials with a fast rising phase and in denervated muscles it was assumed that the former end plate was in the centre of the muscle close to the degenerating nerve.

The maximum rate of rise and fall of the action potential were obtained by the use of a RC derivating circuit. The threshold or critical membrane potential ($E_{crit.}$) was taken as the potential level at which the first sign of an active response was observed. When the active response failed to exceed the zero potential level of the cell it was considered to be a local response otherwise an action potential. As a measure of the time course of the action potential the duration of "overshoot" at zero potential was taken.

The oxygenated bath fluid had the composition described by Liley (1956) with the difference that the concentration of calcium was 4 instead of 2 mM (Redfern and Thesleff 1971 a). The temperature of the organ bath was $29 \pm 0.5^\circ C$. When the sodium concentration of the bathing fluid was reduced to 20 mM osmolality was maintained by adding choline chloride. Tetrodotoxin crystalline 3x was obtained from Sankyo Co. Ltd. Tokyo and the isolated *Naja naja siamensis* neurotoxin 3 from Dr D. Eaker, Institute of Biochemistry, University of Uppsala, Sweden. Desensitization of cholinergic receptors was produced by the addition to the bathing fluid of 0.5 $\mu g/ml$ of the diethylaminoethyl ether of diphenylpropyl acetic acid (SHF525A) followed by carbachol ($10^{-4} M$) (Magazanik 1970). When the drugs were added to the bathing fluid at least 30 min was allowed for equilibration before the experiment.

Results

In the innervated rat diaphragm muscle we confirmed the observation of Nastuk and Alexander (1973) in the frog that the maximum rate of rise of the action potential is higher in the end plate region than in other areas of the muscle fibre. As shown in Table I the mean maximum rate of rise of the spike at the end plate was 300 V/s but it was only 302 V/s outside this region, i.e. there was a statistically significant difference of 18%. Similarly was the amount of overshoot greater at the end plate than in non junctional areas.

TABLE II The effect of TTX on action potential generation in normal and denervated rat diaphragm muscle fibres

TTX Conc (M)	Days Elap	Site	Action Potentials (Number)	Local responses (Number)	Total number of fibres
5×10^{-7}	Normal	A	11	4	15
		B	8	7	15
10^{-6}	Normal	A	0	38	49
		B	0	3	49
5×10^{-6}	Normal	A	0	2	26
		B	0	0	30
10	1 day	A	7	12	23
		B	0	10	23
5×10^{-5}	1 day	A	6	5	30
		B	0	0	30
10^{-4}	2 days	A	16	5	22
		B	2	13	22
5×10^{-4}	2 days	A	27	3	30
		B	8	12	30
10	3 days	A	23	0	23
		B	21	2	23
5×10^{-4}	3 days	A	28	2	30
		B	9	14	30
10^{-3}	7 days	A	26	0	26
		B	21	7	29
5×10^{-3}	7 days	A	30	0	30
		B	6	16	30
10^{-2}	14 days	A	15	0	15
		B	11	3	15
5×10^{-2}	14 days	A	46	0	46
		B	19	18	45

enhances the rate of desensitization (Magazanik 1970 Magazanik and Vyskocil 1973) and in our experiments carbacholine (10^{-4} M) depolarized the end plate region by only about 5 mV before complete desensitization occurred.

As shown in Table I desensitization or blockade of the cholinergic receptor system had little effect on the difference in maximum rate of rise of action potentials recorded from end plate or non junctional zones.

When TTX was added to the bathing fluid at a concentration of 5×10^{-7} M action potentials could be elicited from most fibres at the end plate region but from about only half the total tested from non junctional zone (Table II). When TTX concentration was increased to 10^{-6} M action potentials could no longer be elicited from any part of the muscle fibre but a local response was present in most fibres (38 out of 49) at the end plate region as shown by Fig. 1. In extrajunctional regions of the muscles cathodal current pulses of increasing intensity gave rise only to larger and larger electrotonic potentials and with the highest level of cathodal depolarization to delayed rectification. In 5×10^{-6} M TTX local responses were

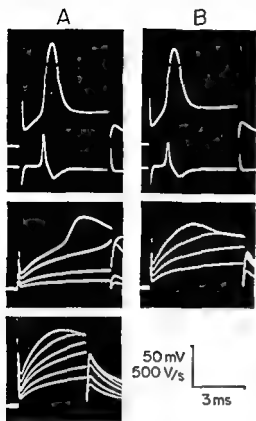


Fig. 1. Intracellular records of typical responses to direct stimulation (A) at the end plate and (B) in non-junctional areas of innervated rat diaphragm muscles. The upper records show action potentials and their first derivative in normal bathing fluid. The break in the upper traces indicates zero potential. The middle record shows a local response in the end plate region in the presence of TTX (10^{-6} M) and electrotonic potentials with delayed rectification in non-junctional areas. The local response in TTX (10^{-6} M) at the end plate region is abolished in the presence of low (20 mM) external sodium concentration (lower record).

present in only 2 out of 26 fibres tested at the end plate and were totally absent from 30 fibres tested extrajunctionally.

To establish the nature of the conductance change responsible for the local response in the presence of 10^{-6} M TTX at the end plate, the external sodium ion concentration was reduced from 135 to 20 mM, osmolarity being maintained with choline chloride. This reduction of sodium completely abolished the local response (Fig. 1). An increase in calcium ion concentration from 4 to 16 mM in low sodium solution failed to restore the response, indicating that sodium was the main ion responsible for the local response in the junctional part of the muscle fibre. It would therefore seem that sodium ionophores in the post-junctional muscle fibre membrane are more resistant to the effects of TTX than are ionophores in extra-junctional areas of the membrane. A complete resistance to the blocking effect of the drug is not observed, however.

Following surgical denervation, the maximum rate of rise of the action potential is reduced, its duration is prolonged, and the spike becomes resistant to the blocking action of 10^{-6} M TTX (Redfern and Thiesleff 1971 a, b). It was of interest to establish whether the difference noted between action potentials generated in junctional and non-junctional areas of innervated muscles was maintained after denervation. From Table I, it is evident that this is indeed the case up to 14 days after

denervation In denervated diaphragm fibres it was also found that E_{crit} was greater (i.e. more negative) at end plate zones than the overshoot was greater and that the duration of the spike at zero potential was longer than in non junctional zones

In confirmation of earlier experiments it was noted that the action potential in denervated fibres was not blocked by 10^{-6} M TTX and that this resistance develops during the first two days after denervation From Table II it can be seen that the action potential in end plate regions is more resistant to the blocking effect of TTX as is evident from results obtained in 5×10^{-6} M TTX It should be noted from Table 1 however that 5×10^{-6} M TTX exerts a greater effect on the end plate action potential of 7 day denervated fibres than does 10^{-6} M TTX

Discussion

The results of the present study show that the maximum rate of rise of the direct action potential is greater at the end plate zone than in non junctional regions of mammalian skeletal muscle fibres This difference is maintained and exaggerated after surgical denervation

A greater rate of rise could be explained by a difference in electrical membrane constants at the end plate compared with other parts of the muscle cell or alternatively by assuming a greater density of functional sodium channels per unit area of post junctional membrane There is at present however, no indication that membrane constants at the end plate are sufficiently different from those of the extrajunctional membrane (W. L. Nastuk Personal communication)

This present study has shown that the action potential in innervated end plate regions contains a mechanism which is partially resistant to the blocking action of TTX From this and earlier studies (Redfern and Thesleff 1971 b) it is apparent that the action potential in denervated muscle becomes to a large extent resistant to the blocking action of this drug It therefore appears that mammalian muscle fibres have two types of regenerative response one being sensitive and the other relatively insensitive to the blocking effect of TTX In an innervated muscle TTX insensitive sites seem to be present only in the end plate region whilst after denervation they appear in the extrajunctional membrane the density of these sites remains higher in the post junctional membrane however Of interest was the present observation that in denervated muscles TTX affected the action potential at the end plate to a lesser extent than it did in non junctional zones It could be that these TTX insensitive sites which are located apparently in greater number within the areas exhibiting action potentials with the greatest rate of rise are responsible for the observed difference between junctional and non junctional regions

The mechanism which allows regenerative responses presumably carried by sodium ions (Redfern and Thesleff 1971 b) in the presence of TTX is unknown at present The possibility exists of some barrier preventing the access of the TTX molecule to the sodium ionophore While this could explain the observed TTX

resistance it cannot explain the greater rate of rise of the action potential in the end plate area.

The close parallelism of the TTX resistant mechanism with the presence of cholinergic receptors could suggest that the regenerative response is activated through sodium ionophores belonging to the receptor. We have tried to investigate this possibility by desensitizing or by irreversibly blocking cholinergic receptors in the innervated end plate. Neither of these procedures had any effect on action potentials recorded. TTX resistant action potentials in denervated muscles are also unaffected by similar treatment (Harris and Thesleff 1971). Such negative findings do not, due to our limited knowledge of receptor function, exclude the involvement of cholinergic receptor ionophores in action potential generation.

The difference in efficacy of the action potential between end plate and non-junctional regions increased following denervation and was doubled in 3–7 days denervated muscles (Table I). This marked difference may explain the observation that fibrillation potentials in denervated muscles are preferentially generated in the former end plate area of the muscle fibre (Belmar and Eyzaguirre 1966).

One of us (M.R.W.) was supported by a Wellcome European Travelling Research Fellowship. The work was supported by a grant (B74 14\ 3112 04C) of the Swedish Medical Research Council.

References

- BELMAR, J. and C. EYZAGUIRRE. Pacemaker site of fibrillation potentials in denervated mammalian muscle. *J. Neurophysiol.* 1966, 29, 425–441.
- HARRIS, J. B. and S. THESLEFF. Studies on tetrodotoxin resistant action potentials in denervated skeletal muscle. *Acta physiol. scand.* 1971, 83, 382–388.
- LILEY, A. W. An investigation of spontaneous activity at the neuromuscular junction of the rat. *J. Physiol. (Lond.)* 1956, 132, 650–666.
- MAGAZANIK, L. G. On the mechanism of influence of diethylaminoethyl ether of α -phenyl- β -lactic acid (SAP 525 A) on neuromuscular synapses. *Bull. exp. Biol. Med.* 1960, 51, 10–14. (In Russian.)
- MAGAZANIK, L. G. and F. VYSKOČIL. Desensitization at the motor end plate. *Drug Receptors*, Ed. H. J. Rang (Macmillan, London), 1973, 105–119.
- NILNER, W. I. and J. T. ALEXANDER. Non homogeneous electrical activity in single muscle fibres. *Exp. Neurol.* 1973, 37, 333.
- REDFERN, P. and S. THESLEFF. Action potential generation in denervated rat skeletal muscle. *J. Physiol. (Lond.)* 1971, 231, 557–564.
- REDFERN, P. and S. THESLEFF. Action potential generation in denervated rat skeletal muscle. *J. Physiol. (Lond.)* 1971, 231, 565–578.

Effects of 5, 5'-Cyclic Adenosine Monophosphate, 5 Hydroxytryptamine, Noradrenaline and Theophylline on the Simultaneous Release of Peroxidase and Amylase from the Guinea Pig Submandibular Gland

By

BENGT CARLSÖÖ ÅKE DANIELSSON STEFAN MARKLUND and TORGNY STIGBRAND

Received 10 December 1973

Abstract

CARLSÖÖ B Å DANIELSSON S MARKLUND and T STIGBRAND *Effects of 5' 5 cyclic adenosine monophosphate 5 hydroxytryptamine noradrenaline and theophylline on the simultaneous release of peroxidase and amylase from the Guinea pig submandibular gland Acta physiol scand 1974 91 203—210*

Noradrenaline (NA) 5 hydroxytryptamine (5 HT) and $N^6,2$ -O-dibutyl cyclic adenosine monophosphate (DBcAMP) induced a parallel discharge of peroxidase and amylase from the guinea pig submandibular gland *in vitro*. Theophylline alone at a concentration of 5 mM had only little effect on enzyme secretion but it markedly potentiated the effects of noradrenaline 5 HT and DBcAMP at submaximal concentrations. Adenosine-3 monophosphonic acid (3 AMP) and adenosine-5 monophosphonic acid (5 AMP) were without effect on enzyme secretion. Maximal effects of NA and DBcAMP on enzyme release were obtained at concentrations of 0.01 mM and 3 mM respectively. Dose response curves for the stimulation of peroxidase and amylase release by 5 HT revealed that this amine was a potent secretagogue at the concentrations of 0.1 and 0.3 mM but was less effective at higher concentrations. It is concluded that peroxidase and amylase are simultaneously secreted from the guinea pig submandibular gland and that the release of both enzymes is mediated via cyclic AMP.

Catecholamines which increase the intracellular levels of cyclic 3',5'-adenosine monophosphate (cAMP) by stimulating the adenylate cyclase system (Sutherland and Robison 1966) induce amylase secretion from salivary glands (Bdolah *et al* 1964). Dibutyl cyclic AMP (DBcAMP) provokes amylase release from rat parotid slices *in vitro*; phosphodiesterase inhibitors such as the methyl xanthines have a similar effect (Bdolah and Schramm 1965). It has therefore been concluded that cAMP acts as an intracellular mediator of enzyme secretion from salivary glands. Like the catecholamines 5 hydroxytryptamine (5 HT) induces enzyme secretion from salivary glands *in vitro*. It has been suggested that also this compound may activate the adenylate cyclase system to produce cyclic AMP (Babad *et al* 1967).

Peroxidase is actively secreted from incubated pieces of salivary gland (Carlsson *et al* 1972). In the present investigation the effects of noradrenaline (NA), 5 HT, theophylline and DBcAMP on the release of peroxidase from guinea pig submandibular gland were investigated. For comparison the concomitant discharge of amylase was recorded.

Material and Methods

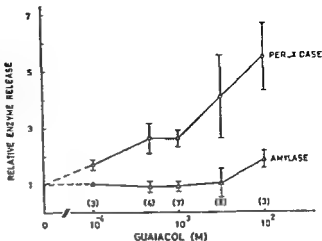
Male guinea pigs 3 months old, weighing roughly 300 g were used for the investigation. The animals were starved overnight prior to sacrifice. They were anesthetized by an intraperitoneal injection of sodium pentobarbital (Nembutal® Abbott). The submandibular glands of both sides were rapidly excised and all extraglandular tissues were removed under a stereomicroscope. In each experiment the glands from 2 animals were used. They were cut into small fragments which were randomly distributed among the incubation vessels. All specimens were incubated for 30 min in 3 ml of bicarbonate buffer (pH 7.4) supplemented with pyruvate, glutamate and fumarate (Krebs 1950) and also containing albumin (5 mg/ml) and glucose (60 mg/ml). After preincubation the medium was replaced by 3 ml of fresh incubation medium containing the different secretagogues. Control incubations without added substances were included in each experiment. Noradrenaline (NA), 5-hydroxytryptamine (5 HT), theophylline, γ -³²P dibutyryl cyclic adenosine monophosphate (DBcAMP), adenosine 3-monophosphoric acid and adenosine 5-monophosphoric acid were tested. Both preincubation and incubation were carried out at 37 °C under continuous gassing with CO₂ in a 5 l/min tubular shaker (Dinshew 1974). After 60 min of incubation the specimens were removed by filtration through a nylon net and homogenized in 5 ml of 50 mM phosphate buffer (pH 6.0) (Dahlqvist 1972) using an Ultra Turrax homogenizer (Janke und Kunkel AG, Staufen, Germany) run at a speed of 1400 rpm for 15–60 s at 4 °C. The homogenates were centrifuged at about 3000 × g for 5 min. Both incubation media and supernatants were assayed for peroxidase and amylase.

Peroxidase assay. Samples from either the supernatants or incubation media were added to 0.2 M pyruvate in 200 mM sodium phosphate buffer (pH 6.0). The total volume was made to 50 ml. Hydrogen peroxide to a final concentration of 1.67 mM was added and the peroxidase activity was calculated from the initial increase in absorbance at 400 nm. Both 5 HT and NA apparently serve as substrates for peroxidase. However, at a high concentration of pyruvate which has a very high reactivity with the peroxidase (Chance 1950) eliminated any interference with the assay.

Amylase assay. The assay was performed as a 30 min wet weight per min. Peroxidase release is expressed as a percentage of the total peroxidase activity in tissue and medium.

Amylase assay. Samples from incubation media and supernatants were appropriately diluted with 0.05 M phosphate buffer and assayed in triplicate for amylase using a microdiffusion technique (dinitro phenyl) (DNS) method with soluble starch as substrate (Dahlqvist 1972). Duplicate incubations of maltose were run in parallel. The test tubes containing 10 µl of the sample and were incubated with 10 µl of the starch solution for 10 min at 37 °C. The reaction was interrupted by adding 0.5 µl of the DNS reagent. All tubes were then cooled to 4 °C. After cooling 0.5 µl of distilled water was added. The colour was measured at 540 nm in a 1 cm cuvette. One unit of amylase was defined as the activity liberating 1 µmole of maltose per min. The amylase activity was expressed as a percentage of the activity recorded in the incubation medium.

Chemicals. All reagents were of the highest quality. Dinitrophenyl and pyruvate were obtained from Merck AG. Adenosine 3-monophosphoric acid and adenosine 5-monophosphoric acid were obtained from Boehringer and Soehnle GmbH, Mannheim, Germany. All reagents were of the highest quality. Noradrenaline tartrate was purchased from Koch Light Laboratories Ltd, Colnbrook, Bucks, England and 5-hydroxytryptamine creatinine sulfate from Sigma Chemical Co., St. Louis, MO, USA. Theophylline was from Mann Research Laboratories, New York, NY, USA. γ -³²P dibutyryl adenosine 3-monophosphoric acid and adenosine 5-monophosphoric acid were obtained from C. L. Boehringer and Soehnle GmbH, Mannheim, Germany.



Results

Peroxidase secreted from the salivary gland was found to be inactivated during the incubation procedure. To investigate this phenomenon a homogenate of submandibular gland was prepared as described above and samples of the supernatant were added to fresh bicarbonate buffer and incubated under continuous gassing for 60 min. As much as 80 per cent of the initially recorded peroxidase activity was lost during the incubation period. In the presence of 1 mM guaiacol a hydrogen donor substrate for peroxidase the enzyme activity was fully protected. 5 HT (0.1 mM) was as effective as guaiacol in protecting the enzyme. NA (0.1 mM) prevented enzyme inactivation to about 80 per cent whereas DBcAMP and theophylline displayed no peroxidase protecting activity.

To determine the amount of enzyme inactivated during the incubation period submandibular gland pieces were incubated with different concentrations of guaiacol (Fig. 1). Peroxidase and amylase activities in the media were determined. Since amylase is neither inactivated during incubation nor affected by guaiacol it is a suitable control for the possible enzyme releasing effect of guaiacol. Fig. 1 shows that maximal maintenance of peroxidase activity was obtained with 0.5–1.0 mM guaiacol. Higher concentrations of guaiacol caused a release of enzyme from the gland as indicated by the increase in amylase secretion. These experiments show that at least 100 per cent of the peroxidase released from the submandibular gland pieces was inactivated during incubations in the absence of enzyme protector. In studies on peroxidase secretagogues a 2–3 fold increase of enzyme activity in the medium may thus reflect protection of the enzyme rather than a true enhancement of release.

Dose response curves for the stimulation of amylase and peroxidase release by NA, 5 HT and DBcAMP are shown in Fig. 2 a–c. NA was found to be the most potent secretagogue tested with respect to both peroxidase and amylase release. A maximal effect on enzyme discharge was obtained at a concentration of 0.01 mM (Fig. 2 a).

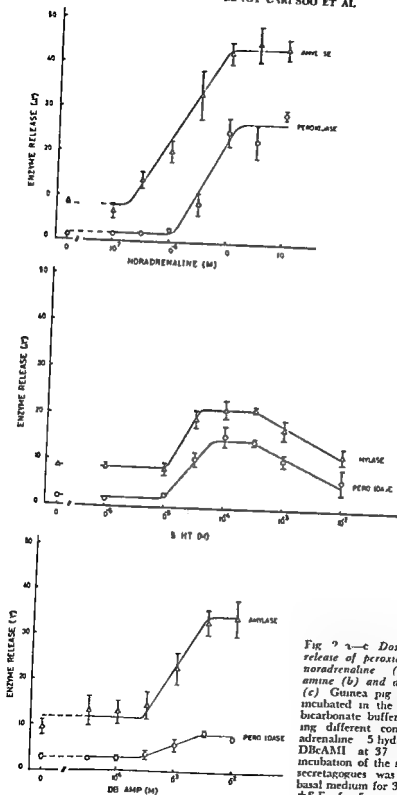


Fig. 2. Dose response curves for release of peroxidase and amylase by noradrenaline (a), 5-hydroxytryptamine (b) and dibutyl cyclic AMP (c). Guinea pig submandibular slices incubated in the supplemented Krebs bicarbonate buffer (pH 7.4) containing different concentrations of noradrenaline, 5-hydroxytryptamine and DBcAMP at 37°C for 60 min. Preincubation of the slices without added secretagogues was performed in the basal medium for 30 min. Mean values \pm S.E. for 5 separate experiments.

TABLE I *In vitro* effects of theophylline (5 mM) on peroxidase secretion from the guinea pig submandibular gland. Guinea pig submandibular slices preincubated for 30 min at 37°C in supplemented Krebs bicarbonate buffer (pH 7.4). Incubations were then performed for 10 min with added theophylline and the listed submaximal concentrations of noradrenaline, 5-hydroxytryptamine and DBcAMP. The peroxidase activity is expressed as ΔA_{415} /g wet weight \pm S.E. in 5 separate experiments. The enzyme release is expressed as percentage of the total peroxidase activity in tissue and medium.

Test substances	Peroxidase activity in medium	Peroxidase activity in homogenate	Percentage peroxidase released
Control	2.3 ± 0.46	191.8 ± 27.01	1.7 ± 0.29
Theophylline 5 mM	4.3 ± 0.74	212.1 ± 26.56	2.2 ± 0.68
Noradrenaline 0.003 mM	12.0 ± 3.07	174.7 ± 30.29	6.5 ± 1.31
Noradrenaline 0.003 mM + theophylline 5 mM	23.0 ± 4.30	173.3 ± 22.41	12.2 ± 1.91
5-HT 0.03 mM	13.1 ± 1.74	180.5 ± 34.70	7.3 ± 1.23
5-HT 0.03 mM + theophylline 5 mM	52.1 ± 8.67	166.3 ± 22.21	23.6 ± 3.41
DBcAMP 1 mM	7.6 ± 1.27	198.4 ± 35.56	3.7 ± 0.28
DBcAMP 1 mM + theophylline 5 mM	16.4 ± 3.82	160.8 ± 18.24	9.2 ± 1.78

which caused a 25 and 45 per cent release for peroxidase and amylase respectively. 5-HT was less effective than NA on enzyme secretion (peroxidase and amylase secretion 15 per cent and 25 per cent respectively) and higher concentrations were required to obtain maximal effect. With 5-HT maximal discharge of both enzymes was obtained at a concentration of 0.1 mM. Higher concentrations of this agent (1 mM and 10 mM) were less effective (Fig. 2b).

TABLE II *In vitro* effects of theophylline (5 mM) on amylase secretion from the guinea pig submandibular gland. The determinations were performed on the same samples as used in Table I. The amylase activity is expressed as units/g wet weight \pm S.E. The amylase release is expressed as percentage of the total amylase activity in tissue and medium.

Test substances	Amylase activity in medium	Amylase activity in homogenate	Percentage amylase released
Control	87 ± 16	1272 ± 903	1.1 ± 0.84
Theophylline 5 mM	161 ± 28	1220 ± 189	11.4 ± 0.90
Noradrenaline 0.003 mM	408 ± 10	1123 ± 245	2.2 ± 0.40
Noradrenaline 0.003 mM + theophylline 5 mM	651 ± 81	974 ± 135	38.3 ± 3.10
5-HT 0.03 mM	197 ± 28	1713 ± 299	15.0 ± 1.68
5-HT 0.03 mM + theophylline 5 mM	563 ± 89	1043 ± 183	35.5 ± 4.41
DBcAMP 1 mM	236 ± 54	1154 ± 154	16.2 ± 2.65
DBcAMP 1 mM + theophylline 5 mM	418 ± 70	1080 ± 158	30.8 ± 2.06

DBcAMP (Fig. 2 c) caused a release of 8 per cent peroxidase and 35 per cent amylase. A plateau was reached at 3 mM DBcAMP.

Table I and II summarize the effects of theophylline on amylase and peroxidase secretion from the guinea pig submandibular gland. Although theophylline alone had little effect it markedly enhanced the effects of NA, 5-HT and DBcAMP. Statistical evaluation of these results revealed that true potentiation occurred and that the effect was not merely additive.

3'-AMP and 5'-AMP were found to be without effect on enzyme secretion.

Discussion

The present study has shown that more than 80 per cent of the peroxidase of the guinea pig submandibular gland is inactivated during an incubation period of 60 min. The enzyme is however fully protected in the presence of 1 mM of the hydrogen donor substrate guaiacol. This would seem to indicate that the inactivation is due to instability of the lactoperoxidase peroxide compounds formed by H_2O_2 which in turn is produced by oxidases in the tissue and/or by autooxidative processes. The peroxide compounds of horseradish peroxidase are known to undergo a slow ($t_{1/2} = 20$ min) irreversible degradation in the presence of very low concentrations of H_2O_2 (Mørklund 1973). Lactoperoxidase has been reported to be even more sensitive to H_2O_2 than horseradish peroxidase (Chirace 1956). In the present investigation 5-HT (0.1 mM) and NA (0.1 mM) were found to protect the peroxidase activity during incubation indicating that these compounds may serve as hydrogen donor substrates.

DBcAMP has been shown to be more effective than the parent compound cAMP, in eliciting an amylase secretory response from salivary glands *in vitro* (Birind *et al* 1967). Furthermore it has proved to be some 80 times more potent than cAMP in stimulating enzyme release from the rat pancreas (Björndal *et al* 1971). DBcAMP is more lipid soluble and seems to be more resistant to degradation by phosphodiesterase than cAMP. At least in some tissues its penetration of cell membranes is reported to be more rapid than that of its analogue (Henson *et al* 1967). Blecher and Hunt (1972) have shown that cell free extracts from various rat tissues contain O-butyryl esterases and N⁶-butyryl amino hydrolases capable of deacylating DBcAMP to monobutyryl cyclic AMP or to cAMP. These authors concluded that DBcAMP could serve as a source of intracellular cAMP.

It has been suggested that several hormones exert their effects on target organs by altering the intracellular level of cAMP. Modulation of secretory activity in various exocrine glands seems to be mediated by this nucleotide. In the present investigation DBcAMP induced a marked release of both peroxidase and amylase which suggests that cAMP is involved in the regulation of the discharge of these enzymes from the guinea pig submandibular gland. Moreover theophylline was found to stimulate peroxidase and amylase secretion. This substance is known to

inhibit phosphodiesterase an enzyme which degrades cAMP to 5 AMP. Theophylline (5 mM) also strongly potentiated the effects of DBcAMP, 5 HT and noradrenaline on enzyme release. It is reasonable to assume that theophylline inhibits the degradation of cAMP which would result in an increased intracellular level of this compound. An inhibitory effect of theophylline on guinea pig submandibular phosphodiesterase activity has recently been shown by Bhoola and Lemon (1972).

Catecholamines stimulate adenylate cyclase activity in different organs. This enzyme associated with cellular membranes catalyzes the formation of cAMP (Sutherland and Robison 1966). Schramm and co workers have shown that cAMP is an intermediate in the catecholamine induced secretion of amylase from the rat parotid gland (Babad *et al* 1967). Furthermore recent studies have clearly established that adenylate cyclase activity in salivary glands is increased by isoproterenol (Malamud 1972). From these observations and the present findings it seems reasonable to assume that the noradrenaline induced release of amylase and peroxidase from the guinea pig submandibular gland is due to activation of the adenylate cyclase system.

5 HT was also found to be a potent stimulator of both peroxidase and amylase secretion. The biological significance of 5 HT in salivary gland metabolism is not clear. Noradrenaline on the other hand is the physiological transmitter of the autonomic sympathetic nervous system and the guinea pig submandibular gland is richly innervated by adrenergic nerves (Alm *et al* 1973). However 5 HT has been shown to enhance adenylate cyclase activity in the liver fluke (Stone and Mansour 1966) and the ciliated protozoan *Tetrahymena pyriformis* (Rozensweig and Kandler 1972). Fluid secretion from the abdominal salivary gland of the blow fly *Calliphora erythrocephala* is markedly increased by 5 HT (Berridge 1970) and it has been established that cAMP serves as an intracellular messenger (Prince *et al* 1972). The only mammalian tissue in which a stimulatory effect of 5 HT on cAMP formation has been demonstrated is brain (Kakiuchi and Rall 1968; Shimizu *et al* 1970). According to Robison *et al* (1971) the relatively minor effect of 5 HT in mammalian tissues compared to that of the catecholamines may reflect the decreasing importance of 5 HT in higher organisms. It is clear from the present findings that 5 HT is less potent than NA in eliciting a secretory response from the guinea pig submandibular gland.

Although there was a striking similarity between the peroxidase and amylase secretory response induced by different secretagogues certain differences were also apparent. Somewhat higher concentrations of NA seemed to be required to stimulate peroxidase release as compared with amylase release. In the presence of DBcAMP the ratio between amylase and peroxidase release was higher than that observed in the presence of 5 HT. These deviations from a strict correlation between peroxidase and amylase release may be due to the different capacities of NA, 5 HT and DBcAMP to protect the secreted peroxidase from inactivation.

Taken together the results strongly suggest that salivary gland peroxidase should be classed among the exportable proteins and that the cellular mechanisms govern

ing the release of this oxidative enzyme are very much the same as those regulating the release of amylase

References

- ALM P G D BLOOM and B CARLSSON Adrenergic and cholinergic nerves of bovine guinea pig and hamster salivary glands *Z Zellforsch* 1973 138 407-420
- BARAD H R BEN-ZVI A BDOLAH and M SCHRAMM The mechanism of enzyme secretion by the cell 4 Effects of inducers substrates and inhibitors on amylase secretion by rat parotid slices *Europ J Biochem* 1967 1 96-101
- BAUDIN H L ROCHUS D VINCENT and J F DELMONT Role of cyclic 3'5' AMP in the action of physiological secretagogues on the metabolism of rat pancreas *in vitro Biochim biophys Acta (Amst)* 1971 25 171-183
- BDOLAH A R BEN-ZVI and M SCHRAMM The mechanism of enzyme secretion by the cell II Secretion of amylase and other proteins by slices of rat parotid gland *Arch Biochem* 1964 104 58-66
- BDOLAH A and M SCHRAMM The function of 3'5' cyclic AMP in enzyme secretion *Biochem biophys Res Commun* 1965 18 457-459
- BERRIDGE M J The role of 5-hydroxytryptamine and cyclic AMP in the control of fluid secretion by isolated salivary glands *J exp Biol* 1970 53 171-186
- BIHOLA K D and M J C LEMON Comparison of the phosphodiesterases in the submaxillary gland brain and liver *Brit J Pharmacol* 1972 45 141P
- BLECHER M and N H HUNT Enzymatic deacylation of mono- and dibutyl derivatives of cyclic adenosine 3'5' monophosphate by extracts of rat tissues *J Biol Chem* 1972 247 1470-1484
- CARLSSON B A DANIELSSON S MARKLUND and T STENBRAND Simultaneous release of amylase and peroxidase from the guinea pig submandibular gland *FEBS Letters* 1972 25 69-72
- CHANCE B Catalases and peroxidases V Properties of the enzyme substrate compounds of lactoperoxidase *J Amer chem Soc* 1950 72 1571-1573
- DAHLQVIST A A method for the determination of amylase in intestinal content *Scand J Clin Lab Invest* 1967 14 145-151
- DANIELSSON A Techniques for measuring amylase secretion from pieces of mouse pancreas *Analyt Biochem* In press
- HENSON W F E W SUTHERLAND and T POSTERNAK Effects of derivatives of adenosine 3'5' phosphate of liver slices and intact animals *Biochim biophys Acta (Amst)* 1967 14P 101-113
- KAKEI H S and T W RALL Studies on adenosine 3'5' phosphate in rabbit cerebral cortex *Mol Pharmacol* 1968 4 379-389
- KREIB H A Body size and tissue respiration *Biochim biophys Acta (Amst)* 1950 4 244-244
- M JAMALI D Amylase secretion from mouse parotid and pancreas: role of cyclic AMP and histamine *Biochim biophys Acta (Amst)* 1972 279 373-376
- MARKLUND S Mechanisms of the irreversible inactivation of horseradish peroxidase caused by hydroxylamine hydroperoxide *Arch Biochem* 1973 154 614-622
- PRINCE W I M J BERRIDGE and H RASMUSSEN Role of calcium and adenosine 3'5' cyclic monophosphate in controlling rat salivary gland secretion *Proc nat Acad Sci (Wash DC)* 1973 503-557
- ROBINSON C A R W BUTCHER and E W SUTHERLAND Cyclic AMP p 32 Academic Press New York and London 1971
- ROZENSWAIG Z and S H KANDLER Epinephrine and serotonin activation of adenylyl cyclase from *tetrahymena* *in vitro* *FEBS Lett* 1972 221-223
- SHIMIZU H C R CREVELING and J DALY Stimulated formation of adenosine 3'5'-cyclic phosphate in cerebral cortex: synergism between electrical activity and biogenic amines *Proc nat Acad Sci (Wash DC)* 1970 65 1033-1039
- STONE D B and T E MALLER Phosphofructokinase from the liver fluke *Fasciola hepatica*. I Activation by adenosine 3'5' phosphate and by serotonin *Mol Pharmacol* 1966 3 161-166
- SUTHERLAND E W and G A ROBINSON Metabolic effects of catecholamines A The role of cyclic 3'5' AMP in responses to catecholamines and other hormones *Pharmacol Rev* 1966 18 145-161

Method for Gravimetric Registration of Changes in Tissue Volume

By

P O GRANDE J JARHULT and S MELLANDER

Received 10 December 1973

Abstract

GRANDE P O J JARHULT and S MELLANDER *Method for gravimetric registration of changes in tissue volume* Acta physiol scand 1974 91 211-215

A technique is described by which changes of tissue volume of a muscle region enclosed in a plethysmograph can be followed in terms of water displacements measured with an electronic gravimetric transducer. Experimental tests show that the method provides accurate recordings of vascular capacitance responses and of transcapillary fluid movements.

The plethysmographic technique described by Mellander in 1960 for continuous recording of changes of tissue volume combined with measurements of blood flow and arterial and venous pressures has been widely used for concomitant quantitative studies of the resistance exchange and capacitance functions in the peripheral circulation (for review of literature see Mellander and Johansson 1968). In more recent modifications of the technique various transducers have been used for monitoring blood flow and pressures on an electronic recording unit but no reliable electronic transducer has been available for recording changes of tissue volume.

Volume changes were therefore usually registered by an airfilled volume piston recorder on a separate mechanical recording unit (e.g. kymograph). This disadvantage has been eliminated by the present approach where a tissue volume change is followed in terms of water displacement between the plethysmograph and a reservoir the extent of which is accurately recorded by an electronic gravimetric transducer. The present paper describes the application of the technique to the study of changes in tissue volume of the lower leg muscles in the cat.

Description of method

The general design of the apparatus is shown schematically in Fig. 1. It consists of a double-walled cylindrical perspex plethysmograph (I) and a unit (II) for gravimetric recording of the fluid displacements to or from the plethysmograph.

resulting from changes of tissue volume. The lower leg muscle region, prepared *in situ* according to Kjellmer (1963) is inserted through the opening in the proximal base of the plethysmograph using the shaved skin freed from the underlying tissue as a cover of the muscles and for waterproof closure of the plethysmograph with the screws (A) and the two perspex flanges (B) (for details see Mellander 1960). The muscle region is firmly fixed and kept in place by two metal holders (C) penetrating the walls of the plethysmograph and applied to the lower part of the tibia and by two other ones (D) applied to the femur outside the plethysmograph. The plethysmograph is filled with water of neutral temperature ($\approx 36^{\circ}\text{C}$) through the inlet (E) so that water overflows in the polyethylene tubing (F) and the firmly fixed glass tubing (G) until the reservoir (H) is about half filled. The hydrostatic water pressure inside the plethysmograph is determined by the water level in the reservoir and can be adjusted to desired levels by varying the height of the reservoir via the stand (I). The pressure at the midlevel of the muscle region is measured by a water manometer (J). Minor air bubbles if present are trapped in the upper somewhat elevated proximal part of the plethysmograph and therefore do not interfere with water movements to unit II. The space (K) between the outer and inner cylinder of the plethysmograph serves the purpose of keeping temperature inside the plethysmograph measured by the thermometer (L) constant. This is accomplished by continuous recirculation of water of constant temperature through space (K) from a thermostatically regulated water bath via the inlet (M) and outlet (N). An alternative but somewhat less exact method for thermoregulation is to fill the space (K) with water of neutral temperature (36°C) through the inlet (M) and keep temperature constant throughout the experiment by the heating coil system (O) which is positioned a few cm from the bottom midline so as to cause water circulation and even heat distribution in space (K). Further detail about the temperature control are given below. A given change of tissue volume lead to a corresponding change of the water volume in the reservoir (H) the magnitude of which is recorded gravimetrically via a Grass FT 10 transducer (P) on a Grass Polygraph. To avoid water evaporation or disturbances from air movement in the environment the reservoir and the transducer are enclosed in a perspex container Q with an opening (R) which maintains atmospheric air pressure in the container.

Experimental. The apparatus is primarily designed for quantitative measurements of changes of tissue volume as caused by alterations of tone in the capacitance vessels affecting regional blood volume and by net transcapillary fluid movements. From previous studies (see Mellander and Johansson 1968) it is known that a maximal constrictor or dilator response of the capacitance vessels in the cat lower leg muscle region (weigh about 50 g) corresponds to a decrease or increase of regional blood volume (tissue volume) by about 0.5 ml and such a response to an abrupt physiological stimuli is usually fully developed within 20–60 s. Transcapillary fluid movements produced by stimuli which alter capillary hydrostatic pressure occur at a maximal rate of about 11 ml/min in this muscle region. The

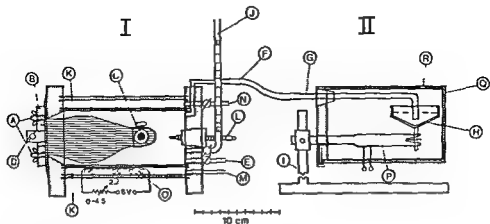


Fig 1 Schematic illustration of the device

technique thus should permit reliable recordings of circulatory effects within this range

To avoid undue high frequency disturbances a low frequency response of the recording system is to be preferred which still permits adequate recordings of the mentioned circulatory events. A rise time (0–90% of full scale deflection) of about 1 s for an instantaneous volume increase was found suitable and it is adjusted to this value via the Polygraph driver amplifier. The sensitivity of the recording system may be set so as to cause a scale deflection of 1 cm/0.1 ml tissue volume change. For calibration a known water volume is injected from a syringe through the opening (R) in the container (Q) into the reservoir (H) (Fig 1). Baseline adjustment can be accomplished by the same procedure.

Experimental tests of the device were performed to evaluate possible methodological errors as caused by spontaneous movements of the muscle region, temperature variations, water evaporation, hydrostatic pressure changes and capillary forces.

Spontaneous movements of the muscle region were found effectively prevented by the firm fixation with the holders (C, D).

A temperature change in the plethysmograph (water volume ≈ 0.4 l) of 1°C was found to cause a volume change of about 0.1 ml. Temperature therefore must be kept reasonably constant and this was accomplished by either of the two methods described. The body temperature of the animal was thermostatically controlled at $38 \pm 0.05^\circ\text{C}$. With a plethysmograph temperature control via the water bath (thermostat delay 1°C , circulating fluid volume 200–400 ml/min) the temperature variation in the vicinity of the muscle region (as measured by thermometer L) was found negligible even in long term (2–4 h) experiments. With the heating coil system (O) after initial adjustment to establish equilibrium temperature ($\approx 36.5^\circ\text{C}$ reached 15–30 min after insertion of the muscle region) temperature was found to be maintained virtually constant throughout longlasting experiments.

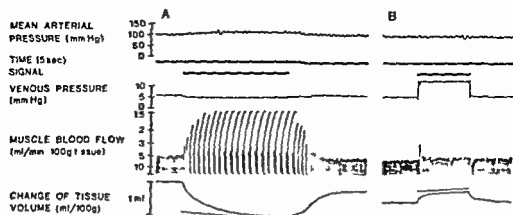


Fig. 2 Polygraph tracings with technique shown in Fig. 1 of effects on resistance and capacitance vessels and on net transcapillary fluid movement during vasoconstrictor fibre stimulation (panel A) and during a determination of the capillary filtration coefficient (panel B) in a cat muscle region.

without further adjustments of (O). Occasionally, and in particular if body temperature control of the animal was neglected there could be a continuous drift of up to $0.5^{\circ}\text{C}/\text{h}$. Such a drift could be lessened by fine manual adjustments of (O), or by insertion of a thermostat relay in the circuit (O—L). Yet the latter type of temperature control is usually not necessary for short term acute experiments in fact it may be disadvantageous due to the induced temperature oscillations.

The container (Q) effectively prevented water evaporation from the reservoir (H). For practical purposes it could be considered negligible ($< 0.025\text{ ml/h}$).

A volume change in the plethysmograph alters the water level in the reservoir (H) and thereby the hydrostatic pressure in the plethysmograph. With the present dimensions of the reservoir the induced pressure change is quite small or about $0.5\text{ mm H}_2\text{O/ml}$ volume change which implies that the consequent change of tissue pressure in most cases can be considered negligible. Besides the effect of changed hydrostatic water pressure on transcapillary fluid movements it can cause a minor dislocation of the skin flap used for closure of the plethysmograph. The inherent latter error in the volume measurement was found to be about 1% .

The capillary force between the glass tube (G) and the water in the reservoir (H) causes an error in the volume measurement of about 1% .

Experimental tracings. Fig. 2 gives examples of the use of the present technique for recording capacitance responses and transcapillary fluid movements. Panel A illustrates changes of blood flow (recorded with an optical drop flowmeter) and of tissue volume in the cat lower leg muscles (weight 50 g) in response to adrenergic nerve fibre stimulation at 8 Hz . This caused a constriction of the resistance vessels increasing vascular resistance by 280% and of the capacitance vessels causing a blood mobilisation of $0.95\text{ ml}/100\text{ g}$ tissue (initial decline of tissue volume) and a subsequent transcapillary absorption of extravascular fluid at a rate of 0.08

ml/min \times 100 g tissue (indicated by dashed line below the volume curve) In panel B a determination of the capillary filtration coefficient was performed by increasing venous outflow pressure 7 mm Hg. The capillary filtration coefficient was 0.010 ml/min \times 100 g \times mm Hg. These effects are typical for a skeletal muscle region (cf Mellander and Johansson 1968).

Comments

The principle for gravimetric recording of volume displacement used here bears some relation to a previously described gravimetric method for measuring minute flow rates in the anterior chamber of the eye (Barany 1966). The present apparatus as evidenced by the experimental tests provides reliable measurement of changes of tissue volume in a muscle region as caused by capacitance responses and by transcapillary fluid movements. It permits more accurate recordings than with the previously used mechanical volume transducer (Mellander 1960).

To facilitate separation between blood volume changes (capacitance responses) and transcapillary fluid movements the capacitance responses can be followed simultaneously by monitoring variations in radioactivity of the red cells tagged with ^{51}Cr via an external scintillation detector placed outside the plethysmograph (see Ablad and Mellander 1963, Kjellmer 1965). By combining the plethysmographic and radioactive tracer measurements with recordings of blood flow and arterial and venous pressure concomitant tracings can be obtained on a multichannel polygraph of the different parameters needed for a quantitative evaluation of reactions evoked in pre and postcapillary resistance vessels, precapillary sphincters and capacitance vessels as well as of transcapillary fluid movements (see Mellander and Johansson 1968).

Several modifications of the plethysmograph unit have been described which are designed to fit other organs than muscle such as skin, intestine, glandular and adipose tissue in experimental animals and the hand, forearm and calf in the human being (for ref. see Mellander and Johansson 1968). The present equipment for electronic registration of changes of tissue volume can be used for these plethysmographs as well.

This work was supported by grant B74 14\ 7710 08C from the Swedish Medical Research Council. Invaluable technical aid from Mr L. Åkesson, Mr B. Clementz and Miss Margaretha Rahm is gratefully acknowledged.

References

- ABLADE B and S. MELLANDER. Comparative effects of hydralazine, sodium nitrite and acetylcholine on resistance and capacitance blood vessels and capillary filtration in skeletal muscle in the cat. *Acta physiol. scand.* 1963 58 319-379.
- BARANY E. H. Doyne memorial lecture. The mode of action of myotics on outflow resistance. A study of pilocarpine in the rhesus monkey *Cercopithecus ethiops*. *Trans. ophthal. Soc.* 1966 86 539-558.
- KJELLMER I. Studies on exercise hypertension. *Acta physiol. scand.* 1965 64 Suppl. 244 1-2.
- MELLANDER S. Comparative studies on the adrenergic neuro-hormonal control of resistance and capacitance blood vessels in the cat. *Acta physiol. scand.* 1960 50 Suppl. 176 1-36.
- MELLANDER S. and B. JOHANSSON. Control of resistance, exchange and capacitance functions in the peripheral circulation. *Pharmacol. Rev.* 1968 20 117-196.

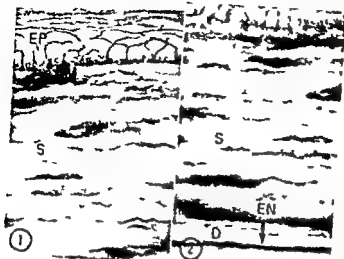


Fig 1 NaK ATPase reaction in the cornea of the rat. Note the strong enzyme activity localized at the cell membranes of the epithelium (EP). High activity can be seen near the Bowman's membrane (BM). In the stromal area (S) Schwann cells, nerve fibers and possibly keratocytes also show enzyme activity. Magn $\times 430$.

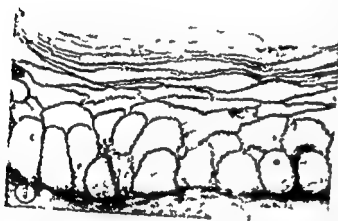


Fig 2 NaK ATPase activity in the rat cornea. A dark precipitation indicating the reaction activity can be seen in the endothelial cells (EN). On the other hand, no precipitation can be seen in the Descemet's membrane (D). Magn $\times 430$.

Fig 3 High magnification of the epithelial cells of the cornea demonstrating NaK ATPase activity localized all over the cell membranes. Magn $\times 1000$.

accordance with stages 1, 2, 3 and 5 (see above) the solutions usually contained ouabain in a corresponding concentration as that used in the pre incubation solution.

The effect of ouabain was also checked *in vivo* by injecting the drug diluted in distilled water intra vitreally. The intraocular concentration thus obtained corresponded to about 10^{-4} M. An equal volume of 0.9% saline was injected into the contralateral eye. The animals were killed 80 to 90 hr after injection. The corneas were treated as described above in order to demonstrate the enzyme activity histochemically.

B Effect of sodium and potassium. The concentrations of sodium and potassium in the incubation solution were varied from 0 to 145 mM and from 0 to 200 mM respectively.

C Substrate concentration. The primary substrate 3.0 mM ATP was replaced either by 3.0 mM of ADP or β -glycerophosphate. The effect of total absence of the substrate from the incubation solution was also checked.

D Omission of the coupling agent. In some experiments the sections were incubated in the ordinary incubation solution but lead was omitted.

Results

Localization of the NaK ATPase activity

The NaK ATPase activity in the tissue sections was estimated by comparing the sections incubated with sodium and potassium with the controls without these

Fig 4 The section has been treated in the absence of the two activators (Na and K) thus resulting in decreased precipitation. However reaction activity can be noted at all original sites (epithelium stromal fibers and endothelium (arrow)) Mg⁺⁺ × 460

Fig 5 The section has been pre incubated in the presence of 3×10^{-4} M ouabain prior to fixation. Subsequently it has been fixed and incubated in the presence of the substrate and the activators (Na and K) in the usual way. As can be noted the reaction activity is clearly decreased at all those sites which normally exhibit a high enzyme reaction (EP = epithelium, BM = Bowman's membrane, S = Descemet's membrane and EN = endothelium). This indicates that the decreased activity which is sensitive to ouabain is due to the specific pump enzyme activity. Mg⁺⁺ × 430



activators or with the sections pre incubated and incubated in the presence of ouabain. Therefore the circumstances during the different stages of the procedure must be exactly the same. In this study the optimal fixation time was one hr at 4°C and the incubation lasted 30 min at 37°C .

In the presence of sodium and potassium NaK ATPase activity was localized at the cell membranes of all the epithelial cells of the cornea (Fig 1 and 3). A strong dark brown precipitate was seen at the basal part of the epithelium near Bowman's membrane (Fig 1—3).

In the stromal area darkly stained deposits were seen these were obviously localized in the Schwann cells and possibly also in the membranes of keratocytes (Fig 1 and 2). In the whole mount preparations it can be seen that the cell membranes of the endothelial cells were active (Fig 6).

Control studies When sodium and potassium were omitted from the incubation solution a similar localization was obtained as when these ions were present but the reaction intensity was significantly lower (Fig 4). When the concentrations of sodium and potassium were higher than 70 mM the reaction intensity began to fall again.

In the presence or absence of sodium and/or potassium but in the presence of ouabain in the pre incubation and incubation solutions the reaction activity was clearly inhibited as well (Fig 5). However in the presence of ouabain the nerves

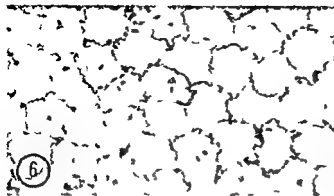


Fig 6 A whole mount section of the cornea which has been photographed so that the endothelium is in focus. The reaction product indicating the localization of NaK ATPase activity is seen in the cell membranes of the endothelium. Men $\times 380$.

in the stroma still showed a reaction of moderate intensity. A preincubation carried out at 22 °C for 1 hr in the presence of 3×10^{-4} M ouabain seemed to be sufficient to cause a marked inhibition of the reaction.

When ouabain was injected intravitreally 80–90 hr before enucleation the NaK ATPase activity was clearly inhibited too (Fig 7). Only a weak reaction was visible in the cell membranes of the epithelial cells and in the stromal structures.

The sections incubated without ATP or lead or by using α or β glycerophosphate as a substrate all remained negative. When ADP (dibarium salt) was used as the substrate no reaction could be demonstrated. This salt of ATP was observed to give a more intense reaction than dibarium ATP.

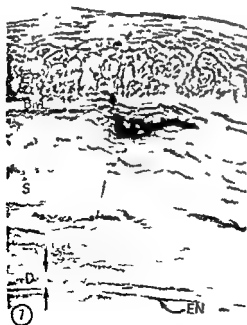


Fig 7 The section has been cut from the eye into which ouabain has been injected intravitreally 80 hr prior to enucleation. A clear inhibition of the NaK ATPase activity can be seen in all normal reaction areas (compare Fig 5 and 1–3). Men $\times 400$.

Discussion

A series of works in our laboratory has shown that a specific histochemical demonstration of NaK ATPase activity is highly dependent on the proper composition of the incubation solution (Palkama and Uusitalo 1970 Uusitalo and Palkama 1970 and Harkönen *et al* 1972). A highly important factor is the correct concentration of Pb^{++} , ATP and Mg^{++} . A too low concentration of Pb can be responsible for a free diffusion of the enzyme induced liberation of phosphate groups which are thus not precipitated rapidly enough. On the other hand a too high concentration of Pb evidently causes not only inhibition of the enzyme but also an unspecific precipitation of this agent. According to our findings a Pb^{++} concentration of 1 mM and Pb^{++}/ATP ratio of 1 is the best. A too high concentration of Mg^{++} or an old incubation solution causes nuclear staining. The optimal concentration of Mg^{++} also seems to be about 3 mM.

When ouabain is used before fixation and the ionic concentration is correct a clear-cut inhibition of the histochemical reaction for NaK ATPase is noted. On the other hand the reaction is activated by the presence of 70 mM of Na⁺ and K⁺. Thus the method used in this study can be regarded as specific for the enzyme studied.

It should be pointed out that in the biochemical analyses carried out in our laboratory (Harkönen *et al* 1972) concerning the effects of different fixatives on the NaK ATPase activity it has been observed that a mild fixation leaves enough activity to produce a visible reaction in the sections.

In accordance with the technique used the NaK ATPase activity was localized in the cornea: 1) at the epithelial cell membranes, 2) in the Schwann cells and nerve fibers and possibly in keratocytes and 3) in endothelial cell membranes.

The sites of the enzyme activity confirm the earlier works on corneal ATPase activity (Ehlers 1963, Kaye and Tice 1966, Maeda and Sakaguchi 1963 and Tervo and Palkama 1974).

There exists several theories about the direction of ion and water transport in the cornea (e.g. Dikstein and Maurice 1972, Green 1966, Hodson 1971, Maurice 1972). We cannot as yet judge whether the ion transport is directed towards the corneal stroma through the endothelium or the epithelium or whether the pumping direction is such that one of these layers is transporting ions and water in and the other out of the cornea. However at present it can be pointed out that both the epithelium and the endothelium are rich in NaK ATPase and that the epithelium contains by far the largest surface area for active pumping. Thus it seems evident that both the epithelium and the endothelium are of great importance for the ion and water metabolism and balance of the cornea. These active sites are obviously responsible for the correct equilibrium of corneal water transport as far as the corneal transparency for light is concerned.

The enzyme activity present in the stroma i.e. in the Schwann cells and in the nerve fibers is possibly important from the nutritional point of view of these structures.

This work is part of a research project carried out at the Eye Research Laboratory of the Anatomy Department of Helsinki University Finland. It has been supported by a grant from the Sigrid Juselius Foundation Helsinki Finland to A.P.

References

- ANDERSON, P. Purification and quantitation of glutaraldehyde and its effect on several enzyme activities in skeletal muscle. *J Histochem Cytochem* 1967 15 657-661.
- BONTING, S. L., K. A. SEMON and N. M. HARRIS. Studies on sodium potassium activated adenosine triphosphatase. I. Quantitative distribution in several tissues of the cat. *Arch Biochem* 1961 93 416-423.
- DIKSTEIN, S. and B. M. MARICE. The metabolic basis to the fluid pump in the cornea. *J Physiol (Lond)* 1970 271 29-41.
- EHLERS, V. Corneal adenosine triphosphatase. A histochemical investigation. *Exp Eye Res* 1965 4 48-53.
- GREEN, K. Dependence of corneal thickness on epithelial ion transport and stromal sodium. *Amer J Physiol* 1966 221 1169-1177.
- HODSON, S. Evidence for a bicarbonate-dependent sodium pump in corneal epithelium. *Exp Eye Res* 1971 11 20-29.
- HARKONEN, M., A. PALKAMA and R. LUOTALO. Functional dependence of the ciliary epithelium ATPase activity and intraocular pressure on the autonomic nervous system. *Acta physiol scand* 1970 80 327-341.
- KAYE, G. I. and L. W. TICE. Studies on the cornea. A electron microscopic localization of adenosine triphosphatase activity in the rabbit cornea in relation to transport. *Invest Ophthalmol* 1966 5 22-32.
- MAEDA, K. and K. SAKAGUCHI. Studies on sodium potassium activated adenosine triphosphatase in the cornea. Electron microscopic observations on the rat cornea. *Jap J Ophthalmol* 1965 9 195-199.
- MARRICE, D. M. The localization of fluid pump in the cornea. *J Physiol (Lond)* 1970 271 43-54.
- MCGILVERAY, J. T. A method for the cytochemical demonstration of sodium activated adenosine triphosphatase. *J Histochem Cytochem* 1961 12 651-658.
- NOVIKOFF, A. B. Enzyme localization with Wachstein Meisel procedures: real or artifact? *J Histochem Cytochem* 1967 15 353-354.
- PAKARINEN, P. Preservation of the cornea for penetrating keratoplasty. An experimental study. *Acta ophthalmol (Nbh)* suppl 106 1965.
- PALKAMA, A. and R. LUOTALO. The histochemical demonstration of sodium potassium activated adenosine triphosphatase activity in rabbit ciliary body. A methodological study. *Ann Med exp F* 1970 48 42-55.
- ROSENTHAL, A. S., H. I. MOSES, I. TICE and C. E. GAYOT. Lead ion and phosphatase histochemistry. III. The effects of lead and adenosine triphosphate concentration on the incorporation of phosphate into fixed tissue. *J Histochem Cytochem* 1967 17 608-611.
- TERVO, T. and A. PALKAMA. Histochemical findings on sodium potassium activated adenosine triphosphatase (NaK ATPase) activity in the cornea. *Acta Ophthalmol scand* 1974. In press.
- LUOTALO, R. and A. PALKAMA. Localization of sodium potassium stimulated adenosine triphosphatase activity in the rabbit ciliary body using light and electron microscopy. *Ann Med exp F* 1970 48 84-88.
- WACHSTEIN, M. and F. MEISEL. Histochemistry of hepatic phosphatase at a physiological pH. *Amer J Pathol* 1957 72 13-23.

Parallel Activation of Dynamic Fusimotor Neurones and a Climbing Fibre System from the Cat Brain Stem

I Effects from the Rubral Region

By

TORVALD JENSEN

Received 21 December 1973

Abstract

JENSEN T. Parallel activation of dynamic fusimotor neurones and a climbing fibre system from the cat brain stem. I Effects from the rubral region. Acta physiol scand 1974 91 223-242

Climbing fibre activity in the cerebellar paramedian lobule as well as hind limb dynamic fusimotor activation caused by electrical stimulation in the rubral region were studied in halothane anesthetized cats. A dorsal stimulating region which was somatotopically arranged, could evoke climbing fibre activity in 3 longitudinal projection areas. This stimulating region was situated in the dorsal parts of the red nucleus and at caudal levels also dorsally to this structure. It was suggested that a synapse was interposed in this descending pathway at rostral rubral levels. From a ventral region situated in the ventral parts of but also extending ventrally and caudally to the red nucleus only a hind limb projection area could be activated. The two pathways relay through the inferior olive and share olivary climbing fibres with each other and with ascending spino-olivocerebellar paths. A marked similarity in the extent of stimulating areas activating hind limb dynamic fusimotor neurones and climbing fibres to one hind limb zone is demonstrated as well as a close similarity in minimum stimulating thresholds for the two effects. The results are discussed in relation to a current hypothesis on the role of climbing fibre systems in motor control.

A descending system influencing dynamic fusimotor neurones of the lumbar spinal cord was indicated by Appelberg (1963) and further identified by Appelberg and Molander (1967). This system was activated by repetitive electrical stimulation within a restricted area of the mesencephalon in the vicinity of the red nucleus. The effective area for stimulation was in the caudal parts of the red nucleus but also extended dorsally and caudally to this structure. Appelberg and Emonet-Denand (1965) showed that the system specifically activated dynamic fusimotor neurones, i.e. neither static fusimotor neurones nor skeletomotor neurones were co-activated when the stimulus intensity was kept low and the tip of the electrode was optimally placed in the mesencephalon. The system seemed to excite extensor as well as flexor dynamic fusimotor neurones.

This descending system was further investigated (Appelberg and Jeneskog 1969 1972) and it was shown that the system proceeds in the dorsolateral funiculus of the spinal cord although it is identical with neither the rubrospinal nor the corticospinal tract. Another descending system primarily influencing static fusimotor neurones and proceeding in the ventrolateral funiculus of the spinal cord was also described by Appelberg and Jeneskog (1972).

It is therefore by now well established that selective effects on static and dynamic fusimotor neurones respectively may be evoked from the rubral region. Restricted areas influencing only one or the other class of neurones may readily be identified (for detailed description see Appelberg and Jeneskog 1972). It has earlier been demonstrated that most parts of the mesencephalic brain stem may exert diverse effects on the fusimotor system (*c.f.* Eldred and Fujimori 1958). According to their maps however these authors mainly studied the reticular formation and paid little attention to the nearby rubral region. In the present investigation the region which selectively influences dynamic fusimotor neurones as judged by the behaviour of spindle primary afferents to central stimulation during extension and twitch tests was investigated.

Single shock stimulation in the same area of the mesencephalon evoked activity in the posterior lobe cortex of the cerebellum as well as in a medullary region overlapping the homolateral inferior olivary nucleus (Appelberg 1967) and it was suggested that a rubro-olivary pathway was simultaneously mediating facilitatory effects on dynamic fusimotor neurones and information to the cerebellar cortex. This suggestion was based upon the finding that the medullary region when electrically stimulated influenced the dynamic fusimotor neurones in an almost identical way to the mesencephalic region. Furthermore the medullary region showed signs of postsynaptic activity as a result of single shock stimulation within the mesencephalic area and stimulation in the medullary region also evoked activity in the posterior cerebellar cortex. In addition lesions in the medullary region prevented the mesencephalic stimulus from influencing the muscle spindle dynamic sensitivity. On double shock stimulation in the mesencephalon at various conditioning test intervals the time course of amplitude modulation of the test response evoked in the cerebellum was found to follow the same pattern as the time course of excitability changes typical for inferior olivary climbing fibres (Armstrong and Harvey 1966).

Recent investigations concerning spinocerebellar paths terminating as climbing fibres in the anterior cerebellar lobe (see Oscarsson 1969 1973) have revealed a sagittal organization of the cerebellar cortex. The different paths terminate in restricted longitudinal zones and show a complex convergence pattern which seems to be established at the inferior olivary level. Such a convergence is not only found between ascending climbing fibre paths but descending climbing fibre paths from the cerebral sensorimotor cortex (Miller Nezlina and Oscarsson 1969 a) and from two areas in the mesencephalon (Miller Nezlina and Oscarsson 1969 b) have also been shown to share climbing fibres with ascending paths. Furthermore Cooke

Oscarsson and Sjöfönd (1972) have demonstrated that the ascending climbing fibre paths through branching of their last order neurones also terminate in the paramedian lobule of the posterior cerebellar lobe in a longitudinal projection pattern.

The physiological demonstration of a longitudinally organized olivocerebellar projection pattern is supported by anatomical findings. Voogds (1969) myeloarchitectonic studies have indicated that the cerebellar cortex is arranged in several narrow longitudinal zones which he denoted A, B, C1, C2, C3 and D in the medio-lateral direction. These zones may be followed along the whole rostro-caudal extent of the cortex and thus a specific zone in the anterior lobe has its counterpart also in the posterior lobe. This author further demonstrated that restricted inferior olivary lesions result in longitudinally oriented bands of degeneration in the cerebellum.

The apparent similarity between stimulating regions in the mesencephalon for activation of dynamic fusimotor neurones (Appelberg and Molander 1967, Appelberg and Jeneskog 1972) and for activation of descending climbing fibre paths (Appelberg 1967, Miller *et al.* 1969 b) was the main reason for the undertaking of the present study. It was of interest to compare more closely, by threshold mapping, the stimulating regions in the same experiment thereby possibly revealing that a single descending system may exert both types of effects. Such an organization of a descending motor system would support the hypothesis of Miller and Oscarsson (1970) suggesting that descending command signals for motor activities may also be sent to the cerebellum via collaterals to the inferior olivary neurones.

The results of this investigation confirm and extend earlier findings concerning climbing fibre activation from the mesencephalon, particularly the rubral region. Three climbing fibre projections to the paramedian lobule are described and furthermore a somatotopic organization of the stimulating areas in the rubral region is demonstrated. A more wide spread climbing fibre projection to the anterior lobe than previously found is also shown. A striking coincidence between stimulating areas in the rubral region for climbing fibre activation and for activation of hind limb dynamic fusimotor neurones is revealed as well as a marked similarity in minimum stimulating threshold for the two effects.

A corresponding study of the inferior olivary region has been performed simultaneously and these results are presented in a separate paper (Jeneskog 1974 b). Two preliminary reports of some of the results have appeared (Appelberg and Jeneskog 1973, Jeneskog 1974 a).

Methods

The results to be presented were obtained in experiments on 28 cats. They were anesthetized with halothane (Fluothane ICI) administered via a Fluotec Mark II vaporizer. Most experiments were performed with an air halothane mixture and the others with an O_2 - N_2O halothane mixture containing 10% O_2 . Breathing was spontaneous and the end tidal CO_2 was continuously monitored with a Beckman Medical Gas Analyzer (Model LB-1). Blood pressure was continuously measured via a femoral artery cannula and prevented from falling below 75 mm Hg by administration of dextrane solution (Macrodex Pharmacia). Glucose (5.5%) and Ringer solutions were infused intermittently at low rates.

Operation After tracheal venous and arterial cannulations a low thoracic (Th12—Th13) laminectomy was performed. The dura was opened and the dorsal funiculi and the right spinal half were transected and removed over approximately one segment. Additional spinal cord lesions could be performed during the experiment with the aid of watchmakers forceps. A second laminectomy (L7—L5) exposed the dorsal roots S₁, L₁ and L₆ which were cut close to the cord on the left side after opening the dura. All other roots were left intact.

The left hind limb was denervated as completely as possible except for the flexor digitorum longus muscle (a physiological toe extensor). The muscle tendon was dissected free distally cut and later connected to an electromagnetic puller via a strain gauge for tension recording.

Two craniotomies were performed, one over the right mesencephalon to allow stereotaxic electrode penetrations to the rubral region and the other over the posterior parts of the cerebellum to allow stereotaxic electrode penetrations to the right inferior olivary region (Jeneskog 1974) and exposing also the left paramedian lobule for surface recordings. The dura was opened in both craniotomies.

Slight variations in the described procedure were sometimes made and will be noted in connection with the Results. In a few experiments where only climbing fibre responses were studied the lower laminectomy and the leg operation were omitted.

Mounting The animal's head was mounted in a stereotaxic frame where the electrode holders could be oriented according to Horsley Clark coordinates. The back was fastened with pins in the pelvis and a clamp in the spinous process of the L₄ vertebra and the left hind limb was sufficiently fixed via a clamp around the foot. The skin of all exposed regions was tied up and the pools were filled with heated mineral oil.

Recording One or more primary muscle spindle afferents from the muscle were isolated usually in the L₇ dorsal root by successive splitting under a dissecting microscope. A functional single fibre was identified as a primary muscle spindle afferent by the pause in the discharge during a muscle twitch and by observing the dynamic sensitivity of the ending to extension. Only very seldom was it necessary to determine the conduction velocity of the fibre studied in order to differentiate between primary and secondary spindle afferents.

Evoked activity in the paramedian lobule was recorded via a spring mounted silver ball electrode on the cerebellar surface with the indifferent electrode placed in the temporal muscles.

All signals were amplified and displayed on a Tectronix double beam storage oscilloscope for monitoring and simultaneously on a Tectronix 565 for film recording (Grass kymograph Camera).

The rectal temperature of the cat as well as the temperatures in the pools were monitored and kept within normal limits (rectal 38—39°C, pools 35—38°C) with the aid of radiant heat from above and a plastic tube spiral with circulating thermostatically regulated water under the belly of the animal.

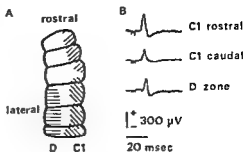
Stimulation The muscle nerve was stimulated via a bipolar hook electrode with single shocks to evoke single muscle twitches. A similar electrode was used for surface stimulation of the dorsolateral part of the spinal cord in the 13th thoracic segment (the rubrospinal tract antidromically and the hind limb component of the dorsolateral spino-olivocerebellar path orthodromically).

Stimulation in the mesencephalon was performed via a stereotaxically guided medio-lateral grid of three electrodes (interelectrode distance 1 mm). They were electrolytically sharpened glass insulated platinum-iridium wires with a free tip of 60—90 μ m (tip diameter approx 10 μ m) and an impedance of 10—100 kohm at 1 kHz. The stimulator delivered constant current pulses (cathodal 0.2 ms) via isolation units. The maximum current used was 100 μ A. Trains of 3 pulses at 600 Hz were used when testing climbing fibre responses and long trains at 300 Hz when testing dynamic fusimotor activation. The indifferent electrode was a platinum-iridium wire in contact with the cerebral surface through the craniotomy. The mesencephalic electrode could also be used for recording of antidromic field potentials.

The mechanical stimulus to the muscle was either linear ramp stretches (2—4 min at 2.5—10.0 mm/s) or electrically evoked maximal single twitches at a rate of 0.8—1.0/s (see Appelberg and Jeneskog 1968, 1972).

Histology At the end of each experiment electrolytic lesions were made at known depths in at least one electrode track. The animals were killed with an overdose of pentobarbital (Mebumal 6% ACO) and the head and sometimes also the part of the spinal cord containing lesions (Jeneskog 1974b) were removed. After 14 days of fixation in Holt and Hicks buffered formaldehyde solution the head was mounted again in the stereotaxic frame and relevant blocks of the brain stem were cut out in a plane parallel to the electrode tracks. The blocks were dehydrated, embedded in Cedukol (Merck) and cut in serial sections (30 μ m) which were stained with toluidine blue.

Fig 1 A shows a schematically drawn picture of the left paramedian lobule. Three climbing fibre projection areas activated from the right rubral region are indicated by different hatching. Nomenclature of longitudinal zones according to Voogd (1969). B shows specimen records of surface recorded climbing fibre responses from the three projection areas on rubral stimulation. Time and amplitude calibrations apply to all records.



With this technique the shrinkage of the brain stem due to the histological procedures was generally about 30 %.

Effective stimulating regions could then be fitted on to camera lucida drawings of the histological sections with reference to the electrolytic lesions made in the experiment and often also to the antidromic field potential evoked in the red nucleus on stimulation of the contralateral spinal cord in the 13th thoracic segment.

Abbreviations

CF climbing fibre CFR climbing fibre response CP cerebral peduncle C1 C2 C3 D longitudinal cerebellar cortical zones DI dynamic index DF SOCP dorsal spino-olivocerebellar path DLF SOCP dorsolateral spino-olivocerebellar path fl forelimb hl hind limb HPT habenopeduncular tract IP nucleus interpeduncularis MG medial geniculate body Mm mamillary body N III nucleus of the third cranial nerve PAG periaqueductal gray substance PIAL intermediate part of anterior cerebellar lobe PM paramedian lobule of posterior cerebellar lobe Ret reticular formation RN red nucleus SC superior colliculus STI spindle twitch index Thal thalamus III third cranial nerve

Results

Climbing fibre responses (CFRs) in the left paramedian lobule (PM) of the posterior cerebellar lobe caused by electrical stimulation in the right mesencephalon were studied in a total of 25 expts. In the surface recordings employed the following characteristics of the evoked potentials made it possible to identify them as being due to climbing fibre (CF) activation of Purkyne cells.

1 The potentials were not evenly distributed over the surface of the lobule but instead confined to certain longitudinal areas (e.g. Oscarsson 1969, 1973).

2 From a single stimulating point in the mesencephalon sharply rising positive potentials were found in some recording points and negative potentials or no evoked potential at all in others. As has been shown by several investigators (e.g. Oscarsson and Uddenberg 1966, Armstrong and Harvey 1968) the sharply rising surface positive potentials indicate synchronous CF activation of many Purkyne cells (a CFR) just beneath the recording point. The negative potentials have been presumed to represent spread of the electrical fields generated by the Purkyne cells in a nearby CF projection area (Oscarsson 1968).

3 The amplitude of the positive potentials fluctuated in an unpredictable manner between successive stimulations in the mesencephalon even at repetition rates as

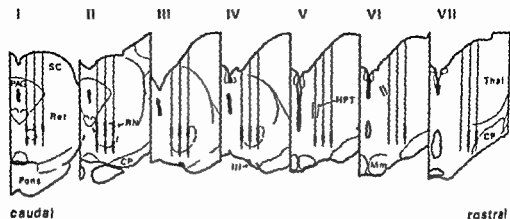


Fig. 2 I—VII are camera lucida drawings of transverse histological sections through the brain stem viewed from behind. I is at the caudal border of the red nucleus and the distance to successive diagrams is approx. 1 mm. The rostral pole of the red nucleus is between diagrams IV and V. The three parallel vertical lines in each diagram represent the electrode tracks and their thickened parts indicate low threshold regions ($\leq 10 \mu\text{V}$) for evoking climbing fibre responses in the contralateral paramedian lobule. There are two regions at caudal and middle rubral levels (I—III) and only one at rostral rubral levels (IV) and also rostrally to the nucleus (V—VII).

low as one per second (Armstrong and Harvey 1968; Miller and Oscarsson 1970). Sometimes the amplitude fluctuated in a cyclic manner with a period of tens of seconds (Miller and Oscarsson 1970).

Distribution of evoked climbing fibre activity in the paramedian lobule to mesencephalic stimulation

As mentioned above, the CFRs evoked from the mesencephalon were not evenly distributed over the surface of the PM but instead they showed an organized longitudinal projection pattern. This has earlier been found in the projections of the ascending Cf paths to the anterior lobe (Oscarsson 1969) and to the PM (Crnik *et al.* 1972) as well as in the descending projection from the mesencephalon to the anterior lobe (Miller *et al.* 1969 b).

Fig. 1 A shows a schematically drawn picture of the left PM as seen on exposure of the posterior cerebellar lobe. The caudalmost 2—3 folia of the PM are not included because they are bent forward and hence not accessible to surface recording. Three distinct projection areas were disclosed and specimen records of CFRs in the three areas evoked from the rubral region are shown in Fig. 1 B. A projection area was defined as the area where the amplitude of the positive surface potential was at least half the maximal one (the amplitude of the CFRs varied in different parts of the PM and was 100—1000 μV in different experiments). Adopting the nomenclature introduced by Voogd (1969) and based upon his anatomical observations, the three sagittal zones in the PM are denoted C1, C2 and D in the medio-lateral direction. A C3 zone is also present in the most rostral part laterally to the C2 zone and rostrally to the D zone. One projection area activated from the mesencephalon is thus within the D zone and the other two areas comprise the C1

zone the first being the three most rostrally situated folia and the other the three accessible caudal folia

From a single stimulating point in the mesencephalon often only one or two of the projection areas were activated. When for instance large positive potentials were recorded from the D zone negative potentials were often seen in the rostral C1 zone (cf Fig 3)

Positive potentials confined to the C2 zone were never found in this series. A possible C3 zone projection in the PM will be described in connection with the somatotopic aspects of the mesencephalic stimulating region (see below)

To summarize in addition to the D zone projection expected from other investigations (Miller *et al* 1969b; Cooke *et al* 1972), the present study demonstrated two further projection areas in the PM activated from the mesencephalon. Both of them are confined to the C1 zone.

The stimulating region in the mesencephalon as revealed by threshold mapping

The CFRs studied in the PM were all evoked from the medial parts of the brain stem at the mesencephalic level. Effective stimulating points were situated within or close to the red nucleus. 45 electrode penetrations at different rostro-caudal levels were made in the 25 expts.

The results are summarized in Fig 2. The diagrams (I—VII) were drawn from transverse histological sections through the brain stem; the interval between them being approximately 1 mm. The 3 parallel vertical lines in each diagram represent the electrode tracks and their thickened parts indicate the effective stimulating region at each level. The results of an individual experiment were projected onto the nearest diagrams in the illustrated series. The threshold for evoking CFRs varied in different experiments and was at caudal levels typically 15–30 μ A (with 3 pulses at 600 Hz). The bars in the diagrams of Fig 2 show the extent of the stimulating regions as mapped with 70 μ A stimulation. At caudal and middle levels of the red nucleus (diagrams I—III) two regions were found with a definite threshold increase ($> 100 \mu$ A) in between. These regions will be referred to as the dorsal and ventral regions respectively. In the most rostral part of the red nucleus (diagram IV) and also rostrally to this structure (diagram V—VII) only one region was found. This will be referred to as the rostral region. In one experiment the rostral region was found to extend rostrally in a slightly lateral direction and possibly reach the cerebral peduncle (diagram VII). The ventral region evoked CFRs only in the D zone while the dorsal and rostral regions could evoke CFRs in all three projection areas.

Usually a train of 3 impulses was needed to activate the pathways properly, but from the dorsal site sometimes 2 or even 1 impulse was enough provided that the tip of the stimulating electrode was really in the low threshold center and the stimulating intensity was raised a bit above the threshold for the 3 impulses.

The shortest latency of the evoked potentials from the dorsal region was in different experiments 7.8–8.6 ms (mean 8.1 ms, $n = 16$). The ventral region was

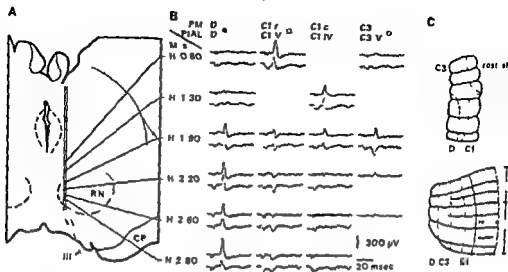


Fig 3 A is a drawing of a transverse histological section through the brain stem at the level of the red nucleus. The vertical line represents the electrode track and the dots mark the stimulating points at different depths in the track. The 2 lateral electrodes in the grid were not tested in this particular experiment and are omitted in the drawing. The four columns in B show the responses evoked at 4 different points in the paramedian lobule (upper trace in each pair) and in the intermediate part of the anterior lobe (lower trace in each pair) from the indicated stimulating points in the brain stem. C upper diagram shows the recording points in the paramedian lobule and lower diagram the recording points in the anterior lobe. Nomenclature of longitudinal zones according to Voogd (1969) and of lobules according to Larsell (1953). The simultaneously recorded points are marked in the same way in the 2 diagrams of C and above the 4 columns of traces in B. Time and amplitude calibrations apply in all records.

rather variable in its ability to evoke CFRs and the latency was always longer than that from the dorsal region (90–108 ms, mean 98 ms, $n = 6$). The shortest latency of the CFRs evoked from the dorsal region did not differ in the three projection areas of the PM. The possible fourth projection to the C3 zone is an exception (see below). At rostral levels of the red nucleus (diagram IV in Fig 2) it was found that supra threshold stimulation yielded a latency which was comparable to that from the dorsal region. On lowering the stimulating intensity to near threshold the latency increased abruptly by about 1 ms. From levels rostrally to the red nucleus the CFRs were quite variable and only the longer latency response could be evoked. In short, at caudal rubral levels two stimulating regions were found which evoked CFRs in the PM. The latency from the dorsal region was shorter than that from the ventral region. Furthermore, when the dorsal region was followed rostrally a step increase in the latency of the CFR was found at rostral rubral levels.

Somatotopy in the projection path from the mesencephalon to the paramedian lobule and to the intermediate part of the anterior lobe

It was noted in the preceding section that stimulation at rostral mesencephalic levels and in the dorsal region at rubral levels could evoke CFRs in three different areas of the PM.

The dorsal region at rubral levels was shown to be somatotopically organized so that in a certain electrode position the use of a suitable stimulating intensity activated only one or two of the three projection areas Fig 3 shows the results obtained in one experiment, where anterior as well as posterior lobes of the cerebellum on the left side were exposed This made it possible to compare anterior and posterior lobe projections activated from the mesencephalon Fig 3 A shows the stimulating electrode track through the mesencephalon The CFRs evoked simultaneously in the PM (upper trace in each pair) and in the intermediate part of the anterior lobe (PIAL lower trace in each pair) from 6 different depths in the same penetration are shown in Fig 3 B The four columns of traces represent 4 recording points as marked in Fig 3 C With only one exception (4th column) it is seen that when a stimulus evoked a CFR in a certain part of the PM a CFR could also be found in a corresponding part of the PIAL The points simultaneously recorded from were chosen according to the projection areas of ascending CF paths (Cooke *et al* 1972) From the dorsal parts of the dorsal stimulating region (H -0.80) CFRs were evoked only in the rostral C1 zone of the PM and in the C1 zone of lobulus V (Larsell 1953) of the PIAL These parts are forelimb areas according to the termination of ascending CF paths (Cooke *et al* 1972) From this depth there were no potentials found (positive or negative) in the caudal C1 zone of the PM or in the C1 zone to lobulus IV (Larsell 1953) of the PIAL i.e. in the hind limb areas (not illustrated) Further down in the stimulating region a hind limb part appears with the C1 zone projection first (H -1.30) and deeper in the track the D zone projection (H -1.90) In the forelimb C1 zones the CFRs from H -1.30 in the mesencephalon looked much the same as those from H -0.80 (not illustrated) Depth H -2.80 was still in the dorsal region as defined in the preceding section but from H -3.0 no positive or negative potentials were recorded in any point studied The latencies of the CFRs evoked in the PIAL were 1-1.0 ms shorter than those in the PM although the recording points were in corresponding areas

A C3 zone projection in the PIAL could not be detected (negative wave from H -1.90 is a mirror image from the D zone projection) although such a projection was found in the most rostral folium of the PM It should be noted that the negative wave in the PIAL (C3 zone) has shorter latency than the positive wave in the PM (C3 zone) That CFR is not thought to be a rostral extension of the D zone projection because the latency is longer than in the more caudal part of the D zone In fact the latency decreased suddenly on moving the recording electrode from the most rostral folium to the second one The anterior lobe was exposed in only one experiment but it is surprising that a C3 zone projection could not be found in the PIAL (neither lob IV nor lob V) though it was found in the PM

From the ventral region as defined in the preceding section only a D zone projection to the PM was found even when CFRs in the C1 zone were especially looked for (16 penetrations in 13 expts)

The results presented in this section confirm earlier results (Miller *et al* 1969 b) with regard to the D zone projection from the dorsal mesencephalic region Further,

more it is demonstrated that this region is somatotopically organized with a forelimb part dorsally and a hind limb part ventrally. The C1 zone projection in the PIAL and the possible C3 zone projection in the PM have not been shown previously.

Convergence from ascending paths in the climbing fibre projections activated from the mesencephalon

For the surface recordings of CFRs employed in the present series a special procedure was used to demonstrate a possible convergence from the mesencephalon and the spinal cord. This convergence is postulated to take place in the inferior olive the source of CFs in these systems. There is a long period (up to more than 100 ms) of heavily depressed excitability of the inferior olivary neurones after they have discharged (Armstrong and Harvey 1966). If a conditioning test procedure is applied the amplitude modulation of the test response would show the same time course as the excitability changes of inferior olivary neurones provided that there is a convergence.

Miller *et al.* (1969b) described 2 mesencephalic regions corresponding to the dorsal and ventral regions in this paper which both projected to the D zone of the PIAL. These regions activated CFs which were also activated by the hind limb component of the spino-olivocerebellar path running in the dorsolateral funiculus (DLF—SOCP). Considering the branching of CFs to project to both the PIAL and the PM (Cooke *et al.* 1972), a convergence also in the PM between CFRs evoked from the mesencephalon and from the spinal cord was investigated by means of the conditioning test procedure. As expected convergence between the D zone projections from both mesencephalic regions and the hind limb component of the DLF—SOCP could be demonstrated.

Figs 4 A—C are from such an experiment. In Fig 4 A is shown the convergence between the pathways activated in the dorsal mesencephalic region and the hind limb component of the DLF—SOCP activated in the 13th thoracic segment. The upper trace shows the test response of the DLF—SOCP alone and the lower trace shows that a conditioning stimulus to the dorsal mesencephalic region causes a 100% depression of the test response (interval approx. 50 ms). Fig 4 B shows the same thing between the pathways activated in the ventral mesencephalic region and the hind limb component of the DLF—SOCP (interval approx. 50 ms). Furthermore dorsal and ventral regions also activate at least partly the same CFs destined for the D zone of the PM (Fig 4 C) as shown by the CFR from the ventral region as test response. The 2 C1 zone projections show the same type of convergence from the dorsal region and the spino-olivocerebellar path running in the dorsal funiculus (DLF—SOCP) activated in the second cervical segment of the spinal cord (Fig 4 D).

Fig 4 E shows graphically the temporal pattern of a conditioning test series using the D zone CFR from the dorsal region as conditioning stimulus and the CFR of the hind limb component of the DLF—SOCP as test stimulus (*cf.* Fig 4 A). The

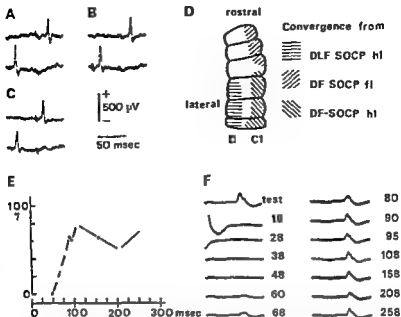


Fig 4 A upper trace shows the climbing fibre response evoked in the D zone of the left paramedian lobule on stimulation of the left DLF in Th13 (6 shocks at 600 Hz). Lower trace shows interaction from right dorsal rubral region (interval approx 50 ms) B same as A but interaction from right ventral rubral region (interval approx. 50 ms) C upper trace shows the climbing fibre response evoked in the D zone from the entral rubral region. Lower trace shows 100% depression of this response when it is preceded (approx 50 ms) by a conditioning stimulus to the dorsal rubral region. Time and amplitude calibrations apply to Fig 4 A-C D convergence patterns from ascending paths in the climbing fibre projections activated from the dorsal rubral region E shows graphically the relationship of the amplitude of the test response in the left paramedian lobule (D zone) to different conditioning test intervals. Test stimulus given to the left DLF in Th13 and conditioning stimulus to the right dorsal rubral region. 100% is the amplitude of the test response alone. The graph is constructed from the recordings in F which show the averaged ($n = 75$) test responses. Conditioning test interval in ms is indicated on the right side of each record. Uppermost trace is the test response alone. The end of the conditioning response is visible in the second and third traces of the left column. Whole traces in F are 48 ms and small wavelets indicate the 6 stimulus shock artifacts.

traces from which the graph was constructed are shown in Fig 4F. They are averaged (Didac 800) test responses (25 stimulations at approx 1 Hz) at indicated conditioning test intervals. This averaging was performed because of the spontaneously occurring variations in the amplitude of the surface potentials. It is seen that the depression of the test response is 100% up to approx 50 ms interval. The amplitude of the test response then gradually recovers to reach a maximum at around 100 ms interval followed by a new depression which is not very pronounced. This relationship is very much the same as the one described for the excitability changes of inferior olivary neurones by Armstrong and Harvey (1960) and also correspond closely to the curve obtained by Appelberg (1967) on double shock stimulation in the mesencephalic region influencing muscle spindle dynamic sensitivity.

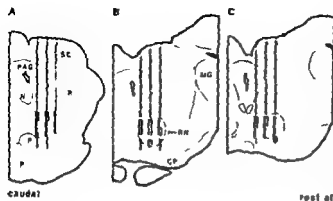


Fig. 5. A—C are transverse histological sections through the brain stem viewed from behind. A = approx 0.5 mm caudally to the caudal pole of the red nucleus and B and C approx 2 mm and 3 mm respectively rostrally to A. The 3 parallel vertical electrode tracks are marked in each diagram. Black bars on the left side of each track indicate low threshold region for eliciting dynamic spindle effects. Black bars on the right side of each track indicate low threshold region for evoking climbing fibre activity. The D zone of the contralateral paramedian lobe.

Comparison of stimulating areas in the rubral region for activation of climbing fibre and dynamic fusimotor neurones

It was mentioned in the Introduction that one important purpose of this investigation was to directly compare low threshold stimulating regions for activation of CFs and of hind limb dynamic fusimotor neurones. In order to exclude possible misinterpretations between experiments this comparison ought to be performed in the same experiment.

The stimulating effects were stable enough to allow a detailed comparison in 7 expts. and scattered observations in a number of other experiments are in agreement with those presented. It was found that the mesencephalic region activating CFs to the D zone of the PM coincided most closely with the region activating dynamic fusimotor neurones to the hind limb toe extensor flexor digitorum longus. Dynamic fusimotor activation was detected indirectly by observing the response of primary muscle spindle afferents to the twitch test and sometimes also to linear extension of the muscle under control conditions as well as during repetitive mesencephalic stimulation (cf. Appelberg and Jøneskog 1968, 1972 and Fig. 6).

The threshold for dynamic fusimotor activation was 10–30 μ A in the experiments with caudal mesencephalic electrode penetrations and somewhat higher in those with rostral penetrations. This is in agreement with earlier findings (Appelberg and Jøneskog 1972). The threshold for evoking D zone CFRs in the PM in the same experiments was 15–45 μ A at caudal levels and 30–60 μ A at rostral levels. The difference between thresholds for the two effects was small in a single experiment (< 10 μ A caudally and < 30 μ A rostrally). The combined results from the 7 expts. are shown in Fig. 5 where the experiments have been fitted to three mesencephalic levels. Level A is approximately 0.5 mm caudally to the caudal border of the red nucleus (cf. diagram 1 in Fig. 2) and levels B and C are approximately 2.0 mm and 3.0 mm rostrally to level A. Black bars on the left side of

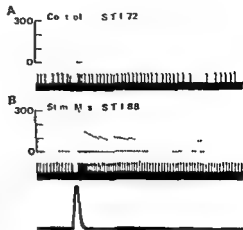


Fig 11 In A is shown the response of a primary muscle spindle afferent to a muscle twitch under control conditions. The upper part is the instantaneous frequency plot (imp/s) and the lower part is the original spike record. B same as A but during repetitive stimulation ($60 \mu\text{V}$) in the dorsal rubral region. Lowermost traces in B are twitch tension record and 100 ms time calibration.

each track indicate the low threshold region ($\leq 70 \mu\text{V}$) for activation of dynamic fusimotor neurones and black bars on the right side of each track indicate the low threshold region ($\leq 70 \mu\text{V}$) for activation of CFs to the D zone of the PM. As seen in Fig 5A, CFRs were evoked from two regions (the dorsal and ventral regions described in an earlier section) while effects on dynamic fusimotor neurones were obtained from an area covering in the dorso-ventral direction both these regions. However from this area two different descending systems both acting on dynamic fusimotor neurones may be activated as demonstrated by Appelberg and Jeneskog (1972). These authors described a dorsal and a ventral mesencephalic region which both influenced hind limb fusimotor neurones. At caudal rubral levels and also caudally to the nucleus the two regions were often confluent but it was demonstrated that effects from the dorsal region proceed in the dorso-lateral funiculus of the spinal cord while effects from the ventral region take a ventrolateral spinal course. The CFRs evoked from the ventral region in the present investigation were always more variable than those from the dorsal region (see above) and thus part of the ventral stimulating region for evoking CFRs might have been overlooked in the experiment illustrated in Fig 5A. This suggestion was supported by the findings in another experiment performed using chloralose anaesthesia where the stimulating region for evoking CFRs (stimulation level close to that in Fig 5A) was continuous i.e. the dorsal (short latency CFR) and ventral (longer latency CFR) regions followed each other without a definite threshold increase in between. That experiment has not been included here because the activation of dynamic fusimotor neurones was untypical probably because of the anaesthetic used. The fusimotor activation in that experiment always ceased within a few seconds after the repetitive stimulation had begun although the stimulation continued. At the caudal rubral level (Fig 5B from 4 expts) the coincidence between the stimulating regions for the two effects is remarkably close. At mid rubral levels (Fig 5C from

2 experiments) there is again a continuous region for dynamic fusimotor activation but two separate regions for evoking CFRs. However the region covered by both types of effects seems to be the same.

An example of dynamic fusimotor activation from the dorsal rubral region is presented in Fig. 8 where the behaviour of a muscle spindle primary afferent to a muscle twitch both under control conditions and during mesencephalic stimulation is shown. The central stimulation raised the spindle twitch index (STI; see Appelberg and Jenesko 1972) from 72 to 88 indicating a rather strong dynamic fusimotor activation of this muscle spindle. On testing the same spindle afferent with linear extension of the muscle (2 mm at 2.5 mm/s) the dynamic index (DI) raised from 64 in the controls to 92 during the mesencephalic stimulation.

Discussion

The present investigation dealt with two problems: firstly the activation from the rubral region of descending climbing fibre systems and their relation to ascending climbing fibre paths and secondly the correlation of one of these systems with a known descending path influencing hind limb dynamic fusimotor neurones.

Climbing fibre responses could be evoked in the contralateral paramedian lobule from two separate low threshold regions at the rubral level: one dorsal and the other ventral.

The dorsal region will be discussed first. It is situated in the dorsal parts of the red nucleus and caudally also dorsally to this structure and its stimulation may evoke responses in three separate longitudinal areas of the paramedian lobule. One projection area is in the caudal parts of the lateral third of the lobule i.e. within the D zone according to the nomenclature of Voogd (1969). The two other projection areas are confined to the rostral and caudal parts respectively of the medial third i.e. within the C1 zone of Voogd. From the dorsal parts of the dorsal stimulating region only the rostral C1 zone projection is activated while from the ventral parts of this region climbing fibre responses are evoked in the caudal C1 zone and in the D zone. There is sometimes slight overlap and in these cases all three projection areas may be activated from a single stimulating point (cf. H. 190 of Fig. 3) when stimulating intensities are well above threshold. According to Cooke *et al.* (1972) the rostral C1 zone is a forelimb projection area and the caudal C1 zone and the D zone are hind limb projection areas with respect to ascending climbing fibre paths. The convergence demonstrated in this series in the D zone projection from the hind limb component of the DLF—SOCP and in the two C1 zone projections from the DF—SOCP allows the conclusion that the dorsal rubral region is somatotopically arranged with a forelimb part dorsally and a hind limb part ventrally. Miller *et al.* (1969b) described a D zone projection in the anterior cerebellar lobe from their dorsal mesencephalic region. This projection was confirmed in the present study and furthermore a C1 zone projection to the anterior lobe was revealed both to lobulus V and to lobulus IV (Larsell 1953) which are fore- and hind limb areas.

respectively with regard to ascending climbing fibre paths (e.g. Oscarsson 1969). When recording simultaneously from anterior and posterior lobes it was noted that the amplitude variations of the climbing fibre responses occurred in parallel although the amplitude of the surface response was always larger in the paramedian lobule. From this it is suggested that the anterior and posterior lobe responses are evoked at least partly via a single group of climbing fibres which by axonal branching reach corresponding zones in both parts of the cerebellum. This suggestion was also made by Armstrong, Harvey and Schild (1969, 1971, 1973a, b, c) and by Cooke *et al.* (1972) in studies of ascending climbing fibre paths terminating in the anterior and posterior cerebellar lobes.

There is a remarkable doubling of projection areas of ascending climbing fibre paths in the anterior lobe so that forelimb components reach both C1 and C3 zones of the lobulus V and hind limb components both C1 and C3 zones of the lobulus IV (Oscarsson 1969). This doubling has been shown to depend at least partly on axonal branching of single climbing fibre neurones which also reach the C1 zone of the paramedian lobule (Armstrong *et al.* 1971, 1973a, b, c). However from the dorsal rubral region climbing fibre responses were detected only in the C1 zone of the anterior lobe with the evoked potentials in the C3 zone of the anterior lobe always being negative. A climbing fibre response was indeed evoked in the most rostral folium of the paramedian lobule at its lateral border and this part is a C3 zone according to Voogd (1969). The latency of this response was however longer than those in the other projection areas and it was thus probably evoked via an indirect path. It was not possible to find even such a long latency response in the C3 zone of the anterior lobe. Thus lack of short latency climbing fibre responses in the C3 zones of the anterior lobe as well as of the paramedian lobule from the rubral region was observed in only one experiment. There is however no reason to believe that the lack of short latency C3 zone responses was the result of damage to the preparation as climbing fibre responses were readily evoked in other areas and negative potentials with short latencies were easily recorded within the C3 zone of the anterior lobe (e.g. Fig. 3B from H. - 190).

The dorsal stimulating region was followed in the rostral direction well beyond the rostral pole of the red nucleus. From such levels the evoked climbing fibre responses were variable but they could be recorded in all 3 projection areas of the paramedian lobule. Low intensity (threshold) stimulation at rostral rubral levels yielded a climbing fibre response with a latency which abruptly shortened about 1 ms on raising the stimulus intensity. From stimulating levels rostrally to the red nucleus only the longer latency response was evoked. The described latency increase at the level of the rostral red nucleus as well as the marked variability in the climbing fibre responses evoked from levels rostrally to this structure indicate that a synapse in the descending pathway to the cerebellum is interposed in the rostral parts of the red nucleus. From these facts it is suggested that effects from the dorsal stimulating region at rubral levels represent the activation of an uncrossed rubro-olivary tract with cell bodies located in the rostral part of the red nucleus and that

effects from the rostral extension of the stimulating region represent the stimulation of presynaptic fibres to these rubral cells. The origin of these prerubral fibres is not known but possibly they come from the ipsilateral cerebral peduncle. In fact, the course of the prerubral stimulating region is strongly suggestive of the course of cortico-rubral fibres, as described by Rinvik and Walberg (1963). These authors showed that fibres from the forelimb area of the motor cortex end in the red nucleus predominantly dorsally to fibres from the hind limb cortical area. This somatotopic pattern is in good agreement with the pattern found for the rubro-olivocerebellar path in this investigation.

Considering the convergence on to the inferior olivary climbing fibres from this descending path and the DLF—SOCP and the DF—SOCP, it must be concluded that the rubro-olivary tract reaches at least the dorsal accessory olive, because the ascending paths are known to relay in this part of the inferior olive (Oscarsson 1969). However this is not in agreement with the anatomical observation that rubro-olivary fibres reach only the dorsal lamella of the principal olive (Walberg 1956, Edwards 1972) and the physiological observation that stimulation of the paramedian lobule antidromically activates inferior olivary neurones only in the ventral lamella of the principal olive (Armstrong and Harvey 1966). This disagreement could be explained if the rubro-olivary tract described here activates the climbing fibre neurones via an interneurone. However this is probably not the case as will be further discussed in a forthcoming paper (Jeneskog 1974 b). A poor correlation between anatomical and physiological observations was also found for the cortico-olivocerebellar path (Miller *et al* 1969 a).

The ventral stimulating area overlaps the ventral part of the red nucleus in its caudal parts but extends also caudally and ventrally to this structure. This was shown in the histological reconstructions of effective stimulating areas and also physiologically by demonstrating that the ventral region extends ventrally to the antidromic field potential evoked in the red nucleus on stimulation of the contralateral spinal cord in the 13th thoracic segment. Antidromic stimulation at this level activates only the hind limb rubrospinal neurones and their cell bodies are known to be situated in the ventrolateral parts of the red nucleus (Pompeiano and Brodal 1957). From the ventral region climbing fibre responses were evoked only in the D zone of the paramedian lobule although responses were also looked for in the CI zone. This D zone projection and the effective stimulating area are in agreement with the findings of Miller *et al* (1969 b) in their study of anterior lobe projections from the rubral region of the mesencephalon. The longer latency of the D zone climbing fibre response evoked from the ventral region as compared to the latency of the response from the dorsal region as well as the marked variability of the evoked responses indicate that this pathway to the cerebellum is an indirect one as was also suggested by Miller *et al* (1969 b).

As mentioned in the Introduction Appelberg (1967) found that posterior cerebellar lobe activity probably mediated via inferior olivary climbing fibres, is evoked from the same mesencephalic region as the one giving excitation to hind limb

dynamic fusimotor neurones (Appelberg and Molander 1967) Climbing fibre activation from this perirubral region has since been studied by Miller *et al* (1969 b) and also more thoroughly in this investigation The purpose of this was to make a direct comparison of effective low threshold regions for evoking climbing fibre responses and for activating hind limb dynamic fusimotor neurones Such a comparison was made in a number of experiments with stimulation at several different rostro caudal me encephalic levels The closest similarity between low threshold stimulating regions for the two types of effects was found when the region influencing dynamic fusimotor neurones was compared to the region evoking climbing fibre responses in the D zone of the paramedian lobule It is an important factor for the hypothesis to be discussed below that dynamic fusimotor neurones to a hind limb muscles are activated from the same rubral area as climbing fibres which are also influenced by the hind limb component of an ascending spino-olivocerebellar path (DLF—SOCP)

The slight differences in ventral borders of the stimulating areas may be explained in several ways One possibility is that part of the ventral stimulating region for activation of climbing fibres might have been overlooked because the responses evoked from this region were quite variable This suggestion is supported by the findings in a chloralose anesthetized preparation as described in the Results section Another possibility is that the ventral region although giving climbing fibre responses in the D zone has nothing at all to do with the descending DLF system to hind limb dynamic fusimotor neurones It might instead be related to another descending system proceeding in the ventrolateral funiculus of the spinal cord which may also activate dynamic fusimotor neurones (Vedel and Mouillac Baudevin 1969) This system is often coactivated from the rubral region (Appelberg and Jeneskog 1972)

Beside the marked similarity in the extent of the stimulating regions for the two effects there was also a close similarity in minimum stimulating thresholds The slightly higher intensity sometimes needed for the climbing fibre responses to be evoked was probably the result of the experimental procedure as the threshold mapping of the region giving dynamic fusimotor activation was always done during the first electrode penetration of a single experiment Then the electrode grid was drawn back to a level well above the effective area and the threshold mapping of the region giving climbing fibre responses was performed in a second penetration with the same rostro-caudal and medio lateral coordinates Thus slight damage to the tissues of the first penetration may have caused the occasionally occurring threshold increase A further coincidence concerning stimulating threshold was that the minimal effective intensity rose in parallel when the electrodes were moved from caudal to more rostral rubral levels This type of threshold increase has been noted before in connection with the activation of dynamic fusimotor neurones (Appelberg and Jeneskog 1972)

It is tempting to interpret the close coincidence between stimulating regions in the rubral area for the two effects as well as the marked similarity in mi

stimulating thresholds as an indication that the two effects are mediated by one and the same descending system. Such an organization would support the hypothesis of Miller and Oscarsson (1970) that descending command signals for motor activities to spinal cord segments (or lower brain stem centers) may also be sent to the cerebellum via collaterals to inferior olivary climbing fibres. These same neurones are informed a little later by ascending paths of what occurred in the segment (or at the low brain stem level) as a consequence of the descending activity and its integration with peripheral inputs to the cord segment (or the lower brain stem). The convergence from the descending motor system described in this paper on to climbing fibres which are also activated by the hind limb component of the DLF—SOCP makes it possible for the inferior olive to integrate this specific descending motor activity with the activity of a particular ascending system. Accepting such an interpretation this investigation has demonstrated a specific motor function of which the cerebellum is informed via a climbing fibre path.

The studies of Chambers and Sprague (1955a, b) have indicated that the cerebellar vermis is concerned with posture and locomotion of the entire body while more lateral parts are concerned with spatially organized and skilled movements of an ipsilateral limb. The termination of the path from the red nucleus in the D zone of the cerebellum indicates that this descending system might have some relation to ipsilateral skilled movements rather than to whole body equilibrium. The ascending DLF—SOCP which terminates only in the non vermal part of the cerebellum (C and D zones, Larson, Miller and Oscarsson 1969) should thus also monitor activity concerning ipsilateral skilled movements. This has been indicated by Larson *et al.* (1969) who found that the adequate stimulus for evoking activity in the DLF—SOCP is cutaneous stimulation of the pads. From that fact these authors assumed that the DLF—SOCP might be related to reflex arcs specifically activated from the plantar surface of the foot such as the magnet reaction (Rademaker 1931) and the extension reflex described by Engberg (1964). Both the e reflexes may be included in the group called spatially organized and skilled movements by Chambers and Sprague (1955a, b).

This work was supported by the Swedish Medical Research Council Project No. 041333 and by The Medical Faculty, Umeå.

References

- APPELBERG B. Central control of extensor muscle spindle dynamic sensitivity. *Life Sci.* 1963 9: 106—103.
- APPELBERG B. A rubro-olivary path and II Simultaneous action on dynamic fusimotor neurones and the activity of the posterior lobe of the cerebellar cortex. *Exp Brain Res* 1967 3: 337—349.
- APPELBERG B. and F. EMMET DUNN. Central control of static and dynamic sensitivities of muscle spindle primary endings. *Acta physiol scand* 1963 63: 487—494.
- APPELBERG B. and T. JENESKOG. Extension and twitch of muscle as tests of muscle spindle static and dynamic sensitivities. *Lif Sci* 1968 Part I 7: 1271—1287.
- APPELBERG B. and T. JENESKOG. A dorso-lateral spinal pathway mediating information from the mesencephalon to dynamic fusimotor neurones. *Acta physiol scand* 1969 77: 159—171.
- APPELBERG B. and T. JENESKOG. Mesencephalic fusimotor control. *Exp Brain Res* 1970 35: 97—112.

- APPELBERG B and T JENESKÖG Parallel activation from the cat brain stem of hind limb dynamic fusimotor neurones and climbing fibres to the cerebellar paramedian lobule *Brain Res* 1973 58 229-233
- APPELBERG B and C MOLANDER, A rubro-olivary pathway. II Identification of a descending system for control of the dynamic sensitivity of muscle spindles *Exp Brain Res* 1967 3 372-381
- ARMSTRONG D M and R J HARVEY Responses in the inferior olive to stimulation of the cerebellar and cerebral cortices in the cat *J Physiol (Lond)* 1966 187 553-574
- ARMSTRONG D M and R J HARVEY Responses of a spino-olivo-cerebellar pathway in the cat *J Physiol (Lond)* 1968 194 147-168
- ARMSTRONG D M R J HARVEY and R F SCHILD Branching of individual olivo-cerebellar axons to terminate in more than one subdivision of the feline cerebellar cortex *J Physiol (Lond)* 1969 202 106P-108P
- ARMSTRONG D M R J HARVEY and R F SCHILD Distribution in the anterior lobe of the cerebellum of branches from climbing fibres to the paramedian lobule *Brain Res* 1971 20 203-206
- ARMSTRONG D M R J HARVEY and R F SCHILD Branching of inferior olivary axons to terminate in different folia, lobules or lobes of the cerebellum *Brain Res* 1973 a 54 365-371
- ARMSTRONG D M R J HARVEY and R F SCHILD Cerebello-cerebellar responses mediated via climbing fibres *Exp Brain Res* 1973 b 18 19-39
- ARMSTRONG D M R J HARVEY and R F SCHILD The spatial organization of climbing fibre branching in the cat cerebellum *Exp Brain Res* 1973 c 18 40-58
- CHAMBERS W W and J M SPRAGUE Functional localization in the cerebellum I Organization in longitudinal cortico-nuclear zones and their contribution to the control of posture both extrapyramidal and pyramidal *J comp Neurol* 1955 a 103 105-129
- CHAMBERS W W and J M SPRAGUE Functional localization in the cerebellum II Somatotonic organization in cortex and nuclei *Arch Neurol Psychiat (Chic)* 1955 b 74 653-680
- COOKE J D O OSCARSSON and B SJÖLLIN Termination areas of climbing fibre paths in paramedian lobule *Acta physiol scand* 1972 84 37 A-38 A
- EDWARDS S B The ascending and descending projections of the red nucleus in the cat: an experimental study using an autoradiographic tracing method *Brain Res* 1972 48 45-63
- ELROD E and B FUJIMORI Relations of the reticular formation to muscle spindle activation. In *Reticular Formation of the Brain* (ed H H Jasper) pp 275-283 Little Brown & Co Boston 1951
- EVENSEN I Reflexes of foot muscles in the cat *Acta physiol scand* 1964 62 Suppl 235 64 p
- JENESKÖG T Convergence from the mesencephalon and the spinal cord in climbing fibre projections to the paramedian lobule *Acta physiol scand* 1974 a Suppl 396 69
- JENESKÖG T Parallel activation of dynamic fusimotor neurones and a climbing fibre system from the cat brain stem. II Effects from the inferior olivary region *Acta physiol scand* 1974 b In press
- LARSEN O The cerebellum of the cat and the monkey *J comp Neurol* 1953 99 195-200
- LARSEN O S MILLER and O OSCARSSON Termination and functional organization of the dorsolateral spino-olivocerebellar path *J Physiol (Lond)* 1969 203 611-640
- MILLER S and O OSCARSSON Termination and functional organization of spino-olivocerebellar paths. In *The Cerebellum in Health and Disease* (eds W S Fields and W D Willis Jr) pp 172-200 W H Green St Louis Mo 1970
- MILLER S A NEZLINA and O OSCARSSON Projection and convergence patterns in climbing fibre paths to cerebellar anterior lobe activated from cerebral cortex and spinal cord *Brain Res* 1969 a 14 230-233
- MILLER S A NEZLINA and O OSCARSSON Climbing fibre projection to cerebellar anterior lobe activated from structures in midbrain and from spinal cord *Brain Res* 1969 b 14 234-236
- OSCARSSON O Termination and functional organization of the ventral spino-olivocerebellar path *J Physiol (Lond)* 1968 196 453-478
- OSCARSSON O The sagittal organization of the cerebellar anterior lobe as revealed by the projection patterns of the climbing fibre system. In *Neurobiology of Cerebella: Evolution and Development* (ed R Llinas) pp 525-533 AFA Chicago 1969
- OSCARSSON O Functional organization of spinocerebellar path. In *Handbook of Sensory Physiology Volume II Somatosensory System* (ed A Iggo) pp 339-380 Springer Berlin-Heidelberg-New York 1973

- OSCARSSON O and N LIDENBERG Somatotopic termination of spino-olivocerebellar path. *Brain Res* 1966 3 204—207
- POMPEIANO O and A BRODAL, Experimental demonstration of a somatotopical origin of rubro-spinal fibres in the cat. *J comp Neurol* 1957 103 225—252
- RADEMAKER, G G J *Das Stehen* Monographien a. d ges geb Neurologie u Psychiatrie 59 416 p Springer Berlin 1931
- REINIK E. and F WALBERG Demonstration of a somatotopically arranged cortico-rubral projection in the cat. An experimental study with silver methods. *J comp Neurol* 1963 120 393—407
- VEDEL J P and MOUILLAC-BALDEVIN Etude fonctionnelle du controle de l'activite des fibres lussmotorices dynamiques et statiques par les formations reticulées mesencephalique pontique et bulbaire chez le Chat. *Exp Brain Res* 1969 9 325—345
- VOORD J The importance of fibre connections in the comparative anatomy of the mammalian cerebellum. In *Neurobiology of Cerebellar Evolution and Development* (ed R Liima) pp 493—514 AHA Chicago 1969
- WALBERG F Descending connections to the inferior olive. An experimental study in the cat. *J comp Neurol* 1956 104 77—173

Titratable Acid, P_{CO_2} , Bicarbonate and Ammonium Ions along the Rat Proximal Tubule

By

BERTIL KARLMARK and BO G DANIELSON

Received 23 December 1972

Abstract

KARLMARK B and B G DANIELSON *Titratable acid P_{CO_2} , bicarbonate and ammonium ions along the rat proximal tubule* Acta physiol scand 1974 91 243-258

The proximal tubule of cortical nephrons of male albino rats were studied. The intratubular pH was measured with antimony microelectrodes. The concentrations of bicarbonate ions, the ammonium ions and titratable acid were measured in the same free flow samples from single tubules using a recently developed ultramicroanalytical system, which also permits the estimation of intratubular P_{CO_2} . The concentration of titratable acid, which is thought mainly to emanate from phosphate, was found to be constant, about 1 mM along the proximal tubule. This is explained as a gradient limited transport process for phosphate as well as for hydrogen ions. The concentration of ammonium ions was found to be about 2 mM along the convoluted proximal tubule in spite of water reabsorption, indicating some reabsorptive mechanisms for ammonium or the base ammonia. Furthermore the present investigation indicates a high P_{CO_2} in the untreated proximal tubule which could explain the phenomenon of disequilibrium pH.

The hydrogen ions delivered into the renal tubules are generally considered to emanate from the intracellular hydration of carbon dioxide (Rector 1971). This production is slow however if uncatalyzed but will deliver nearly inexhaustible amounts of hydrogen ions in the kidney under the influence of carbonic anhydrase (Maren 1969). Recent histochemical studies on the rat kidney indicate that carbonic anhydrase is present in the entire convoluted tubular wall of the rat cortical nephron (Lonnnerholm 1971). Full knowledge of the enzyme's role in the kidney however is still lacking (Kunau 1972). With the presence of an intraluminal enzyme an accumulation of carbonic acid is prevented and the intratubular pH is kept at a higher value than otherwise in an uncatalyzed reaction. Walser and Mudge (1960) after re-examination of data by Roughton (1944) discussed also this possibility as did Rector *et al* (1960). But whether the carbonic anhydrase located in the brush

border of the proximal tubule is functioning intracellularly or intraluminally is as yet not possible to judge from a histochemical point of view.

An experimental indication of the possible role of an intraluminal carbonic anhydrase outlined above was given by Rector *et al* in 1965. Assuming constant bicarbonate concentrations at different P_{CO_2} (Clapp *et al* 1963, Karlmark and Schell 1973) they found that during the administration of a carbonic anhydrase inhibitor the proximal tubule had an intratubular pH of about 0.85 pH units lower than the same fluid when collected and equilibrated in a quinhydrone electrode. This difference was called an acid disequilibrium pH and was thought to be due to a delayed dehydration of carbonic acid during carbonic anhydrase inhibition which would favour an accumulation of free hydrogen ions. The same conclusions were drawn by Vieira and Malmic (1968) using antimony microelectrodes for the *in situ* pH measurements but their disequilibrium was lower 0.41 pH units.

But reabsorption of bicarbonate ions might however also account for urine acidification at least in the turtle bladder as shown by Schulz and Brodsky (1972). In mammals Maren (1969) calculated that about one third of the bicarbonate filtered is reabsorbed as carbon dioxide and the rest is reabsorbed actively as bicarbonate ions. The quantitative roles of the two main factors proposed for urine acidification (the hydrogen ion secretion and the bicarbonate reabsorption) are not fully elucidated however. The buffer loading experiments purposed for calculation of maximal rates of hydrogen ion secretion are difficult to interpret in this respect because the buffer handling of the tubular wall is as yet incompletely defined. One approach to these problems might be the titration of hydrogen ions bound to the different urine buffers. Such methods are as yet not used however in renal micro-puncture research, mainly due to the technical difficulties in the titration of nanoliter samples. A new method for the direct measurement of titratable acid (TA)* in samples of a few nanoliters (Solomon and Alpert 1969) has recently been modified for the use on samples collected intratubularly from the rat nephron (Karlmark 1973). This modified method is used in the present investigation.

Finally, the output of ammonium ions** is another acid eliminating mechanism of the mammalian kidney. The renal output of ammonium is not merely the result of the elimination of that ion from the blood but is also a result of formation of ammonia in the renal tubular cells as was shown by Nash and Benedict (1971). The aforementioned found that in dogs the ammonium concentration in renal venous blood was twice as high as that in the arterial blood and in blood from the caval vein, a fact later confirmed by Denis *et al* (1964).

The base ammonia is uncharged, highly diffusible and penetrates cell membranes very rapidly. Pitts (1971). As established by Stone *et al* (1967) the am-

* Titratable acid in urine is defined in this paper as the base necessary to titrate a bicarbonate-free urine from its initial pH to a pH of 7.4 (Siggard Andersen 1966).

** Ammonia is used for the base (NH_3). The corresponding acid (NH_4^+) is called ammonium. The sum of ammonia and ammonium concentrations in a solution will be referred to as the total ammonia.



Fig. 1 The metal kidney cup with small drilled holes for buffer solutions

monia brought to the kidney in arterial blood and that produced within the tubular cells form a common pool. The diffusible base rapidly gains entrance to the interstitial fluid, the peritubular blood and the tubular fluid of the whole kidney (Balogh Baruch 1971).

Ammonia binds hydrogen ions to form ammonium with a pK_a above 9 (Jacquez *et al.* 1959). This ion is restricted when penetrating cell membranes according to Jacobs (1940). It follows then that ammonia already diffused into an acid solution surrounded with a biological membrane will be locked or trapped as ammonium. Assuming a constant partial pressure of ammonia (P_{NH_3}) in different such solutions, the highest ammonium concentration will be obtained in the most acid one.

Rather few experiments on ammonium excretion are performed with micro-puncture technique probably due to the fact that the microdiffusion technique for the analysis of ammonium in such experiments requires large sample volumes (50–200 nanoliter) which sometimes necessitates pooling of urine from different tubules. The pH measurements intended for the calculation of P_{NH_3} were furthermore performed *in vitro* with quinhydrone micro electrodes (Pierce and Montgomery 1935). These electrodes have certain disadvantages however in that they always measure the pH under conditions of chemical equilibrium in a P_{CO_2} assumed to exist in the tubule. Moreover, the equilibration time is long in the electrodes if the sample volume is 50 nl or more (Rector *et al.* 1963) — a volume which is at least required in such experiments.

The purpose of the present investigation was to determine the main acid base parameters in the same sample from the proximal tubule of the rat cortical nephron. The possibility to use recently developed analytical technique for titratable acid bicarbonate and ammonium ions, intratubular pH and P_{CO_2} , made it possible to evaluate some of the mechanisms behind the urine acidification (Karlmark 1973, Karlmark and Sothell 1973).

Material and Methods

Male albino rats (Sprague Dawley Strain, Anticimex, Stockholm, Sweden, weighing 200–310 g) were used in this study. They were fed on a standard commercial rat pellet diet (Anticimex, Sweden) and had food and water ad libitum until the start of the experiment. Anesthesia was induced by an intraperitoneal injection of Inactin® (Chem. Fabrik Promonta GmbH, Hamburg, West Germany) with a dose of 120 mg/kg b.wt. No additional anesthetic was administered during the course of the experiments. The body temperature was kept constant at 38°C with a heating lamp.

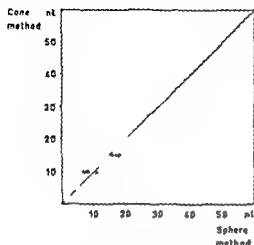


Fig. 2 A comparison between the two volume measurement methods described with the use of four consecutive pipettes for the cone volumes. The line is that of identity.

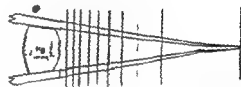


Fig. 3 The tip of a sampling pipette approximated to a cone and divided into ten equal volumes.

Surgical Procedures. The animals were tracheotomized with a polyethylene tube (id 1.7 mm) reaching half the distance between the larynx and the upper teeth. Catheters were inserted in the right jugular vein for infusions and in the left common carotid artery for blood sampling and blood pressure measurements. The pressure was registered using a Siatham transducer (P23AA Siatham Hato Rey, Puerto Rico) and a potentiometer recorder (LER 124 Yokogawa Works Ltd Tokyo Japan). The urinary bladder was drained through a short catheter since pilot studies showed a diminished urine flow rate from the experimental kidney when the bladder was filled. The left kidney was exposed via a flank incision and suspended in an aluminium kidney cup seen in Fig. 1.

The kidney was imbedded with oil-filled cotton wool and the loose capsule was carefully retracted around a minor part of the dorsal kidney surface. Evaporation of most surface fluid was permitted but the kidney was not allowed to be dried. The renal surface was thereafter superfused with filtered and heated mineral oil saturated with water and pre-equilibrated with 5% carbon dioxide and 20% oxygen in nitrogen at room temperature. The oil's P_{CO_2} (Karlmark and Sothell 1973) was checked after each experiment and was found to range between 30 and 51 mm Hg. The left ureter was finally catheterized with the catheter tip in the renal pelvis.

Infusions. Immediately after catheterization of the left jugular vein a prime dose of Polyfrucosan S (Inutest[®] Lacton Gesellschaft Lanz Austria termed inulin in the following) was administered intravenously. Saline with 12.5% inulin was used in a priming dosage of 4.8 ml/kg bwt. Immediately afterwards a continuous infusion was begun with the same solution at a rate of 4.8 ml/kg bwt and hour (Sage Pump 35[®] Sage Instr. Inc. New York USA). The infusion had progressed for at least 1 h and a half before any sampling occurred. This inulin infusion was a plasma concentration of about 120 mg.

The Choice of Tubular Infusion. Measuring of blood pressure with lysamine green observed during pilot studies and following reports on changed membrane properties with the use of lysamine green (Björk and Nagel 1969; Heller 1971; and Christensen and Fredriksen 1972) disqualified this technique for identification of different parts of the nephron. For accuracy no other technique was used. Instead the nephrons which seemed to be technically convenient for good measurements and good sampling were chosen. The puncture site was identified in terms of degree of fluid reabsorption at that special site. The inulin concentration in the tubular fluids as compared to plasma (IF/P inulin) in this case represented a scale from 1.0 to 4.2. No values were found between 3.15 and 3.70. All values below 3.15 then were regarded as proximal and these results are used in this paper.

Intratubular pH. Measurement of the intratubular pH was performed in a manner similar to that described by Vietra and Malnic (1968). The manufacturing of the electrodes used is

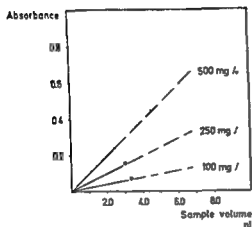
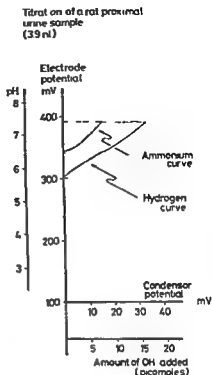


Fig 4 The plot of extinction against the sample volume giving concentration lines for inulin in the different solutions

Fig 5 Original titration curves from the analysis of a rat proximal urine sample



described elsewhere (Harlmark 1973). In the present investigation the antimony electrodes had a shorter tip however and were ground to a diameter of about $5 \mu\text{m}$. The Ag/AgCl reference electrode had a liquid junction of 3 cm agar in 3 M NaCl ending in a tip of about $10 \mu\text{m}$. Previous studies showed that the location of the reference electrode in the kidney did not influence the intratubular pH measurements in the proximal tubule. For convenience then the reference tip was inserted peripherally in the kidney assuring a small damage of the tubules. The reference tip had to be freshly prepared to avoid irrelevant tip potentials. The potential of the measuring system was read on a battery-driven mV meter free from ground (Radometer Copenhagen Denmark).

Intratubular Sampling. Ground pipettes with a tip to $6\text{--}8 \mu\text{m}$ were filled with mercury and connected to a water filled glass syringe. A high pressure was necessary to fill the very tip with the metal. The high surface tension of the mercury forced the tip meniscus backward but it was kept at the tip by a continuous high pressure in the syringe. By balancing this pressure the position of the tip meniscus was easily controlled. Assuming the tip of the pipette is a cone every position of the tip meniscus corresponds to a certain tip volume which can be estimated from an ocular scale of a microscope. Fig 2 shows a comparison between saline volumes measured with this "cone method" and a reference sphere method measuring the diameter of the droplet in the oil according to Hellman *et al* (1967). It can be seen that up to $20\text{--}25$ nanoliter the results of the two methods are similar. Above that volume the cone method underestimated the true volume. This is understandable since no corrections were made for the convex surface of the mercury. Fig 3 shows a pipette with an unfilled cone which is divided into ten equal volumes. The sampling rate used in this study was about 3.5 nl/min for 10 min and one tenth of the cone was continuously filled each min.

Prior to each sampling (which took place through the same hole as used for the intratubular pH measurements) about 0.2 nl mineral oil colored with Sudan Black and equilibrated

with 12% CO₂ was aspirated into the mercury filled pipette. The injection of this oil in the tubule prior to the sampling confirmed the passage of urine around the tip of the pipette. When the sampling was finished about one nanoliter of that mineral oil superfusing the kidney was aspirated to prevent evaporation.

Inulin Determination The spectrophotometric Antrone method described by Hilger *et al* (1958) was used but in a modified manner. One part of the micropuncture aliquot was divided into three or more 4–7 nl samples the exact volumes of which were determined with the sphere method (Hellman *et al* 1961). After incubation with the reagents the extinction was determined in a Beckman DU spectrophotometer adapted for a microcuvet. The absorbances of the same solution have been plotted in Fig 4. The coefficient of variation in this method = 7% or less.

Intratubular P_{CO} and Bicarbonate Determinations The samples collected intratubularly were equilibrated with different P_{CO} whereas the pH was measured by means of antimony micro electrodes. The pH/log P_{CO} line thus represented the buffer curve. With the intratubular pH measured *in situ* the corresponding P_{CO} could be determined using this curve. Using the Henderson Hasselbalch equation the bicarbonate concentration could then be calculated for that particular P_{CO}. Theoretical and practical aspects on these determinations have been described by Karlmark and Sjötiell (1973).

Determination of Titratable Acid (TA) After sampling and the bicarbonate determinations (Karlmark and Sjötiell 1973) 3–5 nl samples were put into a thermostated oil bath pre-equilibrated with 20% oxygen in nitrogen. Due to the loss of carbon dioxide to the oil the pH of the samples always rose above 7.4 units. To make determinations possible according to the previously given definition of TA the HCO₃ ions were eliminated by adding about 0.5 nl 25 mM HCl. In such way the pH of each sample was reduced to below 7 units. Titration of the samples was then performed with hydroxyl ions liberated from the antimony trioxide electrode system as described by Karlmark (1973). Simultaneous pH measurements with another antimony electrode system in the droplet made it possible to record a titration curve on an X-Y recorder. Original titration curves are shown in Fig 5. The attainment of the ammonium curve in this figure is described below.

As the solution is artificially acidified the entire titration curve does not reflect the hydrogen ions produced *in vivo*. The TA is therefore calculated as the amount of hydroxyl ions necessary to titrate the sample from the intratubular pH to the actual blood pH. In this investigation the mean actual blood pH was 7.47 ± 0.06 (SD). Due to the slight differences in TA (less than 5% error) using pH 7.4 as opposed to the actual blood pH a pH of 7.4 was used as the titration end point for convenience. In cases of alkalosis and acidosis however this discrepancy must be taken into account.

The amount of hydroxyl ions liberated by the antimony electrode system was calculated assuming that each electron stored in the capacitor corresponded to one hydroxyl ion.

Ammonium Determination The ammonium content in the tubular urine was determined according to Karlmark (1973). This method utilizes the phenomenon that ammonium ions will react with formaldehyde to form hexamethylenetetramine. The hydrogen ions liberated in this reaction are then titrated with the hydroxyl ions liberated from an antimony trioxide electrode system (see Fig 5). This ultramicro method is designed for samples of a few nanoliters the coefficient of variation is 10% or less. The values given in the present study are the mean values of duplicates.

The ammonia concentration was calculated using the logarithmic form of the law of mass action

$$\text{pH} = \text{pK}_a + \log \frac{\text{NH}_3}{\text{NH}_4}$$

The pK_a used was 9.0 (Bink and Schwartz 1960). P_{NH} was calculated as follows

$$P_{\text{NH}_3} = \frac{\text{NH}_3 (22.09)}{\alpha}$$

α stands for the Bunsen solubility coefficient (liter NH₃/liter H₂O mm Hg) and was given the value 0.626 in accordance with Jacques *et al* (1959). Ammonia concentration in mole per liter gives P_{NH} in mm Hg.

Acid Base Status of the Blood The acid base status of the blood was determined as described by Siggaard Andersen (1967). In spite of the fact that the terminology and nomenclature used are intended for man they can be used for animals too (Siggaard Andersen personal communication). The normal values compared to man are different however.

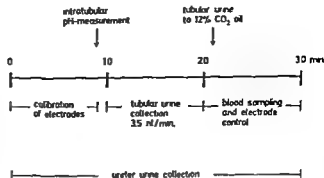


Fig 1 The working schedule during one experimental period

500 μ l were taken from the arterial catheter into heparinized glass capillaries (Radiometer) without suction. About 300 μ l were used for the equilibration with two gases and making actual pH measurements and about 100 μ l were used for the insulin determinations. After the blood sample had been taken and the catheter flushed with saline the surface of the kidney sometimes exhibited a paleness. Even if the kidney surface seemed to be quite normal after such a paleness no further experiments were performed with that animal.

The Experimental Periods: The experiments were performed in periods of 30 min (Fig 6) showing the different procedures during one experimental period.

Occasionally the scheme could not be properly held. In these cases a discrepancy of a few minutes occurred due to trouble with the electrodes. The intratubular pH however was always measured just prior to the sampling.

Results

The pilot study prior to the experiments presented in this paper showed a transient decrease in blood pressure 10–20 mm Hg and a slight fall in GFR after sampling of 0.5 ml blood. This sampling however occurred at the end of the experimental period (Fig 6) so the decrease in GFR was thought to have a minor influence on urine production during this period. The results from the pilot study also created the criterion that no experimental period was started if the blood pressure was below 100 mm Hg. Finally a maximal blood sampling of 1.0 ml was permitted from each animal.

The blood acid base status showed a mean pH value of 7.47 ± 0.06 (S.D.) a base excess of $-0.8 \text{ mEq} \pm 2.4$ (S.D.) and a P_{CO_2} in arterial blood of $33 \text{ mm Hg} \pm 5$ (S.D.). Since no experimental periods were started with a blood pressure below 100 mm Hg the animals investigated were considered fairly normal. The mean GFR was $3.1 \pm 1.2 \text{ ml/min bwt}$ on the kidneys examined. The results are summarized in Table I.

Intratubular pH: Positioning the electrode tips differently in the tubules strongly influenced the potential measured as has also been reported with other types of electrodes (e.g. Fromter and Hegel 1966). When the antimony electrode was manipulated to the periphery of the lumen the potential immediately changed by 20–40 mV. By moving the tip back to the center of the lumen the potential again became stable at the initial value. This deviation is compatible with that from

TABLE I Results from Seventeen Proximal Tubular Samples taken from 11 Rats

Tubule	TF/P Inulin	Intra- tub pH (mea- sured)	HCO mM/l	Intra- tub Pco ₂ mm Hg	Blood Pco ₂ mm Hg	Bise Excess mM/l	Intra- tub pH at blood Pco ₂	Dis- equil pH	NaH ₂ P ₄ mM	P _{NaH} x 10 ⁴ mm Hg	TA mM
1	2.01	6.46	6.9	95			6.99	-0.53	1.9	185	0.9
2	1.58	6.56	9.0	98	29	+8.5	7.12	-0.56	2.0	245	0.9
3	1.58	6.58	6.2	64			6.91	-0.36	1.8	231	0.5
4	1.33	6.89	1.6	8	36	+2.2			3.0	786	0.8
5	1.58	6.83	11.4	67	38	+1	7.22	-0.39	2.4	548	0.6
6	1.00	6.74	9.3	67	38	+1	7.10	-0.36	1.4	260	0.9
7	1.91	6.71	1.7	83	33	+1.5	7.10	-0.39	1.8	312	0.6
8	1.44	6.98	7.2	30	33	-1	6.91	+0.04	2.7	871	0.6
9	1.49	6.81	12.2	75	32	±0	7.54	-0.33	2.4	593	0.7
10	2.89	6.63	5.2	48	40	+0.5	6.86	-0.23	3.3	598	0.9
11	2.18	6.63	4.9	45	28	-0.5	6.94	-0.31	2.6	471	0.6
12	2.23	6.45	5.6	79	37	-0.8	7.07	-0.62	2.2	209	1.0
13	1.37	6.70	8.9	70	38	+1	6.07	-0.17	2.2	379	1.2
14	2.09	6.59	3.5	36	19	+0.2	6.80	-0.21			1.0
15	9.58	6.78	5.8	38	33	-0.8	6.85	-0.07	1.8	360	0.9
16	2.48	6.71	3.4	26	33	-0.5	6.57	-0.14	1.5	260	0.8
17	3.15	6.51	3.1	38	35	-1	6.51	±0	2.0	197	1.8

touching an electrode against the luminal cell membrane. In one previous study saline loading diminished the risk of this artefact perhaps due to a widening of the lumen. In the present study the lowest stable intratubular measurement was taken as the true value.

Fig. 7 shows the intratubular pH measurements as related to the functional length of the tubule (TF/P inulin).

The Intratubular Bicarbonate Concentrations The concentration of bicarbonate along the nephrons is shown in Fig. 8. The values were calculated using the intratubular pH described previously but have been corrected for the $\text{CO}_2\text{--HCO}_3^-$ influence on the antimony electrode system (Karlmark and Sothell 1973).

The constants used in the Henderson Hasselbalch equation were $\text{pH}_a = 6.09$ and $S = 0.031$ (Hastings and Sendroy 1925 and Van Slyke *et al.* 1928). These calculated values fit well with those measured in plasma filtrate (Siesjö 1962 *a* and *b*, Mitchell *et al.* 1965 and Johnell 1971) which is assumed to have approximately the same constants as rat proximal tubular urine.

The Intratubular Pco_2 Fig. 9 shows the corresponding pattern for Pco_2 along the proximal tubule. These values were calculated by means of the equilibration curve and the actual pH as described previously. The results show a wide scatter but most values are higher than the corresponding arterial Pco_2 . As shown in the figure the intratubular Pco_2 tends to decline from high values in the most proximal part of the tubule to values closer to that of the arterial blood in the more distal parts examined.

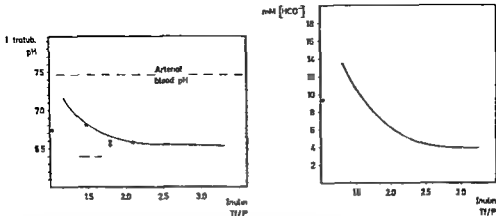


Fig 7 The intratubular pH in seventeen rat proximal tubules and their respective TF/P inulin. The solid line is drawn to the best visual fit. The broken line indicates the mean arterial blood pH.

Fig 8 The intratubular concentration of bicarbonate. The values have been corrected by a factor of 1.43 as described by Larimark and Sotell (1973).

Titrateable Acid Fig 10 shows the TA plotted against the corresponding TF/P inulin as the mean of duplicates.

In the Bowman's capsule the pH becomes equal to the plasma pH. The TA is then equal to zero as the titration end point is already reached (pH 7.4).

The ammonium concentrations are shown in Fig 11 plotted in a relation to the functional length of the proximal tubule.

According to Table I and Fig 11 there is no indication of a change in ammonium concentration along the proximal tubule in spite of the increased intratubular acidity. The mean ammonia pressure was found to be $402 \cdot 10^{-6}$ mm Hg.

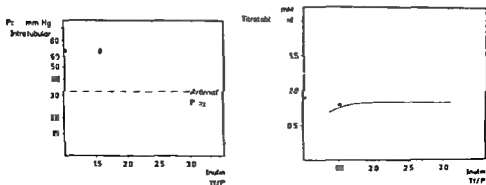


Fig 9 Pco₂ in the proximal urine samples plotted against the functional length of the tubule. The dashed line indicates the mean arterial blood Pco₂. One value (Pco₂ = 8) is excluded.

Fig 10 Titratable acid along the rat proximal tubules. The line is drawn by eye.

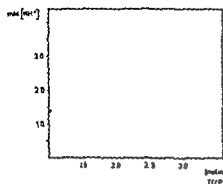


Fig 11 The ammonium concentration in seventeen rat proximal tubules as related to their respective TFP/inulin as an indicator of the functional length of tubule

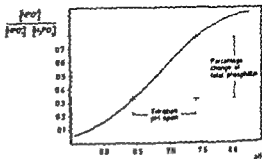


Fig 12 Titration of a phosphate buffered solution from an initial pH of 6.45 to a pH of 7.40. The total phosphate concentration in the solution is determined as described in the text. The concentrations of H_2PO_4^- and PO_4^{3-} are approximated to zero in the pH range studied

Discussion

The normal blood acid base status of the rats in the present investigation was somewhat different from that found at other laboratories (Rector 1965; Malmic *et al* 1972; Levine 1971) but Persson (1969) has shown that undisturbed awakened rats of the strain used in Uppsala and adapted to an arterial catheter exhibit such an acid base status of the blood. The same condition has also been confirmed in Uppsala by Ramner (1972). The rats in the present investigation are therefore considered to be in a good condition in spite of the anesthesia and the surgical trauma.

The results presented in Table I show a difference between the pH measured intratubularly and the pH measured in the tubular samples equilibrated at the arterial PCO_2 , i.e. a disequilibrium pH in accordance with Rector *et al* (1965). Assuming the main route for bicarbonate reabsorption is via a hydrogen ion secretion the reasons for this disequilibrium might be at least twofold: (1) a state of chemical non equilibrium and (2) a state of disequilibrium PCO_2 . The latter of these means that the intratubular PCO_2 differs from that in the arterial blood. The two mechanisms behind a disequilibrium pH cannot be separated with the methods as yet used but one advantage with the equilibration method used in this investigation is the possibility to quantify a hypothetical disequilibrium PCO_2 . Which one of the two reasons for disequilibrium pH dominates can only be judged in an indirect manner for each experimental condition.

Chemical Non Equilibrium This phenomenon is discussed in detail by Rector *et al* (1965) and Vieira and Malmic (1968). The dehydration of carbonic acid is thought to be normally catalyzed by an intraluminal carbonic anhydrase in the proximal tubule. The explanation given is that during carbonic anhydrase inhibition the intraluminal dehydration of carbonic acid is delayed. This delay could

lead to an accumulation of carbonic acid ($pH = 3.57$) and thus an increased acidity and a low pH. The normal uncatalyzed rate of carbonic acid dehydration is 30/s (Maren 1969) which means a half time for this reaction of $\ln 2/30 = 0.023$ s. The dehydration is thus a rapid process even when uncatalyzed. It could be rate limiting under uncatalyzed conditions however if the diffusion of carbonic acid into the tubule cell is instantaneous.

Disequilibrium P_{CO_2} . The results in this investigation indicate that the disappearance of bicarbonate from the proximal tubule (measured as mmol/s) might be more rapid in the early proximal tubule than in the late proximal tubule. Providing most of the bicarbonate ions filtered are reacting with the hydrogen ions secreted the formation of carbon dioxide should be more rapid in the early parts of the tubule. If the diffusion of carbon dioxide from the lumen is restricted in some manner a high P_{CO_2} would be the result. This explanation is difficult to prove however because data on the transmembrane diffusion rate in the kidney tubule of carbon dioxide is lacking.

In the rat kidney tubule Malmic and Mello-Aires (1971) using the split oil droplet technique showed that the half time for the out (and in) diffusion of carbon dioxide across the luminal cell membrane was in the range 0.5–1 s. This time should be compared with the uncatalyzed dehydration of carbonic acid which was as previously mentioned. In conclusion then the uncatalyzed dehydration of carbonic acid in the lumen may be at least 20 times more rapid than the diffusion of carbon dioxide from the lumen. Under such conditions an accumulation of carbon dioxide intratubularly can be expected. The disappearance rate of carbon dioxide $t_{1/2} = 15$ s due to the hydration reaction probably plays no role in this respect.

The preceding discussion thus indicates that the uncatalyzed dehydration reaction of carbonic acid is unlikely to be the limiting step in the bicarbonate reabsorption mediated by a hydrogen ion secretion. The physiological significance of an intraluminal carbonic anhydrase has also been questioned by Maren (1967). Thus the indication is that the disequilibrium pH found in this investigation might be due to a disequilibrium P_{CO_2} . Fig. 9 (see Results) was drawn under this assumption. The disequilibrium seems to be highest in the early proximal tubule (Table I and Fig. 9). The data in this paper thus suggests that under the experimental conditions presented (1) a disequilibrium is present in the early proximal tubule (2) the disequilibrium will be less in the middle part and (3) in the final part there will be an equilibrium pH.

For comparison the data by Rector *et al.* (1965) should be mentioned. The mean disequilibrium was 0.11 pH units for four tubules analyzed under comparable conditions. Vieira *et al.* (1968) found a corresponding disequilibrium pH of 0.14 (not significantly different from zero however). The other results in the papers described deal with animals treated with bicarbonate carbonic anhydrase or carbonic anhydrase inhibitors and therefore can hardly be compared with those presented here.

A further finding of interest in this field is that of Enns (1967). In an *in vitro* system Enns found evidence for function of carbonic anhydrase other than the catalysis of the hydration-dehydration reaction of carbonic acid and proposed that the enzyme had a carrier function for carbon dioxide across a membrane system. If this mechanism acts *in vivo* one physiological function of the carbonic anhydrase in the brush border of the proximal tubule could be to transport carbon dioxide to the cell. If this function is inhibited by carbonic anhydrase the disequilibrium pH found during this inhibition could be the result of an intratubular carbon dioxide accumulation. This paper proposes that such a phenomenon in fact occurs in proximal tubules of untreated rats.

The intratubular pH found in this investigation agrees on a whole with that reported by Vieira and Mulaic (1968) and Rector *et al.* (1965) when measured under similar conditions.

The absence of a falling pH along the proximal tubule found by the former investigators cannot be confirmed in this study, however. Since the initial parts of the tubules are not accessible to puncture in the rat strain used, the steep fall in pH in this part of the nephron proposed in Fig. 7 cannot be caught. The rather constant pH along the largest part of the nephron might indicate a gradient-limited hydrogen secretory process—the amount of hydrogen ions secreted will balance the backward transport—both due to diffusion and due to solvent drag (the fluid reabsorption). Assuming a constant reabsorption per unit area, the hydrogen secretory ability should be the same throughout the proximal tubule. The amount of TA in a tubular segment will then be determined by the amount of buffers in the fluid. The concentrations of these buffers were in the present investigation, however, also constant as judged from the constant pH and constant TA. The latter finding thus indicates a gradient-limited reabsorption of buffering substances as well. Due to this phenomenon, the amount of TA passing down the proximal tubule will successively decrease. The results suggest that an increased acidification ability of the proximal tubule could be created both by an increased hydrogen ion activity (pH) difference and larger concentration differences of buffers.

The main buffering anions in urine are phosphate, creatinine, and uric acid (Gyorv *et al.* 1964). The pK_{a_2} for creatinine is about 4.7 and that for uric acid pK_{a_2} is about 5.8, which means that their buffering properties are very slight at the intratubular pH measured here. The pK_{a_2} for phosphate is about 7.2, but due to the ionic strength in the urine in the proximal tubule it should be corrected to 6.8 (Schwartz *et al.* 1954). During the titrations performed in this investigation, phosphate was approximated to be the only buffer titrated.

Fig. 12 shows a titration of a phosphate solution providing a pK_{a_2} of 6.8. The pH at the start of the titration was 6.45 (corresponding to sample 12 in Table I).

As shown in the figure, 45% (0.77–0.32) of the total phosphate content was titrated. The TA concentration in sample No. 12 was 1.0 mM. Thus the approxi-

* The gradient limitation means that a transport system has the ability to build up a limited concentration difference across the membrane.

mate phosphate concentration in this sample could be calculated to be 2.2 mM the mean phosphate concentration in this study 2.7 ± 0.8 (SD) Strickler *et al* (1964) and Frick (1968) using a spectrophotometric phosphate method found proximal concentrations of inorganic phosphate similar to those suggested in this paper. The constant proximal concentrations furthermore constant proximal concentrations furthermore support the conclusions of Amiel *et al* (1970) who found evidence for a reabsorption of phosphate in the proximal tubule. They concluded that this transport was concentration gradient limited which is well in accordance with the findings in the present investigation.

In conclusion then the constant TA concentration along the proximal tubule seems to be the result of concentration gradient limitations for a transport of phosphate as well as for a transport of the hydrogen ion.

The mean concentration of ammonium found in this investigation was 2.2 ± 0.5 (SD) mM. The values are somewhat higher than those found in the rat by Glabman *et al* (1963) and Hayes *et al* (1964). These investigators using the microdiffusion technique found approximately 1 mM ammonium in the end proximal tubule, while Oelert *et al* (1967) with a similar technique found about 0.5 mM. This difference could hardly be explained by the presence of amino groups. From a chemical point of view amino acids are known to interfere with ammonium determinations using the present formaldehyde method (Sorensen 1908) in such a manner that amino groups will react with the formaldehyde releasing hydrogen ions from the carboxyl groups. The presence of amino acids thus will give falsely high ammonium concentrations. As recently shown by Bergeron and Morel (1969) however the maximal capacity for reabsorption of amino acids by the proximal tubule far exceeds the normal filtered load. This means low normal intratubular concentrations of amino acids already in the middle and distal parts of the tubule. These conclusions agree well with those of Ruzskowski *et al* (1962).

Since ammonia is a volatile base and highly lipid soluble its quantitative analysis is technically difficult—especially in nanoliter samples. Ammonium and ammonia in a solution occurs in a proportion which is determined by the actual pH. If ammonia is diffused into the surroundings a new pH will follow thus a new chemical equilibrium. The amount of ammonium lost in this manner will increase with increasing capacity of the solution to buffer hydrogen ions. To avoid the loss of ammonia the pH of the sample should be held both as low and as long as possible in the methods used by other investigators and until the addition of formaldehyde in the present method. The highest pH measured in the samples in this investigation prior to the formaldehyde adding was 8.6 (tubule No. 4) in the 17 samples the mean was 8.0 ± 0.3 (SD). The latter means that about 10% of the total ammonia is in its basic form the loss of ammonia has therefore not been corrected for.

The P_{NH_3} in this study coincides with the apparent P_{NH_3} measured by Hayes *et al* (1966) during acetazolamide infusion. Assuming an equilibrium pH in the proximal tubule of the untreated rat however they corrected this apparent P_{NH_3} .

to an actual P_{NH_3} . The basis for this calculation is dubious however since the intratubular pH measured with a quinhydrone method, was corrected after data by Rector *et al* (1965) who in that study used another type of carbonic anhydrase inhibitor. The cortical actual P_{NH_3} would then be about 15 % of the "apparent" value. As pointed out earlier the existence of a proximal equilibrium pH in the untreated rat is questioned.

The P_{NH_3} found by Oelert *et al* (1967) in the rat cortex was about 20 % of the value found in this investigation. The reasons for this discrepancy are unclear but seems to emanate from differences in experimental design and from the use of quite different analytical methods.

In the present study the concentrations of ammonium found along the proximal tubule have no clear tendency to increase with increasing TF/P Inulin and decreasing intratubular pH. This indicates an ammonia/ammonium reabsorption along the proximal tubule parallel to the water reabsorption. This reabsorption could then occur either as ammonium or ammonia. The latter process is dependent upon a high permeability in the tubular wall and a rapid decomposition from ammonium so that chemical ammonia/ammonium equilibrium exists at all instances. A direct reabsorption of ammonium ions can however not be excluded even though the permeability for this ion probably is low (Jacobs 1940). Such a mechanism is compatible with findings in the toad bladder where Guggenheim *et al* (1971) have proposed a membrane transport competition between ammonium and potassium.

For the technical assistance during this work we are greatly indebted to Mrs Birgitta Gronvall and Miss Kerstin Planhammar.

This work was supported by grants from The Swedish Medical Research Council, The Medical Faculty of the University of Uppsala, The Swedish Society for Medical Research and Forenade Liv Life Insurance Company.

References

- AMIEL, G. H. HANSEN and C. RICHTER. Micropuncture study of handling of phosphate by proximal and distal nephron in normal and parathyroidectomized rat. Evidence for distal reabsorption. *Pflug. Arch. Physiol.* 1970 317 93-109.
- BALACRA, BARUCH S. Renal metabolism and transfer of ammonia. *The Kidney Academic Press* 1961 111 33-3.
- BANK, N. and W. B. SCHWARTZ. Influence of certain urinary solutes on acidic dissociation constant. *Am. J. Physiol.* 1960 198 125-127.
- BERGERON, M. and F. M. REID. NH_4^+ acid transport in rat renal tubules. *Am. J. Physiol.* 1963 165 33-34.
- CHRISTENSEN, P. and C. FREDRIKSEN. The effect of some L-lysine derivatives on gallbladder fluid absorption and bile electrolyte transport in vitro. *Pflug. Arch. ges. Physiol.* 1972 331 160-171.
- CLAPP, J. R., J. F. WATSON and R. W. BERLINER. Osmolality, bicarbonate concentration and water reabsorption in peritubular fluid of dog nephron. *Am. J. Physiol.* 1963 205 212-213.
- DENIS, G. H. PHELPS and R. F. PITTS. The function of tubular cells. *J. clin. Invest.* 1964 43 571-587.
- DOKKE, A. and W. NAEFEL. Die Wirkung von L-Asparagin auf den Natriumtransport an der isolierten Bauchhaut von *Rana temporaria*. *Pflug. Arch. Physiol.* 1969 313 11-18.

- ENNS T Facilitation by carbonic anhydrase of carbon dioxide transport *Science* 1967 155 44-47
- FRICK A Reabsorption of inorganic phosphate in the rat kidney *Pflugers Arch ges Physiol* 1968 304 351-364
- FROMTER, E and U HEGEL Transtubuläre Potentialdifferenzen an proximalen und distalen Tubuli der Rattenniere *Nahrung-Schmiedeberg's Arch exp Path Pharmacol* 1966 204 107-120
- GLABMAN S R M KLOSE and G GIEBISCH Micropuncture study of ammonia excretion in the rat *Amer J Physiol* 1963 205 (1) 177-182
- GLOGENHEIM H J J BOLLENGIER and S KLAHR Inhibition by ammonium of sodium transport across toad bladder *Amer J Physiol* 1971 220 1651-1659
- GYORY A E A NEGRIN and K D G EDWARDS Urinary excretion of titratable acid and its relationship to urinary pH and inorganic phosphorus excretion *Austr Ann Med* 1968 17 3 236-241
- HASTINGS A B and J SENDROY The effect of variation in ionic strength on the apparent first and second dissociation constants of carbonic acid *Biol Chem* 1925 65 445-450
- HAYES C P J S MALSON E E OWEN and R R ROBINSON A micropuncture evaluation of renal ammonia excretion in the rat *Amer J Physiol* 1964 207 77-83
- HAYES C P E E OWEN and R R ROBINSON Renal ammonia excretion during acetazolamide on sodium bicarbonate administration *Amer J Physiol* 1966 210 744-750
- HELLER J The influence of Lysamine Green on tubular reabsorption of electrolytes and water in rats *Pflugers Arch ges Physiol* 1971 373 27-33
- HELLMANN B H R ULFENDUHL and B G WALLIN Microphotometry utilizing a shrinking droplet technique *Anal Biochem* 1967 18 439-443
- HILGER H H J D KALLMAYER and K J ULLRICH Wasserresorption und Ionentransport durch die Sammelrohrzellen der Säugetieriere *Pflugers Arch ges Physiol* 1958 267 218-237
- JACOBS M H Some aspects of cell permeability to weak electrolytes *Cold Spr Harb Symp quant Biol* 1940 8 30-39
- JACQUEZ J A J W POPELL and R JELTYCH Solubility of ammonia in human plasma *J appl Physiol* 1959 14 255-258
- JOHNELL H E The first dissociation constant for carbonic acid and the solubility of carbon dioxide in human amniotic fluid *Scand J clin Lab Invest* 1971 27 233-238
- KARLMARK B The determination of titratable acid and ammonium ions in picomole amounts *Analyt Biochem* 1973 57 69-82
- KARLMARK B and M SCHTELL The determination of bicarbonate in nanoliter samples *Analyt Biochem* 1973 53 1-11
- KUHAL R T The influence of the carbonic anhydrase inhibitor Benzolamide (CL 11 366) on the reabsorption of chloride sodium and bicarbonate in the proximal tubule of the rat *J clin Invest* 1972 51 294-306
- LEVINE D Z Effect of acute hypercapnia on proximal tubular water and bicarbonate reabsorption *Amer J Physiol* 1971 221 1164-1170
- LOFVERHOLM G Histochemical demonstration of carbonic anhydrase activity in the rat kidney *Acta Physiol scand* 1971 81 433-439
- MALNIC G and M DE MELLO-AIRES Kinetic study of bicarbonate reabsorption in proximal tubule of the rat *Amer J Physiol* 1971 220 1759-1767
- MALNIC G M DE MELLO-AIRES and G GIEBISCH Micropuncture study of renal tubular hydrogen ion transport in the rat *Amer J Physiol* 1971 221 147-158
- MARON T H Carbonic anhydrase Chemistry physiology and inhibition *Physiol Rev* 1967 47 595-781
- MARON T H Renal carbonic anhydrase and the pharmacology of sulfonamide inhibitors *Handb exp Pharm* 1969 24 193-256
- MITCHELL R A D A HERBERT and C T CARMAN Acid base constants and temperature coefficients for cerebrospinal fluid *J appl Physiol* 1963 20 27-30
- NASH T P and S R BENEDECT The ammonia content of the blood and its bearing on the mechanism of acid neutralization in the animal organism *J Biol Chem* 1921 48 443-488
- OELETT H E ULLRICH and A G MILLS Messungen des Ammoniakdrucks in den corticalen Tubuli der Rattenniere *Pflugers Arch ges Physiol* 1963 300 35-48
- PERASON A E G Chloride and water transport in rat cortical nephrons *Acta u n Lepidolensis* 1969 10
- PIPERCK J A and H MONTGOMERY The microquinhydrone electrode Its application to the determination of the pH of the glomerular urine of the nocturnal *J Biol Chem* 1935 110 763-772

- PITTS R F The role of ammonia production and excretion in regulation of acid base balance *New Engl J Med* 1971 3rd 32—38
- RAMMER L Intravascular coagulation fibrinolysis inhibition and post traumatic renal failure A study in burned rats Acta Univ Upsaliensis 1977
- RECTOR F C Renal secretion of hydrogen The Kidney Academic Press Vol III 1971 200—252
- RECTOR F C A W CARTER and D W SELDIN with the technical assistance of A C NOLL The mechanism of bicarbonate reabsorption in the proximal and distal tubules of the kidney *J clin Invest* 1965 44 278—290
- RECTOR F C D W SELDIN A D ROBERTS and J S SMITH The role of plasma CO_2 tension and carbonic anhydrase activity in the renal reabsorption of bicarbonate *J clin Invest* 1960 39 1709—1721
- ROUGHTON F J W Some recent work on the chemistry of carbon dioxide transport by the blood *Harey Lect* 1944 39 96—142
- RSZAKOWSKI M C ARASIMOWICZ J KAPROWSKI J SYEFFFEN and K WEISS Renal reabsorption of amino acids *Amer J Physiol* 1967 203 891—896
- SCHILB T P and W A BRODSKY CO_2 gradients and acidification by transport of HCO_3^- in turtle bladder *Amer J Physiol* 1977 227 272—281
- SCHWARTZ W H N BANA and R W P CUTLER The influence of urinary ionic strength on phosphate pH_a and the determination on titratable acid *J clin Invest* 1959 38 347—356
- SIESJO B K The solubility of carbon dioxide in cerebral cortical tissue of cats With a note on the solubility of carbon dioxide in water 0.16 M NaCl and cerebrospinal fluid *Acta physiol scand* 1962 a 33 323—341
- SIESJO B K The bicarbonate/carbonic acid buffer system of the cerebral cortex of cats as studied in tissue homogenates II The pH_a of carbonic acid at 37.5 °C and the relation between carbon dioxide tension and pH *Acta neurol scand* 1962 b 38 121—141
- SJOGAARD ANDERSEN O In Current Concepts of Acid Base Measurement *Ann N Y Acad Sci* 1966 133 41—58
- SJOGAARD ANDERSEN O *The Acid Base Status of the Blood* Munksgaard Copenhagen 1961 3rd Ed
- VAN SLUYKE D D J SENDROV A B HASTING and J M NEILL Studies of gas and electrolyte equilibria in blood The solubility of carbon dioxide at 38 °C in water salt solution, serum and blood cells *J Biol Chem* 1928 18 163—199
- SOLOVON M and H ALPERT A method for determining titratable acidity in nanoliter samples of biological fluids *Analys Biochem* 1969 37 291—296
- STONE W S S BALAGURA and R F PITTS with the technical assistance of L M SHIRLAND Diffusion equilibrium for ammonia in the kidney of the acidotic dog *J clin Invest* 1967 46 1603—1608
- STRICKLER J C D D THOMPSON R M KLOSE and G GIEBISCH with the technical assistance of J V GLICK and J B VALCHAY Micropuncture study of inorganic phosphate excretion in the rat *J clin Invest* 1964 43 1596—1601
- SORENSEN S P I Enzym studies *Biochem Z* 1908 7 43—101
- WALFRUM M and G H MOORE Renal excretory mechanisms Mineral Metabolism Academic Press New York and London Vol 1 1968 282—326
- WEIERA F I and G MALNIC Hydrogen ion excretion by rat renal cortical tubules as studied by an antimony microelectrode *Amer J Physiol* 1968 214 710—718

Cardiorespiratory Responses to Graded Exercise at Increased Ambient Air Pressure

By

LENNART FAGRAEUS, CARL MAGNUS HESSER and DAG LINNARSSON

Received 27 December 1973

Abstract

FAGRAEUS L, C M HESSER and D LINNARSSON. *Cardiorespiratory responses to graded exercise at increased ambient air pressure*. Acta physiol scand 1974 91 259-274.

The separate and combined effects of increased inspired oxygen and nitrogen pressures on cardiorespiratory and metabolic responses to graded exercise (50, 100 and 150 W) were assessed by comparing data from identical work experiments performed under three different ambient conditions *etc.* with the subjects breathing (A) air at 1.0 ATA, (B) oxygen at 1.0 ATA, and (C) air at 4.5 ATA (same inspired P_{O_2} as in B). In general the physiological responses to the various work loads were qualitatively similar in the three conditions, but for a given load quantitative differences were observed. By comparing Condition C with A it was found that a rise in both the O_2 and N_2 pressures resulted in the following changes at the highest work load: significant increments in \dot{V}_{O_2} , \dot{V}_{CO_2} , end-tidal and mixed expired P_{CO_2} and oxygen pulse (\dot{V}_{O_2} per heart beat); significant reductions in heart rate, \dot{V}_D , \dot{V}_D/\dot{V}_T and ventilatory equivalents for oxygen (\dot{V}_E/\dot{V}_{O_2}) and carbon dioxide (\dot{V}_E/\dot{V}_{CO_2}); and no consistent changes in \dot{V}_E and respiratory exchange ratio. When related to \dot{V}_{O_2} *etc.* in the metabolic rather than the ergometric load, \dot{V}_E was lower in C than in A. By comparing Condition B with A and C with B, evidence was obtained that the above changes in \dot{V}_E , P_{CO_2} , ventilatory equivalents, oxygen pulse and heart rate were caused in part by the rise in O_2 pressure and in part by factors related to the rise in N_2 pressure, whereas the changes in \dot{V}_D and \dot{V}_D/\dot{V}_T were due mainly to the raised O_2 pressure and the changes in \dot{V}_{O_2} and \dot{V}_{CO_2} to the raised N_2 pressure.

It is generally recognized that physiological responses to muscular exercise at increased ambient air pressures are influenced by the action of a number of factors such as the increased oxygen and nitrogen pressures, the increased gas density, and the pressure itself (Lanphier 1964; Bennett and Elliott 1969; Shilling and Werts 1973). However, little information exists concerning the relative contributions of these factors to the ventilatory, circulatory and metabolic changes that occur in man performing light, moderate or heavy exercise in hyperbaric environments.

Accordingly, an attempt has been made to evaluate the separate and combined effects of high inspired oxygen and nitrogen pressures on cardiorespiratory and metabolic responses to graded submaximal exercise in normal human subjects. This was done by comparing data obtained in identical exercise experiments performed under three different ambient conditions *etc.* with the subjects breathing air at am-

TABLE I Physical characteristics and work capacity of 7 subjects

Subject	Age yrs	Height cm	Weight kg	\dot{V}_{O_2} max l/min STPD
SL	31	180	70	54
JB	36	174	73	32
NP	23	178	73	30
IL	23	182	75	40
IJ	32	187	80	40
BW	31	183	80	38
YG	23	181	77	36

\dot{V}_{O_2} max = aerobic work capacity predicted according to Åstrand (1960)

bient pressures of 1.0 and 4.5 atmospheres absolute (ATA) and oxygen at 1.0 ATA. Part of this study has been reported briefly (Hesser, Fagraeus and Linnarsson 1968).

Methods

Seven healthy experienced R. Sw. Navy divers served as subjects (Table I). All studies were carried out within a dry compression chamber the temperature of which was adjusted to approximately 23°C. Each subject performed graded exercise under three different ambient conditions: (1) while breathing (A) air at 1.0 ATA, (B) oxygen at 1.0 ATA and (C) air at 4.5 ATA. Ambient temperature, density of inspired gas mixtures and partial pressures of inspired gases in the three conditions are shown in Table II. The two trials at normal pressure were performed on the same day with an intervening rest period of 1–2 h (4 subjects started with the O₂ expts and 3 subjects with the air expts) while the 4.5 ATA trials were performed on a separate day. Every other subject had the 4.5 ATA trials first.

The subjects were seated on a directly calibrated cycle ergometer (Monark, Sweden) and inhaled air or oxygen from a 200-liter Douglas bag via a mouthpiece, a low dead space (10 ml) respiratory valve (cf. Dobeln 1949), a Venturi type low resistance flowmeter (Wigertz 1969) and smooth bore tubings (inside diameter 3.8 cm). The Douglas bag was partially filled with water to secure saturation of the respiratory gases with water vapor. The resistive pressures offered by the inspiratory circuit at flow rates of 1.0 and 2.0 l/s amounted to 1.2 and 2.9 cm H₂O at 1.0 ATA and to 2.9 and 8.5 cm H₂O at 4.5 ATA respectively. At corresponding flow rates the resistive pressures of the expiratory circuit (mouthpiece, respiratory valve, wide bore tubings, a 3-way stopcock and a 200-liter Douglas bag) were 0.9 and 2.5 cm H₂O at 1.0 ATA and 2.0 and 7.5 cm H₂O at 4.5 ATA respectively.

Tidal volume (\dot{V}_T), respiratory frequency (f) and inspired minute volume (\dot{V}_I) were continuously recorded on a breath-by-breath basis (Åstrand and Wigertz 1966) using the Venturi type flowmeter in combination with online digital computation techniques (cf. Broman and Wigertz 1971). The flowmeter was calibrated in each experiment with rotameters precalibrated for air or oxygen at 1.0 ATA. In the 4.5 ATA experiments the flowmeter was connected with rotameters outside the chamber through an outlet in the chamber wall, calibration being accomplished by use of appropriate conversion factors. Heart rate (HR) was recorded beat by beat from chest electrodes and a linear cardiotachometer (Lindborg, Wigertz and Odman 1969) and ECG was monitored continuously outside the pressure chamber. To obtain the stable state values for \dot{V}_I and HR the time averages of these variables over the final two minutes of rest and over the 5th minute of work at each work level were computed online by an integrating voltmeter. During these periods expired gas was collected into plastic Douglas bags from which duplicate samples were drawn into mercury receivers for subsequent analysis by the micro Scholander technique (Scholander 1947). Rectal temperature was measured in 3 subjects using a thermistor probe (Yellow Springs Instruments Inc. No. 401).

For the continuous recording of end-tidal O₂ and CO tensions a special breath-by-breath sampler (Brisman, Hesser and Matell 1962) was used in connection with a paramagnetic O₂ analyzer (Model F 3, Beckman Instruments Inc., Calif.) and an infrared CO analyzer (Model

TABLE II Ambient pressure and temperature density of inspired gas mixture and partial pressures of inspired gases in 3 experimental conditions

Condition	Inspired gas mixture	Ambient pressure		Ambient temp C	Density of inspired gas mixture g/l BTPS	Partial pressures of inspired gases mm Hg		
		ATA	mm Hg			CO ₂	O	N
A	Air	1.0	755	24.0	1.10	0.2	148	560
B	Oxygen	1.0	755	23.4	1.22	—	708	—
C	Air	4.5	3445	23.3	5.12	1.0	711	2686

Values are means $n = 7$

LB-1 Beckman Instruments) located outside the chamber. Before and after each experiment the O₂ and CO₂ analyzers were calibrated with known mixtures of CO₂ and air or CO₂ and oxygen saturated with water vapor.

Inpiratory gas flow (\dot{V}_T), \dot{V}_I and tidal volume (V_T) and F_{O_2} and F_{CO_2} and HR were recorded continuously and simultaneously on an 8 channel ink recorder (Brush Mark 200). From the collected data and by using standard equations the following variables were computed: oxygen uptake (\dot{V}_{O_2}), carbon dioxide elimination (\dot{V}_{CO_2}), respiratory exchange ratio (R), mixed expired (P_{ECO_2}) and end tidal CO₂ tensions, ventilation equivalents for oxygen (\dot{V}_I/\dot{V}_{O_2}) and carbon dioxide (\dot{V}_I/\dot{V}_{CO_2}) and oxygen pulse ($\dot{V}_{O_2}/\text{heart rate}$).

Procedure. All experiments were run in the morning after a light meal. The general plan for the 4.5 ATA expts was as follows. After entering the chamber together with an observer, the subject sat on the cycle ergometer and the pressure in the chamber was raised to 4.5 ATA at a rate of 1–2 ATA/min. Following a 5 min period which was allowed for the subject to become adjusted to the conditions and for chamber temperature to attain equilibrium, the subject put on a nose clip and started to breathe from the Douglas bag. After an additional 12 min rest period the subject started to exercise for 6 min at each of three consecutive work loads of 50, 100 and 150 W (approx. 300, 600 and 900 kpm/min) and at a pedalling rate of 50 rpm. During the final 2 min of the rest period and the last minute of each work period, expired gas was collected into Douglas bags and the stable-state values for \dot{V}_I and HR were determined (see above). Decompression to atmospheric pressure was accomplished on air according to standard naval decompression tables.

Except for the compression and decompression, the same general procedure was used in the two trials performed at normal atmospheric pressure.

Analysis of data. In order to disclose the combined and separate effects of high inspired O₂ and N₂ pressures the data obtained in the 3 experimental conditions have been compared in the following ways. **Comparison I.** The combined effects of increased inspired O₂ and N₂ pressures, gas density and pressure per se were determined by comparing data from the expts at 4.5 ATA with those from the expts at 1.0 ATA. **Comparison II.** The separate effects of using the inspired O₂ pressure to the same level as in the expts at 4.5 ATA were estimated by comparing data obtained on oxygen and on air at 1.0 ATA. **Comparison III.** The effects of increasing the inspired N₂ pressure, gas density and pressure per se to the same level as at 4.5 ATA breathing air were evaluated by comparing data from the experiments on air at 4.5 ATA with those on oxygen at 1.0 ATA.

Conventional statistical methods have been applied and the Student's *t* test for paired samples was used to determine the significance of differences in Comparisons I, II and III.

Error in \dot{V}_{O_2} determined. When used shortly after a rapid rise in ambient air pressure the Douglas bag method will yield \dot{V}_{O_2} values which are too low due to increased nitrogen uptake from the lungs. That this error in \dot{V}_{O_2} was of insignificant magnitude in the present study can be shown as follows. From published data on the dynamics of N₂ washout during oxygen breathing (Lundin 1933, 1960) it can be calculated that the rate of N₂ uptake in our 4.5 ATA expts amounted to about 40 ml/min STPD when the first collection of expired gas was started 15 min after the change in ambient pressure (cf. Hessler 1965). With a breathing threshold \dot{V}_{O_2} uptake will cause an underestimation in \dot{V}_{O_2} of only about 8 ml/min STPD.

Results

Table III presents mean values and standard deviations for measured and computed variables in the 7 subjects at rest and during the stable state of exercise at loads of

TABLE III Ventilation, gas exchange and heart rate at rest and during the stable state of exercise at ergometric loads of 50, 100 and 150 W in three different ambient conditions

Variable	n = 7	Rest				Exercise	
		10 ATA		4.5 ATA		1.0 ATA	
		air		air		air	
Pulmonary ventilation (\dot{V}_E) l/min BTPS	M SD	12.0 2.3	10.9 1.0	12.5 1.5	21.7 1.3		
Tidal volume (V_T) l BTPS	M SD	1.58 0.93	1.40 0.81	1.63 0.76	2.27 1.27		
Respiratory rate (f) breaths/min	M SD	9.2 3.5	8.9 3.1	8.7 3.1	11.9 5.0		
O ₂ uptake (\dot{V}_{O_2}) l/min STPD	M SD	3.9 1.0	3.9 0.5	4.5 0.5	9.8 1.0		
CO elimination (\dot{V}_{CO_2}) l/min STPD	M SD	3.5 0.7	3.2 0.5	3.7 0.3	8.0 0.7		
Resp. exchange ratio (R)	M SD	9.0 1.3	8.4 1.2	8.2 1.1	8.1 1.1		
Mixed expired P_{CO_2} mm Hg	M SD	25.2 2.9	25.0 2.7	27.1* 3.4	32.0 2.6		
End-tidal P_{CO_2} mm Hg	M SD	33.3 2.6	32.8 2.0	34.0 3.0	40.4 1.9		
Heart rate beats/min	M SD	62.5 2.4	61.6 8.7	56.9 5.4	88.1 10.1		
Ventil. equivalent for O ₂ (\dot{V}_E/\dot{V}_{O_2})	M SD	31.8 7.5	29.4 6.1	28.2 2.8	22.3 2.7		
Ventil. equivalent for CO ₂ (\dot{V}_E/\dot{V}_{CO_2})	M SD	35.0 4.2	34.9 3.7	34.1 4.3	27.4 2.5		
O ₂ gen. pulse (\dot{V}_{O_2} heart rate) ml O ₂ /heart beat	M SD	6.3 1.9	6.5 2.1	8.0* 1.3	11.3 2.1		

50, 100 and 150 W while breathing air at 1.0 ATA, oxygen at 1.0 ATA and air at 4.5 ATA. Results of the statistical analyses are also given in Table III.

Oxygen uptake increased linearly with the ergometric load both at 1.0 ATA and at 4.5 ATA (Fig. 1). At the highest load \dot{V}_{O_2} was 12% greater ($p < 0.01$) in the high pressure environment. Since it has been shown (Asmussen and Nielsen 1955) that substitution of oxygen for air at normal ambient pressure does not cause any significant changes in \dot{V}_{O_2} at rest or during submaximal exercise, it was assumed that the stable state \dot{V}_{O_2} values in the present O₂ experiments equalled those observed in the air experiments at 1.0 ATA.

Carbon dioxide elimination also increased linearly with the ergometric load in all 3 conditions. While for a given load there was no significant difference in \dot{V}_{CO_2} between the 2 conditions with normal ambient pressure, \dot{V}_{CO_2} was somewhat greater at all work loads in the high pressure condition. However, this increase in \dot{V}_{CO_2}

100 W				150 W			
1.0 ATA O	4.5 ATA air	1.0 ATA air	1.0 ATA O	4.5 ATA air	1.0 ATA air	1.0 ATA O ₂	4.5 ATA air
20.6	22.4	32.3	30.9	30.2	44.7	40.5*	41.4
2.0	2.0	2.4	3.0	3.2	3.6	3.9	2.2
1.99	2.09	2.44	2.92	2.73	2.70	2.53	2.71
83	51	73	62	67	69	68	44
11.8	11.3	14.2	14.8	11.7	17.5	16.8	15.6
4.3	3.7	3.9	3.8	3.2	4.5	4.7	2.5
98 ⁺⁺	1.06	1.51	1.51 +	1.60 +	1.99	1.99 ⁺⁺	2.23 +
	05	07		07	11		09
73	8 ⁺⁺	1.29	1.26	1.31	1.76	1.73	1.94
04	03	08	06	11	10	10	11
77	77	83	83	82	89	88	87
11	05	04	06	07	05	03	06
31.4	33.3	34.7	35.3	39.1	34.3	37.5*	40.0 ⁺⁺
1.8	3.1	1.8	2.4	3.6	1.4	2.1	3.3
39.6	41.7 ⁺	44.0	44.7	48.3 +	45.4	47.8*	54.9 ⁺⁺
1.9	3.2	1.6	3.1	3.6	1.5	2.1	4.0
82.1	76.5 +	108.4	104.7	96.0 ⁺⁺	129.5	122.2*	122.5*
10.4	7.4	9.1	11.7	8.3	11.8	14.0	12.2
21.3	21.1	21.5	20.6	18.9	22.5	20.3*	18.6 +
4.1	2.4	2.0	2.6	1.9	1.8	1.7	1.4
27.6	27.3	25.1	24.6	23.1*	25.4	23.1*	21.4 +
1.6	2.6	1.4	1.7	2.1	1.1	1.3	1.6
12.1	14.0 ⁺⁺	14.0	14.6	16.8*	15.5	16.5	18.3
2.2	1.7	1.7	2.0	2.2	1.8	2.4	1.6

Values are means and standard deviations. * Difference between 4.5 ATA air and 1.0 ATA air (Comparison I) or between 1.0 ATA O₂ and 1.0 ATA air (Comparison II) is statistically significant $p < 0.05$. + Difference between 4.5 ATA air and 1.0 ATA O₂ (Comparison III) is statistically significant $p < 0.05$. ++ Assumed value (see text).

was proportional to the increase in \dot{V}_O as indicated by the fact that the respiratory exchange ratio did not change significantly when the pressure was raised to 4.5 ATA (Table III).

Pulmonary ventilation at a given ergometric load became somewhat reduced when the inspired O₂ pressure was raised to about 710 mm Hg by substituting oxygen for air at normal ambient pressure. At the highest load ($\dot{V}_{O_2} \sim 2.0$ l/min STPD) \dot{V}_I thus decreased by about 9%, i.e. from a mean value of 44.7 l/min BTPS at 1.0 ATA air to 40.5 l/min at 1.0 ATA O₂ ($p < 0.01$). When in addition the inspired N₂ pressure was raised to 3.5 ATA by increasing the ambient air pressure to 4.5 ATA

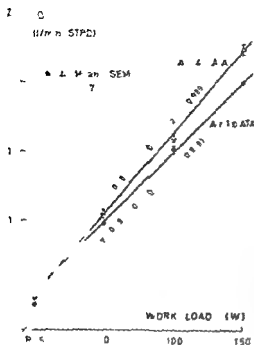


Fig. 1. Oxygen uptake (y) in relation to ergometric work load (x) in subjects breathing air at 1.0 ATA and at 4.5 ATA. Heavy lines are least-squares regression lines, each line being based on 21 individual observations. Mean values \pm one standard error of the means ($n = 7$) are also shown in the figure.

no significant further change occurred in V_I (Table III). However, since the metabolic expenditure (V_{O_2}) at a given ergometric load was greater in the high pressure environment, V_I was less for a given V_{O_2} at 4.5 ATA than at 1.0 ATA breathing O_2 .

Fig. 2. From data obtained at loads of 100 and 150 W it was calculated that this lowering of V_I averaged 3.3 l/min BTPS at a V_{O_2} of 2.0 l/min STPD. As shown in Fig. 3 V_I for a given V_{CO_2} also decreased with a rise in the O_2 and in the N_2 pressure respectively. That the pulmonary ventilation was reduced by high inspired O_2 and N_2 pressures is also reflected by the fact that the ventilatory equivalents for oxygen (V_I/V_{O_2}) and for CO_2 (V_I/V_{CO_2}) were reduced at 100 and 150 W when oxygen was substituted for air at 1.0 ATA and further reduced when the ambient pressure was raised to 4.5 ATA (Table III).

Tidal volume and respiratory rate increased approximately linearly with the ergometric work load in the two conditions with normal ambient pressure. In the high pressure condition V_T first increased with the work load to attain an average value of 2.73 l BTPS at 100 W, but then remained essentially unchanged with a further increase in work load to 150 W. In this latter situation the increase in V_I thus was caused solely by an increase in breathing frequency. In comparison to the values observed at 1.0 ATA O_2 , V_T for a given work load was larger and f was lower at 4.5 ATA air (Table III), although only the difference in V_T at 100 W was statistically significant ($p < 0.05$).

End tidal P_{CO_2} (Fig. 4) and mixed expired P_{CO_2} increased with the work load in all three conditions (Table III). However, because of the concomitant reductions of

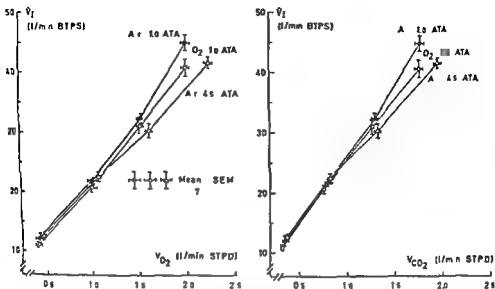


Fig 2 Relationship between minute ventilation and oxygen uptake at rest and during exercise (50, 100 and 150 W) in subjects breathing air at 1.0 ATA (filled circles), oxygen at 1.0 ATA (open circles) and air at 4.5 ATA (open triangles). Each point is the mean value for seven subjects. Vertical and horizontal bars indicate \pm one standard error of the mean.

Fig 3 Relationship between minute ventilation and carbon dioxide elimination under the same conditions as in Fig 2. Symbols as in Fig 2.

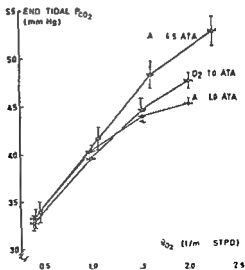


Fig 4 End tidal CO_2 tension in relation to oxygen uptake under the same conditions as in Fig 2. Symbols as in Fig 2.

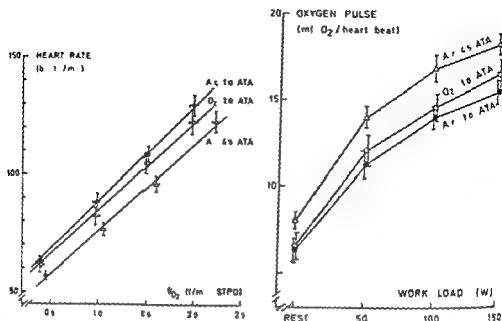


Fig 3 Heart rate (y) in relation to oxygen uptake (x) under the same conditions as in Fig 2. Heavy lines are least squares regression lines each line being based on 28 individual observations. Symbols as in Fig 2. Regression equations: Air 1.0 ATA $y = 48.2 + 40.2x$ ($n = 28$, $r = 0.973$); O₂ 1.0 ATA $y = 47.6 + 37.0x$ ($n = 28$, $r = 0.884$); Air 4.5 ATA $y = 39.2 + 36.5x$ ($n = 28$, $r = 0.945$).

Fig 4 Oxygen pulse (V_o /heart rate) in relation to ergometric work load under the same conditions as in Fig 2. Symbols as in Fig 2.

ventilation P_{CO_2} rose to higher levels at 100 and 150 W when oxygen was substituted for air at 1.0 ATA and to even more elevated levels when the ambient pressure was raised to 4.5 ATA. At the highest load the mixed expired P_{CO_2} thus averaged 34.3 mm Hg at 1.0 ATA air, 37.5 mm Hg at 1.0 ATA O₂, and 42.0 mm Hg at 4.5 ATA air. Corresponding values for end tidal P_{CO_2} were 45.4, 47.8 and 52.9 mm Hg respectively. The differences between these mean values were all statistically significant ($p < 0.01$).

Heart rate increased approximately linearly with the work load in all 3 conditions. However, as compared to the values at 1.0 ATA air, HR for a given ergometric load was lower at 1.0 ATA O₂ and still lower at 4.5 ATA air (Table III). This lowering of the heart rate was even more marked when HR was related to a given V_o (Fig 3), when related to the metabolic rather than to the external ergometric load. From the data obtained at 100 and 150 W it was calculated that the decrement in HR at an O₂ uptake of 2.0 l/min averaged 7 beats/min ($p < 0.05$) when the O₂ pressure was raised by substituting oxygen for air at normal ambient pressure and about 17 beats/min when also the N₂ pressure was raised to 3.5 ATA by increasing the ambient pressure to 4.5 ATA. No abnormalities were observed in the ECG recordings from any subject in any of the conditions studied. Oxygen pulse (V_o /heart

rate) i.e. the amount of oxygen taken up from the lungs per heart beat increased with the ergometric load in all three conditions (Fig. 6). Compared to the control values at 1.0 ATA breathing air the average oxygen pulse at a given load was 0.2–1.0 ml O₂ greater at 1.0 ATA O₂ and 2–3 ml O₂ greater at 4.5 ATA air.

Rectal temperature showed a slight tendency to increase with the work rate from a mean value of 36.6°C at rest to 36.8°C during exercise at 150 W. No consistent differences were observed between the 3 conditions.

While muscular fatigue of the legs at a given load was reported to be approximately the same in all 3 conditions the high work rates were found to be more stressful in the hyperbaric environment by most subjects mainly because of respiratory discomfort due to increased breathing resistance. In no instance were there any overt signs or symptoms of nitrogen narcosis and in no case was the decompression to atmospheric pressure accompanied by bends or other signs of decompression sickness.

Discussion

The present study shows that ventilation, circulation and gas exchange in man at rest and during graded submaximal exercise are affected in several ways by acute exposure to hyperbaric air (Comparison I Table III). Since a rise in ambient air pressure involves simultaneous increases of the inspired O₂ and N₂ pressures gas density and pressure *per se* the cardiorespiratory changes observed may have been caused by either of these factors or by a combination of them. Hence Comparison I cannot be used to evaluate the relative contributions of these factors to the total effects of raised air pressure. However by comparing data obtained in experiments which differed mainly in respect to the inspired O₂ pressure (Comparison II) or in respect to the inspired N₂ pressure gas density and pressure *per se* (Comparison III) the separate effects of these two groups of factors could be estimated. The experimental design and methods used in this study do not allow any distinction between possible influences of raised P_{N₂}, increased gas density and pressure *per se*.

Acute exposure to 4.5 ATA air in the resting state caused no consistent changes in the cardiorespiratory and metabolic variables listed in Table III except for a small reduction of the heart rate and slight increases of the oxygen pulse and mixed expired P_{CO₂}. The observed 1.9 mm Hg rise in mixed expired P_{CO₂} was evidently due in part to the fact that the CO₂ tension of air inhaled at 4.5 ATA is normally about 0.8 mm Hg higher than at 1.0 ATA. As indicated by Comparisons II and III most of the reduction in heart rate was due to the rise in N₂ pressure or some closely related factor whereas the increase in oxygen pulse probably was due in large part or entirely to the reduction in heart rate.

The responses of most variables to graded exercise were qualitatively similar in the three different conditions. Quantitative differences in the responses to a given work load were observed however and in most cases these differences showed a tendency to increase as the ergometric load was increased. At the highest load (150 W Table III) a rise in ambient air pressure to 4.5 ATA thus caused statistically significant

increases in \dot{V}_{O_2} , \dot{V}_{CO_2} , oxygen pulse, mixed expired and end tidal P_{CO_2} , significant reductions in heart rate and ventilatory equivalents for O_2 and CO_2 , whereas no significant changes occurred in \dot{V}_I , \dot{V}_T , f , and respiratory exchange ratio (*Comparison I*). As indicated by *Comparisons II and III*, the changes in oxygen pulse, mixed expired and end tidal P_{CO_2} and ventilatory equivalents for O_2 and CO_2 were caused by the combined effects of raised inspired O_2 and N_2 pressures, whereas the increases in \dot{V}_{O_2} and \dot{V}_{CO_2} were due only to the rise in N_2 pressure and the decrease in heart rate to the rise in O_2 pressure.

The observation that \dot{V}_{O_2} for a given ergometric load increased by approximately 10% when the air pressure was raised to 4.5 ATA (Fig. 1) can probably be attributed entirely to some factor or factors related to the increased N_2 pressure. The rise in O_2 pressure does not appear to be a contributing factor since it is known that a similar rise in O_2 pressure at normal atmospheric pressure has no significant influence on \dot{V}_{O_2} at submaximal work loads (Asmussen and Nielsen 1955). Similarly, the possibility that the increased O_2 consumption at 4.5 ATA was due to the increased N_2 pressure itself or the pressure *per se* seems unlikely as it has been shown that the addition of 4–7 ATA N_2 at an oxygen pressure of 1.0 ATA does not cause any significant change in the O_2 consumption rate of isolated tissues such as the rat diaphragm or brain tissue (Rodgers, Fenn and Craig 1969; Stadie, Riggs and Haugaard 1945). It seems probable, therefore, that the increase of \dot{V}_{O_2} observed at 4.5 ATA can be attributed in large part or entirely to the increase in gas density and hence in airway resistance and work of breathing (Marshall, Lanphier and DuBoué 1956; Buhlmann 1963; Maro and Farhi 1967). The oxygen cost of breathing air at 4.5 ATA is the cost of breathing a gas 4.7 times as dense as air at sea level (Table II) was estimated as follows.

At the highest work load the difference in \dot{V}_{O_2} at 1.0 and 4.5 ATA averaged 240 ml/min STPD, whereas \dot{V}_I amounted to approximately 40 l/min BTPS in both conditions (Table III). The O_2 cost for the extra work done in breathing the denser gas thus amounted to about 6 ml O_2 per liter of inspired gas. Since the metabolic cost of breathing at sea level is in the order of 2 ml O_2 per liter of ventilation at a \dot{V}_I of 40 l/min (Otis 1964), it follows that the total cost of breathing at 4.5 ATA amounted to about 8 ml O_2 per liter of inspired gas at the highest work load. Thus about 15 per cent of the total O_2 uptake at this load was used for the work of breathing, which seems to be a surprisingly high value. However, similar high values for the O_2 cost of breathing high density gases have recently been reported. Thus Glauser, Glauser and Rüggli (1967) found that the O_2 cost of CO_2 -induced hyperpnea at a rate of 36 l/min amounted to 2.7 ml O_2 per liter of ventilation when the density of the inspired CO_2 -air mixture was 1.25 g/l and increased to 7.8 ml O_2 per liter of ventilation when the gas density was increased to 4.9 g/l by substituting sulfur hexafluoride for nitrogen in the inhaled gas mixture. In subjects performing moderate exercise, Salzano, Rausch and Saltzman (1970) observed that the \dot{V}_{O_2} for a given ergometric load increased by approximately 8 ml O_2 per liter of ventilation when the density of the inspired gas was increased 4.4 times by use of a helium-oxygen gas

mixture at 31.3 ATA. In all these studies the work of breathing also included the work done to overcome the resistance to airflow in the external breathing circuit. In our 4.5 ATA expts this external work was estimated (*cf* Otis 1964 p. 470) to be in the order of 0.5 W at a \dot{V}_I of 40 l/min. Thus the values given above for the O_2 cost of breathing high density gases would have been less had no external breathing circuit been used.

When related to the external ergometric load the ventilatory response to graded exercise was similar in all 3 conditions except that a significant 8% reduction of \dot{V}_I occurred at the highest load when the O_2 pressure was raised by substituting oxygen for air at 1.0 ATA (Table III). The observation that a rise in O_2 pressure caused a reduction of ventilation in heavy but not in mild exercise is in agreement with earlier reports (Asmussen and Nielsen 1946, 1958; Bannister and Cunningham 1954; Lambertsen *et al.* 1959). Although \dot{V}_I at a given ergometric load remained essentially unchanged when the N_2 pressure was raised to 3.5 ATA (Comparison III, Table III) the O_2 uptake and CO_2 elimination increased and as a result the ventilatory equivalents for O_2 and CO_2 were significantly reduced at the two highest loads. Hence when related to the metabolic rather than to the ergometric load the ventilation in moderate and heavy exercise was reduced by increased N_2 pressure (Fig. 2). This non-oxygen dependent reduction of \dot{V}_I amounted to about 8% at an O_2 uptake of 2.0 l/min and was thus of the same magnitude as the reduction caused by the rise in O_2 pressure. A reduced ventilatory response to exercise of moderate and high work intensities has also been observed in subjects breathing mixtures of helium-oxygen at 31.3 ATA (Salzano, Rausch and Saltzman 1970) or nitrogen-oxygen at 4 ATA (Lambertsen *et al.* 1973) with normal or nearly normal O_2 pressures.

Previous reports have shown that the ventilatory responses to exercise (Tabakin and Hanson 1960; Cerretelli, Sikand and Farhi 1969) and CO_2 (Cherniack and Snidal 1956; Milic-Emili and Tyler 1963) are diminished when the work of breathing is artificially increased at sea level by addition of an external resistance. It seems likely therefore that the non-oxygen induced reduction of ventilation observed in the present 4.5 ATA expts was due mainly to the increased airway resistance caused by the increased gas density. However, since it is well known that nitrogen at high pressures has a narcotic influence on the central nervous system (Behnke, Thomson and Motley 1935; Bennett 1966) the possibility that the reduced ventilation was due to a respiratory depressant effect of the increased N_2 pressure itself also deserves consideration. In previous breath holding experiments with air and oxygen at normal and at elevated ambient pressures (Hesser 1962, 1965) it was found that a rise in N_2 pressure up to and including 3.8 ATA had no significant influence on the breath holding ability, suggesting that such N_2 pressures have little if any depressant action on the respiratory centers. Recent studies on the ventilatory response to CO_2 in hyperbaric environment (Fagraeus and Hesser 1970; Lambertsen *et al.* 1973) have shown that a rise of the inspired N_2 pressure to 4–6 ATA causes a significant decrease in the slope of the CO_2 response curve with no apparent shift in the position of the curve. The primary effect of artificially increased breathing resistance is also a

increases in \dot{V}_{O_2} , \dot{V}_{CO_2} , oxygen pulse, mixed expired and end tidal P_{CO_2} , significant reductions in heart rate and ventilatory equivalents for O_2 and CO_2 , whereas no significant changes occurred in \dot{V}_I , \dot{V}_T , f and respiratory exchange ratio (Comparison I). As indicated by Comparisons II and III, the changes in oxygen pulse, mixed expired and end tidal P_{CO_2} and ventilatory equivalents for O_2 and CO_2 were caused by the combined effects of raised inspired O_2 and N_2 pressures, whereas the increases in \dot{V}_{O_2} and \dot{V}_{CO_2} were due only to the rise in N_2 pressure and the decrease in heart rate to the rise in O_2 pressure.

The observation that \dot{V}_{O_2} for a given ergometric load increased by approximately 10% when the air pressure was raised to 4.5 ATA (Fig. 1) can probably be attributed entirely to some factor or factors related to the increased N_2 pressure. The rise in O_2 pressure does not appear to be a contributing factor since it is known that a similar rise in O_2 pressure at normal atmospheric pressure has no significant influence on \dot{V}_{O_2} at submaximal work loads (Asmussen and Nielsen 1955). Similarly, the possibility that the increased O_2 consumption at 4.5 ATA was due to the increased N_2 pressure itself or the pressure *per se* seems unlikely as it has been shown that the addition of 4–7 ATA N_2 at an oxygen pressure of 1.0 ATA does not cause any significant change in the O_2 consumption rate of isolated tissues such as the rat diaphragm or brain tissue (Rodgers, Fenn and Craig 1969; Stadie, Riggs and Haugaard 1943). It seems probable therefore that the increase of \dot{V}_{O_2} observed at 4.5 ATA can be attributed in large part or entirely to the increase in gas density and hence in airway resistance and work of breathing (Marshall, Lanphier and DuBois 1906; Buhlmann 1963; Maio and Farhi 1967). The oxygen cost of breathing air at 4.5 ATA is the cost of breathing a gas 4.7 times as dense as air at sea level (Table II) was estimated as follows:

At the highest work load the difference in \dot{V}_{O_2} at 1.0 and 4.5 ATA averaged 240 ml/min STPD, whereas \dot{V}_I amounted to approximately 40 l/min BTPS in both conditions (Table III). The O_2 cost for the extra work done in breathing the denser gas thus amounted to about 6 ml O_2 per liter of inspired gas. Since the metabolic cost of breathing at sea level is in the order of 2 ml O_2 per liter of ventilation at a \dot{V}_I of 40 l/min (Ous 1964), it follows that the total cost of breathing at 4.5 ATA amounted to about 8 ml O_2 per liter of inspired gas at the highest work load. Thus about 15 per cent of the total O_2 uptake at this load was used for the work of breathing, which seems to be a surprisingly high value. However, similar high values for the O_2 cost of breathing high density gases have recently been reported. Thus Glauser, Glauser and Russ (1967) found that the O_2 cost of CO_2 -induced hyperpnea at a rate of 36 l/min amounted to 2.7 ml O_2 per liter of ventilation when the density of the inspired CO_2 air mixture was 1.25 g/l and increased to 7.8 ml O_2 per liter of ventilation when the gas density was increased to 4.9 g/l by substituting sulfur hexafluoride for nitrogen in the inhaled gas mixture. In subjects performing moderate exercise, Salzano, Rausch and Saltzman (1970) observed that the \dot{V}_{O_2} for a given ergometric load increased by approximately 8 ml O_2 per liter of ventilation when the density of the inspired gas was increased 4.4 times by use of a helium-oxygen gas

500 ml BTPS at 150 W. With acute exposure to 4.5 ATA air V_D/V_T decreased significantly to 0.24 at rest and to 0.18 at 150 W, while V_D showed no consistent change in the resting state but decreased to 475 ml BTPS in exercise. When the O_2 pressure alone was raised by substituting oxygen for air at 1.0 ATA, V_D/V_T and V_D showed no significant changes at rest but decreased during exercise to values similar to those found at 4.5 ATA. It may be concluded therefore that acute exposure to 4.5 ATA air caused a significant reduction of the V_D/V_T ratio at rest mainly because of the increased N_2 pressure and significant reductions of V_D/V_T and V_D during exercise at 150 W predominantly due to the increased O_2 pressure.

The observation that the end tidal P_{CO_2} at high metabolic loads increased as the ambient pressure was raised to 4.5 ATA (Fig. 4) indicates that at these loads the alveolar ventilation, like the pulmonary minute ventilation, was reduced in the hyperbaric environment. This conclusion is based on the reasonable assumption that changes in end tidal P_{CO_2} at a given metabolic level are similar to those which occur in mean alveolar P_{CO_2} . The results of *Comparisons II and III* (Table III) indicate that this reduction of alveolar ventilation was due both to the increased O_2 and the increased N_2 pressure.

The fact that the end tidal P_{CO_2} during exercise rose to rather high levels even at normal ambient pressure (Table III) can only in part be explained by the appearance of a negative arterial to end tidal P_{CO_2} difference. Another contributing explanation would be that all our subjects were divers with long diving experience. Thus Goff and Bartlett (1957) have reported the occurrence of elevated end tidal P_{CO_2} and reduced ventilatory response to exercise in trained underwater swimmers, whereas Jarrett (1966) observed that exercise at normal and at increased ambient pressures produced lower alveolar ventilation with correspondingly higher end tidal P_{CO_2} in divers than in subjects without any diving experience.

The old observation by Shilling, Hawkins and Hansen (1936) that high pressures of air have a depressant effect on the cardiac rate both at rest and in exercise was confirmed in the present study (*Comparison I*, Table III). Shilling *et al.* attributed this cardiac depression to the elevated partial pressure of oxygen. The results of *Comparisons II and III* clearly demonstrate, however, that only part of the bradycardia occurring in hyperbaric air can be ascribed to the elevated O_2 pressure, the remaining part being caused by some factor or factors related to the elevated N_2 pressure. Another important observation was that the true magnitude of the non-oxygen-dependent bradycardia will be underestimated if the heart rate in exercise is related to the external rather than to the metabolic load ($\dot{V}O_2$). Thus the heart rate at 150 W showed no significant change with a rise in N_2 pressure to 3.5 ATA when related to the external ergometric load (*Comparison III*, Table III) but decreased significantly by about 10 beats/min when plotted as a function of $\dot{V}O_2$ (Fig. 5).

It is well known that elevated inspired O_2 pressures lead to a reduction of the heart rate in man at rest (Daly and Bondurant 1962; Kenmure *et al.* 1972) and during submaximal exercise (Asmussen and Nielsen 1955; Taunton *et al.* 1970). Daly and Bondurant found that this decrease in heart rate at rest was abolished by atropine

and concluded that oxygen induced bradycardia is brought about mainly by changes in vagal tone. In a recent report (Fagraeus and Linnarsson 1973) evidence was presented however that in exercise the major part of oxygen induced bradycardia can be attributed to a direct myocardial effect of hyperoxia while the remaining part was found to be mediated over parasympathetic pathways.

Cardiac slowing in response to increased inert gas pressures has been reported to occur in man at rest (Flynn, Berghage and Coil 1972) and in exercise (Saltzmann and Saltzman 1970, Bradley *et al.* 1971, Flynn *et al.* 1972). From experiments on humans breathing gas mixtures of varying density at constant or varying ambient pressures Flynn *et al.* obtained evidence suggesting that both the increase in ambient pressure and in gas density contribute to the development of the bradycardia occurring in hyperbaric conditions. In the isolated guinea pig heart preparation Fagraeus (1971) on the other hand was unable to detect any effects of raising the N_2 pressure to 8 ATA or the hydrostatic pressure to 9 ATA on heart rate, myocardial contractile force and the response to sympathetic stimulation suggesting that the non oxygen dependent portion of the bradycardia observed at elevated air pressures is mediated through changes in the autonomic nervous system activity. Recent observations (Fagraeus and Linnarsson 1973) on the effects of high O_2 and N_2 pressures before and after drug induced changes in the autonomic balance suggest that the non oxygen dependent bradycardia in man is mainly caused by a change in the beta adrenergic stimulation of the heart. Whether this change in sympathetic influence on the heart is caused by the increased N_2 pressure, hydrostatic pressure or gas density or by some other factor or factors related to the increase in N_2 pressure cannot be settled at the present time.

The increased oxygen pulse observed in the exercise experiments at 4.5 ATA (Fig. 6) can evidently be ascribed to the same factors that were shown above to be responsible for the increase of \dot{V}_O and the decrease of heart rate that occur at high ambient air pressure. Since the oxygen pulse is equal to the product of the stroke volume and the O_2 difference between arterial and mixed venous blood, the increased oxygen pulse at 1.0 ATA O_2 and 4.5 ATA air implies that in submaximal exercise either the stroke volume, the arterial-venous O_2 difference or both these variables are increased by increased inspired O_2 and/or N_2 pressures. Whichever of these variables is involved, the larger oxygen pulse at high air pressure ensures an undiminished or even increased overall O_2 transport to the tissues in the face of a reduced heart rate.

This work was supported by the Swedish Medical Research Council (Project No. 40\ 689).

References

- ASMUSSEN, E. and M. NIELSEN. Studies on the regulation of respiration in heavy work. *Acta physiol. scand.* 1946, 19, 171-188.
 ASMUSSEN, E. and M. NIELSEN. The cardiac output in rest and work at low and high oxygen pressures. *Acta physiol. scand.* 1955, 35, 73-83.
 ASMUSSEN, E. and M. NIELSEN. Physiological dead space and alveolar gas pressures at rest and during muscular exercise. *Acta physiol. scand.* 1956, 38, 1-21.

- ASMUSSEN E and M NIELSEN Pulmonary ventilation and effect of oxygen breathing in heavy exercise *Acta physiol scand* 1958 43 365-378
- ASTRAND I Aerobic work capacity in men and women with special reference to age *Acta physiol scand* 1960 42 Suppl 169 1-97
- ASTROM T and O WIGERTZ A digital computer for automatic breath by breath calculation of respiratory functions *Report Lab Anat Nat Med Karol Inst Stockholm* March 1966 23 pp
- BANNISTER, R G and D J C CUNNINGHAM The effects on the respiration and performance during exercise of adding oxygen to the inspired air *J Physiol (Lond)* 1954 125 118-137
- BEHNKE A R, R M THOMSON and E P MOTLEY The psychologic effects from breathing air at 4 atmospheres pressure *Amer J Physiol* 1935 117 554-558
- BENNETT P H *The Physiology of Compressed Air for Scuba and Freest Gas Narcosis* Oxford Pergamon Press 1966 116 pp
- BENNETT P B and H H ELLIOTT (Eds) *The Physiology and Medicine of Diving and Compressed Air Work* London Baillière Tindall and Cassell 1969 537 pp
- BRADLEY M E, R L ANTHONIS, J VOROSMARTI and P G LEMKE, Respiratory and cardiac responses to exercise in subjects breathing helium-oxygen mixtures at pressures from sea level to 19° atmospheres In *Underwater Physiology* edited by C J Lambertsen New York Academic Press 1971 pp 375-337
- BRISMAZ, J C, M HESSER and G MATELL, Breath by breath sampling of alveolar (end tidal) gas *Acta physiol scand* 1962 56 299-305
- BROMAN S and O WIGERTZ Transient dynamics of ventilation and heart rate with step changes in work load from different load levels *Acta physiol scand* 1971 81 54-74
- BUHLMAN A A Respiratory resistance with hyperbaric gas mixtures *Proc Second Symposium on Underwater Physiology Natl Acad Sci Natl Res Council Publ 1181* 1963 pp 98-107
- CERRETELLI P, R S SIKAND and L E FARHI Effect of increased airway resistance on ventilation and gas exchange during exercise *J appl Physiol* 1969 27 597-600
- CERNIACK R M Work of breathing and the ventilatory response to CO In *Handbook of Physiology, Respiration* edited by W O Fenn and H Rahn Washington D C Amer Physiol Soc 1965 Sec 3 Vol II Chapt 60 pp 1469-1474
- CERNIACK R M and D P SNIDAL, The effect of obstruction to breathing on the ventilatory response to CO *J clin Invest* 1956 35 1286-1290
- DALY W J and S BONDURANT Effects of oxygen breathing on the heart rate blood pressure and cardiac index of normal men—resting with reactive hyperemia and after atropine *J clin Invest* 1962 41 126-132
- DOBELN W von A respiratory valve with insignificant dead space *Acta physiol scand* 1949 18 34-35
- ENGBROFF H Volumen Ineffizien Bemerkungen zur Frage des schädlichen Raumes *Uppsala Lak Foren F* 1938 44 191-218
- FAGRAEUS L Performance of the isolated guinea pig heart in hyperbaric environment *Report Lab Anat Nat Med Karol Inst Stockholm* July 1971 11 pp
- FAGRAEUS L and C M HESSER Ventilatory response to CO₂ in hyperbaric environments *Acta physiol scand* 1970 80 194-204
- FAGRAEUS L and D L JARSSON Heart rate in hyperbaric environment after autonomic blockade *Forsk medic (Stockh)* 1973 9 260-264
- FLYNN E T, T E BERGMAN and E F COLL, Influence of increased ambient pressure and gas density on cardiac rate in man *Experimental Biology Report 4-72* Washington Navy Yard Washington, DC 1972 35 pp
- GLAUZER S C, E M GLAUZER and B F RUBY Gas density and the work of breathing *Respir Physiol* 1967 9 344-350
- GOFF L G and G BARTLETT JR, Elevated end tidal CO₂ in trained underwater swimmers *J appl Physiol* 1957 10 203-206
- HESSER, C M The role of nitrogen in breath holding at increased pressures In *Man Dependence on the Earthly Atmosphere* edited by R E Sherr New York Macmillan 1969 317-334
- HESSER, C M Breath holding under high pressure In *Physiology of Breath Holding in a Diving Animal of Japan*, edited by H Rahn and T Yokoyama Natl Acad Sci Natl Res Council Publ 1341 1965 165-181
- HESSER C M and B HOLMGREN Effects of raised barometric pressure on expiration in man *Acta physiol scand* 1959 47 28-43
- HESSER C M, L FAGRAEUS and D LINNARSSON Cardiorespiratory responses to exercise in hyperbaric environment *Proc of the International Conference of Physiological Sciences* Vol VII Washington DC 1968 p 191
- JARRETT A S Alveolar carbon dioxide tension increased in ambient pressures *J appl Physiol* 1965 1 158-167
- KENNEDY, A C, F W R MURDOCH, I HUTTON and A J V CAMERON Hemodynamic effects of oxygen at 1 and 2 Atm pressure in healthy subject *J appl Physiol* 1972 39 273-276

and concluded that oxygen induced bradycardia is brought about mainly by changes in vagal tone. In a recent report (Fagraeus and Linnarsson 1973) evidence was presented, however, that in exercise the major part of oxygen induced bradycardia can be attributed to a direct myocardial effect of hyperoxia while the remaining part was found to be mediated over parasympathetic pathways.

Cardiac slowing in response to increased inert gas pressures has been reported to occur in man at rest (Flynn, Berghage and Coil 1972) and in exercise (Salzano, Rausch and Saltzman 1970, Bradley *et al.* 1971, Flynn *et al.* 1972). From experiments on humans breathing gas mixtures of varying density at constant or varying ambient pressures Flynn *et al.* obtained evidence suggesting that both the increase in ambient pressure and in gas density contribute to the development of the bradycardia occurring in hyperbaric conditions. In the isolated guinea pig heart preparation Fagraeus (1971) on the other hand was unable to detect any effects of raising the N_2 pressure to 8 ATA or the hydrostatic pressure to 9 ATA on heart rate, myocardial contractile force and the response to sympathetic stimulation, suggesting that the non oxygen dependent portion of the bradycardia observed at elevated air pressures is mediated through changes in the autonomic nervous system activity. Recent observations (Fagraeus and Linnarsson 1973) on the effects of high O_2 and N_2 pressures before and after drug induced changes in the autonomic balance suggest that the non oxygen dependent bradycardia in man is mainly caused by a change in the beta adrenergic stimulation of the heart. Whether this change in sympathetic influence on the heart is caused by the increased N_2 pressure, hydrostatic pressure or gas density or by some other factor or factors related to the increase in N_2 pressure cannot be settled at the present time.

The increased oxygen pulse observed in the exercise experiments at 4.5 ATA (Fig. 6) can evidently be ascribed to the same factors that were shown above to be responsible for the increase of \dot{V}_{O_2} and the decrease of heart rate that occur at high ambient air pressure. Since the oxygen pulse is equal to the product of the stroke volume and the O_2 difference between arterial and mixed venous blood, the increased oxygen pulse at 1.0 ATA O_2 and 4.5 ATA air implies that in submaximal exercise either the stroke volume, the arterial-venous O_2 difference or both these variables are increased by increased inspired O_2 and/or N_2 pressures. Whichever of these variables is involved, the larger oxygen pulse at high air pressure ensures an undiminished or even increased overall O_2 transport to the tissues in the face of a reduced heart rate.

This work was supported by the Swedish Medical Research Council (Project No. 40\ 689).

References

- ASMUSSEN, E. and M. NIELSEN. Studies on the regulation of respiration in heavy work. *Acta physiol scand* 1946 12: 171-188.
 ASMUSSEN, E. and M. NIELSEN. The cardiac output in rest and work at low and high oxygen pressures. *Acta physiol scand* 1955 35: 13-23.
 ASMUSSEN, E. and M. NIELSEN. Physiological adaptation and alveolar gas pressures at rest and during muscular exercise. *Acta physiol scand* 1957 32: 1-21.

- ASMUSSE E and M NIELSEN Pulmonary ventilation and effect of oxygen breathing in heavy exercise *Acta physiol scand* 1958 43 365-378
- ASTRAND I Aerobic work capacity in men and women with special reference to age *Acta physiol scand* 1960 49 Suppl 169 1-99
- ASTROM T and O WIGERTZ A digital computer for automatic breath by breath calculation of respiratory functions *Report Lab 4 stat 16 at Med Farsol Inst Stockholm* March 1966 23 pp
- BANNISTER R G and D J C CUNNINGHAM The effects on the respiration and performance during exercise of adding oxygen to the inspired air *J Physiol (Lond)* 1954 103 118-137
- BEHNKE A R R M THOMSON and E P MOTLEY The psychologic effects from breathing air at 4 atmospheres pressure *Am J Physiol* 1935 112 534-538
- BENNETT P B *The Physiology of Compressed Air Intoxication and Inert Gas Narcosis* Oxford Pergamon Press 1966 116 pp
- BENNETT P B and D H ELLIOTT (Eds) *The Physiology and Medicine of Diving and Compressed Air* New London Balliere Tindall and Cassell 1969 532 pp
- BRADLEY M E and R ANTHONISSEN J VOROSMARTI and P G LUYKZAVER Respiratory and cardiac responses to exercise in subjects breathing helium-oxygen mixtures at pressures from sea level to 19² atmospheres In *Underwater Physiology* edited by C J Lambertsen New York Academic Press 1971 pp 325-331
- BRISMAAR J C M HESSE and G MATELL Breath by breath sampling of alveolar (end tidal) gas *Acta physiol scand* 1962 36 299-303
- BROMAN S and O WIGERTZ Transient dynamics of ventilation and heart rate with step changes in work load from different load levels *Acta physiol scand* 1971 81 54-74
- BUHLMANN A A Respiratory resistance with hyperbaric gas mixtures *Proc Second Symposium on Underwater Physiology Natl Acad Sci Natl Res Council Publ* 1181 1963 pp 98-107
- CERRETELLI P R S SIKAND and L E FARHI Effect of increased airway resistance on ventilation and gas exchange during exercise *J appl Physiol* 1969 27 597-600
- CHERNIACK R M Work of breathing and the ventilatory response to CO₂ In *Handbook of Physiology Respiration* edited by W O Fenn and H Rahn Washington D C Amer Physiol Soc 1965 Sec 3 Vol II Chapt 60 pp 1469-1474
- CHERNIACK R M and P S IDOL The effect of obstruction to breathing on the ventilatory response to CO₂ *J clin Invest* 1956 35 1286-1290
- DALY W J and S BONDURANT Effects of oxygen breathing on the heart rate blood pressure and cardiac index of normal men—resting with reactive hyperemia and after atropine *J clin Invest* 1967 41 126-132
- DOBELN W von, A respiratory valve with insignificant dead space *Acta physiol scand* 1949 18 34-35
- ENGROFF H Volumen Ineffizien Bemerkungen zur Frage des schadlichen Raumes *Lipsala Lak Form F* 1938 44 191-218
- FAGRAEUS L Performance of the isolated guinea pig heart in hyperbaric environment *Report Lab Anat 16 at Med Farsol Inst Stockholm* July 1971 11 pp
- FAGRAEUS L and C M HESSE Ventilatory response to CO₂ in hyperbaric environments *Acta physiol scand* 1970 80 191-201
- FAGRAEUS L and D LINNARSSON Heart rate in hyperbaric environment after autonomic blockade *Foena mediet (Stockholm)* 1973 9 760-764
- FLYNN E T T E BERGHAUSE and E F CORR Influence of increased ambient pressure and gas density on cardiac rate in man *Experimental Diver's Log Report 4-77* Washington Navy Yard Washington D C 1972 35 pp
- GLAUZER S C E M GLAUZER and H F REIS Gas density and the work of breathing *Respir Physiol* 1967 344-350
- GOTT L G and M BARTLEY JR Elevated end tidal CO₂ in trained underwater swimmers *J Appl Physiol* 1957 10 203-206
- HESSE C M The role of nitrogen in breath holding at increased pressure In *Man Dependence on the Earthly Atmosphere* edited by K E Shaeffer New York Macmillan 1962 37-334
- HESSE C M Breath holding under high pressure In *Physiol J South Beach Held Divn and the Am J Jpan* edited by H Rahn and T Yokoyama Natl Acad Sci Natl Res Council Publ 1341 1963 165-181
- HESSE C M and B HOLMGREN Effects of raised barometric pressure on respiration in man *Acta physiol scand* 1959 47 111-113
- HESSE C M L FAGRAEUS and D LINNARSSON Cardiorespiratory responses to exercise in hyperbaric environment *Proc of the International Conference on Physiology and Medicine Vol VII* Washington D C 1968 p 191
- JARRETT A S Alveolar carbon dioxide tensions at increased ambient pressures *J appl Physiol* 1966 1 158-162
- KENNEDY A C F W R MURDOCH I HUTTON and A J CAMERON Hemodynamic effects of oxygen at 1 and 2 ATA pressure in healthy subjects *J appl Physiol* 1972 33 273-277

and concluded that oxygen induced bradycardia is brought about mainly by changes in vagal tone. In a recent report (Fagraeus and Linnarsson 1973) evidence was presented, however, that in exercise the major part of oxygen induced bradycardia can be attributed to a direct myocardial effect of hyperoxia while the remaining part was found to be mediated over parasympathetic pathways.

Cardiac slowing in response to increased inert gas pressures has been reported to occur in man at rest (Flynn, Berghage and Coil 1972) and in exercise (Salzano, Rausch and Saltzman 1970, Bradley *et al.* 1971, Flynn *et al.* 1972). From experiments on humans breathing gas mixtures of varying density at constant or varying ambient pressures Flynn *et al.* obtained evidence suggesting that both the increase in ambient pressure and in gas density contribute to the development of the bradycardia occurring in hyperbaric conditions. In the isolated guinea pig heart preparation Fagraeus (1971) on the other hand was unable to detect any effects of raising the N_2 pressure to 8 ATA, or the hydrostatic pressure to 9 ATA on heart rate, myocardial contractile force and the response to sympathetic stimulation, suggesting that the non oxygen dependent portion of the bradycardia observed at elevated air pressures is mediated through changes in the autonomic nervous system activity. Recent observations (Fagraeus and Linnarsson 1973) on the effects of high O_2 and N_2 pressures before and after drug induced changes in the autonomic balance suggest that the non oxygen dependent bradycardia in man is mainly caused by a change in the beta adrenergic stimulation of the heart. Whether this change in sympathetic influence on the heart is caused by the increased N_2 pressure, hydrostatic pressure or gas density or by some other factor or factors related to the increase in N_2 pressure cannot be settled at the present time.

The increased oxygen pulse observed in the exercise experiments at 4.5 ATA (Fig. 6) can evidently be ascribed to the same factors that were shown above to be responsible for the increase of $\dot{V}O_2$ and the decrease of heart rate that occur at high ambient air pressure. Since the oxygen pulse is equal to the product of the stroke volume and the O_2 difference between arterial and mixed venous blood, the increased oxygen pulse at 1.0 ATA O_2 and 4.5 ATA air implies that in submaximal exercise either the stroke volume, the arterial-venous O_2 difference or both these variables are increased by increased inspired O_2 and/or N_2 pressures. Whichever of these variables is involved, the larger oxygen pulse at high air pressure ensures an undiminished or even increased overall O_2 transport to the tissues in the face of a reduced heart rate.

This work was supported by the Swedish Medical Research Council (Project No. 40X-689).

References

- ASMUSSEN, E. and M. NIELSEN. Studies on the regulation of respiration in heavy work. *Acta physiol. scand.* 1946, 12, 171-188.
 ASMUSSEN, E. and M. NIELSEN. The cardiac output in rest and work at low and high oxygen pressures. *Acta physiol. scand.* 1955, 35, 73-83.
 ASMUSSEN, E. and M. NIELSEN. Physiological dead space and alveolar gas pressures at rest and during muscular exercise. *Acta physiol. scand.* 1956, 39, 1-21.

- WILSEN E and M NIELSEN Pulmonary ventilation and effect of oxygen breathing in heavy exercise *Acta physiol scand* 1958 43 365-378
- WISTRAND I Aerobic work capacity in men and women with special reference to age *Acta physiol scand* 1960 49 Suppl 169 1-92
- ASTRO T and O WIGERTZ A digital computer for automatic breath by breath calculation of respiratory functions *Report Lab Anat Med Karol Inst Stockholm* March 1961 23 pp
- BALLISTER R C and D J C CUNNINGHAM The effects on the respiratory and perfimane during exercise of adding oxygen to the inspired air *J Physiol (Lond)* 1954 105 118-137
- BEINKE A R R M THOMSON and H P MOTLEY The psychologic effects from breathing air at 4 atmospheres pressure *Amer J Physiol* 1935 117 554-558
- BENNETT P B *Theatology of Compressed Air Intoxication and Inert Gas Narcosis* Oxford Pergamon Press 1966 116 pp
- BENNETT P B and D H ELLIOTT (Eds) *The Physiology and Medicine of Diving and Compressed Air* Work London Baillière Tindall and Cassell 1969 532 pp
- BRADLEY M E and R ANTHONY J VOROSWARTI and I G IYAWIATZ Respiratory and cardiac responses to exercise in subjects breathing helium oxygen mixtures at pressures from 1 to 1 level to 192 atmospheres In *L. dequate Physiol* edited by C J Farnham New York Academic Press 1971 pp 325-337
- BRUNAR J C M HESSEN and G WATTELL Breath by breath sampling of alveolar (enititil) gas *Acta physiol scand* 1967 56 299-305
- BROWAN S and O WIGERTZ Transient dynamics of ventilation and heart rate with increasing work load from different load levels *Acta physiol scand* 1971 81 54-71
- BULHMAN A A Respiratory resistance with hyperbaric gas mixtures *Proc 5th Int Symp on Lung Respi Physiol Natl Acad Sci Natl Res Council Publ* 1961 1963 pp 11-107
- CERRATELLI P R S SIKAND and L E FARON Effect of increased airway resistance on ventilation and gas exchange during exercise *J Appl Physiol* 1969 27 397-400
- CERNIACH R M Work of breathing and the ventilatory response to CO₂ In *Handbook of Physiology* 1962 Sec 3 Vol II Chapt 60 pp 1469-1474
- CERNIACH R M and D H SIDAAL The effect of obstruction to breathing on the ventilatory response to CO₂ *J Clin Invest* 1956 35 1285-1290
- DALY W J and S BONDURANT Effects of oxygen breathing on the heart rate and stroke volume at cardiac index of normal men—resting with reactive hyperemia and after air p₂₁ *J Clin Invest* 1969 41 126-132
- DONALD W von Respiratory alveolar with insignificant dead space *Acta physiol scand* 1911 10 34-35
- EVONOFF H Volumen Ineffizien Bemerkungen zur Frage des schädlichen Raums *Arch f. Physiol Lab Fm Fh* 1938 44 191-218
- FAGRAEUS L P Performance of the isolated guinea pig heart in hyperbaric environment *Respi Lab Anat Med Karol Inst Stockholm* July 1971 11 pp
- FAGRAEUS L and C M HESSEN Ventilatory response to CO₂ in hyperbaric environment *Acta physiol scand* 1970 80 193-204
- FAGRAEUS L and D LINNARSSON Heart rate in hyperbaric environment after autotransfusion *Forskn Med (Stockholm)* 1973 2 260-264
- FLYNN E T T F BERGHAUSE and F F COU Influence of increased ambient pressure on the denaturation of cardiac rate in man *Exp Metabol Dis Lung Respiol* 1977 5 35 pp
- GLAESER C E M GLAESER and B F RUSV Gas denaturation and the work of breathing *J Physiol* 1967 2 344-350
- GORE L M and G BARTLEY JR Elevated end tidal CO₂ in train 1 unit water swim *J Appl Physiol* 1957 10 203-206
- HESSEN C M The role of nitrogen in breath holding and increased pressure *Acta Physiol* 1961 10 2 327-334
- HESSEN C M Breath holding and high pressure *In Physiol of the Human* 1963 1 11-14
- HESSEN C M and D LINNARSSON Effects of increased barometric pressure on the respiratory response to hypobaric environment *Proc 5th Int Symp on Lung Respi Physiol Natl Acad Sci* 1961 1963 165-181
- HESSEN C M and D LINNARSSON Cardiorespiratory response to hypobaric environment *Proc 5th Int Symp on Lung Respi Physiol Natl Acad Sci* 1961 1963 165-181
- JARRETT A S Volatile carbon dioxide desaturation at increased ambient pressure *J Appl Physiol* 1966 21 158-166
- KENNEDY A C F W R MURDOCH I HUTTON and J J L CAMPBELL The effect of oxygen at 1 and 2 atm pressure on healthy subjects *J Appl Physiol* 1966 21 158-166

- LAUBERTIEN C J, R GELFAND M J, LEYER G, BODANHER N, TAKANO T, A. REED J C, DICKSON and P T WATSON. Respiration and gas exchange during a 14-day continuous exposure to 5.2 O in N_2 at pressure equivalent to 100 FSW (4 ata). *Aerospace Med* 1973 44 844-849
- LAUBERTIEN C J, S G OWEN, H WENDEL M W, STROUD A, LURIE W, LOCHNER and G F CLARK. Respiratory and cerebral circulatory control during exercise at 21 and 20 atmospheres inspired pO_2 . *J appl Physiol* 1959 14 966-982
- LAUFHIER, E H. Man in high pressures. In *Handbook of Physiology: Adaptation to the Environment* edited by D H Dill, E F Adolph and C G Wilber. Washington D C: Amer Physiol Soc 1964 Section 4, Chapt 58 pp 893-909
- LINDBOOG B, O WIGERTZ and TH ÖRMAN. A beat to beat heart rate meter with linear analog output for muscular exercise studies. *Report Lab Arterial Med Karol Inst Stockholm Dec* 1969 23 pp
- LUNDIN G. Nitrogen elimination during oxygen breathing. *Acta physiol scand* 1953 30 Suppl 111 130-143
- LUNDIN G. Nitrogen elimination from the tissues during oxygen breathing and its relationship to the fat-muscle ratio and the localization of bends. *J Physiol (Lond)* 1960 137 167-175
- MAIO D A and L E FARHI. Effect of gas density on mechanics of breathing. *J appl Physiol* 196 23 687-693
- MARSHALL R, E H LAUFHIER and A B DUBOIS. Resistance to breathing in normal subjects during simulated dives. *J appl Physiol* 1956 9 5-10
- MATTELL G. Time-courses of changes in ventilation and arterial gas tensions in man induced by moderate exercise. *Acta physiol scand* 1963 58 Suppl 206 1-53
- MILIC EMIL J and J M TELER. Relation between work output of respiratory muscles and end tidal CO_2 tension. *J appl Physiol* 1963 18 497-504
- OTIS A B. The work of breathing. In *Handbook of Physiology: Respiration* edited by W O Fenn and H Rahn. Washington D C: Amer Physiol Soc 1964 Section 3, Vol I Chapt 17 pp 463-476
- RODGERS E H, W O FENN and A B CRAIG JR. The oxygen consumption of rat tissues in the presence of nitrogen helium or hydrogen. *Respir Physiol* 1969 6 168-177
- SALZANO J, D C RAUSCH and H A SALTZMAN. Cardiorespiratory responses to exercise at a simulated seawater depth of 1000 feet. *J appl Physiol* 1970 28 34-41
- SCHOLANDER, P F. Analyzer for accurate estimation of respiratory gases in one half cubic centimeter samples. *J Biol Chem* 1947 167 235-250
- SEVERINGHAUS J W and C P LANSOY JR. Respiration in anesthetized. In *Handbook of Physiology: Respiration* edited by W O Fenn and H Rahn. Washington D C: Amer Physiol Soc 1964 Section 3, Vol II Chapt 49 pp 1219-1264
- SINILLIN C W, J A HANSEN and R A HANSEN. The influence of increased barometric pressure on the pulse rate and arterial blood pressure. *U S Navy Med Bull* 1936 34 39-47
- SINILLIN C W and M F WERTS. *Underwater Medicine and Related Sciences*. New York: Plenum Publ Corp 1973 630 pp
- STAGIE W, C B C RIGGS and N HAGGARD. Oxygen poisoning. III. The effect of high oxygen pressures upon the metabolism of brain. *J Biol Chem* 1945 160 191-208
- TANAKA B S and J S HANSON. Responses to ventilatory obstruction during steady state exercise. *J appl Physiol* 1970 10 579-582
- TAYLOR J E, E W BANISTER, T R PATRICK, P OFORSAGD and W R DUNCAN. Physical work capacity in hyperbaric environments and conditions of hyperoxia. *J appl Physiol* 1970 28 421-427
- WASSERMAN K, A I VAN KESSEL and G G BURTON. Interaction of physiological mechanisms during exercise. *J appl Physiol* 1967 22 71-83
- WIGERTZ O. A low resistance flow meter for wide range ventilatory measurement. *Respir Physiol* 1969 253-260
- ZECHMAN F F, C HALL and W E HELL. Effects of graded resistance to tracheal airflow in man. *J appl Physiol* 1970 30 36-362

Regression of Structural Cardiovascular Changes after Reversal of Experimental Renal Hypertension in Rats

By

YEN LUNDGREN

Received 15 January 1974

Abstract

LUNDGREN Y: Regression of structural cardiovascular changes after reversal of experimental renal hypertension in rats. *Acta physiol scand* 1974 91 275-285.

Renal hypertension was induced in young normotensive male Wistar rats by constriction of one renal artery. This constriction was released 3-4 weeks later when pressure had stabilized around 180 mm Hg and when the structural cardiovascular adaptation to this hypertensive level was largely completed (Folkow *et al* 1973, Lundgren *et al* 1974). 1, 3, 7, 14 and 25 days later paired hindquarter perfusions were performed on one declipped renal hypertensive rat (DRHR) and one normotensive control rat (NCR) exploring the design of the resistance vessels as expressed by the resistance at maximal vasodilatation, the maximal slope of the dose-response curve to noradrenaline and the maximal pressor response (cf Folkow *et al* 1970b). At the same time intervals the left heart ventricles of all animals were weighed. Already one day after declipping arterial pressure was normalized while the hemodynamic analysis indicated that the DRHR resistance vessels like the left ventricle still showed largely unchanged hypertrophic changes characterizing hypertension. Then however a rapid regression of these changes occurred being considerable already after 7-14 days and after about 3 weeks the design of both heart and resistance vessels had become fully readapted to normotensive levels.

Like earlier hemodynamic studies in man with essential hypertension, hemodynamic studies on spontaneously hypertensive rats (SHR, Okamoto 1969) and renal hypertensive rats (RHR) show that the resistance vessels exhibit a structural adaptation of great hemodynamic importance (cf Folkow *et al* 1973, Lundgren *et al* 1974). Thus their wall/lumen ratio is enhanced due to an increased media thickness in combination with a lumen that is reduced even during maximal dilatation. These changes considerably raise resistance without necessitating any increased smooth

muscle tone. Like the wellknown left ventricular hypertrophy (Pickering 1968), this structural vascular adaptation is induced by any sustained increase in average blood pressure and it develops so rapidly (Folkow *et al* 1973 b, Lundgren *et al* 1974) that it becomes of great importance for the maintenance and even for the creation of hypertension whatever the initiating functional mechanism. The process seems to be qualitatively the same in rats predisposed to hypertension (SHR) and in genetically normotensive rats (RHR) but it might be quantitatively somewhat more pronounced in SHR than in RHR (see Folkow *et al* 1973 a).

It is obviously of great interest to know what happens with vascular design if pressure is decreased to or below normal levels. Intense treatment of SHR with hypotensive drugs leads to considerable regression of the mentioned hypertensive vascular changes already after 5 weeks though this regression appears to become lower and less pronounced the more advanced the hypertension state (Weiss 1974). If more drastic and abrupt pressure reductions are induced *e.g.* regionally by arterial obstructions regression can be traced already after 3 days and is largely completed in 3–5 weeks (Folkow and Svertsson 1968, Weiss and Hallbäck 1974). These studies illustrate that vascular design is greatly dependent on the local pressure and that it seems to be rapidly adjusted to pressure changes at least in young individuals.

The present study was performed in order to investigate how rapidly and to what extent the hypertensive structural changes of heart and resistance vessels show regression in renal hypertension when pressure is normalized by removing the renal artery clip.

Methods

Renal hypertension was induced during ether anesthesia in 15 male Wistar rats, 6–7 weeks old by placing a silver clip on the left renal artery leaving the right kidney intact. The rise in arterial pressure was followed by intraarterial measurements in the caudal artery during awake conditions the artery being cannulated during brief ether anesthesia. After 3–4 weeks when both hypertension and the structural changes of heart and resistance vessels were well established (*cf.* Lundgren *et al* 1974) the clip was removed and the reduction in blood pressure was followed, also now by intraarterial measurements. Paired perfusion experiments were then performed on hindquarters of one declipped renal hypertensive rat (DRHR) and one normotensive control rat (NCR) 1, 3, 7, 14 and 23 days after declipping each group consisting of 1–16 pairs. For details concerning the exact experimental procedure, the construction of the resistance curves and their key points see Folkow *et al* (1970 b, 1971). Thus as described earlier (Lundgren *et al* 1974) the pressure flow relationships during complete smooth muscle relaxation were examined (1–40 ml/min \times 100 g) and then dose response curves to noradrenaline (NA) were constructed for each paired experiment. The different key points *i.e.* resistance at maximal dilatation threshold dose of NA, maximal steepness of the resistance curve and maximal pressor response were deduced for each pair of curves and the mean \pm S.E. of these parameters were calculated for each group of DRHR and NCR. The mean difference \pm S.E. and the degree of significance between DRHR and NCR within each group were calculated by the pairing design *t* test. The differences between the various DRHR groups were analysed by a group comparison *t* test of the mean differences DRHR–NCR. The left heart ventricles from all animals were weighed and the mean \pm S.E. of the percentage left heart ventricle weight/body weight was calculated for all groups.

TABLE I Presents the mean values \pm SE for renal hypertensive rats (RHR) before and 1 3 7 14 and 25 days after declipping (D RHR) and for their normotensive control rats (NCR). Also the mean differences \pm SE and the degree of significance are given concerning arterial pressure resistance at maximal dilatation (flow = 30 ml/min \times 100 g) maximal steepness of the resistance curve (tangent of the angle) and maximal pressor response

	Arterial blood pressure mm Hg	PRU ₉₀ at maximal dilata- tion (flow 30 ml/min)	Tangent of the angle	Maximal pressor response mm Hg
RHR n = 12	180 \pm 6	1 66 \pm 0 07	5 0 \pm 0 3	352 \pm 7
NCR n = 12	111 \pm 3	1 33 \pm 0 05	3 8 \pm 0 3	271 \pm 11
mean difference	69 \pm 8	0 33 \pm 0 02	1 2 \pm 0 4	81 \pm 12
significance	p < 0 001	p < 0 001	p < 0 02	p < 0 001
D RHR 1 day n = 18	105 \pm 3	1 63 \pm 0 06	4 6 \pm 0 2	360 \pm 7
NCR n = 16	110 \pm 2	1 40 \pm 0 03	3 7 \pm 0 2	268 \pm 7
mean difference	-5 \pm 4	0 23 \pm 0 06	0 9 \pm 0 3	97 \pm 10
significance	ns	p < 0 005	p < 0 07	p < 0 001
D RHR 3 days n = 15	105 \pm 2	1 69 \pm 0 06	4 7 \pm 0 2	330 \pm 10
NCR n = 15	108 \pm 2	1 47 \pm 0 03	3 6 \pm 0 3	270 \pm 6
mean difference	-3 \pm 3	0 22 \pm 0 05	1 1 \pm 0 2	60 \pm 11
significance	ns	p < 0 005	p < 0 001	p < 0 001
D RHR 7 days n = 15	107 \pm 2	1 55 \pm 0 03	4 2 \pm 0 3	325 \pm 12
NCR n = 15	104 \pm 2	1 46 \pm 0 05	3 3 \pm 0 2	278 \pm 10
mean difference	3 \pm 2	0 09 \pm 0 07	0 9 \pm 0 4	47 \pm 12
significance	ns	ns	p < 0 05	p < 0 005
D RHR 14 days n = 14	117 \pm 2	1 66 \pm 0 07	3 8 \pm 0 3	316 \pm 10
NCR n = 14	109 \pm 2	1 52 \pm 0 07	3 5 \pm 0 2	281 \pm 10
mean difference	8 \pm 3	0 14 \pm 0 06	0 3 \pm 0 3	35 \pm 11
significance	p < 0 02	ns	ns	p < 0 01
D RHR 25 days n = 12	117 \pm 3	1 60 \pm 0 05	3 3 \pm 0 2	307 \pm 6
NCR n = 12	110 \pm 2	1 48 \pm 0 03	3 3 \pm 0 2	290 \pm 7
mean difference	7 \pm 4	0 12 \pm 0 06	0 0 \pm 0 2	12 \pm 5
significance	ns	ns	ns	ns

Results

Before unclamping the left renal artery the directly measured arterial pressure during awake resting conditions was considerably increased in RHR compared to NCR (p < 0 001) being 180 \pm 6 mm Hg and 111 \pm 3 mm Hg respectively. Already 1 day after removing the clip blood pressure of the declipped RHR (D RHR) was reduced to 105 \pm 3 mm Hg after which there was again some increase pressure being 117 \pm 3 mm Hg after 25 days Shamoperated RHR where the clips were left *in situ* remained hypertensive and they did not differ in pressure compared to unoperated RHR.

Paired perfusion experiments were performed on the hindquarters of one D RHR in parallel with one NCR 1 3 7 14 and 25 days after unclamping the left renal artery as described in Methods. The mean values \pm SE for the different groups concerning the various hemodynamic parameters thus obtained are presented in

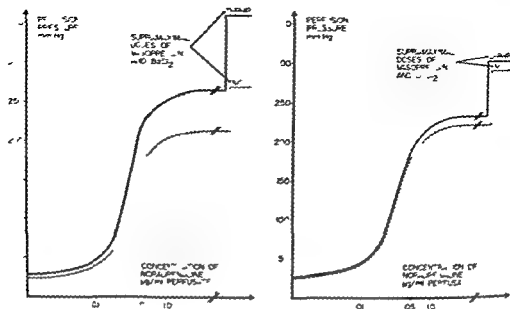


Fig. 1. Left part: Mean resistance curves from 16 paired hindquarter perfusions of renal hypertensive rats 1 day after declipping (D RHR, blood pressure 103 ± 3 mm Hg) and normotensive control rats (NCR, blood pressure 110 ± 2 mm Hg) showing the resistance responses to increasing concentrations of noradrenaline (NA) during constant flow conditions. Maximal pressor response is ensured by supramaximal doses of vasopressin and benzathine. Log NA concentration ($\mu\text{g/ml}$ perfusate) is given on the abscissa and the perfusion pressure (mm Hg) on the ordinate. — The D RHR resistance curve shows significant increases in resistance at maximal dilatation, in maximal steepness and in maximal pressor response, compared to NCR (right part). Mean resistance curves from 12 paired hindquarter perfusions of D RHR 23 days after declipping (blood pressure 117 ± 3 mm Hg) and their matched NCR (blood pressure 110 ± 2 mm Hg). There is no longer any significant difference between the two resistance curves concerning resistance at maximal dilatation, maximal steepness or maximal pressor response.

Table I together with the mean differences \pm S.E. and the degree of significance between D RHR and NCR in each experimental group. The data for RHR before renal artery unclamping given in this table are taken from a recent series of experiments (Lundgren *et al.* 1974).

However, before describing the results compiled in Table I some technical aspects should first be briefly commented. Since all the experiments were run as equally treated pairs, mean differences and degree of significance could be calculated by the pairing design *t* test. Further accidental interferences (e.g. differences in viscosity, temperature or composition of the perfusate) could thereby be largely cancelled out concerning the comparison of RHR and D RHR with their matched NCR. It is on the other hand probably such interferences that mainly

TABLE II Shows mean values \pm S.E. concerning body weight, arterial blood pressure, left ventricular weight and percentage left ventricular weight/body weight for renal hypertensive rats (RHR) before and 1, 3, 7, 14 and 23 days after declipping (D RHR) and for matched normotensive control rats (NCR). The degree of significance between RHR and their weight matched NCR and between D RHR and their matched NCR is also given.

	Body weight g	Arterial blood pressure mm Hg	Left ventricular weight, g	Percentage left ventricular weight/body weight
RHR n = 17	217 \pm 7	178 \pm 4	0.651 \pm 0.027	0.307 \pm 0.011
NCR n = 17	216 \pm 8	108 \pm 2	0.471 \pm 0.017	0.218 \pm 0.003
significance	n.s.	$p < 0.001$	$p < 0.001$	$p < 0.001$
D RHR 1 day n = 16	228 \pm 7	105 \pm 3	0.604 \pm 0.019	0.265 \pm 0.006
NCR n = 16	235 \pm 7	110 \pm 2	0.438 \pm 0.013	0.186 \pm 0.007
significance	$p < 0.005$	n.s.	$p < 0.001$	$p < 0.002$
D RHR 3 days n = 15	273 \pm 8	105 \pm 2	0.650 \pm 0.021	0.238 \pm 0.004
NCR n = 15	274 \pm 10	108 \pm 2	0.509 \pm 0.016	0.187 \pm 0.006
significance	n.s.	n.s.	$p < 0.001$	$p < 0.001$
D RHR 7 days n = 15	272 \pm 6	107 \pm 2	0.591 \pm 0.014	0.216 \pm 0.005
NCR n = 15	270 \pm 7	104 \pm 2	0.496 \pm 0.015	0.184 \pm 0.004
significance	n.s.	n.s.	$p < 0.001$	$p < 0.001$
D RHR 14 days n = 14	293 \pm 5	117 \pm 2	0.584 \pm 0.014	0.200 \pm 0.004
NCR n = 14	293 \pm 5	109 \pm 2	0.521 \pm 0.013	0.179 \pm 0.004
significance	n.s.	$p < 0.02$	$p < 0.002$	$p < 0.001$
D RHR 23 days n = 12	292 \pm 5	117 \pm 3	0.545 \pm 0.020	0.185 \pm 0.006
NCR n = 12	289 \pm 5	110 \pm 2	0.507 \pm 0.013	0.175 \pm 0.005
significance	n.s.	n.s.	n.s.	n.s.

explain why the mean values of the various NCR groups differ slightly. For example even though the perfusate was the same within each paired group it was sometimes necessary to use e.g. different batches of Ficoll for some of the groups as a result of a limited supply. This may of course somewhat affect e.g. the viscosity of the perfusate and hence also the measured values. Such unavoidable though minor differences only serve to illustrate the necessity of using paired experiments in quantitative comparative studies of this type. Further the maximal pressor responses will to a slight degree be affected by a somewhat varying edema formation which moderately raises tissue pressure and correspondingly reduces transmural vascular pressure. This factor is increasingly important towards the end of the experiments and usually to the greatest extent in NCR implying that it tends to slightly reduce the difference between RHR—D RHR and NCR with respect to the maximal pressor response.

Anyhow Table I shows that already 1 day after unclamping the left renal artery mean arterial pressure of D RHR is normalized and after 3 weeks of normotension the hypertensive structural changes of the resistance vessels have largely disappeared.

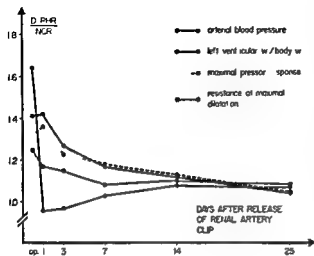


Fig 2 Time course and extent of regression of the hypertensive changes in cardiovascular design after reversal of renal hypertension. Days after declipping are plotted along the abscissa and along the ordinate the ratios between renal hypertensive rats (RHR) before and after (D RHR) declipping and their normotensive control rats (NCR), concerning 1) arterial pressure 2) left ventricular weight/body weight 3) maximal pressor response and 4) flow resistance at maximal dilatation (flow = 30 ml/min \times 100 g). Thus the cardiovascular system still displays structural hypertensive changes one day after declipping but rapid regression then occurs with normalization after about 3 weeks.

Concerning details of the regressive changes it is seen that already 3 days after unclamping there is a slight though not yet significant decrease of the resistance at maximal dilatation in D RHR. After 1 week however this parameter reflecting the luminal size is almost normalized since there is no longer any significant difference between D RHR and NCR and no further significant decrease in resistance at maximal dilatation occurred later.

The maximal steepness of the dose response curve to NA is on the other hand still significantly increased in D RHR 1 week after declipping but after 2 weeks it hardly differs from that of NCR and after 3 weeks it is completely normalized. This indicates a full regression by that time of the earlier enhanced wall/lumen ratio. Likewise the maximal pressor response reflecting primarily the bulk of contractile tissue in relation to the lumen shows rapid regression even though it is still significantly raised in D RHR compared to NCR 2 weeks after declipping. However at that time D RHR differs significantly also from control RHR when comparing the mean differences between D RHR—NCR and RHR—NCR by the group comparison *t* test. After about 3 weeks D RHR and NCR no longer differ indicating a largely complete regression of the earlier present media hypertrophy. Concerning vascular sensitivity to noradrenaline there was at no stage any difference between RHR or D RHR and NCR to judge from the threshold dose of NA i.e. the dose raising resistance 25% above the level of maximal dilatation.

The left part of Fig 1 presents the mean resistance curve of D RHR 1 day after

declipping and that of their matched NCR while the right part presents those of D RHR and NCR 25 days after unclamping. It can be seen that one day after declipping the D RHR resistance curve shows a significantly increased flow resistance at maximal dilatation ($p < 0.005$) an exaggerated curve steepness ($p < 0.02$) and a raised maximal pressor response ($p < 0.001$), compared with NCR indicating hypertensive changes in vascular design. However 25 days after unclamping (right part) there is a largely complete regression of these changes when the D RHR and NCR resistance curves are compared. Thus the earlier hypertensive vascular bed has now become structurally fully readapted to normal pressure conditions.

Table II shows that the regression of the left ventricular hypertrophy after declipping of RHR closely parallels the regression of the structural vascular changes particularly that of the media hypertrophy as judged mainly by the changes in maximal pressor response. This is also clear from Fig. 2 which diagrammatically illustrates the time course of the decrease in blood pressure in comparison with the regression of vascular and cardiac hypertrophy. Days after operation (declipping) are here plotted along the abscissa and on the ordinate are plotted the ratios of RHR/NCR and D RHR/NCR with respect to 1) arterial pressure 2) percentage left ventricular weight/body weight 3) maximal pressor response and 4) resistance at maximal dilatation.

Discussion

Regional hemodynamic studies in man with essential hypertension suggest that the well documented resistance increase during resting tone may be almost entirely ascribed to a structural adaptation of the resistance vessels showing clear signs of an increased wall/lumen ratio in association with a lumen that is reduced even at maximal dilatation (Folkow, Grimby and Thulesius 1958, Conway 1963, Sivertsson 1970 cf Folkow *et al* 1972 a, 1973 a). The findings are supported and extended by more detailed studies on spontaneously hypertensive rats (SHR, Okamoto 1969) and on renal hypertensive rats (RHR) involving experiments on both the entire systemic circuit of SHR (Folkow *et al* 1970 a) and on the isolated hindquarter vascular bed of SHR and RHR (Folkow *et al* 1970 b, Lundgren *et al* 1974). Briefly this type of changed design of the resistance vessels implies that a raised resistance can be maintained at a normal smooth muscle tone and that exaggerated resistance shifts are elicited for given changes in muscle activity. Quantitative morphological analyses of the resistance vessels by Suwa's group (Furuyama 1962, Suwa and Takahashi 1971) and morphological and chemical studies on the thoracic aorta of renal hypertensive rats by Wolinsky (1970, 1971) also document the presence of a media hypertrophy.

Enforced reductions in pressure, either regionally by arterial obstructions or generally by hypotensive drug treatment induce rapid regression of the hypertensive vascular changes (e.g. Folkow and Svertson 1968 Weiss 1974 Weiss and Hallback 1974). Further immunosympathectomy in newborn SHR or aortic obstruction in young SHR largely prevent the development of the mentioned hypertensive vascular changes (Folkow *et al* 1971 Folkow *et al* 1972b). These studies strongly suggest that the changes mainly represent a regional structural adaptation to the average pressure load.

The present study on rats was performed in order to investigate how rapidly and to what extent regression of the mentioned hypertensive vascular changes and the left ventricular hypertrophy in renal hypertension occurs if the renal artery clip is eliminated. According to an earlier study (Lundgren *et al* 1974) cardiovascular hypertrophy is fully developed 3–4 weeks after renal artery constriction in young normotensive male Wistar rats. At this time when the cardiovascular system seems to have adapted completely to the raised blood pressure, the renal artery constriction was released and arterial pressure was normalized already after one day. The paired hindquarter perfusions, performed on one declipped RHR (D RHR) and one matched NCR, 1 3 7 14 and 25 days after declipping and the changes in left ventricular weight revealed that 1 and 3 days after operation there was not yet any significant difference in cardiovascular design compared to unoperated RHR. However both the cardiac and vascular hypertrophic changes rapidly diminished during the subsequent days and weeks and were fully eliminated after about 3 weeks. Resistance at maximal dilatation seemed to be the parameter most rapidly normalized already after about 1 week indicating a rapid increase of the vascular lumina to normal size. Thereafter the increased steepness of the D RHR resistance curve disappeared indicating a largely normalized wall/lumen ratio closely followed by the maximal pressor response representing mainly the bulk of contractile wall tissue together with the left ventricular weight which were normalized in about 3 weeks. Thus the time course and the extent of the regression of the left ventricular hypertrophy and the parameters indicating vascular media hypertrophy were nearly identical suggesting a close similarity in structural adaptation of cardiac and vascular smooth muscles.

These results are in good agreement with those of Wolinsky (1971 1972) who found a considerable decrease in the smooth muscle component of rat thoracic aorta after reversal of renal hypertension. However Wolinsky did not observe any complete regression of media thickness in the thoracic aorta after declipping at least not in male rats. This apparent difference from the present findings is probably due both to the different durations of hypertension 4 weeks in the present experiments and 10 weeks in Wolinsky's experiments and to the difference in design between the true resistance vessels and the aorta in which the relative proportions of collagen and elastin are much higher. In Wolinsky's experiments the increased amounts of elastin and collagen in the aorta did not show any appreciable regression after

reversal of renal hypertension. In the resistance vessels proper, where the relative proportions of such elements are normally much smaller, a substantial increase of collagen content may call for a fairly longlasting hypertension. However, once a substantial collagen invasion has occurred also in the resistance vessels its regression may be about as sluggish as in the aorta. Thus the structural hypertensive changes of the resistance vessels might be far more persistent if for example renal hypertension had lasted for many months instead of 4 weeks as in the present experiments which are now being explored.

From the present study it is clear that blood pressure in early renal hypertension of rats decreases to normal level already one day after release of the renal artery constriction despite the presence of considerable hypertrophic cardiovascular changes. This may at first sight seem surprising but earlier studies (see Ledingham 1971, Funder *et al* 1970) have shown that this rapid pressure normalization is due to the fact that declipping brings about a sharp reduction in cardiac output while resistance if anything further increases at least in short term measurements (6–7 h). It is possible that the sudden overperfusion of the earlier obstructed kidney initiates complex neurohormonal and fluid shifts where among other possibilities the neurogenic tonic influences might even become subnormal. This situation is indeed exceedingly complex and calls for much further attention. Whatever the mechanism the reduced blood pressure will lead to a rapid and full regression of the structural cardiovascular changes and hence to a stabilization of the normotensive state. If however the clipped kidney is instead extirpated the hypertensive state tends to prevail compared to equally treated normotensive animals indicating extrarenal pressor mechanisms (e.g. Pickering 1945, Floyer 1950, Funder *et al* 1970). It is possible that the presently documented "structural autoregulation" of the resistance vessels is in reality identical with the proposed extrarenal pressor mechanisms.

Further together with the results of e.g. Wolinsky (1971, 1972) and Weiss (1974) the present results also illustrate the advantages of an early induction of anti-hypertensive therapy. Also the results by Toban and coworkers (1969) point in such a direction since no substantial decrease in mesenteric arteriolar wall thickness was observed after reversal of longstanding renal hypertension (9 months duration) apart from some decrease in water content. This decreased water content of arteriolar walls after declipping in longlasting hypertension may reflect that some water logging occurs in later stages (see also Lundgren *et al* 1974) though such a factor will hardly affect the wall/lumen ratio of the resistance vessels as much as media hypertrophy or collagen invasion. If however blood pressure is normalized by suitable therapy before substantial increases of elastin and collagen occur the more rapidly established hypertrophic wall changes may well disappear completely and rather rapidly to judge from the present results. This has also the great advantage that the tendency of a vicious circle inherent in the potentiation concerning the pressor effects between these adaptive hypertrophic changes and functional excitatory influences (*cf* Folkow *et al* 1973) may be effectively interrupted.

This study has been sponsored by grants from the Swedish Medical Research Council (No B74 14\ 16 10C) from the Swedish National Association against Heart and Chest Diseases and from the Medical Faculty University of Göteborg

AB Hassle generously covered part of the expenses for a technician

References

- CONNAY J Vascular abnormality in hypertension Study of blood flow in the forearm *Circulation* 1963 27 520—529
- FLOYER M A Further studies on the mechanism of experimental hypertension in the rat *Clin Sci* 1955 14 163—181
- FOLKOW B G GRIBBY and O THULESSON Adaptive structural changes of the vascular walls in hypertension and their relation to the control of the peripheral resistance *Acta physiol scand* 1958 44 255—272
- FOLKOW B M GURBACH M HALLBACK Y LUNDGREN and L WEISS Hemodynamic consequences of regional hypotension spontaneously hypertensive and normotensive rats *Acta physiol scand* 1971 83 532—541
- FOLKOW B M HALLBACK Y LUNDGREN R SIVERTSSON and L WEISS The importance of adaptive changes in vascular design for the establishment and maintenance of primary hypertension as studied in man and SHR *Spontaneous Hypertension* Ed A Okamoto Igaku Shoin Ltd Tokyo 1972 a 103—115
- FOLKOW B M HALLBACK Y LUNDGREN R SIVERTSSON and L WEISS Importance of adaptive changes in vascular design for establishment of primary hypertension studied in man and in spontaneously hypertensive rats *Circulat Res* 1973 a 32—33 Suppl I 1 2—13
- FOLKOW B M HALLBACK Y LUNDGREN and L WEISS Structurally based increase of flow resistance in spontaneously hypertensive rats *Acta physiol scand* 1970 a 79 373—378
- FOLKOW B M HALLBACK Y LUNDGREN and L WEISS Background of increased flow resistance and vascular reactivity in spontaneously hypertensive rats *Acta physiol scand* 1970 b 80 93—106
- FOLKOW B M HALLBACK Y LUNDGREN and L WEISS Effects of immunosympathectomy on blood pressure and vascular reactivity in normal and spontaneously hypertensive rats *Acta physiol scand* 1972 b 84 512—523
- FOLKOW B M HALLBACK Y LUNDGREN and L WEISS Time course and extent of structural adaptation of the resistance vessels in renal hypertensive rats (RHR) as compared with spontaneously hypertensive rats (SHR) *Acta physiol scand* 1973 b 87 10A—11A
- FOLKOW B and R SIVERTSSON Adaptive changes in reactivity and wall/lumen ratio in rat blood vessels exposed to prolonged transmural pressure difference *Life Sci* 1968 7 1783—1289
- FUNDER J W J R BLAIR WEST M C CAIRN K J CATT J P COOGLAN D A DEVTON J F NELSON B A SCOCORNS and R D WRIGHT Circulatory and humoral changes in the reversal of renovascular hypertension in sheep by unclipping the renal artery *Circulat Res* 1970 27 249—258
- FURUYAMA M Histometrical investigations of arteries in reference to arterial hypertension *Tohoku J exp Med* 1962 76 388—414
- LEDINCHAM J M Mechanisms in renal hypertension *Proc roy Soc Med* 1971 64 409—418
- LUNDGREN Y M HALLBACK L WEISS and B FOLKOW Rate and extent of adaptive cardiovascular changes in rats during experimental renal hypertension *Acta physiol scand* 1974 91 103—115
- OKAMOTO K Spontaneous hypertension in rats *Int Rev exp Path* 1969 7 227—270
- PICKERING C W The role of the kidney in acute and chronic hypertension following renal artery constriction in the rabbit *Clin Sci* 1945 5 229—247
- PICKERING C W *High blood pressure* London J & A Churchill 1968
- SIVERTSSON R Hemodynamic importance of structural vascular changes in essential hypertension *Acta physiol and* 1970 Suppl 343 6—56
- SUWA N and T TAKAMIZU *Morphological and morphometrical analysis of circulation in hypertension and ischemic kidney* Munich—Berlin—Wien Urban and Schwarzenberg 1971
- TOLIAN L R OLSON and G CHESLEY Water content of arteriolar wall in renovascular hypertension *Amer J Physiol* 1969 216 22—24
- WEISS L Long term treatment with antihypertensive drugs in spontaneously hypertensive rats Effects on blood pressure survival rate and cardiovascular design *Acta physiol scand* 1974 91 393—408

- WEISS L and M HALLBÄCK Time course and extent of structural vascular adaptation to regional hypotension in adult spontaneously hypertensive rats (SHR) *Acta physiol scand* 1974 91 365—373
- WOLINSKI H Response of the rat aortic media to hypertension *Circulat Res* 1970 26 507—527
- WOLDEN H Effects of hypertension and its reversal on the thoracic aorta of male and female rats *Circulat Res* 1971 28 622—637
- WOLINSKI H Long term effects of hypertension on the rat aortic wall and their relation to concurrent aging changes *Circulat Res* 1972 30 301—309

Dependence of Basic Secretion of Antidiuretic Hormone on Cerebrospinal Fluid $[Na^+]$

By

KERSTIN OLSSON and RIGOR KOLMODIN

Recently it was shown that the secretion of antidiuretic hormone (ADH) in the non hydrated goat subsides during intracarotid infusions of slightly hypertonic solutions of galactose and glycerol (Olsson and Kolmodin 1974). The results appear incompatible with the idea that the basic release of ADH from the neurohypophysis in non hydrated subjects is due to a continuous stimulation of a hypothalamic osmoreceptor mechanism (Verney 1947). Previous studies in the goat (cf Andersson 1971) suggest that a central $[Na^+]$ sensitive receptor system near the third cerebral ventricle participates in the regulation of the ADH release. Therefore it was assumed that the ultimate cause of the inhibition of the ADH release observed during intracarotid infusions of galactose and glycerol solutions might have been a lowering of the $[Na^+]$ of the cerebrospinal fluid (CSF). The experiments reported here provide further support for the idea that intracarotid infusions of certain non electrolyte solutions inhibit the ADH secretion by reducing the $[Na^+]$ of the CSF.

6 adult female goats were used. The animals were routinely kept in metabolism cages where all the experiments were conducted. All goats had polyvinyl catheters permanently implanted into the carotid artery. During the infusions the free end of the vascular catheter was connected to a perfusion pump via a polyethylene tubing.

In addition to the vascular catheters two of the goats were provided with a permanent three-cannula system in one of the lateral cerebral ventricles (Åkerlund, Andersson and Olsson 1973). During intraventricular infusions the free end of the inner cannula of this system was connected to an infusion pump via a polyethylene tubing.

The osmolality of the urine was determined by use of an "Advanced Instruments" osmometer. Since previous studies had revealed a mean plasma osmolality of 294 mosm/kg in the non hydrated goat (Fricksen, Fernández and Olsson 1971) this value was used for calculations of renal free water clearance (C_{H_2O}) in the present experiments.

Intracarotid infusions. The 90 min intracarotid infusions of 0.5 M galactose ($n=11$) (Fig. 1, circles) and of 0.5 M d-glucose ($n=6$) at the rate of 3.75 ml/min invariably induced a water diuresis in the non hydrated goats. The initially negative renal C_{H_2O} became positive about 50 min after onset of the infusion. It continued to rise during the following 20 min and then remained at a high level throughout the infusion period. After cessation of the infusion renal C_{H_2O} began to fall and became negative again within 30 min. Intravenous injections of 3 mU of arginine

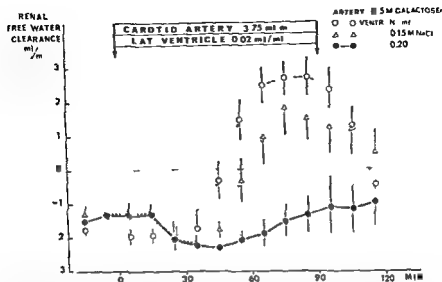


Fig 1 **Circles** Induction of a pronounced water diuresis in non hydrated goats by the intra carotid infusion of 0.5 M galactose solution (10 expts 4 goats) **Dots** Total blocking of this water-diuretic response by the simultaneous low infusion of slightly hypertonic NaCl into the lateral cerebral ventricle (7 expts 2 goats) **Triangles** Delayed and reduced water diuresis during the combined infusion of 0.5 M galactose into the carotid artery and isotonic NaCl into the lateral ventricle (6 expts 2 goats) Each symbol represents mean Vertical bars = S.E.

vasopressin were made when the renal C_{H_2O} had risen to a positive value during one of the intracarotid d glucose and one of the intracarotid galactose infusions (not included in Fig 1) This administration of exogenous ADH rapidly reversed the positive renal C_{H_2O} to negativity The inhibition of the water diuresis lasted for 30 min in the galactose and for 40 min in the glucose experiment i.e just before respectively 10 min after cessation of the intracarotid infusions

Combined intracarotid and intraventricular infusions In another series of experiments isotonic (0.15 M) or slightly hypertonic (0.2 M) NaCl solutions were infused for 90 min into the lateral cerebral ventricle at the rate of 0.02 ml/min concomitantly with the intracarotid infusions of 0.5 M galactose. When isotonic NaCl was infused into the lateral ventricle ($n = 6$) the water-diuretic response to the intracarotid galactose infusion was delayed and reduced (Fig 1 triangles) No water diuresis at all developed during intracarotid infusions of galactose performed simultaneously with the intraventricular infusion of 0.2 M NaCl ($n = 7$) (Fig 1 dots) Thus arrest of the water diuresis was obtained regardless of whether the intraventricular infusion of NaCl was performed ipsilaterally or contralaterally to the intracarotid galactose infusion

Studies of central sodium angiotensin interaction have given rise to the suggestion that an alternative to hypothalamic osmoreceptors in Verney's (1947) sense may

be receptors in the vicinity of the third ventricle which are affected by the $[Na]$ of the CSF (Andersson 1971). Experiments in the goat involving a lowering of the $[Na]$ of the CSF, without reduction of its osmolality lend support to this idea. The ADH releasing and dipsogenic effects of intracarotid infusions of hypertonic NaCl can be blocked by slow infusions of isotonic or hypertonic saccharide solutions into the CSF of the lateral cerebral ventricles (Olsson 1973). The aim of this study was to obtain additional evidence that the observed arrest of the ADH secretion was due to a reduced CSF $[Na]$ and was not related to the osmolality of the solutions infused into the carotid artery. Such evidence has been provided by the following observations. The water diuretic response to intracarotid infusions of 0.5 M galactose was as pronounced as that observed during previous infusions of 0.35 M galactose (Olsson and Holmodin 1974) and it was arrested effectively by a slow infusion of slightly hypertonic NaCl into the CSF of the lateral ventricle. This happened regardless of whether the NaCl was administered into the CSF of the ventricle located ipsilateral or contralateral to the carotid galactose infusion. It indicates that the Na ions acted below the lateral ventricle probably in the anterior part of the third ventricle as judged from the effects of intraventricular infusions of hypertonic NaCl in this species (Andersson, Dallman and Olsson 1969).

In conclusion the results of this study support the idea that the basic release of ADH in non-hydrated normovolemic subjects is due to a continuous weak stimulation of periventricular Na-sensitive receptors.

This work was supported by the Swedish Medical Research Council (Project No 3399).

References

- ANDERSSON, L. E. I., ANDERSSON, K. and OLSSON, K. A cannula system for frequent infusions into the CSF of the cerebral ventricles of the goat. *Physiol. Behav.* 1973, 10, 161—162.
- ANDERSSON, L. E. I. Thirst and brain control of water balance. *Amer. Scientist* 1971, 59, 400—411.
- ANDERSSON, L. E. I., DALLMAN, M. J. and OLSSON, K. Observations on central control of drinking and the release of antidiuretic hormone (ADH). *Life Sci* 1969, (1), 0, 425—432.
- ERIKSSON, L. O., FERNANDEZ, J. and OLSSON, K. Differences in the antidiuretic response to intracarotid infusions of various hypertonic solutions in the conscious goat. *Acta physiol. scand.* 1972, 83, 551—562.
- OLSSON, K. Further evidence for the importance of CSF $[Na]$ concentration in central control of fluid balance. *Acta physiol. scand.* 1973, 88, 183—189.
- OLSSON, K. and R. HOLMODIN. Inhibition of ADH secretion by intracarotid infusions of slightly hypertonic non-electrolyte solutions. *Acta endocr. (Copenh.)* 1974, 76, 53—58.
- VERNEY, E. B. The antidiuretic hormone and the factors which determine its release. *Proc. roy. Soc. B* 1971, 171, 105.

Action of Drugs on the Innervated and Denervated Urinary Bladder of the Rat

By

MATS ELMER

Received 13 November 1973

Abstract

ELMER M: Action of drugs on the innervated and denervated urinary bladder of the rat. *Acta physiol scand* 1974 91 289-297

In the normally innervated rat bladder methacholine, acetylcholine, adrenaline and phenylephrine elicited contraction of the detrusor muscle *in situ*, while isoprenaline caused relaxation. The response to noradrenaline varied but was most often relaxation. Experiments with dihydroergotamine and propranolol indicated the presence of both excitatory α receptors and inhibitory β receptors in the detrusor muscle. The bladder developed supersensitivity to parasympathomimetic agents and in the case of α receptor mediated effects also to sympathomimetic agents after parasympathetic decentralization and denervation and after sympathetic denervation. Regarding the adrenergic β receptor effects however no supersensitivity developed after any of the denervation procedures. Parasympathetic denervation or decentralization uncovered a contractile response to noradrenaline most often masked by predominant relaxation in the normal bladder.

Lesions to the motor nerves of the urinary bladder give rise to a spastically paralytic bladder showing autonomous contractions. This phenomenon occurs in man (Lapides *et al* 1962), in the dog (Jacobson 1945) and in the cat (Carpenter and Root 1961). Lapides *et al* showed an increased bladder response to stretch after administration of urecholine to patients with motor nerve lesions and proposed that the autonomous bladder is a result of supersensitivity of the detrusor muscle to acetylcholine.

The urinary bladder of man, cat and dog contains intramural ganglia which means that section of both pelvic nerves results in a parasympathetic decentralization of the bladder. Development of supersensitivity in the parasympathetically decentralized bladder has not yet been studied in experimental animals (Taira 1972). In contrast to other species the rat bladder receives parasympathetic axons from ganglia situated outside the organ and it is possible to perform a postganglionic parasympathetic denervation (Carpenter and Rubin 1967). In earlier work the sensitivity of the rat bladder to acetylcholine or carbachol was not found to be significantly

changed 4–8 days after total bilateral denervation (Carpenter and Rand 1965) or 14 days after unilateral denervation (Carpenter and Rubin 1967)

In the present study the sensitivity of the urinary bladder of the rat was examined after parasympathetic decentralization and denervation as well as after sympathetic denervation

Methods

95 male albino rats of the Sprague Dawley strain were used. The animals weighing about 350 g were 8–11 months old when studied.

Denervation procedures. Postganglionic sympathetic denervation was performed in one group of rats by section of the hypogastric nerves distal to the hypogastric ganglia below the bifurcation of the aorta. In another group the bladder was parasympathetically decentralized by section of the pelvic nerves proximal to the pelvic plexa which in the male rat form distinct ganglia located on the lateral surface of the prostate gland (Langworthy 1963). Bilateral postganglionic denervation was achieved by extirpation of the pelvic ganglia. This procedure results in sympathetic as well as parasympathetic denervation since the postganglionic sympathetic fibres of the hypogastric nerves pass through the pelvic ganglia. In one group of rats the bladder was both parasympathetically decentralized and sympathetically denervated. The operations were performed aseptically using ether anaesthesia. In the rats with divided parasympathetic nerves the bladder had to be emptied daily by manual pressure using ether anaesthesia. Despite this treatment these bladders always contained some residual urine and often weighed over 3 times more than controls when examined about 2 weeks after the nerves had been cut. To avoid bacterial infection the animals were given a sulfonamide (Sulfino® Nordmark Werke 20 mg/day) subcutaneously.

Intravesical pressure recording. 14–18 days after the operations the intravesical pressure was recorded *in situ* by way of a glass cannula inserted into the bladder through an incision in the exposed urethra as described earlier (Elmer 1973). The rats were anesthetized with orolose (100 mg/kg) given through a cannula in a femoral vein after induction with ether.

Drugs. The substances used were methacholine chloride, acetylcholine chloride, adrenaline bitartrate, noradrenaline bitartrate, phenylephrine hydrochloride, isoprenaline sulphate, atropine sulphate, dihydroergotamine methanesulphonate and propranolol hydrochloride. The drugs were injected through the cannula in the femoral vein.

Statistical analysis. For statistical evaluation of the data Student's *t* test for unpaired sample was used. The 0.05 level of probability was accepted as significant.

Results

Normally innervated bladders. Methacholine (Fig. 1a), acetylcholine, adrenaline (Fig. 3) and phenylephrine elicited contraction of the detrusor muscle while isoprenaline caused relaxation. The response to noradrenaline was a relaxation of 1–2 mm Hg in 10 rats (Fig. 2a) and a contraction of 1–3 mm Hg in 4 rats. Atropine 1 mg/kg totally abolished the contractile response to methacholine and acetylcholine given in doses up to 10 µg/kg but did not affect the responses to 0.1–10 µg/kg of adrenaline, phenylephrine, noradrenaline or isoprenaline. After injection of dihydroergotamine 2 mg/kg the contraction caused by adrenaline was changed into a relaxation which could be inhibited by the administration of propranolol 2–4 mg/kg (Fig. 3). After propranolol the contraction caused by adrenaline was increased by 1–3 mm Hg. Noradrenaline given after propranolol always caused a contraction which was abolished by dihydroergotamine.

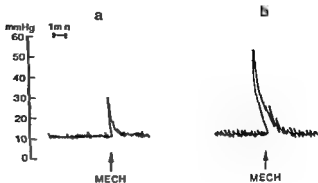


Fig 1 Pressure response to methacholine $1 \mu\text{g/kg}$ (MECH) a, Normally innervated bladder b 17 days after total denervation

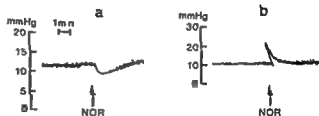


Fig 2 Pressure response to noradrenaline $1 \mu\text{g/kg}$ (NOR) a, Normally innervated bladder b 17 days after total denervation

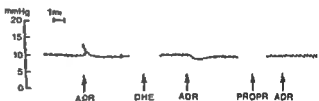


Fig 3 Pressure response to adrenaline $1 \mu\text{g/kg}$ (ADR) in a normally innervated bladder DHE dihydroergotamine 2 mg/kg PROPR propranolol 2 mg/kg

Denervated bladders The threshold doses and the pressure responses above a resting level of about 10 mm Hg of the denervated bladders to a suprathreshold dose of each drug are compared to normally innervated control bladders in Fig 4—7. The resting level and the small spontaneous contractions present in the normal bladders were not affected by denervation.

Methacholine and acetylcholine An increased sensitivity to methacholine and acetylcholine was found after parasympathetic denervation and decentralization (Fig 4). The supersensitivity to methacholine was less marked after decentralization than after denervation ($p < 0.05$). After sympathetic denervation the threshold doses were lowered but the responses to $1 \mu\text{g/kg}$ were not significantly changed. However, the responses were increased more after combined sympathetic denervation and parasympathetic decentralization than after parasympathetic decentralization alone ($p < 0.05$). Fig 1 shows the response to methacholine ($1 \mu\text{g/kg}$) which is more than doubled 17 days after total denervation.

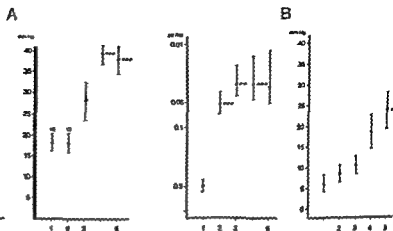


Fig 4 A Methacholine B Acetylcholine

Threshold doses (to the left) and pressure responses to 1 μ g/kg (to the right) of the normally innervated (1) sympathetically denervated (2) parasympathetically decentralized (3) totally denervated (4) and parasympathetically decentralized and sympathetically denervated (5) urinary bladder. The vertical lines represent \pm standard error of mean. The figures above the vertical lines indicate the number of rats examined.

* $p < 0.05$ **

$p < 0.01$ *** $p < 0.001$

Adrenaline The sensitivity of the bladder to adrenaline was increased after sympathetic denervation as well as after parasympathetic denervation and decentralization (Fig 5 a). Sympathetic denervation seemed to be the most effective denervation procedure in lowering the threshold dose to adrenaline and parasympathetic denervation appeared more effective than decentralization but the differences were not significant.

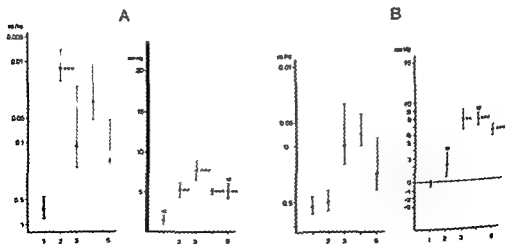


Fig 5 A Adrenaline B Noradrenaline

Threshold doses (to the left) and pressure responses to 0.5 and 1 μ g/kg respectively (to the right). Symbols as in Fig 4.

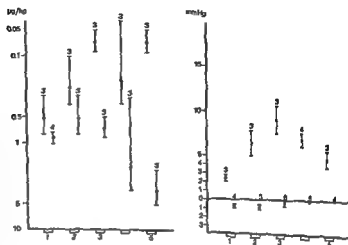


Fig 6 Threshold doses of noradrenaline (to the left) and pressure responses to 1 μ g/kg (to the right) after propranolol 4 mg/kg (closed circles) and after d hydroergotamine 11 mg/kg (open circles). Symbols as in Fig 4

Noradrenaline Sympathetic denervation did not sensitize the bladder to noradrenaline (Fig 5 b). Parasympathetic denervation or decentralization however not only lowered the threshold doses but also turned the predominant relaxation of the bladder into a contraction (Fig 2). The supersensitivity was somewhat less marked after decentralization than after denervation. When the pelvic ganglia were extirpated immediately before the experiment the response to noradrenaline was still a relaxation of the detrusor muscle and the sensitivity was not increased.

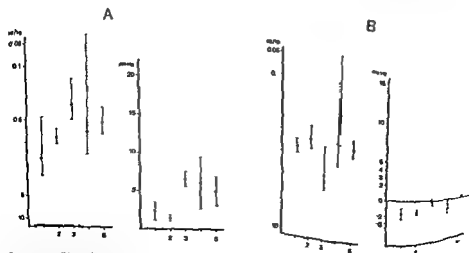


Fig 7 A Phenylephrine B Isoprenaline Threshold doses (to the left) and pressure responses to 1 μ g/kg (to the right) in Fig 4

After the administration of propranolol 4 mg/kg the contractile response to noradrenaline was increased after sympathetic denervation as well as after parasympathetic denervation and decentralization (Fig 6). The relaxation caused by noradrenaline after the injection of 2 mg/kg of dihydroergotamine was however not changed by any of the denervation procedures.

Phenylephrine and isoprenaline The sensitivity of the detrusor muscle to phenylephrine was not significantly changed by sympathetic denervation, which may be explained by the small number of animals studied. Parasympathetic decentralization however caused an increased response to 1 μ g/kg (Fig 7 a). None of the denervation procedures caused any change of the sensitivity of the bladder to isoprenaline (Fig 7 b).

Discussion

The excitatory effect of parasympathomimetic agents on the detrusor muscle shown by Edmunds and Roth (1920) in the cat by Carpenter (1963) in the rat *in vitro* and by Vano (1965) in the rat *in situ* was also found in this study.

However the responses to adrenaline and noradrenaline were not found by Vano (1965) using pithed rats and recording the responses of the bladder as contractions in the axis from the urethra to the vertex instead of changes in the intravesical pressure.

The responses to the catecholamines can be expressed in terms of adrenergic α and β receptors (Ahluwist 1948) as is the case in the urinary bladder of cats and rabbits (Edwards and Setcklen 1968, Sjostrand, Sjogren and Schmitterlow 1972) and dogs (Dhasmana, Gupta and Bhargava 1970). In the present experiments the β stimulating agent isoprenaline imitated the inhibitory response to noradrenaline and after β receptor blockade the response to noradrenaline was always a contraction. The excitatory response to adrenaline was mimicked by the α stimulating agent phenylephrine and after α receptor blockade adrenaline caused relaxation of the bladder. Adrenaline exerted its effect mainly on the excitatory α receptors but the increased contraction caused by adrenaline after β receptor blockade indicates that normally the inhibitory β receptors were also stimulated. These results indicate that the detrusor muscle of the rat contains both excitatory α receptors and inhibitory β receptor.

The increased tone and the autonomous contractions described in other species after denervation (Lapides *et al.* 1962, Jacobson 1945, Carpenter and Root 1961) were not found in this study in the rat. A reason for this may be that the bladders in the present paper were studied about 2 weeks after denervation while the autonomous activity described in the other species did not appear until 3 or more weeks after the operations.

The increased sensitivity of the denervated bladder to parasympathomimetic agents found in this study was not obtained by Carpenter and Rand (1965). This may be explained by the different method used. They stated that section of the

pelvic nerves caused lesions of the blood supply to the bladder¹ furthermore instead of emptying the bladder daily by manual pressure they placed a ligature around the bladder neck above the ureters. Unilateral denervation does not cause any supersensitivity to parasympathomimetic drugs probably because the axons from either side distribute bilaterally in the detrusor muscle (Carpenter and Rubin 1967).

The sensitization of the urinary bladder shows the general characteristics of a denervation supersensitivity as described by Cannon and Rosenblueth (1949)

1 The threshold doses to the drugs were lowered

2 A suprathreshold dose of a drug caused a larger response in the denervated than in the control bladder. This increase could partly be due to the hypertrophy of the detrusor muscle after parasympathetic denervation but the response increased also after sympathetic denervation when no hypertrophy was found. Sympathetic denervation was in most cases not so effective in causing supersensitivity as parasympathetic decentralization which may partly be explained by the sparse adrenergic innervation of the detrusor (El Badawi and Schenk 1966). Moreover the sympathetic denervation was probably incomplete since sympathetic fibres outside the hypogastric nerve have been described. Giannuzzi (1863) predicted the existence of an accessory hypogastric nerve in the cat on the basis of stimulation experiments and morphological studies have shown adrenergic nerve fibres in the pelvic nerve of the cat (Hamberger and Norberg 1965) and of the rat (Alm and Elmer unpublished observation).

3 The supersensitivity at least to some drugs was found to be less marked after parasympathetic decentralization than after denervation in agreement with the law of denervation (Cannon 1939). This is also the case in the parotid gland which like the rat urinary bladder receives postganglionic parasympathetic axons from ganglia situated outside the organ making it possible to perform a parasympathetic denervation (Stromblad 1955). In the sphincter of the pupil which also belongs to the few structures in which the postganglionic parasympathetic fibres can be cut supersensitivity develops both after decentralization and after denervation (Anderson 1905; Shen and Cannon 1936). In this case however denervation was not found to be more effective than decentralization.

4 The sensitization was unspecific either parasympathetic or sympathetic denervation causing supersensitivity to both parasympathomimetic and sympathomimetic agents. The β receptor mediated effect on the bladder however was not increased by any of the denervation procedures. This is in contrast to the secretory effect on the submaxillary gland of the rat which is also supplied with both α and β receptors and in which denervation supersensitivity develops both to α and β stimulating agents (Emmelin, Holmberg and Ohlin 1965). It is on the other hand in accordance with the finding that denervation in the inhibitory nerve-muscle system does not result in greater irritability to the inhibitory action of adrenaline (Elliott 1905).

The finding that the response to noradrenaline was unchanged in the acutely denervated bladder indicates that the altered responses of the chronically den-

erated detrusor muscle were due to supersensitivity and not to changes in the blood flow to the bladder or any other effect of the denervation

The relaxation caused by exogenous noradrenaline in most of the normally innervated bladders is not consistent with the finding that stimulation of the sympathetic fibres in the hypogastric nerve causes contraction in the cat and monkey (Sherrington 1892) in the dog cat and rabbit (Langley and Anderson 1895) and in the rat (Elmer unpublished observation) Sigg and Sigg (1964) investigated whether sympathetic denervation could make the cat bladder super sensitive to exaggerate a contractile response to exogenous noradrenaline that might be masked by predominant relaxation in the normal bladder However the sympathetically denervated bladder did not become supersensitive to respond with contraction to noradrenaline when no adrenergic blocking agents were used Because of these findings Sigg and Sigg proposed that a cholinergic mechanism is involved in sympathetic nerve bladder transmission In the present investigation however a contractile response to noradrenaline was obtained after parasympathetic denervation and decentralization These findings indicate that the excitatory receptors of the detrusor muscle described in this paper after sensitization can be stimulated by exogenous noradrenaline and accordingly it is not necessary because of this evidence to assume a non adrenergic mechanism to be involved in sympathetic nerve bladder transmission

This work was supported by grants from the Medical Faculty University of Lund
Sulfuno was kindly supplied by Nordmark-Werke Hamburg

References

- ANLIQUIST R P A study of the adrenergic receptors *Amer J Physiol* 1948 133 586—600
ANDERSON H K The paralysis of involuntary muscle Part II On paralysis of the sphincter of the pupil with special reference to paradoxical constriction and the functions of the ciliary ganglion *J Physiol (Lond)* 1905 33 156—174
CANNON W B A law of denervation *Amer J med Sci* 1939 198 737—750
CANNON W B and A ROSENBLUTH *The Supersensitivity of Denervated Structures* Experimental Biology Monographs New York Macmillan 1949
CARPENTER F G Excitation of rat urinary bladder by coaxial electrodes and by chemical agents *Am J Physiol* 1963 204 727—731
CARPENTER F G and S A RAND Relation of acetylcholine release to responses of the rat urinary bladder *J Physiol (Lond)* 1963 180 371—382
CARPENTER F G and W S ROOF Effect of parasympathetic denervation on feline bladder function *Am J Physiol* 1951 166 686—691
CARPENTER F C and R M RILEY The motor innervation of the rat urinary bladder *J Physiol (Lond)* 1961 112 609—617
DHARMAN H M G P GUPTA and K P BHARADVAJ Analysis of the adrenergic receptors in the urinary tract of dog *Jap J Pharmacol* 1970 20 461—466
EDMUNDS C W and G B ROY The point of attack of certain drugs acting on the periphery I Action on the bladder *J Pharmacol exp Ther* 1920 15 189—199
EDVARDSEN P and J SEIERSTEDT Distribution of adrenergic receptors in the urinary bladder of cats rabbits and guinea-pigs *Acta pharmacol toxiol* 1968 26 437—445
EL BADAWI A and E A SUTSK Dual innervation of the mammalian urinary bladder *Amer J Anat* 1966 119 407—428
ELLIOTT T R The action of adrenaline *J Physiol (Lond)* 1905 32 401—467
ELMER M Degeneration activity in the rat urinary bladder *Acta physiol scand* 1973 87 223—227
EMMELIN N J HOLMBERG and P OHLIN Receptors for catechol amines in the submaxillary glands of rats *Brit J Pharmacol* 1965 22 134—138

- GIANNULZI M J Recherches physiologiques sur les nerfs moteurs de la vessie *J Physiol* (Paris) 1863 6 22-29
- HAMBERGER B and K. A. NORBERG Studies on some systems of adrenergic synaptic terminals in the abdominal ganglia of the cat *Acta physiol scand* 1965 65 235-247
- JACOBSON G E Neurogenic vesical dysfunction *J Urol* (Baltimore) 1945 53 610-695
- LANGLEY J N and H. K. ANDERSON The innervation of the pelvic and adjoining viscera Part II The bladder *J Physiol* (Lond) 1895 19 71-84
- LANGWORTHY O R Innervation of the pelvic organs of the rat *Intest Urol* 1965 2 491-511
- LAVIDES J C R FRIEND E P AJEMIAN and W S REIS Denervation supersensitivity as a test for neurogenic bladder *Surg Gynec Obstet* 1962 114 241-244
- SHEN S C and W B CANNON Sensitization of the denervated pupillary sphincter to acetylcholine *Chin J Physiol* 1936 10 359-372
- SHERRINGTON C S Notes on the arrangement of some motor fibres in the lumbosacral plexus *J Physiol* (Lond) 1897 13 671-772
- SICC E B and T D SICC Sympathetic stimulation and blockade of the urinary bladder in cat *Int J Neuropharmacol* 1964 3 241-251
- SJOSTRAND M E C SJOGREN and C G SCHMITZELLOW Responses of the rabbit and cat urinary bladders *in situ* to drugs and to nerve stimulation *Acta pharmacol (Kbh)* 1972 31 241-254
- STROMBLAD R Sensitivity of the normal and denervated parotid gland to chemical agents *Acta physiol scand* 1955 33 83-98
- TAIRA N The autonomic pharmacology of the bladder *Ann Rev Pharmacol* 1972 12 197-208
- VANOV S Responses of the rat urinary bladder *in situ* to drugs and to nerve stimulation *Brit J Pharmacol* 1965 24 591-600

Characteristics and Distribution of Spinal Focal Synaptic Potentials Generated by Group II Muscle Afferents

By

T C FU¹ M SANTINI and E D SCHOMBURG²

Received 26 November 1973

Abstract

FU T C M SANTINI and E D SCHOMBURG *Characteristics and distribution of spinal focal synaptic potentials generated by group II muscle afferents* Acta physiol scand 1974 91 298-313

The location of the segmental relays of group II afferents in the spinal cord was investigated by recording extracellular focal synaptic potentials (FSP) generated by group II afferents in the gastrocnemius soleus nerve. Three types of group II FSPs were differentiated by their location and latency. (1) The dorsal group II FSP was located in the dorsal horn dorsolateral to the intermediate nucleus. Its short latency from the incoming group II volley (0.6-1.0 ms) led to the conclusion that at least the onset is monosynaptically generated.

(2) The ventral group II FSP was found between the intermediate nucleus and the motor nucleus. This type of FSP had a longer central latency ranging from 1.2-2.5 ms which made it difficult to decide whether the linkage was monosynaptic or disynaptic. However when considering other results (Fu and Schomburg 1974) it seems probable that the ventral FSPs in the low range of central latencies were generated monosynaptically. (3) The late group II FSP had a long and varying central latency and was found over a wider region although less regularly than the other FSPs. Presumably the late FSP represents the postsynaptic effect in second and third order neurones. It seems likely that at least the main part of the investigated dorsal and ventral group II FSPs was generated by secondary afferents from muscle spindles.

There is only scanty knowledge concerning the intraspinal pathway and termination of group II muscle afferents. We have now made an attempt to locate the segmental relays of group II afferents in the spinal cord by recording extracellular focal synaptic potentials (FSP). These potentials are now generally regarded as caused by the current flow generating postsynaptic potentials in neurones (Eccles *et al* 1954 *cf* also Brooks and Eccles 1947, Lorente de No 1947, 1953, Lloyd 1952). So far the recording of FSPs has been used mainly to investigate monosynaptic con-

Present address:

¹ Department of Physiology, College of Medicine, National Taiwan University, Taipei, Taiwan

² Istituto Farmacologia, Via V. Sar 103, 10122 Milano, Italy

³ Institute of Physiology, University of Göttingen, Göttingen, Germany

neurons from different fibre systems. In their classical study of the group I FSPs Eccles *et al* (1954) established that group Ia afferents have monosynaptic excitatory connections with neurones both in the intermediate region and the motor nucleus. Ib afferents on the other hand connect only with neurones in the intermediate region. Coombs *et al* (1956) employed this method to show that large cutaneous afferents terminate in the dorsal horn (*cf* also Fernandez de Molina and Gray 1957). Recording of monosynaptic FSPs has also been used to investigate the termination of descending fibre systems (Grillner *et al* 1970, Hongo *et al* 1972).

Coombs *et al* (1956) made a first attempt to localize the interneuronal relays from group II muscle afferents. They found a group II FSP in a region extending from the dorsal horn to the ventral part of the intermediate zone. Their latency measurements suggest that early components of this FSP were monosynaptically evoked but they made no attempt to differentiate this component from the later ones.

We have extended their observation, the aim being

- 1) to establish reliable criteria for identification of monosynaptic group II FSPs
- 2) to clarify the spinal distribution of gastrocnemius soleus (GS) group II FSPs.

Throughout this report the term 'group II fibres' will be used for muscle afferent fibres conducting in a range from 72 m/s (Hunt 1954) to 20 m/s (Matthews 1972, p. 116) irrespective of their receptor origin (*cf* Discussion).

Methods

Preparation. Experiments were carried out on cats (2.7–4.0 kg). Dissection was made under ether anaesthesia. After discontinuation of the ether anaesthesia (about 3 h before recording) the animals were maintained under chloralose anaesthesia (50–60 mg/kg *iv*) or in 4 experiments with a combination of chloralose (30–40 mg/kg) and pentobarbital sodium anaesthesia (Nembutal Abbott 4–10 mg/kg). The findings in both groups were essentially the same. All cats were immobilized with gallamine triethiodide (Flaxedil, May and Baker Ltd) and artificially ventilated. The end tidal CO₂ concentration was monitored and adjusted to 38–44%. During the experiment the mean blood pressure normally ranged from 90–120 mm Hg. A drop in blood pressure was compensated by infusion of a mixture of low and high molecular weight dextran or if more severe (below 80 mm Hg) by slow intravenous infusion of noradrenaline. The rectal temperature was kept within 36–39°C. After laminectomy from L4–L7 the left ventral roots L6–S1 were cut and in most experiments the ventral root L7 was mounted for antidromic stimulation.

The left hindlimb was extensively denervated. The cut nerves to gastrocnemius soleus (GS), posterior biceps semitendinosus (PBSt) and plantaris (Pl) were dissected and mounted on bipolar silver electrodes for stimulation.

Stimulating procedures. The mounted nerves were stimulated with constant voltage rectangular pulses (duration 0.1 ms, repetition rate 2.5/s in 6 experiments or 50/s in 3 experiments).

The stimulation intensities are given in multiples of threshold for group I fibres.

For determination of maximal group I stimulus strength and for better separation between group I and group II fibres the double volley technique was used as described for differentiation between group I afferent fibres (Bradley and Eccles 1953, Eccles *et al* 1957). Two stimuli were applied to the peripheral nerve: the second one within the refractory period of a preceding group I volley (stimulus interval ranged from 0.5–0.8 ms in the different experiments). When the first stimulus reached maximal group I strength the second group I volley disappeared and a pure group II volley resulted from the second stimulus.

was suprathreshold for group II afferents. With this method the separation between the group I FSP and the group II FSP is clear. This gains in importance if the group I FSP is big in relation to the group II FSP as it was in most recordings (cf. Fig. 6A, B).

During mapping in the spinal cord the first stimulus was adjusted to the group I maximum (1.6–2.5 T) while the second stimulus was kept in the low to medium group II range (3.5–5.0 T) in order to avoid group III contamination. Single and double stimuli were generally applied in an alternating manner.

Recording procedures. In 3 experiments the dorsal root incoming volley evoked by the peripheral nerve stimuli was recorded with a surface electrode at middle or caudal L7. In the other experiments the afferent volley was recorded monopolarly from the cut dorsal root S1 or the cranial part of this root.

The FSPs were recorded with glass microelectrodes (1.5–2 MΩ) filled with 3 M NaCl. All records were obtained extracellularly; negativity of the microelectrode was recorded as a downward deflexion. The procedure for mapping the potential fields at the different levels of the lumbar cord was described by Eccles *et al.* (1954). For each track the surface contact of the electrode was set at zero on the micromanipulator. Then the electrode was slowly inserted just beyond the desired level, usually the ventral border of the motor nuclei or an equivalent depth. Afterwards the electrode was withdrawn in steps of 0.2 mm or 0.25 mm. The FSPs were recorded after each withdrawal. Disturbances of the potentials by large unitary discharges of nearby neurones were seldom observed with this method (cf. Eccles *et al.* 1954). Normally they could be easily recognized and avoided as far as possible by adjusting the electrode to another "clean" level. When different nerves were tested in the same track a separate passage of the electrode was performed through the track for each nerve.

In most experiments the transverse exploration of the group II FSP was done by tracking with different transverse angles of the microelectrode ranging from 15° ventro-medially to 35° ventro-laterally. For each transverse level the same surface penetration point was used (11–14 mm to the left of the midline of the dorsal column). For technical reasons all tracks had an additional ventro-cranial angle of 10° or 15°. The depth of the recordings was given as the distance between recording point and surface point of that track irrespective of the angle used. The actual depth of the recording sites in the track was calculated according to the following formula:

$$x = d \cos \alpha \cos \beta$$

Here α and β are the longitudinal and the transverse angles of the electrode both referred to the perpendicular axis. For example the depth of 2 mm in a track with the most commonly used angles of 15° longitudinally and of 10° or 20° transversally would give a corrected perpendicular depth of 1.90 mm or 1.82 mm respectively, i.e. an error of less than 10% in relation to the scale readings.

In the last track of each relevant transverse exploration a reference electrode was left in the cord and its position checked histologically. The position of the electrode tracks and of the field potential areas in the maps of Fig. 6 and 7 are based upon these histological controls. In Fig. 6 a 20% shrinkage of the cord during fixation is taken into account and the error caused by the ventro-cranial angle of the electrode is corrected.

At each point the recorded potentials were taken directly (4–6 sweeps superimposed) and also averaged (50–100 sweeps per record). Averaging was performed in an alternating manner for the responses to single and double stimulation. For averaging a computer with an integrating analog-to-digital converter was used with a time resolution of 125 μs/address. Latencies to the onset of FSP which generally were taken from averaged records contained an error of about ±0.1–0.2 ms. The size of the FSP was calculated from the averaged records for group I FSPs were measured from their negative peak to the baseline; group II FSPs were measured from their negative peak in relation to the waning slope of the group I FSP. For this purpose the recording of the pure group I FSP (single stimulation) was superimposed on the recording of the group I–II FSP (double stimulation) or the decay phase of the group I FSP was superimposed on the part where the group II FSP occurred. The rising time of the group II FSP was measured from the beginning of the FSP to its maximal peak. In case the group II FSP wave was not uniform but had two or more clearly discrete peaks the rising time was measured to the first peak.

The term "central delay" will be used for the delay between the stimulus-generated afferent volley recorded in the dorsal root entry zone at L7 or S1 and the onset of the FSP, thus including the central conduction time and the synaptic delay.

Throughout this report group I includes groups Ia and II because no clear separation between the two components could be seen in the present series.

Abbreviations: ISI, focal synaptic potential; GS, gastrocnemius-soleus; ISL, posterior biceps-semitendinosus; PL, plantar; T, threshold strength for group I afferents (cf. Methods).

TABLE I Peripheral excitability conduction time and velocity of group I and group II fibres of GS

	Excitability		Minimal conduction time ms	Maximal conduction veloc m/s
Group I	max.	1.6-2.3 (1.9) T	1.4-1.6	91-117 (103)
Group II	thresh	1.5-2.3 (1.8) T	2.3-2.7	57-69 (64)

() = mean values

T = stimulus strength in relation to group I threshold

max = stimulus strength for maximal group I excitation

Results

A summary of the observed excitability and peripheral conduction velocity of GS afferents is given in Table I. All data in this table are based on 11 expts. Latencies were always referred to the beginning of the incoming volley or the FSP. This means that Table I gives the range of conduction time and velocity in the different experiments for the fastest group I and group II fibres and that the central delay of the different FSP waves (*cf.* Table II) applies only to these fibres.

Three different types of group II spinal FSPs were observed. These could be discerned by their local distribution and their latency from the group II incoming volley: a dorsal FSP with short latency (monosynaptic dorsal group II FSP), a ventral FSP with longer latency (ventral group II FSP) and a late FSP not so strictly defined with respect to location (late group II FSP *cf.* Table II). The different FSPs generated by group II afferents from gastrocnemius will be described separately in the sections A-C.

A The monosynaptic dorsal group II focal synaptic potential (FSP) from GS

1 *Experimental criteria for identification of monosynaptic group II FSP.* The identification of a monosynaptic group II FSP required its differentiation from a mono- or polysynaptic group I FSP, a di- or polysynaptic group II FSP and a monosynaptic group III FSP.

Fig. 1 illustrates the procedure for the differentiation between group I and group II monosynaptic FSPs by grading the stimulus strength in single stimuli. The left column (I) shows the nonaveraged FSPs (upper traces: 4-5 sweeps superimposed) and the incoming volley from an SI filament (lower traces); the right column (II) the averaged FSPs (100 samples/record). With stimuli (S) in the range of group I below group II threshold (A) a pure group I FSP occurred. It shows the characteristic time course which is well known from investigations by Eccles *et al.* (1954) and Coombs *et al.* (1956). Following the initial biphasic presynaptic spike (latency from the incoming group I volley 0.1-0.2 ms) there is a prolonged negative wave (a) with steep onset (latency from the incoming volley 0.6-0.7 ms) and a slower decay. From its latency and stimulus strength relation

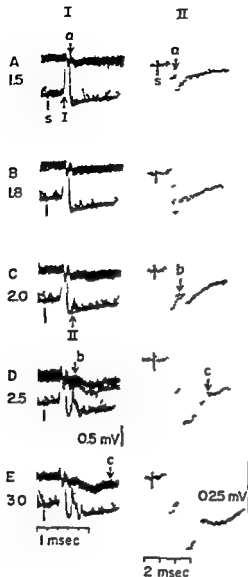


Fig 1

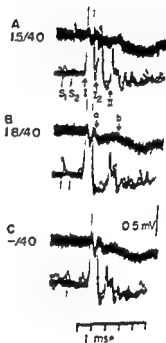


Fig 2

Fig 1 Differentiation between group I and group II FSPs by their relation to the incoming afferent volley. In column I the upper traces are intraspinally recorded focal potentials (same experiment and position as in Fig 2) and the lower traces incoming volleys evoked from G.S. stimulation recorded from an S1 dorsal root filament. Each record consists of 4-5 superimposed traces. Column II shows averaged (100 records) focal potentials evoked at the same strength as the corresponding records in column I. Stimulus strength indicated beside the records in relation to Ia threshold. A stimulus (1.5 T) submaximal for group I (I group I incoming volley a, group I FSP). B stimulus (1.8 T) maximal for group I (cf Fig 2) subthreshold for group II. C stimulus (2.0 T) just suprathreshold for group II (II group II incoming volley b early group II FSP). D stimulus strength (2.5 T) threshold for a late group II FSP. c. E stimulus strength 3.0 T. Arrows indicate incoming group I and II volleys and onset of group I (a) and group II (b, c) FSPs. Voltage calibration for focal potential separately for non-averaged and averaged record. Time 1 ms/div for non-averaged records 2 ms/div for averaged records.

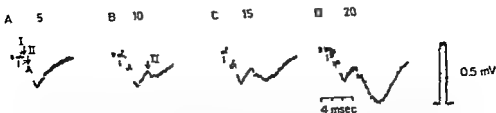


Fig 3 Differentiation of group II FSP and group III FSP by their latency and threshold to graded G-S nerve stimulation. Averaged records of FSPs (80 samples/record) all with single stimuli graded from 5 T to 20 T. Threshold for group II FSP (II) 2.0 T threshold for group III FSP between 7 and 10 T. Stimuli indicated by arrows at the beginning of the records. Time 4 ms/div.

(threshold 1 T maximal with group I at 1.8 T) this FSP can be clearly attributed to postsynaptic current events evoked monosynaptically by group I afferents (*cf* Brooks and Eccles 1947 Eccles *et al* 1954). In B with a stimulus strength just at group II threshold (1.8 T) a trace of a second FSP wave occurred on the decay slope of the group I FSP. When the stimulus strength was further increased to 2.0 T (C) a distinct small group II incoming volley (II) occurred (latency from stimulation 2.6 ms conduction velocity of its fastest fibres 60 m/s). Now the second FSP wave (b) was well developed and grew in parallel with the increasing group II incoming volley when the stimulus strength was increased (D—E). From the close relations of threshold and the short latency (0.7 ± 0.1 ms) from the group II incoming volley this potential can be presumed to be a *monosynaptic group II FSP*. The possibility of a dis- or polysynaptic group I FSP can be excluded since a polysynaptic group I FSP should at least occur with group I maximum (i.e. in this case at 1.8 T (for determination see Fig 2 which was taken from the same experiment). The late FSP (c latency from the stimulus 14 ± 0.3 ms) occurring in D with a threshold of 2.5 T will be described in section C.

In the example presented in Fig 1 the group I FSP was small compared to the group II FSP. However normally it was the other way around. Therefore it was necessary to have a clearer separation between the two groups. This was performed

Fig 2 Double volley stimulation for determination of maximal group I excitation and separation of group I and group II FSPs. Upper records focal potentials recorded at a depth of 2 mm in middle L7 dorso-lateral to the maximum of the group I FSP. Lower records incoming volley from G-S stimulation recorded from an S1 dorsal root filament. For each record 4–5 traces are superimposed. Stimuli (S1–S9) indicated by vertical bars below the records of the incoming volley. Stimulation strength in relation to group I threshold is indicated for first and second stimulus beside the records. A first stimulus (S1 = 1.5 T) sub-maximal for group I incoming volley (I). Second stimulus (S2 = 4.0 T) in the low to medium group II range (*cf* Fig 1) induces a second group I (I') and a group II (II) incoming volley. B first stimulus (1.8 T) maximal for group I second stimulus (4.0 T) as in A induces pure group II incoming volley no second group I volley left. The group I FSP (a) and group II FSP (b) are better separated than in C where the second stimulus (4.0 T) is given alone. Voltage calibration refers to focal potentials. Time 1 ms/division.

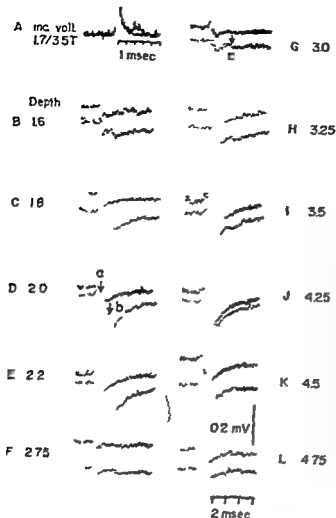


Fig. 4. Dorsal-ventral location of group I and group II FSP. A: superimposed traces of incoming volley in S1 dorsal root filament evoked by single and double stimulation of G5 single or first stimulus 17 T maximal for group I second stimulus 35 T. B-L: averaged records taken at the indicated depths (mm) of one track shown in Fig. 7A. At each depth the upper records were taken with single stimulation (17 T) the lower ones with double stimulation (17/35 T): a: group I FSP; b: dorsal group II FSP; c: ventral group II FSP. Time 1 ms/div in A; 2 ms/div of the calibration below L for B-L. Voltage calibration 0.2 mV for B-L. For more details see text.

by the aid of the double volley technique as demonstrated in Fig. 2. The recordings were taken in the same experiment and with the same recording conditions as Fig. 1. In left column: upper traces: FSP; lower traces: incoming volley. A second group I volley (I') occurred after the second stimulus ($S_2 = 40$ T) as long as the first stimulus (S_1) was submaximal for group I (lower trace A). This second group I volley disappeared in B when the first stimulus reached maximal group I strength (1.8 T in this case). No: the second stimulus induced a group II incoming volley alone (II) which is better separated from the group I volley than after a single stimulus of the same strength (C: threshold of group II in this experiment 18–20 T, cf. Fig. 1). The advantage of this separation for the recognition of monosynaptic group II FSP (b) becomes evident if B and C are compared. In C the second stimulus is given alone.

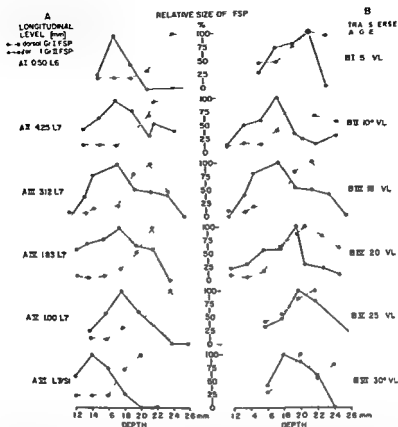


Fig 5 Depth relation between dorsal group II FSP and dorsal group I FSP at different longitudinal levels (A) and transverse angles (B). All tracks are performed in one experiment stimulation at G S nerve. For each track the maximal dorsal group I FSP and the maximal dorsal group II FSP were set as 100 and the size of the FSPs recorded at other depths are given in per cent. The relative size of the dorsal group I FSPs and the dorsal group II FSPs then was plotted against the recording depth. Longitudinal position of the tracks in A: AI in L6 0.5 mm cranial to the border L6/L7, AII—AV in L7 distance to the border of L7/S1 is indicated in mm. Total length of L7 root entrance was 5.9 mm. A VI at the border of L7/S1. The transverse experimental angle of the tracks in B was 5° to 30° up of the electrode going ventrolaterally (VL). The longitudinal level of the tracks equals that of A III. The transverse position of the tracks of A and B is indicated in Fig 6 C and D. The maximal size of the dorsal group I FSP and dorsal group II FSP is shown in Fig 6 A and B.

2 Transverse and longitudinal spinal distribution of the monosynaptic dorsal G S group II FSP

Transverse distribution. The data of this section refer to investigations of the L7 spinal segment mainly in its middle third.

Fig 4 shows a series of recordings of one track (position indicated in Fig 7 A) which demonstrates the characteristic dorsoventral location of the different group I and group II FSPs generated by G S stimulation. In A the incoming volleys of a S₁ dorsal root filament induced by single and double stimuli were superimposed

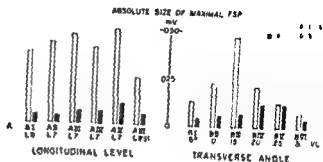
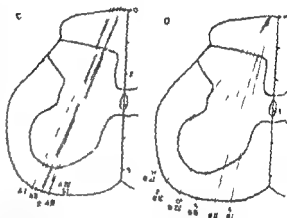


Fig. 4B. Relation between maximal size of dorsal group II and dorsal group I FSP at different longitudinal (A) and transverse (B) levels. A: maximal absolute size of the FSP recorded in the track shown in Fig. 3A. B: maximal absolute size of the FSP recorded in the tracks of Fig. 3B (C-D). In diagram of the transverse position of the tracks which were investigated in Fig. 3A and C and those which were investigated in Fig. 3B and D.



Since a relatively small number of the dorsal and lateral group III cells were active in most experiments, the demonstration of group III FSPs was done by their dorsal latencies as is shown in Fig. 3. While the group II FSP (II) had a threshold of 1.0-1.5 ms and a latency of 1.0-1.5 ms in the stimulus of 3.3-3.7 ms, the group III FSP (III) occurred with a threshold of 1.0-1.5 ms and had a latency of 1.0-1.5 ms. Generally all FSPs with latencies in the peripheral (5) stimulus of more than 7 ms (cf. Connors et al. 1956) and a threshold of 1.0-1.5 ms (cf. R. M. Eccles and Lundberg 1957) were assumed to be of the dorsal group III which have their main representation among group III afferents.

Among the first stimulus (1.7 ms) maximal for group I second stimulus (3.7 ms) threshold for group II in this experiment (6.1 ms). In B-1 the upper records were taken with single stimulation thus giving the fairly pure group I FSP (1). Traces of later FSP were in C-D and 1-11 can be attributed to the small group II component. The lower records were taken with double stimulation thus the additional FSP was visible occurring in these records were of group II origin. As described by Eccles et al. (1954) the group I responses (a latency to the group I incoming volley of 0.7 ms for the dorsal FSP 0.6-0.8 ms for the ventral one) had their maximum in the intermediate region (at a depth of 2.2 mm) and in the ventral horn (at 1.0 mm). The dorsal response was relatively small in this case due to the laterality of the track. The monosynaptic dorsal group II FSP (b in B-1) latency from the group II incoming volley 0.6-0.8 ms had its maximum at 2.0 mm i.e. slightly dorsal to that of the dorsal group I FSP. The somewhat later group II FSP occurring with a more ventrally located maximum (depth 2.3-3.5 mm) will be included in section B.

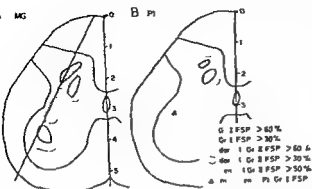


Fig 7 Transverse distribution of group I and group II FSP of G-S (A) and PI (B). A The map of G-S FSP is composed from the results of 13 transverse tracks at two levels in the middle third of the L7 segment. The hatched areas include the regions where group I FSP or dorsal group II FSP respectively exceeded 60% of their maximal size. The maxima for the dorsal and the ventral group I FSP were determined separately. The dotted or broken line respectively includes areas

with FSP size of more than 50% of the maximum. The area where ventral group II FSPs were found with a size of 50% of the maximal observed size is surrounded by a crossed line. The indicated track refers to Fig 4 B. This map of PI FSP is composed of the results of 7 tracks which were performed in the same experiment and at the same longitudinal levels as those in A. It is drawn similar as the map in A except that the ventral group I FSP is only indicated by its maximum and an indication of the ventral group II FSP is omitted because it was quite inconsistent.

The dorso-ventral relation between the dorsal group I FSP and the monosynaptic dorsal group II FSP is shown more detailed in Fig 5 and 6. Fig 5 shows the relative size of the dorsal group II and the dorsal group I FSP in relation to the depth from the cord dorsum. For each track the size of the maximal dorsal group I FSP or dorsal group II FSP was set as 100% and the size of the FSPs recorded at other depths was set in relation to this value. In A the tracks were performed at different longitudinal levels from caudal L6 to the border of L7/S1. In B all tracks were taken at the same level and surface penetration point in the middle L7 (equal to the level of A III) but with different angles of the electrode so that most of the gray matter is transversally covered at that level. The position of the tracks is indicated in Fig 6 C and D. In all tracks except in B I the maximum of the early group II FSP is dorsal to the maximal group I FSP and even in B I the mean value of the three maximal values of the dorsal group II FSP is dorsal to that of the group I FSP.

The absolute size (in mV) of the maximal dorsal group I and group II FSP recorded in the same tracks is shown in Fig 6 A and B. From Fig 6 B it can be seen that the maximal size of the dorsal group II FSP was found in more lateral tracks (B IV-B V) than the maximum of the dorsal group I FSP (B III).

The transverse spinal distribution of the different G-S group I and group II FSP is given in Fig 7 A. The map is composed from the measurements of one experiment (same experiment as Fig 4) with 13 transverse tracks performed at two levels in the middle of the L7 segment. Observe that the main region of the monosynaptic dorsal group II FSP is located dorso laterally to the dorsal group I FSP.

Longitudinal distribution From the caudal L6 to the cranial S1 segment the size and transverse distribution of the monosynaptic dorsal group II FSP was approxi-

mately the same. Fig. 5A shows the dorso-ventral relation between the dorsal group II FSP and the dorsal group I FSP at different levels from caudal L6 (A I) to the border of L7/S1 (A VI). At each level the relative size of the FSP was plotted against depth from the cord dorsum as described for the transverse distribution in Fig. 5B. At all levels the maximum of the dorsal group II FSP was dorsal to the dorsal group I FSP. The absolute values of the maximal FSP observed in the different tracks are shown in Fig. 6A and the position of the tracks in Fig. 6C in which all tracks are projected on the same transverse plane in middle L7 (level of A III).

In the middle of L6 small monosynaptic dorsal group II FSPs were observed only occasionally (latency from stimulus 3.1–3.3 ms, depth of the maximal observed sizes 1.8–2.4 mm). The size of the dorsal group I FSP was mostly unchanged at this level. Its latency (2.2–2.3 ms) and depth of maximal size (2.0–2.4 mm) was about the same as in L7.

At the cranial L6 and caudal L5 level no monosynaptic dorsal group II FSPs were observed. At this level the dorsal group I FSP was 20–40 % of its size in L7. It occurred at about the same depth (depth of maximal size 2.0–2.6 mm) but with slightly longer latency from the stimulus (2.3–2.6 ms) than in L7.

The caudal borders of the group II FSP were not investigated systematically. It is noteworthy, however, that after transection of the S1 dorsal root the monosynaptic dorsal group II FSP about 2 mm caudal to the most cranial root entrance of S1 was of the same size as in caudal L7.

B. The ventral group II FSP from G-S

In the track shown in Fig. 4 at the depth of 2.2–3.5 mm (E–I) a second group II FSP (c) occurred with a latency from the incoming group II volley of 2.0–2.4 ms. Such ventral group II FSPs, which were located ventrolateral to the region of the intermediate group I FSP and dorsomedial to the motor nuclei, often reaching into these regions (cf. Fig. 4 and Fig. 7A) were found in about 50–70 % of the tracks in L7 in which dorsal group II FSPs were observed. The ventral FSP was generally less distinct and its distribution was not so well defined as that of the dorsal group II FSP. Therefore the indication of the distribution of the ventral group II FSP in Fig. 7A which is taken from the results of one experiment (cf. Section A) has to be regarded with certain reservations. In other experiments ventral group II FSPs of comparable size were also found more medially and dorsally than in Fig. 7A, reaching into the region of the dorsal group I FSP.

The threshold for the occurrence of the ventral group II FSP was the same or slightly higher (1–1.2 times group II threshold) than that for the generation of the dorsal group II FSP.

The latency of the ventral group II FSP from the group II incoming volley observed in different experiments was 1.2–2.5 ms (1.6–2.0 ms in more than 10 % of cases) and thus clearly longer than that of the dorsal group II FSP. As demonstrated in Fig. 4 no gradual transition in the latency of the dorsal and the ventral

group II FSP was observed but there was every time a jump in latency when going from the dorsal to the ventral region. In the transitional zone between these regions both FSPs occurred in a few cases in the same recording.

In the region between caudal L6 and cranial S1 the threshold value, latency and transverse distribution of the ventral group II FSP was about the same. In middle L6 the size and the depth of the maximal ventral group II FSP was still in the same range but the latency to the stimulus was slightly longer (5.0–5.3 ms) probably due to longer conduction distance. At the cranial L6 and caudal L5 level group II FSP were still observed. The maxima occurred at 2.2–2.6 mm depth and the latency from the stimulus ranged from 5.2 to 6.2 ms. With these long latencies there is some difficulty in differentiating the responses from the late group II FSP described in the next section particularly since no extensive tracking was performed.

C The late group II FSP from G-S

In Fig 1 D–E another discrete third type of group II FSP (c) with longer latency (latency from stimulation 6.4 ± 0.3 ms) appeared at somewhat higher stimulus strength (2.5 T) than the monosynaptic dorsal group II FSP but still in the low threshold group II range. Similar late group II FSPs with latencies of 4.9–7.5 ms (5.1–6.3 ms in more than 70% of cases) to the G-S stimulus and with thresholds about 1.3–1.5 times higher than group II threshold (i.e. clearly below group III threshold) were seen in most experiments. In the L7 segment the late group II FSP was normally well separable from the ventral group II FSP by its longer latency. A sliding transition between the latencies of these different FSPs in relation to the recording depth was not seen. For example in one track at middle L7 a late group II FSP was found at a depth of 2.8–3.5 mm with a latency from the stimulus ranging between 5.0–5.7 ms while in the same track a ventral group II FSP occurred between 2.0–2.6 mm with a latency of 4.3–4.4 ms. Sometimes the late group II FSP appeared together with dorsal or ventral group II FSPs (cf Fig 1 D–E).

TABLE II Latency and location of group I and group II FSP of GS

	Latency to stimulus ms	Central delay ms	Depth of max FSP mm
Dorsal group I FSP	1.9–2.3	0.4–0.7	1.8–2.8 (2.2–2.4)
Ventral group I FSP	1.9–2.4	0.4–0.8	3.2–4.3
Dorsal group II FSP	3.0–3.7 (3.1–3.3)	0.6–1.0 (0.6–0.8)	1.4–2.2 (1.8–2.0)
Ventral group II FSP	3.8–4.8 (4.1–4.5)	1.2–2.5 (1.6–2.0)	2.0–3.2 (2.2–2.8)
Late group II FSP	4.9–7.5 (5.1–6.3)	2.4–3.1 (2.5–3.8)	1.4–4.4

() = values observed in more than 70% of cases

* total distribution: no clear maximum for this FSP

D Data from nine investigations in L7 segment. Latency and central delay relate to the beginning of the FSP wave and the stimulus artifact of the beginning of the incoming group I or group II volley respectively.

The occurrence and spinal distribution of the late group II FSP was less regular and less well defined than that of the dorsal and ventral group II FSP. Late group II FSPs were observed occasionally at depths from 1.4 to 4.4 mm, sometimes over a wide region, sometimes restricted to small spots in a few tracks. Therefore a clear maximum could not be determined for this FSP.

The effect of pentobarbital upon the group II FSPs was tested in two experiments. The late group II FSP was greatly diminished after a small dose of pentobarbital (15 mg/kg); only about 20% of the control size was left. The latency of the late group II FSP was also greatly prolonged (4.9 ms in control, 5.6 ms after 10 mg/kg, 6.2 ms after 20 mg/kg). However, the dorsal group I and group II FSPs decreased only about 20% after a total dose of 15–20 mg/kg. The ventral group II FSP was more sensitive to pentobarbital than the dorsal one; it was reduced to about 50% after a total dose of 10 mg/kg but then remained unchanged up to 25 mg/kg. The latency of both group I and group II FSP (ventral and dorsal) was not prolonged even after 30 mg/kg of pentobarbital.

Summarizing the group I and II FSPs. Table II gives a summary of the latency to the stimulus, the central delay and the depth of maximal size for the different group I and group II FSPs investigated in L7 segment. The latency and central delay are measured from the stimulus artefact or the beginning of the incoming group I or group II volley, respectively, to the beginning of the FSPs. The data are gathered from different experiments and present the extreme values. The values which were observed in more than 70% of measured cases are given in parentheses. For the late group II FSP the total range of depth where it was found is indicated, since no clear maxima were determinable in this case (cf. above).

The rise time of the dorsal and ventral group II FSP was quite variable (0.3–3.0 ms for dorsal group II FSPs, 0.4–0.9 ms in 80% of measured cases). In some cases the rising slope was observed to depend on the stimulus strength, being less steep with stimuli just above threshold and getting steeper with increasing stimuli although the size did not particularly increase.

D. Group II FSPs from P1 and PBS1

An investigation of the FSPs evoked in the L7 segment by afferents from P1 (Fig. 7B map composed from seven tracks in the same experiment and levels as Fig. 7A) showed that the distribution of monosynaptic dorsal group II FSP and dorsal group I FSP is similar to that of the corresponding GS FSPs. Ventral group II FSPs from P1 occurred at about the same latencies as those from GS and they also seemed to be mainly located ventrally to the dorsal group I FSP. They were less consistent than GS group II FSPs and were thus less systematically investigated, so that their distribution cannot be described in detail.

Group II FSPs from PBS1 were obtained irregularly. Only in one out of four experiments did we record a clear monosynaptic dorsal group II FSP with a latency of 2.5–2.9 ms from the stimulus (latency of group I FSP 1.6–1.8 ms). In the other experiments only sporadic dorsal group II FSP were found dorsally to the intermediate region. Ventral and late group II FSPs with a latency of 3.1–5.2 ms were observed more often than the dorsal group II FSPs. They were very scattered and ventral to the intermediate region.

Discussion

The results showed three types of spinal FSPs generated by group II afferents in the G S nerve which could be differentiated by their latency and location in the spinal cord. The dorsal group II FSP was located dorsolateral to the group I FSP found in the intermediate region (*cf Eccles et al 1954*). This FSP was related very closely to the threshold and size of the group II incoming volley at the dorsal root L7 or S1. Its short latency from the incoming group II volley indicates that at least its onset is monosynaptically generated. The varying sometimes fairly long rising time of the FSP might be attributed to different causes: firstly a contribution to the FSP from fibres with different conduction velocities; secondly a contribution of monosynaptic and polysynaptic events to the FSP; thirdly a variable delay of impulses in excited interneurons which may influence the FSP. The latter assumption would be supported by the finding that the rising slope of the dorsal group II FSP was steepened in some cases with increasing stimulus strength without a concomitant significant change in the size of the FSP. It could not be decided to which an extent slower conducting group II fibres and polysynaptic effects contribute to the late part of the dorsal group II FSP.

The second type denoted ventral group II FSP was mainly found ventrolateral to the group I FSP of the intermediate region and dorsomedial to the group I FSP of the motor nucleus, sometimes reaching into both these regions. It was evoked with the same or slightly higher threshold than the dorsal group II FSP. The duration and the large range of central latencies (12–25 ms) as well as its less well defined distribution complicate the interpretation of this type of FSP and may suggest that it is not generated by a homogeneous group of neurones. Particularly for those FSPs in the lower range of central latencies it was not possible to decide if the linkage was disynaptic or monosynaptic either from slow conducting group II afferents or fast group II fibres with slow intraspinal conduction. However, Fu and Schomburg (1974) have shown that group II muscle afferents have branches beyond the region where the dorsal group II FSP was recorded and also found that the conduction velocity is appreciably slowed down in these ventral branches. From these results it seems probable that at least part of the ventral group II FSP is monosynaptically generated (*cf Discussion in Fu and Schomburg 1974*).

In the case of the late group II FSP with its long central latency and inconsistent distribution it seems safe to postulate that they are not evoked monosynaptically but represent the postsynaptic effect in second or third order neurones. The finding that a somewhat higher stimulus strength was required to evoke the late group II FSP than the dorsal FSP discussed above may be explained by the summation required for excitation of first order group II interneurons. The strong depression of late group II FSPs by pentobarbital also supports the postulate that they were generated polysynaptically.

The distribution of group II FSPs described by Coombs *et al* (1956) covered part of the region where our dorsal and ventral group II FSPs were recorded. Since they used pentobarbital anesthesia it would seem less likely that late FSPs gave any appreciable contribution in their experiments.

So far the term group II was attached to muscle afferents with conduction velocities within the appropriate range (*cf.* Introduction). The question now arises to which extent the group II FSPs may be generated by receptors of non muscle spindle origin. Different investigations have shown that an uncertain number of fibres conducting in the group II range cannot be allocated to muscle spindles. The computations of Barker *et al.* (1962), which are based upon histological studies of the soleus muscle and nerve suggested a very high percentage (35–42%) of group II fibres not originating from muscle spindles and a similar figure was mentioned by Paintal (1960). In contrast the electrophysiological investigations of Hunt (1964) and the more recent calculation of Boyd and Davey (1968) suggested that group II afferents in the nerves to the medial gastrocnemius and soleus consist almost entirely of fibres from muscle spindles (Boyd and Davey p. 37). According to Boyd and Davey (1968) there may be a contribution of about 7% from other receptors *e.g.* Ruffini spray and pressure pain receptors. It seems very unlikely that impulses in afferents from these receptors contributed appreciably to the initial part of the dorsal or ventral group II FSPs. These afferents conduct mainly in the range below 40 m/s (Paintal 1960; Boyd and Davey 1968) and would thus not be expected to contribute to the low threshold early group II effects. Moreover the main fraction of these afferents is in the group III range. If a small part of them exerted a clear influence in the low threshold group II range this effect should gradually rise with the stimulus strength in the group III range. However the threshold of the group III FSP was well defined and clearly separate from the group II FSP.

Accordingly it seems likely that at least the main part of the investigated dorsal and ventral group II FSPs was generated by secondary muscle spindle afferents. This postulate is supported by findings regarding the intraspinal termination of muscle afferents with secondary endings (Fu and Schomburg 1974).

The authors are sincerely grateful to Professor Anders Lundberg for his continuous valuable suggestions and his inspiring critical discussions throughout this work. Our thanks are also due to Mrs Rauni Larsson for excellent technical assistance. This work was supported by the Swedish Medical Research Council (Project No. 14 \-94). E. D. Schomburg was supported by a grant from the Deutsche Forschungsgemeinschaft.

References

- BARKER, D. M. C. JR and M. N. ADAL. A correlation between the receptor population of the cat's soleus muscle and the afferent fibre diameter spectrum of the nerve supplying it. In *Symposium on Muscle Receptors*, ed. Barker D. M. C. Jr, pp. 251–261. Hong Kong: Hong Kong University Press, 1961.
- BOYD, I. A. and M. M. DAVEY. *Composition of Peripheral Nerves*. Edinburgh: Livingstone, 1968.
- BRADLEY, K. and J. C. ECCLES. Analysis of the fast afferent impulses from thigh muscles. *J. Physiol. (Lond.)* 1953, 100, 462–473.
- BROOKS, C. MC and J. C. ECCLES. Electrical investigation of the monosynaptic pathway through the spinal cord. *J. Neurophysiol.* 1947, 10, 751–764.
- COOMBS, J. S., D. R. CURTIS and S. LAURENCE. Spinal cord potentials generated by impulses in muscle and cutaneous afferent fibres. *J. Neurophysiol.* 1956, 19, 451–467.
- ECCLES, R. M. and A. LUNDBERG. Synaptic action in motoneurons by afferents which may evoke the flexion reflex. *Arch. ital. Biol.* 1953, 97, 119–221.

- ECCLES J C R M ECCLES and A LUNDBERG Synaptic actions on motoneurons in relation to the two components of the group I muscle afferent volley *J Physiol (Lond)* 1957 136 527—546
- ECCLES J C P FATT S LANDGREN and G J WINSBURY Spinal cord potentials generated by volleys in the large muscle afferents *J Physiol (Lond)* 1954 125 590—606
- FERNANDEZ DE MOLINA A and J A B GRAY Activity of the dorsal spinal grey matter after stimulation of cutaneous nerves *J Physiol (Lond)* 1957 137 126—140
- FL T C and E D SCHOMBURG Electrophysiological investigation of the projection of secondary muscle spindle afferents in the cat spinal cord *Acta physiol scand* 1974 91 314—329
- GRILLNER S T HONGO and S LLOYD The vestibulospinal tract Effects on alpha motoneurons in the lumbosacral spinal cord in the cat. *Exp Brain Res* 1970 10 94—120
- HONGO T E JANKOWSKA and A LUNDBERG The rubrospinal tract IV Effects on interneurons *Exp Brain Res* 1972 15 54—78
- HUNT C C Relation of function to diameter in afferent fibres of muscle nerves *J gen Physiol* 1954 38 117—131
- LLOYD D P C Electrical manifestation of action in neurons In *The Biology of Mental Health and Diseases* pp 135—158 New York P B Hoeber 1952
- LORENTE DE NÓ R Action potential of the motoneurons of the hypoglossal nucleus *J cell comp Physiol* 1947 29 207—287
- LORENTE DE NÓ R Conduction of impulses in the neurons of the oculomotor nucleus pp 132—179 In *Ciba Foundation Symposium The spinal cord* London J and A Churchill Ltd Boston Little Brown and Co 1953
- MATTHEWS P B C *Mammalian Muscle Receptors and Their Central Actions* London Edward Arnold (Publ) Ltd 1972
- PAINTAL A S Functional analysis of group III afferent fibres of mammalian muscles *J Physiol (Lond)* 1960 152 250—270

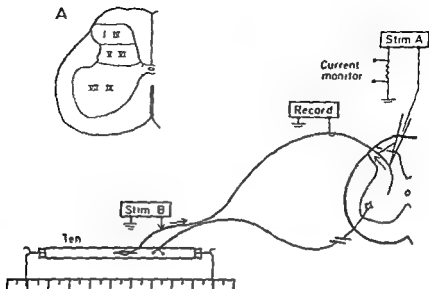


Fig. 1. *Experimental arrangement.* Recording in a dorsal root filament from an identified single secondary muscle spindle afferent from tenuissimus (Ten). A: stimulation of an intraspinal fibre branch with glass microelectrode (current monitor *cf.* Methods). B: stimulation of the Ten nerve for determination of the afferent conduction velocity and for identification of the antidromic spike by collision (see text *cf.* also Fig. 2). Inset A: spinal layers in L7 according to Rexed (1954) supplementary to Table 1.

appropriate filament with a single group II fibre from the innervated part of Ten or VIG was found. The identification of a secondary muscle spindle afferent depended on the following criteria: the afferent impulse induced by stimulation of the peripheral Ten or VIG nerve branch had to be all or none from threshold up to stimulation intensities of 10–70 nT. The fibres were attributed to group II by their peripheral conduction velocity. The dividing limit was set at 17 m/s between group I and II (Hunt 1954) and 20 m/s rather than 24 m/s (Matthews 1972, p. 116) between group II and III. The extreme values of the group II fibres recorded from Ten were 27 and 56 m/s from VIG 34 and 62 m/s (*cf.* Table 1).

The muscle spindle origin of the group II fibres was proved by its reaction to stretch and twitch contraction of the muscle. All recorded afferents gave a roughly linear relation between muscle length and tonic discharge frequency and showed a pause during muscle contraction even if the pause was not very pronounced in most Ten spindle afferents. But in no case was an increased activity observed during contraction. In each fibre the variability of the interspike interval (standard deviation/mean) was determined from several samples at different muscle lengths with afferent firing frequencies between 20–50 imp/s. The values in Table 1 are the mean values of the different calculations.

After identification of the afferent fibre the microelectrode was inserted into the cord and an attempt was made to stimulate its spinal axonal branches. The actual origin of the spinal fibre branches from the identified fibre was proved by the collision technique (*cf.* Schmidt *et al.* 1961). As long as the stimulus in the cord was subthreshold for the group II fibre the peripheral stimulus evoked an orthodromic spike (*cf.* Fig. 2A). As soon as the cord stimulus exceeded threshold the peripherally induced impulse was collided out by the earlier appearing antidromic impulse elicited by the cord stimulus (Fig. 2C). Threshold stimulation at the cord evoked an regular alternation of the impulse responding to the cord stimulus or to the peripheral stimulus (Fig. 2B). Due to multiple antidromic discharges in other fibres an antidromic group II impulse induced by suprathreshold cord stimulation could not be recognized in 3 out of 10 investigated fibres. However in these cases the colliding-out effect of the central stimulation upon the peripherally induced impulse was accepted as criterion for the continuity between the excited spinal axonal branch and the afferent group II

TABLE I Peripheral characteristics of the investigated group II muscle spindle afferents comparing data for group I afferents and a survey about the intraspinal regions from which the group II fibres were antidromically activated

Group II Unit No	Peripheral characteristics group II fibres							Group II antidromically activated from intraspinal regions Rexed layers			
	cond veloc m/s	thresh α T	static sens Imp/s mm	intersp variab	cond veloc m/s	thresh α T	intersp variab *	d f	I-IV	V-VI	VII-VIII
Ten-I 22	44	43	05					(+)	+	(+)	+
Ten-II 26	43	17	04					-	(+)	-	+
Ten-III 37	20	22	04					-	(+)	(+)	(+)
Ten-IV 41	25*	10	07					+	+	(+)	+
Ten-V 47	14	05	05	108	08			-	+	(+)	+
Ten-VI 52		21	05					+	+	+	+
Ten-VII 56	15	31	06	170	05			(+)	+		
MG-I 34	16	33	04	86	08	15		(+)	(+)	+	+
MG-II 46	15	17	08	103	06	88		+	+	+	+
			[23]			[171]					
MG-III 62	13	61	04	99				+	+	+	+

cond veloc threshold peripheral conduction velocity threshold in relation to α fibre threshold (α T)

static sens static sensitivity to graded stretch

intersp variab variability of the interspike intervals

thresh here in relation to Ia threshold

[] variability of the interspike interval before deafferentation

d f dorsal funiculus

+ antidromically activated from this area with less than 10 μ A

(+) antidromically activated from this area with 10-20 μ A (Ten) or 10-20 μ A (MG)

- no antidromic activation with less than 20 or 20 μ A

fibre The regions from which the axonal branches of a group II fibre could be excited were mapped out as follows. The electrode was inserted into the cord dorsum to a tip position of 4.5-5 mm from the cord dorsum and slowly (2.5 \times 10-15 μ m/s) withdrawn under continuous maximal microelectrode stimulation and stimulation with 5-10 α T of the peripheral Ten or MG nerve branch. As soon as the orthodromic impulse in the root filament was collated out the threshold current for excitation of the spinal axonal branch at that place was determined. Then the electrode was retracted in steps of 50 or 100 μ m and at each position the threshold current for antidromic activation was measured. The exploration in the cord was done by tracking with different transverse angles of the microelectrode in steps of 5 or 7.5°. The electrode was always inserted through the same surface spot in about the middle between the midline and root entry zone. An angling of 10-15° ventro-medially to 20-35° ventro-laterally normally covered the entire gray matter except the most dorsolateral part of the ventral horn and the most dorsomedial and dorsolateral part of the dorsal horn. Due to the richness of the blood vessels on the cord dorsum a systematic transverse exploration of these regions was impossible in most cases.

The position of the tracks was histologically verified by placing one reference electrode in one track at each relevant level of transverse exploration. A shrinkage of the cord during histological preparation of 10 μ m was taken into account. This value was taken from the transverse shrinkage which was determined in two experiments where reference electrodes were inserted into the cord in a known transverse distance.

Abbreviations: Hamstring HS, medial gastrocnemius MG, lateral gastrocnemius LG, cutaneous Tn. α T in context of stimulus intensities means "times threshold for efferent fibres".

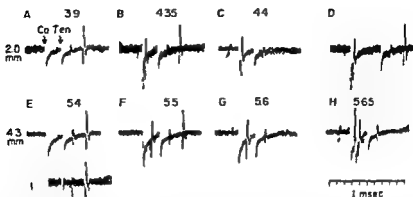


Fig. 2. Identification of impulses in a Ten group II fibre (Ten I 47 m/s) antidromically activated from two different intraspinal sites (same transverse level). In each record 5 traces are superimposed: I stimulation of the peripheral Ten nerve alone; A—H intraspinal (Co) and peripheral (Ten) stimulation together. A—D intraspinal stimulation at an electrode depth of 2.0 mm; E—H at 4.3 mm. Current strength for intraspinal stimulation is indicated in μ A. In A and E the cord stimulus was subthreshold. In B and F the cord stimulus was just at threshold strength; the impulses were induced irregularly from the cord stimulus or from the peripheral stimulus. In C and G the cord stimulus was suprathreshold and the peripherally induced impulse was collided out. D: demonstration of the critical interstimulus interval for collision (see text). H: additional antidromically induced larger and faster impulse, presumably of a group I fibre. Time: 1 ms/division.

Results

1. Identification of the fibres as secondary spindle afferents

Seven group II spindle afferents from the tenuissimus (Ten) and three from the medial gastrocnemius (MG) muscle were investigated. They had a conduction velocity between 22–62 m/s and a static sensitivity between 0.5–6.1 imp/s/mm. After de-efferentation the variability of the interspike intervals in these fibres ranged from 0.4–0.8% and thus remained well below the 2% limit (Matthews and Stein 1964).

The effect of de-efferentation upon the interspike variability was checked in one case (fibre MG II). Here the typical diminution was evident. Details about the characteristics of each fibre are given in Table I. In some cases, additionally to the group II fibre, an active group I fibre was included in the recorded filament. For comparison, the data of these group I fibres are also given in Table I (column 5 to 7). The labelling of the group II fibres in the text and figures refers to the numbers in Table I.

2. Transverse intraspinal distribution of thresholds for antidromic stimulation

Tenuissimus. Fig. 2 shows recordings from a Ten secondary spindle afferent (Ten V). In record I the peripheral stimulus at the Ten nerve is given alone. The peripheral orthodromic group II impulse had a latency of 30 ms (cond. veloc. 47 m/s). Another small impulse appeared after 13 ms (cond. veloc. 103 m/s) and

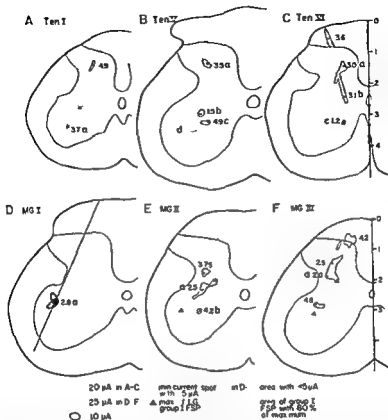


Fig 3 Intraspinal areas from which the secondary spindle afferents were antidromically activated. Each map was composed from the results of transversal tracking at one level. The indication of the fibres (A—C Ten D—F MG) refers to the numbers in Table I. Areas from which the fibres were activated with a threshold of less than $20 \mu\text{A}$ (in A—C) or $25 \mu\text{A}$ (in D—F) are surrounded by a dotted line; those with a threshold of less than $10 \mu\text{A}$ by a solid line. The minimal threshold point within the latter areas was marked with a dot and the threshold current was indicated if the current was less than $5 \mu\text{A}$. The indications a—d refer to Table III. Black triangle in D—F: maximum of focal synaptic potentials (FSP) generated by group I from LG. In D: horizontally hatched area indicates antidromic excitation with less than $5 \mu\text{A}$; vertically hatched area: area of group I FSP from LG with a size of more than 80% of its maximum.

was presumably generated by cut group I afferents: its size varied considerably with slight changes in the recording conditions. In the records A—H both peripheral and spinal stimuli were applied: the latter at two different sites with minimal threshold for antidromic excitation of the fibre, at a depth of 2.0 mm (A—D) and at 4.3 mm (E—H), both at the same transverse level (stimulus sites marked by a and d in Fig 3 B). The stimulus strength is given in μA . In A and E the intraspinal stimulus was subthreshold for antidromic excitation and an impulse is induced from the Ten stimulus. When the intraspinal stimulus was at threshold (B and F) the pike was elicited with irregular alternation either from the intraspinal or from the

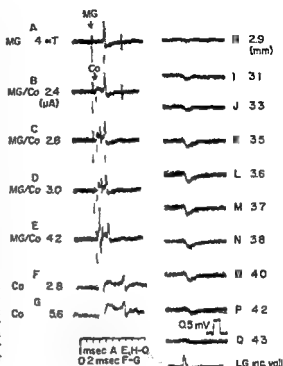
peripheral Ten stimulus. With slightly suprathreshold stimulation in the cord the spikes were exclusively evoked by the intraspinal stimulus (C and G).

The latency for the antidromically conducted spike was 0.35 ms at the depth of 2.0 mm (C) and 1.07 ms at 4.3 mm (G). In D the interval between the two stimuli is enhanced to show the critical latency for collision (first stimulus intraspinal strength as in C). Sometimes the peripheral Ten stimulus now evoked a spike even if the intraspinal stimulus had suprathreshold strength. As expected the critical interstimulus interval was reached when the interval between the end of the first antidromic spike and the peripheral Ten stimulus (second stimulus) exceeded the conduction time of the orthodromically conducted spike. When the stimulus strength was slightly enhanced another antidromic spike was evoked from the deep spinal stimulus site (H). The size of this impulse was 1.5 times larger than that of the group II one and its latency to the stimulus was about half as long (0.5 ms). Similar antidromic spikes 1.5 to 3 times larger and about twice as fast as those of the identified group II fibres were observed in several experiments (*cf.* Fig. 4 E and Table III). They could not be identified peripherally but were assumed to originate from group I afferents. Data for group I fibres are given in Table III for comparison with group II fibres data.

The depth of the second intraspinal stimulus site in Fig. 2 (4.3 mm) indicated that branches of secondary spindle afferents from Ten were found not only in the intermediate region and dorsally to it but also in the ventral horn (Fig. 3 (A-C)) and Table I summarizes the regions from which Ten secondary spindle afferents were antidromically excited. In Fig. 3 those areas from which the fibres were excited with 20–25 μ A or less are surrounded by a dotted line; those with thresholds of less than 10 μ A by a solid line. Threshold minima with less than 5 μ A within this area are marked with a dot and the minimal current is given.

In Table I the regions from which the fibres were excited are defined according to the classification of layers by Rexed (1954) (*cf.* insert A in Fig. 1). Here a plus sign without parenthesis indicates that the fibre could be excited with less than 10 μ A. The parenthesis means that excitation was seen with 10–20 μ A. The drawing of Fig. 3 were made from the results of transverse tracking at one level only while the information in Table I was collected from all results obtained for the fibre. The asterisk denotes fibres from two or more levels. Most of the investigated fibres (5 out of 7) entered an ascending branch into the dorsal funiculus (for data about the longitudinal course see below). The negative finding of 2 experiments in the dorsal funiculus was practically without meaning since the dorsal funiculus was not sufficiently explored. All fibres were antidromically excited in the dorsal horn in most cases at less threshold (less than 10 μ A). The most excitable region was usually dorsal to dorso-lateral to the intermediate region where the maximal group I focal synaptic potentials from the posterior biceps-semi-tendinosus muscle are found (*cf.* Eccles *et al.* 1954). Antidromic activation was obtained from the intermediate region in 3 cases (*cf.* 6) but usually with higher threshold than in the dorsal horn.

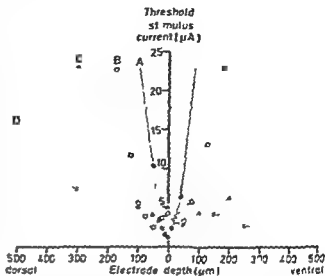
Fig 4 Antidromic activation from the region of the motor nucleus of a secondary spindle afferent. Fibre MG I. Five traces superimposed in each record. A stimulation of the MG nerve (MG) evoking a group II spike (latency 4.7 ms) and a large group I volley (latency 18.5 ms). B—E peripheral stimulus and cord stimulus (Co) together. In B—D electrode depth 3.675 mm, in E 3.675 mm in the track marked in Fig 3. Cord stimulus in H subthreshold for antidromic fibre activation, in C threshold in D suprathreshold. The current strength is indicated in μA . In E intraspinal threshold stimulation for an additional antidromic spike presumably in a group I fibre. F—G cord stimulus alone (same stimulus site as B—D) in F threshold current, in G after doubling of the threshold current both with expanded time display. H—Q group I focal synaptic potentials (FSP) generated by LG nerve stimulation (stimulus strength 5 aT) recorded at the indicated electrode depth. Same track as for stimulation in B—G (marked in Fig 3 D). The incoming volley to LG stimulation recorded at L7 root entrance is displayed below Q. Voltage calibration for H—Q is given below P. Time 1 ms/division for A—E and H—Q, 0.2 ms/division for F—G.



Surprisingly in all cases the fibres were antidromically excited from a region within the ventral horn in most cases with low threshold (less than 10 μA in 5 out of 8 cases in three of them less than 5 μA). The most excitable spots were medial to dorso medial of motor nucleus or reaching into it.

Medial gastrocnemius The intraspinal threshold measurements from MG secondary spindle afferents were correlated with the distribution of the group I focal synaptic potentials evoked from the lateral gastrocnemius nerve. The position of the maximal focal potentials is marked in Fig 3 (D—F) by a triangle. From Fig 3 (D—F) and from Table I it appears that the intraspinal distribution of areas from which the gastrocnemius group II spindle afferents were antidromically excited was similar to that of the tenuissimus afferents. They all sent an ascending branch into the dorsal funiculus and were antidromically excited from regions in the dorsal horn and the intermediate region. Moreover in all three cases regions for excitation with low threshold current (minima between 2.8 and 4.8 μA) were found in the ventral horn in two cases dorsal and dorsomedial to the maximum of the lateral gastrocnemius motor nucleus (E and F) and in one case reaching into it (D fibre MG—I). In Fig 3 (D) for the latter experiment the area in the ventral

Fig 3 Different pattern of threshold-depth relations. The graphs indicate the threshold current for antidromic activation of the intraspinal group II fibre branches. Zero depth means the depth of minimal threshold for A and the mean depth of the stimulating points with lowest thresholds for B—D. The other positions of the electrode tip are indicated as the distance dorsal or ventral to this depth. A curve of Ten 11 zero depth corresponds to an electrode depth of 3.16 mm. B MGI 0 = 3.6 mm depth. C MGI 0 = 0.60 mm depth. D MGI 0 = 1.70 mm depth.



horn from which the group II spindle afferent was excited with a stimulation strength of less than 5 μ A is hatched horizontally while the area where the size of the group I focal synaptic potentials was more than 80% of the maximum is hatched vertically. Both areas are clearly overlapping.

The original records in Fig 4 show that the minimal threshold site for antidromic excitation (2.8 μ A) of this group II fibre (MGI 1) lay in the region of the maximal group I focal synaptic potential. In A the peripheral stimulus at the medial gastrocnemius nerve was applied alone the group II fibre spike had a latency of 4.7 ms (cond. veloc. 34 m/s) while some simultaneously recorded group I fibres had a latency of 1.85 ms (cond. veloc. 86 m/s). B—Q are recorded in a track which was marked in Fig 3 D. B—D show the procedure for determination of the threshold for antidromic excitation of the fibre at the site of the minimal threshold at 3.6 mm electrode depth as described for the fibre in Fig 2. H—Q show the group I focal synaptic potentials at the indicated electrode depth. It is evident that the maximum of these potentials were located at 3.6—3.7 mm i.e. at the depth of the minimal threshold for antidromic group II fibre excitation. E shows another example of a fast large spike which could be excited antidromically additionally to the group II spike with its site of minimal threshold close to that of the group II spike (0.05 mm ventrally to the stimulus site of B—D).

3. Relation of the threshold current to electrode tip position

In the graph shown in Fig 3 the threshold current for antidromic activation of the fibres was related to the depth of the stimulating electrode. Zero depth in Fig 3 is the depth of minimal threshold (for A) or the mean depth of the stimulating sites with the lowest thresholds (for B—D); the other positions of the electrode tip are indicated as distance dorsally or ventrally to this depth. The curves

TABLE II Longitudinal distribution of spinal branches of secondary spindle afferents

	Distance between root entrance and stimulation level (mm)			
	dorsal fun. c.	dorsal horn	intermed. reg.	ventral horn
cranial last +	6.6	3.2	3.0	3.2
first □	—	4.6	3.2	4.6
caudal last +	0.4	1.0	0.8	0.4
first □	0.5	—	1.0	0.5

last + = distance to the extreme cranial or caudal stimulation level from which antidromic activation occurred with less than 20–25 μ A.

first □ = distance to the first cranial or caudal stimulation level from which fibres were not activated.

The Table gives the extreme values obtained from different experiments (6 Ten and 3 MG fibres of text).

represent characteristic examples of the three main different patterns of threshold depth curves. The first type (curve A) has a well defined minimum and a symmetrical steep threshold increase on both sides (cf Jankowska and Roberts 1972). In the second type (B and C) the minimal threshold current was not so clearly restricted being scattered (about ± 1 –2 μ A) around a mean minimal value in a zone of about 100 to 300 μ m. However the slope of the rise of the threshold current away from the borders of the low threshold zone resembled that of the first type. In the third type (D) the zone of low threshold current was even larger (more than 500 μ m) and the scatter around the mean minimal current more pronounced (about ± 3 –4 μ A). Moreover the change to the rising slope of the threshold curve beyond the zone of low threshold was often less steep (cf D dorsal side). These three types were not strictly separated so that intermediate shapes were observed.

In consideration of the investigations of Jankowska and Roberts (1972) it is assumed that stimulation sites in the gray matter with thresholds of about 3.0 μ A had a distance to the activated fibre of less than 160 μ m. In most of the above described threshold depth relations of the first or second type the rise from minimal threshold current values of 1.2–5 μ A to the values of 20–25 μ A occurred within 75–225 μ m. It can thus be estimated that the electrode tip-to-axon distance is at less than 400 μ m if the threshold current was less than 20–25 μ A.

4 Longitudinal mapping

A systematical longitudinal mapping for each fibre could not be performed. Therefore the findings regarding the longitudinal distribution of 6 Ten and 3 MG fibres were combined. The results are summarized in Table II. The longitudinal position of the intraspinal stimulation site is given as distance to the level of the

TABLE III Central antidromic delay and effective antidromic intraspinal conduction velocity

Group II Unit No	group II impulses					group I impulses	
	periph cond veloc. m/s (2)	stim depth mm (3)	thresh current μ A (4)	central antidr delay ms (5)	intrasp cond veloc m/s (6)	central antidr delay ms (7)	intrasp cond veloc m/s (8)
Ten-II	26	31 33	9.5 6.5	1.15 0.9	5.6 8.3		
Ten-IV	41	2.8	6.6	0.85			
Ten-Va	47	2.0	3.5	0.35	15.5	0.25	19.8
b		3.7	1.5	0.67	9.6		
c		5.9	5.8	0.72	10.0	0.35	20.2
d		4.3	5.5	1.07	7.0	0.50	14.9
		4.3	7.0	0.93	9.6	0.35	26.7
Ten-VIa	52	1.4	5.0	0.45			
b		2.4	3.1	0.55			
MG-Ia	34	3.6	2.8	0.74	10.9	0.25 0.35	32.3 22.0
MG-II	46	2.3	4.25	0.6	6.2	0.3	11.8
a		2.4	7.0	0.7	9.7		
b		3.3	4.2	0.85	8.7		
MG-IIIa	62	2.0	2.0	0.5	9.4		
		2.4	5.7	0.8	6.4		

(2) peripheral conduction velocity of the group II fibres

(3) depth of antidromic intraspinal stimulation (group II and group I)

(4) threshold current for antidromic group II activation

(5) central antidromic delay of the group II impulses

(6) effective antidromic intraspinal conduction velocity of the group II impulses (for calculation see text)

(7) comparing data for antidromic group I impulses (cf. text)

cord entrance of the fibre. For the different spinal regions is given the most cranial or caudal stimulation site from which a fibre was antidromically activated with less than 20–25 μ A (last +). The distance of the first investigated level beyond this position is the first level from which a fibre could no longer be activated with this stimulus strength is also given (first ϕ). In the gray matter branches of the secondary spindle afferents were found up to about 3.2 mm cranial of the fibre entrance and down to 0.4 to 1 mm caudal of it. The ascending branch in the dorsal funiculus was traced cranially only up to 0.6 mm and no further investigation was performed.

5 Central antidromic delay and intraspinal conduction velocity

Table III gives the delay between the intraspinal stimulus at different depth and the antidromic spike in the dorsal root filament (central antidromic delay). The depth given in column 3 is the observed electrode depth and due to the angling of the manipulator this depth has to be reduced by 5–15% to get the approximate perpendicular depth from the cord dorsum (cf. Fu *et al.* 1974).

The indication a—d in column 1 of Table III refers to the labelling in Fig 3. These stimulation sites were close to or identical with the sites of minimal threshold marked in the figure. The central antidromic delay (column 5) was generally measured with slightly suprathreshold stimulation current. This means a stimulus strength which just induced constantly an antidromic spike with a stable latency (about 1.1—1.2 times threshold current). The effect of increasing current strength upon the central antidromic delay was not systematically investigated. In a few cases however when the current was increased to 1.5 or 2 times threshold (threshold 2—4 μ A) the delay was reduced by less than 0.1 ms. In the example of Fig 4 (F, G) doubling of the threshold current induced a shift of the antidromic spike of only 0.04 ms. Since the recordings were taken from the dorsal root at a distance of 4.4—8.5 mm from the cord entrance the conduction time in the root must be subtracted to get the real intraspinal antidromic delay. Assuming the same conduction velocity in the root as in the periphery the root conduction time was 0.3 ms for Ten—II in the range of 0.1 ms for the other group II fibres and presumably about half as long for the group I fibres.

No positive relation was found between the peripheral conduction velocity of the fibre and its central antidromic delay, i.e. there was no clear evidence that faster group II fibres had a shorter delay (stimulation at comparable depths). For example the delay of MG—II (46 m/s) was 0.7 ms at 2.4 mm depth with MG—III (62 m/s) 0.8 ms at the same depth.

A clear relation however was seen between the central delay and the depth of the site from which the fibre was antidromically activated. This relation was particularly evident for fibre Ten—V where the delay could be measured exactly for antidromic spikes elicited at different depths. But this relationship also appears if the results of all experiments are combined. From sites within the dorsal horn (depth 1.4—2.0 mm) the delay was 0.35—0.5 ms (mean 0.43 ms) from those within the intermediate region (depth 2.3—2.8 mm) 0.55—0.85 ms (mean 0.7 ms) and from those within the ventral horn (depth 3.1—4.3 mm) 0.67—1.15 ms (mean 0.88 ms). As mentioned in section 2 antidromic group I impulses were sometimes recorded in the same filament (*cf.* Fig 2 H and Fig 4 E). For comparison the group I data are given in Table III column 7 and 8. The antidromic central delay of group I spikes was half to a third as long as that of group II spikes (identical stimulation sites ± 0.1 mm).

For a rough calculation of the effective antidromic intraspinal conduction velocity of group II afferents the simplifying assumption is made that the fibres were running in a uniform bow from the entrance level ventrally to the depth at which stimulation was performed and then straight cranially or caudally to the stimulating point at this depth. The conduction velocity in the dorsal root is assumed to be the same as in the periphery and the conduction time in the root was subtracted from the antidromic delay. Furthermore in calculating the conduction velocities given in Table III column 6 the utilization time was disregarded. The velocity thus calculated showed a wide scatter (for example 7.0—15.5 m/s for fibre Ten V).

However, in all measured cases the value was distinctly smaller than the peripheral conduction velocity the reduction being in the range of 3–10 times (mean 5.3). A strict relationship between the calculated intraspinal conduction velocity and the peripheral velocity was not seen.

The antidromic intraspinal conduction velocity of group I fibres (Table III column 8 same assumptions for calculation as for group II) was in all cases 2–3 times higher than that of group II fibres. Assuming a peripheral conduction velocity of 100 m/s the reduction of intraspinal versus peripheral velocity of group I fibres is 3–9 times i.e. in the same range as for group II fibres.

In order to eliminate the utilization time as a source of error it is more appropriate to calculate the effective intraspinal conduction velocity between two stimulating sites. The measurements from group II fibre Ten V (periph. cond. veloc. 47 m/s) allow a calculation between two sites at the same transverse level. Here between the stimulating sites in the dorsal horn (a in Fig. 3B) and in the ventral horn (b and d in Fig. 3B) the conduction velocity was 3.0–5.3 m/s. These values are even lower than the values in Table III. Thus somewhat surprising finding may be caused by different factors. Firstly, the error of disregarding the utilization time may be small compared to the error which is induced by the simplifying assumptions for the calculation of the intraspinal conduction velocity. The variations of the values from different stimulus sites at comparable depths may indicate that the latter error can be considerable. Secondly, the effective conduction velocity may get a progressive reduction within the cord possibly due to branching and/or a less straight course in the more ventral regions (cf. Table III). Ten V a-d conduction velocity from 2.0 mm depth 15.5 m/s from 4.3 mm 7.0 and 9.6 m/s.

Discussion

The methods employed allowed an investigation of the intraspinal projection of single group II fibres which were functionally identified as muscle spindle afferents. The most remarkable result was that these fibres project not only to the dorsal horn and intermediate region but also to the ventral horn close to the motor nucleus or even into it.

The threshold mapping may give information both regarding the trajectory of the stem axon and its main branches and the region of presynaptic branching and synaptic termination. Before discussing the termination it is necessary to consider the shape of the depth threshold curves and the significance of the special low threshold regions in some detail. In those cases when the region of low threshold antidromic stimulation was very restricted (cf. Fig. 3A stimulation point marked a in Fig. 3Cc) and the shape of the depth threshold curve was of the simple type (first type Fig. 5A) forming a sharp minimum it may be assumed that only one axonal branch was stimulated and that the direction of the tracks was reasonably transverse to the axon. Stonev *et al.* 1968; Jankowska and Roberts 1972; Roberts

and Smith 1973). In other cases when the depth threshold curve has a broad minimum (curve B in Fig. 5) the explanation may be either that the fibre was branching or that the electrode track was not transverse but more or less axial to the direction of the fibre. The latter type of curve was frequently found in the dorsal horn and in the ventral horn. The hypothesis of branching is made rather likely if the curve is found in combination with non-elongated large low threshold foci without any interconnecting low threshold stripe between them (e.g. Fig. 3Ba and Da). Such a stripe would rather have been expected if the results were due to stimulation of the stem axon or main branches from it. It is rather unlikely that the transverse plane chosen for detailed exploration would coincide exactly with the region where the stem of the investigated group II fibre runs ventrally in the grey matter. Moreover the low threshold foci had a longitudinal extension of several mm. Accordingly the most simple explanation of the finding of two distinct low threshold regions in the dorsal horn and in the ventral horn is that a branching network of the group II fibre is stimulated in these regions presumably preterminally or very close to the synaptic terminals.

In case of the dorsal low threshold region the group II focal synaptic potential mapping (Fu *et al.* 1974 *cf.* also Coombs *et al.* 1956) did reveal monosynaptic action exactly in this region so there is close agreement between the results of the two investigations employing different techniques. With regard to the more ventral region the very fact that the fibres cannot be stimulated from more ventral sites suggests proximity to a terminal region. However whereas in this case there is also a good local correlation to the focal synaptic potential measurements the time relation requires a more detailed discussion. The reason is that the latency of the ventral focal synaptic potential was so long that a disynaptic effect could not be excluded (central delay 1.2–2.5 ms mean 1.6–2.0 ms Fu *et al.* 1974). The long central antidromic delay which is found in group II fibres after stimulation in the ventral horn (0.67–1.15 ms mean 0.88 ms) suggests that at least a part of these focal potentials was generated monosynaptically.

In this context it should be mentioned that the central antidromic delay has to be considered with some caution firstly if the values are compared with data of other intraspinal investigations which used records of the incoming volley at the root entrance (the root conduction time must be subtracted). Secondly the utilization time for the antidromic excitation is disregarded in most of the measurements. Thirdly it is not sure if the intraspinal antidromic conduction time is equal to the orthodromic one. It may be that the antidromic invasion from small to large branches takes more time than the reverse orthodromic conduction. However if the observed antidromic central delay of impulses in presumed group I fibres (0.2–0.45 ms corrected in relation to the root entrance) is compared to the central delay of orthodromic induced group Ia EPSP in interneurons of the intermediate region (0.35–0.6 ms Eccles *et al.* 1960) or in motoneurons (0.45–0.8 ms Brock *et al.* 1957; Eccles *et al.* 1957 a, b) they both prove to be in a reasonable coherent order. Thus it can be assumed that the time difference for antidromic and orthodromic

conduction is not a serious complication probably not exceeding the inaccuracy of measurement and the error which is induced by latency variations due to small differences in stimulation strength in relation to the threshold current. In consideration of these precautions the shortest observed antidromic delay of group II fibres from the ventral horn (0.57–0.62 ms corrected in relation to the root entrance) would support the assumption that even for the fastest group II EPSPs recorded in motoneurons (central delay at least 1.3 ms Eccles and Lundberg 1959) one interneurone must be interpolated.

To summarize: The present findings in conjunction with the results regarding group II focal synaptic potentials (Fu *et al.* 1974) suggest the existence of two main populations of first order interneurons recruited from secondary spindle afferents located in the dorsal and ventral horn respectively. Due to slow intraspinal conduction velocity of secondary spindle afferents the ventral group of interneurons may be monosynaptically activated after a relatively long central delay.

The authors are sincerely grateful to Professor Anders Lundberg for his continuous valuable suggestions and his inspiring critical discussions throughout this work. Our thanks are also due to Mrs Ragni Larsson for excellent technical assistance. This work was supported by the Swedish Medical Research Council (Project No 14\94). T. C. Schomburg was supported by a grant from the Deutsche Forschungsgemeinschaft.

References

- BARKER, H. M. C. IP and M. N. ADAL. A correlation between the receptor population of the cat's soleus muscle and the afferent fibre diameter spectrum of the nerve supplying it. In *Symposium on Muscle Receptors* ed. Barker D. (pp. 157–261) Hong Kong: Hong Kong University Press, 1967.
- BOVE, I. A. and M. R. DAVIS. *Composition of Peripheral Nerves*. Edinburgh: Livingstone, 1968.
- BROOK, J. C. J. S. LOOMBS and J. C. ECCLES. The recording of potentials from motoneurons with an intracellular electrode. *J. Physiol. (Lond.)* 1957, 117, 431–460.
- CLARK, J. S. D. R. CURTIS and S. LUNDBERG. Spinal cord potentials generated by impulses in motoneuron and cutaneous afferent fibres. *J. Neurophysiol.* 1956, 19, 457–467.
- CLARK, R. M. and A. LUNDBERG. Synaptic actions in motoneurons by afferents which may evoke the flexion reflex. *Arch. ital. Biol.* 1953, 97, 109–271.
- ECCLES, J. C. R. M. ECCLES and A. LUNDBERG. Synaptic actions on motoneurons in relation to the conduction velocity of the group I muscle afferent volley. *J. Physiol. (Lond.)* 1957, 136, 537–541.
- ECCLES, J. C. R. M. ECCLES and A. LUNDBERG. The convergence of monosynaptic excitatory afferents on motoneurons of different species. *J. Physiol. (Lond.)* 1957, 137, 41–50.
- ECCLES, J. C. R. M. ECCLES and A. LUNDBERG. Influx of neurone in and around the intermediate cell of the lumbar spinal cord. *J. Physiol. (Lond.)* 1960, 151, 89–114.
- ECCLES, J. C. P. L. ECCLES, S. LUNDBERG and C. J. WILSON. Spinal cord potentials generated by volleys in the flexor digitorum profundus. *J. Physiol. (Lond.)* 1953, 103, 500–401.
- FU, T. C. M. SANTINI and F. D. SCHOMBURG. Characteristics and distribution of spinal focal synaptic potentials elicited by group II muscle afferent. *Acta physiol. scand.* 1974, 91, 298–313.
- HUNT, C. C. Relation of fibre diameter in afferent fibres of muscle nerves. *J. gen. Physiol.* 1954, 38, 11–131.
- JANKOWSKI, E. and M. J. R. BIRN. An intracellular recording technique of the axonal projections of single spinal interneurons in the cat. *J. Physiol. (Lond.)* 1972, 257, 677–697.
- JANKOWSKI, E. and D. O. SMITH. Antidromic activation of Rexed cells and their axonal projections. *Acta physiol. scand.* 1973, 88, 198–211.

- MATTHEWS P B C *Mammalian Muscle Receptors and Their Central Actions* London Edward Arnold (Publ) Ltd 1972
- MATTHEWS P B C and R B STEAD The regularity of primary and secondary muscle spindle afferent discharges *J Physiol (Lond)* 1969 207 59—82
- PAINAL A B Functional analysis of group III afferent fibres of mammalian muscles *J Physiol (Lond)* 1960 152 250—270
- REYER B A cytoarchitectonic atlas of the spinal cord in the cat *J comp Neurol* 1954 100 297—379
- ROBERTS W J and D O SMITH Analysis of threshold currents during microstimulation of fibres in the spinal cord *Acta physiol scand* 1973 89 384—394
- SCHMIDT R F J SENGES and M ZIMMERMANN Excitability measurements at the central terminals of single mechano-receptor afferents during slow potential changes *Exp Brain Res* 1967 9 220—233
- STONEY B D JR, W D THOMPSON and H ASANUMA Excitation of pyramidal tract cells by intracortical microstimulation Effective extent of stimulating current *J Neurophysiol* 1968 31 659—669
- WALL P D, W S McCulloch, J Y LETTVIN and W H PITTS The terminal arborization of the cat's pyramidal tract determined by a new technique *1956 J Biol Med* 1956 78 457—464

Uptake of Iodinated Oxytocin by Some Tissues and Organs in the Male Rat

By

ANDERS AGUO

Received 10 December 1973

Abstract

AGUO A Uptake of iodinated oxytocin by some tissues and organs in the male rat
Acta physiol scand 1974 91 330-338

The tissue distribution of ^3I -oxytocin was studied shortly after injection of 40 mU into male rats. There appeared to be a gradual accumulation of radioactivity in the neurohypophysis and a specific uptake was observed in the vas deferens. The radioactivity content was also studied in extracts prepared from the hypophysis in animals killed 30 or 240 s after injection. There appears to be a very rapid catabolism both in the neuro- and adenohypophysis since radioactivity was found in several substances already 30 s after injection of intact hormone. The uptake pattern in the various tissues is discussed in relation to known or suggested functions of oxytocin in the male.

Oxytocin is known to induce contractions in the uterus and the mammary gland. This effect is generally believed to be mediated via oxytocin receptors in the muscle cells and the myoepithelial cells resp. in these target organs. By using purified oxytocin it has recently been shown that the hormone is taken up in the uterus (Sjoholm and Riden 1969) and the mammary gland (Soloff, Swartz and Saffran 1972) of the rat. Oxytocin analogues further compete with oxytocin for uptake in proportion to their known oxytocic activities (Soloff *et al.* 1973).

It has been known that oxytocin initiates or stimulates contractions in vas deferens in the rabbit (Melin 1970) and in the ram (Knight 1972). It is also known that oxytocin stimulates contractions in tubuli in the testis (Niemi and Kormanio 1963). Furthermore, several authors have suggested that oxytocin liberates gonadotropins (Marini *et al.* 1969; Wenner 1965; Melin 1971) and it has been established by radioimmunoassay that oxytocin specifically liberates FSH in males (Franchimont and Legros 1969). It has finally been reported that oxytocin stimulates sexual activity in the male rabbit (Melin and Kihlstrom 1963). As oxytocin certainly exerts at least some of these effects it should be possible to demonstrate uptake of oxytocin by some of the above mentioned tissues in the male. The usual vas of

studying such a problem has been to inject tritiated oxytocin and measure the radioactivity content in various tissues. However the specific activity of the tritiated preparations is much too low to allow measurement in small tissue samples after injection of physiological doses.

Since it has been shown by Thompson, Freychet and Roth (1972) that iodinated oxytocin retains at least some of its biological activities and since it is possible to prepare iodinated oxytocin with high specific activity (500–1000 $\mu\text{Ci}/\mu\text{g}$) we decided to use the radioiodinated hormone in order to study the distribution of oxytocin after intravenous injection in the male rat. Besides measuring uptake of the hormone we also prepared extracts from the hypophysis after injection and subjected the \equiv to thin layer chromatography to get some idea of the fate of the oxytocin.

Materials and methods

Radioiodination: Synthetic oxytocin (450 IU/mg, Sandoz) in a quantity of 2 IU per iodination was iodinated with ^{125}I (NHS 30 Radiochemical Centre, Amersham, England) according to Greenwood, Hunter and Glover (1963) as modified for oxytocin by Chard, Kitau and Landon (1970). However saline instead of tris buffer was used for the final dilution of the reaction mixture. The yield (incorporation of ^{125}I in oxytocin) of each radioiodination varied between 83 and 90 per cent.

Unreacted iodine was removed by the addition of 11 g Dow ion exchange resin (2 \times 8 50–100 mesh, Dow Chemical Co.) followed by vigorous shaking for 2 min. After the resin had settled 10 μl of the supernatant was subjected to electrophoresis on Whatman 3 MM paper (13 V/cm, 90 min in veronal buffer, pH 8.0, ionic strength 0.1). The proportion unreacted iodine never exceeded 4%. Upon thin layer chromatography (see below) oxytocin and iodine were found together with some material remaining at the application point. Before the Dow treatment two unknown spots were regularly found in the chromatograms. The solution was divided in 3 ml aliquots and stored below -25°C until used (always within 30 days). Iodine, a substance which except in the thyroid gland is mainly extracellular, was chosen as a convenient control substance. For the control experiments ^{125}I alone as mixed with exactly the same solutions as the oxytocin, excepting the addition of Dowex.

Injection of iodinated oxytocin or iodine: The rats (male Sprague Dawley rats, 300 g, Anticimex, Sollentuna, Sweden) were anesthetized with 25% urethane injected intraperitoneally at a dose of 0.5 ml/100 g b.wt. The external jugular vein on the left side and the common carotid artery on the opposite side were cannulated with thin polyethylene tubings. Oxytocin 40 mU approx. 30 μCi or iodine approx. 50 μCi ($< 35\text{ ng}$) were injected in the jugular veins at a volume of 0.5 ml.

Preparation of tissue samples: At different times after the injection 0.4 ml blood was taken from the carotid artery and immediately thereafter the animals were killed by exsanguination. The skull was quickly opened and the brain removed. Within 3 min after the death of the animal the hypophysis had been taken out and the neural lobe separated from the adenohypophysis. Additional tissue samples (cerebral cortex, hypothalamus, skeletal muscle, vas deferens, testis, epididymus, seminal vesicle, prostate and coagulating gland) were all rapidly dissected out and carefully freed from connective tissue. All samples were then washed in saline to remove any blood which might have adhered to their surfaces. They were carefully dried on a filtering paper put in preweighed polyethylene tubes and weighed to the nearest tenth of a milligram. Cerebral cortex was usually taken from the right side. The hypothalamus

was cut out with a sharp scalpel blade or with a small pair of scissors rostrally immediately in front of the optic chiasm to a depth of about 3 mm dorsal to the base of the brain and caudally in the rostral end of the pons to the same depth. The tissues in the polyethylene tubes were dissolved with 1 ml of 30% KOH per tube to obtain equal geometry in the gamma-counter. The radioactivity content in all samples was counted in an Autowell II automatic gamma counter, the efficiency of about 12% and a background of 16–20 cpm.

Extraction and thin layer chromatography: Animals used for these studies were cannulated only in the external jugular vein, the carotid artery being left intact. At certain intervals after injection of the radioactive material the animals were killed by decapitation.

TABLE I Radioactivity content in some tissues and organs at varying times after the injection of 125 I oxytocin Dpm/mg Each value represents the mean from 5 animals The variation indicated is the standard error of the mean

Tissue/organ	Time between injection and killing of animal (seconds)			
	30	60	90	240
Blood	3161 \pm 562	2995 \pm 120	1474 \pm 278	1553 \pm 79
Adenohypophysis	1481 \pm 701	1690 \pm 201	745 \pm 211	1009 \pm 49
Neurohypophysis	1651 \pm 363	1725 \pm 63	1005 \pm 154	1310 \pm 90
Hypothalamus	118 \pm 17	145 \pm 13	63 \pm 16	110 \pm 8
Skeletal muscle	110 \pm 56	177 \pm 26	141 \pm 41	170 \pm 30
Testis	74 \pm 515	114 \pm 14	73 \pm 18	115 \pm 13
Epididymus	55 \pm 12	124 \pm 31	77 \pm 20	153 \pm 33
Vas deferens	352 \pm 98	238 \pm 33	170 \pm 37	216 \pm 49
Seminal vesicle	192 \pm 40	219 \pm 30	190 \pm 44	235 \pm 193
Coagulating gland	195 \pm 54	199 \pm 27	233 \pm 90	245 \pm 29
Prostate	261 \pm 53	233 \pm 35	193 \pm 15	408 \pm 16
Cerebral cortex	141 \pm 12	122 \pm 12	85 \pm 14	95 \pm 6

The heads were immediately dropped into a mixture of *n*-hexan and dry ice After 10 min the heads were removed and stored below -25°C for a few days before extraction A total of eighteen rats were used in this part of the study The hypophysis was dissected out of the still frozen head thawed and separated into neuro- and adenohypophysis Immediately there after the parts were dropped into 250 μl 10% ice cold acetic acid and homogenized Three hypophyses were pooled and extracted as has been previously described for bovine neurohypophysis by Pliska, Thorn and Vilhardt (1971)

The dried tissue extracts were dissolved in 50 μl 5% acetic acid and 10 μl of this solution and standard solution of oxytocin iodine and tyrosine were subjected to thin layer chromatography on silicagel plates (DC Fertigplatten Kieselgel 60 Merck in either of two systems (a) butanol acetic acid water 3:1:1 or (b) butanol pyridine acetic acid water 15:10:3 (v/v)) The distance between the start and the front was about 13 cm Each extract was chromatographed twice in both systems These systems have been used by Pliska, Birch and Thorn (1971) for chromatography of vasopressin metabolites

The dried plates were covered with Ilford Industrial X-ray film and stored in the dark at $+4^{\circ}\text{C}$ for 5 to 60 days The X-ray film was developed in Kodak D 19 X-ray developer

TABLE II Radioactivity content in some tissues and organs at varying times after injection of 125 I Dpm/mg Each value represents the mean from 5 rats The variation indicated is the standard error of the mean

Tissue/organ	Time between injection and killing of animal (seconds)			
	30	60	90	240
Blood	1713 \pm 243	9126 \pm 143	1276 \pm 291	555 \pm 71
Cerebral cortex	121 \pm 4	78 \pm 6	101 \pm 90	107 \pm 93
Adenohypophysis	3072 \pm 491	3561 \pm 317	536 \pm 191	371 \pm 59
Neurohypophysis	1111 \pm 319	1293 \pm 193	1519 \pm 803	703 \pm 11
Hypothalamus	15 \pm 19	116 \pm 17	105 \pm 17	77 \pm 3
Skeletal muscle	114 \pm 11	215 \pm 15	114 \pm 28	51 \pm 11
Testis	86 \pm 21	71 \pm 11	257 \pm 57	58 \pm 7
Epididymus	109 \pm 45	73 \pm 4	77 \pm 93	155 \pm 91
Vas deferens	219 \pm 33	215 \pm 21	175 \pm 48	142 \pm 9
Seminal vesicle	163 \pm 31	241 \pm 50	181 \pm 51	111 \pm 9
Coagulating gland	171 \pm 43	219 \pm 43	171 \pm 52	144 \pm 8
Prostate	205 \pm 29	194 \pm 30	167 \pm 47	120 \pm 23

TABLE III Radioactivity content in neuro- and adenohypophysis expressed relative to that of the blood after injection of ^{125}I -oxytocin or ^{125}I Mean \pm S.D.

Time after injection	Adenohypophysis		Neurohypophysis	
	^{125}I -oxytocin	^{125}I	^{125}I oxytocin	^{125}I
30 s	0.46 ± 0.147	1.79 ± 1.311	0.51 ± 0.088	0.88 ± 0.437
60 s	0.52 ± 0.097	1.47 ± 0.903	0.45 ± 0.173	0.54 ± 0.690
90 s	0.44 ± 0.074	0.42 ± 0.067	0.78 ± 0.083	1.27 ± 0.781
240 s	0.58 ± 0.049	0.53 ± 0.110	0.91 ± 0.064	1.28 ± 0.592

Results

Distribution of ^{125}I oxytocin

The disappearance of radioactivity from the blood was slower after injection of ^{125}I -oxytocin than after ^{125}I (Table I and II). The radioactivity content of the neurohypophysis was not significantly changed between 30 and 240 s after injection of ^{125}I oxytocin. A statistically insignificant decrease was obtained when ^{125}I was injected (Table II). The data obtained at 30 and 60 s after iodine injection was extremely variable between different animals (Table II and III). The adenohypophysis showed the same general pattern as the neurohypophysis. If the radioactivity content of the hypophysis is expressed relative to that of the blood at the same time (Table III) it is seen that oxytocin is gradually accumulated in the neurohypophysis whereas iodine is not. The difference between 90 s and 240 s is statistically significant ($p < 0.025$) for both the neuro- and adenohypophysis after oxytocin injection but not after iodine injection.

The radioactivity content in the other tissues and organs studied at varying times after injection of oxytocin or iodine is also shown in Table I and II. As can be seen no other tissues or organs approached the levels found in the neuro- or adenohypophysis.

The vas deferens is different from most other samples as its radioactivity content is at a maximum 30 s after injection of both oxytocin and ^{125}I . There were no significant differences between the various values obtained after oxytocin injection but when iodine was injected the radioactivity content was significantly lower at 240 s than at 30 s ($p < 0.05$). Another pattern is obtained with the prostate. Here the value at 240 s is higher than the others ($p < 0.05$). The latter is also the case for the testis and epididymis after ^{125}I -oxytocin ($p < 0.05$). When ^{125}I was injected none of these organs shows the same pattern as after oxytocin injection. The radioactivity content in the prostate decreased between 30 and 240 s ($p < 0.05$) whereas that of the testis and epididymis was not significantly changed after iodine injection.

Thin layer chromatography

As the R_F -values of the substances studied were rather similar it proved necessary to use two different developing systems in order to separate oxytocin from tyrosine

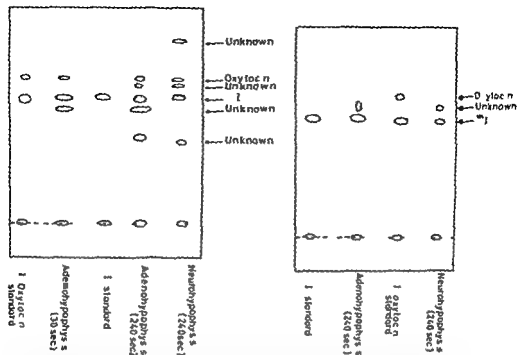


Fig 1 Thin layer chromatogram (pyridine system) of various extracts obtained after intravenous injection of 40 mU ¹²⁵I oxytocin. Figures in brackets refer to time between injection and killing of the animal.

Fig 2 Thin layer chromatogram (pyridine system) of various extracts obtained after injection of ¹²⁵I. Figures in brackets refer to time between injection and killing of the animal.

a metabolite which is found very soon after injection of oxytocin (Sjöholm and Riden 1969).

In the chromatogram of the adenohypophysis extract prepared from rats killed 30 s after injection of oxytocin three distinctive and one weak radioactive spot are found in the pyridine system (Fig 1). One corresponds to intact oxytocin and one to ¹²⁵I. The weak one and the third distinctive spot are unknown. In the pyridine free system at least five spots are obtained. The significance of the unidentified spots is at present unknown. At 240 s there is another unknown spot in the pyridine system (Fig 1). The size and blackening of the other spots seem to be generally the same.

The extract from the neurohypophysis prepared 30 s after oxytocin injection and chromatographed in the pyridine system contains detectable amounts of only oxytocin and ¹²⁵I. Even these spots were very faint and exposure times of more than 50 days had to be used before they could be detected at all. At 240 s after injection there are at least 3 spots (Fig 1). These are oxytocin, iodine and 3 unknown. In the pyridine free system are found the same but very weak spots as in the extract from the adenohypophysis at 30 s.

DISTRIBUTION OF OXYTOCIN

After injection of iodine alone 3 distinctive spots were found in the extract both the adeno- and neurohypophysis. One of these corresponds to ¹²⁵I-1 other 2 unknown. A third very weak spot was sometimes observed (Fig. 2).

Discussion

One could imagine that a re uptake of oxytocin in the neurohypophysis is performed by a mechanism similar to that known to operate in the catecholaminergic neurons. Pliska, Thorn and Vilhardt (1971) found accumulation of intact 3H vasopressin and some of its metabolites after *in vitro* incubation of the neurohypophysis from oxen and similar results were obtained with rat and pig neurohypophysis by Edwards (1971a). On the other hand Edwards (1971b) could find no evidence of intact intracellular oxytocin using essentially the same methods as Pliska. Barth and Thorn (1971), Willumsen and Bie (1969) studied the *in vivo* uptake of 3H vasopressin in the rat and found a very high content in the hypophysis 12 min after injection. Aroskar *et al.* (1964) observed a high radioactivity content in the hypophysis 20 min and one hour after injection of 3H oxytocin.

The high doses used in the above mentioned studies (1—10 IU/rat) are entirely unphysiological. It is for example known that about 14 mU of oxytocin is released during suckling in the lactating rat (Grosvenor and Turner 1957). Moreover Sjöholm and Ryden (1969) and Willumsen and Bie (1969) have shown that breakdown products appear in the blood within 120 s after injection of oxytocin or vasopressin. Thus we know a great deal about the uptake and distribution of oxytocin or vasopressin metabolites but very little about the uptake of intact hormone *in vivo*. However, already 30 s after injection we found in this study oxytocin in both the adeno- and neurohypophysis. At the same time there was also some other iodinated substance in the extract prepared from the adenohypophysis suggesting a fast breakdown of oxytocin in at least that part of the hypophysis. It is not very likely that this substance is taken up from the blood at this time since the injected preparation does not contain any detectable substances other than oxytocin and iodine and the time is probably too short to allow an extrahypophysial breakdown of oxytocin. It is on the other hand likely that oxytocin penetrates the cell membranes in the hypophysis since the enzymes responsible for its degradation probably are intracellular. That there are enzymes in the neurohypophysis capable of degrading neurohypophysial hormones is evident from the work by Pliska, Thorn and Vilhardt (1971) and Edwards (1971a). Whether such enzymes also exist in the adenohypophysis is not known but the aminopeptidases degrading oxytocin and vasopressin are of very low specificity and it is reasonable to assume that there are aminopeptidases in the adenohypophysis which may inactivate these hormones. In sum then it is tentatively concluded that oxytocin is taken up by and rapidly degraded in the neurohypophysis most likely in the nerve terminals or axons. It is also evident that oxytocin is taken up and rapidly degraded in the adeno-

hypophysis. Thus these results cannot be explained simply as a result of some neuronal re uptake mechanism. It may be noted that the amount of iodine taken up in the neurohypophysis is as high as the amount of ^{125}I oxytocin. It has actually been shown that iodine is accumulated in the neurohypophysis after intravenous injection (Jentzer 1953).

As mentioned earlier it has been suggested by several authors that oxytocin releases gonadotropins. From this point of view the uptake of oxytocin in the adenohypophysis is conceivable. The extremely rapid degradation is still surprising and no reasonable explanation can be offered. One possibility is that the extraction procedure in some way caused degradation of oxytocin but this procedure has been used successfully by Pliska, Barth and Thorn (1971) for vasopressin extraction and it is not likely that oxytocin is more unstable than vasopressin at the conditions used. Even if the ^1I is more loosely bound to the tyrosine residue than is ^{125}I , it is unlikely that it is incorporated into any other substances and it seems reasonable to conclude that oxytocin actually is rapidly degraded in both the adeno- and neurohypophysis.

Of the other samples studied the vas deferens showed a peculiar uptake pattern where the radioactivity content not significantly changed between the various times. Another oxytocin target organ, the uterus, showed a somewhat similar uptake pattern in Sjöholm and Rydén's (1969) study. Our study suggests, with all reservations, that the effects of oxytocin observed by Melin (1970) on the vas deferens are mediated via a local action of the hormone in this organ. It is not justifiable to suppose that the quantitative aspects of the uptake in the vas deferens are similar for the natural and the iodinated hormone. In fact there are reasons to believe that oxytocin is much more strongly bound to and faster taken up by the receptors than is ^1I -oxytocin. This has been shown to be the case for ^{125}I insulin where binding to the diaphragm lessens and becomes slower with increasing degrees of iodination and specific activity (Bouman, Couert and Jaspers 1972).

Niemi and Hormino (1965) found clearest effect of oxytocin on the muscular element in the testis. It has accordingly been possible to demonstrate an uptake of oxytocin in the testis. The uptake pattern differed from that in the vas deferens in that it was at a maximum at 240 s. The amount taken up in the testis was smaller than the amount taken up in skeletal muscle or vas deferens. This can be understood if some attention is paid to the histology of the testis. This consists mainly of tubuli with wide lumen and thin walls with some contractile elements. The proportion of the organ consisting of muscular tissue is very small and if it were possible to determine the weight of the muscular tissue in the organ and express oxytocin uptake relative to that, then this would certainly alter the picture.

Oxytocin may occasionally stimulate contraction of the seminal vesicle (Melin 1970). This was the reason for including this the coagulating gland and the prostate. Only in the prostate was oxytocin specifically taken up.

This study has shown that besides in the hypophysis oxytocin is also taken up in some organs in the male rat, all of which have been suggested to be oxytocin

- SJÖHOLM I and G RYDÉN Uptake of oxytocin in tissues after intravenous administration of irradiated oxytocin in rats *Acta endocr (Abh)* 1969 61 432—440
- SOLOFF M T SWARTZ and M SAFFRAN Specific uptake of radioactivity from ^3H oxytocin by surviving segments of mammary gland *Endocrinology* 1972 91 213—216
- SOLOFF M T SWARTZ M MORRISON and M SAFFRAN Oxytocin receptors Oxytocin analogs but not prostaglandins compete with ^3H -oxytocin for uptake by rat uterus *Endocrinology* 1973 92 104—107
- THOMPSON E E P FAEYCHET and J ROTH Moniodo-oxytocin Demonstration of its biological activity and specific binding to isolated fat cells *Endocrinology* 1972 91 1199—1205
- WEINER, R Test zur Stimulation der gonadotropen Funktion des Hypophysenvorderlappens mit Oxytocin *Arch Gynak* 1965 207 191—195
- WILLIAMS N B S and P BIZ Tissue to plasma ratios of radioactivity in the rat hypothalamo-hypophyseal system after intravenous injection of ^3H lysine⁸-vasopressin and ^3H mannitol *Acta endocr (Abh)* 1969 60 389—400

Stimulation of Glucose Metabolism in Rat Mast Cells by Antigen, Dextran and Compound 48/80, Used as Histamine Releasing Agents

By

NIRMAL CHAKRAVARTY and HANS JORGEN SORENSEN

Received 14 December 1973

Abstract

CHAKRAVARTY N and H J SORENSEN *Stimulation of glucose metabolism in rat mast cells by antigen dextran and compound 48/80 used as histamine releasing agents* Acta physiol scand 1974 91 339-353

Histamine release in aerobic medium from rat peritoneal mast cells by anaphylactic reaction dextran and compound 48/80 was associated with a stimulation of exogenous glucose metabolism as determined by carbon dioxide and lactate production. There was generally a correlation between the amount of histamine released and the degree of metabolic stimulation. In anaerobic medium a stimulation of lactate production was observed in most of the experiments when histamine was released by anaphylactic reaction and dextran. Compound 48/80-induced histamine release in presence of oligomycin was not however associated with any appreciable change in lactate production. Galactose and fructose were metabolized by rat mast cells to CO_2 and lactate but the rate of CO_2 production was only 18% and 29% respectively and that of lactate production (aerobic) 5% and 36% respectively as compared to the metabolism of glucose to these products under the same conditions. 0.1 mM concentration of fructose was ineffective.

Earlier observations on the oxygen requirement of anaphylactic histamine release and its dependence on pH and temperature suggested that an enzymatic reaction is activated in the process (Parrot 1942 Mongar and Schild 1957 1958 Chakravarty 1960 Uvnas and Thon 1961). Inhibitors of the respiratory chain and of glycolysis were also shown to block the release (Moussatche and Prouvost Danon 1962 Chakravarty 1962). Furthermore in the guinea pig lung succinate stimulates anaphylactic histamine release apparently through its oxidative metabolism while inhibitors of the tricarboxylic acid cycle block the release (Moussatche and Prouvost Danon 1962 Chakravarty 1962 Chakravarty and Sorensen 1973).

Lately pure populations of rat peritoneal mast cells have been used to study the relationship of the energy metabolism of mast cells to histamine release. It has thus been shown that a stimulation of mast cell respiration occurs for a short period after

the bath was brought down to ca. 70°C and shaking continued for another 2 h. In control experiments in which mast cells were exposed to the same concentration of H_2SO_4 at $0-4^{\circ}\text{C}$ for 5 min and then incubated with uniformly labeled ^{14}C -glucose at 37°C for 30 min no CO was produced showing that the reaction was stopped by H_2SO_4 . Other control experiments done previously with $\text{NaH}^{14}\text{CO}_3$ solution showed that the trapping of $^{14}\text{CO}_2$ was essentially complete after equilibration for 2 h (Chakravarty 1968 b). The rubber stopper was removed after 2 h and the center well transferred to a scintillation flask containing 10 ml 0.4% omnifluor in toluene.

Lactate production in aerobic medium was determined in the incubation fluid of the same experiments described above. After the trapping of carbon dioxide by hyamine hydroxide was completed the flasks were opened and the incubation medium transferred to a centrifuge tube. The flask was washed twice with 1 ml distilled water the wash fluid being added to the centrifuge tube. The combined fluid was then neutralized with sodium hydroxide solution to pH ca. 7. The tube was centrifuged and the supernatant collected for ion exchanged chromatography. The deposit was shaken with 2 ml distilled water and centrifuged again the supernatant being added to the sample collected for chromatography. In some experiments the deposit after the last centrifugation was dissolved in solvent 100 to determine the remaining radioactivity which was found to be negligible. The total amount of supernatant was then run slowly through a column of anion exchange resin viz BIO RAD AG2 X8 100-200 mesh converted to the formate form. The column was then washed with 40 ml distilled water and thereafter eluted with 15 ml 8% formic acid. The formic acid eluate was freeze-dried and dissolved in 1 ml 80% ethyl alcohol. 300 μl of the alcoholic solution was then placed as a single spot on a 0.25 mm thick silica gel C (Merck) thin layer plate. The chromatogram was run at ca. 20°C for about 2 h with ethyl acetate-formic acid (210/30) saturated with water. The plate was dried at room temperature by blowing air and autoradiographed. The spot identified as lactate constituted over 80% of the radioactivity applied to the plate. In three experiments the samples were run by two dimensional chromatography with the first run as described above and the second either in ethyl alcohol-ammonium hydroxide-water (168/8/3%) or in benzene-methanol-acetic acid (79/14/7). Lactate migrated in both the solvents used for the second run as a single spot. The total amount of radioactivity in the zones below and above the spot in the second run constituted less than 1% of the radioactivity in the spot.

The amount of lactate produced from exogenous glucose by the mast cells was determined from the radioactivity in the lactate spot in the thin layer chromatogram. The radioactivity was determined by scraping the area of the plate corresponding to the lactate spot and transferring the material to aquasol in a scintillation flask. For each experiment along with the samples from the experiment, 2 samples of uniformly labeled ^{14}C lactate in 2 ml Krebs-Ringer solution (with 1 mg/ml serum albumin) were also analyzed to determine the lactate recovery. As in case of the incubation fluid H_2SO_4 was added to these control samples which were then neutralized and run simultaneously with the samples from the experiment through the entire procedure viz ion exchange chromatography, freeze-drying and thin layer chromatography. The mean of the two quantitative recoveries of ^{14}C -lactate was used to correct the unknown value for lactate in the samples. There was no loss of radioactivity during the ion exchange chromatography. The average recovery after freeze-drying was 75% and that after thin layer chromatography 80%. In all the experiments a sample was incubated with radioactive glucose without cells as a control for any radioactivity appearing in the CO trapping agent or in the lactate area of the thin layer chromatogram (see below).

Lactate production from exogenous glucose associated with glucose-dependent histamine release was studied by blocking oxidative metabolism with oligomycin or using nitrogen or helium as the gas phase. Oligomycin was dissolved in ethyl alcohol to give 1% conc. and then diluted as required with Krebs-Ringer solution. Samples of mast cells were incubated at 37°C with oligomycin $1\text{ }\mu\text{g/ml}$ for 10 min before adding glucose and 1 min later the histamine releaser was added. Incubation was continued for 14 min more when the reaction was stopped by adding H_2SO_4 . In experiments in which nitrogen or helium was used the samples in 15 ml Warburg flasks were preincubated at 37°C for 30 min under air to reduce the endogenous substrates and were then exposed to a flow of nitrogen or helium for 45 min at $0-4^{\circ}\text{C}$. Thereafter glucose was added to the cells and the samples transferred to the 37°C bath. The histamine releasers were added 3 min later and the incubation continued for another 12 min before terminating the reaction with H_2SO_4 . Glucose and the releasers were added to the cells from the sidearms without opening the flasks. Lactate production was determined by following the conversion of uniformly labeled ^{14}C glucose to ^{14}C -lactate by the method described above.

¹ Oxygen contamination of nitrogen was $<0.02\%$ and of helium $<0.0005\%$.

Uniformly labeled glucose used in these experiments was purified for the first few experiments by two dimensional thin layer chromatography using 0.4 mm microcrystalline cellulose plates (DS O Camag). The plates were run first in ethyl acetate pyridine water (15:10:20) and then in isopropanol pyridine acetic acid water (8:8:1:4). After identifying radioactive glucose by autoradiography the area was scraped and glucose eluted with water. It was freeze-dried and dissolved in Krebs-Ringer solution for the experiments. This rather long process of purification was later shortened by simply filtering radioactive glucose through several layers of Whatman DE81 DEAE cellulose paper and thereafter freeze-drying the filtrate. This method of purification was found to be as effective as the two dimensional thin layer chromatography.

It appears that some impurities in ^{14}C glucose produced by the radioactive disintegration are acidic in nature and a part of the impurities is sufficiently volatile to be taken up by hyamine hydroxide. It was therefore essential to purify ^{14}C -glucose before use. The purification mentioned above reduced the radioactivity obtained from the samples without cells but did not completely eliminate it. The relatively small number of counts obtained in this way did not interfere with the experiments when appropriate corrections were made. Control samples without cells gave in hyamine hydroxide 50–100 d.p.m. which was 1/10–1/100 of the counts from the samples with the cells. For lactate determination the area of the thin layer chromatogram from control samples without cells corresponding to the lactate spot gave around 1000 d.p.m. constituting less than 1/30 of the counts obtained from the lactate spots of the samples with cells. Both CO_2 and lactate blank counts were deducted from the corresponding values for samples containing cells.

The production of carbon dioxide and lactate from fructose and galactose was studied using the same methods as described above with the difference that the incubation time was 30 min and the concentration of the sugars was 5 mM. Samples in this series of experiments were also incubated with glucose in the same way as fructose and lactose for comparison. The sugars were purified by two dimensional thin layer chromatography and control samples without cells were included in the experiments as described above for glucose.

All radioactivity determinations were carried out in a Nuclear Chicago Mark II liquid scintillation spectrometer. Quenching corrections were made by internal standardization. The counting efficiency for ^{14}C was 90–92%.

Uniformly labeled ^{14}C glucose, galactose, fructose and lactic acid (sodium salt) were purchased from The Radiochemical Centre, Amersham, Omnisfluor (98% PPO + 2% p-bis-o-methylstyryl benzene) and aquasol were purchased from New England Nuclear GmbH and hyamine hydroxide and solvane 100 from Packard Instruments Company Inc. Compound 48/80 was kindly supplied by AB Leo, Helsingborg, Sweden. (Thio)phosphoryl serine (92% pure) was obtained from Schwarz/Mann and dextran (m.w. 80,000) from Pharmacia. Sterile 30% and 3% bovine serum albumin in Tyrode buffer solution were obtained from Miles Laboratories. Cold d-glucose (Analar) was purchased from B.D.H. Chemicals Ltd. and cold fructose and d-galactose from Sigma Chemical Co. On enquiry we were informed by Sigma Chemical Co. that fructose used by us gave only one spot in three systems of paper chromatography and may be essentially considered free from glucose. Galactose according to the same source contained only 0.0006% glucose. Oligomycin (15% oligomycin A + 8% oligomycin B) was also purchased from Sigma Chemical Company. Other chemicals used were of analytical grade.

Results

Changes in glucose metabolism of mast cells by anaphylactic reaction in aerobic milieu

The metabolism of exogenous glucose to carbon dioxide and lactate in sensitized mast cells incubated with antigen is shown in Table I. The production of carbon dioxide and lactate has been determined during incubation for 15 min at 37°C in aerobic milieu. Of this period the cells were in contact with the releaser for 13 min. Expressed as p moles glucose converted to carbon dioxide per 10^6 cells, the mean CO_2 production may be seen in expts. 1–5 Table I to be increased from 61 to 111. There was 57–261% (average 159%) stimulation in CO_2 production from mast cells exposed to antigen. The amount of anaphylactic histamine release was 8–

TABLE I Changes in the metabolism of exogenous glucose in peritoneal mast cells of Wistar rats associated with anaphylactic histamine release. The conversion of ^1C -glucose to ^1CO and ^{14}C -lactate after incubation at 37°C for 15 min

Expt	Phosphatidyl serine $\mu\text{g/ml}$	Hista mine	p mol glucose \rightarrow $\text{CO}/10^6$ cells			p mol glucose \rightarrow lactate/ 10^6 cells		
			without releaser	with releaser	stimulation	without releaser	with releaser	stimulation
1	0	13	94	148	57	8260	11500	40
2	0	14	38	137	261	4240	8270	94
3	0	13	63	135	114	6840	7280	0
4	0	17	47	144	206	$P > 0.1$		
5	0	8	62	158	155			
Mean (Expts 1-5)		12	61	144	159	6447	9017	71
6	25	45	78	355	355	4970	8520	47
7	25	59	86	367	327	6050	9110	51
8	25	42	111	286	158	5510	9100	65
9	25	49	77	303	294	2950	8130	108
Mean (Expts 6-9)		49	88	378	284	4870	8215	74

0.6×10^6 to 1.5×10^6 mast cells in Krebs-Ringer solution were incubated with or without antigen egg albumin 0.2 mg/ml . Uniformly labeled ^1C -glucose $5.1-5.9 \mu\text{Ci}$ were added to each sample. Glucose concentration $0.85-0.9 \text{ mM}$, sp. activity $3 \text{ Ci}/\mu\text{M}$. Gas phase air. p mol glucose converted to CO and lactate shown. P determined by paired comparison.

14% (averaged 12%). The mean increase in the conversion of glucose to lactate (aerobic glycolysis) was 47% but this is not statistically significant. It appears however from the individual values that the lactate production was stimulated.

TABLE II Control experiments with peritoneal mast cells from non sensitized Wistar rats showing the effect of egg albumin in the absence and the presence of phosphatidyl serine on the metabolism of exogenous glucose. The conversion of ^1C -glucose to CO and ^1C -lactate after incubation at 37°C for 15 min

Expt	Phosphatidyl serine $\mu\text{g/ml}$	p mol glucose \rightarrow $\text{CO}/10^6$ cells			p mol glucose \rightarrow lactate/ 10^6 cell		
		without egg albumin	with egg albumin	stimulation	without egg albumin	with egg albumin	stimulation
1	0	71	83	17	3820	4570	20
2	0	24	28	17	1850	1970	4
3	0	57	66	16	1220	1350	11
Mean		51	59	17	2297	2613	1
4	25	76	117	54	5840	6500	11
5	25	107	140	37	2430	2160	0
6	25	105	145	38	4000	4040	1
7	25	69	84	-			
Mean		88	122	38	4090	4333	4

0.4×10^6 to 1.0×10^6 mast cells in Krebs-Ringer solution were incubated with or without egg albumin 0.2 mg/ml . Uniformly labeled ^1C -glucose $4.3-5.6 \mu\text{Ci}$ were added to each sample. Glucose concentration $0.72-1.03 \text{ mM}$, sp. activity $3 \text{ Ci}/\mu\text{M}$. Gas phase air. p mol glucose converted to CO and lactate shown. P determined by paired comparison.

TABLE III Changes in the metabolism of exogenous glucose in peritoneal mast cells of Wistar and Sprague Dawley rats associated with dextran induced histamine release in presence of phosphatidyl serine $25 \mu\text{g/ml}$. The conversion of ^{14}C -glucose to $^{14}\text{CO}_2$ and ^{14}C lactate after incubation at 37°C for 15 min

Expt	Species of rats	Histamine release %	p moles glucose \rightarrow CO_2 / 10^6 cells			p moles glucose \rightarrow lactate* 10^6 cells		
			without releaser	with releaser	stimulation %	without releaser	with releaser	stimulation %
1	W	31	78	172	121	4730	450	74
2	W	24	99	165	67	6990	9400	34
3	W	31	64	157	145	5210	9701	77
			$P < 0.005$			$P < 0.05$		
Mean (Expts 1-3)		29	80	165	111	4977	7787	67
4	SD	13	84	133	58			
5	SD	10	234	294	26			
6	SD	16	114	216	89			
7	SD	11	95	158	66			
8	SD	13	90	126	40			
			$P < 0.005$					
Mean (Expts 4-8)		13	123	185	56			

0.1-10 to 2.7×10^6 mast cells in Krebs Ringer solution were incubated with or without dextran 5-8 mg/ml. Uniformly labeled ^{14}C -glucose 4.2-6.2 μCi were added to each sample. Glucose concentration 0.70-1.03 mM sp. activity 3 $\mu\text{Ci}/\mu\text{M}$. Gas phase air p moles glucose oxidized to CO_2 and lactate shown. P determined by paired comparison.

10% and 94% in 2 of the 3 expts. It may also be pointed out that the lactate production was stimulated most (94%) in the same experiment in which the stimulation of CO_2 production from glucose was also the highest (261%). Egg albumin in non sensitized rats did not cause any significant increase in the production of CO_2 and lactate (see Table II Expts 1-3).

It was felt that anaphylactic reaction with a higher amount of histamine release than in expts 1-3 of Table I might better reveal the changes in glucose metabolism. The next series of experiments were therefore performed with phosphatidyl serine which has been shown to potentiate anaphylactic histamine release from rat mast cells (Goth et al 1971; Monger and Svec 1972). These experiments (6-9) differ from expt 1 of Table I in having 25 $\mu\text{g/ml}$ phosphatidyl serine in the medium. It may be seen that the histamine release was very much higher in this group (42-59%). The production of CO_2 from glucose was also remarkably stimulated in all the 4 expts, the average stimulation being 284%. The conversion of glucose to lactate was also stimulated 31-108% with an average of 74%. It may be pointed out that some stimulation of the conversion of glucose to CO_2 was caused by the incubation of mast cells from non sensitized rats with egg albumin in presence of phosphatidyl serine (see Table II Expts 4-7). The degree of stimula-

TABLE IV Changes in the metabolism of exogenous glucose in peritoneal mast cells from Sprague Dawley rats associated with compound 48/80-induced histamine release. The conversion of C-glucose to CO and C-lactate after incubation at 37°C for 15 min

Expt	Histamine release	p mol glucose → CO /10 ⁶ cells			p mol glucose → lactate/10 ⁶ cells		
		without releaser	with releaser	stimulation	without releaser	with releaser	stimulation
1	38	99	179	81	4590	7070	54
2	35	90	167	86	4850	7200	48
3	22	126	190	51	3810	4730	11
4	35	135	262	94	7130	9620	35
5	45	56	143	155	4940	8450	71
		P < 0.005			P < 0.005		
Mean 35		101	188	93	5066	7314	44

1.6 × 10⁶ to 4.4 × 10⁶ mast cells in Krebs-Ringer solution were incubated with or without compound 48/80 0.4–2.0 µg/ml. Uniformly labeled C-glucose 4.9–6.2 µCi were added to each sample. Glucose concentration 0.82–1.03 mM, sp. activity 3 µCi/µM. Gas phase air. p mol glucose converted to CO and lactate shown. P determined by paired comparison.

tion in non sensitized rats was however low i.e. an average stimulation of 38% as compared to 284% in the sensitized rats. The lactate production was not however significantly altered when mast cell from non sensitized rats were incubated with egg albumin in the presence of phosphatidyl serine. Egg albumin produced very little histamine release from non sensitized rat mast cells. The average release with 0.2 mg/ml egg albumin was 1.1% in the absence of phosphatidyl serine and 3.2% in its presence after deduction of the spontaneous histamine release.

Changes in glucose metabolism of mast cells by dextran in aerobic milieu

The studies on glucose metabolism during incubation with dextran were carried out both in mast cells from Wistar and Sprague Dawley rats. Phosphatidyl serine was always added to the medium because histamine release from isolated pure populations of mast cells by dextran alone tends to be poor (Chakravarty *et al.* 1973). Although glucose inhibits dextran induced histamine release (Beraldo *et al.* 1962) Chakravarty and his coworkers (1973) found that the inhibition of the release induced by 1 mg/ml dextran from mixed peritoneal cells of Wistar rats was 58% even with 20 mM glucose. We felt therefore that the metabolic studies could very well be carried out in presence of the small amount of radioactive glucose required in our experiments by increasing the concentration of dextran to 5–8 mg/ml because of the competitive nature of the glucose inhibition shown by Dias da Silva *et al.* (1965). Indeed as shown in Table III the histamine release from Wistar rat mast cells by dextran in presence of 0.7–1 mM glucose was quite good i.e. 24–31%. The table further shows that the oxidation of glucose to CO in Wistar rat mast cells was increased by dextran in all the 3 expts 67–145% above the values for the cells incubated without dextran. Simultaneously aerobic glycolysis was stimulated as shown by 34–77% increase in lactate production by dextran. It may be pointed out that the amount of histamine released shows good correlation to the degree of stimulation of CO and lactate production.

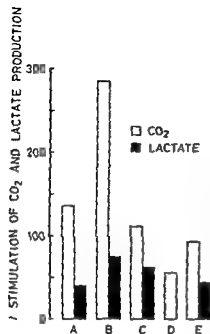


Fig 1

Comparison of the average stimulation of the conversion of exogenous glucose to CO₂ and lactate (aerobic glycolysis) during histamine release induced by anaphylactic reaction dextran and compound 48/80. A Anaphylactic reaction in Wistar rat mast cells average histamine release 12%. B Same as A except that phosphatidyl serine was added to the medium average histamine release 49%. C Wistar rat mast cells incubated with dextran in presence of phosphatidyl serine average histamine release 79%. D Same as C except that Sprague Dawley rat mast cells were used average histamine release 13%. E Sprague Dawley rat mast cells incubated with compound 48/80 average histamine release 35%.

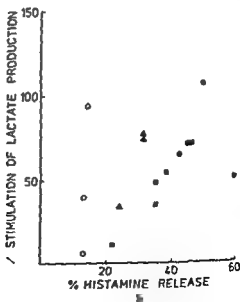
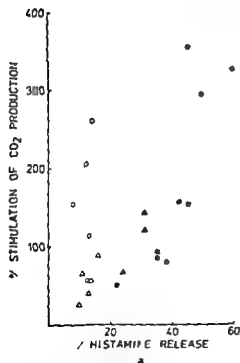


Fig 2 Correlation of histamine release to the stimulation of (a) CO₂ and (b) lactate production from exogenous glucose in aerobic medium. Histamine releasing agents: ○ Antigen, ● Antigen in presence of phosphatidyl serine, ▲ Dextran (Wistar rats), ■ Compound 48/80.

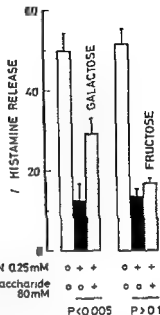


Fig 3 The effect of 80 mM galactose and fructose on the cyanide inhibition of histamine release induced by compound 48/80 from mixed peritoneal cells of Sprague Dawley rats. Mean values \pm SE in 4 expts with galactose and 5 expts with fructose. Conc of compound 48/80 0.5–1 μ g/ml. Fructose was essentially free from glucose (see methods). Galactose contained 0.0006 \circ glucose. Spontaneous histamine release (0–2 \circ) deducted.

The oxidation of glucose to CO was also studied in Sprague Dawley rats (expts 4–8 Table III). There was a stimulation of CO production varying from 26 to 89 % in the mast cells from which 10–16 % histamine was released by dextran. As expected the histamine release was less pronounced than from Wistar rat mast cells and the stimulation of CO production was also moderate (average 56 %). Here also the highest histamine release (16 %) is associated with the highest stimulation of CO production (89 %).

Changes in glucose metabolism of mast cells by compound 48/80 in aerobic milieu
The changes in the metabolism of glucose caused by compound 48/80 is shown in Table IV. With histamine release varying from 22 to 45 % there was 51 to 150 % stimulation in the oxidation of glucose to CO and 11–71 % stimulation of the conversion of glucose to lactate (aerobic glycolysis). It may be pointed out that the minimal histamine release (22 %) corresponds to the minimal stimulation of CO and lactate production while the maximal histamine release (45 %) is associated with the maximal metabolic stimulation.

The average stimulation of the conversion of exogenous glucose to CO and lactate in aerobic milieu associated with histamine release induced by anaphylactic reaction dextran and compound 48/80 is presented in Fig 1 for comparison. The histamine release with the three agents in the individual experiments has been plotted against the stimulation of CO and lactate production in Fig 2. In spite of the diversity of the material the figures show that there is a relationship between the amount of histamine released and the degree of stimulation of the metabolism of exogenous glucose.

TABLE V Conversion of exogenous glucose by rat peritoneal mast cells to lactate under anoxic conditions in relation to glucose dependent histamine release induced by anaphylactic reaction dextran and compound 48/80 Incubation time 15 min at 37 °C

Expt	Releaser	Inhibitor of oxidative metabolism	Histamine release %			p moles glucose → lactate/ 10 ⁶ cells		
			with glucose	without glucose	inhibition	without releaser	with releaser	stimulation
1	Antigen	Nitrogen	27	9	67	10 540	10 670	1
2	Antigen	Helium	29	17	42	11 720	7 440	11
3	Antigen	Helium	13	3	77	7 600	9 550	26
4	Antigen	Helium	27	11	100	7 030	11 280	60
Mean			24	7	72	7 973	9 723	25
5	Dextran	Helium	15	0	100	7 790	10 330	33
6	Dextran	Helium	10	0	100	4 210	7 370	75
Mean			13	0	100	6 000	8 850	54
7	Compd 48/80	Oligomycin	34	3	97	5 910	5 700	0
8	Compd 48/80	Oligomycin	14	5	65	5 250	5 090	8
9	Compd 48/80	Oligomycin	27	8	71	5 080	5 110	0
Mean			25	5	76	5 413	5 500	3

Expts 1-6 0.5×10^6 to 1.5×10^6 mast cells from Wistar rats in Krebs-Ringer solution were incubated with or without the antigen egg albumin 0.2 mg/ml in Expts 1-4 and with or without dextran 0.5 mg/ml in Expts 5-6 Gas phase nitrogen or helium Phosphatidylserine 25 µg/ml added to the medium Expts 7-9 1.0×10^6 to 1.2×10^6 mast cells from Sprague Dawley rats in Krebs-Ringer solution were incubated with or without comp 48/80 2 µg/ml Oligomycin 1 µg/ml in medium Gas phase air Uniformly labeled C-glucose 4.7-6.0 µCi were added to each sample Glucose concentration 0.79-1.00 mM sp activity 3 µCi/µM p mol glucose converted to lactate shown Paired comparison for Expts 1-6 $P < 0.05$

Changes in anaerobic glycolysis of mast cells associated with glucose dependent histamine release

Although lack of oxygen or inhibition of oxidative metabolism blocks histamine release this effect may be counteracted and the release induced if glucose is added to the medium (Diamant and Uinas 1961; Rothschild *et al* 1961). In the experiments shown in Table V we have followed the anaerobic metabolism of exogenous glucose to lactate associated with glucose dependent histamine release induced by anaphylactic reaction dextran and compound 48/80. Oxidative metabolism was blocked in Expts 1 by oligomycin 1 µg/ml and in the others by replacing the gas phase by nitrogen (1 expt) or helium (5 expts). Histamine release induced by antigen in an anaerobic milieu in presence of glucose varied from 13 to 29% which was reduced to 0-17% in the absence of glucose showing that histamine release from isolated rat peritoneal mast cells is inhibited by anoxia. The lactate production associated with the release was variable from practically no stimulation in Expts 1 and 2 to a moderate stimulation (26% and 60%) in Expts 3 and 4. The anaphylactic experiments were performed in presence of phosphatidylserine. It seems unlikely that egg albumin would have any appreciable direct effect on

TABLE VI Metabolism of galactose and fructose in peritoneal mast cells from Sprague Dawley rats. The conversion of uniformly labeled ^1C monosaccharides to ^1CO and ^1C -lactate is shown. Incubation time 30 min at 37°C in aerobic milieu.

Monosaccharide	p mol monosaccharide \rightarrow CO/10 ⁶ cells	p mol monosaccharide \rightarrow lactate/10 ⁶ cells
Galactose 5 mM	43 \pm 5.3	570 \pm 83
Fructose 5 mM	69 \pm 5.4	410 ^a
Glucose 5 mM	240 \pm 22.3	11 500 ^b

For all values except a and b mean \pm S.E. from 3 expts. are shown.

a Mean of 2 expts. (individual values 300–470).

b 1 expt. With 1 mM glucose in the medium 5066 p mol glucose was converted to lactate in 10 min (see Table IV). The lactate production at this lower concentration of glucose (1 mM) in 10 min may thus be taken to be from $2 \times 5070 = 10\,132$ p mol glucose as the fall of lactate production rate during this period (30 min) would be negligible (Chakravarty 1965). This rate is thus about the same as the value (11 500 p mol glucose \rightarrow lactate) obtained here with 5 mM glucose.

Uniformly labeled ^1C monosaccharides were used. Approximately 5 μCi labeled sugar were added to each sample. Gas phase air. p mol monosaccharide converted to CO and lactate shown.

lactate production in presence of phosphatidyl serine as judged from the study of unsensitized mast cells shown in Table II (expts 4–6).

Dextran gave 10–15% histamine release in presence of glucose and this was inhibited completely by anoxia in the absence of glucose. The lactate production in the two experiments with dextran (expts 5 and 6 Table V) was increased 33% and 75% above the control values.

During compound 48/80 induced histamine release oxidative metabolism was inhibited by 1 $\mu\text{g/ml}$ oligomycin. As oligomycin blocks oxidative phosphorylation (Lardy *et al.* 1958) the metabolic pathway likely to be open would be anaerobic glycolysis. The histamine release was 14–34% in presence of glucose and 3–8% in its absence. As shown in Table V (expts 7–9) the production of lactate from glucose during the histamine release was not altered.

The metabolism of galactose and fructose

The metabolism of these two sugars was studied because the anoxic inhibition of histamine release has been reversed by glucose but not by galactose and fructose (Drimant and Uinas 1961) and the reversal by glucose is assumed to be caused by anaerobic glycolysis of glucose. Table VI shows that both galactose and fructose are oxidized to CO but the rate of oxidation is slow being 18% for galactose and 29% for fructose as compared to the oxidation of glucose to CO. The aerobic glycolysis of glucose at 5 mM glucose conc. is shown in the table for only 1 experiment but this value is not essentially different from the average aerobic conversion of glucose to lactate in Sprague Dawley rats at about 1 mM glucose conc. as reported in Table IV (see also footnote Table VI). The aerobic production of lactate from galactose and fructose was thus 5% and 3.6% respectively as compared to the aerobic lactate production from exogenous glucose.

TABLE VII Glycolysis in rat peritoneal mast cells

Expts	Species of rats	Glucose conc mM	Phosphatidyl serine $\mu\text{g/ml}$	Inhibitor of oxidative metabolism during anaerobic glycolysis	Glycolysis $\times 10^{11}$ mol lactate/cell hour	
					aerobic	anaerobic
1 Present expts	Wistar	1	2	Nitrogen or helium	3.8	5.9
2 Present expts	Spr Dawley	1	11	Oligomycin $1 \mu\text{g/ml}$	4.1	4.3
3 Expts of Chakravarty 1963	Spr Dawley	5	0	Nitrogen	4.15	7.6

The glycolysis values give lactate production from only exogenous glucose for groups 1 and 2 and total glycolysis (exogenous and endogenous) for group 3

Since a fraction of galactose and fructose is converted to lactate the effect of a high concentration of these sugars on cyanide inhibited histamine release was explored. These experiments shown in Fig. 3 were performed with mixed peritoneal cells from Sprague Dawley rats using compound 48/80 as the histamine releasing agent. It may be seen that the inhibition of histamine release caused by cyanide was partially reversed by 80 mM galactose while fructose in the same concentration was ineffective.

Discussion

As shown in Table VII the average rate of glycolysis from glucose expressed as lactate molecules produced per cell per hour is in the present experiments 3.8×10^{11} mol and 5.9×10^{11} mol for aerobic and anaerobic glycolysis respectively in mast cells from Wistar rats the corresponding figures for Sprague Dawley rat mast cells being 4.1×10^{11} mol and 4.3×10^{11} mol respectively. Glycolysis in mast cells has previously been studied by one of us by the Cartesian diver technique using Sprague Dawley rats. The glycolysis rate in presence of glucose was then estimated to be 4.15×10^{11} mol/cell/h in the aerobic medium and 7.6×10^{11} mol/cell/h in the anaerobic medium (Chakravarty 1963). The present values for lactate production from exogenous glucose in Sprague Dawley rats is thus about the same as reported previously for the total glycolysis—both exogenous and endogenous—in the aerobic medium. The values for anaerobic glycolysis using oligomycin in the present experiments are however somewhat lower.

The average CO_2 production from exogenous glucose in the present experiments has been 0.14×10^{11} m/cell/h in Wistar rat mast cells and 0.24×10^{11} m/cell/h in Sprague Dawley rat mast cells using about 1 mM glucose concentration. The rate of oxidation of exogenous glucose to CO_2 is thus higher in Sprague Dawley as

compared to Wistar rats ($P < 0.025$). The total glucose utilization is however similar in the two species. From the average values for the metabolism of exogenous glucose for Wistar rat mast cells obtained in the present experiments it may be calculated that 1.9×10^{-11} mol glucose is utilized (converted to CO and lactate) per cell per hour. The corresponding value for Sprague Dawley rat is 2.1×10^{-11} mol glucose utilized per cell per hour.

The rate of glucose oxidation to CO by Wistar rat mast cell reported earlier must be regarded as too high and the same is true for galactose and fructose (Chakravarty 1968 b). That was also the reason why a stimulation of CO production from glucose in relation to compound 48/80 induced histamine release could not be demonstrated earlier. The radioactive sugars used in those experiments were 99% pure but no further purification was employed. We have pointed out in the present report under Methods that the impurity in ^{14}C marked sugars can give an appreciable blank value in the CO trapping agent in control samples incubated without cells. This source of error has now been eliminated by purifying the sugars before use and in addition by using a larger number of cells and deducting the small blank value in each experiment. The rate of oxidation of galactose and fructose to CO has now been estimated to be 18% and 29% respectively of the rate for glucose oxidation to CO (Table VI). Thus the conclusion made from the previous observation that galactose and fructose are taken up by mast cells and metabolized to CO remains the same but concerning the quantitative data as explained above the values presented here should be considered more accurate. A part of galactose and fructose is metabolized by the Embden Meyerhof pathway as shown by their conversion to lactate although the rate of lactate production is only 5% and 3% respectively compared to the rate of lactate production from glucose (Table VI). Consistent with this finding galactose in high conc (80 mM) partially reversed the cyanide inhibition of histamine release while fructose still remained inactive (Fig. 3).

Both the oxidation of glucose to CO and its aerobic glycolysis to lactate have been shown to be stimulated—the former to a higher degree—by all the 3 histamine releasing agents viz antigen dextran and compound 48/80 (Fig. 1). In addition there is a correlation between the amount of histamine released and the degree of stimulation of glucose metabolism (Fig. 2). Generally a parallelism may also be observed between the stimulation of CO and of lactate production suggesting that glucose uptake and utilization by the Embden Meyerhof pathway was enhanced. Since around 80% of the acid metabolites of glucose was lactate the sum of CO and lactate reflects the glucose uptake.

Histamine is released from mast cells in response to all the three agents employed within 1/2 min (Bloom *et al* 1967, Bloom and Chakravarty 1970, Chakravarty *et al* 1973). The metabolism of glucose has been studied during 15 min starting 1–3 min before the addition of the releaser. It is thus difficult to say from the present findings whether the metabolic stimulation is directly related to the histamine release process or is initiated by the changes induced in the mast cell by the re-

leasing agents. Further studies are required to explore this problem primarily by determining the time course of the metabolic stimulation.

The present observation on glucose metabolism is consistent with the previous finding that anaphylactic histamine release from mast cells is accompanied by a stimulation of their respiration lasting 15–20 min (Chakravarty 1968a). Furthermore a good correlation has recently been shown between the ATP content of mast cells and the amount of histamine released, the release being blocked when the ATP content is drastically reduced (Johansen and Chakravarty 1972, 1973).

The changes of lactate production from glucose when histamine was released under anoxic conditions were variable: essentially no change was associated with compound 48/80 induced histamine release while a stimulation of lactate production was observed in 2 out of 4 anaphylaxis experiments and in both the experiments with dextran (Table V). As we do not know how much stimulation of anaerobic glycolysis is produced by glucose itself it is difficult to interpret this result. It is also possible that any stimulant effect could be better shown by using a shorter incubation time in close relation to histamine release. As reported earlier compound 48/80 induced histamine release may differ from anaphylactic histamine release (Chakravarty 1968c) while there is a similarity between anaphylactic and dextran induced histamine release both being stimulated by phosphatidyl serine (Goth *et al.* 1971). We have therefore treated the results for anaphylactic and dextran induced release statistically as a group. Paired comparison of these results (expts 1–6 Table V) shows that there is a significant increase in lactate production associated with the release ($P < 0.025$). Further work is required to evaluate if the lack of stimulation of lactate production with compound 48/80 is influenced by oligomycin used in this series to block oxidative metabolism.

Phosphatidyl serine has been used in some of the experiments on anaphylactic histamine release (Table I) and in all the experiments on dextran induced histamine release. Phosphatidyl serine itself also stimulates glucose metabolism. It may be seen by comparing CO_2 production from mast cells without releaser in Table I that there was a 44% stimulation caused by phosphatidyl serine ($P < 0.01$). In two other experiments not reported here in which the effect of phosphatidyl serine alone was studied the CO_2 production from the mast cells was stimulated by the phospholipid. This observation is of interest in view of the reported stimulation of anaphylactic and dextran induced histamine release by phosphatidyl serine (Goth *et al.* 1971; Moller and Sver 1972; Chakravarty *et al.* 1973).

A grant from the Carlsberg Foundation for this work is gratefully acknowledged. Our thanks are due to Mrs. Lone Bruus for her skilful technical assistance.

References

- BERALLO W. T., W. DIAS D. S. and A. D. LAMOS FR. AUSTON: Initial effects of carbohydrates on histamine release and mast cell disruption by dextran. *Brit. J. Pharmacol.* 1972, 19, 405–413.
- BLOM C. B. and N. CHAKRAVARTY: The course of anaphylactic histamine release and morphological changes in rat peritoneal mast cells. *Acta physiol. scand.* 1970, 78, 410–414.

- BLOOM G H and FREDHOLM O and HAEGERMARK Studies on the time course of histamine release and morphological changes induced by histamine liberators in rat peritoneal mast cells *Acta physiol scand* 1967 71 270-282
- CHAKRAVARTY N The mechanism of histamine release in anaphylactic reaction in guinea pig and rat *Acta physiol scand* 1960 48 146-166
- CHAKRAVARTY N Aerobic metabolism in anaphylactic reaction in vitro *Amer J Physiol* 1962 a 203 1193-1198
- CHAKRAVARTY N Inhibition of anaphylactic histamine release by 2-deoxyglucose *Nature (Lond)* 1962 b 194 1187-1184
- CHAKRAVARTY N Glycolysis in rat peritoneal mast cells *J cell Biol* 1965 20 123-128
- CHAKRAVARTY N Respiration of rat peritoneal mast cells during histamine release induced by antigen antibody reaction *Exp Cell Res* 1968 a 49 160-168
- CHAKRAVARTY N Uptake and oxidative utilization of glucose fructose and galactose by rat mast cells *Biochem Pharmacol* 1968 b 17 643-645
- CHAKRAVARTY N Further observations on the inhibition of histamine release by 2-deoxyglucose *Acta physiol scand* 1968 c 72 425-437
- CHAKRAVARTY N and H J SØRENSEN Potentiation of anaphylactic histamine release from guinea pig lung by maleate and succinate *Acta physiol scand* 1973 88 401-411
- CHAKRAVARTY N and E ZELTHEN Respiration of rat peritoneal mast cells *J cell Biol* 1965 25 113-121
- CHAKRAVARTY N A GOTTI and P SZY Potentiation of dextran induced histamine release from rat mast cells by phosphatidyl serine *Acta physiol scand* 1973 88 469-480
- DE MANT B and B UVNAS Evidence for energy requiring processes in histamine release and mast cell degranulation in rat tissue induced by compound 48/80 *Acta physiol scand* 1961 53 315-329
- DIAS DA SILVA W and A D LEMOS FERNANDES Study of the mechanism of inhibition produced by hexoses on histamine release activity of dextran *Experientia (Basel)* 1965 21 96-97
- GOTTI A H R ADAMS and M ANOCHTZEN Phosphatidylserine Selective enhancer of histamine release *Science* 1971 173 1034-1035
- JOHANSEN T and N CHAKRAVARTY Dependence of histamine release from rat mast cells on adenosine triphosphate *Vaughn-Schmiedeberg's Arch exp Path Pharmacol* 1972 270 457-463
- JOHANSEN T and N CHAKRAVARTY The relation of adenosine triphosphate content of rat mast cells to anaphylactic and compound 48/80-induced histamine release *Acta physiol scand* 1973 Suppl 396 B 121
- LARDY H A D JOHNSON and W C McMURRAY Antibiotics as tools for metabolic studies I A survey of toxic antibiotics in respiratory phosphorylation and glycolytic reactions *Arch Biochem* 1958 78 587-597
- MONGAR J L and H O SCHILD Effect of temperature on the anaphylactic reaction *J Physiol (Lond)* 1957 135 370-378
- MONGAR J L and H O SCHILD The effect of calcium and pH on the anaphylactic reaction *J Physiol (Lond)* 1958 140 277-284
- MONGAR J L and D SYEC The effect of phospholipids on anaphylactic histamine release *Brit J Pharmacol* 1972 46 741-759
- MOLSSATCHE II and A PROUST DAXON Influence of sodium succinate and malonate on the histamine release in the anaphylactic reaction in vitro *Arch Biochem* 1958 77 108-111
- MOLSSATCHE II and A PROUST DAXON Influence of inhibitors of the respiratory chain on the release of histamine during the anaphylactic reaction in vitro Action of antimycin A and carbon monoxide *Biochem Pharmacol* 1967 11 603-603
- PARROT J L Sur la réaction cellulaire de l'anaphylaxie Son caractère aérobie *C R Soc Biol (Paris)* 1947 136 361-36
- ROTHSCHILD A M I VILGMA and M ROCHA E SILVA Metabolic studies on the release of histamine by compound 48/80 in the rat diaphragm *Biochem Pharmacol* 1961 7 748-755
- SIRORE P A A BURKHALTER and V H CONN JR A method for the fluorometric assay of histamine in tissues *J Pharmacol exp Ther* 1959 127 187-186
- UVNAS B and I L THON Evidence for enzymatic histamine release from isolated mast cells *Exp Cell Res* 1961 23 45-57

Protein Concentration and Colloid Osmotic Pressure of Rat Skeletal Muscle Interstitial Fluid

By

K. AUKLAND and H. M. JOHNSEN

Received 20 December 1973

Abstract

AUKLAND K. and H. M. JOHNSEN *Protein concentration and colloid osmotic pressure of rat skeletal muscle interstitial fluid* Acta physiol scand 1974 91 354-364

Protein concentration and colloid osmotic pressure (COP) were estimated in the fluid contained in nylon wicks after implantation in skeletal muscle of rats for 1 to 3 h. After 1 and 2 h implantation wick fluid showed an albumin/total protein ratio of 0.44 compared to 0.61 in plasma. Average concentrations relative to that of plasma were 0.37 for albumin, 0.57 for total protein and 0.76 (calculated by difference) for non albumin protein. After 3 h implantation these ratios had increased significantly to 0.49, 0.69 and 1.07 respectively, presumably indicating beginning inflammation. The unexpected excess of non albumin wick fluid protein had an electrophoretic mobility like that of plasma β globulins but its origin—*from plasma or muscle*—is uncertain. Wick fluid COF averaged 8.7 mm Hg as compared to a plasma COP of 18.9 mm Hg.

While the microcirculation of skeletal muscle has been extensively studied in terms of regulation of total flow, capillary pressure, effective capillary area and permeability, rather little is known about protein concentration of interstitial fluid. Since in interstitial fluid colloid osmotic pressure (COP) is a codeterminant of transcapillary water flux, it is obvious that the extravascular protein concentration of this large tissue must be of great importance for fluid balance, not only in the muscle itself but for the whole body.

It seems generally assumed that interstitial fluid COP in skeletal muscle is a few mm Hg only. It is also assumed for interstitial fluid from most other tissues. However, the few direct observations available indicate that the protein concentration of muscle interstitial fluid is by no means negligible. Thus Katz *et al.* (1970) found an extravascular albumin concentration in excised rat skeletal muscle amounting to 50-60 % of that in plasma. Somewhat lower albumin concentration, 42 % of that in plasma, was obtained in interfibre fluid collected by glass capillary tubes from skeletal muscle of guinea pigs by Creese, D'Silva and Shriv (1962). Furthermore, if lymph is considered representative of interstitial fluid with respect to protein content, the only estimate of muscle lymph we are aware of indicates a protein

content of about 50 % of that in plasma for cats and dogs (Jacobsson and Kjellmer 1964). Since none of these determinations seems to have been widely acknowledged we decided to study protein concentration and COP of skeletal muscle interstitial fluid obtained by the wick method recently described for sampling interstitial fluid from subcutaneous tissue (Aukland and Fadnes 1973, Johnsen 1974).

The results obtained on rat skeletal muscle largely confirmed the data referred to above of a protein concentration of about half that of plasma and also provided the first direct estimate of interstitial fluid COP with an average of 8.7 mm Hg. However further analysis of the wick fluid also showed an unexpectedly high concentration of a protein with electrophoretic mobility like that of plasma β globulins the origin of which has not been satisfactorily elucidated by the present study.

Methods

All experiments were made on Wistar rats weighing 300–450 g. In order to standardize the experimental conditions all animals were anesthetized. Sodium pentobarbital (Nembuto) was given intraperitoneally as an initial dose of 60 mg/kg and in longlasting experiments additional doses of 5 mg/kg were given to prevent muscle activity. The rat was placed prone on a heating pad. After shaving the back a midline incision was made through the skin from the lower dorsal vertebrae to sacrum, exposing the muscles on each side of the spine. This region was chosen for wick implantation because the m. erector spinae, m. quadratus lumborum and m. iliopsoas constitute a fairly extensive continuous muscle mass. Wicks were sewn into the muscle by means of 5 cm long slightly blunted round and somewhat curved mending needles. The needle was introduced in the upper lumbar region and pushed 4–5 cm in caudal direction 3–8 mm under the surface. The position of the wick was checked by dissection in several experiments and in every instance it was found to be in muscle tissue. Penetration to the peritoneal cavity was never observed. By this method two wicks were placed on each side of the spine about 4 and 8 mm from the midline and the skin incision was then closed by wound clips. The wicks used in these experiments were three stranded multifilamentous Pearsall unbounded nylon thread (James Pearsall & Co. Taunton Somerset, England) with a diameter of about 0.6 mm. The actual wick consisting of doubled thread contained about 500 filaments. Before use the wicks were soaked in ethanol for 24 h to remove spinning oil, washed in distilled water and thereafter soaked in sterile 0.9 % saline.

After a predetermined time—1, 2 or 3 h—the wicks were pulled out one by one. Both ends were cut off and the wick immediately transferred to saline for elution of proteins or to mineral oil for centrifugation for electrophoresis or measurements of colloid osmotic pressure. Arterial blood for the same analyses was sampled from the cut carotid artery immediately after removing the wicks.

Determination of total protein, albumin and hemoglobin after 24 h elution in 2 ml saline was performed on a total of 97 individual wicks in 23 rats as described in a previous paper (Aukland and Fadnes 1973). Albumin was determined spectrofluorimetrically by ANS (1 Amino naphthalene-8 sulfonic acid) using rat albumin as a standard and total protein was determined by Amidoschwartz 10B. The total protein in plasma was also measured with the method of Klungsoyr (1969) using Seronorm (Nyegaard & Co. A/S Oslo) as standard. Hemoglobin concentration was measured with a benzidine method as previously described (Aukland and Fadnes 1973).

For electrophoresis and COP determination wick fluid was isolated by centrifugation under mineral oil in a special glass tube provided with a funnel which kept the wick up from the bottom. It has been shown by Johnsen (to be published) that the fluid recovered in this way from wicks soaked in different plasma dilutions has a COP identical to that of the respective test solutions. To provide sufficient amounts of fluid for protein determinations COP or electrophoresis 2–4 wicks from each animal were centrifuged together. Bloodstained wicks were excluded since in this case hemoglobin determination was not suitable for testing blood contamination because the red cells were sedimented during isolation.

COP was determined on 5–10 μ l samples by the membrane osmometer recently described by Aukland and Johnsen (1974). Amicon membranes LM10 or more usually PM30 were used.

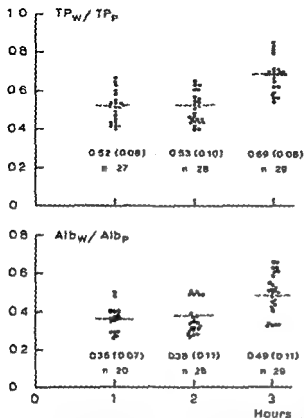


Fig. 1. Wick fluid (W)/plasma (P) concentration ratios for total protein (TP) and albumin (Alb) for single wicks after 1, 2 and 3 h implantation. Mean values with SD and wick numbers given below.

Electrophoresis was run on 2 cm broad cellulose acetate membranes using a barbital buffer pH 6.8 and ionic strength 0.1 and a current of 0.8 mA per strip for 45 min (slightly modified from Kaplan and Savory 1965). The strips were stained with Ponceau red S and read on a Densicord densitometer. No correction for different affinity to various proteins were made.

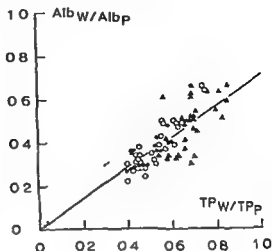
Results

Protein determinations were made on fluid eluted from a total of 97 wicks after implantation in 25 rats for 1 h (33 wicks), 2 h (32 wicks) and 3 h (32 wicks). Some wicks were clearly bloodstained and a hemoglobin concentration in wick fluid of 0.1 to 0.5 g/100 ml was found in 13 wicks which also showed significantly higher total protein but not higher albumin concentration than the remaining 84 wicks. In these 84 wicks no correlation was found between hemoglobin (average 0.03 g/100 ml) and albumin or total protein concentrations. A hemoglobin concentration of less than 0.1 g/100 ml was therefore chosen as criterion for acceptance.

Albumin and total protein concentrations

Considerable scatter was observed both between wicks from the same rat and between wicks from different animals. Also plasma protein concentrations varied considerably not only as random variations but unfortunately also between different

Fig 2 Wick fluid (W)/plasma (P) ratios for albumin (Alb) for each wick correlated to W/P ratios for total protein (TP) of corresponding wicks. Closed circles 1 h, open circles 2 h and triangles 3 h implantation.



batches of rats. For this reason, comparison between rats has been facilitated by calculating wick fluid/plasma ratios and albumin/total protein concentration ratios for wick fluid and plasma.

Fluid of wicks implanted for 1 and 2 h had a total protein concentration about half that of plasma. The concentration was significantly higher ($p < 0.01$) 85% of plasma concentration in wicks implanted for 3 h (Fig 1). In spite of considerable scatter between wicks, it is also evident from Fig 1 that the wick fluid/plasma ratio for albumin was considerably less than that for total protein, averaging 0.37 after 1 and 2 h implantation. Like total protein, also wick fluid albumin concentration increased significantly and to about half that of plasma in the interval from 2 to 3 h implantation. Somewhat less scatter was observed when the ratios for all wicks in each rat were averaged, as evident from Table I. However, the finding of

TABLE I Protein concentration in plasma (P) and wick fluid (W)

Implant at on time		Total prote n				Album n				Non albumin protein			
		P		W/P		P		W/P		P		W/P	
		n	g/100 ml		n	g/100 ml	n		g/100 ml				
1 h	Mean	9	5.93	3.10	51	7	3.37	1.20	36	7	2.57	1.75	72
	SD		48	57	07		31	19	04		67	17	18
2 h	Mean	8	5.36	2.82	53	8	3.46	1.33	39	8	1.90	1.0	80
	SD		7	37	07		28	22	07		35	26	11
3 h	Mean	8	6.09	4.16	69	8	4.02	1.96	49	8	2.12	2.20	107
	SD		58	17	06		31	37	09		49	46	14

Calculated as the difference between total protein and albumin concentrations.

* Significantly different ($p < 0.01$) from corresponding values after 1 and 2 h implantation.

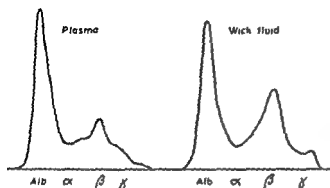


Fig. 3. Cellulose acetate electrophoretic pattern of plasma and wick fluid.

a significantly lower wick fluid/plasma ratio for albumin than for total protein is not due to averaging a large number of data. As is evident from Fig. 2, this relationship was found in all wicks with one single exception.

Table I also shows concentrations of nonalbumin protein calculated as the difference between total protein and albumin concentrations. This difference obviously accumulates analytical errors from both analyses including standardization in accuracies and therefore shows even greater variation than albumin and total protein. The very high wick fluid/plasma ratio of 0.7–0.8 after 1 and 2 h implantation is striking. In fluid from wicks implanted for 3 h, nonalbumin protein concentration had increased to the plasma level—but not significantly higher—an increase approximately proportional to the increase in albumin concentration. The average wick fluid composition after 1 and 2 h implantation is summarized in Table II, showing the marked dominance of nonalbumin protein in wick fluid as compared to plasma.

Electrophoresis

The dominance of nonalbumin protein in wick fluid from two rats was confirmed by electrophoresis (Fig. 3). The excess nonalbumin protein had a mobility like that of plasma β globulins. Practically identical patterns were observed in another rat. The electrophoretic albumin/total protein ratios in wick fluid 0.46 and 0.45

TABLE II. Average composition of plasma and wick fluid after 1 and 2 h implantation

	TP	Alb	NAP			COP
	g/100 ml	g/100 ml	g/100 ml	Alb/TP	Alb/NAP	mm Hg
Plasma	5.60 (44)	3.42 (21)	2.18 (10)	0.61 (08)	1.64 (10)	18.9 (12)
Wick fluid	2.23 (4)	1.21 (21)	1.02 (37)	0.44 (06)	0.81 (12)	8.7 (14)

Alb = albumin; TP = total protein; NAP = nonalbumin protein; COP = colloid osmotic pressure. Data are means \pm SD in parentheses. Protein determinations in 12 rats; all 12 in the figures are mean \pm SD in parentheses.

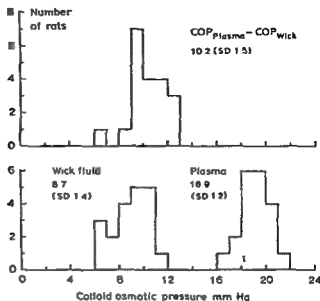


Fig 4 Lower panel Distribution of colloid osmotic pressure (COP) in wick fluid and plasma from 20 rats Upper panel Differences between COP of plasma and of wick fluid in the 20 rats

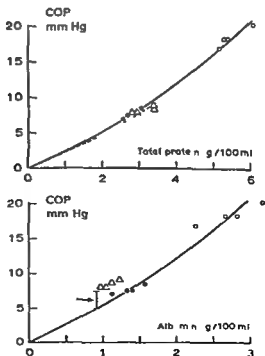


Fig 5 Upper panel Colloid osmotic pressure (COP) of plasma (open circles) of plasma diluted 1:1 (closed circles) and of wick fluid (triangles) from 4 rats related to total protein concentration. Unbroken line drawn to fit plasma/plasma dilutions. Broken line COP calculated from protein concentration according to Landis and Pappenheimer (1963). Lower panel COP related to albumin concentration. Symbols as above. Arrow points to difference between wick fluid COP and corresponding plasma dilution. Further explanation in text.

and in plasma 0.57 and 0.60 were somewhat higher in both rats than the corresponding ratios calculated from the chemical determinations (ANS and Amidoschwartz) 0.40 and 0.36 in wick fluid and 0.51 and 0.52 in plasma. This discrepancy may well be due to a higher affinity of Ponceau Red to albumin than to globulins. A similar difference in affinity is also present for Amidoschwartz but in the case of total protein determination this error has been counteracted by calibration against standard plasma. The γ globulin content was low in plasma as has previously been observed in rats (Deutsch and Goodloe 1945) and was also low in wick fluid.

Colloid osmotic pressure (COP)

COP of wick fluid and arterial plasma was determined in 20 rats after 1 h wick implantation. In each animal fluid was centrifuged from 2–4 wicks—bloodstained wicks being excluded in an attempt to satisfy the same criteria as for protein determination ($\text{Hgb} < 0.1 \text{ g/100 ml}$). Wick fluid COP averaged 8.7 (SD 1.4) mm Hg as compared to an average plasma COP of 18.9 (SD 1.2) mm Hg. Identical values were obtained both on plasma and wick fluid with the two types of dialyzing membranes nominally excluding molecular weights higher than 10 000 and 30 000 respectively. The distribution of the measurements is shown in Fig. 4 which also shows the plasma—wick fluid COP difference calculated for each rat, a value which averaged 10.2 (SD 1.5) mm Hg.

In 4 rats determination of albumin and total protein was made on the same samples as used for COP measurements. In order to correlate COP to protein concentration COP was also measured on 1:1 dilution of the plasma samples with 0.9% saline. This group of rats had plasma and wick fluid albumin concentrations somewhat below average but the wick fluid/plasma ratios were fairly close to the average for the whole material being 0.40 for albumin and 0.58 for total protein. As shown in the upper panel of Fig. 5 total plasma protein concentration and COP showed the well known curvilinear relationship in good agreement with the formula given by Landis and Pappenheimer (1963) for human plasma (broken line in Fig. 5). Furthermore in spite of its different protein composition the wick fluid showed practically the same relationship. In the lower panel of Fig. 5 COP is plotted against albumin concentration showing the wick fluid COP lying about 2.5 mm Hg higher than that of plasma dilutions (arrow in Fig. 5). The difference may be interpreted as follows. If plasma is diluted until its albumin concentration equals that of wick fluid any excess of colloid osmotic pressure of wick fluid (wick fluid COP—diluted plasma COP) must be due to an excess of nonalbumin protein. The average excess of nonalbumin protein in wick fluid (wick fluid non-albumin—diluted plasma non-albumin protein concentration) was 0.95 (range 0.75–1.20) g/100 ml. This difference may be compared to the COP of about 2.5 mm Hg exerted by 1 g/100 ml albumin in the concentration range 1–2 g/100 ml (Landis and Pappenheimer 1963). Thus the COP of the excess non-albumin protein in wick fluid is about the same as that of equal amounts of

albumin suggesting a molecular weight of about 70 000. However, considering the small number of observations and the rather small deviation in COP, a cautious conclusion should probably be that the nonalbumin protein is unlikely to be much smaller than albumin and is also unlikely to have a molecular weight as high as twice that of albumin.

Discussion

The albumin concentration of wick fluid after 1 and 2 h implantation, 37 % of plasma albumin concentration, is considerably lower than that previously found in subcutaneous tissue with the same method in rats (Aukland and Fadnes 1973) and humans (Poulsen 1973). However, as in subcutaneous wicks the albumin concentration rose after more than 2 h implantation, the rise probably being caused by an inflammatory increase of capillary permeability to proteins. As previously discussed in the case of subcutaneous wicks, the constancy of albumin and total protein concentrations from 1 to 2 h implantation suggests a constant and presumably normal capillary permeability in this period.

Similar albumin concentrations, 44 % of that in plasma, were observed by Creese *et al.* (1962) in fluid collected by blind puncture with glass capillaries into skeletal muscle of guinea pigs. Somewhat lower values, 21 to 35 % of plasma albumin concentration, were estimated in excised skeletal muscle from man by Rothschild *et al.* (1955). On the other hand, higher albumin concentration, 55 % of the plasma level, was found in skeletal muscle of rats in a careful study by Katz *et al.* (1970). A higher average ratio (0.59) but also greater scatter (0.20–0.87) was also observed in muscle lymph from cats and dogs by Jacobsson and Kjellmer (1964). Even if these results differ considerably, possibly due to differences between species and experimental conditions, they all agree with the present results in that there is a rather high albumin concentration in interstitial fluid of skeletal muscle.

Whereas the albumin concentration of wick fluid appears to be a reasonable value for normal interstitial fluid, the considerably higher wick fluid/plasma ratio for total protein was unexpected and might be an artifact due to the sampling technique. When compared to plasma which had been diluted to give the observed wick albumin concentration, the wick fluid contained an excess of nonalbumin protein of about 1 g/100 ml. This is unexpected because the plasma globulins are supposed to pass the normal capillary wall with greater difficulty than the smaller albumin molecule, as indicated by numerous studies of protein composition in lymph from various organs (Loffey and Courtice 1970). It should be emphasized, however, that the present study does not answer the question whether the excess nonalbumin protein is a plasma protein or a protein derived from the muscle itself. In either case, its presence in the wick fluid could represent an artifact due to the sampling technique. Obviously, the introduction into the muscle of a needle and a wick of thickness several times that of the muscle cells must distort the anatomy and might well be envisaged to damage capillaries and muscle cells. However, excess

and in plasma 0.57 and 0.60 were somewhat higher in both rats than the corresponding ratios calculated from the chemical determinations (ANS and Amidoschwartz) 0.40 and 0.36 in wick fluid and 0.51 and 0.52 in plasma. This discrepancy may well be due to a higher affinity of Ponceau Red to albumin than to globulins. A similar difference in affinity is also present for Amidoschwartz but in the case of total protein determination this error has been counteracted by calibration against standard plasma. The globulin content was low in plasma as has previously been observed in rats (Deutsch and Goodloe 1945) and was also low in wick fluid.

Colloid osmotic pressure (COP)

COP of wick fluid and arterial plasma was determined in 20 rats after 1 h wick implantation. In each animal fluid was centrifuged from 2–4 wicks—bloodstained wicks being excluded in an attempt to satisfy the same criteria as for protein determination ($\text{Hgb} < 0.1 \text{ g/100 ml}$). Wick fluid COP averaged 8.7 (SD 1.4) mm Hg as compared to an average plasma COP of 18.9 (SD 1.2) mm Hg. Identical values were obtained both on plasma and wick fluid with the two types of dialyzing membranes nominally excluding molecular weights higher than 10 000 and 30 000 respectively. The distribution of the measurements is shown in Fig. 4 which also shows the plasma—wick fluid COP difference calculated for each rat a value which averaged 10.2 (SD 1.5) mm Hg.

In 4 rats determination of albumin and total protein was made on the same samples as used for COP measurements. In order to correlate COP to protein concentration COP was also measured on 1:1 dilution of the plasma samples with 0.9% saline. This group of rats had plasma and wick fluid albumin concentrations somewhat below average but the wick fluid/plasma ratios were fairly close to the average for the whole material being 0.40 for albumin and 0.58 for total protein. As shown in the upper panel of Fig. 5 total plasma protein concentration and COP showed the well known curvilinear relationship in good agreement with the formula given by Landis and Pappenheimer (1963) for human plasma (broken line in Fig. 5). Furthermore in spite of its different protein composition the wick fluid showed practically the same relationship. In the lower panel of Fig. 5 COP is plotted against albumin concentration showing the wick fluid COP lying about 2.5 mm Hg higher than that of plasma dilutions (arrow in Fig. 5). The difference may be interpreted as follows. If plasma is diluted until its albumin concentration equals that of wick fluid any excess of colloid osmotic pressure of wick fluid (wick fluid COP—diluted plasma COP) must be due to an excess of nonalbumin protein. The average excess of nonalbumin protein in wick fluid (wick fluid non-albumin—diluted plasma non-albumin protein concentration) was 0.73 (range 0.73–1.20) g/100 ml. This difference may be compared to the COP of about 2.5 mm Hg exerted by 1 g/100 ml albumin in the concentration range 1–2 g/100 ml (Landis and Pappenheimer 1963). Thus the COP of the excess non-albumin protein in wick fluid is about the same as that of equal amounts of

lander wick method) transcapillary fluid balance thus demands a mean capillary pressure of about 11 mm Hg. This estimate is higher than observed with micro-puncture technique and in isogravimetric studies (Landis and Pappenheimer 1963) but agrees reasonably well with more recent isovolumetric measurements in cats (12–15 mm Hg) where care was taken to avoid increased capillary filtration (Eliassen *et al* 1973). However if the excess nonalbumin protein in wick fluid is not a normal constituent of interstitial fluid the true COP would be about 6 mm Hg giving an estimated mean capillary pressure of about 14 mm Hg. In any case the magnitude of interstitial fluid COP in skeletal muscle is such that it should not be neglected when discussing transcapillary fluid balance. As in other tissues the relatively high interstitial protein concentration and COP may well be an important buffer against edema formation (Starling 1896, Wiederhielm 1968, Aukland 1973, Fadnes 1973). Under conditions with increased capillary pressure or reduced plasma colloid osmotic pressure increased net capillary filtration and lymph flow will lower interstitial COP and thereby tend to reduce net transcapillary filtration forces and prevent overt edema.

H. M. Johnsen is a Student Research Fellow of the Norwegian Research Council for Science and the Humanities. This support, and grants from Norsk Medisinaldepot are gratefully acknowledged. The authors wish to thank Mrs. Signid Lepsoe for expert technical assistance and Mr. S. Elsaev for help with electrophoresis.

References

- AUKLAND, K. Autoregulation of interstitial fluid volume. Edema preventing mechanisms. *Scand. J. clin. Lab. Invest.* 1973, 31, 247–254.
- AUKLAND, K. and H. O. FADNES. Protein concentration of interstitial fluid collected from rat skin by a wick method. *Acta physiol. scand.* 1973, 88, 350–358.
- AUKLAND, K. and H. M. JOHNSEN. A colloid osmometer for small fluid samples. *Acta physiol. scand.* 1974, 90, 485–490.
- CREESE, R. J. L. D. SILVA and D. M. SHAW. Interfibre fluid from guinea pig muscle. *J. Physiol. (Lond.)* 1962, 162, 44–53.
- DEUTSCH, H. F. and M. B. GOODPASTER. An electrophoretic survey of various animal plasmas. *J. Biol. Chem.* 1945, 161, 1–20.
- ELIASSEN, E., B. FOLKOW, B. HILTON, B. ÖBERG and B. RIPPÉ. Pressure volume characteristics of the interstitial fluid space in the skeletal muscle of the cat. *Acta physiol. scand.* 1974, 90, 583–593.
- FADNES, H. O. Interstitial fluid pressure and albumin concentration in experimental hypoproteinemia. *Acta physiol. scand.* 1973, Suppl. 396, 61.
- GARLICK, O. G. and E. M. REISCHL. Transport of large molecules from plasma to interstitial fluid and lymph in dogs. *Amer. J. Physiol.* 1970, 219, 1593–1605.
- GODART, S. Studies of the physiology of lymphatic vessel by microcirculation methods. *Lymphology* 1968, 1, 80–87.
- GUYTON, A. C., H. J. GRANGER and A. M. TAYLOR. Interstitial fluid pressure. *Physiol. Rev.* 1971, 51, 577–563.
- JACOBSSON, J. and I. HJELLMER. Flow and protein content of lymph in resting and exercising skeletal muscle. *Acta physiol. scand.* 1964, 60, 278–283.
- JOHNSEN, H. M. Measurement of colloid osmotic pressure of interstitial fluid. *Acta physiol. scand.* 1974, 91, 14–144.
- KAPLAN, A. and J. SAVORY. Evaluation of a cellulose acetate electrophoresis system for serum protein fractionation. *Clin. Chem.* 1965, 11, 937–942.
- KATZ, J. G., B. BONORRIS, B. GOLDEN and A. L. SELLERS. Extravascular albumin mass and exchange in rat tissues. *Clin. Sci.* 1970, 39, 65–72.
- ALLANSON, L. Quantitative estimation of protein. Separation of albumin protein-copper complex from excess copper on Sephadex G 25. *Analyt. Biochem.* 1969, 7, 91–98.

- LANDIS E. M. and J. R. PAPPENHOFER Exchange of substances through the capillary walls *Handbook of Physiology* Section 2 Circulation Vol II Eds W. F. Hamilton and P. Dow Amer. Physiol. Soc. Washington D.C. 1963 961—1034
- LEE J. E. Analysis on diffusion and convection of protein in tissue *J. appl. Physiol.* 1977 32 254—256
- POLLSEN H. L. Subcutaneous interstitial fluid albumin concentration in long term diabetes mellitus *Scand. J. clin. Lab. Invest.* 1973 32 167—173
- RENYI VAMOS F. *Das innere Lymphgefäßsystem der Organe* Verlag der Ungarischen Akademie der Wissenschaften Budapest 1960 411—414
- RODERMUND O. E. Zur Verteilung von Plasmaproteinen in Blut und Haut *Arch. klin. exp. Derm.* 1970 237 684—689
- ROTHSCHILD M. A. A. BAUMAN R. S. YALOW and S. A. BERSON Tissue distribution of ¹²⁵I labeled human serum albumin following intravenous administration *J. clin. Invest.* 1955 34 1354—1358
- SCHULTZE H. E. and J. F. HEREMANS *Molecular biology of human proteins* Vol 1 Elsevier Publ. Comp. Amsterdam—London—New York 1966 487—507
- STARLING E. H. On the absorption of fluid from the connective tissue spaces *J. Physiol. (Lond.)* 1896 19 312—326
- SZABO G. Z. MAOYAR and G. MOLNAR Lymphatic and venous transport of colloids from the tissues *Lymphology* 1973 6 69—79
- WIEDERHILM C. A. Dynamics of transcapillary fluid exchange *J. gen. Physiol.* 1968 52 294—635
- YOFFEY J. M. and F. C. COURTICE *Lymphatics lymph and the lymphomylod complex* Academic Press London New York 1970

Time Course and Extent of Structural Vascular Adaptation to Regional Hypotension in Adult Spontaneously Hypertensive Rats (SHR)

By

LILIAN WEISS and MARGARETA HALLBÄCK

Received 28 December 1973

Abstract

WEISS L. and M. HALLBÄCK. *Time course and extent of structural vascular adaptation to regional hypotension in adult spontaneously hypertensive rats (SHR)*
Acta physiol scand 1974 91 365—373

In female spontaneous hypertensive rats 8—19 months old and consequently with considerable structural changes in their resistance vessels the aorta was ligated below the renal arteries markedly lowering the hindquarter blood pressure 3, 7, 14, 21 and 135 days later the hindquarters of these rats and of control rats were subject to paired perfusions from maximal dilatation up to maximal pressor responses thus exploring hemodynamically the rate and extent of regressive changes in vascular design. — Already after 3 days clear signs of regression of the hypertensive vascular changes were found and in about 3 weeks the resistance vessels had almost completed the considerable adjustment to the low pressure situation with widened lumina and a reduced bulk of contractile media. However still after another 17 weeks they displayed signs of a wall/lumen ratio elevation compared with the situation in similarly treated young SHR (Folkow *et al* 1971 a). — It is concluded that even though a considerable hypotension a readjustment of vascular design takes place also in adult SHR with established hypertension. It is generally more difficult to induce full regression the higher the age and the longer the duration of the disease presumably due to the gradual addition of less reversible vascular changes such as collagen invasion of the media.

Hemodynamic analyses in man as well as in spontaneously and renal hypertensive rats suggest that the increased resistance in hypertension may be ascribed mainly to a structural adaptation of the resistance vessels where media hypertrophy is associated with narrowed lumina even during maximal dilatation (*cf* Folkow *et al* 1973, Lundgren *et al* 1974).

By producing regional hypotension in one of the hindlimbs of cats Folkow and Sivertsson (1968) showed that the resistance vessels adapted in the direction of a reduced wall/lumen ratio compared to the control limb within 3—5 weeks evidently reflecting a general tendency of vessels to adjust their design to the current pressure level. Further when the abdominal aorta of 3 week old NCR and SHR which had not been exposed to any pressure rise was ligated below the renal arteries so that

their hindquarters were supplied via collaterals at a reduced pressure head the characteristic hypertensive vascular alterations failed to develop (Folkow *et al* 1971a). It was concluded that also the resistance vessels of hypertensive animals adapt structurally to the prevailing pressure level even when it is low. This was so despite the fact that largely the same neurohormonal influences affected both the hypotensive vessels in the hindquarters and the hypertensive ones in the upper part of SHR.

Further intense but rather brief (3 weeks) antihypertensive treatment with guanethidine and hydralazine could bring blood pressure of adult SHR down to normotensive levels and subsequent hemodynamic evaluation of the characteristics of their hindquarter vessels revealed a considerable regression of the hypertensive structural changes also in this rather advanced state of hypertension (Folkow *et al* 1971b; Weiss 1974).

In the present study the time course and extent of such vascular adaptation was examined in 8–12 month old SHR with established hypertension where the hindquarters had been made hypotensive by aortic constriction for periods of 3, 7, 14, 21 and 135 days after which paired hemodynamic comparisons with NCR were performed as briefly outlined above.

Methods

The aorta was ligated 5 mm distally to the renal arteries during ether anesthesia in 56 8–12 month old female SHR which tolerate this operation far better than male rats. Attempts to produce graded aortic constriction failed because of aneurysm formation. A group of matched female NCR were exposed to dissection of the abdominal aorta though no lesion was performed. These shamoperated rats were subsequently used as controls in paired perfusion experiments performed on the isolated hindquarters 3, 7, 14, 21 and 135 days after the aortic ligation. In addition 12 untreated female SHR were used. At each time interval 8–13 pairs of NCR SHR or NCR aortaligated SHR were investigated. The blood pressure was first measured simultaneously in the cannulated carotid and caudal arteries of the unanesthetized Nembutal® 50 mg/kg i.a. animals in order to estimate the pressure difference in the aortic constriction in SHR. The pressure flow relationship at maximal vasodilatation in the isolated hindquarter vascular bed was then explored after which the response to intravenous adrenalin (NA) in doses from subthreshold to supramaximal levels and to late doses of vasopressin and BaCl₂ were investigated during constant flow perfusion. To get an estimate of the perfused hindquarter weight without edema the weight of all parts of the vessel bed of the hindquarter was subtracted from the total body weight.

The technique used for hindquarter perfusion, the recordings of the resistance changes, the construction of the resistance curves characterizing the individual vascular bed and the result evaluation have been described in detail earlier (Folkow *et al* 1970, 1971).

Results

The arterial blood pressures (mean \pm SE) in the carotid artery under anesthesia were in the control SHR 181 ± 6 , in the constricted NCR 173 ± 3 and in the constricted aortaligated SHR 174 ± 5 mm Hg. When arterial pressure was measured in the tail artery during awake conditions in control SHR and NCR it was 160 ± 4 and 114 ± 5 mm Hg respectively. Evidently carotid artery obstruction raised the pressure

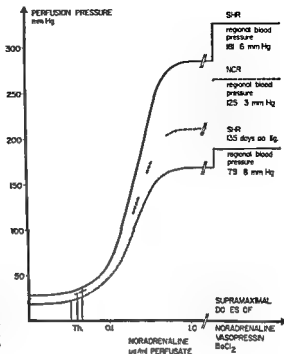


Fig 1 Relationships between mean resistance curves from constant flow perfusions of isolated hindquarters in female adult SHR, NCR and SHR that had been aortalgated for 135 days (cf Table I)

somewhat but this procedure was necessary for evaluation of the pressure drop across the aortic constriction

Immediately after aortic ligation the caudal blood pressure fell to 20–30 mm Hg but then it gradually rose evidently due to improved collateral circulation. Thus caudal artery pressure (mean \pm S.E.) in the aortalgated SHR was 26 ± 2 after 3 days, 44 ± 4 after 7 days, 57 ± 8 after 14 days and 59 ± 6 after 21 days to reach 79 ± 8 mm Hg after 135 days.

In the paired perfusion experiments where the isolated hindquarters of aorta ligated SHR were perfused in parallel with those of unligated sham-operated NCR a pressure flow run was first performed during maximal dilatation varying flow between 5 and 40 ml/min $\times 100$ g. From the calculated pressure flow curve the average resistance to flow in terms of peripheral resistance units per 100 g tissue (PRU₁₀₀) was determined at flows of 10 ml and 30 ml/min $\times 100$ g. For the evaluation of the structurally determined resistance at maximal dilatation the flow of 30 ml/min $\times 100$ g is more illustrative of the hemodynamic situation in maximally vasodilated skeletal muscle of intact organisms. The reason is that the distending pressure is then closer to normal allowing differences in vascular distensibility to be taken into account (Hallback, Lundgren and Weiss 1974).

Subsequently flow was kept constant at about 10 ml/min $\times 100$ g and noradrenaline (NA) was infused from subthreshold to supramaximal amounts, definite maximal pressor responses being ensured by vasopressin and barium chloride injections. Resistance curves were constructed as described earlier (Folkow *et al*

their hindquarters were supplied via collaterals at a reduced pressure head, the characteristic hypertensive vascular alterations failed to develop (Folkow *et al* 1971a). It was concluded that also the resistance vessels of hypertensive animals adapt structurally to the prevailing pressure level, even when it is low. This was so despite the fact that largely the same neurohormonal influences affected both the hypotensive vessels in the hindquarters and the hypertensive ones in the upper part of SHR.

Further intense but rather brief (5 weeks) antihypertensive treatment with guanethidine and hydralazine could bring blood pressure of adult SHR down to normotensive levels and subsequent hemodynamic evaluation of the characteristics of their hindquarter vessels revealed a considerable regression of the hypertensive structural changes also in this rather advanced state of hypertension (Folkow *et al* 1971b; Weiss 1974).

In the present study, the time course and extent of such vascular adaptation was examined in 8–12 month old SHR with established hypertension where the hindquarters had been made hypotensive by aortic constriction for periods of 3, 7, 14, 21 and 135 days after which paired hemodynamic comparisons with NCR were performed as briefly outlined above.

Methods

The aorta was ligated 5 mm distally to the renal arteries during ether anesthesia in 56 8–12 month old female SHR which tolerate this operation far better than male rats. Attempts to produce graded aortic constriction failed because of aneurysm formation. A group of matched female NCR were exposed to dissection of the abdominal aorta though no ligation was performed. These shamoperated rats were subsequently used as controls in paired perfusion experiments performed on the isolated hindquarters 3, 7, 14, 21 and 135 days after the aortic ligation. In addition 15 untreated female SHR were used. At each time interval 8–13 pairs of NCR SHR or NCR aortaligated SHR were investigated. The blood pressure was first measured simultaneously in the cannulated carotid and caudal arteries of the two anesthetized (Nembutal® 50 mg/kg) animals in order to estimate the pressure difference across the aortic constriction in SHR. The pressure-flow relationship at maximal vasodilatation in the isolated hindquarter vascular bed was then explored after which the resistance responses to noradrenaline (NA) in doses from subthreshold to supramaximal levels and to large doses of vasopressin and BCl₂ were investigated during constant flow perfusion. To get an exact measure of the perfused hindquarter weight without edema the weight of all parts of the rat except the hindquarters was subtracted from the total body weight.

The technique used for hindquarter perfusion, the recordings of the resistance changes, the construction of the resistance curves characterizing the individual vascular beds and the results evaluated have been described in detail earlier (Folkow *et al* 1970, 1971a).

Results

The arterial blood pressures (mean \pm SE) in the carotid artery under anesthesia were in the control SHR 181 ± 6 , in the compiled NCR 125 ± 3 and in the compiled aortaligated SHR 174 ± 5 mm Hg. When arterial pressure was measured in the tail artery during awake conditions in control SHR and NCR it was 160 ± 4 and 114 ± 5 mm Hg respectively. Evidently carotid artery obstruction raised the pressure

1970) and Fig. 1 illustrates the mean resistance curves for *A* Unligated female SHR tail artery pressure 181 ± 6 mm Hg during carotid artery occlusion (see above) *B* Unligated female NCR tail artery pressure being 125 ± 3 mm Hg during carotid artery occlusion and *C* Female SHR after 135 days of aortic ligation when the changes in vascular design to local hypotension appear to be stabilized tail artery pressure being then 79 ± 8 mm Hg during carotid artery occlusion. The structurally determined changes in resistance to flow as reflected by the resistance curves can be defined by

- 1 The resistance at maximal dilatation reflecting the size of the structurally determined lumina of the resistance vessels
- 2 The steepness of the resistance curve predominantly reflecting a changed wall/lumen ratio
- 3 The maximal pressor response reflecting the maximal strength and hence the relative thickness of the smooth muscle component of the vessel walls
- 4 NA threshold i.e. the NA dose producing a 25 % increase in resistance from the state of maximal dilatation reflects the sensitivity of the contractile elements

Concerning point 4 earlier experiments have revealed that there is no important difference in smooth muscle sensitivity between NCR and SHR or aorta ligated SHR (Folkow *et al.* 1970 1971 a Hallback Lundgren and Weiss 1971) and attention was therefore focussed mainly on the resistance at maximal dilatation the steepness of the resistance curve and the maximal pressor response

All experiments were run in parallel with matched controls thereby largely eliminating the impact on the comparisons of accidental disturbances such as differences in perfusate composition temperature viscosity NA content etc. As can be seen from Table I there is a slight variation in the NCR values between the different experimental groups. This illustrates the usefulness of the paired experimental procedure which also allows the statistical analysis to be performed according to the principle of pairing design *t* test. The results in Table I represents the mean values (\pm S.E.) the mean difference (\pm S.E.D.) and the degree of significance between the sham operated NCR and the aorta ligated SHR for each experimental group. Already 3 days after abrupt reduction in regional blood pressure in the ligated SHR (to 26 mm Hg) a rapid structural vascular adjustment has taken place since there is no longer any statistical difference between NCR and aorta ligated SHR in neither resistance at maximal dilatation steepness of resistance curve nor maximal pressor response (Table I). After 7 days these adjustments are still more pronounced the resistance at maximal dilatation in the aorta ligated SHR being now significantly lower than that in NCR and after 14 days this is true also for the maximal pressor response. After 21 days the regressive adjustment of vascular design seems to be almost completed though a slight further adjustment seems to take place. Considering the fact that the regional blood pressure is increased another 20 mm Hg after 135 days this delayed adjustment is presumably associated to the gradual improvement of the collateral circulation by passing the aortic obstruction.

TABLE I Mean values (\pm S.E.) mean differences (\pm S.E.D.) and degree of significance of the differences between SHR aortaligated SHR and NCR

Group of pairs	Caudal pressure mm Hg	Carotid pressure mm Hg	PRU at 10 ml/min \times 100 g	PRU at 30 ml/min \times 100 g	Steepness (Tg)	Maximal pressor response mm Hg
SHR "control"	181 \pm 6	181 \pm 6	2.44 \pm 0.10	1.54 \pm 0.03	5.0 \pm 0.4	317 \pm 17
NCR	130 \pm 6	130 \pm 6	2.17 \pm 0.09	1.37 \pm 0.04	3.6 \pm 0.4	257 \pm 11
mean difference	51 \pm 8	51 \pm 8	0.27 \pm 0.06	0.17 \pm 0.04	1.4 \pm 0.5	60 \pm 14
n = 12						
significance	p < 0.001	p < 0.001	p < 0.001	p < 0.001	p < 0.05	p < 0.002
SHR 3 days	26 \pm 2	157 \pm 5	2.17 \pm 0.11	1.38 \pm 0.06	3.3 \pm 0.3	273 \pm 13
NCR	113 \pm 7	113 \pm 7	2.29 \pm 0.09	1.41 \pm 0.06	3.5 \pm 0.4	276 \pm 14
mean difference	-87 \pm 9	44 \pm 10	-0.12 \pm 0.12	-0.03 \pm 0.08	-0.2 \pm 0.2	-3 \pm 17
n = 12						
significance	p < 0.001	p < 0.005	n.s.	n.s.	n.s.	n.s.
SHR 7 days	44 \pm 4	179 \pm 5	1.91 \pm 0.08	1.27 \pm 0.03	3.4 \pm 0.4	240 \pm 11
NCR	127 \pm 7	127 \pm 7	2.28 \pm 0.10	1.38 \pm 0.05	3.4 \pm 0.4	238 \pm 14
mean difference	-83 \pm 7	52 \pm 8	-0.37 \pm 0.09	-0.11 \pm 0.03	0.0 \pm 0.2	2 \pm 14
n = 13						
significance	p < 0.001	p < 0.001	p < 0.005	p < 0.05	n.s.	n.s.
SHR 14 days	57 \pm 8	174 \pm 9	1.77 \pm 0.08	1.16 \pm 0.04	2.8 \pm 0.3	208 \pm 14
NCR	129 \pm 5	129 \pm 5	2.24 \pm 0.12	1.38 \pm 0.06	3.1 \pm 0.4	247 \pm 14
mean difference	-72 \pm 9	46 \pm 8	-0.47 \pm 0.15	-0.22 \pm 0.07	-0.4 \pm 0.2	-39 \pm 12
n = 11						
significance	p < 0.001	p < 0.001	p < 0.01	p < 0.01	n.s.	p < 0.01
SHR 21 days	59 \pm 6	174 \pm 5	1.91 \pm 0.09	1.20 \pm 0.06	3.2 \pm 0.6	185 \pm 12
NCR	130 \pm 4	130 \pm 4	2.54 \pm 0.07	1.45 \pm 0.03	3.7 \pm 0.4	238 \pm 16
mean difference	-71 \pm 7	44 \pm 7	-0.43 \pm 0.12	-0.25 \pm 0.08	-0.5 \pm 0.7	-72 \pm 11
n = 8						
significance	p < 0.001	p < 0.001	p < 0.01	p < 0.05	n.s.	p < 0.001
SHR 135 days	79 \pm 8	176 \pm 11	1.85 \pm 0.10	1.11 \pm 0.04	2.5 \pm 0.2	189 \pm 14
NCR	117 \pm 4	117 \pm 4	2.49 \pm 0.10	1.49 \pm 0.05	2.8 \pm 0.3	264 \pm 20
mean difference	-38 \pm 7	59 \pm 11	-0.64 \pm 0.11	-0.37 \pm 0.07	-0.3 \pm 0.3	-75 \pm 20
n = 12						
significance	p < 0.001	p < 0.001	p < 0.001	p < 0.001	n.s.	p < 0.001

Further to obtain a comparison between the NCR—aortaligated SHR groups and the NCR—SHR control groups the differences from the respective groups of pairs were analysed by means of the group comparison t test. This type of comparison revealed a significant decrease in resistance at maximal dilatation ($p < 0.05$) in steepness of the resistance curve ($p < 0.005$) and in maximal pressor response ($p < 0.05$) between the aortaligated SHR and untreated control SHR already 3 days after aortic obstruction.

Fig. 2 illustrates diagrammatically the regional blood pressure fall and the extent of the structural adaptation of the resistance vessels in relation to time. The mean values for regional blood pressure resistance at maximal dilatation and maximal pressor response for each time interval are here expressed as the ratio between aortaligated SHR (or ordinary SHR) hindquarters and the NCR control hindquarters. As can be seen the changes occurring during the first 2—3 weeks are

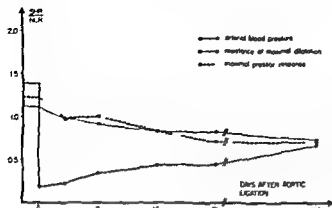


Fig 2 Diagrammatic illustration of the regional blood pressure drop and the extent of structural vascular adaptation in the hindquarters with time after aortic ligation in SHR. All values are expressed as ratios for SHR/ Δ CR and for aortaligated SHR/NCR

considerable and rapid as described above. After 135 days there is an almost perfect adjustment to the local pressure level (0.68) of the resistance at maximal dilatation (0.75) and the maximal pressure response (0.72). However, the ratio for the steepness of the resistance curves (0.89 Table I) remains increased in the ligated SHR in relation to the arterial pressure levels which might indicate the presence of e.g. collagen elements that do not show such rapid regression as the smooth muscle component (cf Wolinsky 1972).

Discussion

If the structural adaptation of resistance vessels in hypertension (cf Folkow *et al* 1973) is considered as an exponent of a *per se* normal tissue response to changes in load like that characterizing the heart it is evident that also a decrease in pressure should affect the vascular bed and then in the opposite direction. Accordingly Folkow and Sverrisson (1968) observed in cats that the arterial vessels within few weeks adapted markedly to a pressure reduction with respect to their design in the direction of a reduced wall/lumen ratio as judged from both structural and hemodynamic changes.

The time course and extent of such a structural vascular adaptation is of course of great interest also for the evaluation of hypertension its development as well as its treatment. Therefore the earlier described hindquarter preparation of SHR has been used as a model for studying shifts in structural design of the resistance vessels induced by e.g. reductions in local arterial pressure (Folkow *et al* 1970 1971a). For this purpose the aorta was in the present study ligated below the renal arteries in adult female SHR in the phase of manifest hypertension (age 8–12 months) as a comparison to the earlier study in young, prehypertensive SHR. Only females were used since adult males in contrast to the earlier studied 3 week old males (Folkow *et al* 1971a) did not usually survive aortic ligation presumably mainly because of differences between the sexes in collateral circulation via the genital organs. It has further been suggested (Jaffe and Rowe 1972) that hormonal dif-

ferences might contribute to the ability to develop collateral vessels. In any case the adult females managed this initially drastic local reduction in pressure to 20–30 mm Hg quite well without obvious tissue lesions and after 2 days the animals seemed to use their hindquarters largely in the normal way. Further, no gross muscle atrophy could be demonstrated since the weight of the hindquarters in per cent of total body weight of the aortaligated SHR did not differ significantly from that of the matched NCR.

The mean level of arterial pressure in the hypotensive hindquarters during the initial 3 week period was of the order of 40–60 mm Hg with exception for the first few days when it was still lower. In response to this drastic lowering of pressure which corresponded to about 40–50 % of the pressure level in the shamoperated NCR the SHR resistance vessels exhibited a rapid and fairly extensive change in design to judge from the alterations of the resistance curves 3 days after aortic ligation when the rats moved around normally without signs of ischemia. The first clear change in vascular design was found expressed as a decrease in resistance at maximal dilatation, a reduced steepness of the resistance curve and a reduced maximal pressor response. In a few experiments performed already 1 day after operation when the rats still had signs of relative ischemia the results showed no clear signs of vascular structural regression. After about 3 weeks the adaptive structural changes of the resistance vessels appeared to be almost completed and both the resistance at maximal dilatation and the maximal pressor response were then significantly lower than in NCR ($p < 0.05$). The results cannot be ascribed to any ischemic interference with smooth muscle contractility since the vascular changes would then have been most severe during the first few days when pressure and flow were at their lowest levels. Therefore the gradual reduction in *e.g.* maximal contractile strength of the resistance vessels can thus only be explained by a reduction in their media mass. It is possible that part of the decreased resistance at maximal dilatation reflects an addition of newly formed microvessels but such a possibility calls for a microscopic evaluation of the vascular arborization.

The decreased maximal contractile strength together with the reduced steepness of the resistance curve and the decreased resistance at maximal dilatation strongly suggest a rapid and considerable adjustment in design of the previously hypertrophic resistance vessels towards wider lumina and thinner walls partly compensating for the pressure fall. Already after 21 days this change is almost completed though a slow further increase in collateral capacity bypassing the aortic occlusion takes place during the subsequent 15–17 weeks. Then the ratio for the ligated SHR hindquarter blood pressure to that of NCR was 0.68 while the SHR/NCR ratios for the resistance at maximal dilatation and for the maximal pressor response were 0.75 and 0.72 respectively. Thus an almost perfect adjustment of the vascular design to fit the regional pressure level was at hand (Fig. 2). However the steepness of the resistance curve reflecting mainly the wall/lumen ratio of the resistance vessels never became fully balanced to the lowered pressure in these old SHR since the ratio SHR/NCR was here as high as 0.89. When instead young prehypertensive

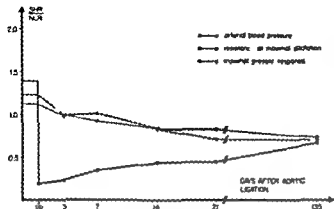


Fig 2 Diagrammatic illustration of the regional blood pressure drop and the extent of structural vascular adaptation in the hindquarters with time after aortic ligation in SHR. All values are expressed as ratios for SHR/NCR and for aortaligated SHR/NCR.

considerable and rapid as described above. After 135 days there is an almost perfect adjustment to the local pressure level (0.68) of the resistance at maximal dilatation (0.70) and the maximal pressor response (0.72). However the ratio for the steepness of the resistance curves (0.89 Table I) remains increased in the ligated SHR in relation to the arterial pressure levels which might indicate the presence of e.g. collagen elements that do not show such rapid regression as the smooth muscle component (cf Wolinsky 1972).

Discussion

If the structural adaptation of resistance vessels in hypertension (cf Folkow *et al* 1973) is considered as an exponent of a *per se* normal tissue response to changes in load like that characterizing the heart it is evident that also a decrease in pressure should affect the vascular bed and then in the opposite direction. Accordingly Folkow and Sverrisson (1968) observed in cats that the arterial vessels within few weeks adapted markedly to a pressure reduction with respect to their design in the direction of a reduced wall/lumen ratio as judged from both structural and hemodynamic changes.

The time course and extent of such a structural vascular adaptation is of course of great interest also for the evaluation of hypertension its development as well as its treatment. Therefore the earlier described hindquarter preparation of SHR has been used as a model for studying shifts in structural design of the resistance vessels induced by e.g. reductions in local arterial pressure (Folkow *et al* 1970 1971a). For this purpose the aorta was in the present study ligated below the renal arteries in adult female SHR in the phase of manifest hypertension (age 8–12 months) as a comparison to the earlier study in young prehypertensive SHR. Only females were used since adult males in contrast to the earlier studied 3 week old males (Folkow *et al* 1971a) did not usually survive aortic ligation presumably mainly because of differences between the sexes in collateral circulation via the genital organs. It has further been suggested (Jaffe and Rowe 1972) that hormonal dif-

- FOLKOW B, M HALLBACK, Y LUNDGREN and L WEISS Effects of intense treatment with hypotensive drugs on structural design of the resistance vessels in spontaneously hypertensive rats *Acta physiol scand* 1971 **6** 83 280—287
- FOLKOW B, M HALLBACK, Y LUNDGREN, R SIVERTSSON and L WEISS Importance of adaptive changes in vascular design for establishment of primary hypertension studied in man and spontaneously hypertensive rats *Circulat Res* 1973 **32**—33 Suppl 1 1 2—1 13
- FOLKOW B, M HALLBACK, Y LUNDGREN and L WEISS Effects of immunosympathectomy on blood pressure and vascular "reactivity" in normal and spontaneously hypertensive rats *Acta physiol scand* 1972 **84** 512—523
- FOLKOW B, Y LUNDGREN and L WEISS The effect of prolonged propranolol treatment on blood pressure and structural design of the resistance vessels in young spontaneously hypertensive rats (SHR) *Acta physiol scand* 1972 **84** ■ A—9 A
- FOLKOW B and R SIVERTSSON Adaptive changes in "reactivity and wall/lumen ratio in cat blood vessels exposed to prolonged transmural pressure difference *Life Sci* 1968 **7** 1283—1289
- FRIS ■ D, D RAGAN H, PILLSBURG III and M MATHEWS Alteration of the course of hypertension in the spontaneously hypertensive rat *Circulat Res* 1972 **31** 1—7
- HALLBACK M, Y LUNDGREN and L WEISS Reactivity to noradrenaline of aortic strips and portal veins from spontaneously hypertensive and normotensive rats *Acta physiol scand* 1971 **81** 176—181
- HALLBACK M, Y LUNDGREN and L WEISS Distensibility of the resistance vessels in spontaneously hypertensive rats as compared with normotensive control rats *Acta physiol scand* 1974 **90** 57—68
- JAFFE M D and P W ROWE The mechanism by which female hormones enlarge collateral arteries *Michigan Med* 1972 **71** 605—606
- LUNDGREN Y Regression of cardiovascular changes after reversal of experimental renal hypertension in rats *Acta physiol scand* 1974 **91** 275—285
- LUNDGREN Y, M HALLBACK, L WEISS and B FOLKOW Rate and extent of adaptive cardiovascular changes in rats during experimental renal hypertension *Acta physiol scand* 1974 **91** 103—115
- OKAMOTO K Spontaneous hypertension in rats *Int Rev Exp Path* 1969 **7** 227—270
- SMIRK F H The prognosis of untreated and of treated hypertension and advantages of early treatment *Amer Heart J* 1972 **83** 875—840
- WEISS L Long term treatment with antihypertensive drugs in spontaneously hypertensive rats (SHR) Effects on blood pressure, survival rate and cardiovascular design *Acta physiol scand* 1974 **91** 393—408
- WOLINSKY H Effects of hypertension and its reversal on the thoracic aorta of male and female rats *Circulat Res* 1971 **28** 622—637
- WOLINSKY H Long term effects of hypertension on the rat aortic wall and their relation to concurrent aging changes Morphological and chemical studies *Circulat Res* 1972 **30** 301—309

Discharge Properties of Motor Units in Relation to Recruitment Order in Voluntary Contraction

By

JAN HANNERZ

Received 10 January 1974

Abstract

HANNERZ J *Discharge properties of motor units in relation to recruitment order in voluntary contraction* Acta physiol scand 1974 91 374—384

The discharge pattern and recruitment order of single motor units in voluntary contraction of the normal human anterior tibial muscle was studied with an electrode having a high selectivity and a high positional stability in the muscle. In sustained contractions each motor unit was activated at a characteristic level of tension. The higher the threshold of the motor unit in sustained contraction the higher was the frequency when the unit attained a discharge at regular intervals and the higher tended the maximum frequency of the unit to be. Motor units with low thresholds in sustained contractions exhibited a continuous or tonic discharge in strong sustained contractions whereas units with high thresholds tended to exhibit a discontinuous or phasic discharge. For some units the threshold of activation remained stable for others it increased during activity. In twitch contractions the recruitment order of motor units differed considerably from that in sustained contractions.

When a motor unit is activated at a low frequency it discharges at irregular intervals. The intervals become more regular as the frequency is increased. Previous investigators have estimated the minimum frequency at which motor units attain a discharge at regular intervals to be about 5—9/s (e.g. Adrian and Bronk 1929, Smith 1934, Milner Brown, Stein and Yemm 1973). Haglund and Lippold (1954) showed that motor units with a low threshold in sustained contraction have a lower minimum frequency than have units with a higher threshold. Tokizane and Shimazu (1964) estimated the minimum frequency at regular intervals for different motor units by correlating the standard deviation of the discharge intervals with the discharge frequency. They found two distinct groups of units in all muscles tested although the minimum frequencies differed between different muscles. In the anterior tibial muscle they found one group discharging at regular intervals at a

frequency of about 7/s and one group at a frequency of about 12/s. However these authors were not in a position to study systematically single motor units in more than about 25% of the maximum tonic tension. The maximum frequency has previously been difficult to record owing to the fact that in strong contractions the interference activity of many motor units obstructs the identification of single units. The displacement of the recording electrode which occurs in strong contractions is an additional obstacle.

Some investigators (Seyffarth 1940, 1941, Weddell, Feinstein and Pattle 1944, Bigland and Lippold 1954) have avoided these difficulties by recording the potentials of motor units in partially denervated muscle where only a few functioning units remain. However recordings in paretic muscles are not comparable to those obtained from normal muscles since the discharge pattern of a motoneurone varies with changes in the afferent inflow (Tokizane and Shimazu 1964).

Because of these difficulties and differences in experimental conditions and also probably because different muscles were studied, the results from previous investigations have been contradictory, resulting in different hypotheses as to the discharge pattern of motor units in sustained voluntary contraction.

An electrode has now been designed which has a high selectivity and is not prone to displacement even at maximum contraction (Hannerz 1974). With the use of this electrode the discharge pattern of different motor units has been studied and related to their recruitment order in sustained and twitch voluntary contractions as briefly reported earlier (Hannerz 1973).

Methods

This study is limited to the motor units of the anterior tibial muscle. Most experiments were performed on the author but the findings were confirmed on other subjects. The subject was seated in a chair with the knee bent at an angle of about 140° and the foot at an angle of about 90° to the lower leg. His shoe was firmly fastened to a myograph. The signal of the myograph was linear for tensions up to 30 kg. The maximum voluntary tension of the anterior tibial muscle recorded in this way was about 25 kg for subjects in this study.

When the recruitment order of motor units in twitch contractions was studied, the muscle was relaxed as much as possible before each twitch contraction in order to avoid subliminal facilitation before the activation (*cf.* Hannerz and Grimby 1973).

The recording electrode was placed proximally near the tibia and comparatively near the muscle surface. Histochemical investigations have shown that muscle fibres of both type I and type II are located within the area studied (Grimby and Hannerz 1970).

The potentials of the motor units were recorded with a bipolar electrode which has been described earlier (Hannerz 1974). It consists of three diamel-coated silver wires 100 μ m in diameter. The ends of the wires are insulated by repeated dipping in lacquer. Minimal holes are made in the insulated ends of two of the wires and at the side of the third wire with a spark from an induction coil. The wires are glued together in such a way that the holes at the recording surfaces are close to each other. The wire with the hole on the side has its protruding end bent to form a hook which minimizes the displacement of the electrode in the muscle in strong contractions. The electrode is inserted into the muscle with the use of an injection needle which is then withdrawn. The 3 recording points allow three different recording combinations as bipolar electrode. In order to obtain a recording with a high selectivity of potentials while at the same time preserving the characteristics of the potentials of the motor units, the impedance of two of the recording wires should be about 750 kilohms and one about 4 megohms as measured at 1000 Hz. Since the properties of the recording surfaces may change during the insertion of the electrode and in the position of the

TABLE 1 The minimum frequency of motor units with different thresholds in tonic contraction

Recruitment tension	Minimum frequency			
	7-12/s	13-15/s	16-24/s	25-35/s
0-25	31	7		
26-50	2	17	3	
51-75		4	18	
76-100 %			4	11

electrode is impossible to change once the electrode has been inserted, considerable patience is called for and reiterated trials are usually required to obtain conclusive registrations.

The potentials of the motor units were amplified and displayed on EMG recording system Medelec MS 6. This had a frequency response from 40-1600 Hz which was limited to 10-1000 Hz by the capacity of the tape recorder used. The results obtained were checked by repeated playbacks and film recordings. Only those recordings were included in which the potentials could be identified by their characteristic shape throughout the experiment.

Results

Recruitment order of motor units in sustained contractions

The recruitment order of motor units in sustained contraction has earlier been found to be stable (Smith 1934; Bigland and Lippold 1954). Each motor unit is also activated at a characteristic level of tension and stops discharging when the tension decreases below this level (Bigland and Lippold 1954; Norris and Gasteiger 1955). These findings are confirmed in this study though in the case of some motor units only when these are not fatigued (see below).

A motor unit can thus be described by reference to the percentage of the maximum tonic tension at which it is activated.

Minimum frequency in sustained contractions

Each motor unit was examined to ascertain when it attained a discharge at regular intervals. The regularity of the discharge was never total. The Tokizane-Shimizu mode of calculating the standard deviation of the discharge intervals at different discharge frequencies was used. The minimum frequency was defined as the minimum frequency a motor unit has to attain in order to have a standard deviation of less than 10 ms counted from at least 50 successive intervals in a sustained contraction.

The 100 motor units studied had minimum frequencies ranging from about 7/s to about 35/s. The motor units with a low threshold in sustained contraction had a low minimum frequency. The higher the threshold of the unit in sustained contraction the higher was its minimum frequency (Table 1).

Fig. 1 shows the recruitment of 3 different motor units in slowly increasing contractions. The motor units were recruited at 15%, 60% and 90% of the maxi-

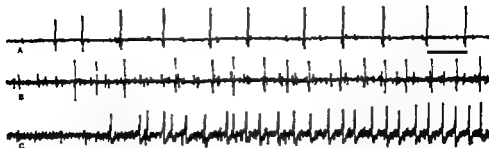


Fig 1 shows 3 motor units recruited at 15%, 60% and 90% of the maximum sustained tension respectively. The "15%" motor unit (A) attained its discharge at regular intervals at about 10/s, the 60% motor unit (B) at about 20/s and the 90% motor unit (C) at about 35/s. Time bar 100 ms.

imum tonic tension respectively. The 15% motor unit attained its minimum frequency at about 10/s (A), the 60% motor unit at about 20/s (B) and the 90% motor unit at about 35/s (C).

As mentioned in the introduction Tokizane and Shimazu, by calculating the standard deviation of the discharge intervals at different discharge frequencies, found two distinct groups of motor units: the tonic and the kinetic ones in the anterior tibial muscle. In Fig 2 these two groups are compared with four motor units with different thresholds in tonic contraction found in this study. A differentiation of the motor units in the anterior tibial muscle into two distinct groups could not be verified.

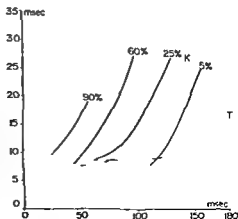


Fig 2 Standard deviation of the discharge intervals (ordinate) at different discharge intervals (abscissa) for four different motor units with different thresholds in sustained contraction. The solid curves represent 4 units which were recruited at about 5%, 25%, 60% and 90% of the maximum sustained contraction. The broken curves represent the tonic (T) and the kinetic (K) group of units found by Tokizane and Shimazu.

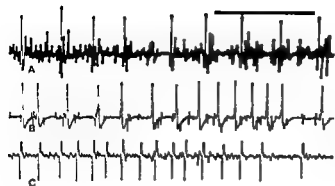


Fig. 3 shows 3 motor units discharging in maximum sustained contraction. They were recruited at about 15% (A), 60% (B) and 90% (C) of the maximum tonic tension respectively. Time bar 100 ms.

Maximum frequency in sustained contractions

It was found to be difficult to keep some motor units with high thresholds in sustained contractions activated maximally for as long as a whole second. The maximum frequency was therefore calculated from a period of 250 ms.

The 63 motor units studied had different maximum frequencies ranging from about 20/s to about 65/s (Table II). The maximum number of discharges during 250 ms was 16. Table II shows that units with low thresholds in sustained contraction tend to have a low maximum frequency and units with a high threshold a high maximum frequency. In general the higher the threshold the higher the maximum frequency, although there are exceptions to this rule. Thus units with a maximum frequency of about 30/s are mostly found among units with low thresholds in sustained contraction but they also occur among units with high thresholds.

Fig. 3 shows the frequency of 3 motor units at maximum tonic voluntary contraction. The 3 units are recruited at about 15%, 60% and 90% of the maximum tonic tension respectively. At maximum voluntary tension the 15% motor unit

TABLE II The maximum frequency of motor units with different thresholds in tonic contraction

Recruitment tension	Maximum frequency			
	25–30/s	31–35/s	36–50/s	51–65/s
0–25%	13	4		
26–50	1	12	4	
51–75		6	11	
76–100		4	2	6

The numbers of motor units in the tables are not representative of the percentages of units with different properties in the anterior tibial muscle since a selection of units was made with a view to studying units having properties as different as possible.

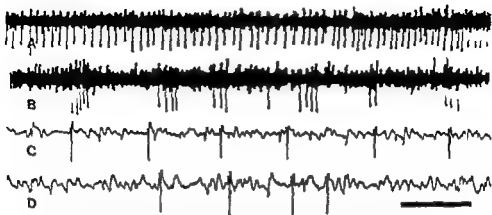


Fig 4 shows a motor unit with an intermittent discharge pattern. It was first recruited at about 35 % of the maximum tonic tension. In A it discharges at regular intervals at about 40 % of the maximum tonic tension. In B the unit has ceased to discharge at regular intervals and has begun to discharge in bursts at about 60 % of the maximum tonic tension. C and D are from A and B respectively at 10 times faster sweep to show the characteristics of the potentials. Time bar in A and B 500 ms. in C and D 50 ms.

discharges at a frequency of about 30/s (A) the 60 % motor unit at about 45/s (B) and the 90 % motor unit at about 60/s (C)

Continuous and intermittent discharge pattern in sustained contractions

Certain motor units discharge in sustained contractions without pauses as long as the tension is above the minimum frequency and do not show any signs of fatigue in their discharge pattern. After the minimum frequency has been attained their frequency increases steadily in proportion to the tension increase until the maximum tension is almost attained. In general all motor units of this type have approximately the same frequency when they are active simultaneously, i.e. they start discharging at regular interval at the frequency already attained by the previously activated units. However the motor unit does not have the same frequency as the previously activated units until it has attained its minimum regular frequency. Nor do all units of this type have the same frequency at tensions above 90 % of the maximum tonic tension at this level they begin to differ from one another as to maximum frequency.

Other motor units discharge discontinuously even at tensions above that for minimum frequency. Having attained their maximum frequency they can begin to discharge in bursts with pauses of 1 s or more. Fig 4 shows such a motor unit activated at about 35 % of the maximum tonic tension. It discharges at regular interval at about 40 % of the maximum tonic tension (A) but discharges in bursts

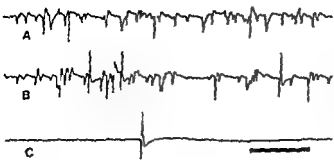


Fig 5 A Motor units activated in a sustained contraction of about 20% of the maximum tonic tension. B The recruitment of a new motor unit upon an increase of the contraction strength to about 25% C The recruitment of the 25% motor unit alone in a twitch contraction Time bar 100 ms

at about 60% of the maximum tonic tension (B) The thresholds of these bursts tend to increase progressively so that ultimately it is not possible to recruit the motor unit at all until after a period of rest

All motor units recruited in the first 30% of the maximum tonic tension were of the continuously discharging type The units recruited above 80% of the maximum tonic tension were all of the intermittently discharging type Most of the units recruited between 30–80% of the maximum tonic tension were of the continuously discharging type There may however have been a methodological bias due to the fact that continuously discharging motor units are easier to discover

Recruitment order in twitch contractions

It was shown in previous papers that the recruitment order of motor units in twitch contractions is different from that in sustained contractions and that the difference increases the more relaxed the muscle is before the twitch contraction and the more rapid the twitch contraction is (Grimby and Hannerz 1968 1970 1974 Hannerz and Grimby 1973)

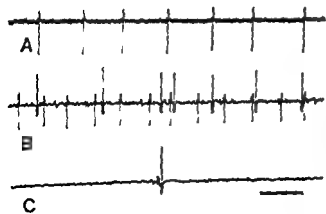


Fig 6 A A motor unit recruited upon tonic contraction at about 33% of the maximum tonic tension B Another unit recruited upon an increase of the contraction strength to about 40% of the maximum tonic tension C The recruitment of the 40% motor unit alone in a twitch contraction Time bar 100 ms

In this study a series of rapid twitch contractions was performed in each recording. The greatest differences from the recruitment order in sustained contractions are shown in Fig. 5 and 6.

Fig. 5A shows a sustained voluntary contraction of about 20% of the maximum tonic tension. The active motor units were recruited successively when the contraction was increased from 0 to about 20% of the maximum tonic tension. A new unit was recruited when the contraction was increased to 25% (B). In Fig. 5C the 25% motor unit was activated alone in a rapid voluntary twitch contraction without the activation of the motor units with lower thresholds in sustained contraction.

Fig. 6A shows a sustained voluntary contraction with a motor unit recruited at about 18% of the maximum tonic tension. A second motor unit was recruited when the tension was increased to about 40% (B). Fig. 6C shows the 40% motor unit being activated alone in a rapid voluntary twitch contraction.

Discussion

It is generally agreed that there is a progressive recruitment of motor units upon a gradually increasing contraction. It has, however, been disputed whether any new motor units are recruited in the last 25% of the maximum tonic tension (Clamann 1970). It was found in the present study that new motor units are recruited at all levels of tension: not only in the first 75% of the maximum tonic tension.

It was also found that different motor units have a different discharge frequency range. The range is about 7–20/s for the units with the lowest thresholds in sustained contraction and can be about 35–60/s for the units with the highest thresholds.

The values for highest voluntary discharge frequency of motor units found in extremity muscles in previous studies differ. Some authors did not find frequencies higher than about 20/s (Smith 1934; Dasgupta and Simpson 1962; Clamann 1970). Other investigators found frequencies of about 45/s (Adnan and Bronk 1929; Lindsley 1935; Wedell, Fernsten and Pattle 1944; Bigland and Lippold 1954). Seyffarth (1941) found frequencies of 30–40/s in the anterior tibial muscles and of 55–60/s in the elbow flexors. One study reports frequencies of 60–140/s (Norris and Gasteiger 1955). The discrepancies may be due to the fact that different muscles were investigated and that different ways of measuring the maximum frequency were used. Some authors have counted the number of discharges during a whole second. Others have calculated the highest frequencies from 5–10 discharges only. The very high frequency of 140/s was calculated from the shortest single intervals found. Admittedly, the procedure here used of measuring the maximum frequency from the highest discharge frequency in only 200 ms in

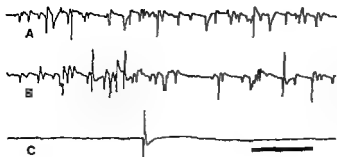


Fig 5 A Motor units activated in a sustained contraction of about 20% of the maximum tonic tension B The recruitment of a new motor unit upon an increase of the contraction strength to about 25% C The recruitment of the 25% motor unit alone in a twitch contraction Time bar 100 ms

at about 60% of the maximum tonic tension (B) The thresholds of these bursts tend to increase progressively so that ultimately it is not possible to recruit the motor unit at all until after a period of rest

All motor units recruited in the first 30% of the maximum tonic tension were of the continuously discharging type The units recruited above 80% of the maximum tonic tension were all of the intermittently discharging type Most of the units recruited between 30–80% of the maximum tonic tension were of the continuously discharging type There may however have been a methodological bias due to the fact that continuously discharging motor units are easier to discover

Recruitment order in twitch contractions

It was shown in previous papers that the recruitment order of motor units in twitch contractions is different from that in sustained contractions and that the difference increases the more relaxed the muscle is before the twitch contraction and the more rapid the twitch contraction is (Grimby and Hannerz 1968 1970 1974 Hannerz and Grimby 1973)

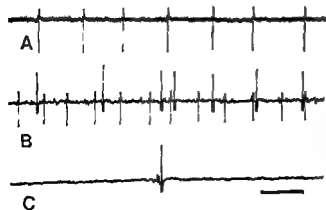


Fig 6 A A motor unit recruited upon tonic contraction at about 18% of the maximum tonic tension B Another unit recruited upon an increase of the contraction strength to about 40% of the maximum tonic tension C The recruitment of the 40% motor unit alone in a twitch contraction Time bar 100 ms

not support the suggestion by Freund *et al.* (1973) that the difference in recruitment order between sustained and twitch contractions previously described (Grimby and Hannerz 1968) is merely a change between motor units with very similar thresholds. In fact the mode of activation may be even more significant than could be shown here since motor units tend to synchronize in rapid twitch contractions and this makes the recruitment order difficult to determine. Moreover only motor units active in twitch contractions as well as sustained contractions are studied and the existence of motor units active only in twitch contractions cannot be excluded.

The finding that a motor unit with a low discharge frequency is always recruited before a motor unit with a higher discharge frequency in sustained contractions indicated that motor units with slow twitch fibres predominate in weak to moderate sustained contractions. The earlier recruitment of motor units with higher discharge frequency in twitch contractions indicates a greater role for units with fast twitch fibres in voluntary twitch contractions.

This investigation was supported by research grants from the Swedish Multiple Sclerosis Society Stockholm.

References

- ADRIAN E. D. and D. W. BROOK. The discharge of impulses in motor nerve fibres. Part II. *J. Physiol. (Lond.)* 1979 67 131—151.
- BIGLAND B. and O. C. J. LIPPOLD. Motor unit activity in the voluntary contraction of human muscle. *J. Physiol. (Lond.)* 1954 123 322—335.
- BLCHTHAL F. and H. SCHMALBRUCH. Contraction times and fibre types in intact human muscle. *Acta physiol. scand.* 1970 79 435—452.
- BURKE R. E., D. N. LEVINE, F. E. ZAJAC, P. TSAIRIS and W. K. ENGEL. Mammalian motor units: Physiological histochemical correlation in three types in cat gastrocnemius. *Science* 1971 174 709—712.
- CLAMANN H. P. Activity of single motor units during isometric tension. *Neurology (Minneapolis)* 1970 20 254—260.
- DASGUPTA A. and J. A. SIMPSON. Relation between firing frequency of motor units and muscle tension in the human. *Electromyography* 1962 2 117—128.
- EDSTROM L. and E. KUGELBERG. Histochemical composition, distribution of fibres and fatigability of single motor units. *J. Neurol. Neurosurg. Psychiat.* 1968 31 424—433.
- FREUND H. J., V. DIETZ, C. W. WITA and H. KAPP. Discharge characteristics of single motor units in normal subjects and patients with supraspinal motor disturbances. In J. E. Desmedt (Ed.) *New Developments in Electromyography and Clinical Neurophysiology* Vol. 3. Karger, Basel, 1973, pp. 247—250.
- GRIMBY L. and J. HANNERZ. Recruitment order of motor units on voluntary contraction: changes induced by proprioceptive afferent activity. *J. Neurol. Neurosurg. Psychiat.* 1968 31 565—573.
- GRIMBY L. and J. HANNERZ. Differences in recruitment order of motor units in phasic and tonic flexion reflex in spinal man. *J. Neurol. Neurosurg. Psychiat.* 1970 33 562—570.
- GRIMBY L. and J. HANNERZ. Differences in recruitment order and discharge pattern of motor units in the early and late flexion reflex component in man. *Acta physiol. scand.* 1974 90 555—564.
- HANNERZ J. Discharge properties of motor units in man. *Excerpta (Basel)* 1973 9 45—46.
- HANNERZ J. An electrode for recording single motor unit activity during strong muscle contractions. *Electroenceph. clin. Neurophysiol.* 1974. In press.

with electronic registering, but they claimed to be unable to demonstrate a statistically significant difference in the two situations (see however later under Discussion).

It was therefore thought to be of interest to study the effect of a wider variation of energy implanted in the muscles during the preparatory movement preceding a jump. This was done by not only performing a counter movement as Marec and Demy, and Cavigna *et al* did, but also by letting the subject jump down to the force platform from levels of different heights.

Material

The experimental data were collected from 19 young subjects: 14 males and 5 females. Their mean body weight was 71.0 kg (51.0 to 91.1 kg).

Methods

A force platform was constructed in such a way that the pressure registered by it was independent of the position of the subject on the platform (Bonde Petersen 1974). The platform was slightly under-damped and had a natural frequency of about 50 Hz.

For registering of the pressures on the platform a Beckel 581 DIII strain gauge bridge and amplifier was used. The signal, which was a linear function of the load within the applied range, was passed on to a Brush Mark 220 ink writer operated at paper speed 125 mm/s.

In order to vary the energy level of the subject prior to the jump, 5 different situations were utilized. In one situation the subject jumped from a semi-squatting position. No preparatory counter movement was allowed. In a second situation the subject was allowed a preparatory counter movement starting standing erect on the platform.

In the last three situations the subject jumped down from one of the three different platforms I to III, the heights of which were 0.233, 0.404 and 0.693 m respectively above the surface of the force platform. The jump down was immediately without stop continued in the vertical upward jump. Examples of the records obtained during the jumps are shown in Fig. 1.

The height of the jump—the vertical lift of the subject's center of gravity—was calculated from the time of flight t_f seconds measured directly from the records (distance 4 to 5 in Fig. 1). This presupposes that the subject leaves and lands on the platform with the body held in the same position. The subject therefore were instructed to keep the legs merely extended at landing and to keep the arms at the sides with only slightly flexed elbows.

If the flight the subject will take off with a certain upward directed velocity v_f m/s, which will decrease and become zero at the apex of the jump. During the subsequent downward movement velocity will again increase and reach numerically the same value v_f m/s at touch down. The time spent moving upwards or downwards will be the same and equal to $\frac{1}{2} t_f$ s. As the acceleration of gravity is 9.81 m/s² it follows that $v_f = \frac{1}{2} t_f \times 9.81$ m/s. The average velocity upwards or downwards will be $v_f/2$ m/s or $\frac{1}{4} t_f \times 9.81$ m/s. The distance d covered at this average velocity in the time $\frac{1}{2} t_f$ —i.e. the height of the jump—will then be $\frac{1}{4} t_f \times 9.81 \times \frac{1}{2} t_f = \frac{1}{8} (t_f)^2 \times 9.81$ or $d = 1.226 \times (t_f)^2$ m.

At the top of the flight the increase in energy level of the jumper over that in the position standing on the force platform will then be $w \times d$ kpm, in which w is the weight of the subject in kp.

Correspondingly the increase in energy level of the subject at the moment he reaches the force platform after jumping down from platforms I, II and III respectively (at point 1 in Fig. 1 C) can be calculated as $w \times h$ kpm, in which w is the weight in kp of the subject and h is the height in m of platform I—III.

In the case of jumping after a preparatory counter movement (Fig. 1 B) the maximum increase in energy level of the subject at point 2 is calculated as kinetic energy from $E_k = mv^2$. In this formula m , the inertial mass of the subject equals weight divided by the acceleration of gravity i.e. $w/9.81$ and velocity v is calculated from $F \times t = m \times v$.

$F \times t$ (F = force, t = time) is measured planimetrically from the records (hatched area between 1 and 2 in Fig. 1 B). E_k thus becomes $(F \times t)^2 / 2w \times 9.81$ kpm.

* v_f was also calculated from the registered force-time integral using the formula $F \times t = m \times v_f$ in which $F \times t$ was measured planimetrically. The two ways of calculating v_f gave identical results showing that also dynamic forces applied to the platform were registered correctly.

Fig 1 Examples of records from force platform. Ordinate force in kp, abscissa time in sec. In A the subject jumped from a semi squatting position. In B the subject made a preparatory counter movement starting standing erect on the force platform. In C the subject jumped down from a platform 0.233 m above the force platform. 1 indicates the start of the downward movement when in contact with the force platform. 2 is the time of maximum downward velocity. 3 indicates the time of maximum upward velocity. 4 the time of take-off and 5 the time of touch down. The dotted line indicates the weight of the subject.

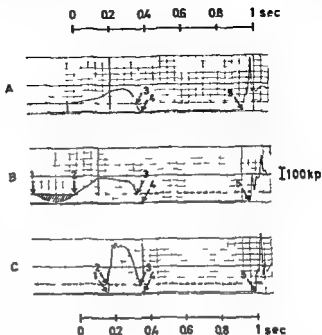


TABLE I Height of vertical jump d in m calculated from the time of flight (sec text) without or with preparatory movements

subject				after jumping down from platforms I - III			
no	sex	body weight kg	from squatting position	with a counter movement	I height 0.233 m	II height 0.404 m	III height 0.690 m
1	m	75.8	0.450	0.515	0.515	0.515	0.491
2	m	87.5	0.316	0.307	0.320	0.307	0.345
3	m	70.1	0.320	0.328	0.372	0.394	0.404
4	m	61.5	0.483	0.519	0.538	0.555	0.557
5	m	70.0	0.444	0.484	0.493	0.529	0.473
6	m	73.6	0.356	0.342	0.340	0.354	0.357
7	m	69.7	0.443	0.408	0.441	0.429	0.442
8	m	79.1	0.340	0.397	0.399	0.432	0.336
9	m	79.4	0.347	0.370	0.399	0.386	0.372
10	m	91.1	0.466	0.503	0.470	0.473	0.470
11	m	83.5	0.399	0.413	0.413	0.424	0.412
12	f	57.6	0.373	0.351	0.350	0.388	0.301
13	m	71.0	0.366	0.448	0.486	0.517	0.473
14	f	59.6	0.218	0.215	0.228	0.245	0.206
15	f	62.6	0.373	0.304	0.311	0.307	0.298
16	m	72.0	0.370	0.355	0.349	0.386	0.396
17	m	74.0	0.410	0.401	0.425	0.447	0.384
18	f	59.1	0.250	0.269	0.277	0.280	0.253
19	f	51.0	0.340	0.381	0.389	0.403	0.410
Σ		71.0	0.366	0.386	0.396	0.408	0.389
SD		—	0.071	0.083	0.083	0.086	0.086
SE		—	0.016	0.019	0.019	0.019	0.019

TABLE II Maximum energy levels at start (E_{neg}) and end (E_{pos}) of the period preceding the take off Δkpm indicates the gain in E_{pos} for each jumping condition over E_{pos} during the jump from the squatting position. In the last column Δkpm is expressed in per cent of E_{neg}

jumping condition	E_{neg} kpm	E_{pos} kpm	Δkpm	$\frac{\Delta kpm \times 100}{E_{neg}} \%$
squatting	0	26 II	—	—
counter movement	6 I	27 4	1 4	22 II
I height 0.233 m	16 6	28 2	2 2	13 2
II height 0.404 m	28 7	29 0	3 0	10 5
III height 0.690 m	49 0	27 6	1 6	3 3

Results

The individual results of jumping from a squatting position, with a counter movement or after jumping down from heights I~III are shown in Table I. The table shows that the height of the jump d becomes increasingly greater if a counter movement or a jump down from a height precedes the actual jump—but only up to height II (0.40 m). After jumping down from height III (0.69 m) d again becomes smaller although still greater than when jumping from a squatting position.

These differences are all statistically significant at a 0.02 level (Student's t test paired samples).

The energy levels of the subjects (averages of all only) are calculated as described in Methods and tabulated in Table II. In this Table E_{neg} signifies the highest level of energy in the downward movement before the jump. In jumping from a squatting position E_{neg} has the value of zero. E_{pos} correspondingly signifies the highest energy level reached during the upward movement. The Table shows that the energy is 26 II kpm when jumping from a squatting position and increases stepwise up to 29.0 kpm with increasing steps of E_{neg} preceding the jump. At the highest level of E_{neg} however this trend is reversed and E_{pos} becomes smaller again. The gain in E_{pos} Δkpm over E_{pos} from the jumps from the squatting position is shown in the Table also as a percentage of the corresponding value of E_{neg} .

Discussion

In jumping from the squatting position (Fig. 1 A) it must be assumed that the subjects exerted themselves maximally right from the start of the jump. The recorded force however rose very slowly and the maximum was not reached until after about 300 ms. The reason for this probably is that a certain amount of the liberated energy was wasted in taking up the slack and stretching the elastic components of the muscles (cf. Hill 1970). In human muscles it has been demonstrated also by Asmussen and Sorensen (1971). When a counter movement was performed before the jump (Fig. 1 B), a certain amount of energy E_{neg} was implanted into the body in excess

of the energy liberated by the muscle contractions, which again are assumed to be maximal. Part of this must have degenerated into heat but another part most probably was absorbed by the elastic components of the muscles so that less of the energy subsequently liberated by the muscles was wasted as internal work. As a consequence more energy was available for external work resulting in a greater height of the jump. E_{pos} was increased by a value that represents about 23% of E_{neg} (Table II).

When the subjects jumped down from heights I—III respectively still more energy was made available for tautening and stretching the elastic components (Table II). More energy could therefore be made useful for the jump. The highest increase in E_{pos} over that gained in a jump from a squatting position was on an average 3.0 kpm. Inspection of Table I shows though that several individuals gained even more: subject no. 13 for instance 10.7 kpm when jumping from height II. That is 37.7% of the implanted E_{neg} . Others on the other hand gained nothing some even performing worse when jumping down from a height (e.g. subject no. 15). Fig. 1 C illustrates how the maximum tension typically is 2–3 times as large as in situation A. It is therefore justifiable to assume that the elastic components not only were stretched corresponding to the maximum tension that can be developed voluntarily by the contractile mechanism but that a certain tension above that was produced temporarily by the rapid stretching of the elastic components by gravity. This tension was liberated immediately thereafter adding to the amount of energy provided by the contractile mechanism. Such high tensions (3–400 kp) should not astonish as we know that strong persons can produce tensions of up to 1000 kp as isometric contractions with their leg extensor muscles.

It will be noticed from Table II comparing height I to height II that the increase in E_{neg} of $28.7 - 16.6 = 12.1$ kpm was accompanied by an increase in E_{pos} of $29.0 - 28.2 = 0.8$ kpm i.e. a net gain as E_{pos} of 6.6% of the extra E_{neg} . The two situations were technically alike and directly comparable. The most likely explanation would also here be that these 6.6% were energy transferred from E_{neg} to E_{po} via stored elastic energy. The situation is similar to the one studied by Asmussen and Sørensen (1971) where a maximal eccentric muscle contraction was continued without relaxation as a maximal concentric contraction. Depending on the speed of movement a considerable gain in work could be achieved—up to 70% for the very first part of an arm flexion at high speed.

Increasing the height of the downward jump from 0.40 m to 0.69 m—i.e. E_{neg} from 28.7 kpm to 49.0 kpm—was not followed by a further increase in d or in E_{pos} but rather by a decrease. The reason for this is probably that the forces developed during the braking of the fast downward movement were so great that they might endanger the jumpers who consequently did not exert themselves maximally. Whether this decrease in ΔE_{pos} was due to a conscious or to a reflex inhibition cannot be decided.

A prerequisite for the explanation given above is that the structures that absorb the negative energy from the counter movements possess such properties that they

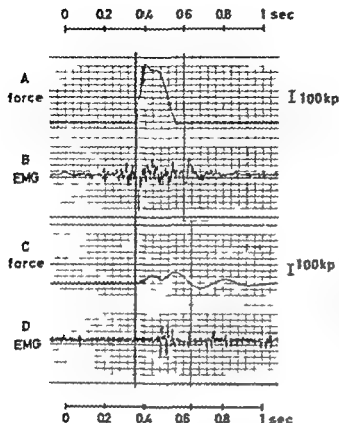


Fig 2 The record from the force platform (A and C) and the EMG (arbitrary units) from the soleus muscle (B and D) during two different procedures. In A and B simultaneous records were obtained as the subject jumped down from a height of 0.404 m. continuing in a maximal vertical jump. C and D were simultaneously recorded as a sudden pressure was applied vertically downward to the shoulders of the subject standing tip-toes on the force platform.

are able to store appreciable amounts of elastic energy — i.e. they must show a high degree of elastic stiffness. As already Fenn (1930) pointed out, resting muscles can be dismissed from consideration because of their very low stiffness in the physiological range of movement. Active muscles on the other hand have a much higher degree of stiffness within the same range (Buchthal and Løyer 1951, p. 96, Fig. 4). It would accordingly be very unlikely if the muscles of the legs in the present experiments were not active at the moment of touch-down (cf. Fig. 1 C).

In order to prove this, electromyographic records were obtained by means of a Disa electromyograph connected to the Brush ink writer and surface electrodes glued to the skin over the soleus muscle and the vastus lateralis muscle. Fig. 2 A–B shows the EMG from the soleus and the record from the force platform when a subject jumped down from a height of 0.404 m preliminary to a vertical jump. It is obvious that the touch-down was preceded by an increased electrical activity of the soleus — due to an anticipatory increase in muscle tone beginning about 100 ms before contact with the force platform was made (cf. McNeill Jones and Watt 1971). A simple myotatic reflex elicited by the stretching of the muscles at landing would be too slow for counteracting the fall. Fig. 2 C–D shows how a sudden downward pressure applied to the shoulders of the subject standing on tip-toes on the force platform

elicited a reflex in the soleus muscles. This is demonstrated by the increased electrical activity (Fig. 2 D) and by the subsequent oscillations in the record from the force platform (Fig. 2 C). The reflex time was about 120 ms, i.e. more than half the time spent in contact with the platform in a jump (Fig. 2 A) (cf. also Grillner 1972).

It may be argued that even though the whole muscle—in *casu* soleus—is active during the time of energy absorption—i.e. from touch down to the start of the upward movement—its individual muscle fibers may pass through periods of relaxation in which all stored elastic energy would be lost. A voluntary contraction of a whole muscle is the result of the summated contractions of numerous muscle fibers, some of which may perform series of single twitches while others may be tetanized—all depending on the natural frequencies of the nervous impulses to the muscle. But even in the former case the duration of a single twitch is so long (74 ± 11 ms for the time to crest in the soleus muscle according to Buchthal and Schmalbruch 1970) that it covers an appreciable part of the negative phase in the jump. The duration of the negative phase t_x of the jump while in contact with the force platform can be estimated from the following arguments.

Let the *downward movement* from touch-down to the movement has been completely stopped last t_x s have an initial velocity of v_b , a final velocity of zero and an average velocity therefore of $\frac{1}{2}v_b$ m/s. The distance covered in this movement will then be $t_x \times \frac{1}{2}v_b$. Calling the total time of contact with the force platform (point 1 to point 4 in Fig. 1 C) t_{tot} the subsequent *upward movement* on the platform will last $(t_{tot} - t_x)$ s. The initial velocity will be zero, the final velocity v_{fin} and therefore the mean velocity $\frac{1}{2}v_{fin}$. The distance covered in this movement must be the same as in the downward movement hence

$$t_x \times \frac{1}{2}v_b = (t_{tot} - t_x) \times \frac{1}{2}v_{fin} \text{ and solving for } t_x$$

$$t_x = (v_{fin} - t_{tot}) / (v_b + v_{fin})$$

v_{fin} is calculated from the height of the jump ($h = \frac{1}{2}(v_{fin}^2/g)$) v_b correspondingly from the height from which the subject jumped down and t_{tot} is measured on the record from the force platform from touch down to take off (1 to 4 in Fig. 1 C).

In the case of the counter movement v_b is determined as described under E_{neg} .

Calculated in this way the average values \pm S.D. for t_x —the durations of the negative phase during which the possible storing of elastic energy takes place—were found to be 0.268 s after the counter movement and 0.190 ± 0.064 and 0.162 ± 0.006 and 0.141 ± 0.047 s after jumping down from heights 0.233, 0.404 and 0.690 m respectively.

Accordingly the active period even of single twitches determined as time to crest by Buchthal and Schmalbruch (1970) occupies one half to one third of the negative phase of the jumps and thus provides good opportunities for storing of energy in stiff muscle fibers.

Our results have shown that a phase of negative work preceding the jump significantly increases the jumping height up to a certain limit. This confirms the results of Marey and Demy (1885). Cavagna *et al.* (1971) calculated from their experiments that such an enhancement was not demonstrable at a significant level. However a Student's *t* test performed on the data of Cavagna

et al reveals that a counter movement *de facto* results in a significant increase in the velocity of take-off of 6.4 % ($P < 0.01$) corresponding to an increase in height or E_{pos} of 11.3 % i.e. twice the average increase in our data (*cf* Table I)

The possible storage of elastic energy in muscles under other conditions (*e.g.* running and walking) has recently attracted renewed attention (Cavagna *et al* 1964, 1971 Lloyd and Zacks 1972 Grillner 1972). The present experiments should add to the understanding of the importance of storage of elastic energy in the contracted muscle during eccentric conditions as a mediator for increasing the total work output during short bursts of muscle activity.

References

- ASMUSSEN E and SØRENSEN The wind up movement in athletics *Trial Human* 1971 **24** 147-155
- BONDE PETERSEN F A simple force platform *Europ J appl Physiol* 1974 To be submitted
- BLICHTHAL F and E. KASER The rheology of the cross striated muscle fibre with particular reference to isotonic conditions *Dan Biol Medd* 71 No 7 1951
- BLICHTHAL, F and H SCHMALBRICH Contraction times and fibre types in intact human muscle *Acta physiol scand* 1970 **79** 435-452
- CAVAGNA G A H DUTMAN and M MARGARIA Positive work done by a previously stretched muscle *J appl Physiol* 1968 **24** 21-32
- CAVAGNA G A L HOMMEN G CITTERIO and R MARGARIA Power output of the previously stretched muscle In *Medicine and Sport & Biomechanics II* 159-167 Basel 1971
- FENN W O Frictional and kinetic factors in the work of sprint running *Am J Physiol* 1930 **9** 583-611
- FENN W O and B S MARSH Muscular force at different speeds of shortening *J Physiol (Lond)* 1935 **85** 277-297
- GRILLNER, S The role of muscle stiffness in meeting the changing postural and locomotor requirements for force development by the ankle extensors *Acta physiol scand* 1972 **86** 97-108
- HILL A V *First and last experiments in muscle mechanics* Cambridge University press 1970
- LEVY A and J WYMAN The viscous elastic properties of muscle *Proc roy Soc B* 1977 **101** 218-243
- LLOYD B H and R M ZACKS The mechanical efficiency of treadmill running against a horizontal impeding force *J Physiol (Lond)* 1972 **223** 355-363
- MAREY M and M G DEMÉNY Locomotion humaine: mécanisme du saut *C R Acad Sci (Paris)* 1885 **101** 489-494
- MELVILL JONES G and D G D WATT Observations on the control of stepping and hopping movements in man *J Physiol (Lond)* 1971 **219** 709-727

Long term Treatment with Antihypertensive Drugs in Spontaneously Hypertensive Rats (SHR) Effects on Blood Pressure, Survival Rate and Cardiovascular Design

By

LILIAN WEISS

Received 18 January 1974

Abstract

WEISS L. Long term treatment with antihypertensive drugs in spontaneously hypertensive rats (SHR) Effects on blood pressure survival rate and cardiovascular design Acta physiol scand 1974 91 393-408

Three age groups of SHR were treated orally with hydralazine and guanethidine. The first prehypertensive group was treated from 2.5 until 8 months of age and thereafter pressure was followed for another 6 months. A delayed and quite modest pressure increase then occurred and average life span was prolonged compared with untreated SHR or SHR treated only from 12 months of age. — The second 8 months old group representing established hypertension was treated for 5, 10 or 20 weeks, the last subgroup being followed for another 2 weeks without treatment. Arterial pressure, left ventricular weight and design of the resistance vessels as explored by quantitative hemodynamic analyses were studied at these intervals. After 11 weeks pressure was normalized with some regression of hypertrophic vascular changes, particularly in females, though the increased wall/lumen ratio appeared to remain and heart weight was only slightly reduced. After 20 weeks with and 2 weeks without treatment cardiac and vascular design were still the same as during treatment but pressure had now risen considerably. — The third 11 months old group with advanced hypertension was treated for 13 weeks causing only modest pressure reduction and vascular regression. — This suggests that early treatment has great advantages, that females exhibit more regression of vascular structural changes than males and that late treatment gives less regression, presumably due to addition of less regressive wall components like collagen.

During the last decades quantitative hemodynamic estimations of parameters reflecting the structural characteristics of the resistance vessels (cf Folkow et al 1972a, 1973) indicate that the resistance increase in particularly primary hypertension is mainly a matter of a changed vascular design rather than the consequence of a raised smooth muscle tone as commonly believed. Thus the resistance vessels exhibit a hypertrophic increase in wall/lumen ratio with a reduced lumen even at maximal dilatation which resets the resistance equilibrium to a higher level and tends to amplify the range of dilatation-constriction. This structural adaptation

which is of the same general nature as the wellknown left ventricular hypertrophy (cf Suwa and Takahashi 1971) appears to be a rapid essentially local response to increases in average pressure. It is thus largely completed about 3 weeks after induction of renal hypertension in rats (Lundgren *et al* 1974) and it is about as rapidly reversed whenever pressure is reduced, whether locally (Folkow and Svertson 1968; Weiss and Hallböök 1974) or generally (Lundgren 1974). Moreover if part of the vascular bed in young prehypertensive SHR (Okamoto 1969) is protected from the subsequent pressure rise (Folkow *et al* 1971a) or if neurogenic excitatory influences are generally interfered with by e.g. immunosympathectomy in newborn SHR (Folkow *et al* 1972b) the mentioned structural vascular adjustments largely fail to develop. This is also the case after prolonged treatment of young SHR with adrenergic β receptor antagonists (Folkow, Lundgren and Weiss 1972; Weiss, Lundgren and Folkow 1974).

Against such a background it was considered of interest to analyse quantitatively in different age groups of SHR the effects of intense treatment with hypotensive drugs on blood pressure and survival rate, on cardiac hypertrophy and on vascular design explorations that would be very difficult to carry out in man due to technical problems, drug side effects, inhomogenous groups *etc*. Part of the present results have earlier been briefly reported (Folkow *et al* 1971c).

Methods

General experimental arrangement and material Three different age groups of SHR were utilized to explore the effects of prolonged treatment with hypotensive drugs applied at different stages of hypertension. Thus young "prehypertensive" SHR (SHR₁) were used to explore both an early period of treatment affects (1; blood pressure development in later phases of life and 2; survival rate in comparison with untreated SHR, or SHR treated only in later phases of life. No analyses of the immediate effects of such "preventive" treatment on cardiovascular design were made in this group of animals since these particular aspects have been explored in another study (Weiss, Lundgren and Folkow 1974).

Adult SHR (SHR₂) with "established" hypertension and old SHR (SHR₃) with advanced hypertension as compared with normotensive control rats (NCR) were used mainly to explore 3; how prolonged hypotensive treatment affects already established structural changes in the heart and resistance vessels with special emphasis on the degree of regression that may be induced in these later stages of hypertension. — The special procedures used to accomplish these goals are described below in more detail under 1, 2 and 3.

Treatment and treatment With exception for a few animals (see 2 below) hydralazine and guanethidine¹ were used for treatment, a common drug combination in Sweden in severe hypertension when rapid and extensive pressure reductions are required. The two drugs were administered in the drinking water corresponding to an estimated dosage of 2 and 70 mg/kg b.wt. and 74 h respectively. During the first 3 weeks intraperitoneal injections of guanethidine 1 mg/kg were added once a week.

Indirect pressure estimations were used to check the effects of treatment and were performed as follows. The rats were first exposed to indirect heating for some 20 min which elicited a considerable tail vasodilatation. The hyperemic pink tail was then emptied of its blood content by enclosure in a pressure tube whereupon a cuff was suddenly inflated and then slowly released in a standardized way by the same trained technician. The cuff pressure level was noted when the tail suddenly turned from white to pink. The values thus obtained

¹We are indebted to Ciba-Geigy Ltd, Basel, Switzerland for generous gifts of Apresoline® and guanethidine.

can of course only be used as an approximate estimation of arterial pressure for a group of animals but the method has the advantage that measurements of the approximate pressures for all the groups could be frequently and rapidly performed throughout the experimental period. Further these indirect pressure estimations were finally checked against intraarterial pressure measurements also performed during awake conditions after the tail artery had been cannulated under brief ether anesthesia.

1) *Preventive treatment effects on blood pressure development* 5 female and 6 male SHR₁ were treated with hydralazine guanethidine as described above from the age of 2.5 months when they still were in a prehypertensive phase with an indirectly measured arterial pressure around 145 mm Hg as compared with about 120 mm Hg in matched normotensive control rats (NCR). Treatment was continued and its effects followed by the indirect blood pressure measurement method until the age of 8 months whereupon all treatment was interrupted. Blood pressure was then followed for another 6 months but by means of direct intraarterial measurements in the awake state 17, 32, 70, 100 and 175 days after cessation of treatment and compared with the pressures in untreated matched SHR and NCR. No hemodynamic evaluation of the design of the resistance vessels was performed particularly since such information was available in a related study in which chronic "preventive" treatment with β -adrenergic receptor antagonists had largely prevented the rise in pressure otherwise occurring in SHR (Weiss Lundgren and Folkow 1974).

2) *Preventive treatment effects on survival* For comparative purposes 3 different groups of male SHR were used. The first group comprised the 6 male SHR₁ mentioned above to which were added 6 male SHR₂ treated for the same time period but with propranolol 100 mg/kg and 24 h also given in the drinking water (cf. Weiss Lundgren and Folkow 1974). Since these 2 types of preventive treatment had largely similar effects on blood pressure and survival they could be pooled together for comparisons with the other 2 groups of male SHR. One of these 2 groups was made up by 14 entirely untreated male SHR and the other of 14 male SHR in whom treatment with the same doses of hydralazine and guanethidine was first initiated at the age of 12 months.

These 3 groups of SHR were then followed between age 12 and 20 months under identical living conditions except for the continued hypotensive drug treatment of one of the groups. Handling and blood pressure measurements were limited to a minimum in order to avoid any undue influence on the survival rate. This allowed for an estimate of the effect of late and early treatment on mortality.

3) *Effects of treatment on cardiovascular design* Treatment schedule As mentioned above two main groups of SHR were used for this particular study: a) SHR₁ and b) SHR₂ representing established and "advanced" phases of hypertension respectively. They were throughout compared with untreated matched SHR and NCR.

a) The SHR₁ group consisted of 16 male and 12 female SHR 3 months old at the start of treatment when their directly measured mean arterial pressure was around 170 mm Hg or slightly higher. Originally they were divided into three subgroups treated for 5, 10 and 20 weeks respectively. The purpose was here to follow changes in cardiovascular design along with the normalization of pressure which occurred already within 5 weeks of treatment. However no further adjustments in cardiovascular design were observed subsequent to the initial 5 week period of treatment while a considerable difference became apparent in steady state consequently animals treated for 5 and 10 weeks were pooled into separate groups below denoted as male and female SHR₁ 5 or 10 weeks of treatment. At the end of the treatment periods they were all used for paired perfusion experiments with NCR as described below.

The last subgroup of SHR₁ treated for 20 weeks as initially observed concerning the rate of rise of the arterial pressure during 2 weeks after cessation of the treatment. After those 2 weeks they were exposed to paired perfusion experiments in comparison with NCR to explore whether the resistance vessels had again readjusted themselves to the rising pressure. As a comparison to SHR₁ a small group of NCR (NCR₁ 5 males) was exposed to the same drug treatment for 13 weeks to find out whether even a normotensive cardiovascular system is significantly affected by this type of antihypertensive treatment. b) The SHR₂ group consisted of 14 month old male SHR with advanced hypertension the directly measured mean arterial pressure being around 180–190 mm Hg. They were all exposed to hydralazine guanethidine treatment for 13 weeks whereupon they were exposed to paired perfusion experiments together with matched NCR.

Acute perfusion experiments After completed treatment all SHR₁, NCR₁ and SHR₂ were exposed to acute paired perfusion experiments in comparison with untreated matched NCR. Arterial pressure was first measured directly in the awake state by means of a cannula in the tail artery subsequently used for pressure recording during the perfusion experiment. The isolated hindquarter vascular beds were then subject to paired hemodynamic quantitative analyses.

during artificial constant flow perfusion (for details see Folkow *et al* 1970 b 1971 a)

After maximal vasodilatation had been ensured in both animals by papaverine a pressure flow run was first performed at flows varying between 11 and 40 ml/min \times 100 g for exact estimations of resistance in peripheral resistance units/100 g (PRU₁₀₀) at the flow levels of 10 and 30 ml/min. Thereafter flow was kept constant at 10 ml/min \times 100 g which is fully representative for resting flow in vivo and low enough to avoid undue edema formation. Then noradrenaline (NA) dissolved in the perfusion medium was infused in a stepwise fashion from subthreshold to supramaximal concentrations (0.01–5.0 μ g/ml perfusate) both preparations always receiving the same NA concentrations. Definitely maximal pressor responses were ensured by slug injections of 10 IU vasopressin and 150 mg BaCl_2 .

Flow resistance at maximal dilatation together with the resistance responses to NA and the other pressor drugs were then calculated for each pair of hindquarter preparations and resistance curves were plotted with log NA dose per ml perfusate on the abscissa and the pressor response on the ordinate. Each resistance curve exhibits the following key points reflecting the structurally determined characteristics and the smooth muscle sensitivity of the resistance vessels: 1) Resistance at maximal dilatation illustrating average luminal width; 2) NA threshold i.e. the NA dose required to achieve a 25 per cent increase in resistance from the level of maximal dilatation thus reflecting smooth muscle sensitivity to NA; 3) Steepness of the resistance curve to NA reflecting primarily the wall/lumen ratio and 4) The maximal pressor response reflecting the bulk of contractile wall tissue in relation to the lumen (see Folkow *et al* 1970 b).

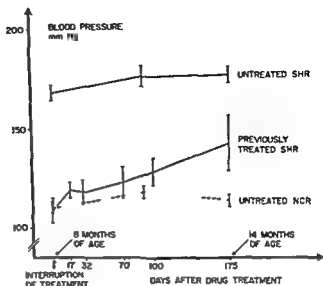
From these figures mean values of each group of animals and paired group difference were calculated for comparisons. — Since guanethidine interferes with the adrenergic nerves and therefore causes some smooth muscle supersensitivity to catecholamines in the treated animals causing a shift to the left of the resistance curve (see also Folkow *et al* 1972 b) attention was mainly focused on the resistance at maximal dilatation, the slope of the resistance curve and the maximal pressor response together reflecting the design of the resistance vessels and further on the weight of the left heart ventricle as related to body weight. — Statistical analysis was performed utilizing pairing design *t* test. To obtain a comparison between groups the difference between NCR and treated SHR was compared to the difference between NCR and untreated SHR controls by means of group comparison *t* test. At *p* values below 0.05 the difference was considered as significant.

Results

1 *Preventive treatment effects on blood pressure development* Young 'prehypertensive' rats (SHR_Y) were treated from the age of 2.5 months when their indirectly estimated arterial pressure only slightly exceeded that of their matched NCR (145 versus 120 mm Hg). During drug treatment their indirectly measured blood pressure was kept around 125 mm Hg and at the end of a 5 1/2 month period of treatment when mean blood pressure was instead measured directly in the renal artery during awake conditions it was 113 ± 6 mm Hg. Then all treatment was stopped and mean arterial pressure was followed intermittently for nearly 6 months by the same direct approach during awake conditions.

As can be seen from Fig. 1 there was only a very slow pressure increase with time and still after a total period of nearly 6 months of pressure recordings pressure had reached only moderately hypertensive levels. It was then 143 ± 14 mm Hg compared with 175 ± 4 mm Hg in untreated matched SHR and 115 ± 4 mm Hg in untreated matched NCR. In contrast when blood pressure was followed for 2 weeks in SHR_Y after a 20 week period of treatment a far more rapid pressure rise was observed. Here pressure rose from 116 mm Hg up to 156 mm Hg compared with 175 mm Hg in untreated matched SHR (mean values for males and females). As measured

Fig 1 Changes in intra arterially measured blood pressure (\pm SE) of 11 SHR previously treated between 2 1/2 and 8 months of age and followed for 6 months after treatment was interrupted as compared to 15 NCR and 15 untreated SHR.



indirectly pressure had after 3 days risen from 120 to 140 mm Hg after 6 days to 155 and after 10 days to 170 mm Hg

Thus treatment during a fairly early period of life seems to reduce the rate and extent of pressure increase after interruption of therapy compared with the situation when animals in the established phase of hypertension have been exposed to a prolonged period of treatment

2 Preventive treatment effects on survival Fig 2 shows the survival rate of a group of 12 SHR males which had been exposed to an early period of treatment (from 2 1/2 up to 8 months of age) either with hydralazine and guanethidine or with propranolol (see Weiss Lundgren and Folkow 1974) both treatments yielding similar survival rates. This compiled group is compared with the survival rate of 2 groups of equally old SHR males i.e. 14 entirely untreated ones and 14 that were treated with hydralazine and guanethidine only after the age of 12 months. Fig 2 illustrates the considerably higher survival rate of the SHR males that had been exposed to a period of early hypotensive treatment also compared with those SHR that actually were under treatment though it was started in a fairly advanced stage of hypertension

3 Effects of treatment on cardio-vascular design a) In the intermediate age group (SHR₁) drug treatment was started at the age of 8 months i.e. in the established phase of hypertension. After 4–5 weeks of treatment the indirectly measured arterial pressure was largely normalized. When pressure was measured also directly in the tail artery during awake conditions in the SHR₁ subgroup used for hindquarter perfusion at this stage it was 121 ± 4 mm Hg. In the subgroup exposed to hindquarter perfusion after 10 weeks of treatment the directly measured

during artificial constant flow perfusion (for details see Folkow *et al* 1970b 1971a)

After maximal vasodilatation had been ensured in both animals by papaverine a pressure flow run was first performed at flows varying between 5 and 40 ml/min \times 100 g for exact estimations of resistance in peripheral resistance units/100 g (PRU₁₀₀) at the flow levels of 10 and 30 ml/min. Thereafter flow was kept constant at 10 ml/min \times 100 g which is fairly representative for resting flow *in vivo* and low enough to avoid undue edema formation. Then noradrenaline (NA) dissolved in the perfusion medium was infused in a stepwise fashion from subthreshold to supramaximal concentrations (0.04—50 μ g/ml perfusate) both preparations always receiving the same NA concentrations. Definitely maximal pressor responses were ensured by slug injections of 10 IU vasopressin and 100 mg BaCl₂.

Flow resistance at maximal dilatation together with the resistance responses to NA and the other pressor drugs were then calculated for each pair of hindquarter preparations and resistance curves were plotted with log NA dose per ml perfusate on the abscissa and the pressor response on the ordinate. Each resistance curve exhibits the following key points reflecting the structurally determined characteristics and the smooth muscle sensitivity of the resistance vessels: 1) Resistance at maximal dilatation illustrating average lumenal width. 2) NA threshold i.e. the NA dose required to achieve a 25 per cent increase in resistance from the level of maximal dilatation thus reflecting smooth muscle sensitivity to NA. 3) Steepness of the resistance curve to NA reflecting primarily the wall/lumen ratio and 4) The maximal pressor response reflecting the bulk of contractile wall tissue in relation to the lumen (see Folkow *et al* 1970b).

From these figures mean values of each group of animals and paired group difference were calculated for comparisons. — Since guanethidine interferes with the adrenergic nerves and therefore causes some smooth muscle supersensitivity to catecholamines in the treated animals causing a shift to the left of the resistance curve (see also Folkow *et al* 1972b) attention was mainly focussed on the resistance at maximal dilatation, the slope of the resistance curve and the maximal pressor response together reflecting the design of the resistance vessels and further on the weight of the left heart ventricle as related to body weight. — Statistical analysis was performed utilizing pairing design *t* test. To obtain a comparison between groups the difference between NCR and treated SHR was compared to the difference between NCR and untreated SHR controls by means of group comparison *t* test. At *p*-values below 0.05 the difference was considered as significant.

Results

1 *Preventive treatment effects on blood pressure development* Young prehypertensive rats (SHR_y) were treated from the age of 25 months when their indirectly estimated arterial pressure only slightly exceeded that of their matched NCR (145 versus 120 mm Hg). During drug treatment their indirectly measured blood pressure was kept around 125 mm Hg and at the end of a 5 1/2 month period of treatment when mean blood pressure was instead measured directly in the tail artery during awake conditions it was 113 ± 6 mm Hg. Then all treatment was stopped and mean arterial pressure was followed intermittently for nearly 6 months by the same direct approach during awake conditions.

As can be seen from Fig. 1 there was only a very slow pressure increase with time and still after a total period of nearly 6 months of pressure recordings pressure had reached only moderately hypertensive levels. It was then 143 ± 14 mm Hg compared with 175 ± 4 mm Hg in untreated matched SHR and 115 ± 4 mm Hg in untreated matched NCR. In contrast when blood pressure was followed for 2 weeks in SHR_y after a 20 week period of treatment a far more rapid pressure rise was observed. Here pressure rose from 116 mm Hg up to 156 mm Hg compared with 175 mm Hg in untreated matched SHR (mean values for males and females). As measured

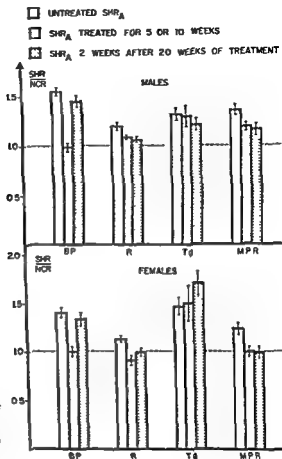


Fig 3 The mean ratio (\pm SE) between untreated treated and previously treated SHR and their respective NCR concerning blood pressure (BP) resistance at maximal dilatation (R) steepness of the resistance curves (Tg) and maximal pressor response (MPR). For details see text and Table I

towards the end of the paired perfusions was almost regularly more pronounced in NCR than in SHR. This moderately elevates tissue pressure particularly in NCR and correspondingly reduces the transmural vascular pressures during the final recordings of the maximal pressor responses. Consequently such an interference leads to a slight underestimation of the difference in maximal pressor response between SHR and NCR and some overestimation of the true maximal pressor responses.

In Table I the mean values \pm SE with the mean difference \pm SE D (pairing design t test) are summarized while Table II illustrates the significance of the differences between pairs of untreated SHR₁ and their NCR and treated SHR₁ and their NCR (group comparison t test). This allows an evaluation of the relationship between treated and untreated SHR₁ via their respective differences to NCR. Fig 3 again illustrates the extent of the changes in blood pressure in resistance at

TABLE I Mean values \pm S.E. mean difference \pm S.E.D. and degree of significance for paired experiments on adult treated spontaneously hypertensive rats (SHR_A) and untreated matched SHR as compared with matched normotensive control rats (NCR ns = non significant) The average age of rats at acute experiments was 10 months males and females are given separately

Group	Caudal pressure mm Hg	PRU ₁ at 30 ml/min	Steeptness tangent of the angle	Maximal pressor response mm Hg
<i>Males</i>				
Untreated SHR	186 \pm 5	1.90 \pm 0.09	4.2 \pm 0.5	3.0 \pm 1.7
NCR	121 \pm 4	1.64 \pm 0.03	3.2 \pm 0.3	2.75 \pm 1.9
n = 14 pairs				
d	66 \pm 4	0.31 \pm 0.07	1.0 \pm 0.3	95 \pm 13
p <	0.001	0.001	0.01	0.0001
Treatment for 5 or 10 weeks SHR _A				
NCR	118 \pm 4	1.63 \pm 0.04	4.9 \pm 0.3	3.16 \pm 7
	121 \pm 3	1.51 \pm 0.03	3.8 \pm 0.4	2.68 \pm 8
n = 9 pairs				
d	-3 \pm 4	0.12 \pm 0.04	1.1 \pm 0.2	49 \pm 9
p <	ns	0.01	0.005	0.001
Treatment for 20 weeks + 2 weeks without treatment				
SHR _A	167 \pm 7	1.77 \pm 0.04	3.6 \pm 0.2	3.49 \pm 13
NCR	116 \pm 4	1.69 \pm 0.03	3.0 \pm 0.2	3.04 \pm 12
n = 7 pairs				
d	51 \pm 6	0.09 \pm 0.05	0.6 \pm 0.2	43 \pm 18
p <	0.001	ns	0.05	0.05
<i>Females</i>				
Untreated SHR	159 \pm 4	1.56 \pm 0.06	4.4 \pm 0.3	3.18 \pm 18
NCR	114 \pm 5	1.38 \pm 0.04	3.0 \pm 0.1	2.56 \pm 12
n = 12 pairs				
d	45 \pm 5	0.18 \pm 0.04	1.4 \pm 0.5	62 \pm 15
p <	0.001	0.005	0.003	0.003
Treatment for 5 or 10 weeks SHR _A				
NCR	117 \pm 6	1.24 \pm 0.03	4.2 \pm 0.4	2.69 \pm 8
	116 \pm 5	1.36 \pm 0.06	2.8 \pm 0.4	2.57 \pm 9
n = 8 pairs				
d	1 \pm 6	-0.12 \pm 0.07	1.4 \pm 0.4	6 \pm 19
p <	ns	ns	0.03	ns
Treatment for 20 weeks + 2 weeks without treatment				
SHR _A	146 \pm 2	1.58 \pm 0.09	4.8 \pm 0.3	3.53 \pm 17
NCR	109 \pm 6	1.59 \pm 0.03	2.8 \pm 0.2	2.56 \pm 39
n = 4 pairs				
d	38 \pm 7	-0.01 \pm 0.07	2.0 \pm 0.2	-3 \pm 15
p <	0.03	ns	0.01	ns

maximal dilatation in maximal pressor response and in steepness of the resistance curves in males and females presented as the ratios between untreated treated and previously treated SHR_A and their respective NCR. Both females and males show reductions in pressure in resistance at maximal dilatation and in maximal pressor

TABLE II Group comparison: test of the mean differences (from Table I) between treated SHR NCR and untreated matched SHR NCR (ns = non significant)

Groups	Caudal blood pressure	PRU at 30 ml/min \times 100 g	Tangent of the angle	Maximal pressure response
<i>Males</i>				
SHR NCR untreated compared to SHR NCR treated for 5-10 weeks	$p < 0.001$	$p < 0.07$	ns	$p < 0.05$
SHR NCR ₁ untreated compared to SHR NCR 2 weeks after treatment	$p < 0.05$	$p < 0.08$	ns	$p < 0.05$
<i>Females</i>				
SHR NCR untreated compared to SHR NCR treated for 5-10 weeks	$p < 0.001$	$p < 0.001$	ns	$p < 0.05$
SHR NCR untreated compared to SHR NCR 2 weeks after treatment	ns	$p < 0.05$	ns	$p < 0.05$

response already after 5 weeks of treatment the situation being largely the same after 10 weeks. However a comparison of females with males (the closely similar values obtained after 5 and 10 weeks of treatment are then pooled) indicates that the mentioned signs of structural regression are significantly greater in the females ($p < 0.01$ for the resistance at maximal dilatation and $p < 0.05$ for the maximal contractile strength). Concerning the steepness of the resistance curves reflecting primarily the wall/lumen ratio it should be noted that this parameter is not significantly reduced in any of the groups (see also Table I and II). — The apparent rise in steepness in the female group treated for 20 weeks (see Fig. 3) may well be accidental since this particular material was quite small.

After 20 weeks of treatment followed by 2 weeks without treatment blood pressure had as mentioned again risen to 167 mm Hg in males and to 146 mm Hg in females at the end of the 2 week period compared with 186 mm Hg in untreated males and 159 mm Hg in untreated females. However as seen from Fig. 3 the vascular bed still exhibited largely the same structural characteristics as during treatment but it should again be stressed that treatment in this age group did not significantly reduce the enhanced slope of the resistance curve which mainly reflects the wall/lumen ratio of the resistance vessels. This may be of considerable relevance for the rapid increase in blood pressure in SHR₁ compared with the very slow and modest pressure increase after interrupted medication in young rats.

Concerning left ventricular weight in SHR₁ only a small reduction of the order of 10% occurred after treatment compared with untreated controls. Therefore their left ventricular weight was still some 60 per cent above normal levels implying

that it is difficult to influence the cardiac muscle once this rather advanced stage of SHR hypertension is reached

In the small group of treated adult normotensive rats (NCR₁) there was a modest pressure decrease after 13 weeks of treatment pressure being 100 ± 5 mm Hg vs 113 ± 3 mm Hg in the matched untreated NCR. There was also a slight though significant reduction in resistance at maximal dilatation ($p < 0.05$) which was true also for the maximal pressor response ($p < 0.05$), but there was no change in the steepness of the resistance curve

b In the group of 14 month old SHR (SHR₀) with 'advanced' hypertension treatment was started first when general age changes of the cardiovascular system are known to be present also in NCR and when the longstanding hypertension in SHR has usually caused lesions in e.g. kidneys vessels and heart (Okamoto 1969). As shown in Table III blood pressure directly measured in the awake situation was after 13 weeks of treatment still as high as 150 mm Hg compared with 187 mm Hg in untreated SHR and 114 mm Hg in matched NCR illustrating a less efficient hypotensive effect in these old rats than in SHR₁. The hemodynamic analyses of the SHR₀ resistance vessels showed that the resistance at maximal dilatation was normalized but even though the maximal pressor response was significantly decreased compared to untreated SHR it was still considerably higher than in NCR ($p < 0.005$) and there was no reduction of the slope of the resistance curve (Table III). Further there was no reduction in left ventricular weight as compared to untreated matched SHR₀. Thus it seems to be especially difficult in old SHR to normalize blood pressure with hypotensive drug treatment or to induce any considerable regression of the structural changes in heart and resistance vessels

Discussion

Hemodynamic studies in man and in spontaneously hypertensive rats (SHR) suggest that the resistance increase in primary hypertension is mainly the result of a media thickening and a luminal restriction of the resistance vessels present even at maximal vasodilatation (Folkow *et al* 1970 a, b Folkow *et al* 1972 a, 1973). Recent morphological studies on resistance vessels (Furuyama 1962 Suwa and Takahashi 1971) as well as histochemical studies on the rat thoracic aorta (Wolinsky 1970 1971) further support the findings of such vascular structural changes which are of the same general nature as the well known left ventricular hypertrophy. For any given degree of smooth muscle tone these structural changes reset the resistance to a higher level and they appear to develop rapidly whenever vessels are exposed to sustained changes in average pressure. Thus the adaptive changes are largely completed in about 3 weeks when genetically normotensive rats are provoked into renal hypertension (Lundgren *et al* 1974) and opposite changes occur about as rapidly in animals where pressure is lowered instead (Folkow and Svertsson 1968 Lundgren 1974 Weiss and Hallback 1974).

TABLE III Upper part Mean values \pm S.E. mean difference \pm S.E. II and degree of significance for the paired experiments on old treated spontaneously hypertensive rats (SHRo) or untreated matched SHR as compared with matched normotensive control rats (NCR). Only male rats average age at acute experiments was 18 months. Lower part Group comparison t test for the differences between on the one hand untreated SHR and their NCR and between treated SHR and their NCR on the other

Group	Caudal blood pressure mm Hg	PRU ₁ at 30 ml/min \times 100 g	Steepness tangent of the angle	Maximal pressor response mm Hg
Untreated SHR	182 \pm 5	1.80 \pm 0.08	4.1 \pm 0.3	360 \pm 10
NCR	114 \pm 3	1.53 \pm 0.06	3.1 \pm 0.2	243 \pm 15
d	68 \pm 6	0.33 \pm 0.07	1.0 \pm 0.3	117 \pm 15
n = 10 pairs				
p <	0.001	0.005	0.03	0.001
SHRo Treatment for 15 weeks	150 \pm 4	1.46 \pm 0.03	4.9 \pm 0.3	314 \pm 18
NCR	118 \pm 2	1.59 \pm 0.10	3.1 \pm 0.2	253 \pm 23
d	33 \pm 4	-0.13 \pm 0.11	1.8 \pm 0.2	61 \pm 18
n = 8 pairs				
p <	0.001	ns	0.001	0.03
Untreated SHR NCR as compared to SHRo NCR	p < 0.001	p < 0.003	p < 0.05	p < 0.03

Changes of this nature may be considered as a slower structurally based correlate to the principle of functional autoregulation of flow resistance which occurs promptly upon changes in regional pressure. The above mentioned studies show that this type of structural autoregulation of the resistance vessels becomes of crucial importance for the development and maintenance of chronic hypertension and may also by virtue of its positive feedback nature invite a vicious circle by potentiating the hemodynamic impact of functional excitatory influences.

The positive feedback nature of this adaptive structural change of the resistance vessels has however the potential advantage that also rapid regression may take place whenever pressure is lowered at least as long as hypertrophic changes in wall/lumen ratio are not complicated by less reversible changes like collagen invasion or true wall lesions (e.g. Wolinsky 1970, 1971, 1972; Okamoto 1969). Concerning the situation in man a great number of studies of various types of hypotensive drug treatment indicate a clear decrease in blood pressure in peripheral resistance (e.g. Lund Johansen 1970) and also in terms of retinal vascular changes heart volume etc (e.g. Dorph *et al.* 1970). Population studies further show the value of treatment in terms of e.g. decreased mortality rate in treated hypertensives as compared to untreated individuals (Pickering 1969; Breckenridge, Dollery and Farry 1970; Freis 1971 a, b; Arnold 1970; Smirk 1972).

Towards such a background it was considered of interest to study in more detail what happens with the design of the resistance vessels if blood pressure in SHR, a model of essential hypertension in man, is kept lowered by hypotensive drugs similar

to those employed in treatment of man. This was earlier explored in a pilot study (Folkow *et al* 1971c) and it is the main topic of the present investigation. Prolonged treatment was employed with hydralazine and guanethidine in three different age groups *ie* young prehypertensive SHR (SHR₁), adult SHR with established hypertension (SHR₁) and old SHR with advanced hypertension (SHR₀). In general, the results show that this combination of hypotensive drugs in longterm administration more or less effectively normalizes arterial pressure and also leads to some regression of the hypertensive vascular changes as reflected by the reductions in resistance at maximal dilatation and in the maximal pressor response. However the older the animals and the more advanced their hypertension the poorer the results concerning regression of the structural cardiovascular changes.

The treatment of SHR_Y may be considered as mainly preventive in nature since hypertension in these young rats is still mild while the situation in SHR₁ and, particularly in SHR₀ is probably complicated by both collagen invasion and lesions of the vascular walls. Both age and sex are likely to affect the degree and time course of the structural vascular adaptation and its regression as illustrated *eg* in recent studies by Wolinsky (1971, 1972) on the thoracic aorta of rats. Aging *per se* was here found to lead to collagen invasion but much more so when hypertension was present. Further particularly the collagen component showed very poor regression towards normal levels especially in male rats.

Apart from the influence of age and sex the time needed to induce regression of structural vascular changes may well be longer in hypotensive drug treatment than when pressure is suddenly and drastically lowered by other means. Thus in *eg* aorta ligated SHR a significant change in design is traced already 3 days after pressure reduction (Weiss and Hallback 1974). Regression is almost as rapid when the renal artery clips are removed in young rats with renal hypertension where complete normalization of both heart and resistance vessels occurs already after 3 weeks (Lundgren *et al* 1974). However also here the pressure reduction is prompt and considerable occurring within one day while hypotensive drug treatment generally lowers pressure more gradually.

In the present study SHR_Y were used mainly to explore the changes of arterial pressure after interruption of preventive treatment between the age of 2.5 and 8 months. In a related study on young SHR (Folkow, Lundgren and Weiss 1972, Weiss, Lundgren and Folkow 1974) treatment was instead carried out with adrenergic β receptor blockers also from the age of 2.5 up to 8 months. Also in these animals pressure was largely normal after interrupted treatment and so was the design of their resistance vessels to judge from a quantitative hemodynamic analysis of their hindquarter vascular beds. Freis *et al* (1972) treated young SHR with a combination of reserpine, hydralazine and chlorothiazide up to the age of 13 months after which the animals were observed for a considerable period. In these rats a slow pressure increase occurred towards hypertensive levels but pressure always remained below that of untreated SHR and vascular lesions largely failed to appear.

Upon interruption of treatment of the present SHR₁ arterial pressure rose so slowly that still after 2—3 months it was almost normal and at the end of a 6 month period it was only around 145 mm Hg compared with 175 mm Hg in untreated matched SHR. Further their survival rate after 12 months of age was calculated and compared to entirely untreated SHR and to SHR treated only from the age of 12 months. A comparison after 8 months of observation revealed a 70 per cent survival rate of the earlier treated SHR₁ compared with only 25 per cent for untreated SHR and also for SHR treated only from the age of 12 months.

In the group of adult SHR with established hypertension (SHR₁) the course of both the blood pressure reduction and the regression of hypertensive structural changes were followed. Here blood pressure as measured directly in the awake animals had reached normal levels after 5 weeks of treatment. At the same time both the resistance at maximal dilatation and the maximal pressor response had become almost normalized and another 5 weeks of treatment did not further change these parameters significantly. However the steepness of the resistance curves was not decreased in SHR₁ suggesting a remaining increase of wall/lumen ratio that may in part be a result of e.g. collagen invasion which as earlier mentioned seems to occur gradually and does not display as prompt a regression as smooth muscles. A clear but small difference between the sexes was further observed where females exhibited significantly larger decreases than the males concerning resistance at maximal dilatation and maximal pressor response which remained somewhat elevated in males.

After a total of 20 weeks of treatment followed by 2 weeks without treatment blood pressure in SHR₁ had again increased from about 120 to about 165 mm Hg in males and from 120 to 145 in females though being still 15—20 mm Hg lower than in matched untreated SHR. Their vascular beds had by then not yet re-established all the signs of hypertrophic changes but it should be stressed that the increased wall/lumen ratio was never reduced perhaps indicating collagen invasion in the vascular walls at this age as mentioned above. A pre-erred increase in wall/lumen ratio will independent of its background tend to exaggerate the resistance increase induced when smooth muscle activity is again normalized after treatment.

The group of adult normotensive male rats (NCR₁) which was exposed to similar prolonged treatment showed a small reduction of resting arterial pressure and the hemodynamic analyses of the hindquarter vascular beds revealed modest regressive changes in the same direction as in treated SHR₁. Presumably the casual pressure measurements slightly underestimate the average pressure load during daily life particularly when one compares periods with and without treatment since treatment may considerably curtail transient pressure rises in connection with environmental excitatory stimuli.

In the old rats with advanced hypertension (SHR₀) a significant lowering of blood pressure occurred though even after 13 weeks of treatment they were still well above the normal pressure range. This may indicate lesional elements like renal damage etc. superimposing a renal hypertension and hence complicating the treat-

ment The subsequent hemodynamic analyses of the SHR₀ hindquarter vascular bed showed that the resistance at maximal dilatation was normalized but the maximal pressor response, reflecting the bulk of contractile media in relation to the lumen was only slightly lowered Further no reduction was seen concerning the steepness of the resistance curve which mainly reflects the wall/lumen ratio of the resistance vessels, a parameter which is not only influenced by smooth muscle elements but also by collagen invasion water logging, etc The reason may be that a substantial collagen invasion has occurred which, according to Wolinsky's studies (1971) on the aorta shows very poor regression compared with that characterizing smooth muscle hypertrophy Further this may also keep the walls stiffer at the site of the arterial baroreceptors thereby hindering their resetting to a lower pressure equilibrium (Aars 1969)

As is seen in these old SHR, and also in adult SHR there seems to be a remaining increase in the thickness of the vascular wall after treatment (see also Weiss, Lundgren and Folkow 1974) although it does not imply also a reduced lumen This and the findings of an increased wall/lumen ratio in combination with a reduced resistance at maximal dilatation in the renal vascular bed of SHR (Folkow *et al* 1971b) suggest that an increased wall thickness might be present without encroaching upon the lumen Hence it seems as if the luminal width is *per se* influenced also by factors like the nutritional flow conditions and prevailing vascular tone while the wall thickness appears to adjust itself primarily to the current level of wall tension

When taken together the present study on SHR of different ages illustrates that prolonged treatment of young SHR started when they are still barely hypertensive largely protects them against the development of both hypertension and structural vascular changes Further if this treatment is interrupted later in life there is only a very slow and modest progression of hypertension and survival is considerably improved — In established hypertension in adult and even in old SHR where substantial and more complicated structural changes of heart and resistance vessels seem to be present it is still possible to decrease pressure and to reduce at least part of already existing vascular changes Thus also here treatment interferes to some extent with the vicious circle inherent in the interaction between functional and structural factors raising the resistance to flow However, the further the disease has progressed the more difficult it obviously is to fully reverse the structural changes especially in male SHR to a great extent presumably due to late changes like an increasing collagen invasion in vascular walls (Wolinsky 1971 1972) and even manifest lesions (Okamoto 1969) It is therefore hardly surprising that pressure rapidly returns to hypertensive levels upon interruption of treatment in such animals

These results of model studies in rats with primary hypertension may therefore justify the conclusion that early, fairly intense treatment has a considerable chance to induce adequate regression of hypertrophic vascular changes thereby efficiently interrupting the vicious circle inherent in the consequent potentiation of the hemo-

dynamic effects induced by smooth muscle activations. The more advanced the structural changes, particularly when complicated by degenerative instead of purely hypertrophic elements, the more difficult it is to induce regression and consequently the smaller the chances to avoid a prompt return of the hypertensive state if treatment is interrupted.

This study was supported by grants from the Swedish Medical Research Council (No B74 14\ 16 10C) from the Swedish National Association against Heart and Chest Diseases and from the Medical Faculty, University of Göteborg.

AB Hassle generously covered part of the expenses for a technician.

References

- AARS H. Relationship between aortic diameter and aortic baroreceptor activity in normal and hypertensive rabbits. *Acta physiol scand* 1969 75 406—414.
- ARNOLD O H. *Therapie der arteriellen Hypertonie*. Springer Verlag Berlin—Heidelberg—New York 1970.
- BRECKENRIDGE A C, T DOLLERY and E H O PARRY. Prognosis of treated hypertension. *Quart J Med* 1970 39 411—429.
- DORFEL S A, LETH B, DEGNOL and A FROM. Visceral changes in severe hypertension and their response to drug treatment. *Acta med scand* 1970 187 411—417.
- FOLKOW B, M GUREVICH, M HALLBACK, Y LUNDGREN and L WEISS. Hemodynamic consequences of regional hypotension in spontaneously hypertensive and normotensive rats. *Acta physiol scand* 1971 a 83 532—541.
- FOLKOW B, M HALLBACK, Y LUNDGREN, R SIVERTSSON and L WEISS. The importance of adaptive changes in vascular design for the establishment and maintenance of primary hypertension as studied in man and SHR. In *Spontaneous Hypertension*. Ed K Okamoto. Igaku Shoin Ltd Tokyo 1972 a.
- FOLKOW B, M HALLBACK, Y LUNDGREN, R SIVERTSSON and L WEISS. Importance of adaptive changes in vascular design for establishment of primary hypertension studied in man and spontaneously hypertensive rats. *Circulat Res* 1973 32—33 Suppl 1 2—13.
- FOLKOW B, M HALLBACK, Y LUNDGREN and L WEISS. Structurally based increase of flow resistance in spontaneously hypertensive rats. *Acta physiol scand* 1970 a 79 373—378.
- FOLKOW B, M HALLBACK, Y LUNDGREN and L WEISS. Background of increased flow resistance and vascular reactivity in spontaneously hypertensive rats. *Acta physiol scand* 1970 b 80 93—106.
- FOLKOW B, M HALLBACK, Y LUNDGREN and L WEISS. Renal vascular resistance in spontaneously hypertensive rats. *Acta physiol scand* 1971 b 83 96—105.
- FOLKOW B, M HALLBACK, Y LUNDGREN and L WEISS. Effects of intense treatment with hypotensive drugs on structural design of the resistance vessels in spontaneously hypertensive rats. *Acta physiol scand* 1971 c 83 280—287.
- FOLKOW B, M HALLBACK, Y LUNDGREN and L WEISS. Effects of immunosympathectomy on blood pressure and vascular reactivity in normal and spontaneously hypertensive rats. *Acta physiol scand* 1972 b 84 512—523.
- FOLKOW B, Y LUNDGREN and L WEISS. The effect of prolonged propranolol treatment on blood pressure and structural design of the resistance vessels in young spontaneously hypertensive rats. *Acta physiol scand* 1972 84 8A—9A.
- FOLKOW B and R SIVERTSSON. Adaptive changes in reactivity and wall/lumen area in cat blood vessels exposed to prolonged transmural pressure difference. *Life Sci* 1968 7 1283—1289.
- FRIS E D. Effectiveness of drug therapy in hypertension: present status. *Circulat Res* 1971 28—29 Suppl II 11—12 70.
- FRIS E D. The chemotherapy of hypertension. *J Amer med Ass* 1971 218 1009—1015.
- FRIS E D, D RAGAN, H PILLSBURY III and M MATHEWS. Alteration of the course of hypertension in the spontaneously hypertensive rat. *Circulat Res* 1972 31 1—7.
- FURUYAMA M. Histometrical investigations of arteries in reference to arterial hypertension. *Tohoku J exp Med* 1967 76 388—414.
- HALLBACK M, Y LUNDGREN and L WEISS. Distensibility of the resistance vessels in spontaneously hypertensive rats as compared with normotensive control rats. *Acta physiol scand* 1974 90 5—68.

- LUNDGREN Y. Regression of cardiovascular changes after reversal of experimental renal hypertension in rats *Acta physiol scand* 1974 91 275—283
- LUNDGREN Y, M HALLBACK, L WEISS and L FOLKOW. Rate and extent of adaptive cardiovascular changes in rats during experimental renal hypertension *Acta physiol scand* 1974 91 103—115
- LUND-JOHANSEN P. Hemodynamic changes in long term diuretic therapy of essential hypertension *Acta med scand* 1970 187 509—518
- OKAMOTO K. Spontaneous hypertension in rats *Int Rev exp Path* 1969 7 727—770
- PICKERING G W. *High blood pressure* London J & A Churchill Ltd 1969
- SMITH F H. The prognosis of untreated and of treated hypertension and advantages of early treatment *Amer Heart J* 1972 83 825—840
- SLAWA N and T TAKAHASHI. *Morphological and morphometrical analysis of circulation in hypertension and ischemic kidney* München—Berlin—Wien Urban and Schwarzenberg 1971
- WEISS L and M HALLBACK. Time course and extent of structural vascular adaptation in regional hypotension in adult spontaneously hypertensive rats (SHR) *Acta physiol scand* 1974 91 365—373
- WEISS L, Y LUNDGREN and B FOLKOW. Effects of prolonged treatment with adrenergic beta receptor antagonists on blood pressure, cardiovascular design and reactivity in spontaneously hypertensive rats (SHR) *Acta physiol scand* 1974 91 447—457
- WOLINSKY H. Response of the rat aortic media to hypertension *Circulat Res* 1970 26 507—522
- WOLINSKY H. Effects of hypertension and its reversal on the thoracic aorta of male and female rats *Circulat Res* 1971 28 622—637
- WOLINSKY H. Long term effects of hypertension on the rat aortic wall and their relation to concurrent aging changes. Morphological and chemical studies *Circulat Res* 1972 30 301—309

Blood Pressure and Vascular Design in Renal Hypertension in Rats after Prolonged Propranolol Treatment

By

YEN LUNDGREN

Received 28 January 1974

Abstract

LUNDGREN Y *Blood pressure and vascular design in renal hypertension in rats after prolonged propranolol treatment* Acta physiol scand 1974 91 409—416

To study the effect of β adrenergic blockade on the development of renal hypertension propranolol was given by administration in the drinking water to 4 week old normotensive male Wistar rats. After 3 weeks of treatment the left renal artery was constricted by a silver clip in order to induce renal hypertension on the same procedure being performed in a group of matched untreated controls. — The incidence and degree of hypertension 4 weeks after renal artery constriction was about the same in both groups but heart rate was considerably lower in the propranolol treated animals and heart rate responses to isoprenaline were diminished. Treatment was continued until 4 weeks after constriction when quantitative hemodynamic analysis of the hindquarter vascular beds revealed the same degree of structural vascular changes in both treated and untreated renal hypertensive rats. — Another group of rats in which renal hypertension and hypertensive cardiovascular changes were already established was treated with propranolol for 3 months. No effect on arterial pressure was noticed but heart rate was considerably reduced. Thus renal hypertension appears to be unaffected by adrenergic β receptor blockade in contrast to the situation in early phases of hypertension in spontaneously hypertensive rats (Folkow, Lundgren and Weiss 1972).

The importance of changes in cardiac output (CO) for the development of renal hypertension has been much debated in recent years. Several investigators, e.g. Ledingham and coworkers (*cf* Ledingham 1971) have noted a transient CO increase after induction of renal hypertension and suggested that it may be essential for the subsequent resistance rise. It is further widely assumed that the increased renin-angiotensin formation in early renal hypertension is of great importance (*cf* Page and McCubbin 1968) and angiotensin may here act partly by facilitating sympathetic discharge via bulbar structures (*e.g.* Ueda *et al* 1969, Jov 1971).

It is for such reasons possible that the adrenergic excitatory control of the heart is of considerable importance for inducing CO increases in early renal hypertension. The present study was performed in order to investigate whether such mechanisms

really are essential in this respect β adrenergic receptor antagonists were therefore given particularly since such drugs considerably interfere with the development of spontaneous hypertension in rats (Folkow, Lundgren and Weiss 1972). Thus one group of rats was given preventive propranolol treatment before and during the induction of renal hypertension while another group was exposed to propranolol treatment first after renal hypertension was established. The incidence and degree of hypertension in both groups were compared with untreated renal hypertensive rats and quantitative hemodynamic analyses were finally performed to study whether drug treatment had influenced the design and reactivity of the hindquarter vascular bed.

Methods

A. Preventive treatment with propranolol 16 normotensive male Wistar rats were from 4 weeks of age exposed to propranolol treatment about 100 mg per kg and 24 h administered in the drinking water. The dose of propranolol was based on long term measurements of the average water consumption per rat and 24 h in cages with 5 rats/cage. After 3 weeks of treatment a silver clip was placed on the left renal artery during ether anesthesia, leaving the right kidney intact. On the same occasion and in exactly the same manner renal hypertension was induced in 16 7 week old male Wistar rats which were not exposed to any pharmacological treatment.

Treatment in the first mentioned group was continued until 4 weeks after renal artery constriction when arterial pressure and heart rate were directly measured in the caudal artery during awake resting conditions. Concomitantly the degree of β adrenergic blockade in the treated group was tested by comparing the heart rate response to 0.1 μ g of isoprenaline (about 0.4 μ g/kg) given in the caudal artery with that of the untreated group.

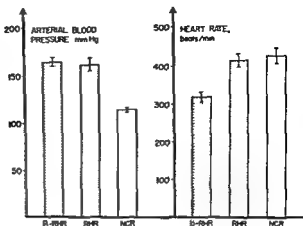
Acute perfusion experiments were then performed on the isolated hindquarters of the propranolol treated (β RHR, $n = 13$) and untreated (RHR, $n = 11$) renal hypertensive rats which had reached a mean arterial pressure of 150 mm Hg or more. This was done in parallel with hindquarters of matched normotensive control rats (NCR). For details concerning experimental procedure, recordings and construction of resistance curves in the paired experiments see Folkow *et al.* (1970, 1971). Briefly the pressure flow relationships were first examined during maximal vasodilatation for exact determinations of resistance at flows of 10 ml and 30 ml/min \times 100 g. Flow was then kept constant at 10 ml/min \times 100 g and noradrenaline (NA) was infused from subthreshold up to supramaximal concentrations (0.04–5 μ g/ml) after which 10 IU of vasopressin and 150 mg of barium chloride were added to ensure a definitely maximal pressor response. Resistance curves were plotted with the following parameters as key points: 1) resistance at maximal dilatation, 2) NA threshold (i.e. the NA concentration producing 25 per cent increase in resistance), 3) steepness of the curve (tangent of the angle) and 4) maximal pressor response (Folkow *et al.* 1970).

B. Propranolol treatment in RHR with established hypertension. In this group a silver clip was placed on the left renal artery leaving the right kidney intact in 16 7 week old normotensive male Wistar rats. Intraarterial pressure and heart rate measurements 4 weeks later showed that 10 of the rats had developed considerable hypertension (≥ 150 mm Hg). After 4 weeks duration of renal hypertension when the hypertrophic cardiovascular changes seem to be largely completed (Folkow *et al.* 1973, Lundgren *et al.* 1973) propranolol 100 mg per kg and 24 h was administered in the drinking water for another 3 months. Intraarterial recordings of blood pressure and heart rate were made after 1 and 3 months of treatment.

Results

A. Preventive treatment with propranolol 13 of the 16 propranolol treated animals developed hypertension (≥ 150 mm Hg) i.e. 82 per cent while 11 of the 16 untreated rats i.e. 69 per cent became hypertensive. Thus the treated group showed

Fig 1 Mean values of arterial pressure and heart rate measured in the caudal artery during awake conditions 4 weeks after renal artery constriction in 16 propranolol treated rats (β RHR) 16 untreated renal hypertensive rats (RHR) and 16 normotensive control rats (NCR). The β RHR and RHR groups include also those rats which did not develop hypertension



if anything the highest incidence of hypertension. Mean values for awake resting arterial pressure and heart rate 4 weeks after renal artery constriction are shown in Fig 1 concerning propranolol treated (β RHR) and untreated renal hypertensive rats (RHR) together with normotensive control rats (NCR). The mean values include those rats which later did not develop hypertension. It is seen that mean arterial pressures of β RHR and RHR were both considerably higher than that of NCR ($p < 0.001$) and did not differ from each other (165 ± 5 mm Hg and 162 ± 7 mm Hg respectively). Heart rate was significantly decreased in β RHR compared to both NCR ($p < 0.001$) and RHR ($p < 0.001$) which in this respect were largely equal.

Also when only those animals were compared which really did develop hypertension β RHR and RHR did not differ in degree of hypertension, mean arterial pressures being then 172 ± 4 mm Hg and 176 ± 6 mm Hg respectively. Heart rate was however significantly lower in the propranolol treated group compared to both untreated RHR and NCR ($p < 0.001$). To test the degree of β adrenergic blockade in the propranolol treated group (β RHR) heart rate responses to injections of $0.1 \mu\text{g}$ of isoprenaline (about $0.4 \mu\text{g/kg}$) were measured. Heart rate increased only 3 per cent in β RHR (11 ± 4 beats/min) compared to 11 per cent (42 ± 5 beats/min) in untreated RHR and 11 per cent (40 ± 13 beats/min) in NCR, the β RHR response being significantly smaller than that of RHR or NCR indicating a considerable blockade of the cardiac β receptors.

The upper part of Table I summarizes mean values \pm S.E. for resting arterial pressure and heart rate together with the different hemodynamic characteristics of the perfused hindquarters of 13 β RHR, 11 RHR and their matched NCR. Since all β RHR and RHR were perfused in parallel with matched NCR, the degree of significance within the groups is tested by the pairing design *t* test. By using such paired experiments interferences of e.g. differences in temperature, viscosity and

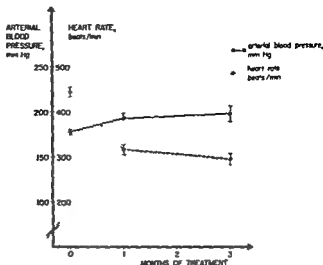
TABLE I Upper part Mean values \pm SE for blood pressure heart rate and the hemodynamic characteristics of the hindquarter resistance vessels (resistance at maximal dilatation steepness of the resistance curve and maximal pressor response) of propranolol treated renal hypertensive rats (β RHR) and their normotensive controls (NCR) and of untreated RHR and their NCR. The degree of significance between β RHR and their NCR and between RHR and their NCR is tested by the pairing design t test. Lower part Mean differences \pm SE between β RHR and their NCR and between RHR and their NCR and the degree of significance between β RHR NCR and RHR NCR tested by a group comparison t test

	Arterial blood pressure mm Hg	Heart rate beats/min	PRU ₁ at max dil (flow = 30 ml/min)	Steepness of the curve (tangent of the angle)	Maximal pressor response mm Hg
β RHR	172 \pm 4	317 \pm 9	1.60 \pm 0.06	4.9 \pm 0.4	337 \pm 9
NCR	112 \pm 2	418 \pm 17	1.34 \pm 0.04	3.7 \pm 0.3	284 \pm 17
n = 13 pairs degree of significance	p < 0.001	p < 0.001	p < 0.001	p < 0.005	p < 0.001
RHR	176 \pm 6	423 \pm 18	1.68 \pm 0.07	5.0 \pm 0.3	353 \pm 8
NCR	113 \pm 3	443 \pm 14	1.35 \pm 0.04	3.8 \pm 0.3	271 \pm 12
n = 11 pairs degree of significance	p < 0.01	ns	p < 0.001	p < 0.01	p < 0.001
mean difference β RHR NCR	59 \pm 5	-101 \pm 16	0.26 \pm 0.05	1.1 \pm 0.3	53 \pm 17
mean difference RHR NCR	63 \pm 6	-20 \pm 21	0.32 \pm 0.06	1.2 \pm 0.4	82 \pm 13
degree of significance	ns	p < 0.001	ns	ns	ns

composition of the perfusate will be largely ruled out (see Lundgren 1974) but may of course somewhat affect the mean values of NCR of the different groups. — The lower part of Table I presents the mean differences \pm SE between β RHR and NCR and RHR and NCR respectively. The degree of significance with respect to the differences between the two groups is analysed by a group comparison t test.

Compared to matched NCR both β RHR and RHR showed 1) a significantly increased flow resistance at maximal dilatation indicating a luminal narrowing, 2) an exaggerated slope of the resistance curve indicating an enhanced wall/lumen ratio and 3) a considerably raised maximal pressor response indicating an increased bulk of contractile tissue in relation to the lumen. Concerning NA threshold on the other hand the groups did not differ significantly from each other. The mentioned signs of hypertensive structural changes of the resistance vessels which are largely completed about 3 weeks after renal artery constriction (Lundgren *et al* 1974) were thus very similar in β RHR and RHR though the resistance at maximal dilatation and the maximal pressor response tended to be slightly lower in β RHR. However when comparing the mean differences β RHR

Fig 2 Mean values of arterial pressure and heart rate in 10 rats with established renal hypertension (RHR) treated with propranolol for 3 months from the age of 11 weeks. Months of treatment are plotted along the abscissa and arterial pressure and heart rate along the ordinate.



NCR and RHR NCR by a group comparison *t* test they did not differ significantly.

B Propranolol treatment in RHR with established hypertension When propranolol treatment was started 4 weeks after construction of the left renal artery, awake resting arterial pressure was 178 ± 3 mm Hg and heart rate 444 ± 11 beats/min. At this time after induction of renal hypertension the hypertrophic changes in cardiovascular design are largely completed (Lundgren *et al* 1974). Fig 2 illustrates the changes in pressure and heart rate during the subsequent 3 months of propranolol treatment. Thus compared with the values before induction of treatment heart rate is considerably decreased ($p < 0.001$) when measured after 1 and 3 months treatment while arterial pressure was slightly though significantly ($p < 0.05$) increased after 3 months. Evidently prolonged propranolol treatment has no appreciable effect on arterial pressure in established renal hypertension in rats even though it considerably reduces heart rate.

Discussion

Since Goldblatt's classical studies (see Pickering 1968, Page and McCubbin 1968) the background of renal hypertension has been intensely debated. Particularly the involvement of changes in cardiac output (CO) and its possible importance has recently attracted much interest. Thus several groups report early phases of increased stroke volume and CO (e.g. Ledingham and Pelling 1967) in renal hypertension in rats. A transient increase in CO gradually followed by more persistent increases in total peripheral resistance has been found in dogs with renal hypertension (Ferrario, Page and McCubbin 1970, Bianchi *et al* 1972). Results like these

have often been taken to support the 'autoregulation theory' of Ledingham and also Guyton (see Ledingham 1971 Guyton and Coleman 1969 Coleman Granger and Guyton 1971) but it is still an open question whether the transfer from an increased cardiac output towards a raised resistance is solely or even mainly due to autoregulatory precapillary adjustments. In any case the phase of increased output coincides well with the increased renin angiotensin formation according to Bianchi *et al* (1972), and angiotensin may influence the circulating blood volume via the aldosterone control of sodium excretion as well as the neurogenic cardiovascular control perhaps mainly via bulbar structures (*e.g.* Ueda 1969 *et al* Joy 1971). On the other hand immunization against angiotensin does not prevent the development of renal hypertension (Eide and Aars 1970 Johnston Hutchinson and Mendelsohn 1970 MacDonald *et al* 1970 Eide 1972). This either indicates that the kidneys possess other means for raising pressure when their perfusion is threatened or that the immunizations were not capable of suppressing all angiotensin actions.

Another factor becomes rapidly involved in renal hypertension i.e. an adaptive structural increase in wall/lumen ratio of the resistance vessels as triggered by the enhanced pressure load. This process completed after about 3 weeks in rats may be called a structural autoregulation and serves to rapidly reset pressure towards higher levels by amplifying the resistance increases produced by smooth muscle activations (*cf.* Folkow *et al* 1973). Because of its rapidity such a factor may considerably contribute not only to the maintenance but also to the development of renal hypertension.

The present study was performed to explore whether the initiating functional elements in renal hypertension were interfered with if the adrenergic control of the heart and the renin secretion were blocked by β adrenergic receptor antagonists (Frohlich *et al* 1968 Buhler *et al* 1972). This was considered of interest since enhancements of cardiac output may as mentioned be of great importance. Further propranolol treatment has considerable beneficial effects when used in early phases of spontaneous hypertension in rats of the Okamoto strain (Folkow Lundgren and Weiss 1972 Weiss, Lundgren and Folkow 1974). However the present results indicate that renal hypertension develops just as readily despite preventive treatment with propranolol in dosages which greatly interfered with the adrenergic control of the heart. Further the resistance vessels of the treated animals exhibited the same degree of rapid structural adaptation as in untreated RHR. Also in already established renal hypertension prolonged propranolol treatment was without effects on arterial pressure but heart rate was also here considerably reduced.

These results hardly support the view that adrenergically mediated increases of cardiac output or/and renin release should be decisive for the pressure rise in renal hypertension. Evidently other mechanisms are well capable of inducing the same degree of pressure rise perhaps also involving initial cardiac output increases even when the mentioned links are blocked. This situation is in contrast to that in spontaneously hypertensive rats where preventive propranolol treatment in early phases of this genetically linked hypertension largely hinders further pressure rise.

and development of structural vascular changes (Weiss Lundgren and Folkow 1974) Evidently there must be essential differences concerning initiating mechanisms in these two types of hypertension However independent of the nature of these initiating mechanisms they induce in both cases considerable structural adaptations of heart and vessels which greatly contribute to the establishment of a chronic hypertensive state

This research has been sponsored by grants from the Swedish Medical Research Council (No B:4 14\ 16-10C) from the Swedish National Association against Heart and Chest Diseases and from the Medical Faculty University of Goteborg

AB Hassle generously covered part of the expenses for a technician Thanks are also due to ICI Ltd Great Britain for generous supply of propranolol

References

- BLANCHI G E BALDOLI R LACCA and P BARBI Pathogenesis of arterial hypertension after the constriction of the renal artery leaving the opposite kidney intact both in the anaesthetized and in the conscious dog *Clin Sci* 1972 42 651-664
- BUSLER F R J H LARAUGH L BAER ■ D VALCHIAN and H R BRUNNER Propranolol inhibition of renin secretion *New Engl J Med* 1972 287 1209-1214
- COLEMAN T G H J GRANGER and A C GUYTON Whole body circulatory autoregulation and hypertension *Circulat Res* 1971 28-79 Suppl II II 76-II 86
- EME I Renovascular hypertension in rats immunized with angiotensin II *Circulat Res* 1972 30 149-157
- EME I and H AARS Renal hypertension in rabbits immunized with angiotensin II *Scand J clin Lab Invest* 1970 25 119-127
- FERRARIO C M I H PAGE and J W MCCLELLAN Increased cardiac output as a contributory factor in experimental renal hypertension in dogs *Circulat Res* 1970 27 799-810
- FOLKOW B M GUREVICH M HALLBACK Y LUNDGREN and L WEISS The hemodynamic consequences of regional hypotension in spontaneously hypertensive and normotensive rats *Acta physiol scand* 1971 83 532-541
- FOLKOW B M HALLBACK Y LUNDGREN and L WEISS Background of increased flow resistance and vascular reactivity in spontaneously hypertensive rats *Acta physiol scand* 1970 80 93-106
- FOLKOW B M HALLBACK Y LUNDGREN and L WEISS Time course and extent of structural adaptation of the resistance vessels in renal hypertensive rats (RHR) as compared with spontaneously hypertensive rats (SHR) *Acta physiol scand* 1973 87 10A-11A
- FOLKOW B Y LUNDGREN and L WEISS The effect of prolonged propranolol treatment on blood pressure and structural design of the resistance vessels in young spontaneously hypertensive rats *Acta physiol scand* 1973 84 8A-9A
- FROHLICH E D R C TARAZI H P DUSTAN and I H PAGE The paradox of beta adrenergic blockade in hypertension *Circulation* 1968 37 417-423
- GUYTON A C and T G COLEMAN Quantitative analysis of the pathophysiology of hypertension *Circulat Res* 1969 24-25 Suppl I I 1-I 19
- JOHNSTON C I J S HUTCHINSON and F A MENDLSON ■ ological significance of renin angiotensin immunization *Circulat Res* 1970 26-27 Suppl II II 215-II 222
- JAY M D The intramedullary connections of the area postrema involved in the central cardiovascular response to angiotensin II *Clin Sci* 1971 41 89-100
- LEDINGHAM J M Mechanisms in renal hypertension *Proc Roy Soc Med* 1971 64 409-418
- LEDINGHAM J M and D PELLING Cardiac output and peripheral resistance in experimental renal hypertension *Circulat Res* 1967 20-21 Suppl II II 187-II 199
- LUNDGREN Y Regress of structural cardiovascular changes after reversal of experimental renal hypertension in rats *Acta physiol scand* 1974 91 223-285
- LUNDGREN Y M HALLBACK L WEISS and B FOLKOW Rate and extent of adaptive cardiovascular changes in rats during experimental renal hypertension *Acta physiol scand* 1974 91 103-115

- MACDONALD G J W J LOUIS V RENZINI G W BOYD and W E PEART Renal-clip hypertension in rabbits immunized against angiotensin II *Circulat Res* 1970 27 197-211
- PAGE I H and J W McCUBBIN Renal hypertension Year Book of Med Publ Inc 1968
- PICKERING G W High blood pressure London J & A Churchill 1968
- LEDA H Y UCHIDA A UEDA T GONDARIA and S KATAYAMA Centrally mediated vasopressor effect of angiotensin II in man *Jap Heart J* 1969 10 243-247
- WEISS L Y LUNDGREN and B FOLKOW Effects of prolonged treatment with adrenergic β receptor antagonists on blood pressure: cardiovascular design and reactivity in spontaneously hypertensive rats (SHR) *Acta physiol scand* 1974 91 447-457

Sympathetic Skin Nerve Activity and Skin Temperature Changes in Man

By

LARS A NORMELL and B GUNAR WALLIN

Received 7 February 1974

Abstract

NORMELL L A and B G WALLIN *Sympathetic skin nerve activity and skin temperature changes in man* Acta physiol scand 1974 91 417-426

Simultaneous recordings of skin temperature and efferent sympathetic impulse activity in cutaneous nerve fascicles were made in two healthy subjects and in one patient with paraplegia due to a transverse lesion of the spinal cord at the level of the first lumbar segment. In the patient the recordings were made below the level of the lesion in a skin area deprived of sensibility but with preserved temperature responses to indirect heating and cooling. The sympathetic nerve activity showed the same characteristics both in the paraplegic patient and in the healthy subjects. Evoked changes in sympathetic nerve activity were followed by changes in skin temperature of the same type in all three subjects. The demonstration of concomitant changes in evoked sympathetic nerve activity in a peripheral nerve and in skin temperature in the corresponding skin area strongly supports the concept that the cutaneous thermoregulatory vasomotor response (CTVR) is a consequence of changes in efferent sympathetic nerve activity. The results demonstrate that loss of somatic sensation and voluntary motor function can be combined with a functionally intact efferent sympathetic pathway below the level of a "complete" lesion of the spinal cord.

It is well established that the blood vessels in the skin are under nervous control. In order to record changes in the nervous influences on the vessels most workers in this field have measured blood flow variations by plethysmographic methods. Skin temperature is a less reliable index of skin blood flow due to the disturbing influence of factors such as ambient climate, sweat evaporation, local metabolism in the underlying tissues and the temperature of the blood returning from distal parts (Sheard 1944, Burton 1948, Bazett *et al.* 1948, Cooper *et al.* 1949, Felder *et al.* 1954, Benzing 1969).

Using a thermographic method Normell (1974) recorded the temperature responses in large areas of skin during indirect heating and cooling under conditions in which ambient climate and sweat evaporation were controlled. A skin temperature change which exceeded that which could be expected from changes in peripheral blood temperature and its local influence on the skin blood vessels was

taken as an expression of a cutaneous thermoregulatory vasomotor response (CTVR) which was presumably mediated via efferent sympathetic nerves. When paraplegic patients were investigated with this method, some patients were found to have preserved CTVR within areas deprived of sensory and motor functions (Nordell 1974). It was postulated that such patients had an intact outflow of centrally evoked sympathetic activity in the peripheral nerves below the level of a complete transverse spinal lesion. Direct evidence supporting this concept has not been available.

With the recent development of a microneurographic technique it has become possible to record sympathetic nerve impulses in peripheral nerves in man (Hagbarth and Vallbo 1968, Delius *et al.* 1972a, b, Hagbarth *et al.* 1972, Wallin *et al.* 1973). By combining the thermographic and microneurographic techniques it might be possible to correlate changes in skin temperature to changes in skin nerve sympathetic activity (SSA) and to obtain direct evidence of sympathetic nervous control of cutaneous vasomotor activity. Recordings were therefore made applying both methods simultaneously on two healthy subjects and a paraplegic man with preserved skin temperature responses to indirect heating and cooling below the level of the spinal lesion.

Material

Subjects

Two healthy female subjects, 22 and 26 years old, and one male paraplegic patient were investigated. For technical reasons, sympathetic nerve recordings are preferably made from a large superficial nerve trunk, such as the posterior tibial nerve. The paraplegic subject selected for the study had preserved skin temperature responses within the innervation zone of this nerve.

Case report. The paraplegic patient was a 30-year-old, previously healthy man who in 1969 sustained a luxation fracture of vertebra L1 resulting in immediate and complete paraplegia. After 6 months he was discharged to his home as a wheel chair patient. The paraplegia remained unchanged with total loss of sensibility and voluntary motor function in the legs below the level of the lesion. Later decubital sores appeared and were treated conservatively and with plastic surgery.

At the time of the present investigation (September 1972) the patient was in good general condition. Well-healed plastic flaps were preserved over the sacrum and tuber regions. There were no signs of cardiac or pulmonary disease. Blood pressure 140/90 mm Hg.

There was a loss of superficial sensibility from the first lumbar dermatome on the right side and the second lumbar dermatome on the left side (Chusid 1970). In addition, deep sensibility was absent in the legs. There was preserved sensibility to bladder distension but urethral sensibility was absent. Volitional muscle activity was absent in the legs except for preserved ability to flex and adduct in the left hip when the weight of the leg was eliminated. Deep reflexes in the upper extremities were normal. The quadriceps reflex was absent on both sides. The Achilles reflex was enhanced. Foot clonus was readily elicited on both sides. Toe flexor reflexes were enhanced. Bulbocavernosus and anal reflexes were present. Babinski sign was present bilaterally. There was normal EMG activity in the musculature corresponding to the spinal segments L1-L5. L1-L11 levels. No volitional EMG activity was recorded below this level. Conductivity in the right posterior tibial nerve was 35 m/s.

There was a neurogenic functional disturbance of the bladder. Voiding was elicited reflexly by straining or by combined anal dilatation and straining. Defaecation was elicited reflexly. Reflex erection could be induced by touch stimuli and could be maintained for a long period of time. The patient had preserved capability to ejaculate. Normal sweating was preserved and occurred simultaneously on the upper body and on the legs. The skin and hair on the legs appeared normal.

Fig 1 Thermograms in black and white showing the back and the trunk and the legs of the paraplegic patient taken during indirect heating and cooling. The black line at waist level indicates the level of sensory loss. Left thermogram taken before heating, middle during heating and right at the end of cooling. Temperature changes (shown by the differences in the gray tone) occur in all skin areas below decubitus scar on the right thigh (note that the thermogram is a mirror image).



Recordings of skin temperature during indirect heating and cooling (Normell 1974) showed a temperature change of 3–5 °C on the back and the backside of the legs including the soles of the feet and the toes (Fig 1). The only exception was a small well-defined area on the outside of the right thigh situated just below a scar after plastic surgery where the temperature did not change. Generalized sweating could be observed underneath the plastic sheet used to prevent evaporation except in the above mentioned area on the right thigh. Thus the patient showed normal changes in skin temperature (Normell 1974) in spite of loss of sensory and motor functions in the lower extremities.

Recording techniques

Thermography

Details of the thermographic method for assessing skin temperature responses during indirect heating and cooling have been described elsewhere (Normell 1974) and only a brief outline will be given here. The infrared radiation from the subject's dorsal side as recorded with a thermocamera (AGA Thermovision® 680 Med cal) and displayed on an oscilloscope screen. Evaporation of sweat was prevented by covering the area of skin under investigation with plastic sheeting. Indirect heating and cooling was carried out by immersing the subject's hands and forearms in water at 42–44 °C or 18–20 °C during periods of 1 h. This procedure normally evoked a skin temperature change of the order of 2–4 °C following a typical time course (Normell 1974).

Since it is difficult to record sympathetic activity from the same electrode position during the prolonged period required for the above mentioned procedure of thermo-provocation a modified thermographic method was used in this study. In order to record small rapid changes in skin temperature a colour monitor (Colour Monitor AGA) was used. This gave a direct picture of the area under investigation with different coloured isotherms corresponding to the different skin temperatures. In this way the skin temperature was continuously monitored and recorded by serial photography with a colour film camera. In parallel with this the temperature changes were also analyzed by a so-called line adaptor (AGA Thermoprobe adaptor). With the aid of this adaptor a signal corresponding to a straight line on the thermogram was taken from the colour monitor and displayed continuously on an oscilloscope screen. The surface temperature of the object along this line was presented graphically and photographed with a Polaroid® camera with a maximal frequency of two pictures per minute (Fig 2). The skin area chosen for temperature recording (sole of foot or finger pulp) was covered with the polyethyoxymethylmethacrylate (Nobecutane®) spray application (0.05 mm) in order to prevent evaporation of sweat. The minimum detectable temperature difference was less than 0.1 °C at +30 °C object temperature.

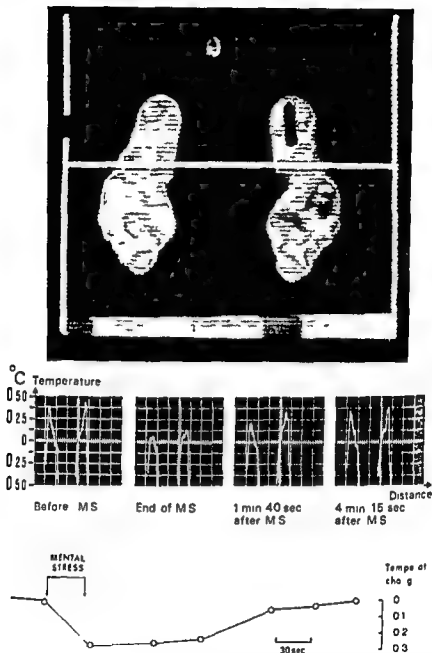


Fig. 1. *Abote Therm* graph—skin temperature recording from foot soles of the paraplegic patient. The top photograph is a black and white picture of the coloured thermoid plate. The differently toned blocks on the plate represent differently coloured temperature intervals (each with the width of 0.1°C). The round area above the heel is the IR radiation reference source. The white line across the soles corresponds to the thermal signal which is displayed via the line adaptor and recorded with a Ilford® camera. Below: Four examples of skin temperature records obtained with the line adaptor positioned across the soles of the feet. The recordings were made before, at the end of and after subjecting the paraplegic patient to mental stress (stressing conversation). The whole time course of the temperature changes in the sole of the left foot is shown by the graph below.

Micro-neurography

The sympathetic nerve activity was recorded with tungsten microelectrodes. Details concerning the characteristics of the electrodes and the recording and display systems have been reported previously (Delius *et al* 1972a). In the illustrations presented in the present study the nerve signals are shown as *mean voltage neurograms* obtained by electronic integration of the original nerve recording (time constant 0.1 s). The recordings were made from the median nerve at the elbow in one healthy subject and from the right posterior tibial nerve in the popliteal fossa in the other healthy subject and in the paraplegic patient. Suitable recording sites in skin nerve fascicles were selected as described previously (Hagbarth *et al* 1972); the only difference being that the paraplegic patient could not feel any insertion paresthesias when the electrode entered the fascicles. As usual the nerve was localized by the muscle twitches from short pulse cathodal electrical stimulation through the needle. As a convenient method of screening the effector organ response to changes in SSA during the recordings skin electrical resistance measurements were made within the receptive field of the impaled fascicle as described previously (Hagbarth *et al* 1972).

Results

Normal subjects

Skin nerve sympathetic activity. At rest the spontaneous SSA was found to have the same characteristics as previously described by Hagbarth *et al* (1972). The impulses were discharged in bursts of varying duration and intensity. The strength of the spontaneous activity was related to the emotional state of the subject in that it increased in stress situations and decreased when the subject relaxed. As observed by Delius *et al* (1972c) it was found that the activity was influenced by the ambient temperature so that it was weaker when the subject felt moderately warm and comfortable and increased during body cooling.

As previously reported (Hagbarth *et al* 1972) bursts of sympathetic impulses could be induced in response to various manoeuvres such as a deep breath, a sudden intense sound or an electric shock applied to the skin anywhere on the body. After a latent period of 1–1.5 s all the reflexly induced bursts and some of the spontaneous ones were followed by transient reductions in the electrical resistance of the skin within the receptive field of the impaled fascicle.

On one occasion when one of the healthy subjects felt warm and sweated (room temperature 32°C) a relatively intense SSA was recorded which decreased strikingly on indirect cooling. This may be explained by a high activity in sudomotor fibres which was inhibited by cooling.

Simultaneous recordings of skin temperature and SSA. When the subject was relaxed and skin temperature equilibrated with the room temperature spontaneous skin temperature fluctuations were minimal and did not exceed 0.1°C over periods of 1–2 min. No clear correlation could be seen between such small occasional changes and sympathetic bursts occurring spontaneously. In contrast when the SSA increased in response to stimuli such as strong arousal stimuli a few repeated deep breaths, mental stress etc. skin temperature decreased in a well defined way which was easy to differentiate from the small spontaneous fluctuations. Fig. 3 shows two examples of the relationship between sympathetic nerve response and the ensuing temperature reaction. It can be seen that the sympathetic nerve responses appear within a second after the beginning of the stimulus and last only a few seconds. The

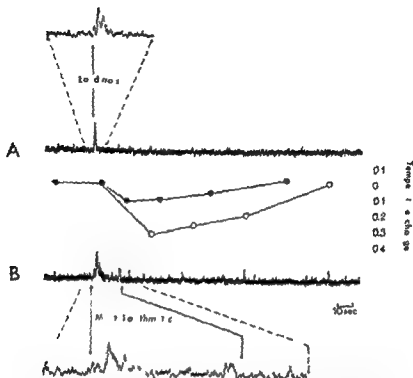


Fig. 3. Two examples of simultaneously recorded evoked SSA and skin temperature changes in a healthy subject. The integrated nerve record in *A* shows the SSA activity elicited by a sudden loud noise. The corresponding temperature change is indicated by filled circles. The upper insert shows part of the nerve record (6 1/2 seconds) with the induced response on an expanded time scale. *B* shows the effect of mental arithmetic. The corresponding temperature record is indicated by the open circles. The lowest tracing shows part of the nerve record (1/2 seconds) on an expanded time scale. Nerve recording from median nerve fascicle and skin temperature recording from the hand within the innervation zone of the unpaired fascicle. Zero on the temperature scale is equivalent to 32 °C.

temperature change which were continuously observed on the colour monitor screen had latencies of about 10–20 s, were maximal after about 30 s and lasted 2–5 min. Mental arithmetic, which constituted a stimulus of longer duration, caused a stronger and more sustained nerve response than the loud noise and also led to a more pronounced temperature reaction (Fig. 3 *B*). Short stimuli such as a single deep breath or a loud noise, which regularly caused a decrease in skin electrical resistance, were not usually followed by detectable temperature changes.

The paraplegic subject

Skin nerve sympathetic activity. During the search for SSA in the paraplegic patient, skin nerve fascicles were identified by the afferent mechanoreceptor discharges that could be evoked by tactile stimuli within the receptive field of the unpaired fascicle. After some probing, sympathetic activity was found in two recording positions in fascicles innervating the skin of the sole of the foot. In one electrode position it was

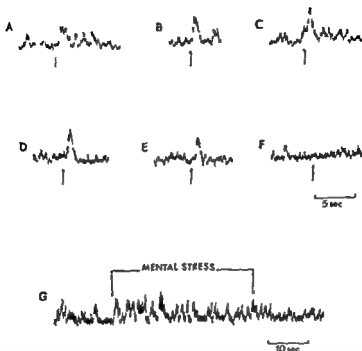


Fig 4 Examples of sympathetic skin nerve responses in the paraplegic patient evoked by A deep breath B external pressure on the thorax C pinching of the skin of the arm D loud noise E electrical stimulation of the skin of a finger F electrical stimulation of the sole of the left foot G mental stress (stressing conversation) Recording from the right posterior tibial nerve

possible to obtain a stable recording for approximately 60 min and during this time several manoeuvres were carried out to establish the characteristics of the nerve activity and the relation between this activity and changes in skin temperature.

The SSA had the same characteristics and prevalence as that recorded in the normal subjects. Spontaneous bursts occurred irregularly and it was possible to induce sympathetic responses to a variety of different stimuli. Fig 4 shows examples of the bursts that were elicited by a single deep breath (A), a sudden pressure on the chest (B), a sudden pinch on the arm (C), a loud noise (D) or by an electric shock to the skin of a finger (E). In contrast to stimuli applied to skin areas above the level of the lesion, no responses were obtained on pinching or electrical stimulation of the skin of the legs, i.e. in areas deprived of their somato-sensory connection with the brain (F). More intense and sustained responses were elicited by mental stress brought about by stressing conversation or by suddenly asking the subject to perform mental arithmetic (Fig 4G). As in healthy subjects, some of the spontaneous and all the reflexly induced sympathetic bursts were followed by transient decreases of skin electrical resistance within the innervation zone of the impaired fascicle.

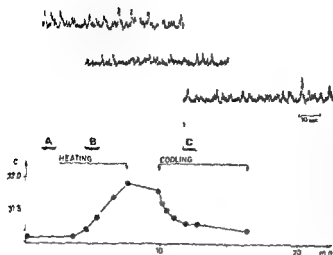


Fig. 5. Simultaneous recordings of SSA and skin temperature in the paraplegic patient during indirect heating and cooling. Nerve records from the right posterior tibial nerve. Skin temperature record from the sole of the right foot. The integrated nerve records shown in the upper 3 tracings were obtained during the time periods marked A, B and C in the temperature diagram. Room temperature 26°C.

Simultaneous recordings of skin temperature and SSA Fig. 2 illustrates the effect of mental stress on the skin temperature of the sole of the foot. The temperature decreased by 0.3°C in a temporal pattern that was similar to that in the healthy subjects (Fig. 3).

The results of simultaneous recordings of skin temperature in the sole of the foot and SSA in the posterior tibial nerve during indirect heating and cooling are shown in Fig. 5. Before the start of the heating the intensity of the SSA was relatively high and the patient felt cold but was not shivering (A). Upon heating skin temperature rose by 0.8°C, the patient started to feel comfortably warm and concomitantly the intensity of the SSA decreased (B). During subsequent cooling the skin temperature fell and the intensity of the nerve activity increased again (C).

Discussion

The sympathetic nature of the nerve activity

The nerve activity recorded in this study was identified as SSA according to characteristics given by Hagbarth *et al.* (1972) and Delius *et al.* (1972c). When human SSA was described by these authors, the evidence for the sympathetic origin of the impulses was discussed in detail. Since evoked neural bursts were followed by reductions in skin electrical resistance and/or plethysmographic evidence of skin vasoconstriction, they suggested that the SSA consisted of a mixture of sudomotor and vasoconstrictor impulses. They also found that the nerve activity was altered in a characteristic way by stimuli altering the emotional state of the subject and also by cooling and heating the subject. Furthermore, it has been shown that the impulses are conducted in efferent fibres at a velocity of slightly less than 1 m/s (Hallin and Torebjörk 1974) and that they can be reversibly blocked by sympathetic ganglion blocking agents (Hagbarth *et al.* 1972; Wallin *et al.* 1973).

In the present study blocking experiments or determinations of the conduction velocity were not considered necessary. There were several other characteristics which agreed so closely with those previously described for efferent SSA that there was no doubt that the activity recorded was of the same nature.

The SSA recorded in the paraplegic patient did not differ from that of the healthy subjects. Thus it can be concluded that normal efferent sympathetic function may be preserved below the level of a complete transverse lesion of the spinal chord. This is in agreement with the findings of Cooper *et al* (1957), who recorded vasomotor responses by means of plethysmography and found that patients with lesions between Th VI and L I could have preserved vasomotor function in the feet even though the feet were deprived of sensibility and motor function. The results can be explained by the special anatomical arrangement of the sympathetic nervous system where the sympathetic chain provides a route by passing a complete spinal lesion.

Correlation between skin temperature changes and SSA. In both healthy and paraplegic subjects arousal stimuli and mental stress gave rise to prompt short lasting increases in SSA which in turn were followed by skin temperature reductions within the innervation zone of the impaled fascicle. Since sweat evaporation was prevented there is little reason to doubt that such temperature changes were due to skin vasoconstriction brought about by increased sympathetic vasoconstrictor activity contained in the multi-unit nerve responses. The decreases in skin temperature were maximal after about 30 s and had a total duration of several minutes. This is a slow and protracted reaction compared to plethysmographically measured blood flow changes brought about by similar stimuli (Mulinos and Shulman 1939; Abramson and Ferns 1940; Wilkins and Eichna 1941; Goetz 1946; Thron *et al* 1960; Delius and Kellerova 1971). For example Delius and Kellerova (1971) found that a deep breath evoked cutaneous vasoconstriction lasting about 20 s in resistance (arterial) vessels and 60 s or more in capacitance (venous) vessels. The maximal responses occurred after 10 and 15/20 s respectively. The sluggishness of the thermographically measured responses compared to the plethysmographically measured ones is explained however by the insulating capacity of the skin tissues which will attenuate and delay all skin surface temperature changes due to blood flow variations. This inertia probably also explains why weak sympathetic bursts did not usually produce detectable skin temperature decreases. The present findings illustrate that recordings of sympathetic effector organ responses always will give incomplete and depending on the recording method more or less distorted pictures of the dynamic variations of the sympathetic outflow seen in direct nerve recording.

The skin temperature changes obtained during indirect heating and cooling (Fig. 5) were more pronounced than those after arousal stimuli and the amplitudes and rates of change were similar to the changes induced during the thermographic procedure for assessing CTR (Normell 1974). The fact that variations in SSA were recorded during arousal stimulation and thermal stimulation with the recording needle in the same position indicates that sympathetic efferent pathways mediate various types of temperature changes, i.e. both small changes after arousal stimuli and larger changes such as in CTR.

This work was supported by grants from Lisa och Johan Grönbergs Stiftelse and Swedish Medical Research Council (B73 01\ 3516 02\). We thank Lars Lofstedt for technical assistance.

References

- ABRAMSON D I and L B FERRIS Responses of blood vessels in the resting hand and forearm to various stimuli *Amer Heart J* 1910 19 541-553
- BAZETT H C L LOVE M NEWTON I EISENBERG R DAY and R FORSTER II Temperature changes in blood flowing in arteries and veins in man *J appl Physiol* 1918 1 3-19
- BENZINGER T H Heat regulation Homeostasis of central temperature in man *Physiol Rev* 1969 49 702-703
- BURTON A C Temperature of skin Measurement and use as index of peripheral blood flow In *Methods in Medical Research* Chicago The Year Book Publishers Inc 1 148 1948
- CHESID J G *Correlative and Functional neuroanatomy* Lange Medical Publications Los Altos California 1970
- COOPER K E A W CROSS A H M GREENFIELD D MCK HAMILTON and H A SCARborough Comparison of methods for gauging the blood flow through the hand *Clin Sci* 1919 8 217-234
- COOPER K E HELLEN M FERRIS and L GUTTMAN Vasomotor responses in the foot to raising body temperature in the paraplegic patient *J Physiol (Lond)* 1957 106 517-555
- DELIS W and E KELLERMAN Reactions of arterial and venous vessels in the human forearm and hand in deep breath or mental stress *Clin Sci* 1971 40 271-282
- DELIS W K E HAGBARTH A HONGELL and B G WALLIN General characteristics of sympathetic activity in human muscle nerves *Acta physiol scand* 1972 a 84 65-81
- DELIS W K E HAGBARTH A HONGELL and B G WALLIN Manoeuvres affecting sympathetic outflow in human muscle nerves *Acta physiol scand* 1972 b 84 82-91
- DELIS W K E HAGBARTH A HONGELL and B G WALLIN Manoeuvres affecting sympathetic outflow in human skin nerves *Acta physiol scand* 1972 c 84 177-186
- FELDER D E RUSSELL H MONTGOMERY and O HORWITZ Relationship in the toe of skin surface temperature to mean blood flow measured with a plethysmograph *Clin Sci* 1954 19 251-258
- GOPPE R H The rate and control of the blood flow through the skin of the lower extremities *Brier Heart J* 1916 31 146-182
- HAGBARTH K E and A B VALLBO Pulse and respiratory grouping of sympathetic impulses in human muscle nerves *Acta physiol scand* 1968 74 96-108
- HAGBARTH K E R G WALLIN A HONGELL H E TONERJÖRN and B G WALLIN General characteristics of sympathetic activity in human skin nerves *Acta physiol scand* 1972 84 144-176
- HALLIN R C and H E TONERJÖRN Single unit activity in sympathetic fibers in human skin nerves 1974 To be published
- MILLING M C and I SHULMAN Vasoconstriction in the hand from a deep inspiration *Amer J Physiol* 1979 129 310-322
- NORMELL L A Recording of normal and impaired cutaneous thermoregulatory vasomotor response by infra red thermography *Scand J clin Lab Invest* 1973 33 Suppl 138
- SHEARD C Temporal regulation of skin and thermal regulation of the body In *Medical Physics* ed by C Clin 1 1523 Chicago Year Book Publishers Inc 1911
- THRON H L K D SIEFFERT and A HINTZE Über das Verhalten der Kapazitäten und der Widerstände der menschlichen Hand im Verlaufe einer durch tiefe willkürliche Inspiration ausgelösten peripheren Vasoconstriction *Pflügers Arch ges Physiol* 1960 270 239-50
- WALLIN B C W DELIS and K E HAGBARTH Comparison of sympathetic nerve activity in normotensive and hypertensive subjects *Circul Res* 1973 33 9-21
- WILKINS R W and J W EICHEN Blood flow to the forearm and calf *Bull Johns Hopk Hosp* 1941 68 425-441

Pulmonary Receptor Recording *in vitro*

By

G W BRADLEY¹

The recording of afferent activity from pulmonary receptors *in vivo* has led to the recognition of a few distinct types of receptors with specific properties. However, the precision with which the linkage between the mechanical event in the lung and the stimulation of the receptor can be studied is limited by continuous gas exchange and blood flow within the lung. The current paper describes a technique by which these problems can be overcome by recording activity from pulmonary receptors *in vitro*.

The chest wall of an anesthetized cat was widely opened and the animal ventilated with 100% oxygen. The trachea was then occluded at end expiration and a lethal dose of Nembutal given. The circulation persisted for long enough to allow the absorption of all the trapped oxygen with consequent collapse of the lungs. The right lung and bronchus together with the trachea and the left bronchus were then quickly removed, care being taken not to damage the right vagus nerve or its pulmonary branches. No attempt was made in the present experiments to preserve the pulmonary circulation intact.

A cannula was inserted into the trachea and the left bronchus tied. The lung was then immersed in a modified Krebs solution (0.150 M NaCl, 0.006 M KCl, 0.002 M CaCl₂, 0.001 M KH₂PO₄, 0.006 M glucose and 0.024 M NaHCO₃) at 37°C which was oxygenated and maintained at a physiological pH by bubbling a mixture of 95% oxygen and 5% carbon dioxide through it. The lung could be inflated with a similar solution to a volume that varied with the experimental procedure. The right vagus nerve was lifted up into liquid paraffin floating on top of the Krebs solution and single fibre activity could then be recorded after dissection of the nerve on a stainless steel platform. The whole procedure could be completed in 20 min and activity recorded for up to 4 h after the death of the animal.

A typical example of a pulmonary stretch afferent discharge is shown in Fig. 1. The frequency of discharge increases with lung inflation and adapts only slowly (see Adrian 1933). This type of activity was by far the most common. In some preparations the discharge pattern remained stable for up to 4 h although in the

¹ Present address: Centre for Respiratory Investigation, Glasgow Royal Infirmary, Glasgow, Scotland.

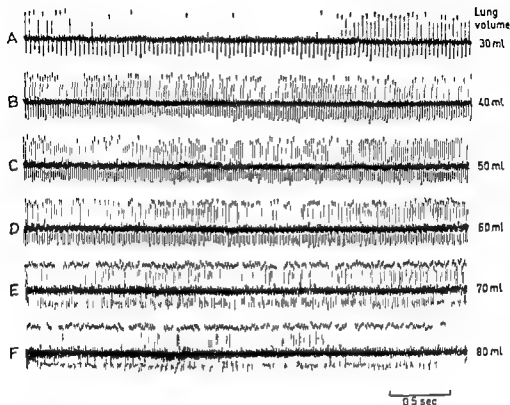


Fig 1 Response of a pulmonary stretch afferent discharge to volume inflation. Lung volumes are measured from the collapsed position. The frequency of discharge was as follows: 30 ml 30 imp/s, 40 ml 52 imp/s, 50 ml 64 imp/s, 60 ml 79 imp/s, 70 ml 97 imp/s and 80 ml 108 imp/s.

majority of cases the discharge became irregular before this time. The onset of irregular activity was usually preceded by a sudden increase in discharge frequency; the irregular activity lasting only a few minutes before electrical silence supervened.

A longer lasting irregular activity was recorded from a few fibres. They showed only a transient response to maintained lung inflation but showed an increase in discharge frequency when histamine was put into the intrapulmonary fluid. They appeared to have the properties of irritant receptors as described by Mill, Sellick and Widdicombe (1969). The effect of histamine and lung inflation on such a discharge can be seen in Fig 2.

J receptor discharge (Paintal 1969) has not so far been identified.

This work was undertaken during tenure of a Swedish Wellcome travelling research fellowship. The encouragement and advice of Prof C. von Euler is gratefully acknowledged. The work has been supported by grants from Karolinska Institutets Fonder and Swedish Medical Research Council project 14X 544.

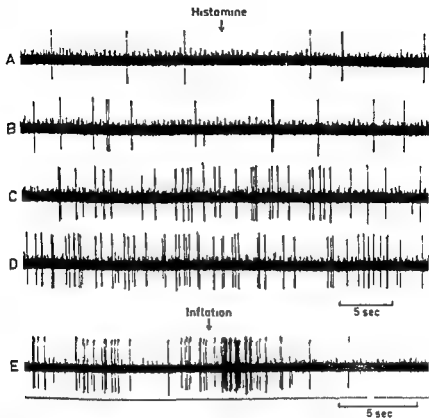


Fig. 2. Irritant receptor discharge. Records A, B, C and D are continuous 750 μ g histamine were added to the intrapulmonary fluid at arrow shown. Record E shows the response to a 20 ml volume inflation.

References

- ADRIAN, E. D. Afferent impulses in vagus and their effect on respiration. *J. Physiol. (Lond)* 1933, 224, 122—126.
- MILLS, J. E. H., SELICK, J. G. and WIDDICOMBE. Activity of lung irritant receptors in pulmonary emboli in anaphylaxis and drug induced bronchoconstriction. *J. Physiol. (Lond)* 1969, 203, 337—357.
- PAINTAL, A. S. Mechanism of stimulation of type J pulmonary receptors. *J. Physiol. (Lond)* 1969, 203, 511—532.

A Note on the Function of the Olfactory Organ of the Hagfish *Myxine glutinosa*

By

KJELL B DOVING and KAJ HOLMBERG¹

The Atlantic hagfish is found on the sea bottoms at depths from 30 to over 1000 m burrowing in the mud. Information about the function of the olfactory organ is largely based on observations on feeding reactions in the laboratory (Gustafson 1935) and in the natural habitat (Strahan 1963). Hagfish are caught by odorous baits and marking experiments indicate a population clustering with return from a release area back to the original catching site (Wahlg 1968 and personal communication). Light and electron microscopical studies on the hagfish olfactory organ (Theisen 1973) on the eye (Holmberg 1972) and the brain (Jansen 1930) indicate that the olfactory organ is the dominant receptor organ. Thus behaviour and histology point to the importance of the olfactory organ in providing the animal with a sensitive sense of smell. The present report is a preliminary description on some functional properties of the hagfish olfactory organ. A more detailed account on the physiology of this organ will appear at a later stage.

Newly caught specimens of hagfish *Myxine glutinosa* were kept in sea water at +4 °C. The animals were decapitated and the dental plates, the ventral tissues and the skin overlaying the dorsal surface of the olfactory organ removed (Fig. 1). Immobilization was secured by removing the brain. A plastic catheter was introduced into the nostril (the hagfish has only one nostril) and a flow of seawater of about 1 ml s⁻¹ at +14 °C was maintained through the olfactory organ.

We tested a variety of solutions of natural substances and 24 pure chemicals made up in the same seawater as used in the nostril flow, and stimuli were introduced by an injecting apparatus into the flow of seawater via a cannula. By varying the speed and amount of injected fluid any desired concentration could be applied. We made DC-recordings with saturated Ag/AgCl electrodes; one electrode was in contact with the flowing seawater, the other a glass electrode filled with seawater was placed on the dorsal surface of the olfactory organ.

Upon stimulation we observed a fast initial rise in potential followed by a decline to a steady level. When the stimulation ceased the potential dropped to the baseline. An example of a response is shown in Fig. 2 A. The polarity of the response was

¹ Present address: Department of Zoology, University of Stockholm, Sweden.



Fig 1 Drawing of the hagfish preparation in sagittal (A) and transverse (B) sections. The position of the transverse section through the olfactory organ is indicated by the vertical line in A. The recording electrode was placed in the middle of the dorsal surface of plane B.

such that the electrode on the olfactory organ went positive in relation to the electrode in contact with the flowing seawater indicating a depolarisation of the olfactory receptors in contact with the seawater. The response peak amplitudes of the olfactory organ to different concentrations of L-Alanine and L-Glutamine are plotted in Fig 2 B. As seen from the graph about 3 times the concentration is needed of L-Glutamine to elicit a response of the same amplitude as obtained with L-Alanine. Other substances found to be potent stimuli were glycine, aminobutyric acid, glutathione and 4-hydroxy L-proline.

We tested the size of the electrical response at different recording positions and found it to be largest in the middle of the olfactory organ. About 3 mm in front of the organ the response could no longer be detected. A continuous flow at a high concentration of KCl greatly diminished the response and eventually abolished it. Responses from the preparation were obtained during periods of 3 h of intermittent stimulation when the seawater was aerated. In view of the observations mentioned above we feel justified to consider the potential changes as a response of the olfactory organ to odours analogous to the electro-olfactogram (EOG) of the olfactory epithelium of other animals and analysed in detail by Ottoson (1956).

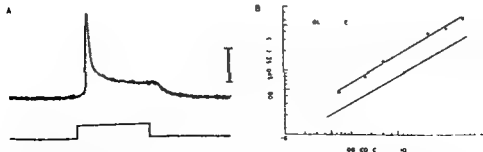


Fig 2 A Response of the olfactory organ of *Myxine glutinosa* to stimulation with $1.4 \cdot 10^{-4}$ M L-alanine. Stimulus duration and indicated by lower trace is 7.5 s. Vertical bar 0.2 mV.

B Relation between peak amplitude of the olfactory response and stimulus strength for 2 amino acids. Each point is the mean value obtained by 4 stimuli.

The preparation of the olfactory organ of hagfish is easily accomplished it is stable for a few hours artefacts are rare events and a multitude of substances can be feasibly tested at accurately determined concentrations. All these properties make it a suitable and attractive subject for odour research. It is hoped that the conveniences of the hagfish preparation make it useful in experiments on the vertebrate olfactory system in student classes.

We are grateful to forsteamanuensis Finn Walvig at the Biological Station University of Oslo Drøbak for supplying the hagfish and to the Swedish Natural Science Research Council for grant R 2935—002.

References

- GLSTAFSON G. On the biology of *Myxine glutinosa* L. *Acta Zool* 1935 28 1—8
- HOLMBERG K. Fine structure of the optic tract in the atlantic hagfish *Myxine glutinosa* *Acta ool* (Stockh.) 1972 53 165—171
- JANSEN J. The brain of *Myxine glutinosa* *J comp Neurol* 1930 49 339—307
- OTTOSSON D. Analysis of the electrical activity of the olfactory epithelium *Acta physiol scand* 1956 33 Suppl 172
- STRANDBY R. The behaviour of myxinooids *Acta zool* (Stockh.) 1963 44 73—102
- THEISEN B. The olfactory system in the hagfish *Myxine glutinosa* I. Fine structure of the apical part of the olfactory epithelium *Acta zool* (Stockh.) 1973 54 271—281
- WALVIG F. Experimental marking of the hagfish (*Myxine glutinosa* L.) *Nytt Mag Zool* 1968 15 35—39

Abstracts from Meeting of the Scandinavian Physiological Society in Oulu 21–22 May 1974

DEMONSTRATIONS

D 1

Changed Sensitivity of Cardiac α and β Adrenoreceptors in Rats following Cold Acclimation

By M N E HARRI, L MELENDER and R TIRRI *Zoophysiological Laboratory, Department of Zoology, University of Turku, Finland*

Cold acclimated rats show an increase in their metabolic response to noradrenaline (NA) (Jansky 1973). Recently it was shown however that cold acclimation results in a temporary decrease in the cardiac chronotropic sensitivity to NA *in vivo* (Tirri *et al.* 1974). In the present study the chronotropic sensitivity of the heart to sympathomimetic amines following cold exposure of rats was studied *in vitro* by using isolated atria. In addition to NA isoprenaline (ISO) and phenylephrine (PHE) as selective β and α stimulants respectively were used.

The basic contraction rate of isolated atria in 37°C Tyrode's solution was 238 beats/min in control rats. Following the exposure of rats to cold (5°C) the rate decreased to 196 beats/min in 7 days and returned to the initial level in 40 days of prolonged cold acclimation.

Cold acclimation did not change the chronotropic sensitivity of isolated atria to ISO measured as the ED₅₀ values of the cumulative dose response curves. Cold exposure for 7 days shifted the dose response curve for NA to the right. The ratio of ED₅₀ of rats acclimated to cold for 7 days to ED₅₀ of control rats was 3.1. This means that cold acclimation for a week decreased the sensitivity of isolated atria by 3.1 times. Cold exposure for 4 and 7 days lowered the sensitivity to PHE by 4.5 and 2.8 times respectively. After 40 days of prolonged cold acclimation the ED₅₀ values did not differ from those of the control animals any more. However the maximum responses to ISO and to NA but not to PHE were now significantly increased.

It is concluded that the lowered chronotropic sensitivity of isolated atria to PHE and to NA after a week's cold exposure results from a decreased sensitivity of cardiac α adrenoreceptors. On the other hand the increased maximum responses to ISO and to NA after 40 days of cold acclimation could be regarded as an increase in the responsiveness of β receptors.

References

- JANSKY, L. *Brit. J. med. Sci.* 1973, 48, 85.
TIRRI, R., M. N. E. HARRI and L. LAHTINEN. *Acta physiol. scand.* 1974, 90, 260–266.

Role of Superficially Bound Ca for Potassium Contracture in Rat Portal Vein

By BENGT UVELIUS, STEFAN M. SIGURDSSON and BORJE JOHANSSON *Department of Physiology and Biophysics University of Lund Sweden*

Fast and slow components in the contractile responses of smooth muscle to various stimulating agents have been attributed to different sources of activator calcium (e.g. Imai and Takeda 1967, Collins Sutter and Teiser 1971, Strin and Bohr 1971, Steinsland Furchgott and Kirpekar 1973). The rat portal vein appears to be critically dependent on extracellular Ca for activation as spontaneous activity is abolished within 3 min of exposure to nominally Ca free solution and responsiveness to K⁺ or noradrenaline is lost within 5 min. The present experiments indicate however the existence of a tissue bound pool of Ca available for contraction but depleted at a relatively slower rate during exposure to Ca free medium. Isometric responses to K⁺ high solution with 2.5 mM Ca were studied after variable periods in Ca free normal medium. A slow contraction with a consistently repeatable time course was found with Ca free periods of 30 min or more (Fig. 1A). With shorter exposure to Ca free solution a faster phase of tension development was observed the rate of which was inversely related to the duration of the Ca free period (Fig. 1A). In the individual preparation the ultimate level of contracture force was about the same irrespective of the previous treatment. Fig. 1B which shows the responses as a percent of the values for the lowest curve at the respective times in Fig. 1A illustrates how the magnitude of the fast component decreases with prolonged exposure to Ca free medium. We conclude that the slow contraction obtained after 30 min or more depends on influx of extracellular Ca whereas the fast component reflects release of Ca from a superficial pool. The fact that Ca free K⁺ high solution fails to induce contraction already after 5 min indicates that the above fast phase represents regenerative release of Ca.

References

- COLLINS G. A., M. C. SUTTER and J. C. TEISER *Can. J. Physiol. Pharmacol.* 1971 **50** 789-799
 IMAI S. and K. TAKEDA *J. Physiol. (London)* 1967 **190** 155-169
 STRIN M. M. and D. F. BOHR *Amer. J. Physiol.* 1971 **220** 1124-1128
 STEINLAND O. M., R. M. FURCHGOTT and S. M. KIRPEKAR *Circ. Res.* 1973 **32** 49-58

D 3

The Hyperpolarisation of Motoneurons by Electrophoretically Applied Amines and Other Agents

By I. ENGBERG, J. A. FLATMAN and K. KADZIELAWA *Institute of Physiology University of Aarhus Denmark*

The transmitter function of biogenic amines in the mammalian central nervous system has been the subject of several studies. Excitatory as well as depressant effects on nerve cells by microelectrophoretically applied noradrenaline, serotonin and

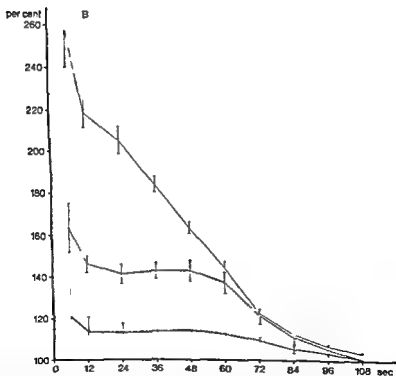
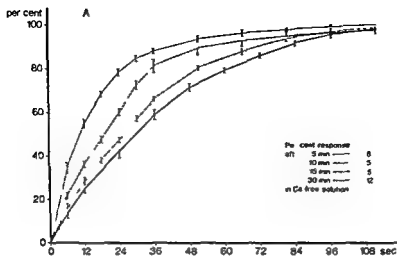


Fig. 1 A Time course of contracture force in per cent of the ultimate value elicited by 100 mM K^+ and 2.5 mM Ca^{2+} after different periods in Ca free medium. Vertical bars represent S.E. B The upper curves in A expressed as a percent of the respective values for the lowest (30 min) curve.

dopamine have been reported, but little is known about the mechanisms of these actions. Intracellular recording has revealed that noradrenaline hyperpolarises motoneurons with a concomitant increase in membrane resistance (Engberg and Marshall 1971, 1973). The hyperpolarization is proportional to the initial membrane potential of the cell (as set by intracellular current injection) and reverses to depolarization at a membrane potential of approximately -20 mV. The increase in membrane resistance reflects a decrease in permeability for one or more ions. A decrease in the Na permeability would cause hyperpolarization. The findings are in contrast with the classical view of inhibitory synaptic mechanisms in the central nervous system.

Extending the above investigations we have found that microelectrophoretically applied noradrenaline, dopamine, octopamine, isoprenaline and serotonin all hyperpolarize motoneurons in a similar way. Both α and β receptor blockers (thymoxamine, propranolol, sotalol, pindolol) do in some cases interfere with the actions of noradrenaline and dopamine as do the neuroleptics chlorpromazine and haloperidol. However, the hyperpolarization produced by these compounds makes assessment of the blockade difficult.

The apparent lack of pharmacological specificity of the amines used in our tests may be due to an indirect action via the liberation of noradrenaline from presynaptic terminals. However, we find that not only amines but also H ions (cf. Marshall and Engberg 1973) and particularly Ca^{++} ions hyperpolarize motoneurons and increase membrane resistance. It is conceivable that all these substances could act directly on charged groups at the membrane thereby influencing the ion permeability. On the other hand it has been suggested that Ca^{++} ions mediate the inhibitory effects of biogenic amines (Phillis *et al.* 1973). We have tested, preliminarily, the chelating agents EDTA and EGTA on motoneurons. EDTA caused a reversible depolarization possibly due to a removal of Ca^{++} . It sometimes blocked the effects of noradrenaline. EGTA did not depolarize but occasionally blocked the effects of Ca^{++} and noradrenaline or dopamine.

References

- ENGBERG I and K. C. MARSHALL *Acta physiol scand* 1971 83 142-144
 ENGBERG I and K. C. MARSHALL *J Gen Physiol* 1973 61 261
 MARSHALL K. C. and I. ENGBERG *Proc Can Fed Biol Soc* 1973 16 33
 PHILLIS J W., N. LAKE and G. YARBROUGH *Brain Research* 1973 53 465-469

D 4

The First Breath

By L. HIRVONEN, R. PELTONEN and T. PELTONEN *Department of Physiology, University of Oulu and Cardiorespiratory Research Unit, University of Turku, Finland*

The rapid transition of the fetus from intrauterine to extrauterine life allows a minimum of time for establishing lung function suitable for gas exchange. The fetal lungs secrete a liquid that fills the future air spaces.

The aeration of the lungs and disappearance of the tracheobronchial fluid was observed by roentgen cinematography in the human baby and the lamb. The film demonstrates the changes in the chest cage and bronchi during the first breath. Pulmonary vessels were visualised by cineangiocardiology before and after the first breath. Simultaneous pressure recordings from pulmonary and systemic circulation were made. In *in utero* conditions the tracheobronchial fluid flows periodically with net outward flow. The fetus swallows it. High blood pressure and scanty blood flow characterise the fetal pulmonary circulation. The duration of the initial phase of the first breath varies. In asphyctic fetus several unsuccessful trials to inspire may be needed but once started the aeration spreads within a period of less than 1 s throughout the lungs. In bronchography the contrast medium injected intratracheally before the first breath spreads up to the alveolar level simultaneously with the aeration of the lungs. Liquid in the pharynx is swallowed. Right ventricular blood pressure falls about 15 mm Hg below the fetal level. The volume of the tracheobronchial tree increases during the first inspiration. When *tegnesium* in saline solution is injected into the bronchi the left heart is visualised within 5 s by gamma camera registration.

It is concluded that the tracheobronchial fluid disappears primarily by absorption into the pulmonary capillaries. Swallowing plays a major role in the elimination of the liquid in the upper airways.

D 5

Renal Cortical Blood Flow during Dehydration in Dogs

By A. KIRKEBO and I. TYSSZBORN *Institute of Physiology, University of Bergen, Norway*

This investigation was performed to study the possible heterogeneity of renal cortical blood flow during dehydration.

Twelve dogs were dehydrated by 200 mg etacrynic acid given orally 24 h before start of the experiments in pentobarbital anesthesia. Total renal blood flow (RBF) and local cortical blood flow were recorded before and after further dehydration by peritoneal dialysis with 7% glucose in saline. Local cortical blood flow was measured by hydrogen clearance recorded simultaneously from 3 platinum electrodes inserted in the outer cortex and 3 electrodes in the inner cortex. RBF was measured by electromagnetic flowmeter.

Etacrynic acid reduced the body weight by 10% and increased hematocrit to 45%. The local blood flow in outer cortex averaged $3.29 \pm \text{SD } 0.80$ ml/min/g and in inner cortex $2.40 \pm \text{SD } 0.47$ ml/min/g giving a ratio of 1.37. Compared to measurements in normally hydrated dogs, flow was significantly reduced in inner (30%) but not in outer cortex (Aukland *et al.* 1973).

After peritoneal dialysis to a mean hematocrit of 60 the average outer cortical flow was reduced to 1.95 ml/min/g and inner cortical flow to 1.41 ml/min/g still showing a ratio of 1.35.

Sudden reductions in desaturation rate at one or more electrode sites were observed in 13 out of 14 expts, indicating marked reductions in local blood flow. Flow remained low zero or up to 80 % of preceding value for 1–60 min and then suddenly rose to preceding value or even higher. These sudden flow changes occurred both in outer and inner cortex, randomly at different electrode sites.

References

- AUKLAND K, A KIERKEBØ E, LOYNING and I TYSSEBØ. Effect of hemorrhagic hypotension on the distribution of renal cortical blood flow in anesthetized dogs. *Acta physiol scand* 1973 87 514–525.

D 6

Stress Induced Ulcer in Spontaneously Hypertensive Rats

By MARGARETA HALLBACK, G MAGNUSSON and LILIAN WEISS. *Department of Physiology, University of Göteborg, Sweden*

Spontaneously hypertensive rats (SHR) display accentuated cardiovascular responses compared with normotensive control rats (NCR) when exposed to acute mental stress (Hallback and Folkow 1974). Thus a more pronounced involvement of the defence reaction which implies an overall sympathetic discharge combined with withdrawal of cardiac vagal tone was observed in SHR, evident as more pronounced increases in both pressure and heart rate compared to NCR.

To evaluate whether mental stress influences SHR more profoundly also concerning other autonomically innervated systems such as the gastrointestinal tract which is predominantly controlled by the parasympathetic nervous system, the incidence of gastric ulcers induced by immobilization stress was studied in SHR and NCR. Even though the exact etiology of such ulcers is not clear, an increased gastric acidity and motility, perhaps combined with impaired mucosal circulation, is of great importance. Vagally mediated influences seem to constitute the key mechanism, since parasympathetic blockade greatly reduces the stress ulcer incidence (Brodie 1968), while sympathetic blockade is of little relevance.

For such purposes 53 SHR and 51 NCR (Wistar, 8 weeks old, both sexes) with blood pressures of 143 ± 2 mm Hg and 108 ± 2 mm Hg respectively were immobilized in metal sheet cylinders for 12 h after a 24 h fasting period. After immobilization stress the rats were killed and the glandular part of their ventricles was inspected for ulcers. Blood pressure was followed during 8 h of immobilization stress in 26 animals, showing a significantly ($p < 0.001$) more pronounced pressure rise in SHR than in NCR (48 ± 5 mm Hg vs 25 ± 2 mm Hg). However, the incidence of gastric ulcers in SHR and NCR did not differ significantly (Chi square test) being 49 % in NCR and 45 % in SHR. To eliminate sympathetic influences on mucosal circulation, 13 SHR and 13 NCR received guanethidine (25 mg/kg/day) for 4 days before and during the immobilization stress, but no significant difference was noticed concerning ulcer formation either between SHR and NCR or between treated and untreated rats.

This implies that centrally mediated autonomic responses to stress seem to affect the vagal control of the gastro-intestinal system to about the same degree in SHR and NCR. Thus the SHR hyperreactivity concerning the adrenergically conveyed defence reaction is apparently not paralleled by any general central hyperreactivity involving also vagally mediated excitatory responses to mental stress

References

- BRODIE D A Experimental peptic ulcer *Gastroent* 1968 50 125—134
HALLBACK M and B FOLKOW Cardiovascular responses to acute mental stress in spontaneously hypertensive rats *Acta physiol scand* 1974 In press

D 7

The Binding of Insulins from Different Animal Species to Rat Fat Cell Receptors
By S GAMMELTOFT and J GLIEMANN *Institute of Medical Physiology C
University of Copenhagen Denmark*

It is generally believed that the cellular actions of insulin are mediated through binding to specific receptors located in the cell membrane (Freychet *et al* 1971 Cuatrecasas 1971). We have shown that isolated rat fat cells possess a major group of receptors with a dissociation constant of 3 nM in a number of 50 000 per cell (Gammeltoft and Gliemann 1973).

In the present study we have determined the binding affinity (i.e. the ability to inhibit the binding of ^3I labelled insulin to fat cell receptors) and the biological potency (i.e. the concentration of insulin required to produce half maximal stimulation of lipogenesis from $2\text{-}^3\text{H}$ glucose in isolated fat cells) of some insulins from different animal species.

It was found that a change in the biological activity relative to porcine insulin was always in agreement with the change in the receptor binding affinity relative to porcine insulin. This finding confirms our previous results on chemically or enzymatically modified insulins (Gliemann and Gammeltoft 1974).

Decreased values of the biological activity and the binding affinity (in % of porcine insulin) was found for insulins from the following animals: Duck (46) hamster (29) rat insulin I (13) and II (53) guinea pig (2) chinchilla (29) and goose fish (24). In contrast insulin from turkey which has been reported to be more potent in rat fat cells than bovine insulin (Weitzel *et al* 1972) showed an increased biological activity and receptor binding affinity relative to porcine insulin (230 %) (Fig. 1). Insulin from chicken has also been reported to exhibit increased activity and binding affinity (Freychet personal communication).

The results are discussed on basis of 1) the primary and tertiary structure of insulin and 2) the nature of the receptor binding.

References

- FREYCHET M I ROTH and D M NEVILLE JR. *Proc Nat Acad Sc U.S.A* 1971 68 1833—183

RECEPTOR BINDING OF INSULIN

PORCINE —●— TURKEY —○—

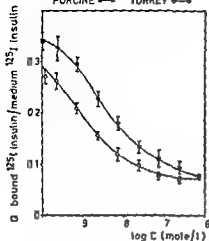


Fig 1 Binding affinity of turkey insulin Isolated fat cells (10 μ l/ml) were incubated at 37 °C with 125 I labelled insulin 0.7 nM either alone (■) or in the presence of porcine insulin (●—●) or turkey insulin (○—○) in the indicated concentrations After 45 min the cells were separated from the buffer by centrifugation through dinonyl phthalate (Gliemann *et al* 1972) Mean \pm S.D. (n = 6)

CUATRECASAS P *J Biol Chem* 1971 246 7265—7274

GAMMELTOFT S and J GLIEMANN *Biochim Biophys Acta* 1973 330 16—32

GLIEMANN J and S GAMMELTOFT *Diabetologia* 1971 10 103—115

WEITZEL G R, RENNER W, KENNELER and K RAYER *Hoppe Seylers Z physiol Chem* 1979 353 980—986

GLIEMANN J, A ØSTERLIND J, VINTEN and S GAMMELTOFT *Biochim Biophys Acta* 1972 286 1—9

D 8

The Relation between Firing Frequency and Input Current in a Nerve Cell Model Based upon a Simplified Form of Hodgkin Huxley's Equations

By E SKALGEN *Departments of Physics and Physiology University of Oslo Norway*

In many nerve cells the membrane shows a more linear response to a subthreshold input current pulse than the giant squid axon described by Hodgkin and Huxley (1952). In these cases a simplified form of Hodgkin—Huxley's equations can be used to describe the nerve membrane. Analytical solutions can then be obtained which in the simplest case are of the form $f = (A \ln(1+B/(1-I_T)) + I)^{1/2}$ (1) where f is the firing frequency and I the input current. A , B , I_T and I are constants determined by measurable membrane properties.

These equations can also be solved in the case of a long term change of the potassium conductance or in the case of an electrogenic Na/K pump. The latter case is the simplest and the steady state current frequency relation can then be given by $I = B \exp(1/(I - I_T)/A)^2 + kI + I_T$ (2) where the symbols f , A , B , I_T , I are the same as in equation (1) and the constant k is determined by the Na/K pump.

The model corresponds well to the behaviour of many types of nerve cells for instance the crayfish stretch receptor. With a step increase of the input current the

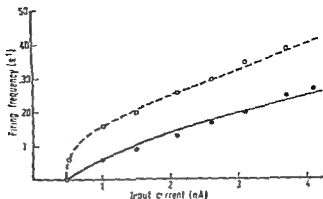


Fig 1 Current frequency relationship in a stretch receptor neuron and in the model

firing frequency increases rapidly, but then decreases to a steady level (adaptation). The figure shows the current frequency relationship of the model when membrane properties of the crayfish stretch receptor are used. An electrogenic Na/K pump is assumed. The experimental points are taken from Sokolov (1972). The unbroken line gives the steady state firing frequency with a constant input current (Experiment filled circles). The broken line gives the firing frequency at the beginning of a sudden increase of the input current from zero to the value shown on the current axis (Experiment open circles).

It is concluded that this model seems to give a simple and quantitative description of the current frequency relationship in some nerve cells.

References

- HODGKIN A. L. and A. F. HUXLEY *J. Physiol.* 117 500
 SOKOLOV P. C. *Biophysical J.* 12 1429

D 9

Linear Subtractive Inhibition produced by Summation of Individual IPSPs

By FEVSTAD G. A. NJA and L. WALLOE *Departments of Mathematics
 Physiology and Physics University of Oslo Norway*

Several authors have reported cases of recurrent inhibition in which the inhibitory effect was proportional to the frequency of firing in the inhibitory fibres over a considerable range (Hartline and Ratliff 1957; Grant and Reinken 1961). Also a constant frequency of firing in the inhibitory fibres caused a constant reduction in the frequency of firing in the cells that were inhibited independent of their level of excitation prior to the onset of the inhibition.

These phenomena are also characteristic for the recurrent inhibition of the slowly adapting stretch receptor neuron of the crayfish. Intracellular recordings from this neuron (Jansen *et al.* 1971) suggest a simple model for the summation of excitation and inhibition. In this model each action potential in the recepto-

neuron is followed by a prepotential increasing from the peak of the afterhyperpolarization to the firing threshold as a linear function of time. Each IPSP instantaneously resets the prepotential to the level of the peak afterhyperpolarization. From this point the prepotential increases again, at just the same rate as after an action potential. This prepotential may either proceed to fire an action potential or it may be interrupted by another IPSP. Receptor firing is always followed by an IPSP with a latency that is k times the duration of an uninterrupted prepotential (t_0). In addition the firing of neighbouring stretch receptors causes IPSPs to occur according to a Poisson point process with mean frequency λ . It can be shown that the mean frequency reduction that is caused by inhibition from the neighbouring stretch receptors in this model of the stretch receptor neuron is

$$\Delta f = \frac{1}{(k+1)t_0} - \frac{1}{kt_0 + \frac{1}{\lambda}(e^{kt_0} - 1)} \quad 0 < k < 1$$

This formula predicts the experimental results with a fair degree of accuracy. It is therefore concluded that the linear properties of the recurrent inhibition in the slowly adapting stretch receptor neuron can be accounted for by the time pattern of the individual IPSPs if the action of each IPSP mainly is to reset a large area of the membrane to a potential close to the level of the peak afterhyperpolarization.

References

- HARTLINE H. K. and F. RATLIFF *J. Gen. Physiol.* 1957 **40** 357-376
 CRANIT R. and B. RESKIN *J. Physiol. (Lond.)* 1961 **158** 461-475
 JÄNSEN J. F., S. A. NIELSEN, K. ØRNSTAD and L. WALLOE *Acta physiol. scand.* 1971 **81** 473-483

D 10

The Kinetics of Splanchnic Elimination of Ethanol and Glycerol in Cats and Related Metabolic Effects

By N. KRARI, J. A. LARSEN and C. OLSEN, *Institute of Physiology, University of Aarhus, Denmark*

In experiments on 8 chloralose anesthetized fasting cats the blood concentration of ethanol or glycerol was raised to about 8 mM by an iv. priming dose and blood samples were then drawn at regular intervals from a femoral artery and a hepatic vein. Hepatic blood flow (HBF) was estimated by Indocyanine Green given continuously. The splanchnic uptake or output of the substance in question was determined by the arterio-hepatic venous difference and HBF. The mean concentration of ethanol or glycerol in the splanchnic blood was calculated as $a - v/\ln a/v$ (a = arterial concentration, v = hepatic venous concentration).

The splanchnic elimination of ethanol appeared to follow Michaelis-Menten kinetics (Fig. 1) and this was further supported by plotting the results as elimina-

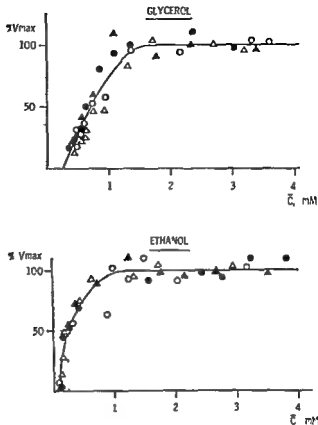


Fig 1 The relation between mean splanchnic concentration and elimination rate (in per cent of maximal elimination rate) of ethanol and glycerol

tion rate against elimination rate over mean concentration (Scatchard plot). The apparent K_m of ethanol was 0.23 mM and v_m 27 ± 2 $\mu\text{mol/kg/min}$. In contrast glycerol elimination did not follow Michaelis-Menten kinetics which may be explained either by a diffusion barrier between blood and hepatocytes or by a splanchnic production of glycerol or a combination of both. The v_{ss} of glycerol was 23 ± 2 $\mu\text{mol/kg/min}$.

At maximal rates of ethanol or glycerol elimination a significant splanchnic lactate output was observed. This was reversed to an uptake when the elimination rate of ethanol was decreased to 90% of V_m and a further decrease in elimination rate did not change the lactate output. The lactate output decreased slightly with glycerol elimination rate but was not changed to an uptake until glycerol was eliminated at a rate of 25% of V_m .

The splanchnic ketone production was not related to ethanol elimination rate. In contrast the ketone production was inversely related to the glycerol elimination rate, indicating an antiketogenic effect of glycerol. The splanchnic oxygen consumption was not related to changes in ethanol or glycerol elimination rate.

Enzyme Activities of Liver Mitochondria from Altitude Exposed Rats

By VUOKKO KINNULI *Department of Physiology, University of Oulu, Finland*

Because the mitochondria are the sites of respiratory activity and dependent on molecular oxygen it would seem appropriate to attach importance to this aspect in hypoxia. In the present investigation the effect of 3 different hypoxic periods were studied and compared with a control group. In both cases rats were exposed to the atmospheric pressure of 380 mm Hg, in the first case the time being 5 h and in the second case 11–16 days. Rat liver mitochondria were isolated in both cases in 0.31 M sucrose solution (pH 7.4) and succinate dehydrogenase activities were determined immediately from the total homogenate and from the isolated mitochondria. Cytochrome oxidase and malate dehydrogenase determinations were carried only from the isolated mitochondria.

During the shorter hypoxic period succinate dehydrogenase activity increased 17% in the total homogenate and 21% in the isolated mitochondria as compared with the control group. Cytochrome oxidase activity increased 21% and no effect on malate dehydrogenase activity was observed.

The longer hypoxic period resulted in decline of the weights of the animals. At the end of the period the liver weight to body weight ratios remained unchanged. Succinate dehydrogenase activity increased 31% in the total homogenate and 23% in the isolated mitochondria. The changes in cytochrome oxidase activities and malate dehydrogenase activities were not significant. In this case the efficiency of oxidative phosphorylation (the P/O ratio) in the isolated mitochondria remained unchanged. The exact mitochondrial protein values as calculated from cytochrome c_{11} concentrations in the total homogenate and in the isolated mitochondria showed 15% decrease as compared with the control group.

As a conclusion can be said that the altered enzyme activities reflect some change in the mitochondrial function. The efficiency of oxidative phosphorylation show that no damage in mitochondria has happened. The changes in the mitochondrial protein values might reflect a decrease in mitochondrial mass that may be a result from a decrease of protein synthesis or from destruction of mitochondria.

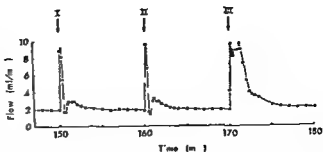
D 12

Chorda Lingual Induced Two phase Vasodilatation in the Saline perfused Cat Submandibular Gland

By J. HIRSHMARK POLANSKY *Institute of Medical Physiology A University of Copenhagen, Denmark*

Gratvik (1970) demonstrated that the vasodilatory response of the cat submandibular gland to stimulation of the chordolingual nerve consisted of 2 phases: a quickly rising primary phase which at cessation of stimulation continued in a second slowly developing but more prolonged phase. It was suggested that the

Fig 1 Flow of venous perfusion fluid from a cat submandibular gland. At I and II the chorda lingual nerve was stimulated by trains of 125 pulses (5 s). At III 1500 pulses were given. Time indicates duration of perfusion with Locke solution.



former was caused by vasodilator nerves while the latter was due to formation of bradykinin from precursors in the plasma. Accordingly only the first phase should be present in long term saline perfused glands.

Cat submandibular glands kept in a thermostated chamber at 37°C were perfused with Locke solution under a hydrostatic pressure of 100–80 mm Hg. The chorda lingual nerve was stimulated electrically (10 V, 1 ms, 25 Hz) by trains of 25, 125 and 1500 pulses. Samples of venous perfusion fluid were taken automatically with intervals of 5–60 s.

Fig 1 shows that brief trains of pulses (125 p, 5 s) elicit two distinct phases of vasodilatation even after perfusion with Locke solution for 2 1/2 h. Though the maximal increase in flow is small during the second phase, the total extra volume of perfusion fluid is comparable to that of the first phase. A longer train of pulses (1500 p, 60 s) causes prolonged vasodilatation.

It is concluded that the two phases of functional vasodilatation observed in the saline perfused cat submandibular gland are due to different mechanisms. The first phase is probably caused by vasodilator nerves while the second phase may be related to increased energy metabolism caused by the simultaneous restitution of intracellular ion concentrations. An involvement of bradykinin formation appears unlikely.

References

- GAUTVÆR, K. *Acta physiol scand* 1970, 79, 174–187.

D 13

Transformation of Spindle Cells into Lymphocyte like Cells in the Blood from Myxine glutinosa

By R. FÄNGE, M. L. JOHANSSON, SJOBECK and M. KÄNJE, Department of Zoo physiology, University of Göteborg, Sweden.

Dibutyl cyclic AMP (db-cAMP) induces morphological differentiation of several cultured neoplastic cells. Thus sarcoma cells resume the typical spindle shape of their normal counterparts (fibroblasts), neuroblastoma cells elaborate axons and

glioma cells obtain multiple thin processes in the presence of c AMP derivatives. These alterations are inhibited if microtubuli are destructed. It has been suggested that c AMP may induce morphological changes of cells by stimulating microtubuli assembly. The purpose of this investigation was to study the transformation of spindle cells into round lymphoid like cells (lymphocytes) as observed in *Myine glutinosa* (Smith 1969). Especially the role of c AMP and microtubuli was considered.

The animals were kept for a week at either 4° C or 15° C. Blood was collected with a heparinized syringe and incubated with or without test substance at 4° C or 15° C. Blood smears were made at different intervals, stained and counted for spindle cells and lymphocytes. The cell counts were expressed as per cent of the total number of non granulated leucocytes.

When the observations started the percentage of spindle cells was 65 regardless of the temperature at which the animals had been kept. Following one hour incubation at 15° C the number of spindle cells decreased to 15 %. Simultaneously the frequency of lymphocytes increased from 35 % to 85 %. If dbc AMP (1 mM) was present there was an initial decrease in spindle cells and an increase in lymphocytes but on prolonged incubation the trends reversed and after one hour the number of the two types of cells equalled that at the beginning. In blood incubated at 4° C no alterations in the proportion of the two types of cells occurred in the control. However in dbc AMP treated blood the lymphocytes increased and the spindle cells decreased in number.

In cultures treated with vinblastine (1 µg/ml) the spindle cells disappeared.

The inverse relationship between the number of spindle cells and lymphocytes suggests that they may represent two stages of the same cell. The transformation of spindle cells into lymphocytes was inhibited by low temperature and by dbc AMP at higher temperature. The effect of vinblastine implies that microtubuli are important for the maintenance of the spindle form. We cannot explain the discrepant effects of dbc AMP at 4° C and 15° C. This demands further investigations.

References

- SMITH R. T. In *Cellular recognition* Ed. R. T. Smith and R. A. Good. North Holland Publ. Co. Amsterdam 1969. 99-109.

B 14

Disynaptic Ia Inhibition of the Interneurons Mediating the Reciprocal Ia Inhibition of Motoneurons

By H. HULTBORN, M. ILLERT and M. SANTINI. Department of Physiology, University of Göteborg, Sweden.

Direct recording from the interneurons mediating the reciprocal Ia inhibition to motoneurons (Hultborn *et al* 1971, Jankowska and Roberts 1972) has now revealed that the Ia inhibitory interneurons themselves receive disynaptic Ia inhibition.

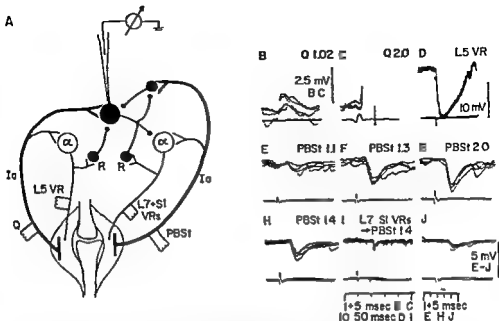


Fig. 1 Disynaptic Ia inhibition of a Ia inhibitory interneurone. Diagram in A is a schematic representation of neuronal connexions in relation to the records shown in B–J. Upper traces are intracellular records. Lower traces are from L6 dorsal root entry zone. Stimulation strength of peripheral nerves is expressed by multiples of threshold of the lowest threshold fibres. Voltage calibration is for intracellular recordings. Time calibrations as indicated. The depressed Ia IPSP shown with a slow time base in I is expanded in J.

tion. These connexions are outlined in Fig. 1A and exemplified in Fig. 1B–J by records from a Ia inhibitory interneurone (*cf.* the recording microelectrode in Fig. 1A). The monosynaptic excitation from the knee extensor quadriceps (Q) nerve (B–C) suggests that the interneurone may inhibit knee flexor posterior biceps semitendinosus (PBSt) motoneurons. Stimulation of Ia afferents from PBSt is seen to evoke a disynaptic inhibition (E–G). It was also established that this Ia IPSP was depressed following antidromic stimulation of S1–L7 ventral roots (I–J). This organization seems to be mutual between flexors and extensors acting at the same joint, since Ia inhibitory interneurons monosynaptically excited from PBSt (thus probably inhibiting Q motoneurons) were found to receive Ia inhibition from Q.

It has turned out that the functionally important activation of Ia afferents occurs during the contraction of the muscle (due to a co-activation of α and motoneurons). A discussion of the possible role of this organization for the reciprocal inhibition of antagonists in relation to the excitation of the agonists has been given elsewhere (Lundberg 1970; Hultborn 1972). The pattern of effects now disclosed (Fig. 1A) would suggest that an increased activity in Ia afferents from the con-

tracting muscles secures an increased excitability of homonymous motoneurons not only by direct monosynaptic excitation but also by releasing them from a possible reciprocal Ia inhibition

References

- HULTBORN H *Acta physiol scand* 1972 Suppl 375 1—42
 HULTBORN H F JANKOWSKA and S LINDSTRÖM *J Physiol (Lond)* 1971 215 613—636
 JANKOWSKA F and W J ROBERTS *J Physiol (Lond)* 1972 222 623—642
 LUNDBERG A. In *Excitatory Synaptic Mechanisms* Eds P Andersen and J K. H. Jansen Universitetsforlaget, Oslo 1970 333—340

D 15

Effects of Lanthanum and Calcium Antagonists on Contractile Responses of Isolated Guinea Pig Gallbladder

By K. E. ANDERSSON, P. HEDNER and C. G. A. PERSSON *Department of Pharmacology, University of Lund Department of Internal Medicine A University Hospital and the Research and Development Department of AB Draco Lund Sweden*

In several types of smooth muscle lanthanum and the calcium antagonists verapamil and D 600 (metoxy derivative of verapamil) have been shown to inhibit calcium movements across the cell membrane and also to interfere with mechanical activity. In addition, lanthanum is able to displace bound calcium from membrane sites (van Breemen 1969 Fleckenstein *et al* 1971, Mayer *et al* 1972). Previous results (Andersson *et al* 1972 a, b) suggested that a decrease in the intracellular content of cyclic AMP leading to an increase in the concentration of free calcium in the myoplasm was of importance for the development of the contraction induced by cholecystokinin and its C-terminal octapeptide (C8 CCK) in isolated guinea pig gallbladder. In order to investigate the effects of interference with the transmembrane movements of calcium on the contractile response to the hormone in this tissue the effects of lanthanum, verapamil and D 600 on C8 CCK induced contraction were investigated. In addition the action of these drugs on the contractile responses to potassium and acetylcholine (ACh) were studied.

Gallbladder strips from guinea pigs were mounted in organ baths containing normal Krebs solution or in experiments with lanthanum a modified solution containing Hepes as a buffer. The solutions were gassed with carbogen and oxygen respectively and kept at 37°C. Isometric tension was recorded.

Lanthanum (0.5—1.0 mM), verapamil (1—10 µg/ml) and D600 (0.5—5 µg/ml) all abolished the phasic part of the potassium contracture and to a variable extent reduced the maximal tension attained during the ensuing "tonic" phase. This effect was similar to that produced by a calcium free medium. In preparations depolarized and contracted by potassium in the presence of verapamil or D 600 C8-CCK and ACh caused a further increase in tension.

Verapamil and D 600 in the concentrations indicated above did not affect or slightly reduced submaximum contractions induced by C-CK, but had a marked inhibitory effect on corresponding contractions elicited by ACh. In the presence of lanthanum (0.5–1.0 mM) the contractile effects of C-CK and ACh were abolished or very markedly reduced. After repeated washing of the preparations their contractile responses to C-CK and ACh were restored.

It is suggested that lanthanum reduces the contractile responses to potassium C-CK and ACh by displacing a fraction of membrane bound calcium necessary for the mediation of the contractile effects of these agents and/or by preventing calcium flow across the membrane. Specific inhibition of calcium inflow through the membrane by means of verapamil and D 600 seems to affect the contractile actions of ACh more than those of C-CK.

References

- ANDERSSON K. E. R. ANDERSSON and F. HEDNER *Acta physiol scand* 1972 a 85 511–516
 ANDERSSON K. E. R. ANDERSSON P. HEDNER and G. G. A. PERSSON *Life Sci* 1972 b 11 723–732
 BREMEN C. VAN *Arch intern Physiol Biochem* 1969 77 710–716
 FLECKENSTEIN A. C. GRAY H. FRITZKY and L. BYON *Klin Wschr* 1971 49 37–41
 MAYER C. J. C. VAN BREMEN and R. CASTELS *Pflügers Arch ges Physiol* 1972 337 333–350

D 16

Proline Dominance in the Intracellular Amino Acid Pool of a Cirripede Crustacean

By H. J. FRYN *Duke University Marine Laboratory Beaufort N. C. 28516 USA* and *Institute of Zoophysiology University of Oslo Blindern Oslo 3 Norway*

The most familiar members of the crustacean order Cirripedia are acorn barnacles and gooseneck barnacles. Acorn barnacles are often abundant in intertidal and estuarine communities and cause extensive fouling of submerged surfaces. Some barnacles are highly tolerant to variations in sea water salinity, however very little is known about the mechanisms allowing this euryhalinity. In the present study the acorn barnacle *Balanus improbus* was long term acclimated to sea water salinities ranging from 0.2 ppt to 63 ppt and the steady state osmotic response investigated.

The intracellular pool of free amino acids of the muscle fibres is dominated by proline. In animals acclimated to hypersaline sea water (63 ppt) the mean proline concentration in muscle is 510^{-3} mol/kg tissue water and this constitutes 86% of the total concentration of free amino acids. With decreasing sea water salinity the proline concentration decreases rapidly to mean values of 120 m mol/kg tissue water at a salinity of 34 ppt to 18 m mol/kg tissue water at 17 ppt and less than 0.5 m mol/kg tissue water at salinities below 11 ppt. In percentage of the total concentration of free amino acids this constitutes 57%, 21% and 2% respectively.

The relative water content of the muscle tissue (mg water/100 mg tissue) decreases much less with increasing salinity than would be expected if the muscle fibers behaved as osmometers. The changes in the relative water content can be accounted for by changes in the specific weight of the tissue and it is concluded that the muscle fibers exhibit a cell volume regulation. Thus the highly adjustable intracellular amount of proline would be of significance as an intracellular osmotic buffer assisting in the cell volume regulation. Analyses of hemolymph osmolality show that *B. improbus* is conforming osmotically to sea water salinities above 10 ppt and regulating hyperosmotically below this salinity. In highly diluted sea water therefore the cells are relieved from the osmotic stress by a regulation of the hemolymph osmolality. In sea waters above 10 ppt however the euryhalinity of *B. improbus* relies on tolerances at the cellular level. The dominance of proline and the sharp increase of its intracellular concentration with increasing extracellular osmolality probably involves proline metabolism as a factor of major importance for the euryhalinity of *B. improbus*.

D 17

Transient Disturbance of Potassium Balance in Rat Liver Induced by Fructose

By M. FOLKE *Institute of Medical Physiology Dept A University of Copenhagen Denmark*

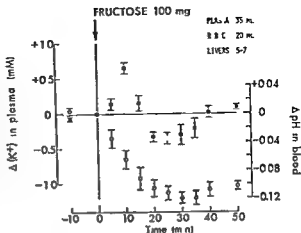
Fructose is eliminated and phosphorylated very rapidly by the liver (Heinz and Junghanel 1969, Sestoft 1974). Within a few minutes administration of fructose reduces the ATP content of rat liver to about one third of normal both *in vivo* (Ravio *et al* 1969) and in the perfused preparation (Woods *et al* 1970). The question arises whether fructose can interfere with hepatic cellular processes believed to require energy in the form of ATP. One such process is the maintenance of a high intracellular potassium concentration in spite of passive potassium efflux from the cells.

Addition of fructose (Fig. 1) to isolated rat livers was followed by release of K⁺ to the medium for approximately 10 min. During this phase measurement of hepatic intracellular potentials revealed a slight depolarization (2–5 mV). During the subsequent potassium uptake occurring after 10 min (Fig. 1) a moderate hyperpolarization (3–8 mV) was observed.

The results indicate that fructose induces an early hepatic net release of K⁺. This may well be due to transient inhibition of active potassium uptake through ATP depletion. A possible increase in membrane permeability leading to augmented passive efflux of K⁺ appears less likely but is not completely excluded as a concurrent phenomenon.

As the hepatic ATP content remains lowered for long periods of time (Woods *et al* 1970) the mechanism of the delayed net uptake of K⁺ is uncertain. If ATP depletion can account for the initial release of K⁺ the subsequent uptake might be expected to proceed in part by mechanisms not directly dependent on ATP. In

Fig 1 Changes in plasma potassium concentration (\blacksquare) and in pH (\square) upon addition of D fructose (555 μ moles) to a portion of heparinized rat blood (55 ml) recirculating through an isolated rat liver. Mean values \pm S.D. of 5 experiments are shown. At zero time (at least 1 h after start of perfusion) plasma potassium concentration was 3.00 ± 0.30 mM and pH was 7.31 ± 0.01 . In the oxygenator of the system the blood was continuously gassed with 5.6% CO_2 in O_2 . Temperature 37°C . Liver donors were moderately fasted (16–18 h).



preliminary experiments delayed potassium uptake occurs even in the presence of 1 mM ouabain which effectively blocks Na^+/K^+ ATPase in rat liver. Potassium uptake in this phase may be related to the marked change in pH (Fig. 1).

References

- HEINZ F and J JUNGHEIM *Hoppe Seyler's Z. physiol. Chem.* 1969 350 859–866
 RAIVIO K, O M P KESKIMÄKI and P H MÄNTYLA *Biochem. Pharmacol.* 1969 18 2615–2624
 SESTOFT L *Biochim. biophys. Acta* 1974 343 1–16
 WOODS H F, L V EGGLESTON and H A KREBS *Biochem. J.* 1970 119 501–510

D 18

Evidence for the Involvement of Separate Enzymes in the Synthesis of Bilirubin Glucosides and Glucuronides in Rat Liver

By J MARNIE H *Department of Physiology, University of Turku, 20520 Turku 52, Finland*

Since the discovery of bilirubin glucoside in dog bile (Heurwegh *et al.* 1970) evidence has accumulated indicating that also the glycosylation besides the glucuronidation is of considerable occurrence and importance as a conjugation pathway of bilirubin in mammals. The problem concerning the possible heterogeneity of the enzyme(s) catalyzing the synthesis of glucosides, UDPglucosyltransferase and its relationship to UDPglucuronosyltransferase(s) is still to be solved. In the present study I have examined the action of several membrane perturbing agents on microsomal bilirubin conjugating UDPglucosyl and UDPglucuronosyltransferase of the liver *in vitro* in order to elucidate the topochemical relationships of these enzymes in the microsomal membrane. Furthermore I have studied the effect of the administration of a polycyclic hydrocarbon, chrysene, on these enzymes *in vivo* to clarify whether they respond in a similar way to the chemical stress. All the mem.

brane perturbants studied (digitonin cetylpyridinium chloride trypsin and phospholipase C) appeared to activate (maximally 6—11 fold) UDPglucuronosyltransferase. Also UDPglucosyltransferase was activated similarly (maximally 3—4 fold) by digitonin, cetylpyridinium chloride and trypsin. UDPglucosyltransferase was found to be, however, more sensitive toward the action of phospholipase C than UDPglucuronosyltransferase. Phospholipase C was clearly inhibitory to UDPglucosyltransferase at concentrations which still activated UDPglucuronosyltransferase about 10 fold. The intraperitoneal administration of chrysene (20 mg/kg) to rats was found to enhance the UDPglucuronosyltransferase activity of liver native microsomes about 1.5 fold while the activity of UDPglucosyltransferase remained unchanged. In the perturbant pretreated microsomes this enhancement was not to be found. The present results suggest a difference in the phospholipid environment of bilirubin UDPglucosyl and UDPglucuronosyltransferase. They also support the existence of different enzymes in the formation of bilirubin glucosides and glucuronides.

References

HEINWECH H, P M G P VAN HEEZ F, COMPERVILLE and J FEVRY *Biochem J* 1970 120: 17p

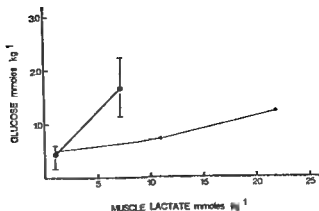
GRANT: This study was financially supported by Emil Aaltonen Foundation

II 19

The Acute Effects of Electrical Stimulation on Metabolites, Enzymes and Fiber Recruitment Pattern in Human Skeletal Muscle

By GERRY WILSON and JAN KARLSSON *Department of Physiology, GIII Stockholm, Sweden S 11433*

Intermittent electrical stimulation was applied to 5 healthy subjects to yield a net of 5 min fused tetanic contraction of the vastus lateralis muscle. Closed biopsies before stimulation (BS), immediately after stimulation (AS) and 2 h recovery (R) provided muscle tissue for a comparative analysis. ATP was reduced 13% AS and further reduced 11% at R as compared to 5.3 mmol \times kg⁻¹ wet muscle (BS). CP was reduced 65% AS from 14.1 mmol \times kg⁻¹ wet muscle (BS) and recovered to 50% of BS value at R. Glycogen concentration was 72 mmol glucose units \times kg⁻¹ wet muscle BS, reduced to 55 mmol AS and increased slightly to 58 mmol at R. Glucose concentration demonstrated a 200% increase AS. This concentration of 1.6 mmol \times kg⁻¹ was twice the concentration for a given lactate value when compared to dynamic work. Glucose at R remained well above BS values. Pyruvate varied between 0.02—0.06 from BS. R. Muscle lactate concentration increased from 1.8 mmol BS to 7.5 mmol AS and remained elevated at 4.5 mmol at R. This is in contrast to dynamic work where at 2 h recovery the lactate has returned to resting values. Enzyme determination showed no alterations from resting values. The glycogen depletion pattern suggested an equal recruitment from both fast and slow twitch fibers by electrical stimulation.



II 20

The Effect of Strength Training on Muscle Enzymes Related to High Energy Phosphate Metabolism

By ALF THORSTENSSON and JAN KARLSSON *Department of Physiology GIH Stockholm Sweden*

The effect of 8 weeks of strength training was studied on 14 students of physical education. The training consisted of 3 training bouts a week and the emphasis was placed on maximal or close to maximal dynamic leg exercise.

Maximal isometric voluntary contraction (MVC) increased from 205 to 232 kp (27% $p < 0.001$) and maximal knee bends (MKB) from 107 to 179 kp (70% $p < 0.001$). Endurance time at 50% of MVC increased from 65 to 78 s (20% $p < 0.005$). No changes were observed in body weight, total body potassium or circumferences of the thigh or the calf muscles with training.

In needle biopsy specimens from vastus lateralis taken before and after training there was no difference in fiber type composition or in fiber area.

Determinations of enzyme activity in crude biopsy homogenates demonstrated changes only for myokinase (MK), the activity of which increased from 1.41×10^4 to 1.52×10^4 mmol \times g⁻¹ \times min⁻¹ (8% $p < 0.005$), whereas the activities of Mg, Ca, and K stimulated ATPase as well as creatine phosphokinase (CPK) were unchanged.

MVC and MKB did not demonstrate any relationship with fiber type composition neither before nor after the training period. The relative increase in MVC was however positively correlated with the individual percentage of slow twitch (ST) fibers ($r = 0.62$). Endurance at 50% of MVC was related to per cent ST fibers but the increase in endurance time after training was independent of fiber type composition. MK activity was related to per cent ST fibers before and after training and the effect of the training was most pronounced in subjects with a low propor-

tion of the ST fiber type Mg^{2+} stimulated ATPase activity showed no relationship with fiber type composition before training ($r = 0.31$) whereas after strength training a positive correlation was observed ($r = 0.67$) between enzyme activity and percentage of FT fibers

It is concluded that strength training had a marked effect on certain force characteristics whereas there were no or minor changes in fiber composition area and activity of certain enzymes. Furthermore since no changes were obtained for the different anatomical parameters it seems reasonable to suggest that the major changes observed were related to neuromuscular functions. The relationship present after training between Mg^{2+} stimulated ATPase activity and the percentage of FT fibers might indicate that not until after vigorous strength training is the enzyme activity in the contracting muscles decisive for performance.

This study was supported by research grants from the Research Council of the Swedish Sports Federation.

D 21

Effect of Polychlorinated Biphenyls on Microsomal Drug Biotransformation in Rat Liver

By H. VUOLTO, Department of Physiology, University of Turku, 205 20 Turku 52, Finland

Polychlorinated biphenyls (PCBs), widely used industrial chemicals, have been detected throughout the world in tissues of a number of animal species including man. PCBs are inducers of steroid hydroxylases in birds (Lincer and Peakall 1970) and of drug oxidizing enzymes in animals (Litterst *et al.* 1972). The present series of investigations was undertaken to delineate the effects of a polychlorinated biphenyl compound Clophen A 50 on microsomal drug monooxygenase complex (cytochrome P-450, NADPH cytochrome c reductase and the overall hydroxylation reactions benzpyrene hydroxylation and *p*-nitroanisole O-demethylation) and UDP-glucuronosyltransferase (*p*-nitrophenol) in rat liver.

Clophen A 50 was administered in oil (15 mg/kg i.p.) once daily for 1, 3 and 6 days. The PCB treatment increased both the proportional liver weight and the amount of microsomal protein per gram of liver wet weight. Benzpyrene hydroxylase and *p*-nitroanisole O-demethylase were enhanced 8 fold and 12 fold in 6 days respectively. The cytochrome P-450 detected was the P-448 form and the concentration of the hemoprotein was increased 3 fold. The subsequent step in microsomal drug metabolism conjugation with glucuronic acid was also enhanced by PCB administration. The enhancement was more pronounced if the latent UDP-glucuronosyltransferase was first revealed by e.g. digitonin phospholipase C or trypsin prior to the determination of the transferase activity i.e. maximally 6-5 or 10 fold respectively as compared to 3 fold in the non activated microsomes.

The data obtained support the assumption that PCBs induce drug metabolism in a way catalytically different from those of the two known types of inducers.

exemplified by phenobarbital and 3 methylcholanthrene (*cf* Vainio and Aitio 1974). The results suggest that PCBs may alter the rate of metabolism of exogenous (endogenous as well) substances thus affecting the responses of the animal towards environmental foreign compounds.

References

- LINGER J L and D H PEAKALL *Nature* 1970 228 783—784
 LITTEREST C L T M FARBER A M BAKER and E J VAN LOON *Toxicol Appl Pharmacol* 1972 23 112—127
 VAINIO H and A AITIO *Acta pharmacol toxicol* 1974 34 130—140

D 22

Lactate Metabolism by the Perfused Rat Liver After Addition of Glycerol

By CHRISTIAN OLSEN *Institute of Physiology University of Aarhus Denmark*

The concentration of lactate in the blood has been shown to increase and the clearance of lactate produced during muscular work to fall when the concentration of glycerol is raised in the man (Olsen and Strange Petersen 1974). A major fraction of the glycerol and the lactate metabolism takes place in the liver (Larsen 1963 Berry 1967) which may be the target organ for this effect of glycerol.

The initial steps in the oxidation of glycerol lead to reduction of NAD to NADH which may drive the reaction

Lactate + NAD \rightleftharpoons Pyruvate + NADH + H⁺ towards the left. Elevated concentrations of pyruvate or decreased intracellular pH exert the same effect.

The effect of glycerol on the hepatic lactate metabolism was studied on the perfused rat liver. The technique was as described previously (Olsen and Krarup 1974) but after an equilibration periode of 40 min with recirculating perfusion medium the perfusion was continued without recirculation to ensure constant composition of the affluent medium throughout the experimental periode. The flow was recorded continuously and related samples of the affluent and effluent medium were taken. The first samples served as controls. Glycerol was then added to a concentration of about 10 mM in the medium.

It appears that the lactate output was insignificant in the control periode but increased significantly after addition of glycerol to the medium. The small output of pyruvate was reversed to a highly significant uptake as a result of the markedly diminished concentration of pyruvate in the effluent medium. There was a slight but consistent increase in the pH of the effluent medium from a mean value of 7.38 to 7.41. The L/P ratio in the effluent medium rose significantly indicating a similar change in the NADH/NAD ratio of the hepatic cytosol (Schmasek 1963).

Thus the rise in the lactate output seems not to be due to elevated concentrations of pyruvate; it may however also be caused by a fall in the intracellular pH but this explanation is unlikely although not excluded as the pH in the effluent medium remained unchanged or even increased slightly.

TABLE I Effects of glycerol on the hepatic output of lactate (L) and pyruvate (P) and on the L/P ratio in the effluent medium

	Lactate output	Pyruvate output	L/P
Control	11.28 ± 0.27	0.06 ± 0.03	17.1
Glycerol	0.72 ± 0.24	-0.12 ± 0.01	44.3
Difference in /	157	-300	159
P	< 0.001	< 0.001	< 0.01

(The lactate and pyruvate output are mean values \pm S.E. expressed in $\mu\text{mol/g}$ wet wt of liver/min $n = 7$)

It is concluded that addition of glycerol to the perfused rat liver results in a significant output of lactate by the liver probably due to increased NADH/NAD ratio

References

- BERRY, M. N. *Proc. R. Soc. Med.* 1967, 60, 52-54.
 LARSEN, J. A. *Acta physiol. scand.* 1963, 57, 224-234.
 OLSEN, C. and N. HANSEN. *Acta pharmacol. et toxicol.* 1974. In the press.
 OLSEN, C. and E. STRANGE-PETERSEN. *Acta physiol. scand.* 1974. In the press.
 SHIMASSEK, H. *Biochem. Z.* 1963, 336, 468-473.

COMMUNICATIONS

C 1

Effects of Prostaglandin E₂ on the Sympathetic Neuroeffector System of the Rabbit Kidney *in Vitro* and *in Situ*

By MADELI E H FRAME and PER HEDQVIST *From the Department of Physiology Karolinska Institute Stockholm Sweden*

It has already been shown that large amounts of prostaglandin E (PGE₂) are present in the renal venous blood of rabbits and that this output is increased on renal nerve stimulation (Davis and Horton 1972). The present study was carried out to examine the hypothesis that PGs of the E series may be involved in the regulation of transmitter release from sympathetic nerve endings (Hedqvist 1973). The isolated rabbit kidney with renal nerve dissected free was used as a model in most experiments although some *in situ* experiments were included in the study as a check on the validity of the *in vitro* situation.

Experiments were carried out to observe the effect of intra arterially infused PGE₂ on (a) vascular response of the kidney to nerve stimulation and exogenous noradrenaline and (b) overflow of tritium labelled noradrenaline during nerve stimulation.

In the (a) experiments infusion of PGE₂ (63–520 ng/ml) into the *in vitro* kidney caused marked inhibition of vascular responses to nerve stimulation whereas the responses to noradrenaline were not significantly altered. In the *in situ* preparation however vascular responses to both nerve stimulation and noradrenaline were inhibited by PGE₂ infusion although its effect on responses to noradrenaline was approximately half of that observed on responses to nerve stimulation.

In the (b) experiments infusion of PGE₂ (63–320 ng/ml) into the *in vitro* kidney caused consistent reduction in overflow of labelled transmitter during nerve stimulation. In addition it was found that this inhibitory effect of PGE₂ varied inversely with the stimulation frequency total number of pulses being kept constant in every stimulation.

In both series of experiments the inhibitory effect of PGE₂ was dose dependent and partial or complete recovery from this effect occurred within 10 to 20 min. The necessity for use of relatively high doses of PGE₂ seemed permissible in view of the rapid metabolism of PGs by prostaglandin dehydrogenase in the rabbit renal cortex (Larsson and Anggard 1973).

It is concluded that PGE₂ acts at both prejunctional and postjunctional levels of adrenergic neurotransmission in the rabbit kidney.

References

- DAVIS H A and E W HORTON *Brit J Pharmacol* 1972 46 658–672
 HEDQVIST P *Adv Biol* 1973 9 461–473
 LARSSON C and E ÅNGGÅRD *Europ J Pharmacol* 1973 21 30–36

C 2

Prostaglandin E_1 on Neuromuscular Transmission

By S E JÄSSON, J HYVÄRINEN, E M TOLPPANEN and J GRIPENBERG
Departments of Anatomy and Physiology, University of Helsinki, Finland

The effects of prostaglandin E_1 (PGE_1) on neuromuscular transmission was studied by intracellular techniques. When a tetanic stimulation was applied to the nerve in a curarized or cut phrenic nerve—diaphragm muscle preparation of the rat PGE_1 (10^{-5} — 10^{-6} M at 38°C) within a few minutes induced intermittent failure and ultimate blockade of the evoked end plate potential (EPP). During the period of intermittent failure the amplitude of the sporadic EPP was often greatly increased. When during this period the frequency of the tetanic stimulation was momentarily decreased the generation of the EPP was normalized only to exhibit a new series of failures as the tetanic stimulation was resumed. When blockade of the EPP was established, recovery was not achieved by decreasing stimulation frequency. The inhibitory effects of PGE_1 occurred without membrane depolarization and there was no effect on the nerve action potential recorded extracellularly from the nerve trunk. The effects were readily reversible upon a few minutes of washing. During all stages of treatment with PGE_1 spontaneous miniature end plate potentials of apparently normal frequency and amplitude were recorded. It appears that at the neuromuscular junction PGE_1 inhibits evoked release of acetylcholine by interfering with some critical step(s) in excitation secretion coupling. Present results are consonant with the idea of PGE playing a regulatory role in transmitter release (Hedqvist 1970) and extend the concept to the cholinergic nervous system.

References

HEDQVIST P. *Acta physiol scand* 1970 Suppl. 345 1—40

C 3

Accumulation of Noradrenaline in the Sympathetic Nerve Trunk Vesicles during Axonal Transport

By H. LAGERCRANTZ. *From the Department of Physiology, Karolinska Institutet, Stockholm S 104 01 Sweden*

The sympathetic nerve axons contain mainly large dense core vesicles or heavy vesicles according to their sedimentation properties. The e vesicles have been found to store relatively low concentrations of noradrenaline (NA) and have therefore been assumed to function only as precursors to the terminal vesicles which are mainly small and light (see Lagercrantz 1971, Smith 1972). The aim of the present investigation was to study the development of the nerve trunk vesicles during their axonal transport.

Bovine splenic nerves were used as a source for the preparation of the nerve vesicles. The nerves were divided in 3 parts: one proximal, one intermediate and one

distal (intrasplenic) segment. Highly purified large dense core vesicles were obtained from these segments by density gradient centrifugation technique (see Lagercrantz 1971). A crude heavy vesicle preparation was also obtained from the spleen.

Biochemical analyses of the nerve vesicle preparations revealed a successive increase of the NA/protein and NA/dopamine β hydroxylase ratios about 17 fold from the proximal to the most distal vesicles. The NA/dopamine β hydroxylase ratio was found to be about 4 fold higher in the vesicle preparation from the spleen than that obtained from the most proximal segment. Furthermore there was a proximo-distal shift of the dopamine β hydroxylase activity towards the heavier regions of the density gradients indicating a successive increase in density of the nerve vesicles. Preliminary studies have shown that the ATP/protein ratio is about the same in the nerve vesicle preparations made from the 3 segments.

The nerve vesicles seem to undergo maturation during their axonal transport which is reflected by their increased densities and NA content. Klein (1974) has reported that NA is stored in 2 pools in these nerve vesicles: one fast pool with rapid amine turnover and one slow pool. The accumulation of NA during axonal transport seems to occur mainly in the fast NA pool.

The NA/protein ratio was estimated to be about 500–600 nmol/mg in the heavy nerve terminal vesicles by comparison with the increase of the NA/dopamine β hydroxylase ratio in the vesicle preparation from the spleen and correcting for the losses during the post mortem delay (cf. Klein 1974). The NA/ATP ratio was estimated to be about 20/1.

It is concluded that the large dense core nerve vesicles have a relatively great NA storage capacity despite their deficit of ATP compared with the chromaffin granules. No evidence for transformation of large dense core vesicles to small ones could be obtained. Consequently, it is believed that the large vesicles are directly involved in neurotransmitter secretion.

References

- KLEIN, R. L. In *Frontiers of Catecholamine research* (Eds E. Usdin and S. Snyder). Pergamon Press, New York, 1973, 423–425.
LAGERCRANTZ, H. *Acta physiol scand* 1971, 82 (Suppl. 366).
SMITH, A. D. *Pharmacol Rev* 1977, 24, 435–457.

C 4

Rectification in Potential Clamped Nodes of Ranvier

By P. ARIÈM and H. FRANKENHAEUSER. *The Nobel Institute for Neurophysiology, Karolinska Institutet, S-10401 Stockholm 60, Sweden.*

The myelinated nerve fibre shows during step polarizations a sequence of specific permeability changes: first a sodium permeability increase followed by a potassium permeability increase. The associated specific currents (I_N and I_K) can relatively satisfactorily be described on the basis of the permeability for these ions and the

electrochemical driving forces as summarized in the constant field equation (Goldman 1943 Hodgkin and Katz 1949 Frankenhaeuser 1960). At large potentials however and under certain circumstances the steady state potassium current deviates from the values predicted by the constant field equation. The current potential curve shows a clear rectification.

It was found in the present investigation that the described rectification can be experimentally induced by increasing the axoplasmic $[Na]$. This was obtained by diffusion through a cut end of the nerve fibre.

External $[Na]$ did not affect the rectification properties. Further it was found that axoplasmic $[Li]$ shifted the potential at which the rectification appeared in negative direction while external $[K]$ shifted the rectification point in positive direction.

An increase in axoplasmic $[K]$ increased the steady state currents in full agreement with the constant field equation but did not shift the rectification point. This means that for the potassium system the concentration and potential are not principally equivalent as driving forces.

In order to describe the potassium system in the myelinated fibres thus strict limitations must be considered: (1) The antagonistic effect of $[K]_o$ and $[Na]$ on the rectification and (2) the dichotomy between concentration and potential as driving forces.

At present it seems that neither a simple pore nor a simple carrier system is a satisfactory model for the transport mechanism for the passive potassium current in the nerve membrane.

References

- FRANKENHAUSER, E. B. *J. Physiol. Lond.* 1960 151 491—501.
 GOLDMAN, D. E. *J. gen. Physiol.* 1943 27 37—60.
 HODGKIN, A. L. and B. KATZ *J. Physiol. Lond.* 1949 108 37—77.

C 5

Effects of Sex Steroids on Prolactin Production by Rat Pituitary Cells in Culture

By E. HALL and K. M. GALTNIK *Hormone and Isotope Laboratory, Akers
 Hospital and Institute of Physiology, University of Oslo, Norway*

Monolayer cultures of rat pituitary tumour cells GH_3 spontaneously synthesize prolactin (PRL) and secrete the hormone into the culture medium. These cells also respond to physiological signals such as different hormones.

We have studied the effect of hypothalamic releasing hormones and sex steroids on the production of PRL and on cell growth. The cells were also tested for synthesis of luteinizing hormone (LH). The cells were cultivated in Ham's complete F10 medium (Ham 1963) supplemented with 18% horse serum and 3% fetal calf serum at 37°C in a humidified atmosphere of 5% CO_2 and 95% air. PRL and LH were measured in the culture medium by separate radioimmunoassays. Tashjian and Hort (1973) have shown that 17 β -oestradiol increased PRL produc-

tion in GH₃ cells. Our data confirm and extend these observations. Treatment with 17 β -estradiol at concentrations as low as 10^{-13} M increased PRL production by 25 % and a three fold increase was observed at an estradiol concentration of $4 \cdot 10^{-8}$ M. The stimulation of PRL production had a lag period of 48 h and maximal effect was observed at 92 h. Cell growth measured as total cell protein was not affected. Testosterone and progesterone had no effect on PRL production or on cell growth.

Three different strains of GH₃ cells which produced PRL did not secrete LH spontaneously. The cells could also not be stimulated to produce LH by treatment with 17 β -estradiol, progesterone, testosterone, LH releasing hormone or thyrotrophin releasing hormone at concentrations which doubled the PRL production.

Estradiol is known to increase serum PRL in the intact animal. We have shown that 17 β -estradiol in physiological concentrations stimulated PRL production by a direct effect on the GH₃ cells. The increased hormone production could not be explained by an increase in cell number. The GH₃ cell system therefore represents a suitable model for further studies on the role of estradiol in the regulation of PRL production.

We are indebted to NIAMD Rat Pituitary Hormone Program for supplying rat PRL and LH.

References

- HAM R G. *Exp Cell Res* 1963 29 515—526
 TASHIRIAN A H JR. and R. F. HOYT JR. *Proceedings of the Symposium on the Molecular Genetics and Developmental Biology* Ed M. SUGIMAN. Prentice Hall, New Jersey 1973 353—387

C 6

Differential Effects of Cyproterone Acetate on Sexual Behaviour and Accessory Sexual Glands in Rabbits

By ANDERS ÅGMO *Institute of Zoophysiology, Uppsala University, Sweden*

Cyproterone acetate (CA) inhibits the binding of 5 α -dihydrotestosterone to cell nuclei in rat seminal vesicle and prostate (Walsh and Korenman 1970). Due to its progestational activity, CA also exerts a negative feedback at the hypothalamic level decreasing gonadotrophin secretion.

In the rat, CA has no effect on the sexual behaviour although it causes atrophy of the seminal vesicle similar to that following castration (Beach and Westbrook 1968, Whalen and Edwards 1969). Both human males and male dogs respond with decreased sexual activity after treatment with CA (Morse *et al* 1973). These differences may very well be caused by species differences in the endocrine regulation of sexual behaviour. The hypothesis put forward by Neumann *et al* (1970) that humans are more dependent on gonadal hormones than rodents are is contradictory to much evidence. To further study the problem of species differences we investigated the effects of CA in male rabbits.

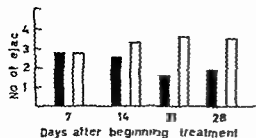


Fig 1 Number of ejaculations achieved during a 10 min mating test after subcutaneous injections of CA or oil vehicle. Black bars CA 20 mg white bars oil vehicle

6 rabbits were once a day subcutaneously injected with 20 mg CA and 5 other animals were injected with oil vehicle only. After 4 weeks the treatment was reversed so that the group formerly given vehicle now was given 20 mg CA and vice versa. Once a week each animal was subjected to a 10 min mating test with a receptive female. Seminal fructose was also determined once a week.

The activity in the accessory sexual glands and also fructose formation is strictly dependent on gonadal hormones and by determining the fructose concentration in semen we can observe the actions of the androgen antagonist on the accessory sexual glands.

The number of ejaculations achieved during a mating test significantly decreased as a result of the CA treatment (Fig 1). The concentration of fructose in semen was unaffected by CA as were the weight of the seminal glands.

References

- BEACH F A and W H WESTBROOK *J Endoc* 1968 42 379-382
 MORSE H C, D R LEACH, M J ROWLEY and C G HELLER *J Reprod Fert* 1973 37 363-378
 NEUMANN F H, von BERNHARDT WALLRADE W, ELGER H, STEINBECK J, D HANN and M KRAMER *Recent Prog Horm Res* 1970 26 337-371
 WALSH P C and S G KORENMAN *Clin Res* 1970 18 126-130
 WHALEN R E and D A EDWARDS *Endocrinology* 1960 84 155-158

C 7

Release and Degradation of Adenosine 3',5'-Monophosphate by the Rat Ovary

By S ROBERT, G SELSTAM and K ÅHRÉN, Department of Physiology, University of Göteborg, Göteborg, Sweden

It is well known that luteinizing hormone (LH) stimulates the formation of adenosine 3',5'-monophosphate (cAMP) in the ovary and it has recently been found that the prepubertal rat ovary releases cAMP to the incubation medium when markedly stimulated by this gonadotrophin (Åhrén *et al* 1974). The aim of the present study has been to test if a low concentration of LH also gives a release of cAMP and to investigate what happens to the extracellular cAMP.

Isolated ovaries from 23 day-old rats were incubated in 1 ml of a modified Krebs bicarbonate buffer as described earlier (e.g. Åhrén *et al* 1974). In one series of

experiments the effect of a low concentration of LH ($0.1 \mu\text{g}$ NIH LH B8/ml medium) was tested. The cAMP content was measured in the tissue and in the medium with a modification of the method described by Gilman (1970). Control ovaries contained $1-1.5 \text{ pmol cAMP/mg wet weight (w/w)}$ at incubation times from 1 to 4 h. No detectable amounts of cAMP were found in the medium at any time. LH did not cause any change in the tissue content of cAMP but a linear increase in medium cAMP was seen from 1 to 4 h. Medium cAMP at 4 h was 12 ± 3 (SE, $n = 5$) pmol/mg w/w . A release of cAMP from the ovary was thus seen in presence of this low LH concentration without any detectable change in the tissue content.

Ovaries were in other experiments incubated in 0.5 ml buffer containing $0.25 \mu\text{M}$ ^3P -cAMP to investigate whether cAMP disappears from the medium. The change in ^3P -cAMP was measured according to Krishna *et al.* (1968). After 1 h 3.4 ± 1.0 ($n = 5$) and after 2 h 6.3 ± 1.5 ($n = 4$) pmol cAMP/mg w/w had disappeared from the medium. This decrease in medium cAMP must be due mainly to phosphodiesterase activity and not to uptake by the ovary, since the total radioactivity in the medium decreased only to a minor extent. Furthermore a phosphodiesterase inhibitor, theophylline markedly lowered the cAMP disappearance. The rate of disappearance of ^3P -cAMP from the medium was not significantly changed when $0.1 \mu\text{g LH/ml}$ was present.

In order to test whether this phosphodiesterase activity was intracellularly located, unlabelled cAMP was added to the medium in a high concentration leading to a marked dilution of any radioactive cAMP formed. A nearly total inhibition of the uptake of ^3P radioactivity was then seen. When $0.25 \mu\text{M}$ ^3H -cAMP was used the uptake of radioactivity was great indicating an uptake of tritiated degradation product(s) but this uptake was also nearly completely inhibited by addition of unlabelled cAMP. Therefore it seems likely that this phosphodiesterase activity is not located intracellularly.

Thus a low concentration of LH causes a release of cAMP from the ovary without a net increase in the total tissue content. Enzymatic degradation of cAMP occurs extracellularly. The release of cAMP occurs without a change in this phosphodiesterase activity. The physiological significance of the ovarian release of cAMP by LH remains to be clarified.

References

- AHREN, K., H. HERLITZ, L. NILSSON, S. ROSEBERG and G. SELSTAM. In *Hormones and polypeptides* Vol. 7. C. H. Li and N. B. Moudgal, eds., Academic Press, New York, 1974. In press.
- GILMAN, A. G. *Proc Nat Acad Sci USA* 1970, 67, 303-317.
- KRISHNA, G., H. WEISS and B. B. BRODIE. *J Pharmacol Exp Ther* 1968, 163, 329-305.

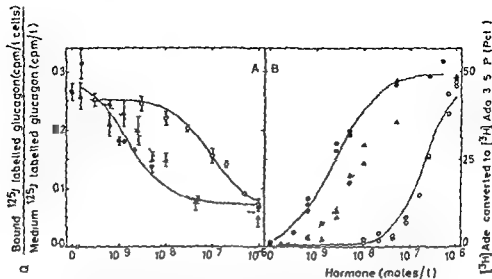


Fig 1 A Binding of ^{125}I labelled glucagon inhibited by glucagon (●—●) monodesamidoglucagon (▲—▲) or des His¹ glucagon (○—○) 0.25 nM of ^{125}I labelled glucagon was incubated with fat cells (10^6 cells/ml) at 37 °C plus the indicated concentrations of unlabeled hormone. After 35 min the cells were isolated from the buffer by centrifugation through dinonyl phthalate. Mean \pm SD ($n=5$). B Stimulation of the adenylyl cyclase by glucagon (●—●) monodesamidoglucagon (▲—▲) or des His¹ glucagon (○—○). Isolated fat cells preincubated with $[8-^3H]$ adenine for 60 min were washed and incubated at 37 °C with the indicated concentrations of hormone in the presence of theophylline (2.5 mM). After 15 min the reaction was stopped by addition of 200 μ l of 0.6 M trichloroacetic acid, unlabelled adenosine 3,5-monophosphate and $[U-^{14}C]$ adenosine 3,5-monophosphate. The adenosine 3,5-monophosphate was isolated and counted in a liquid scintillation counter. The results are expressed as the fraction of the $[8-^3H]$ adenine converted to $[^3H]$ adenosine 3,5-monophosphate with correction for recovery.

C 8

Binding and Stimulation of the Adenylyl Cyclase in Isolated Rat Fat Cells by glucagon and Des His¹ Glucagon

By OLE SONNÉ, J. GLIERMAN and S. GAMSTEDT Institute of Medical Physiology C, University of Copenhagen, Basmannsgade 71, DK-2200 Copenhagen N, Denmark

Isolated rat adipocytes were incubated at 37 °C with ^{125}I labelled glucagon (Sonnen *et al.* 1973) and various concentrations of native glucagon or des His¹ glucagon. The inhibition of binding of ^{125}I labelled glucagon is expressed as the inhibition constant K_i with the 95% confidence limits. The adenylyl cyclase activity was assessed in adipocytes prelabelled with $[8-^3H]$ adenine (Humes *et al.* 1969) by measuring the conversion to $[^3H]$ adenosine 3,5-monophosphate as isolated by the method of Krishna and Burnbaumer (1970).

We found a K_i for glucagon of 12 nM (0.8–22 nM) and a K_i for des His¹ glucagon of 78 nM (44–134 nM) corresponding to an affinity of des His¹ glucagon to about 2% of that of glucagon (Fig. 1 A). The concentration of glucagon and

des His¹ glucagon giving half maximal stimulation of the adenylyl cyclase were 2.6 nM (1.7–3.9 nM) and 340 nM (210–540 nM) corresponding to a potency of des His¹ glucagon of less than 1% (Fig. 1 B). The effects of glucagon and des His¹ glucagon in submaximally stimulating concentrations were additive.

In contrast Rodbell and coworkers (1971) reported that des His¹ glucagon was bound to receptors of liver plasma membranes with an affinity of about 16% of that of native glucagon. Des His¹ glucagon had no stimulatory activity on the adenylyl cyclase of liver plasma membranes and fat cell ghosts and inhibited the action of native glucagon competitively. They concluded that the amino-terminal histidine is non essential for receptor binding but essential for activity.

The effect of des His¹ glucagon seems therefore principally different in the whole fat cell and in liver plasma membranes. A quite close correspondence between the binding affinity and the biological potency was also found for monodesamidoglucagon (potency about 30%) and didesamidoglucagon (potency about 2%). We therefore suggest that in the whole fat cell the degree of stimulation of the adenylyl cyclase is proportional to the occupancy of the receptors with glucagon or glucagon analogues.

References

- HUMES J. L. M. ROUSSELLER and F. A. KUEHL JR. *Anal. Biochem.* 1969 32 210–217
 KRISHNA G. and L. BIRNBAUMER *Anal. Biochem.* 1970 35 393–397
 RODBELL M. L., BIRNBAUMER S. L., POHL and F. SUNDBY *Proc. Nat. Acad. Sci. USA* 1971 68 909–913
 SONNÉ H., J. GLIEMANN and S. GAMMELTOFT *Acta endocr. (Copenh.)* 1973 Suppl. 177 274

C 9

Effect of Nicotine on Left Ventricular Volume in the Dog

By L. HIRVONEN, J. TIMISJARVI and J. MIHKKINEN, *Department of Physiology, University of Oulu, Finland*

Nicotine in moderate doses acts through the existing physiological pathways. The effects depend not only on the way of administration but also on the type, functional state and reactivity of the subject. Cardiovascular effects of nicotine are a result of numerous central and peripheral changes.

In the present study nicotine base was given as a single iv. injection to pentobarbital sodium anesthetized (Nembutal® Abbott) 20 to 35 mg per kg of b.w.) beagle dogs (10 animals of both sexes weighing 7 to 13 kg). Nicotine dose was 0.07 to 0.2 mg per kg of b.w. End-diastolic stroke and residual blood volumes were calculated from angiocardigrams according to the method described by Gribbe *et al.* (1959). It was observed that the end-diastolic volume decreased about 15 per cent, the stroke volume remained unchanged and the residual blood volume decreased about 50 per cent. Cardiac output showed no significant changes. The effect of nicotine was inhibited by beta adrenergic blockade which was carried out by iv. administration of propranolol (Inderal® ICI) dose 0.1 to 0.5 mg per kg.

b.w.) Residual blood volume which in control conditions was only 25 per cent of the enddiastolic volume increased to 50 per cent after propranolol treatment

It is concluded that nicotine has a positive inotropic effect mediated by sympathetic stimulation which may increase the work load of the heart

References

GRIEPE P. L. HIRVONEN J. LIND and C. WEGELIUS *Cardiologia* 1959 34 347-366

C 10

Effect of Vasodilating Drugs on Dental Pulp Blood Flow in Dogs

By H. J. HEYERAS TONDER *Institute of Physiology University of Bergen Norway*

Blood flow of the dental pulp of canine teeth (PBF) in dogs was estimated by measuring H₂-gas clearance with chronically implanted platinum electrodes (Aukland Bower and Berliner 1964 Tonder and Aukland 1974) Control flow averaged 0.16 ml/min g

In preliminary experiments with vasodilating drugs an unexpected observation was made with intraarterial infusion of isoprenaline. Blood flow decreased in spite of practically constant systemic arterial blood pressure suggesting increased pulpal vascular resistance.

To clarify this paradoxical finding a better estimate of perfusion pressure was obtained by cannulating a small artery close to the experimental tooth, usually the lateral nasal artery. Blood flow in the external carotid artery was measured by electromagnetic flowmeter.

Infusion of isoprenaline 0.5-1 µg/min in the external carotid artery caused a 2-3 fold increase in external carotid blood flow (ECBF). Simultaneously local arterial blood pressure (LAP) was reduced by 10-20 mm Hg in spite of unchanged systemic arterial pressure and PBF decreased by 0-25%. Resistance calculated from PBF and systemic arterial pressure increased whereas resistance calculated from LAP showed no consistent change. To test the effect of reduced perfusion pressure PBF was measured during constriction of the external carotid artery. On average PBF fell proportionately more than LAP suggesting a passive vascular bed with passively increased resistance at low perfusion pressure. Thus the reduction in PBF caused by isoprenaline is readily explained by the reduction of local arterial pressure presumably due to marked hyperemia in parallelly coupled vascular beds - stealing. While there is no need to postulate a constrictor effect of isoprenaline on the pulpal resistance vessels a possible dilating effect must be weak.

A similar stealing phenomenon has been observed with acetylcholine and papaverine but with the latter drug the dilating action was sufficient to double pulpal blood flow.

References

- AUKLAND K, B BOWER and R W BERLINER *Circulat Res* 1964 14 164—187
 TONDER K, H and K AUKLAND *Arch oral Biol* 1974 (In press)

C 11

The Effects of N⁶, 2'-O dibutyryl 3,5 cyclic Adenosine Monophosphate (db cAMP) on Hepatosplanchnic Metabolism and Hemodynamics

By N KRARUP, J A LARSEN and A P MUNCK *Institute of Physiology
 University of Aarhus Denmark*

In a previous report it was demonstrated that infusion of glucagon was accompanied by characteristic changes in hepatosplanchnic metabolism and hemodynamics (Krarup and Larsen 1974). The aim of the present study was to examine whether the previous reported effects of glucagon could be reproduced by infusion of db cAMP.

The experiments were performed on fasting cats anesthetized with chloralose and liver function and splanchnic hemodynamics were followed before and during intraportal infusion of db cAMP in various amounts. In one series of 15 expts the total elimination rate of ethanol and the arterial glucose concentration were followed. In all experiments except one db-cAMP infused at rates from 2.5 to 30.0 mg/kg/h caused an increase in the elimination rate of ethanol from 32.5 ± 2.4 to 40.1 ± 3.4 $\mu\text{mol/kg/min}$ accompanied by a maximal increase in arterial glucose concentration of 30—100 %. In 5 expts in which portal blood flow was measured db-cAMP caused a rise in flow from 23.0 ± 3.5 to 35.0 ± 0.8 ml/kg/min. No dose dependence was observed and db-cAMP infused at rates smaller than 2.5 mg/kg/min was without measurable effects.

In another series of 9 expts liver metabolism and splanchnic hemodynamics were followed more closely with the following results. Without showing dose dependence db-cAMP infused at rates from 3—25 mg/kg/h caused a rise in estimated hepatic blood flow from 43.2 ± 6.2 to 51.6 ± 9.4 ml/kg/min with a rise in portal flow from 16.3 ± 1.8 to 23.5 ± 3.4 ml/kg/min and corresponding decrease in resistance of the splanchnic vessels. The splanchnic glucose output increased from 12.0 ± 1.8 to 24.5 ± 3.7 $\mu\text{mol/kg/min}$. Only in 1 expt did db cAMP increase the hepatic elimination rate of ethanol from 32.2 to 38.0 $\mu\text{mol/kg/min}$ accompanied by a rise in hepatic oxygen consumption from 58.1 to 88.8 $\mu\text{mol/kg/min}$. No change in bile production was observed.

Except for the non reproducible effect on hepatic ethanol elimination and oxygen uptake these results are in agreement with the glucagon experiments. They indicate that the previous observed effects of glucagon on hepatosplanchnic metabolism and hemodynamics may be mediated via cAMP and thus support the second messenger hypothesis. However the variable effect of db-cAMP on ethanol metabolism and hepatic oxygen uptake also demonstrate that one or more unknown factors are of importance for the mechanism of action of db cAMP.

References

N. KRARUP and J. A. LARSEN: *Acta physiol scand* 1974 in press

C 12

Autoregulation of Blood Flow in Cortical Regions of the Rat Kidney

By L. O. LINDBOM, Ö. KÄLLSKOG, H. R. ULFENDAHL and M. WOLGAST *Department of Physiology and Medical Biophysics, Biomedical Center, University of Uppsala, Sweden*

The hemodynamic events in the kidney during decreased systemic blood pressure are of longstanding interest in renal physiology. It is known that the renal blood flow remains constant when the perfusion pressure varies between 70 and 180 mm Hg.

In an attempt to study whether this is equally pronounced within different regions of the kidneys, the microsphere technique with two differently radioactive spheres (^{85}Sr and ^{141}Ce) before and during partial constriction of the abdominal aorta was applied. The kidneys were thereafter filled with a silicon rubber compound which made it possible to dissociate between different vascular units within the kidney and to selectively collect glomeruli from different depths within the renal cortex and allowing the study of the juxtamedullary circulation. The kidneys were sliced in different zones and the blood flow per glomerulus or zone was determined.

It was found that the blood flow rate in the superficial glomeruli was proportional to the arterial pressure. In deeper zones, however, the glomerular blood flow was autoregulated and in the juxtamedullary glomeruli even a prominent increase in blood flow was measured at a moderate decrease in blood pressure. It has been proposed that the outer nephrons are salt losing while the deeper ones are considered salt conserving. In this context, the redistribution of blood flow within the kidney found in this study might be relevant as a homeostatic mechanism for electrolyte and water balance.

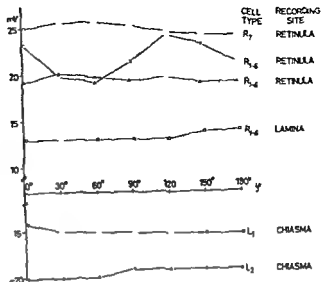
C 13

Polarization Sensitivity of Individual Retinula Cells and Neurons of the Fly *Calliphora* as Studied by an Electrophysiological Staining Method

By M. JÄRVILEHTO and J. MÖRÖG *Department of Physiology, University of Oulu, Finland*

Behavioral and electrophysiological studies have shown that the invertebrates are able to detect the oscillation plane (E vector) of linearly polarized light (for a review see Frisch 1963). It is, however, not known which visual receptor cells or second-order neurons are sensitive to changes in the oscillation plane of polarized light in the fly. In the present work, the polarization sensitivity of these neural elements was studied in the fly *Calliphora erythrocephala*.

Fig 1 Maximal amplitudes of potential responses to polarized light of some visual cells and second-order neurons as a function of the angle of the oscillation plane of light stimulus. Relative light intensity $7 \cdot 10^3$



Dark adapted retinal receptors were stimulated by a squareformed spot like light pulse (duration 100 ms relative intensity $7 \cdot 10^3$). The stimulus was modified by turning the E vector of a polarizing filter 180° (30° steps) around the optic axis of the receptor. The light evoked low potential responses were intracellularly recorded from retinula cells and neurons by very fine glass capillary microelectrodes. The maximal amplitudes of the responses when using different oscillation planes were measured. The cells and neurons were identified with a histological method which uses staining with Procion yellow and localization of the recording site by freeze fixation (Jarvilehto and Zettler 1973).

The present results are based on 13 identified recordings from retinula cells and neurons. In the retinula cell layer both polarization sensitive and insensitive short visual fibers (R_{1-6}) were found. In the lamina all R_{1-6} fibers were insensitive. In the soma of an R cell no polarization sensitivity was detected. No second-order neurons (L_1) could discriminate between the directions of the E vector (Fig 1). None of the recordings did show any spike activity.

In the present study quite few polarization sensitive neural elements were found. It has been suggested that the compound eye of the fly has two functional systems (R_{1-6} and R_{7-8}), R_8 being specialized for the information transmission about the E vector (Hirschfeld 1971). The present results do not lend support for this hypothesis.

References

- FRISCH K. V. D.: *Tanzsprache der Bienen*. Berlin: Springer 1965.
 JÄRVILEHTO M. F. ZETTLER Z.: *Zellforsch.* 1973, 136: 291-306.
 KIRSCHFELD K.: *Naturwissenschaften* 1971, 58: 701-709.

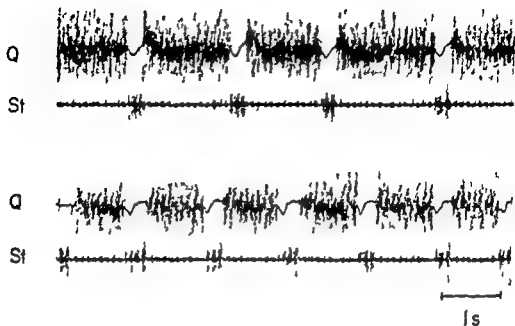


Fig. 1. Rhythmic alternating activity in knee flexors and extensors during bilateral stimulation of dorsal roots L 7. Kitten spinalized (Th 13) at the age of 7 days 2 1/2 months before the experiment. All dorsal roots of the hindlimb girdles (L 3—S 4) were cut. The EMGs from quadriceps (Q) and semitendinosus (St) were recorded bipolarly with thin copper wires inserted into the muscles on an 8 channel inkwriter (Mingograph) with a straight frequency response up to 1200 Hz (Forsberg and Grillner 1973). The two dorsal roots L 7 were stimulated synchronously with 0.2 ms pulses at 5 Hz with approximately equal current strength (upper traces). In the lower traces the ipsilateral stimulation strength was increased with 10. This resulted in an enhanced output frequency by a shortening of the extensor bursts. In general such rhythmic activity could be elicited by bilateral dorsal root stimulation but sometimes stimulation of one side was sufficient. Also antedromic stimulation of the dorsal columns at L 1 gave the same effect. The efficient stimulation frequency varied in different experiments but ranged between 4—100 Hz.

C 14

Locomotor Movements Generated by the Deafferented Spinal Cord

By S. GRILLNER and P. ZANGGER, Department of Physiology, University of Göteborg, Sweden

Brown (1911) evidence for a central generation of locomotion was strongly supported by Sherrington's (1913) finding that bilateral continuous afferent stimulation (50 Hz) could generate rhythmic efferent activity in the otherwise denervated lumbosacral spinal cord (decerebrate cat). These experiments were however reinterpreted by Egger and Wyman (1969) as an experimental artefact and have since been a matter of dispute.

We have repeated the same type of experiment in low spinal preparations (Th 13) in which normal locomotor movements can be elicited on the treadmill (Grillner

1973 Forssberg and Grillner 1973) Fig 1 shows a rhythmic alternating EMG activity (see legend) in an extensor and a flexor at the knee joint evoked by bilateral stimulation (5 Hz) of the cut dorsal roots L 7 in a chronic spinal cat in which both hindlimbs were entirely denervated by transection of the dorsal roots (L 3—S 4) Such results have also been obtained in acute spinal preparations in which 200—500 $\mu\text{g/kg}$ Clonidine 100 mg/kg DOPA or 50 mg/kg Niamid + 50 mg/kg DOPA has been injected iv We have also shown that the extensor activity can coincide at all joints (hip knee and ankle) and similarly the flexor activity so that the deafferented limb actually performs stepping movements Moreover the limbs of the two sides can be coordinated so that the flexor activity of one side coincides with the extensors of the other side i.e. the pattern used in walking or trotting

To assure that phasic information from the remaining afferents was not responsible (L 1 L 2 and possible ventral root afferents Coggeshall *et al* 1973) we have in addition used curarized preparations (recording in peripheral nerve filaments) Also in this case does continuous afferent stimulation result in rhythmic alternating activity

These results show conclusively that the isolated spinal cord itself can generate rhythmic alternating activity coordinated as during locomotion in response to a tonic input

References

- BROWN T G *Proc roy Soc B* 1911 84 308—319
 COGGESHALL R E I D COLLIER and W D WELLS JR *Brain Res* 1973 57 229—233
 EGGES M D and R J WYMAN *J Physiol (Lond)* 1969 207 501—516
 FORSSBERG H and H GRILLNER *Brain Res* 1973 50 184—186
 GRILLNER S *In Control of Posture and Locomotion* Eds R B Stein L G Pearson R S Smith and J B Redford Plenum Press New York 1973 315—335
 SHERRINGTON C S *Proc roy Soc B* 1913 86 233—261

C 15

Oculomotor Outflow During Paradoxical Sleep in the Cat

By J ALIHAJALA S E BJÖRQVIST M OIVAALA J SOINI and P VALLEALA
 Department of Physiology University of Turku Turku Finland

The electrical activity of the medial rectus eye muscles during paradoxical sleep was recorded with intramuscular steel wire electrodes in chronic cats sleeping in dark cages Attention was directed to abruptly starting phasic EMG bursts which often occurred at regular intervals Such phasic EMG bursts may be short twitches of 10—100 ms duration with no activity between the bursts or sudden amplitude increases during ongoing low amplitude EMG activity

For the analysis of oculomotor outflow the time from the start of a phasic EMG burst to the start of the subsequent one was measured without taking notice of the length of the bursts All such burst onset intervals (BOI) were sampled during the long lasting phase of paradoxical sleep in nine cats The distribution of all BOIs is not random but there is a pronounced occurrence of BOIs lasting about 0.4 s

The category of BOIs of about 0.2 s is especially common when dealing with series of EMG bursts in which the successive BOIs are of about the same length.

The electrical activity of an extrinsic eye muscle thus shows a periodicity, whose temporal properties are quite close to the rhythms occurring in certain cerebral structures during paradoxical sleep: the activity of the hippocampus and the lateroposterior part of the thalamus, and the occurrence of so called PGO waves. The similarities to some series of saccadic eye movements in waking cats are also apparent.

C 16

Response to Electric Shock in Rats: Effects of Selective Midbrain Raphe Lesions

By K. HOLT and S. A. LORENTZ, *Institutes of Physiology and Psychology, University of Bergen, Norway*

Lowered brain 5-hydroxytryptamine (5-HT) concentration following p-chloro-phenylalanine (pCPA) administration or lesions in either the septal area or lateral hypothalamic portion of the medial forebrain bundle (MFB) has been correlated with an increased sensitivity to electric shock (Harvey and Lints 1971; Tenen 1967). It is generally agreed that forebrain 5-HT has its primary origin in the midbrain B7-9 cell groups. These cell groups give rise to fibers which ascend in the MFB to innervate a variety of forebrain structures (Dihlstrom and Luxe 1964). Lesions which destroy both the dorsal (B7) and median (B8) raphe nuclei have been shown to facilitate acquisition of a two-way avoidance response but retard acquisition of an one-way avoidance task (Srebro and Lorentz, manuscript submitted for publication 1974). However, it is unclear whether the behavioral effects of such lesions are due to an increase in shock sensitivity.

Lesions were placed electrolytically in either the median ($n = 5$), dorsal ($n = 5$) or both ($n = 6$) midbrain raphe nuclei. Control operations were performed on an additional ten animals. Flinch-jump thresholds were obtained 18-21 days post-operatively and one-way avoidance training conducted 35 days after surgery. The rats were sacrificed on the thirty-ninth post-operative day and their brains rapidly removed and sectioned at the mesencephalic junction. The forebrains were frozen for later serotonin analysis and the brainstems were saved for histological reconstruction of the lesions.

The lesions produced significant reductions in forebrain 5-HT concentration reaching 22% in the median raphe lesion group, 18% in the dorsal raphe lesion group and 70% in the combined lesion group. None of the lesion groups, however, showed any significant differences from controls in pain sensitivity as measured by the flinch-jump technique. On the other hand, one-way avoidance acquisition was greatly retarded in both the median and combined lesion groups. Dorsal raphe lesions, however, did not affect one-way avoidance acquisition except in terms of prolonged escape latencies on the first three trials.

These data suggest that the increased sensitivity to painful stimuli observed following MFB lesions or pCPA administration are not due exclusively to effects on ascending 5 HT fibers arising in the B7 and B8 cell groups. In addition, the results suggest that the effects of midbrain raphe lesions on avoidance learning depend on the locus and extent of the lesions and are not due to an increase in shock sensitivity.

References

- DARLSTROM A and K. FUXE *Acta physiol scand* 1964 62 Suppl 232
 HARVEY J A and C E LINTS *J comp physiol Psychol* 1971 74 28-36
 TAYLOR S S *Psychopharmacologia* 1967 10 204-219

C 17

Effects of Barbiturates *in vitro* on Protein Synthesis, Rapid Axonal Transport and Ultrastructure in the Frog Sciatic System

By H. LARSSON, A. EDSTROM and H. A. HANSSON *Department of Zoophysiology and Inst of Neurobiology University of Goteborg Sweden*

Rapid axonal transport of neuronal components is dependent on local energy generating processes and on the integrity of the microtubular system. Allison and Nunn (1968) suggested that general anesthetics produce narcosis by depolymerization of microtubules. Among other effects, general anesthetics have been shown to depress the synthesis of proteins and nucleic acids *in vitro*. Experiments described here were made to study the effects *in vitro* of barbiturates on the cellular uptake of leucine, incorporation into protein and rapid axonal protein transport (118 mm/day, 18°C) in conjunction with ultrastructural studies.

The preparation, which consists of the spinal ganglia, the sciatic nerve and the gastrocnemius muscle, was placed in Ringer solution in an incubation chamber with 3 compartments (A, B, C) (Edstrom and Mattsson 1972). The parts were separated from each other with silicone grease barriers. H³ leucine was added to comp. A, which made it possible to follow the rapid transport of leucine-labelled proteins from the ganglia along the sciatic nerve towards the muscle. The preparations were incubated for 17 h at 18°C. The transport effect was determined by measuring the amounts of transported labelled proteins which accumulated in front of a ligature placed on the nerve. Paired preparations incubated with and without the addition of the drug to the nerve compartment (comp. B) were used. In separate experiments, ganglia were assayed for incorporation of H³ leucine into TCA insoluble and soluble components. Selected areas of ganglia and nerves were examined in a Siemens 1A electron microscope.

The effects of hexobarbital, pentobarbital, methohexital and thiopental at two concentrations (0.5 mM and 2 mM) were tested. All 4 drugs arrested the transport, pentobarbital being the most and thiopental the least potent one. The drugs did not influence the uptake of H³ leucine into ganglionic cell bodies. Pentobarbital, methohexital and thiopental, but not hexobarbital, depressed incorporation into

TCA insoluble material. In general the rapid transport showed higher sensitivity than protein synthesis to the barbiturates tested. The drugs at concentrations which inhibited axonal transport caused ultrastructural effects which reminded of those caused by colchicine in several systems *i.e.* loss of microtubules and proliferation of neurofilaments.

High concentrations of barbiturates were required to inhibit axonal transport in the present study and still higher to cause corresponding effects on protein synthesis. Normal anesthesia by barbiturates is therefore hardly likely to affect these mechanisms.

References

- ALLISON A. C. and J. F. NELL *Lancet* 1978 2 1326—1329
 EOSTRÖM A. and H. MATTESSON *J. Neurochem.* 1972 19 205—221

C 18

Effects of N-Ethyl maleimide on Rat Phrenic Nerve Terminals and Axons

By ASBJÖRN ROED *Department of Physiology and Biochemistry, Dental Faculty, University of Oslo, Oslo, Norway*

The sulfhydryl blocking agent N-ethyl maleimide (NEM) was observed to increase spontaneous acetylcholine output from rat phrenic nerve terminals and to block the indirectly stimulated phrenic-diaphragm preparation. The following experiments describe this transmitter release and a simultaneous interference with nerve fibre excitability.

Miniature endplate potential (MEPP) frequency increased from ca. 1/s to 500—1000/s in superficial cells upon addition of NEM 25 μ M at 37°C. By recording from single cells during several minutes with intracellular microelectrodes the nerve terminal quantum content was estimated to 3—4/10. Thus NEM probably depletes the releasable store completely (Longenecker *et al.* 1970). Only a part of the MEPP frequency increase could be prevented by leaving out Ca^{2+} in the bathing solution. Accordingly, the NEM-induced transmitter release is partly independent on terminal membrane depolarization.

The neuromuscular block occurred rapidly following a lag period of ca. 20 min after addition of NEM. Simultaneous recordings of high frequent MEPPs and evoked endplate potentials (EPPs) did not disclose any change in MEPP/EPP amplitude ratio. NEM thus left the stimulus-evoked release unaffected. Suddenly, however, the EPPs disappeared whereas the high MEPP frequency could still be recorded for several minutes. Transmitter depletion thus appeared unlikely as the cause of neuromuscular block and recordings of phrenic nerve compound action potentials showed that the overall neuromuscular block could be accounted for by phrenic nerve block. During progression this block could temporarily be cancelled by increasing the stimulating current suggesting a threshold increase.

The failure of previous investigators to disclose this low dose NEM block (Smith 1958) can be explained by the fact that the phrenic nerve contains only A β fibres (Roed 1973). Observations on sciatic nerve compound action potentials with both A α and A β peaks disclosed a selective A β block.

The nerve block and the MEPP frequency increase were irreversible upon washing. Preparations pretreated with the sulphydryl stabilizing agent dithiothreitol were unresponsive to both NEM effects showing that sulphydryl groups were involved in both cases.

The results demonstrate two different functions of sulphydryl groups in motor nerve activity. In the terminals they are essential for keeping the transmitter vesicle stored. In the nerve axons they are necessary for normal excitability especially in A β fibres.

References

- LONGENECKER JR. H. H., W. P. HURLBUT, A. MAURO and A. W. CLARK *Nature* (Lond.) 1970 225 701—705.
 ROED A. *Neuropharmacology* 1973 12 261—267.
 SMITH H. M. *J. cell comp. Physiol.* 1958 51 161—171.

C 19

The Role of Baroreceptor A and C fibres in Reflex Bradycardia

By H. AARS and LISBETH MYHRE *Department of Physiology and Biochemistry, Dental Faculty, University of Oslo, Norway*

About half the population of afferent fibres from baroreceptors are non medullated yet—except for a few reports of selective electrical stimulation of A and C fibres in the carotid sinus and aortic nerves—nothing is known of the participation of C fibres in the baroreceptor reflexes. To study this problem the bradycardic response to a rise of arterial blood pressure was recorded before and after selective anodal blocking of baroreceptor A fibres in the left aortic nerve of Nembutal anesthetized rabbits. Three pairs of electrodes were applied to the nerve for stimulation caudally, block in the middle and recording cranially. The right aortic nerve was cut, the right common carotid artery was used for recording arterial pressure and the left common carotid artery was occluded immediately prior to injection of metaoedrine (40—60 μ g) into the femoral artery. The block was arranged with the positive electrode in the cranial position (Trenchard, Diana W. Thesis, Univ. of London 1970). Spontaneous activity as well as the compound A wave (0.1/s stimulation) was usually obliterated by less than 20 μ A (Constant Current Unit Grass) whereas the double or more was required to extinguish propagation of action potentials in C fibres. Correct functioning of the block was confirmed by abolition of the bradycardic response to A fibre stimulation (100/s, 6 V, 0.02—0.04 ms) and unchanged response to A+C fibre stimulation (20/s, 6 V, 0.5—1.5 ms). The reflex slowing of the heart was assessed by relating the systolic pressure in each heart beat to the time interval between the next two beats (R—R

interval, ECG) prior to and during the rise of pressure resulting from the injection of metaoxedrine

Typically a 20–30 mm Hg rise of pressure caused a 10–12 % slowing of the heart with the aortic nerve intact, and minimal or no change in heart rate when conduction through A fibres was blocked. For 5 rabbits the regression coefficient of the pressure/heart period relationship was 1.82 ± 0.47 (SD) ms/mm Hg with out block as opposed to 0.27 ± 0.01 ms/mm Hg ($P < 0.01$) with only C fibres open.

These preliminary results accordingly demonstrate that C fibres from aortic baroreceptors are not activated by acute, moderate increases in arterial pressure. The reflex bradycardia is solely mediated through afferent A fibres.

C 20

Strong Heat Exposure and Adenohypophyseal Hormone Secretion in Man

By J. LEPPÄLÖFÖ, H. LYBECK, J. PARTANEN, T. RANTA and P. VIRKKUNEN
Institute of Physiology, University of Oulu and University of Helsinki, Finland

Mild heat exposure (46–48°C) has been shown to elicit growth hormone (GH) secretion in man (Okada, Mitsuoka and Kumahara 1972) but information about the secretion of other trophic hormones during exposure to heat is lacking. In the present study the effects of a strong heat stimulus (Sauna bath of 100°C) on the plasma levels of corticotrophin (ACTH), GH, luteinizing hormone (LH) and thyrotrophin (TSH) were investigated.

Five normal male adults were cannulated with venous cubital catheters and blood samples were drawn every 15 min for 90 min. At 30 min the subjects were exposed to the heat of a Sauna bath for 15 min. The temperature at chest level was 100°C and relative humidity 22%. Plasma ACTH, GH, LH and TSH were measured by radioimmunoassays and plasma proteins and glucose by colorimetric assays.

Sublingual temperature rose from 36.8 (mean) to 39.8°C during the 15 min exposure at 100°C. Plasma proteins increased by 5% during the same time but plasma glucose levels were unchanged. Plasma ACTH varied from 20 to 125 pg/ml and plasma TSH from 4 to 12 mU/ml and were not affected by heat. During and subsequently to the heat exposure plasma LH levels rose from 12 to 20 mIU/ml ($p < 0.05$) and then declined to the initial level. The plasma GH level rose to 14 ng/ml at the end of heat exposure but continued the rise up to 60 ng/ml at 45 min when the body temperature was decreasing.

Unchanged plasma ACTH levels during the strong heat exposure are evidently due to the fact that subjects were accustomed to the hot air of the Sauna. The stability of plasma TSH levels during thermal stimuli in man is generally known. The slight increase of another glycoprotein hormone, LH, during the heat exposure was however significant. GH release reached a maximum 20–30 min after the

heat exposure suggesting that heat firstly activated some other mechanism *e.g.* the hypothalamic neurotransmissive system

References

OKADA Y, T MATSUOKA and Y KUMAHARA *J clin endocr* 1972 34 759—763

C 21

The Force Velocity Relation in Venous Smooth Muscle

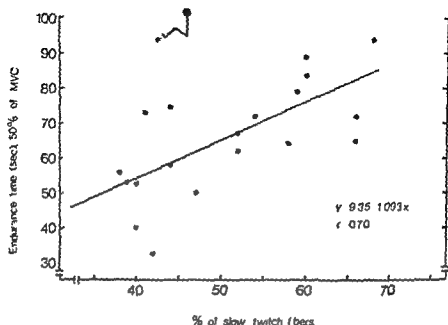
By PER HELLSTRAND and BORJE JOHANSSON *Department of Physiology and Biophysics University of Lund Sweden*

The force velocity relation of muscle provides information on the kinetics of the energy conversion in the contractile apparatus. Only a few reports on this relation in mammalian smooth muscle have been presented and these have mostly been based on studies of afterloaded tetanic contractions (*e.g.* Stephens Kroeger and Mehta 1969 Gordon and Siegman 1971, Meiss 1971). Information is lacking on how variation in the active state affects the force velocity curve in smooth muscle. In the present work instantaneous force velocity curves have been obtained at specified stages of uniform phasic contractions of rat portal vein at 37°C (Johansson 1973) by the method of isotonic quick release. At the maximal intensity of the active state in the rising phase of the isometric contraction the force velocity relation could be described by Hill's (1938) equation $(P+a)(V+b) = b(P_0+a)$. P_0 (force at zero contractile element velocity) and V_m (velocity at zero load) were obtained by extrapolation. The following values were found $a/P_0 = 0.73 \pm 0.04$, $b = 0.54 \pm 0.04$ muscle lengths/s, $V_m = 0.74 \pm 0.02$ muscle lengths/s (mean \pm S.E. $n = 7$). At the time of isometric peak tension V_m has started to decrease whereas P_0 remains essentially unchanged. An explanation for this behaviour might be that deactivation of the preparation does not occur uniformly but rather proceeds longitudinally. As long as one cross section of the muscle is fully active P should remain at its maximal value whereas V_m should decrease as soon as the muscle is not fully active over its entire length. With further decrease in activation after the isometric peak both V_m and P_0 decrease progressively.

The study has shown a maximal velocity of shortening in the rat portal vein which considerably exceeds the V_m values reported for non vascular smooth muscles (*e.g.* Stephens Kroeger and Mehta 1969 Gordon and Siegman 1971 Meiss 1971). Temporal variations in active state are associated with changes in both V_m and P .

References

- GORDON A R and M J SIEGMAN *Amer J Physiol* 1971 211 1223—1230
 HILL A V *Proc Roy Soc B* 1938 126 136—195
 JOHANSSON B *Circ Res* 1973 32 246—258
 MEISS R A *Amer J Physiol* 1971 220 2000—2007
 STEPHENS N L, E KROEGER and J A MEHTA *J Appl Physiol* 1969 26 682—692



C 22

Relationship Between Isometric Endurance and Muscle Fiber Type Composition

By BODIL HULTÉN and JAN KARLSSON *Department of Physiology GIH Stockholm Sæden S 114 33*

Isometric endurance (IE) in man has been demonstrated to be related to maximal voluntary contraction (MVC) a relation which has been referred to as the Rohmert curve. Selective glycogen depletion patterns, assessed by PAS staining indicate that tensions in excess of approximately 20% of MVC recruit only fast twitch fibers (ST). To further elucidate the relationships between IE and fiber type composition 19 subjects had closed biopsies taken from the vastus lateralis for fiber type classification.

Individual MVC and IE at 50% of MVC respectively were also determined. Reinvestigation after 8 weeks of strength training demonstrated increases in both MVC (205 to 232 kp or 27% $p < 0.001$) and IE at 50% MVC (63 to 78 s or 20% $p < 0.001$) without changing the fiber type composition although the fiber area of FT fibers increased slightly. Before as well as after the training IE was related to fiber type composition demonstrating increased performance with higher percent ST fibers. Training only elevated the regression line in parallel with the previous control line. Thus the training effect at this tension was neither in absolute nor in relative terms related to fiber type composition. When IE was tested after training at the pretraining 50% MVC value (45% MVC post training) the mean increased to 99 s or with 53% $p < 0.001$.

Considering the selective glycogen depletion data it seems reasonable to suggest that isometric tensions corresponding to approximately 50% MVC was maintained principally by FT fibers. It then seems that the major significance of ST would be to reduce concentrations of anaerobic metabolites (lactate etc.) formed in FT fibers contractions. This would then reduce factors involved in muscular fatigue and thus prolong performance.

C 23

Control of Breathing in an Amphibious Fish, *Amphipnous Cuchia*

By J P LOMBOIT and K. JOHANSEN *Department of Zoophysiology University of Aarhus Aarhus Denmark*

Many teleost fishes show adaptations for air breathing. *Amphipnous cuchia* inhabits shallow fresh water of India and spends the greater part of its life on land. The gills are rudimentary and the fish depends on aerial gas exchange in a pair of air sacs (lungs) and on skin respiration. The latter accounts for up to 1/3 of oxygen uptake when the fish is in water.

Active branchial ventilation of water never occurred unless the fish was deprived of access to air. O_2 extraction from water ventilation varied between 10–25%. No change in rate of branchial pumping occurred in relation to water PO_2 . At resumption of air breathing branchial pumping stopped instantaneously.

A special respirometer was constructed to monitor air breathing frequency (f), tidal volume (V_T), total ventilation (V_A) and duration of breath cycles in response to altered gas composition in water and/or air.

The normal pattern of air breathing was periodic with long periods of apnoea. Intensity of air breathing varied with water PO_2 (table).

Increasing PO_2 above normal in the gas phase caused reduced V_A suggesting a hypoxic drive to normal breathing. V_A increased moderately ($\times 1.5$) when P_{iO_2} was reduced from normoxia to 75 mmHg, while a further reduction to 40 mmHg caused a fourfold increase in V_A .

CO_2 response curves showed an unchanged V_A when inspired CO_2 was between 0–4%. A further increase in P_iCO_2 increased V_A mainly by an increase in frequency while tidal volume and ventilatory periods were unchanged. A very short response time characterized the change in V_A to altered P_iO_2 and P_iCO_2 .

The data suggest that *Amphipnous* although principally an air breather has retained the piscine mechanism of ventilating the gills (rudimentary) with water. The rate of aquatic ventilation appeared fixed and insensitive to water PO_2 . Air

Water PO_2	Ventil period	Breaths/min (f)	V_T ml/kg
10–20 mmHg	45	n = 34	0.48
ca. 150 mmHg	44	n = 39	0.34
500–600 mmHg	17	n = 17	0.36

ventilation was responsive to gas composition of both water and air. The underlying chemosensitive mechanisms are probably screening blood in the air sacs or its efferent vasculature. Normally occurring changes in ambient and internal gas compositions suggest that ventilation is driven predominantly by a hypoxic stimulus. A lesser importance of CO_2 is in accordance with effective CO elimination through skin correlated with a low gas exchange ratio of the air breathing organs.

C 21

Effects of Mitosis Inhibitors and Anesthetics on Differentiated Mouse Neuroblastoma Cells

By I. J. FRANK and A. LINSTRÖM *Department of Zoophysiology, University of Göteborg, Sweden*

Mouse neuroblastoma cells (L 1300) undergo morphological and physiological differentiation in serum deprived medium in tissue culture. The cells develop processes - or neurites - reminding of normal axons and seem to have many properties in common with normal nerve cells (Schubert *et al.* 1971). In the presence of mitosis inhibitors like colchicine and vinblastine the neurites will retract, an effect which has been ascribed to destruction of the microtubular system. In the present investigation the effects of chlorpromazine, known to have a local anesthetic action, and also that of a standard local anesthetic lidocaine were compared with mitosis inhibitors and a detergent SDS with respect to neurite retraction and membrane effects as observed with Nomarsky microscopy. Since microtubules form a supporting structure in the neurites, neurite retraction was regarded as a criteria for destruction of the microtubular system.

The mitosis inhibitors vinblastine (6×10^{-10} M), colchicine (2×10^{-6} M) and griseofulvin (10^{-5} M) caused neurite retraction in low doses. A 50% reduction in the number of neurites was observed after exposure to the drug for 1 h at the concentration tested. Chlorpromazine and lidocaine had the same effects at 1×10^{-6} M and 8×10^{-4} M respectively. The effects were reversible. In contrast to the other drugs tested SDS produced an irreversible 50% neurite retraction at 1×10^{-5} M. Nomarsky optics furthermore showed that all the drugs, but SDS also caused formation of blebs at the cell surface.

Anesthetics are well known to have surface active properties and are considered to produce this effect by dissolution in the lipid phase of the cell membrane. Alternatively it has been proposed that anesthesia would be due to the reversible depolymerisation of microtubules (Allison and Nunn 1968). SDS is known to dissolve into cell membranes producing the same anti-hemolytic effect on erythrocyte ghosts as anesthetics (Seeman 1972). The present results show that the anesthetics and mitosis inhibitors tested caused similar effects on neuroblastoma cells whereas the detergent SDS had deviating effects. This suggests that chlorpromazine and lidocaine induce neurite retraction by interference with microtubules rather than with the cell membrane system.

References

- ALLISON A C and J F NUNN *Lancet* 1968 2 1326—1329
 SEEMAN P *Pharm Rev* 1972 24 4 583—655
 SCHUBERT D S HUMPHREYS F DEVITRY and F JACOB *Develop Biol* 1971 25 514—546

C 25

Increase in the Potassium Concentration in Brain Extracellular Fluid as a Cause of the No Flow State Following Cerebral Ischemia

By JOHN WADE OLE AMTORP and SOREN CLAUS SORENSEN *Institute of Medical Physiology Dept A University of Copenhagen Juliane Maries Vej 28 Dk 2100 Copenhagen Denmark*

When a tissue is deprived of its blood supply the functional state of the parenchymal cells is generally assumed to be the limiting factor for the ability of the organ to recover its function. However, in the brain inability to restore the local circulation after a period of ischemia might be crucial for the ability to restore normal function (Ames *et al* 1968). In other experiments we found that the potassium concentration in cisternal cerebrospinal fluid rose rapidly following circulatory failure. Because an increase in the extracellular potassium concentration may cause vasoconstriction we wanted to examine if changes in the potassium concentration in brain extracellular fluid following cerebral ischemia could be correlated to changes in cerebral vascular resistance.

Male Sprague Dawley rats weighing 430—470 g were used. The animals were anesthetized with pentobarbital (30 mg) intraperitoneally, tracheotomized and ventilated with a small animal respirator. The ventilator was adjusted in order to keep the arterial P_{CO_2} between 35 and 40 torr. The animals' rectal temperature were kept at 37.5—38°C throughout the experiment using a heating pad. A polyethylene catheter was passed retrograde from the abdominal aorta into the thoracic aorta. Silk thread were placed around the aortic arch, the superior and the inferior venae cava through a thoracotomy. Just prior to stopping the circulation heparin 1 mg was injected through the aortic catheter. Circulatory arrest was induced by occluding the aortic arch, the superior and inferior venae cava simultaneously. At different intervals after the circulatory arrest the cerebral perfusion rate for a solution containing 4% albumin in saline was determined by measuring the uptake of 3H_2O by the brain when the brain was perfused at a constant pressure of 140 mmHg through the aortic catheter. The uptake measured 10, 15, 20 and 25 s after start of the perfusion was found to follow a single exponential function and the perfusion rate (CPR) was calculated according to the formula $CPR = \lambda / 0.693 \cdot T_{1/2}$ where λ is the partition coefficient for 3H_2O between tissue and perfusion fluid $\lambda = 1.20$ and $T_{1/2}$ is the halftime for the wash in of 3H_2O into the brain. In control experiments the perfusion was started immediately after stopping the circulation. In similar experiments samples of cisternal cerebrospinal fluid was obtained at different times after the circulatory arrest and the potassium concentration was measured by flame photometry. The results are shown in Table I.

TABLE I Cerebral perfusion rate (CPR) and the potassium concentration in cerebrospinal fluid following cerebral ischemia

Period of ischemia (min)	CPR ml/100 g/min		[K ⁺] mEq/l
	Cortex	Cerebrum	
0	101	100	3.0
2	103	98	4.1
8	1	34	10.0
16	1	1	12.4

The results show that in control experiments the CPR measured by this method was similar to the cerebral blood flow found in rats when using the Akes technique (Eklund *et al.* 1973) and that after the initial increase in CPR the CPR decreased with increasing duration of the ischemia period. Concomitantly the potassium concentration in cerebrospinal fluid increased to such high levels that it may explain the increase in cerebral vascular resistance. Furthermore, it must be emphasized that the potassium concentration in cerebrospinal fluid increases more slowly than in brain interstitial fluid.

We therefore suggest that the changes in the potassium concentration in brain extracellular fluid following cerebral ischemia is responsible for the changes in cerebral vascular resistance.

References

- AKES, A., R. I. WINDHAGEN, M. KOWADA, J. M. THILANDER and C. MÄYNE (*Am J Pathol* 1973) 77: 437-453.
 EKLUND, B., N. A. LARSEN, J. NILSSON, K. NORRBY and B. H. SÖDER (*Acta physiol scand* 1973) 99: 50-59.

C 26

Pulsatile Hydraulic Power in the Pulmonary Circulation

By H. PETER¹ and A. HALGE, *Institute of Physiology, University of Oslo, Norway*

The pulsatile nature of blood flow puts an extra load on the heart which is not taken into account when one measures the conventional flow resistance only. In the pulmonary circulation this pulsatile hydraulic power normally makes up as much as 1/3 of the total energy output of the right ventricle. Whereas mean flow resistance is determined by vessel dimensions and fluid viscosity, opposition to pulsatile flow depends on fluid inertance, vessel wall compliance and pulse wave reflections in the vascular bed.

We have studied flow and pressure pulse contours in the pulmonary artery of pump perfused rabbit lungs. Flow opposition characteristics of the lung vascular system was analyzed and the external work load was calculated. By changing the

left atrial and the alveolar pressures we found that the peripheral vessels which were affected by such changes had no detectable influence on the pulsatile power load. This part of the external load must then be mainly determined by the compliance and inertance of the large arterial system in spite of a substantial degree of pulsatility in the peripheral vessels. The smooth muscle tension in these large arteries strongly influences the compliance of the vessel walls (Ingram *et al* 1968) and Milnor (1972) has proposed that the function of the musculature in these vessels might be to adjust the pulsatile flow opposition. In addition to the above experiments we changed the compliant and fluid inertive properties of the large arteries by means of vasorelaxants and -constrictors and we found that the pulsatile power load had a minimum at a moderate myogenic tone. The basal vascular tone thus seems to be of importance for minimizing the level of vascular opposition to pulsatile flow.

References

- INGRAM R. H. J. P. SZIDON, R. SKALAK and A. P. FISHMAN *Circ Res* 1968 22 801—815
MILNOR W. R. *New Eng J of Med* 1972 281 1 27—34

¹ Present address: Institute of Medical Biology, University of Tromsø, Norway

C 27

Water Permeability in the Human Forearm Measured by an Osmotic Transient Technique

By T. PALM, S. L. NIELSEN, N. A. LASSEN and P. BIE, *Department of Clinical Physiology, Bispebjerg Hospital and Institute of Medical Physiology C, Copenhagen, Denmark*

The classical technique for measurement of the capillary permeability for water (CFC) is a steady state method using hydrostatic driving force created by venous stasis. It is assumed that the increase in tissue volume observed after some minutes is due to the water flux caused by the change in capillary pressure. It is crucial that other elements of the thermodynamically correct Starling equation remain unchanged but no final proof has been given of these assumptions. Furthermore the method might be too insensitive to show changes in water permeability during pathological conditions.

We describe an osmotic transient method for measurement of water permeability in the vascular bed of the human forearm using an osmotic gradient created by intraarterial infusion of hyperosmolar albumin solution dialysed to contain solutes as normal blood. The hemodilution by interstitial water and infusate is calculated from non permeating tracers in blood and infused solution. It is crucial that hydrostatic pressure does not increase during the infusion (vasodilatation might be caused by hyperosmolar fluids) and venous pressure and forearm volume is therefore controlled during measurement. The suction force of infused albumin is measured as the colloid osmotic pressure in the venous samples. The osmotic transient technique showed a water permeability in the resting forearm 3—6 times as high as that

determined by a conventional Cl/C measurement. Eventually changes in the vascular membrane in pathological states as for instance long term diabetes might be demonstrated by the presented technique.

C 28

Different Temperature Dependence of Luminal and Contraluminal Ion Transport in the Cat Submandibular Gland

By L. P. PETERSEN, J. O. D. NIELSEN and J. HEDENRAB POUlsen, *Institute of Medical Physiology, Dept. 4, University of Copenhagen, Juliane Maries Vej 29, DK-2100 Copenhagen, Denmark.*

Two active Na pumps exist at the acinar level in salivary glands (Petersen 1971). One situated at the luminal membrane is involved in the formation of the primary saliva. The other at the contraluminal membrane is responsible for the maintenance of normal intracellular concentrations in the resting state as well as the reestablishment of these concentrations after stimulation induced changes (Burgess 1966). Since preferential inhibition of the luminal pump by ethacrynic acid was observed (Petersen 1971) concluded that the nature of the two pumps were different. In contrast it was found that both pumps were sensitive to ouabain but depending on the route of administration. It was therefore tentatively concluded that both pumps were ordinary Na/K activated ATPase systems (Poulsen 1974). According to the latter view it should be expected to find the same temperature dependence for the two pumps.

Cat submandibular glands were perfused with phosphate buffered Locke's solution and placed in a chamber where the temperature was kept at 37°C or reduced to 22, 17 or 12°C. The glands were stimulated at each temperature by acetylcholine (10 M). The secretory rate was used as a measure of the activity of the luminal pump. Both the maximal rate of the post-stimulatory uptake of K and the maximal reduction in the venous K concentration (ΔK) were used as measures of the activity of the contraluminal pump.

The luminal pump was more dependent on the temperature than the contraluminal pump. The most pronounced difference was observed at 17°C where the secretory rate was 18% while the rate of K uptake was 38% and ΔK was 41% (mean value relative to values at 37°C, 6 experiments).

It must be admitted that the chosen experimental variables are not exclusively dependent on the state of the pumps involved. Temperature induced changes in passive leaks may influence the results. However the simplest interpretation of the experimental data is that the two pumps are probably not both ordinary Na/K activated ATPase systems.

References

- BURGESS, A. S. V. *J. Physiol.* 1956, 132, 30-39.
 PETERSEN, O. H. *J. Physiol.* 1971, 216, 129-149.
 POULSEN, J. H. In *Secretory Mechanisms of Exocrine Glands*, Eds A. V. THOMAS and O. H. PETERSEN. Munksgaard, Copenhagen, 1974. In press.

Effects of Barbiturates on Synthesis and Rapid Axonal Transport of Protein *in vitro* in the Sciatic System of the Frog

By

ANDERS EDSTROM and HAKAN LARSSON

Received 21 January 1974

Abstract

EDSTROM A and H LARSSON *Effects of barbiturates on synthesis and rapid axonal transport of protein in vitro in the sciatic system of the frog* Acta physiol scand 1974 91 433-440

The effects of hexobarbital, pentobarbital, methohexital and thiopental (0.5 mM and 2 mM) on the synthesis and fast axonal transport of ³H leucine labelled proteins were studied *in vitro* in the sciatic system of the frog. The methodology used made it possible to discriminate between effects on synthesis and transport. All 4 drugs arrested the transport, pentobarbital being the most and thiopental the least potent one. The transport inhibiting effect of 0.5 mM pentobarbital was reversible but not that of the higher concentration. These drugs at concentrations (2 mM) which inhibited axonal transport did not influence the uptake of ³H leucine into ganglionic cell bodies, whereas pentobarbital, methohexital and thiopental, but not hexobarbital, depressed subsequent steps of protein synthesis. Pentobarbital lacked effect on protein synthesis at a concentration (0.5 mM) which arrested axonal transport by 50%. The results indicate that rapid axonal transport shows higher sensitivity than protein synthesis to the barbiturates tested. Fairly high concentrations of barbiturates were required to inhibit axonal transport and still higher to depress protein synthesis in the present study. Normal anesthesia by barbiturates is therefore hardly likely to affect these mechanisms.

Antimitotic drugs like colchicine and vinblastine, well known to interact with microtubule protein subunits (see Olmsted and Borisy 1973), have been found to block rapid axonal transport in a wide variety of nerve preparations (see Wuerker and Kirkpatrick 1972). The microtubular system has therefore been ascribed a central role in the transport machinery. Colchicine is known to arrest mitosis in metaphase, probably by interaction with spindle microtubules. Hexobarbital, a clinically useful barbituric acid derivative, has been reported to cause similar cytological effects on dividing embryonic cells (Grote, Kabany and Schade 1970). Allison *et al.* (1970) demonstrated the reversible disappearance of microtubules in *Actinosphaerium* after exposure to clinical concentrations of several common anesthetics. In contrast, Sauberman and Gallagher (1973) reported the absence of changes in the number and

structure of microtubules in optic nerves of mice anesthetized with halothane or pentobarbital. Furthermore Kennedy, Link and Byers (1972) failed to find inhibition of rapid axonal transport in rabbit vagus nerve exposed to physiological levels of halothane. However, there are to our knowledge no systematic studies made concerning the effects of barbiturates upon axonal transport. The absence of observable ultrastructural changes of microtubules does not exclude that their function could be impaired. Axonal microtubules of the crayfish connectives and of the rat hypothalamo-neurohypophyseal system are as judged with the electron microscope resistant to colchicine at concentrations that arrest transport (Nelson, Hanson and Strand 1971; Simon 1971).

Among other effects barbiturates have been shown to depress the synthesis of DNA, RNA and protein (Whitatt and Gruner 1970; Jackson 1971). Whether this is due to inhibition of cellular uptake processes of precursors of macromolecules and/or of subsequent steps is unclear.

Experiments reported here were made to study the effects of barbiturates on the cellular uptake of leucine, incorporation into protein and rapid axonal transport *in vitro* in the frog sciatic system.

Methods

Frogs *Rana pipiens* were used. After decapitation a preparation was isolated that consisted of two dorsal ganglia (no. 8 and 9), the sciatic nerve and the gastrocnemius muscle. The preparation was placed in an incubation chamber with 3 compartments (A, B and C). The parts were separated from each other by silicone grease barriers. The preparations were incubated in frog Ringer solution of the following composition in mM: NaCl 111.2, KCl 1.9, CaCl_2 1.1, MgSO_4 1.0, NaH_2PO_4 0.45, NaH_2PO_4 1.0 and glucose 5.5. The solution was gassed with oxygen before use and pH was adjusted to 7.4. ^3H -leucine was added to the ganglion compartment A, compartment B, which made it possible to follow the transport of labelled protein from the ganglia along the sciatic nerve, compartment B, toward the muscle compartment C. The preparations and incubation of the system has earlier been described in detail (Edström and Mattsson 1972). It was demonstrated that proteins synthesized in the ganglia were transported within the axon in anterograde direction at a rate of 12 ± 10 mm per day at 18°C (Edström and Mattsson 1972; Edström and Hanson 1973). The two preparations from the same animal were used in each experiment which made it possible to make comparison between paired preparation incubated with and without the addition of the drug. A nylon suture was placed on the nerve (compartment B) 30 mm from the ganglia. The preparation was incubated for 14 h at 18°C. After treatment with trichloroacetic acid (TCA) the distribution of labelled proteins along the nerve was determined as described previously (Edström and Mattsson 1972). In most experiments the transport function was measured by determining only the amount of TCA insoluble radioactivity which accumulated in a fraction equivalent immediately in front of the ligature.

In separate experiments ganglia were assayed for incorporation of ^3H -leucine into TCA insoluble and soluble fractions. After incubation the ganglia were washed twice for 5 min each time with cold Ringer before extraction of TCA soluble radioactivity and then treated as described previously (Anderson, Edström and Mattsson 1972). The radioactivity measured was expressed as TCA insoluble and soluble radioactivity per ganglionic sample. One sample consisted of the two dorsal ganglia (no. 8 and 9). This gave a higher reproducibility than if the radioactivity is referred to the weight or to the protein content (Anderson, Edström and Mattsson 1972).

TCA insoluble samples were dissolved in toluene 350 (Packard) in a 0.55% Permablend III (Packard) solution in toluene and were analysed for radioactivity with a Packard TriCarb (3375) liquid scintillation spectrometer. TCA soluble extracts were counted in Bray's solution (Bray 1960).

Chemicals Aqueous solutions of L-4,5- ^3H leucine (58 Ci/mmol, 1 mCi/ml) were purchased from the Radiochemical Centre Amersham England. Methohexital sodium (brietal), hexobarbital sodium (evipal), thiopental sodium (pentotal) and pentobarbital sodium (nembutal) were kindly supplied by Dr G Åberg AB Nobel Pharma Mölndal.

Results

Effects on axonal transport The preparations were incubated for 17 h at 18°C with ^3H leucine pre-ent in compartment A. In the test preparation the drug was added to compartment B and thus denied access to the nerve cell bodies in the ganglia (compartment A) where proteins for transport are synthesized. After incubation under normal conditions a proximo-distal gradient of TCA insoluble radioactivity is always found along the nerve (cf. Fig. 1). The high radioactivity recovered in front of the ligature is due to a damming up of protein transported within the axons towards the muscle at a rate of 120 mm/day (Edström and Mattson 1972; Edström and Hanson 1973). There is no radioactivity distal to the ligature. The transport effects by the various drugs were determined by comparing the amount of accumulated TCA insoluble radioactivity at the ligature in control and test preparations (Table I). After incubation in the presence of 2 mM hexobarbital, 2 mM pentobarbital or 2 mM methohexital the amount of accumulated radioactivity only represented some per cent of that in corresponding control preparation. Thiopental was less effective and at a concentration of 2 mM reduced the amount of accumulated radioactivity to about 40% of that recovered in the control. Pentobarbital was the most potent of the barbiturates tested and the only one which inhibited the transport when used at the lower concentration of 0.5 mM. Transport was then depressed to 50% of the control values.

Reversibility To test if the inhibitory effects were reversible one preparation was incubated with the addition of one of the drugs to the compartment B while the contralateral preparation was incubated simultaneously in normal Ringer. After incubation for 6 h the drug containing Ringer was replaced by normal Ringer and ^3H leucine was added to compartment A of the test and the control preparation. After incubation for another 15 h the nerves were analysed. The effect of pentobarbital, the most potent of the drugs tested, was reversible at a concentration of 0.5 mM but was largely irreversible when the higher concentration of 2 mM was used (Fig. 1). When the transport is inhibited there is often a damming up of labelled material in the first segment or segments after the barrier as can be seen in Fig. 1. Two experiments were run with each of the 3 other barbiturates at 2 mM concentrations. The transport inhibitory effects induced by hexobarbital and thiopental showed some reversibility. There was in no case complete reversibility. The amount of radioactivity at the ligature of test was in per cent of that recovered in control preparations: 43.61 (hexobarbital), 10.23 (methohexital) and 50.79 (thiopental).

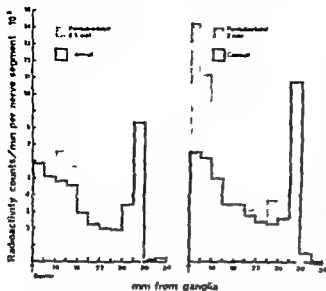


Fig. 1. Distribution of ^3H -leucine labeled TCA-soluble material in the nerve of a frog incubated at 18°C in pentobarbital-containing and in normal Ringer solution. One preparation was used as a control. The other from the same frog post-barbital was added to compartment B. After incubation (see Fig. 1) pentobarbital Ringer was replaced by normal Ringer and ^3H -leucine (5 Ci/mmol) in 1 ml Ringer was added to the compartment A. After another 15 min the nerves were analysed. The position of the literature is shown. Two preparations were run at each drug concentration. Similar results were obtained and one example is shown.

Effects on incorporation into TCA-insoluble and soluble ganglionic components
 In the experiments described above the barbiturates were prevented to reach the ganglia in compartment A. To study their effects on protein synthesis ganglia were separately incubated for 17 h at 18°C and then assayed for TCA-insoluble and soluble radioactivity (Table II). Hexobarbital at a concentration 2 mM which effectively arrested the axonal transport of proteins did not affect incorporation of ^3H -leucine into TCA-insoluble ganglionic components. Pentobarbital at a concentration of 0.5 mM which inhibited the transport by 50% had no significant effect whereas 2 mM pentobarbital depressed the incorporation into TCA-insoluble components to 26% of control values. The latter was accompanied by a several fold increase in the TCA-soluble radioactivity which a priori could be expected if the synthesis but not the precursor uptake mechanisms were inhibited. Likewise the presence of 2 mM methohexital decreased the amount of recovered TCA-insoluble radioactivity and increased the TCA-soluble radioactivity. Corresponding change but much smaller were caused by 2 mM thiopental.

Discussion

The drugs tested hexobarbital, pentobarbital, methohexital and thiopental are all derivatives of barbituric acid with different substituents in position 5. Pentobarbital is mostly described as a short acting sedative hypnotic and the other ones as highly lipid soluble ultrashort acting intravenous anesthetics. The mechanism whereby the barbiturates used blocked axonal transport is not clear. The effects did not correspond to their lipid solubilities. Methohexital having the highest partition coefficient between methylene chloride and water (Bush 1963) was more potent

TABLE I Effects of barbiturates on the accumulation of transported TCA insoluble radioactivity proximal to a ligature placed at the sciatic nerve. The preparations were incubated for 17 h at 18 °C. Compartment A contained 20 µCi ¹⁴C leucine (58 Ci/mmole) in one ml Ringer. One preparation was used as control. To the other from the same animal hexobarbital, pentobarbital, methohexital or thiopental was added to compartment B. The drugs were thereby denied access to the ganglia in compartment A. Results are expressed as mean values \pm S.E.M. P values obtained by use of a paired sample two tailed t test.

	Number of experiments	Counts/min/ nerve segment proximal to ligature	Per cent of control	P
Control	4	10 142 \pm 2 473		
Hexobarbital 0.5 mM	4	18 603 \pm 3 850	94.5 \pm 7.4	> 0.5
Control	4	13 244 \pm 2 410		
Hexobarbital 2 mM	4	1 630 \pm 305	12.8 \pm 0.8	< 0.01
Control	8	21 092 \pm 2 773		
Pentobarbital 0.5 mM	8	11 179 \pm 3 154	52.9 \pm 12.2	< 0.01
Control	4	7 726 \pm 1 234		
Pentobarbital 2 mM	4	273 \pm 63	3.1 \pm 0.9	< 0.01
Control	4	6 275 \pm 967		
Methohexital 0.5 mM	4	7 302 \pm 504	125.6 \pm 29.5	> 0.5
Control	4	8 404 \pm 1 630		
Methohexital 2 mM	4	504 \pm 193	6.7 \pm 2.7	< 0.02
Control	4	4 776 \pm 525		
Thiopental 0.5 mM	4	5 230 \pm 1 335	109.5 \pm 20.0	> 0.5
Control	4	18 637 \pm 863		
Thiopental 2 mM	4	7 285 \pm 1 795	39.1 \pm 9.3	< 0.01

than thiopental in arresting the transport. Pentobarbital, having the lowest partition coefficient, inhibited the transport more effectively than thiopental when used at the same concentrations.

It is possible that the drugs affected the transport secondarily through effects on energy metabolism. The axon depends on continuous supply of ATP to maintain the transport (see Ochs 1972). Barbiturates at concentrations known to produce deep narcosis have been shown to cause some inhibition of respiration of the brain *in vitro*. Fink and Kenny (1970) showed that amobarbital, which is chemically closely related to pentobarbital, caused increased glycolysis of cultured heteroploid mouse cells. It is possible that the cellular ATP content could be maintained by such a metabolic switch if adequate amount of exogenous glucose is available. At least *in vivo* the level of high-energy phosphate compounds does not seem to be influenced after administration of anesthetic doses of barbiturates (Nilsson and Siejko 1970). In spite of a heavy overdose of pentobarbital the oxidative cell metabolism *in vivo* was unaffected (Döring and Olbrisch 1968). Protein synthesis, which is also closely dependent on energy through ATP, was less sensitive than axonal transport to treatment with barbiturates. For instance hexobarbital at a concentration which strongly inhibited axonal transport did not influence protein synthesis. It is therefore possible that the transport inhibitory effects are not mainly due to suppression of ATP formation, which nevertheless could be a contributory factor.

TABLE II Effect of barbiturates on the incorporation of [3 H]leucine into TCA insoluble and soluble ganglionic components. The ganglionic ganglia (nodes B and $\frac{1}{2}$ of one side) were incubated for 17 h at 18°C in 1 ml Ringer's containing 70 μ Ci [3 H]leucine (28 Ci/mmole). The contralateral ganglia of the same animal were incubated with the addition of a substance but otherwise during the same conditions. Results are expressed as mean values of paired preparations. S.E.M. values. Estimate by use of a paired sample *t*-test.

	Number of experiments	TCA insoluble radioactivity (units/min ganglionic sample)	
Control	4	12.78	10.17
Hexobarbital 2 mM	4	81.733	98.303
Control	4	193.05	9.293
Pentobarbital 0.5 mM	4	1119.7	53.4
Control	4	3.3	49.40
Pentobarbital 2 mM	4	110.41	113.1
Control	4	197.131	1.31
Methohexital 2 mM	4	143.545	130.0
Control	9	8.0021	28.391
Pentobarbital 2 mM	4	1.18	11.43

In support of this there was no inhibitory effect by the various barbiturates on the cellular uptake of leucine which has been shown by others to be inhibited by substances which interfere with maintenance of energy metabolism (Appel 1970).

Local anesthetics and barbiturates seem to have some properties especially membrane action in common. Both types of drug probably block the nerve action potential by reducing sodium and potassium conductance increases (Blaustein 1968).

It is therefore of special interest that local anesthetics of the procaine type have been shown to inhibit fast axonal transport of proteins *in vitro* in the rabbit vagus (Link *et al.* 1970) and in the frog sciatic nerve (Anderson and Eidström 1973).

Edström, Hansson and Norström (1973) and *in vivo* of neurosecretory materials in the hypothalamo-neurohypophyseal system of the rat (Edström, Hansson and Norström 1973). Effects on the structure and number of microtubules were observed after drug treatment. Barbiturates when used at clinical concentrations do not seem to produce changes in microtubules observable under the electron microscope (Siu, Berman and Callagher 1973). It remains to be investigated if structural changes are induced during the present *in vitro* conditions when fairly high concentrations of barbiturates were necessary to cause transport inhibition. Considering the latter normal anesthesia by barbiturates is not likely to affect rapid axonal transport. However the possibility of effect after long term exposure to barbiturates should not be excluded.

Barbiturates are from other *in vitro* experiments known as inhibitors of cell growth and macromolecular synthesis. Drugs with these properties have in many cases been shown to be teratogens (see Goldstein, Aronow and Kalman 1969). Jackson (1971) showed that various barbiturates inhibited the incorporation of thymidine, uridine and leucine into their respective macromolecules in mammalian

Per cent of Control	P	TCN-soluble radioactivity Counts/min/ganglionic sample	Per cent of Control	P
		not determined		
103.0 ± 16.9	N.S.			
132.3 ± 16.2	N.S.			
26.3 ± 1.3	< 0.005	40 981 ± 4 848	413.7 ± 48.3	< 0.01
26.3 ± 5.4	< 0.005	159 657 ± 11 365		
66.4 ± 10.3	< 0.01	46 384 ± 5 457	246.5 ± 24.4	< 0.005
		104 884 ± 7 484		
		30 840 ± 2 744		
		37 929 ± 3 776	127.0 ± 13.1	< 0.1

hepatoma cells *in vitro*. It was suggested that nonvolatile anesthetics (thiopental, methohexital and amobarbital) interfere with precursor uptake processes and possibly also macromolecular synthesis. The present results indicate that when similar barbiturates are used at the same concentrations there is no suppression of the cellular uptake of leucine in the present system, whereas its subsequent incorporation into protein is inhibited.

The present work was supported by grants from Statens Naturvetenskapliga Forskningsråd (No 79358) and "C.B. Natfors Vetenkapliga och Allmannnyttiga Stiftelser". Thanks are due to Mrs B. Egner and Miss C. Nyberg for expert technical assistance.

References

- ALLISON, A. C., G. H. HILANDS, J. P. NICK, J. A. KITCHING and A. C. MACDONALD. The effects of inhalational anesthetics on the microtubular system in *Actinosphaerium nucleofilum*. *J. Cell Sci.* 1970, 7: 483-499.
- ANDERSON, K. E., A. EDSTROM and H. MATTSOON. Effects of cytochalasin B on uptake of glucosamine, leucine and sulphate into nerve cells: incorporation into glycoproteins and rapid axonal transport. *Brain Res.* 1972, 48: 343-353.
- ANDERSON, K. E. and A. EDSTROM. Effects of nerve blocking agents on fast axonal transport of proteins in frog sciatic nerves *in vitro*. *Brain Res.* 1973, 50: 125-134.
- APPEL, H. Inhibition of protein synthesis. In *Protein metabolism of the nervous system*. Editor A. Lajtha. Plenum Press, 1970, pp. 671-680.
- BLAUSTEIN, M. Barbiturates block sodium and potassium conductance increases in olfactory clamped lobster axons. *J. gen. Physiol.* 1968, 51: 293-307.
- BUTLER, M. T. Sedatives and hypnotics: Absorption, fate and excretion. In *Physiological pharmacology*, vol. 1. Editors Root, W. E. and F. G. Hofmann. Academic Press—New York, 1963, pp. 183-218.
- DORF, H. J. and R. R. OLBRICH. Das Verhalten der energiereichen Phosphate der Gehirnrinde bei Ausschaltung der elektrischen Aktivität durch hohe Dosen etherischer Narkotika. *Arch. Toxikol.* 1968, 24: 83-90.
- EDSTROM, A. and H. MATTSOON. Fast axonal transport *in vitro* in the cytoskeleton of the frog. *J. Neurochem.* 1970, 19: 705-721.

FINK, M. A. and M. HANSON. Temperature effects on fast axonal transport of proteins in situ in frog sciatic nerves. *Brain Res.* 1973 38 345-354.

EL THOM, A. H. A. HANSEN and A. NORDSTRÖM. Inhibition of axonal transport in vitro in frog sciatic nerves by chlorpromazine and lidocaine. *Z. Zellforsch.* 1973a 143 53-61.

EL THOM, A. H. A. HANSEN and A. NORDSTRÖM. The effect of chlorpromazine and tetracaine on the rapid axonal transport of neurosecretory material in the hypothalamo-neurohypophyseal stem of the rat. *Z. Zellforsch.* 1973b 143 71-81.

FINK, B. R. and C. F. KENNEDY. Local tetracaine reversibly arrests cell growth by antimitotic. *Anesthesiology* 1970 32 300-305.

FINK, B. R., R. D. KENNEDY, A. E. HENDRICKSON and M. F. MARGARIT. Lidocaine inhibition of rapid axonal transport. *Anesth. Analg.* 1972 50 477-481.

GOLDSTEIN, A. L. ARONOW and S. HANMAN. *Principles of drug action*. New York: Harper and Row 1971 11 111-114.

GRÖTE, W., A. KAHARATA and H. SCHÄPE. Auswirkungen eines Barbiturats und zivates auf die Embryogenese von Kaninchen durch Mikrotubulungen. *Humanae nat.* 1970 8 70-73.

JACKSON, S. H. The initial effects of nonvolatile anesthetics on mammalian leg autonomic cells in vitro. *Anesthesiology* 1971 35 718-722.

KENNEDY, R. D., B. H. FINK and M. R. BYRNE. The effect of halothane on rapid axonal transport in the rabbit vagus. *Anesthesiology* 1972 37 433-443.

MARGARIT, M. F. and B. K. SINGH. The effect of anesthetics on the tissue lactate pyruvate phosphorylcreatine (ATP) and AMP concentrations and on intracellular pH in the rat brain. *Acta physiol. scand.* 1970 90 147-149.

NORDSTRÖM, A. H. A. HANSEN and J. SPJÄNNA. Effect of a local anesthetic on axonal transport and ultrastructure of the hypothalamo-neurohypophyseal stem of the rat. *Z. Zellforsch.* 1971 113 271-293.

OGURA, S. Fast transport of materials in mammalian nerve fibres. *Sci. Rev.* 1972 176 237-250.

OLMSTEDT, J. H. and C. C. BURLEY. Microtubules. *Ann. Rev. Biochem.* 1973 42 507-540.

SAMSON, F. F. Mechanism of axoplasmic transport. *J. Neurobiol.* 1971 2 31-36.

SALBERGMANN, A. J. and M. L. GALLAGHER. Mechanisms of general anesthesia. Failure of pentobarbital and halothane to depolymerize microtubules in mouse optic nerve. *Anesthesiology* 1973 38 5-29.

WHITT, P. and J. CRAMER. Barbiturates in cell culture as inhibitors of cell growth and macromolecular synthesis. *Pharmacol. Ther.* 1970 1 211-229.

VERKER, H. B. and J. B. KIRKPATRICK. Neuronal microtubules, neurofilaments and neurofilaments. *Int. Rev. Cytol.* 1972 33 45-15.

The Immediate Effects of Ligation of the Hepatic Artery on Liver Hemodynamics and Liver Function in the Cat

By

NIELS KRARUP and JENS ANKER LARSEN

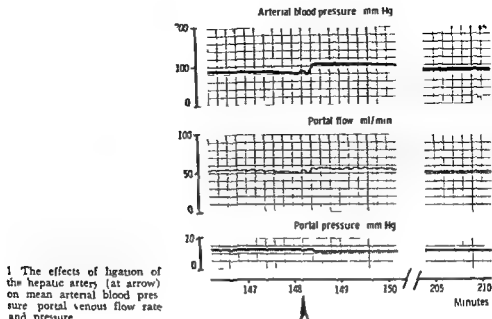
Received 25 January 1974

Abstract

KRARUP N and J A LARSEN *The immediate effects of ligation of the hepatic artery on liver hemodynamics and liver function in the cat* Acta physiol scand 1974 91 441-446

Cats in the postabsorptive state and anesthetized with chloralose were used for the experiments. In 7 out of 8 experiments ligation of the hepatic artery caused no change in the hepatic elimination rate of ethanol, the secretion rate of bile and Indocyanine Green (ICG), the hepatic oxygen consumption or the output of glucose and lactate, whereas a small decrease in hepatic ketone production was noticed. Ligation caused a 16 per cent decrease in ICG clearance and a 60 per cent increase in the extraction ratio of ICG, which can be explained by the reduction in total liver blood flow. In one experiment in which the initial hepatic oxygen consumption was relatively high, ligation caused a fall in hepatic oxygen consumption with marked changes in liver function as a consequence. It is concluded that the main function of the hepatic artery is to supply the liver as a whole with oxygen, whereas no specific functions of the artery were demonstrable.

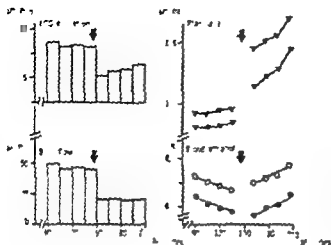
It is generally accepted that one main function of the hepatic artery is to secure an adequate supply of oxygen to the liver. However, reports continue to appear in which it is claimed that the hepatic artery may have more specific functions. Thus, hepatic clearance of Kr^{85} (Hollenberg and Dougherty 1966) and of labelled albumin and erythrocytes (Cohn and Pinkerson 1969) from hepatic arterial and portal venous blood indicate that the two blood streams to some extent may be separated in the sinusoids. Transillumination studies have also revealed that parts of the hepatic lobules are intermittently supplied exclusively with arterial blood (McCurley 1966) and a controlling effect of hepatic arterioles on the distribution and flow rate of portal venous blood in the sinusoids has been suggested by Rapaport et al (1970). Finally, experimental observations suggest that the hepatic artery is of importance for the secretion of bile (Kelly and Kipper 1967) and for the hepatic elimination of dyes (Andrews, Maigrahn and Richard 1956).



The effects of ligation on hepatic and portal blood flow and hepatic oxygen supply from 7 expts are listed in Table I. There is no effect on portal blood flow, oxygen content of portal venous blood or hepatic oxygen consumption. In the control period there was no difference between the oxygen content of portal and hepatic venous blood, but ligation caused a marked increase in the extraction of oxygen from portal venous blood, which with unchanged portal blood flow was sufficient to cover the control oxygen consumption of the liver.

TABLE I The effect of ligation of the hepatic artery on hepatic blood flow, the oxygen content of arterial, portal and hepatic venous blood and the hepato-splanchnic oxygen consumption. The numbers in brackets indicate the oxygen saturation in per cent.

	Control	After ligation	p
Hepatic arterial blood flow ml/kg/min	28 ± 4	4 ± 3	< 0.001
Portal venous blood flow l/kg/min	17 ± 2	20 ± 2	< 0.10
Oxygen concentrations mM			
arterial blood	6.39 ± 0.17 (87)	6.32 ± 0.14 (88)	ns
portal venous blood	3.88 ± 0.23 (5)	4.14 ± 0.20 (58)	< 0.05
hepatic venous blood	3.6 ± 0.40 (50)	1.66 ± 0.94 (23)	0.01
Oxygen consumption μ mol/kg/min			
arterial blood	43 ± 4	44 ± 3	ns
hepatic	69 ± 5	66 ± 6	ns



2 Unusual effect of ligation of the hepatic artery as assessed on ICG excretion, bile flow and plasma/lymph concentrations of ICG and ethanol (from a study in which arterial concentrations of ICG and ethanol were also determined)

The splanchnic elimination of ethanol ($25 \pm 2 \mu\text{mol/kg/min}$) was not changed by ligation and neither was bile flow ($10.5 \pm 1.4 \text{ ml/kg/min}$) nor ICG excretion ($90 \pm 3 \text{ ml/min}$). The steady arterial plasma concentration of ICG in the control period was highly elevated after ligation resulting in a 16% decrease in ICG clearance from 36 ± 0.4 to $30 \pm 0.3 \text{ ml/kg/min}$. The arterio-hepatic venous concentration gradient, however, increased more than the arterial ICG concentration level resulting in a 60% increase in the extraction ratio of ICG from 13 ± 2 to 21 (see calculations).

Ligation did not change the splanchnic lactate output ($82 \pm 20 \mu\text{mol/kg/min}$). Because of exceedingly small pyruvate and acetoacetate concentrations it was only possible to calculate the hepatic venous L/P and Hb/Vc ratios in a few cases in which they remained unchanged. Ligation caused a slight decrease in splanchnic ketone production from 5.7 ± 1.1 to $3.2 \pm 0.4 \mu\text{mol/kg/min}$ but no change in splanchnic output of glucose ($14 \pm 3 \mu\text{mol/kg/min}$) occurred.

In the experiment shown in Fig. 2 a quite different response to ligation was observed. Ethanol elimination as well as bile flow are immediately decreased about 30%. Also the lymph excretion of ICG is decreased and therefore a new steady level of ICG in plasma is not attained. In the control period the splanchnic elimination of ethanol ($38 \mu\text{mol/kg/min}$) and hepatic oxygen consumption ($121 \mu\text{mol/kg/min}$) were significantly higher than normally seen in the fasting state. The extraction of oxygen from portal venous blood after ligation was almost complete (92%) and the hepatic oxygen consumption decreased by 35%. There was a rise in splanchnic output of lactate (from 9 to $30 \mu\text{mol/kg/min}$) and glucose output (from 36 to $85 \mu\text{mol/kg/min}$). The L/P and Hb/Vc ratios could not be calculated. The hemodynamic effect of ligation was similar to those seen in Fig. 1.

Discussion

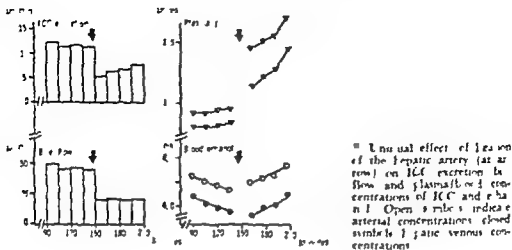
Ligation of the hepatic artery does apparently not influence portal venous hemodynamics to any great extent in accordance with most reports in the literature (Greenway and Stark 1971) and the present experiments confirm that portal blood flow is determined mainly by prehepatic factors. After ligation the estimated arterial blood flow was not significantly different from zero which means that the collateral arterial blood supply to the liver in these experiments is sparse.

In the present experiments the portal fraction of the total hepatic blood flow was decreased to about 40 % by splenectomy in contrast to the normally observed 60 % (Krørup and Larsen 1974). As previously found (Krørup and Larsen 1974) the prehepatic splanchnic oxygen consumption was about 40 % of the total splanchnic oxygen consumption and was unaffected by hepatic artery ligation. Under the conditions the difference in oxygen content between portal and hepatic venous blood is insignificant and the oxygen consumed by the liver is therefore almost completely supplied by the hepatic artery. Even under these circumstances however the portal vein alone was capable of covering the oxygen consumption of the liver in 7 out of 8 experiments aided by an increased extraction of oxygen.

The unaltered hepatic oxygen consumption, splanchnic output of lactate and glucose and L/P and Hb/1c ratios in hepatic venous blood indicate that no substantial part of the liver became hypoxic. This means that portal blood flow after ligation is evenly distributed to all liver sinusoids and that the postulated controlling effect of the hepatic arterioles on the distribution and flow rate of portal flow in the sinusoids therefore must be of minor functional importance. Furthermore the lack of effect of ligation on the splanchnic elimination rate of ethanol, bile flow and ICG excretion makes it unlikely that the liver sinusoids are functionally dependent on the supply of arterial blood. The changes in ICG clearance and extraction ratio after ligation may merely be due to the decrease in total hepatic blood flow in accordance with the model for hepatic dye elimination proposed by Winkler and Gram (1963). The lack of effect on bile flow may indicate that the ductular fraction of the bile in the cat is insignificant or that the bile ductules normally supplied with hepatic arterial blood may be supplied under the present conditions by portal blood through arterio-portal communications.

In only one experiment was ligation of the hepatic artery accompanied by changes in liver function. In this case the hepatic oxygen consumption decreased after ligation while the oxygen extraction in the portal blood was almost complete. The effects may all be explained by a generalized hepatic hypoxia which compromised all liver functions tested. The obvious reason for this marked effect of ligation is the unexplained high initial oxygen consumption of the liver and the experiment illustrates the importance of the arterial oxygen supply in situations where the oxygen consumption of the liver exceeds fasting or near fasting levels.

It may thus be concluded that in the cat the main function of the hepatic artery is to supply the liver as a whole with oxygen whereas no specific functions of the artery were demonstrable in the present acute experiments.



Unusual effect of ligation of the hepatic artery (at arrow) on ICG excretion, bile flow and plasma level concentrations of ICG and ethanol. Open symbols indicate arterial concentrations; closed symbols indicate venous concentrations.

The splanchnic elimination of ethanol ($25 \pm 2 \mu\text{mol/kg/min}$) was not changed by ligation and neither was bile flow ($10.5 \pm 1.4 \text{ ml/kg/min}$) nor ICG excretion ($90 \pm 3\%$ of infusion rate). The steady arterial plasma concentration of ICG in the control period was slightly elevated after ligation resulting in a 16% decrease in ICG clearance from 36 ± 0.4 to $30 \pm 0.3 \text{ ml/kg/min}$. The arterio-hepatic venous concentration gradient however increased more than the arterial ICG concentration level resulting in a 60% increase in the extraction ratio of ICG from 13 ± 2 to $21 \pm 2\%$ (see calculations).

Ligation did not change the splanchnic lactate output ($8.2 \pm 2.0 \mu\text{mol/kg/min}$). Because of exceedingly small pyruvate and acetoacetate concentrations it was only possible to calculate the hepatic venous L/P and Hb/Vc ratios in a few cases in which they remained unchanged. Ligation caused a slight decrease in splanchnic ketone production (from 5.2 ± 1.1 to $3.2 \pm 0.4 \mu\text{mol/kg/min}$) but no change in splanchnic output of glucose ($14 \pm 3 \mu\text{mol/kg/min}$) occurred.

In one experiment shown in Fig. 2 a quite different response to ligation was observed. Ethanol elimination as well as bile flow are immediately decreased about 50%. Also the biliary excretion of ICG is decreased and therefore a new steady level of ICG in plasma is not obtained. In the control period the splanchnic elimination of ethanol ($48 \mu\text{mol/kg/min}$) and hepatic oxygen consumption ($121 \mu\text{mol/kg/min}$) were significantly higher than normally seen in the fasting state. The extraction of oxygen from portal venous blood after ligation was almost complete (92%) and the hepatic oxygen consumption decreased by 35%. There was a rise in splanchnic output of lactate (from 9 to $30 \mu\text{mol/kg/min}$) and glucose output (from 36 to $83 \mu\text{mol/kg/min}$). The L/P and Hb/Vc ratios could not be calculated. The hemodynamic effect of ligation was similar to those seen in Fig. 1.

Effects of Prolonged Treatment with Adrenergic β -receptor Antagonists on Blood Pressure, Cardiovascular Design and Reactivity in Spontaneously Hypertensive Rats (SHR)

By

LILIAN WEISS YEN LUNDGREN and BjÖRN FOLKOW

Received 28 January 1974

Abstract

WEISS L. Y. LUNDGREN and B. FOLKOW *Effects of prolonged treatment with adrenergic β receptor antagonists on blood pressure cardiovascular design and reactivity in spontaneously hypertensive rats (SHR)* Acta physiol scand 1974 91 447-457

Young "p ehypertensive" SHR were treated with two kinds of β adrenergic receptor antagonists from 2 1/2 up to 8 months of age. Arterial pressure largely remained at prehypertensive levels and acute cardiovascular responses to "stress" were considerably modified compared to untreated SHR. Quantitative hemodynamic analyses revealed that resistance vessel design exhibited only slight hypertensive changes when related to untreated controls while the development of left ventricular hypertrophy was far less influenced by the treatment. In part of the group pressure was followed for another 6 months after treatment, showing only a delayed and modest pressure rise compared with untreated matched SHR. When instead adult SHR with "established" hypertension were similarly treated from 8 up to 10 months of age, resting arterial pressure remained unaffected and the resistance vessels exhibited only modest regression of the hypertensive changes with signs of a largely preserved increase of vascular wall/lumen ratio and with negligible regression of cardiac hypertrophy. The results indicate that early "preventive" treatment of SHR with β receptor blockers is of considerable value whichever their exact modes of action, though some regression of vascular changes can be achieved also in established hypertension particularly in females (Weiss 1974).

Like man in early phases of essential hypertension (e.g. Brod *et al* 1962, Julius Pascual and London 1971), young spontaneously hypertensive rats (SHR, Okamoto 1969) appear to display a hyperkinetic hemodynamic pattern (Pfeffer and Frohlich 1973), closely resembling a mild defence reaction and with exaggerated often prolonged pressure and heart rate responses to alerting stimuli (Folkow, Hallback and Weiss 1973, Hallback and Folkow 1974). In general SHR display signs of an intensified activity not only of the sympathico-adrenal system but also of the ACTH-corticoïd and TSH-thyroid systems (Okamoto 1969, Taber *et al* 1972).

Further hemodynamic analyses in both hypertensive rats and man indicate that a structural increase in wall/lumen ratio of the resistance vessels rapidly takes place (Folkow *et al* 1973, Lundgren *et al* 1974) raising resistance and vascular reactivity without necessitating any increased smooth muscle activity. However if the cardiovascular system is protected from functional pressure enhancements the structural vascular changes largely fail to appear, or exhibit considerable regression if already established at least in young organisms (e.g. Folkow *et al* 1972, Weiss 1974, Lundgren 1974). These studies thus suggest that increases in the average pressure are a prerequisite for the mentioned structural adaptation of the resistance vessels which however then reinforces the impact of functional excitatory elements and hence serves to maintain a chronic hypertensive state.

In order to further explore such mechanisms in animals genetically predisposed for hypertension, adrenergic β receptor antagonists were administered to young prehypertensive SHR for 3 1/2 months and to adult SHR for 2 months. Cardiovascular reactivity to altering stimuli was explored during treatment at the end of which hemodynamic analyses of vascular design were performed. In some of the young SHR blood pressure was instead followed for another 6 months after interrupted treatment to explore how a period of early therapy affects the development of hypertension later in life. Part of the results have been earlier briefly reported (Folkow, Lundgren and Weiss 1972).

Methods

Material and type of chronic treatment. Three different SHR groups were subjected to treatment with β adrenergic receptor antagonists administered in the drinking water. One approximate estimate of the daily water and thus drug consumption could be determined from the following: with 3 rats in each wire-meshed bottle the rats would introduce an untreated drinking factor:

4.15 ml and 14 female SHR were treated with pindolol 100 mg/kg and 4 h later the average systolic intra-arterial pressure averaged 135 mm Hg compared with 115 mm Hg in untreated control rats (NCR). Treatment was continued up to 8 months after which pressure in untreated SHR averaged 175 mm Hg. In 5 males and 5 females the drug treatment was then followed for another 6 months by intermittent intra-arterial infusions while the others were used for acute experiments (see below).

10 male and 10 female SHR were treated with H_2O , a cardioselective adrenergic β receptor antagonist. All three experimental groups were used in a dosage of 100 mg per kg and 24 h after 150 mg/kg of pindolol or 100 mg/kg of H_2O when they were used for acute experiments. This drug which has no intrinsic β adrenergic activity is reported to be a β_1 antagonist concerning cardiac effect but has far less effect on β_2 receptors. (Blad, Carlsson and Eriksson 1973). Like propranolol it is orally active and is absorbed upon oral administration and is metabolized in the liver to a large extent in propranolol but has no known active metabolites.

9 male and 9 female SHR and 10 male NCR were treated from 8 to 10 months of age with propranolol 100 mg per kg and 24 h.

12 untreated female and 14 untreated male SHR were used as control and matched to 6 male and 6 female NCR were used in the paired perfusion experiment for comparison with the treated or untreated SHR.

Acute experimental procedure. For evaluation of the effectiveness of the adrenergic β receptor blockade the awake rats were given increasing doses of isoprenaline (0.01–1.5 μ g/100 g) via the tail artery from which the heart rate was recorded. Reproducible heart

rate effects were obtained despite the recirculation situation. The caudal veins are too small to be used in this situation and cannulation of other veins would further disturb the animals. Dose-response curves were constructed and compared for the different groups.

2 In order to evaluate the effect of the chronic treatment on the neurohormonal excitatory influences on the heart and vessels the cardiovascular responses to environmental stress were studied. Thus 6 propranolol treated and 6 H 93/26 treated SHR were compared to matched untreated SHR concerning reactivity in terms of changes in heart rate and blood pressure to standardized "stress stimuli (sudden noise or vibrations) as described in detail elsewhere (Hallback and Folkow 1974).

3 At the end of the treatment period the rats were subjected to paired hemodynamic analyses of their isolated hindquarter vascular beds as earlier described in detail (Folkow *et al* 1970 1971). Mean arterial pressure and heart rate were first measured during awake conditions whereafter the hindquarter perfusion was started. — Pressure flow curves at maximal dilatation and resistance curves to noradrenaline (NA) for the two preparations were constructed and compared concerning A Resistance during maximal vasodilatation reflecting average luminal width B Threshold concentration of NA C Steepness of the resistance curve (tangent of the angle) reflecting mainly the wall/lumen ratio and D Maximal prestor response reflecting the bulk of contractile tissue in relation to the lumen (for details see Folkow *et al* 1970). The left and right heart ventricles were separated and weighed. The compiled results from the various groups of paired animals were subject to statistical analysis according to pairing design t test. The difference between the control groups of SHR \ NCR and the difference between treated SHR \ NCR were compared according to a group comparison t test. At p values below 0.05 the difference was considered as significant.

Results

I *Propranolol treatment from 2.5 months of age* Already at this age mean arterial pressure was slightly though significantly higher than in matched NCR being about 135 and 115 mm Hg respectively ($p < 0.05$). After 5.5 months of treatment intra arterial pressure was 138 ± 4 mm Hg compared with 175 ± 4 mm Hg in untreated age matched SHR. Resting awake heart rate was 273 ± 8 beats/min in the treated SHR compared to 348 ± 13 beats/min in untreated controls.

In those rats where pressure was followed for another 6 months after interruption of all treatment at the age of 8 months arterial pressure reached 150 mm Hg only after more than 3 months when pressure in untreated controls was around 180 mm Hg.

Dose response curves to isoprenaline were considerably displaced to the right for the propranolol treated awake SHR as compared to untreated controls indicating a relative blockade at the time of the test. Further when subjected to standardized stress stimuli such as loud noise and vibrations the treated SHR responded with bradycardia instead of tachycardia which is the most common cardiac response in untreated SHR alerted in a similar manner (see Hallback and Folkow 1974). The bradycardia disappeared after atropine administration. The average rise in pressure was about the same as in untreated SHR but it was delayed and more gradual in onset.

The results from the hemodynamic analyses of the isolated hindquarter preparation with respect to design of the resistance vessels are summarized in Table I. Males and females are here compiled since they did not differ substantially after propranolol treatment. In this Table the means \pm S.E. and the mean difference \pm

YOUNG SHR TREATED WITH PROPRANOLOL OR H 93/26

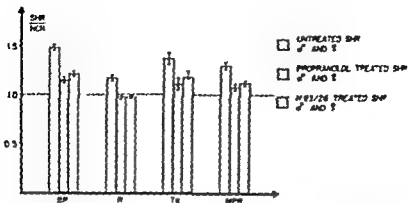


Fig. 1. The mean ratio \pm SE between untreated propranolol or H 93/26 treated SHR from age 17 to 18 months and their respective NCR concerning blood pressure (BP), resistance at maximal dilatation (R), steepness of the resistance curve (Tg) and maximal pressor response (MPV). For details see Table I.

SED are given together with the degree of significance between treated or untreated SHR and NCR and between the different groups of pairs. It is seen that mean arterial pressure after 33 months of treatment was approximately the same as before treatment while it had meanwhile risen some 40 mm Hg in untreated matched SHR. Resistance at maximal vasodilatation was the same in treated SHR and NCR and the steepness of the resistance curve indicating the wall/lumen ratio of the resistance vessels tended to be slightly though not significantly higher in treated SHR than in NCR. The maximal pressor response expressing the bulk of contractile wall tissue in relation to the lumen displayed a small but significant increase in treated SHR compared to NCR. However the difference in this latter parameter was 3–4 times bigger in untreated SHR–NCR. The Δ threshold did not differ in NCR and treated or untreated SHR. In general therefore the structural design of the resistance vessels in the treated SHR as reflected by these hemodynamic parameters appeared to be closely similar to that in untreated SHR at the age of 23 months (unpublished data) suggesting that further progression of hypertensive vascular changes had been largely prevented. To further illustrate the situation the ratios between untreated SHR/NCR and treated SHR/NCR were calculated concerning arterial pressure, resistance at maximal dilatation, slope of the resistance curve and maximal pressor response (Fig. 1). It is here illustrated that the young propranolol treated SHR (like those treated with H 93/26 see below) differ considerably from age matched SHR not only in blood pressure but also in all the parameters reflecting the design of the resistance vessels.

TABLE I Upper part Mean values \pm SE and degree of significance from paired experiments on male and female SHR untreated or treated with propranolol or H 93/26 from age 2 1/2 to 8 months as compared to matched NCR Lower part Group comparison t test of the mean differences between treated SHR—NCR and untreated SHR—NCR.

Group	Mean arterial pressure mm Hg	PRU ₁ at 30 ml/min 100g	Tangent of the angle	Maximal pressor response mm Hg
Untreated SHR	175 \pm 4	1.79 \pm 0.07	4.1 \pm 0.3	347 \pm 13
NCR	118 \pm 3	1.53 \pm 0.04	3.0 \pm 0.2	267 \pm 8
n = 26 pairs				
p <	0.001	0.001	0.001	0.001
Propranolol treated SHR	138 \pm 4	1.54 \pm 0.03	3.9 \pm 0.3	250 \pm 12
NCR	120 \pm 3	1.58 \pm 0.07	3.5 \pm 0.3	231 \pm 10
n = 17 pairs				
p <	0.001	ns	ns	0.05
H 93/26 treated SHR	137 \pm 4	1.54 \pm 0.04	4.0 \pm 0.2	262 \pm 10
NCR	113 \pm 4	1.59 \pm 0.05	3.4 \pm 0.2	235 \pm 8
n = 18 pairs				
p <	0.001	ns	0.003	0.003
Mean differences				
SHR—NCR	57 \pm 4	0.26 \pm 0.05	1.1 \pm 0.2	80 \pm 10
Propranolol SHR—NCR	18 \pm 7	-0.04 \pm 0.03	0.4 \pm 0.2	19 \pm 7
p <	0.001	0.001	0.03	0.001
Mean differences				
SHR—NCR	57 \pm 4	0.26 \pm 0.03	1.1 \pm 0.2	80 \pm 10
H93/26 SHR—NCR	24 \pm 4	-0.04 \pm 0.04	0.6 \pm 0.2	27 \pm 8
p <	0.001	0.001	ns	0.001

Left ventricular weight in per cent of body weight on the other hand revealed that a considerable cardiac hypertrophy had taken place despite treatment since it was only 10 per cent lower in treated SHR than in matched untreated SHR ($p < 0.05$) right ventricular weights being the same. It should here be noted that there is about 70 per cent difference in left ventricular weight between untreated SHR and NCR at this age (8 months).

II *Treatment with a cardioselective adrenergic β receptor antagonist (H93/26) from 2.5 months of age.* After 5.5 months of treatment arterial pressure was 137 \pm 4 mm Hg compared with 175 \pm 4 mm Hg in untreated SHR.

Resting heart rate did not differ from that in untreated SHR at least not when measured during daytime presumably because the oral intake is greater during night and the duration of H 93/26 seems to be shorter than that of propranolol. This probably explains why the responses to increasing doses of isoprenaline varied greatly at the time of the acute experiment. For the same reason there was in these rats a considerable variation in the heart rate responses to the standardized stress stimuli while the acute pressure rises were significantly smaller than in both propranolol treated and untreated SHR.

TABLE II Upper part: Mean values \pm S.E. and degree of significance for paired experiments in male and female SHR untreated or treated with propranolol from 8 till 10 months of age as compared to matched NCR. Lower part: Group comparison test of the mean differences between treated SHR-NCR and untreated SHR-NCR.

Group	Caval blood pressure mm Hg	PRV in III 30 ml/min 100 g	Tangent of the angle	Maximal pressure response mm Hg
Untreated SHR = NCR σ $n = 14$ pairs $p <$	187 ± 5 121 ± 4 0.001	1.95 ± 0.09 1.64 ± 0.03 0.001	4.2 ± 0.5 3.2 ± 0.3 0.01	$3.0 \pm 1^*$ $2.7 \pm 1^*$ 0.001
Propranolol treated SHR σ NCR σ $n = 9$ pairs p	181 ± 3 115 ± 3 0.001	1.74 ± 0.06 1.69 ± 0.04 ns	4.4 ± 0.2 3 ± 0.1 0.003	3.3 ± 8 2.5 ± 8 0.001
Untreated SHR NCR λ $n = 12$ pairs $p <$	159 ± 4 114 ± 5 0.001	1.56 ± 0.06 1.58 ± 0.04 0.005	4.4 ± 0.3 3.0 ± 0.1 0.005	3.18 ± 18 2.5 ± 1 0.003
Propranolol treated SHR NCR λ $n = 12$ pairs $p <$	160 ± 11 127 ± 4 0.05	1.47 ± 0.03 1.53 ± 0.04 ns	4.6 ± 0.3 3.7 ± 0.3 ns	2.94 ± 10 2.8 ± 11 ns
Mean differences SHR-NCR σ Propranolol treated SHR-NCR σ $p <$	66 ± 4 69 ± 5 ns	0.31 ± 0.07 0.05 ± 0.06 0.05	1.0 ± 0.3 1.2 ± 0.3 ns	0.3 ± 13 6.8 ± 7 ns
Mean differences SHR-NCR Propranolol-treated SHR-NCR p	45 ± 5 38 ± 11 ns	0.18 ± 0.04 -0.06 ± 0.08 0.01	1.4 ± 0.3 0.9 ± 0.6 ns	$6^* \pm 15$ ± 10 0.03

The hemodynamic evaluation of the isolated hindquarters showed the same general characteristics as in the propranolol treated rats i.e. the parameters reflecting resistance vessel design of the treated SHR were in good balance with their modestly raised pressure and well below those in untreated SHR (Table I and Fig. 1). However, also in this group left ventricular weight in per cent of body weight was only some 10 per cent below that of untreated matched SHR.

III *Propranolol treatment from 8 months of age* After 2 months treatment of SHR with established hypertension resting arterial pressure was not at all lowered being 184 ± 3 mm Hg in males and 160 ± 11 mm Hg in females. Dose response curves for isoprenaline showed that the heart rate responses were considerably displaced to the right for the treated awake animals indicating a relative β adrenergic blockade at the time of testing.

ADULT SHR TREATED WITH PROPRANOLOL

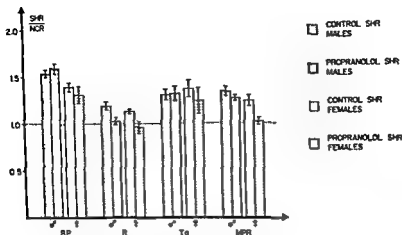


Fig 2 The mean ratio \pm SE between untreated or propranolol treated SHR from age 8–10 months and their respective NCR concerning blood pressure (BP) resistance at maximal dilatation (R) steepness of the resistance curve (Tg) and maximal pressor response (MPR). For details see Table II

Regarding the paired hemodynamic analyses of the hindquarter vascular bed (Table II Fig 2) the difference in resistance at maximal dilatation between treated SHR and NCR had been reduced in both male and female SHR but the steepness of the resistance curve was still considerably raised in both males and females as was also the maximal pressor response in males.

Left ventricular weight in per cent of body weight displayed only slight reduction in treated adult SHR compared to untreated SHR which at this age exhibit about a 70 per cent increase in left ventricular weight when related to age matched NCR.

In adult male NCR treated for 2 months with propranolol there were no significant changes in blood pressure in resistance at maximal dilatation steepness of the resistance curve nor in maximal pressor response.

Summarizing the present results treatment of SHR from a prehypertensive age with adrenergic β receptor antagonists ($\beta_1 + \beta$ or selective β_1) largely prevents the subsequent pressure rise and the development of structural changes of the resistance vessels while a similar treatment started only at the age of 8 months when hypertension is already established seems to exert far less influences in these respects.

Discussion

A raised neurohormonal drive (Okamoto 1969 Tabei *et al* 1972) and cardiovascular hyperreactivity to environmental stimuli (Folkow Haliback and Weiss

1973 Hallback and Follow 1974) seem to be of great importance in SHR to initiating the increased pressure and hence for the development of cardiovascular adaptive changes (see Follow *et al* 1973). Thus functional and structural changes become intertwined in such a way as to cause mutual reinforcements. The same may be true in essential hypertension of man where early phases frequently display a "hyperkinetic" hemodynamic pattern (e.g. Brod *et al* 1962 Julius Pascual and London 1971) closely resembling a mild defence reaction since the raised pressure is associated with increases in cardiac output and muscle blood supply. Further emotionally disturbing stimuli often induce enhanced and more prolonged rises in pressure and heart rate in patients with essential hypertension (e.g. Hales *et al* 1957 Lorimer *et al* 1961).

Against such a background pharmacological interferences with preferentially neurogenic increases of cardiac output might be expected to have beneficial effects and therefore the present study concerning the influence of β adrenergic receptor blocking agents in SHR (cf. Tarazi and Dustan 1972) was initiated. These blocking agents may however well exert important actions also on other relevant points, interfering e.g. with the neurogenic control of renin-angiotensin release (cf. Bahler *et al* 1972) with the baroreceptor modulation of pressure (Dunlop and Shank 1969) or perhaps exerting also central damping influences (Kelliher and Buckley 1970). When treatment was started two of the present SHR groups were only 2.5 months old and still largely prehypertensive, since pressure was barely above normal. Treatment was continued for 7.5 months and had the result that mean arterial pressure and also the design of the resistance vessels were largely the same at 8 months of age as before treatment was started to judge from comparative hemodynamic analyses. At the same age untreated SHR exhibit a markedly raised pressure and considerable structural vascular changes. The early period of treatment had also the consequence that the later development of hypertension was far more benign than in untreated SHR and it considerably improved survival (cf. Weiss 1974).

The β adrenergic antagonists used did not differ significantly with respect to these essential actions despite the fact that propranolol blocks both β_1 and β_2 -receptors while H 93 76 has a selective β_1 blocking effect and perhaps also a shorter duration of action than propranolol. At the present state of knowledge concerning longterm effects of β -receptor antagonists in general it may be fruitless to speculate whether the longterm effects were exerted by identical or partly dissimilar mechanisms. Both may enter central nervous structures and at least part of their longterm effect may be due to a central damping influence on autonomic cardiovascular control which has recently been more and more discussed (e.g. Kelliher and Buckley 1970). Further both drugs undoubtedly reduce adrenergic cardiac stimulation markedly at optimal blood concentrations (Åblad Carlsson and El 1973) which were likely to be present mainly during night and early morning when general activity and consumption are highest in rats. However they modified the acute cardiovascular responses to graded alerting stimuli in somewhat different ways.

the pressure rises being larger though more delayed during propranolol than during H 93/26 treatment. The explanation might be that H 93/26 does not interfere with the β receptor mediated vasodilatation in skeletal muscle induced by the increased adrenaline secretion in connection with alerting stimuli (*cf* Ek *et al* 1973). On the other hand the propranolol treated animals regularly displayed bradycardia responses when exposed to the alerting stimuli. This is only occasionally seen in untreated SHR (Hallback and Follow 1974) and might reflect a partially changed central response pattern.

When adult SHR with established hypertension were exposed to the same propranolol treatment for 2 months their resting arterial pressure remained largely the same as in untreated controls which does not exclude that the average pressure load in daily life might have been somewhat reduced. The resistance vessels exhibited only modest signs of regression of the hypertensive changes: i.e. the resistance at maximal dilatation and the maximal pressor response were somewhat reduced at least in females but there was no significant reduction in the steepness of the resistance curve. This latter parameter reflects mainly the wall/lumen ratio of the resistance vessels where not only the smooth muscle component but also other wall elements contribute such as collagen water logging intimal changes *etc*. Collagen shows very little tendency to be reversed upon pressure reduction at least in the rat aorta (Wolinsky 1971, 1972). Similar results were observed in adult SHR subjected to prolonged treatment with guanethidine and apresoline (Weiss 1974) which lowers pressure and vascular smooth muscle tone considerably. Upon interruption of this intense hypotensive treatment pressure rose far more rapidly in these adult SHR than when young SHR had been similarly treated from prehypertensive age in analogy with the present experiments. It is possible that the less successful treatment of adult SHR in both these studies is to a great extent due to the failure to substantially reduce the wall/lumen ratio of the resistance vessels despite the fact that there were signs of some regression of the muscle component to judge from the moderately reduced maximal pressor response.

Concerning the effects of the present treatment on the weight of the left ventricle only about 10 per cent reduction was achieved in all groups and sexes compared with untreated matched SHR. It should here be realized that left ventricular weight of the treated SHR is still some 60 per cent above that in age matched NCR which in fact means very poor regression (see also Weiss 1974). Thus ventricular hypertrophy is however present already at 6 weeks of age perhaps even earlier which may correspondingly impede regression.

In summary. Longterm treatment from early age with propranolol or with a cardioselective β_1 adrenergic antagonist mainly interfering with sympathetic cardiac excitation kept arterial pressure almost at normal levels and largely prevented further development of structural changes of the resistance vessels. If treatment was later stopped pressure rose only slowly remaining throughout well below that of untreated SHR and the survival rate was considerably improved (see Weiss 1970). Adult rats treated with propranolol were unaffected with respect to resting

arterial pressure but there was in some respects a tendency towards normalization in design of the resistance vessels. However the increased wall/lumen ratio largely remained which may reflect the presence of fairly irreversible wall changes in the resistance vessels at this relatively advanced stage of hypertension. In general therefore the results speak in favour of early treatment when functional excitatory influences are still a dominating feature.

This study was partly supported by grants from the Swedish Medical Research Council (No P74 14), the Medical Faculty, University of Göteborg and from the Swedish National Association against Heart and Chest Diseases.

AB Hassle, Malmö, Sweden, generously covered part of the expenses for a technician and also supplied us with 3176. Thanks are also due to COL Ltd, Gothenburg, for a generous supply of propranolol.

References

- ÅBLAD, B., F. CARLSSON and E. EK: Pharmacological studies of the new cardiovascular adrenergic beta-receptor antagonists. *Life Sci* 1973 17 Part I 10-119.
- BRON, J., J. FENICI, Z. HEJLI, J. JUREK and M. LUBACH: General and regional haemodynamic patterns underlying essential hypertension. *Clin Sci* 1967 33 339-343.
- BUTLER, F. R., J. H. LARSEN, I. BURN, E. H. VALCHIA JR and H. R. BRUNNER: Propranolol inhibition of renin secretion. *N Engl J Med* 1971 285 157-162.
- DANLOP, D. and R. SNEYD: Inhibition of the carotid sinus reflex by the chronic administration of propranolol. *Brit J Pharmacol* 1969 26 137-143.
- EK, E., C. DANIEL, F. CARLSSON, M. LUNDGREN, J. MARRAS and B. ÅBLAD: Hemodynamic effects of two adrenergic beta-receptor antagonists in conscious dogs. *Acta physiol* 1973 Suppl 349 98.
- FOLKOW, B., H. HALLBACK and L. WEISS: Cardiovascular responses to acute mental stress in spontaneously hypertensive rats. *Circ Res* 1973 42 1318-1333.
- FOLKOW, B., J. LUNDGREN and L. WEISS: The effect of prolonged propranolol treatment on blood pressure and structural design of the resistance vessels in young spontaneously hypertensive rats. *Acta physiol* 1974 91 84-89.
- FOLKOW, B., M. HALLBACK, J. LUNDGREN and L. WEISS: Background of increased flow resistance and vascular reactivity in spontaneously hypertensive rats. *Acta physiol* 1974 91 109-113.
- FOLKOW, B., H. HALLBACK, J. LUNDGREN and L. WEISS: Effects of "immunoregulation" on blood pressure and vascular reactivity in normal and spontaneously hypertensive rats. *Acta physiol* 1972 84 51-53.
- FOLKOW, B., M. CARLSSON, M. HALLBACK, J. LUNDGREN and L. WEISS: Hemodynamic consequences of regional hypertension in spontaneously hypertensive and normotensive rats. *Acta physiol* 1972 83 532-541.
- FOLKOW, B., M. HALLBACK, J. LUNDGREN, R. SILVERSTEIN and L. WEISS: Importance of adaptive changes in vascular design for establishment of primary hypertension studied in man and spontaneously hypertensive rats. *Circ Res* 1973 32-33 Suppl I 1-13.
- HALLBACK, M. and B. FOLKOW: Cardiovascular responses to acute mental stress in spontaneously hypertensive rats. *Acta physiol scand* 1974 90 684-698.
- JULIUS, S. A., V. PACEAS and R. LOBOS: Role of parasympathetic inhibition in the hyperkinetic type of borderline hypertension. *Circ Res* 1971 44 413-418.
- KALIS, M. L., E. HARRIS, M. SOKOLOV and L. G. CARPENTER: Response to psychological stress in patients with essential hypertension. *Am J Med Sci* 1957 53 572-578.
- KELLNER, G. J. and J. P. BUCKLEY: Central hypotensive activity of di and d-propranolol. *J Pharm Sci* 1970 59 1276-1280.
- LÖNNER, A. R., P. W. MACFARLANE, G. PROVAN, T. DUFFY and T. D. LAURIE: Blood pressure and catecholamine responses to stress in normotensive and hypertensive subjects. *Cardiovasc Res* 1971 5 163-173.
- LUNDGREN, J.: Regression of structural cardiovascular changes after reversal of experimental renal hypertension in rats. *Acta physiol scand* 1974 91 275-285.

- LINDGREN V, M HALLBACK L, WEISS and B FOLKOW. Rate and extent of adaptive cardiovascular changes in rats during experimental renal hypertension. *Acta physiol scand* 1974 91 103—115
- OKAMOTO H. Spontaneous hypertension in rats. *Int Rev exp Path* 1969 7 277—270
- PFEFFER M A and E D FROMMICH. Haemodynamic and myocardial function in young and old normotensive and spontaneously hypertensive rats. *Circulat Res* 1973 32 1 28—1 35
- TABEI R, T MARUYAMA M, KIMURA and H OKAMOTO. Morphological studies on endocrine organs in spontaneously hypertensive rats. In *Spontaneous Hypertension* Ed H Okamoto Igaku Shoin Ltd Tokyo 1972
- TARAZI R G and H P DUSTAN. Beta adrenergic blockade in hypertension. *Amer J Cardiology* 1972 29 633—640
- WEISS L. Long term treatment with antihypertensive drugs in spontaneously hypertensive rats (SHR). Effects on blood pressure and cardiovascular design. *Acta physiol scand* 1974 91 393—408
- WOLINSKY H. Effects of hypertension and its reversal on the thoracic aorta of male and female rats. *Circulat Res* 1971 28 627—637
- WOLINSKY H. Long term effects of hypertension on the rat aortic wall and their relation to concurrent aging changes. Morphological and chemical studies. *Circulat Res* 1972 30 301—309

Electrical Activity and Isometric Tension in Motor Units of the Cat's Inferior Oblique Muscle

By

GLAUK LÄNNERSTRAND¹

Received 31 January 1974

Abstract

LÄNNERSTRAND G. Electrical activity and isometric tension in motor units of the cat's inferior oblique muscle. *Acta physiol scand* 1974 91 458-474.

Single motor units of the cat's inferior oblique muscle were isolated by partial denervation of the muscle and threshold stimulation of single motor nerve filaments. With electrical tests single innervated SI units multiply innervated conducting MLC units and multiply innervated non-conducting MNC units could be differentiated. SI units conducted impulse activity faster (13 m/s) than MLC units (1 m/s). Single innervated units contracted faster than multiply innervated units. Fusion frequency was found the most useful parameter for a mechanical separation: most SI units fused above 200 pps, most MLC units between 100 and 200 pps and the MNC units below 100 pps. Tetanic tension was high in fast SI units as in slow MLC and MNC units but there was a considerable overlap. The range for the whole material was 25-45 mg. In fast units fusion frequency and the rate of stimulation for maximal tetanic tension coincided. In slow units maximal tetanic tension was reached at stimulus rates of 150-200 pps irrespective of the fusion frequency of the unit. Resistance to fatigue was high in the slow units and in the majority of the fast units.

The attractive properties fit into the motor unit activity pattern determined through multiple recordings in alert animals.

The motor unit is the smallest functional unit in muscle. Based on their isometric twitch characteristics motor units in many mammalian skeletal muscles can be grouped into fast and slow types (Henneman and Olsen 1965, Burke 1966, Andrew and Part 1972, Feig 1972). Usually the fast units show higher tetanic tensions and greater susceptibility to fatigue than slow units (Burke *et al.* 1971). It has been shown that slow units are usually recruited before fast units in different motor acts (see Granit and Burke 1973).

In extraocular muscles the mechanical responses of single motor units have not yet been fully studied except for the cat retractor bulbi where all units are of the fast type (Lännenstrand 1974). Mechanical studies on larger components of the

¹ Visiting Scientist of the Medical Research Council of Canada and of the Smith Kettlewell Institute of Visual Sciences. Present address: The Eye Clinic, Karolinska Hospital, Stockholm, Sweden.

globe rotating muscles (the recti and the oblique muscles) have indicated that a fast and a slow system exist also in these muscles. The experimentation to substantiate this conclusion has recently been reviewed (Bach & Raita 1971, Brenin 1971).

The present study aims at a description of some of the mechanical and electrical properties of single motor units in the inferior oblique muscle of the cat. Such data are necessary for a better understanding of the functional organization of eye movements on the motor unit level. In addition, a few controversial points in eye muscle physiology might be resolved with single unit technique.

The results of previous studies to correlate mechanical properties of the two motor systems with electrical properties of their muscle fibers are somewhat inconclusive. Although all workers agree that the fast system is subserved by singly innervated twitch fibers, it is debatable whether in the slow motor system most fibers are of the classical slow type with non-propagated membrane activity (Hess and Pilar 1963, Pilar 1967) or whether the slow system is composed mainly of fibers intermediate to the typical fast and slow types, multiply innervated but capable of propagating action potentials (Bach & Raita and Ito 1966).

The mechanical properties of the slow component have not yet been sufficiently studied. According to Hess and Pilar (1963) and Bach & Raita and Ito (1966), the fusion frequency (i.e. the rate of tetanic stimulation to reach just fused contraction) is about 30 pulses per sec (pps), but other workers (Barnack, Bell and Rence 1971, Fuchs and Luschei 1971b) could not find evidence for any motor component fusing at such a low stimulus rate.

The long duration of high rate steady discharge recorded from eye muscle motoneuron in alert monkeys (Fuchs and Luschei 1970, 1971a, Robinson 1970, Schuller 1970, Henn and Cohen 1972) and also in human extraocular EMG (Bjork and Kugelberg 1963) indicates that both motor components in eye muscles must fatigue much slower than motor units in other skeletal muscle. However, it has not been experimentally verified that the mechanical properties of individual motor units in the eye muscles can be reconciled with these findings.

With the methods used in this study, three types of motor units could be differentiated in the inferior oblique muscle of the cat. Units with singly innervated twitch fibers (called SI units) were the fastest. Multiply innervated fibers with conducted activity formed units of intermediate mechanical properties (MIC units), while the slowest units were composed of multiply innervated fibers with non-propagated electrical activity (MINC units). All types of units showed a remarkable fatigue resistance. Some of the results have been reported elsewhere in a preliminary form (Lennerstrand 1972, 1973).

Methods

A general description of the methods including most of the surgical procedures and the recording techniques was given in an earlier paper (Lennerstrand 1974). The methodological variations in the present experiments are as follows:

Muscle preparation After detaching the inferior oblique muscle from the globe and enucleating the eye the motor nerve to this muscle was dissected free from surrounding tissue for stimulating purposes and cut close to the ciliary ganglion (see also Bach, Rita and Ito 1966). The number of motor units activated by the stimulation of the motor nerve was reduced by extensive sectioning under microscopic control of nerve branches entering the muscle until one small nerve twig remained. Interference with the circulation of the muscle was carefully avoided. Further isolation of motor units was made by splitting the main motor nerve.

The nerve to the inferior oblique muscle divides into two or three branches. The most distal of them is known to contain a high proportion of thin filers (Sas and Schiøth 1957) which are likely to innervate the slow motor component (Bach, Rita and Ito 1966). It was also observed in the present study that slow units were more readily obtained in stimulation of the distal than of the proximal branches.

Tension recordings Tension was measured at the optimal muscle length (Clare 1959) with a sensitive myograph previously described (Lennestrand 1964). The undamped resonance frequency of the system was 7 kHz.

Electrical recordings Extracellular responses were recorded (i) monopolarly with chlorided silver electrodes, one resting on the tendon the other positioned on the muscle surface at the location of maximal response; the signals were dc amplified (high frequency cut-off 10 kHz); (ii) bipolarly with stainless steel electrodes 0.25 mm in diameter and 0.5 mm apart; the signals were ac amplified (bandwidth 80 Hz–10 kHz); (iii) with glass micropipettes of about 1 megohm impedance filled with 2.6 M KCl connected to a Mentor V-050 in acellular probe system and the signals further ac or dc amplified.

Intracellular recordings were done with glass micropipettes filled with 3 M Procion red dissolved in Ringer solution. The impedance of the pipettes had to be in the range of 40–100 megohms to enable penetration of small muscle fibers and yet allow passage of sufficient amounts of dye into the cells for marking. (The labelled cells were prepared for electron-microscopical examination. A report on this will be published elsewhere.)

In a few cases 2.6 M KCl pipettes of 10–30 megohm impedance were used for the intracellular recordings.

The electrodes were mounted on manipulators accurate to 0.1 mm of positioning. For the conduction velocity and innervation studies the electrodes were moved along the motor unit in a direction roughly parallel to the muscle fibers. Distances read from the manipulator scale were corrected for deviations of the electrodes from a line perpendicular to the muscle surface.

Stimulation The muscle nerve or split filaments thereof were placed over two platinum wires (0.3 mm in diameter) and stimulated with pulses of 0.1 ms duration in single pulses or trains of pulses. The stimulus amplitudes were usually between 0.2 and 1.0 V.

Results

Criteria for single unit isolation In addition to the techniques for motor unit isolation described in Methods II was usually necessary to control stimulus amplitude carefully or several units might be activated simultaneously. Usually only the motor unit with the lowest stimulus threshold was studied. It was identified in high sensitivity recordings by its all-or-nothing responses mechanically and electrically to single stimulus pulses. Tetanic stimulation was then applied at a lower stimulus strength. Sometimes a tension increase in the muscle revealed that a unit with still lower threshold existed in the preparation. Isolation of it was sometimes successful by further splitting of the nerve. The procedure was repeated until the threshold for twitch and tetanic stimulation coincided. In a few slow units no tension change could be recorded to single pulses at a stimulus strength that elicited contraction to repetitive stimulation (see below). Electrical recordings were in these cases used to determine stimulus threshold and to exclude that more than one unit was activated in the tetanic stimulation.

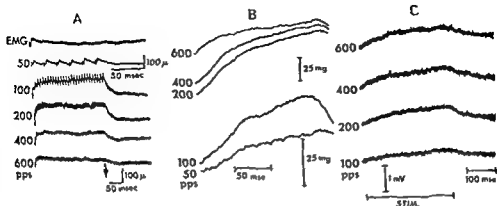


Fig. 1. Electrical recordings (A and C) and mechanical recordings (B) from 2 different MNC units. Baselines shifted between each stimulation. No twitch responses could be obtained in these motor units. A is a dc monopolar recording from the muscle surface; summation of local electrical responses occurred at about 60 pps of stimulation and upwards. The arrow in the 600 pps trace marks stimulus removal. B and C are responses in another unit; mechanogram (B) still unfused at 50 pps stimulation; fusion frequency 60 pps. C is an extracellular dc recording close to the unit with a glass microelectrode for optimal low frequency response. Duration of stimulation indicated by bar.

Electrical properties

A complete extracellular study of electrical properties with both bipolar and monopolar recordings was made in 35 units. From another 25 units only monopolar EMG recordings have been obtained. A few units were intracellularly examined (see Table 1).

Slow units with non propagated activity. All except five units were able to conduct action potentials (see Fig. 2). The five non conducting units showed additive local responses to repetitive stimulation (Fig. 1 A and C). No action potentials were fired even at the highest rates of stimulations of the motor nerve. These units would

TABLE 1. Electrical characteristics of the motor units and their muscle fibers

	Type of unit		
	III	MIC	MNC
Conduction velocity m/s (Mean \pm S.D.)	2.93 \pm 0.41 (n = 16)	1.72 \pm 0.34 (n = 14)	
Intracellular recordings			
Number of units	9	8	1
Number of fibers	15	15	3
Resting potential mV (Mean \pm S.D.)	56 \pm 14.3	42.6 \pm 14.9	52 \pm 18
Number of cells with or without spikes	8	5	0

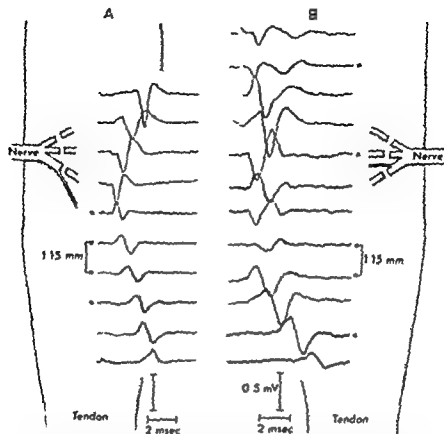


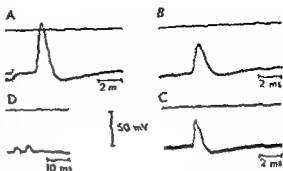
Fig. 1. Bipolar surface EMG recordings along a SI unit. A: with a fusion frequency of 5 pps and a MIC unit II fusing at 140 pps. Three sweeps superimposed. Schematic drawing of muscle preparation to indicate denervated and approximate sites of recording. EMG reversed polarity when the electrodes passed an endplate region on the unit; note multiple reversal in B. Calibration bars at bottom for EMG.

can be composed of low muscle fibers of the type found in amphibian muscle (Kuffler and Vaughan Williams 1953; Orland 1963).

Electrical and mechanical responses to tetanic stimulation of such a unit are presented in Figs. 1B and C. Maximal tension and electrical response was reached at 200 pps. Higher stimulus rates resulted in response decline. Maximal rate of rise in both response occurred at 200–400 pps, compare with the unit labelled "low" in Fig. 7.

Innervation pattern of conducting unit. In muscles with unipulse conducting fibers motor endplate region can be located by exploring the muscle surface in a systematic manner with a bipolar electrode oriented parallel to the fibers (Jarcho *et al.* 1952). The activity generated at the endplates travels in both directions along the fiber. Therefore as a bipolar electrode passes over an endplate region the polarity of the electrical response to single stimuli reverses and the latency of the

Fig 3 Intracellular recordings show an overshoot action potential in a SI unit (A) non overshoot action potentials in two different MIC units (B and C) and low amplitude responses in a MINC unit (D) A from the same unit as Fig 2 A and D from the same unit as Fig 1 B and C Responses to single pulse stimulation of the muscle nerve in A B and C to double stimulus 3 ms apart at two different intensities (threshold and 2 times threshold) in D Top line marks zero potential Dots in D are stimulus pulses distance from zero line indicates stimulus amplitude Note differences in time scales between D and the rest



response reaches a minimum. If the amount of electrical activity in the muscle is restricted to that generated in a single motor unit, the number of reversals would signify the number of endplate areas on that unit. In the inferior oblique about 2/3 or 12–15 mm of the peripheral part of the muscle was available for exploration with a bipolar electrode. (The portion of the muscle closest to the origin could not be exposed without damaging blood vessels to the muscle.) In 16 of the units only one endplate region could be detected (Table I). They were located at the level of the muscle where the nerve entered. Typical recordings along such a unit are shown Fig 2 A.

The remaining 14 units with propagated activity showed two or more endplate areas (see Table I). The unit represented in Fig 2 B had four sites where typical changes in electrical responses took place. These areas were 1–3 mm apart. The innervation of this unit spanned at least 7 mm. In other units with several endplate areas the innervation band ranged between 5 and 8 mm. The endplate regions were absent from the most peripheral part of these units (Fig 2 B).

Thus with respect to electrical properties three kinds of motor units can be differentiated in eye muscles. They are the singly innervated (SI) units, the multiply innervated conducting (MIC) units, and the multiply innervated nonconducting (MINC) units.

Conduction velocity of muscle fibers. The speed of action potential propagation in the conducting units was estimated from monopolar recordings in endplate-free regions. Differences in response latency measured at corresponding points were averaged for 3 or more consecutive recordings. The conduction velocity of the SI unit of Fig 2 A was 3.52 m/s. The MIC unit in Fig 2 B had a conduction velocity of 2.23 m/s. On an average SI conducted at 2.93 m/s and MIC at 1.72 m/s (Table I). A *t*-test showed this difference to be highly significant ($p < 0.001$).

Intracellular responses. Penetrations with glass micropipettes were successful in one or more of the muscle fibers of 9 of the SI units, 3 of the MIC unit, and one of the MINC units. Stable penetrations were hard to obtain since the muscle could

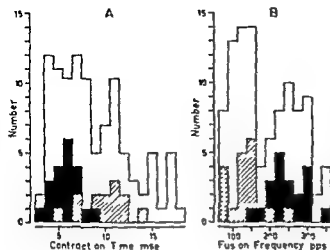


Fig. 4. Histograms of single motor unit twitch contraction time (A) and fusion frequency (B). Enclosed sections mark the electrically identified units: SI units—filled bars; MIC units—striped bars; MINC unit—cross hatched bars. No twitch responses were recorded in MINC units.

not be stretched taut without moving the nerve on the stimulus electrodes which would have endangered the selective activation of the mechanically identified unit. Further, the pipette was easily dislodged by contractions of the penetrated fiber. Undoubtedly the membrane resting potentials and the action potentials of many fibers were reduced because of electrode injury to the cell membrane.

Average resting potentials of fibers in the different types of units are given in Table 1. The values for SI units were slightly higher than those for MIC units. Recordings were made from 3 fibres in the same MINC unit.

Typically the muscle fibers in the SI units responded with an overshoot action potential to nerve stimulation as shown in Fig. 3A for a fiber in the unit of Fig. 2A. Fig. 3B and C depicts the intracellular responses of two fibers in different MIC units. As shown also in Table 1, these fibers less frequently produced overshoot responses.

In the MINC unit only low amplitude intracellular responses were recorded (Fig. 3D). Stimulation with two pulses spaced 35 ms apart was ineffective in generating an action potential. Stronger tetanization was not tried in fear of losing the cell before it could be labelled. The extracellular responses (Fig. 1A and C) were also quite conclusive in excluding the possibility of impulse generation in these slow units.

Mechanical properties

The isometric tension changes to stimulation of single motor units were recorded and twitch contraction time, twitch tension, tetanic tension, rate of tetanic tension rise and fatigability were determined in the same way as described for the retractor bulbi motor units (Iennerstrand 1974). Some 70–80 units including the ones electrically studied have been submitted to complete mechanical testing.

Twitch contraction time was measured from the start to the peak of the twitch response. As shown in the histogram of Fig. 4A the contraction times ranged between 35 and 20 ms. In general SI units contracted faster than MNC units. The MNC units electrically identified did not respond to single pulse stimulation but only to tetanic stimulation.

Fusion frequency was identified as the lowest frequency of tetanic stimulation to produce a fused tetanus with the present recording system. Because of a rather low signal to-noise ratio in the high sensitivity tension recordings, repeated measurements of fusion frequency in the same unit was found more reproducible than those of twitch contraction time. The fusion frequency was therefore chosen to characterize the contractile properties of the unit, i.e. whether it was rapidly or slowly contracting. The inverse relation between fusion frequency and contraction time of a unit is shown in Fig. 5A.

The values of fusion frequency for different units ranged between about 50 and up to 350 pps (Fig. 4B). Of the 5 MNC units four had fusion frequencies below 100 pps (Fig. 1B). In the fifth neither fusion frequency nor twitch characteristics could be determined. The majority of the MNC units fused at frequencies below 200 pps and most of the SI units had fusion frequencies at 200 pps or above. This would indicate again that SI units are fast contracting, MNC units slowly contracting and MNC units are of intermediate contractional speed. It seems reasonable to assume that electrical and mechanical properties are similarly related in all units although in some of them proper electrical tests were not performed.

The histogram of fusion frequencies of the total number of units shows a bimodal distribution statistically verified in a *t* test ($P < 0.001$). In the following description of mechanical properties the units with fusion frequencies above 200 pps will be referred to as fast units. To the greatest part they are the SI units. For the sake of convenience the others will be called slow units, realizing that this means lumping together two groups of units all probably multiply innervated (MNC and MNC) but obviously with quite different membrane properties and probably also different modes of excitation-contraction coupling.

Twitch tension. The diagram to relate twitch tension to fusion frequency (Fig. 5B) shows the values for fast units to be in general slightly higher than those of slow units. The range of twitch tensions was between 4 and 28 mg. However, the variability in repeated twitch amplitude measurements could be up to 30% due to contamination from biological noise (pulse beats and respiratory movements) in the high gain tension readings from this *in situ* preparation.

Tetanic tension. The tetanic tensions determined for different levels of activation are shown in Fig. 6 for two units with fusion frequencies of 300 and 90 pps respectively. Here the variations in individual measurements were much less than for twitch responses. The peak of the tetanic curves represented the maximal tetanic tension of each unit. In Fig. 5C this parameter has been plotted against the fusion frequency. Fast units generally had higher values of tetanic tension than slow ones but there was a considerable overlap. It was further observed in fast units that

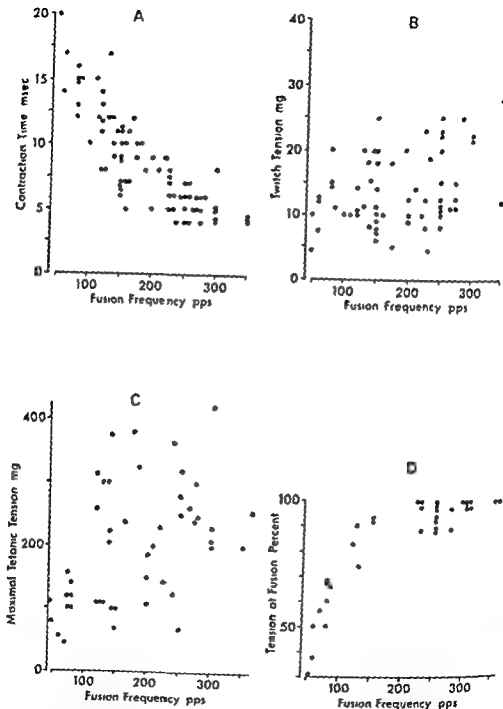
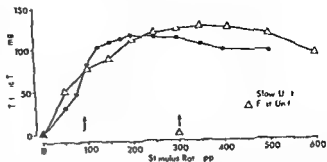


Fig 5 Plots against fusion frequency of contraction time (A) twitch tension (B) maximal tetanic tension (C) and tension at fusion frequency in percent of maximal tetanic tension (D) for single motor units. Tension output in twitch and tetanus is positively correlated to speed of unit contraction (B and C). The slower unit have not reached maximal tetanic tension when stimulated at fusion frequency (D).

Fig 6 Tetanic tension of two single units at different rates of repetitive stimulation. The fusion frequencies of the units were 90 and 300 pps respectively, as marked by the arrows. Note in the slow (VINO) unit the discrepancy between fusion frequency and stimulus rate for maximal tension. In the fast (SI) unit these two values almost coincided.



maximal tetanic tension usually was reached at the fusion frequency of the unit (Fig 6 and 5D). In slow units however maximal tetanic tension required activation at 150–200 pps which is higher than fusion frequency for most of them (Table II). At fusion frequency the force produced in slow units could be as low as 30 percent of the maximal tetanic tension (Fig 5D).

Tetanus twitch tension ratio. In the inferior oblique muscle of the cat Cooper and Eccles (1930) reported a ratio between tetanic tension and twitch tension of 10.7. For isolated motor units in the same muscle higher values would be expected; the twitch response of a single unit would be reduced much more than the twitch response of the whole muscle as an effect of damping by passive muscle elements. The tetanic response measured in steady state would be much less influenced.

In the present motor unit material the average tetanus twitch ratio was 15.1 (± 5.7 SD, $n = 76$). The total range was 6.0–25.6. Values in fast and slow units did not differ significantly (t test $P > 0.05$).

Rate of tension rise. The steepest slope of the rising tension during a tetanic stimulation was taken as a measure on the rate of tension rise in the contraction.

In Fig 7 the rate of tension rise has been plotted against frequency of the repetitive stimulation for a representative sample of motor units identified by their fusion frequencies. As expected the fast units contracted faster than slow units for a certain frequency of stimulation (Fig 8A) and they also reached much higher

TABLE II Stimulus frequency to reach maximal tetanic tension in different groups of units identified from the fusion frequency

Fusion frequency pps	Stimulus rate for maximal tetanic tension pps (Mean \pm S.D.)	Number of observations
50–90	197 \pm 29	13
100–140	108 \pm 24	13
150–190	213 \pm 44	11
200–240	230 \pm 21	8
250–290	283 \pm 39	17
300–350	333 \pm 43	8

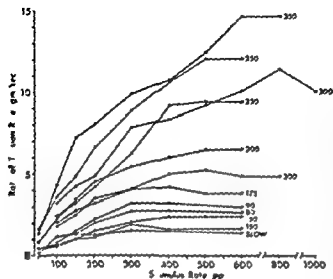


Fig. 7. Rate of tension increase plotted against stimulus frequency for a representative sample of units. Each curve represents values from one unit. The fusion frequency is marked at the end of each curve. In the MNC unit labelled "slow" no fusion frequency could be determined although its rate of tension increase was higher than that of many faster units.

maximal values of speed of contraction. Furthermore the rate of tension increase in fast units continued to rise up to stimulus rates of at least 100–200 pps in some cases even up to 800 pps (Fig. 7). In contrast the slow units had reached maximal speed of contraction at 400 pps or below.

Fatigability. The fatigability of the units was tested with continuous stimulation for about 30 s. Two typical examples are shown in Fig. 9. At 100 pps the fast unit

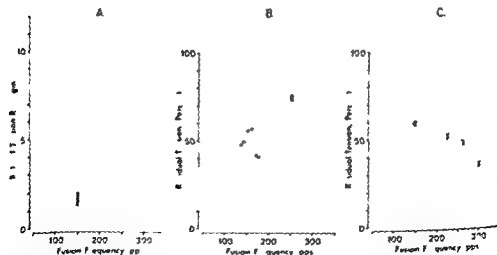


Fig. 8. A. Values for rate of tension increase in different units plotted by their fusion frequency, all stimulated at 400 pps. B and C. Residual tension in the units plotted against fusion frequency. Stimulation at 200 pps B and 300 pps C for 30 s. Tension at the end of stimulation in percent of the maximal tension at stimulus initiation has been used as an expression of fatigue resistance.

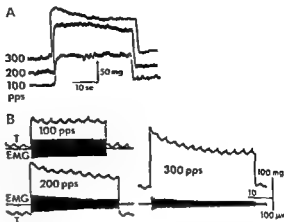


Fig 9 Prolonged stimulation of a slow (MNC) unit (fusing at 80 pps) in *A* and of a fast unit (electrically non identified but fusing at 250 pps) in *B*. Stimulus rates as marked. Tension recordings in *A* baseline shifted between stimulations. Both tension (*T*) and monopolar EMG recorded in *B*. Irregularities in tension curve are due to respiratory coupled movements in the preparation.

(fusion frequency 250 pps) (Fig 9 *B*) showed almost as high fatigue resistance as that of the slow unit (Fig 9 *A*) with a fusion frequency of 80 pps. As the stimulus rate increased the fast unit fatigued proportionally more than the slow unit but the difference was surprisingly small. This is further documented for a sample of units in Fig 8 *B* and *C* where the residual tension after 30 s of stimulation at 200 pps (Fig 8 *B*) and 300 pps (Fig 8 *C*) expressed as a percentage of the initial tension has been taken as a measure of the fatigue resistance of the unit and has been plotted against its fusion frequency. The 200 and 300 pps values were chosen to match approximately the stimulus rates needed for maximal tetanic tension output in slow and fast units respectively (see section on *Tetanic tension* and Table II). Probably the units would not operate at higher firing frequencies during physiological steady state conditions. Even at these levels of activation most fast units could retain 30 % or more of their initial tension. It should be noted that the units that fatigued completely were all in the fast group.

Discussion

It has been shown in this study that extraocular motor units in cats can be separated into singly (SI) and multiply innervated types. In the multiply innervated units the muscle fibers were either of twitch type capable of impulse conduction (MIC units) or of the slow muscle fiber type found in amphibian muscle generating only local responses to nerve stimulation (MNC units).

The SI units formed a group of mechanically fast units. Comments on a possible subdivision of this fast group will be made below. The multiply innervated units formed a group of mechanically slow units with MNC units at the lower and MIC units at the upper end of the range of contractional speed.

Other mammalian skeletal muscle, with the possible exception of middle ear muscles (Fernand and Hess 1969; Teig 1972) consist exclusively of singly innervated fibers.

For example the three types of units that Burke *et al* (1971) could mechanically separate in the gastrocnemius muscle of the cat would with respect to electrical properties all fall in our fast group since they all consisted of singly innervated fibers. There is no reason to believe that the fiber types are mixed in the extracocular or other motor units (Burke *et al* 1971).

Isolation and identification of units Only indirect tests could be used to show that the preparations studied contained single motor units since it was not possible to record from the thin nerve branch left intact (see Methods) and verify that single nerve fibers were activated. However from a comparison with mechanical data obtained in lateral rectus units activated by intracellular stimulation of abducens motoneurons (Goldberg and Lännerstrand in preparation) it could be concluded that single units had been studied also in the inferior oblique muscle.

There was a considerable overlap between tetanic tensions in fast and slow units (fig. 2C). This has been observed also in lateral rectus units (Goldberg and Lännerstrand in preparation). Differences in size between fast and slow motor units would probably not contribute to observed variations in fusion frequency and contraction time on which the mechanical identification rested. The highest fusion frequencies recorded in single fast units were also within the range established for the whole muscle (Cooper and Eccles 1930; Bach, Ritz and Ito 1966).

The tetanus twitch tension ratios were similar for fast and slow units (see Results). As noted by Appelberg and Emonet-Denand (1967) in their study of motor units in the superficial lumbrical muscle this finding would increase the validity of the mechanical identification of motor units from their dynamic properties, i.e. twitch contraction time and fusion frequency. These authors reasoned that if passive elements in series or in parallel had strongly influenced the dynamic behavior of the units, slow units would show higher tetanus twitch tension ratios than fast units.

Electrical properties It could be confirmed that some of the muscle fibers in eye muscles have electrical properties similar to slow fibers in amphibian muscle (Hess and Pilar 1963; Pilar 1967). Such units were rather scarce in the present material. This might be due to the fact that the technique used for activation of single motor units tended to favor the units innervated by low threshold nerve fibers, i.e. predominantly the SI units (Bach, Ritz and Ito 1966).

In the MFC units the velocity of the propagated impulses was generally lower than that of SI units indicating that the fibers in the MFC units were smaller in size. Håkansson (1961) found the speed of impulse conduction of isolated frog muscle fibers to be directly proportional to the circumference of the fibers. In the intact muscle mutual interaction between adjacent active muscle fibers tended to equalize the differences in conduction velocity expected from variations in muscle fiber size (Buchthal, Guld and Rosenfeld 1953). However since single motor units were studied, electrical interference between activity in different fiber types would not occur in the present experiment. Further, in eye muscles where fibers of different sizes are located in separate parts of the muscle, i.e. small fibers predominant

ly in the orbital part and large fibers in the central or global sections of the muscle (Peachey 1971) this interaction might be less important for conduction velocity measurements on the whole slow and fast components

Taking these considerations into account the conduction velocities calculated for the muscle fibers in SI units and in the MIC units correspond fairly well to the values reported by Bach, Rita and Ito (1966) for their fast component (3.00 m/s) and slow component (2.16 m/s). It is therefore conceivable that these components contain SI and MIC motor units respectively. The intracellular data would support this notion. Bach, Rita and Ito (1966) reported lower membrane potentials and higher incidence of non-overshoot action potentials in fibers of the slow component than of the fast component. Similar differences were found in the present material of intracellular recordings from MIC and SI units. As pointed out by Bach, Rita and Ito (1966) these variations may to some extent be due to cell injury by the intracellular electrode which is more prone to occur in the small fibers of the slow conducting units. It is interesting to note that the few fibers impaled in MIC units had as high resting potential as the fibers in the fast units. It has been observed that the slow (amphibia like) fibers in eye muscles located mainly in the central part of the muscle, are of about the same size as the surrounding fast twitch fibers (Harker 1972, Alvarado in preparation) which could account for our findings on their membrane potentials.

The interpretation that the multiple endplate regions identified in the MIC units were located not on the same fiber but on adjacent singly innervated fibers can be rejected on the following grounds. It is known from innervation studies on eye muscles of different species that the singly innervated twitch fibers have a rather thin innervation band about 2 mm wide in the central one third of the muscle (Hess and Pilar 1963, Zenker and Anzenbacher 1964, Dietert 1965). In the MIC units the innervation band extended beyond this distance: it was between 5 and 8 mm wide. This makes it very unlikely that the muscle fibers in MIC units were singly innervated. On the other hand the endplate density is probably much lower on these multiply innervated fibers than on the classically slow fibers. It is interesting to note that fibers either with dense or with more widely spaced multiple innervation have been observed in guinea pig and sheep extraocular muscles (Hess 1961, Harker 1972). The endplate regions were 0.8–1.2 mm apart in the guinea pig muscle (Hess 1961) and 0.5 mm apart in sheep muscle (Harker 1972). * These fibers were smaller than the singly innervated ones. In the guinea pig they were located mainly in the outer orbital layers of the muscles while in the sheep they were located in the core of the muscle (Harker 1972).

These data on innervation, conduction velocity and membrane properties of the fibers of MIC units would indicate that they are identical to the slow twitch fibers found in cat by Bach, Rita and Ito (1966). It might further be suggested that they correspond to the tonic fibers in the rabbit extrinsic eye muscles which are

* Similar innervation of cat eye muscle fibers has just been reported (Alvarado in preparation).

multiply innervated (Ortwa *et al* 1969 Matyushkin and Drabkina 1970) and have lower membrane potentials than the phasic fibers in the same muscle (Matyushkin and Drabkina 1970).

Mechanical properties The tetanic tension of the mechanically slow units i.e. the MFC and MNC units increased steadily with stimulus rate up to 150–200 pps (Fig. 6 Table II). This is far above the fusion frequency for many slow units. In analogy with the behavior of motor units in other mammalian skeletal muscle including the retractor bulbi muscle (Lennerstrand 1974) one would expect the tension output from motor units to saturate at stimulus rates above fusion frequency. On the other hand in amphibian multiply innervated muscle the stimulus frequency for fusion is lower than that for maximal tetanic tension (Floyd and Smith 1971). Results obtained from the tonic component of eye muscles in cat and rabbit by Matyushkin (1964) can be interpreted in the same way. This difference between fast (SI) and slow (MFC and MNC) units in eye muscles supports the idea that slow units contain multiply innervated muscle fibers. In a multi innervated unit differences in conduction time along different nerve terminals would cause temporal variations in addition to the spatial variations in the contraction of its fibers. The net effect might be to smoothen out the overall response of the unit to the individual pulses and fuse the tetanus at a rather low rate of stimulation. This mechanical interaction would become more prominent if a large number of slow units were activated at the same time and would perhaps explain the low fusion frequency of 30 pps for the whole slow motor component reported by Hess and Pilar (1963) and Bach, Ritz and Ito (1966). Other factors in their experimental techniques may also have played a role as pointed out by Bach, Ritz and Ito (1966) and Burmack *et al* (1971).

Evidently the range of firing frequencies over which slow units can increase their steady state tension extends beyond the fusion frequency. In this context it is interesting to note that the maximal firing rates of eye muscle motoneurons in alert monkeys during steady fixation is always above 100 pps and mostly around 200 pps (Fuchs and Luschei 1970, 1971a; Robinson 1970; Schiller 1970; Henn and Cohen 1972). It has been shown in this study that such stimulus rates are needed in order to maximally activate the motor units even of the slow types.

It is possible that observations on the maximal rate of motoneuron firing in saccades can offer a functional means of motor unit identification in alert animals where no assessment of mechanical properties of the unit can be made. Some motoneurons were seen to fire at frequencies up to 800 pps while others for the same movement attained only 300 pps (Fuchs and Luschei 1970; Robinson 1970; Schiller 1970; Henn and Cohen 1972). This could be correlated with the finding in this study that mechanically fast units could increase their speed of contraction with stimulus frequency up to 600–800 pps. In slow units the rate of tension rise levelled off at 400 pps.

Motor units in oculorotatory muscles of man (Bjork and Kugelberg 1953) and monkeys (Robinson 1970) have prolonged periods of activity which for some units

must extend to the whole period of wakefulness. Accordingly it was found in the present study that the resistance to fatigue was high in most fast and in all slow units. However morphological and histochemical studies indicate that not all eye muscle fibers are capable of prolonged contraction: some of the fibers have a low mitochondria content and seem to have a small supply of oxydative enzymes (Peachey 1971, Mayr 1971, Harker 1972, Akarado in preparation). On the other hand the blood flow per volume muscle has been shown to be higher for eye muscles than for any other muscle studied (Wooten and Reis 1972) and this may increase the fatigue resistance of the units. Some of the largest twitch fibers have the same appearance as pale muscle fibers in other muscle known to fatigue quickly (Burke *et al* 1971). Possibly the least fatigue resistant of the fast eye muscle units were composed of such fibers. This would indicate that the mechanically fast group of units could be further subdivided although no clear differentiation could be observed with the other mechanical tests applied in this study.

The valuable advice and criticism by Dr John Outerbridge and Dr Paul Bach y Rita is gratefully acknowledged. This work was supported by a Visiting Scientist Award and by a grant from the Canadian Medical Research Council (No MCR 164-4483) by United States Public Health Service Program Project Research Grant No. E1-00799 by grants from P. E. Lundahl's stipendiefond and from Stiftelsen Vera och Carl J. Michaëlsens donationsfond.

References

- ANDREWS B. J. and N. J. PART: Properties of fast and slow motor units in hind limb and tail muscles of the rat. *Quart J exp Physiol* 1972 57 213-225.
- APPELBERG B. and F. EMOUET-DENAUD: Motor units of the first superficial lumbrical muscle of the cat. *J Neurophysiol* 1967 30 154-160.
- BACH Y. RITA P.: Neurophysiology of eye movements. Pp. 7-45 in Bach y Rita P. and C. C. Collins (eds) *The Control of Eye Movements*. New York: Academic Press 1971.
- BACH Y. RITA P. and F. ITO: In vivo studies on fast and slow muscle fibers in cat extraocular muscles. *J gen Physiol* 1966 49 1177-1198.
- BARNACK N. H., C. C. BELL and B. G. REECE: Tension and rate of tension development during isometric responses of extraocular muscle. *J Neurophysiol* 1971 34 1072-1079.
- BJORCK A. and H. KJØLBERG: The electrical activity of the muscles of the eye and eyelids in various positions and during movement. *Electroenceph clin Neurophysiol* 1953 5 595-602.
- BREIVIN G. M.: The structure and function of extraocular muscle—an appraisal of the duality concept. *Amer J Ophthalmol* 1971 72 1-9.
- BUCHTHAL G., C. GULD and P. ROSENFALCK: Propagation velocity in electrically activated muscle fibers in man. *Acta physiol scand* 1955 34 75-84.
- BURKE R. E.: Motor unit types of cat triceps surae muscle. *J Physiol (Lond)* 1967 193 141-160.
- BURKE R. E., H. N. LEVINE, F. E. ZAJAC III, F. TSURIS and W. K. ENGEL: Mammalian motor units: Physiological histochemical correlation in three types in cat gastrocnemius. *Science* 1971 174 709-712.
- CLOSE R.: Dynamic properties of fast and slow skeletal muscle of the rat during development. *J Physiol (Lond)* 1969 193 74-93.
- COOPER S. and J. C. ECCLES: The isometric responses of mammalian muscle. *J Physiol (Lond)* 1930 69 377-385.
- DIETERT S.: The demonstration of different types of muscle fibres in human extraocular muscle by electron microscopy and choline response staining. *Invest Ophthalmol* 1965 4 51-63.
- FERNAND S. V. and A. HISS: The occurrence, structure and innervation of slow and twitch muscle fibers in the tensor tympani and stapedius of the cat. *J Physiol (Lond)* 1969 200 544-547.
- FLOYD K. and I. C. H. SMITH: The mechanical and thermal properties of frog slow muscle fibers. *J Physiol (Lond)* 1971 13 617-631.

- FUCHS A F and F S FUCHS Firing patterns of abducens neurons of alert monkeys in relationship to horizontal eye movement *J Neurophysiol* 1960 23 387-392
- FUCHS A F and F S FUCHS The activity of single thochlear nerve fibers during eye movements in the alert monkey *Exp Neurol* 1971a 13 78-89
- FUCHS A F and E S FUCHS Development of isometric tension in simian extraocular muscle *J Physiol (Lond)* 1971b 219 155-166
- CRANF R and R E BURKE The control of movement and posture *Brain Res* 1973 33 1-78
- ALLANSON C H Conduction velocity and amplitude of the action potential as related to circumference in the isolated fibre of frog muscle *Acta physiol scand* 1956 27 14-34
- HARKER D W The structure and innervation of sheep superior rectus and levator palpebrae extraocular muscles I Extrasfusal muscle fibers *Invest Ophthalmol* 1972 11 95C-96C
- HEIN A and H GONEN Eye muscle motor neurons with different functional characteristics *Brain Res* 1972 43 381-388
- HENNINGSEN E and C B OLSEN Relations between structure and function in the design of skeletal muscle *J Neurophysiol* 1965 28 581-598
- HEIN A The structure of slow and fast extrasfusal muscle fibers in the extraocular muscles and their nerve endings in guinea pigs *J cell comp Physiol* 1961 28 63-80
- HEIN A and G PILAR Slow fibers in the extraocular muscles of the cat *J Physiol (Lond)* 1963 169 180-199
- JAREMO L W G ELZARTIKER H BERMAN and J I LILIENTHAL JR Spread of excitation in skeletal muscle. Some factors contributing to the form of the electromyogram *Amer J Physiol* 1957 168 446-457
- KÄPFER S W and F M VALCHIAN WILLIAMS Small nerve junctional potentials. The distribution of small motor nerves to frog skeletal muscle and the membrane characteristics of the fibres they innervate *J Physiol (Lond)* 1953 101 289-317
- LENNERSTRAND G Fast and slow units in extrinsic eye muscles of cat *Acta physiol scand* 1971 86 285-288
- LENNERSTRAND G Mechanical and electrical properties of extraocular motor units in the cat *Uio Spring m ting* 1973 63
- LENNERSTRAND G Mechanical studies on the retractor bulbi muscle and its motor units in the cat *J Physiol (Lond)* 1974 236 45-55
- MATYUSHKIN D P Motor systems in the oculomotor apparatus of higher animals *Fed Proc (Transl suppl)* 1961 3 1103-1106
- MATYUSHKIN D P and T M DAVYDINA Electrophysiological characteristics of tonic fibers of the extrinsic ocular muscles *Fiziol Zh (Mosk)* 1970 56 563-569
- MARR R Structure and distribution of fibre types in the external eye muscles of the rat *J Cell Physiol* 1971 3 433-447
- ORLAND R K A further study of electrical responses in slow and twitch muscle fibre of the frog *J Physiol (Lond)* 1963 167 181-191
- ORIMA T Some electrophysiological properties of rabbit extraocular muscle recorded in vivo with intracellular electrode *Jap J Ophthalmol* 1964 8 111-115
- ORIMA T K CHIZAO MINOYA J DAVODOWITZ and G M BREVIN Correlation of potential and fiber type in extraocular muscle *Docum ophthalmol (Den Haag)* 1969 6 197-201
- PEARSON I The structure of the extraocular muscle fibers of mammals Pp 47-66 in B A H RITA I and L C Collins (eds) *The Control of Eye Movements* New York Academic Press 1971
- PILAR G Further study of the electrical and mechanical responses of slow fibers in cat extraocular muscle *J gen Physiol* 1967 50 289-300
- ROBINSON D A Oculomotor unit behavior in the monkey *J Neurophysiol* 1970 33 393-404
- SAS J and R SCHUB Drogenantigen Palisaden Endigungen der Augenmuskeln *Acta morphol und Anat* 1957 2 259-266
- SCHULLER P H The discharge characteristics of single units in the oculomotor and abducens nuclei of the uninected in shes *Exp Brain Res* 1970 10 347-367
- TEIG H Tension and activation time of motor units of the middle ear muscles in the cat *Acta physiol scand* 1971 84 11-21
- WOOTEN G F and B J REI Blood flow in extraocular muscle of cat *Arch neurol* 1976 350-352
- ZENKER W and H VAGENBACHER On the different forms of myo-neural junction in two types of muscle fiber from the external ocular muscles of the rhesus monkey *J cell comp Physiol* 1964 63 273-285

Glycogen Utilization in Leg Muscles of Men during Level and Uphill Running

By

D L COSTILL¹ E JANSSON P D GOLLI² and B SALTIN³

Received 1 February 1974

Abstract

COSTILL D L E JANSSON P D GOLLI² and B SALTIN *Glycogen utilization in leg muscles of men during level and uphill running* Acta physiol scand 1974 91 475-481

Glycogen depletion was followed in the soleus gastrocnemius and vastus lateralis muscles of 3 men during 2 h of treadmill running on the level and uphill (+6°). One subject also ran downhill (-4.5°). Running speed was adjusted in each condition to require 75% of the subjects $V_{O_{2max}}$. Glycogen concentrations were similar in all 3 muscles at rest. From PAS staining glycogen appeared to be evenly distributed between slow and fast twitch fibres. Glycogen depletion of 17, 33 and 44 mmol of glucose units \times kg⁻¹ wet weight occurred in the vastus lateralis soleus and gastrocnemius muscles respectively after running on the level. These values were 50, 46 and 60 mmol \times kg⁻¹ respectively after uphill running. Glycogen depletion in the soleus and gastrocnemius muscles after downhill running was similar to that after running on the level; however in the vastus lateralis it was intermediate to that for uphill and level running. A loss of PAS stain was observed first in the slow twitch fibres in all conditions. The results support the concept of a differential involvement of the leg muscles during running which can be modified by running either uphill or downhill. Thus it is of importance for the representativity of a sample that it is taken from a particular muscle when the local response to exercise or physical training is studied.

Glycogen utilization by human skeletal muscle varies as a function of work intensity (Saltin and Karlsson 1971). Costill and coworkers (Costill *et al.* 1971) have reported differential rates of glycogen depletion in the leg muscles of man during prolonged running. This suggests that there may be different magnitudes of involvement of the leg muscles in running. Such an effect may be attributable to the anatomical location of the muscles or to the mechanics of doing the work.

Present addresses

¹ D L Costill Human Performance Laboratory School of Physical Education and Athletics Ball State University Muncie Indiana

² P D Gollick Department of Physical Education for Men Washington State University Pullman, Washington

³ B Saltin August Krogh Institute Copenhagen University Denmark

The present study was undertaken to extend the earlier work of Costill *et al.* (1971) in studying the differential involvement of the leg muscles during running as judged from the magnitude of the glycogen disappearance. Attempts were made to accentuate any such differences by having the subjects run on the level uphill and downhill. Since a selective glycogen depletion pattern in human skeletal muscle fibres has been observed both in bicycle (Gollnick *et al.* 1973; Gollnick *et al.* 1974) and running (Costill *et al.* 1974), such an analysis was also included in the present study.

Subjects

Physical education students served as subjects for the investigation. Mean values for age, height and weight were 25 ± 3 —28 years, 1.76 — 1.84 m and 69 — 71 kg, respectively. Their maximal oxygen uptake ($\dot{V}_{O_{2\max}}$) averaged 47 — 53 l/min. All subjects were experienced cross-country runners.

Methods and Procedure

Eleven subjects completed a series of 2.1 h submaximal runs on the level and uphill ($+6^\circ$). The speed of the treadmill was adjusted (13.8 and 8.3 km/h) to produce work intensities requiring $\sim 75\%$ of the subjects' $\dot{V}_{O_{2\max}}$ for each experimental condition. One subject also ran downhill (13.0 km/h) at a -4.5° slope but at a high enough speed to elicit a \dot{V}_{O_2} less than 0.2 — 0.3 l/min so that deoxygenation could not be sustained.

Heart rates, finger tip blood samples for lactate determinations and \dot{V}_{O_2} measurements were taken at 10, 30, 50, 70, 85 and 110 min of exercise. Muscle biopsies were taken at rest during a 10 min pause at the end of exercise and at the end of the 2nd h of exercise.

\dot{V}_{O_2} was measured with the Douglas bag technique. The volume of the expired gas was measured in a 1-litre spirometer and its composition determined with the Haldane technique. Heart rate was determined from the electrocardiogram (telemetry). Blood lactate was estimated with an enzymatic technique (Scholz *et al.* 1954). Muscle samples were taken from the lateral portion of the thigh vastus lateralis, gastrocnemius and soleus muscles with the needle technique (Bergström 1969). The incision of the soleus biopsy was made 2—3 cm distal to the lower lateral edge of the gastrocnemius muscle. The samples were immediately divided into portions. One part was frozen in liquid nitrogen and stored at -80°C until analyzed for total glycogen concentration (Kathren, Diamant and Saltin 1971). The remaining portion of the muscle sample was prepared for histochemical analysis as previously described (Gollnick *et al.* 1974; Gollnick *et al.* 1974). Serial sections were stained for myofibrillar ATPase (Padua and Kraman 1955) and for glycogen with the periodic acid-Schiff's (PAS) reaction (Pearl 1961). Muscle fibres were identified as slow twitch (ST) and fast twitch (FT) on the basis of differences in myofibrillar ATPase as described previously (Gollnick *et al.* 1974). Glycogen depletion patterns in the two major fibre types were estimated as previously described (Gollnick *et al.* 1974; Brink *et al.* 1974).

Results

\dot{V}_{O_2} averaged 34 and 37 l/min during level and uphill running, respectively. These values represented about 76 (69—83)% of the subjects' maximal aerobic power. Only minor variations occurred in the \dot{V}_{O_2} during the runs and between level and uphill running (Fig. 1).

Heart rate was similar for the different exercise situations (Fig. 1). An initial increase to about 160 beats/min was observed. Thereafter a gradual increase occurred to a final rate of between 165 and 172 beats/min. The respiratory exchange

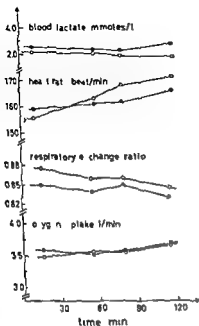


Fig 1

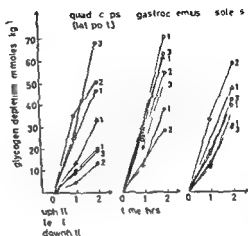


Fig 2

Fig 1 Average blood lactate heart rate respiratory exchange ratio and oxygen uptake for the 3 subjects during 2 h of running on the level (●) and uphill (O)

Fig 2 Glycogen depletion (mmoles of glucose units per kg wet muscle) in the vastus lateralis soleus and gastrocnemius muscles of 3 subjects during 3 h of running on the level and uphill and for one subject during downhill running Data from the individual subjects are indicated by the numbers next to the symbols and stating the condition for the run

ratio (R value) responded similarly throughout the various runs. Average R values of 0.85 and 0.88 were observed for the level and uphill running after 10 min of exercise. Thereafter slight reductions occurred. The mean relative $\dot{V}O_2$ for the subject during downhill running was 3–5% less than in the other conditions. The mean R value was 0.87 and blood lactate and heart rate averaged $2.2 \text{ mmol} \times \text{l}^{-1}$ and $176 \text{ beats} \times \text{min}^{-1}$ respectively. For this particular subject these values are similar to those obtained while running either on the level or uphill and also to the mean values presented in Fig 1. Based on the average $\dot{V}O_2$ and R values it was estimated that the 2 h runs utilized approximately 2100 kcal with 1000 and 1100 kcal being derived from the oxidation of 245 and 270 g of carbohydrates in level and uphill running respectively.

Glycogen concentrations for the 3 muscles examined were relatively constant from day to day and comparable to that normally seen in similar subjects (Gollnick *et al.* 1973, Gollnick *et al.* 1974, Saltin and Karlsson 1971). The small variation that did occur can probably be explained by the fact that no attempt was made to control either the diet or previous activity of the subjects on the days prior to an experiment. One consistent observation was a 5 to 20 mmol (glucose units $\times \text{kg}^{-1}$) lower glycogen concentration in the soleus than in the other 2 muscles.

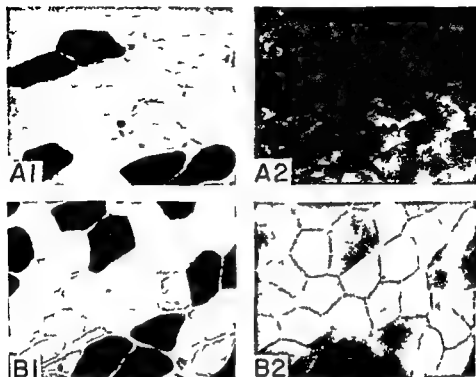


Fig. 3. Photomicrographs ($\times 130$) of the soleus muscle from one subject showing the PAS staining intensity in the SI and IT fibres at rest (A) and after 2 h of running on the level (B). The number 1 series of micrographs are for myofibrillar ATPase showing the dark (FT) and light (ST) stained fibres. The number 2 series of micrographs contains the PAS staining for glycogen. The change in PAS staining was similar for all three muscles and for the different exercise conditions.

A glycogen depletion of 17.44 and 33 mmol of glucose units \times kg⁻¹ wet muscle occurred in the vastus lateralis, gastrocnemius and soleus muscles (Fig. 2) respectively after 2 h of running on the level. These values were 55, 60 and 46 mmol of glucose units \times kg⁻¹ respectively for the same muscles after uphill running. Thus the rate of glycogen depletion was increased in all 3 muscles during uphill running. The soleus and gastrocnemius muscles increased approximately 30% but a 3-fold enhancement of the glycogen utilization occurred in the vastus lateralis. Running downhill resulted in a glycogen depletion in the vastus muscle that was intermediate to that of level and uphill running. No marked difference was present for the soleus and gastrocnemius muscles.

Analysis of the loss of PAS-stainable material from the 2 major fibre types revealed that in all experimental conditions and muscles studied the ST fibres were the first to lose staining intensity. The rapidity of this process was closely related to the glycogen depletion rate observed in a particular muscle. Thus a greater difference in the estimated intensity of the PAS stain existed in the vastus muscle after uphill as compared to level running. In submaximal bicycle exercise a significant

percent of the ST fibres usually are PAS negative before any marked reduction in PAS staining of the FT fibres is detectable (Gollnick *et al* 1974). In the present experiments the loss of PAS staining intensity from FT fibres occurred somewhat sooner in relation to ST fibres than was previously seen during bicycle exercise. However in all cases a faster initial loss of PAS stain occurred in ST fibres. An example of the change in PAS staining after exercise is presented in Fig. 3.

The glycogen depletion pattern during downhill running was not different from running uphill or on the level. However due to the low percentage of FT fibres in the soleus or gastrocnemius muscles no conclusion can be drawn concerning this subject. In fact some samples of the soleus contained 100% ST fibres.

Discussion

In the present study the subjects exercised at the same relative intensity for 2 h on a treadmill where the inclination was changed so that uphill level and downhill running was performed. Heart rate response, blood lactate level and R values were similar in all 3 conditions as was the estimated energy output and carbohydrate combustion. In spite of this clear differences in the rates of glycogen disappearance in the leg muscles existed. This was most pronounced when the vastus lateralis was compared to the soleus and gastrocnemius muscles. Glycogen breakdown was enhanced in all muscles during uphill running. Moreover the increase in the vastus lateralis was so marked that the difference observed between this and the other 2 muscles that existed during running on the level almost disappeared. This can probably be most easily explained by the increased work done by the vastus lateralis in elevating the body during uphill running.

The present results point to the importance of the relative involvement of a particular muscle group in a work task for the local metabolic response taking place. Such estimation of the relative involvement of each muscle group during a given exercise would be of value for a better understanding of intramuscular changes that occur during exercise.

The R value was somewhat higher in uphill as compared to level running. This increase however was not enough to explain the elevated glycogen utilization by the leg muscles during uphill running. The possibilities exist however that the use of carbohydrates was reduced in some muscle groups that were not investigated and that the uptake of glucose by the muscles from the blood stream was reduced.

From the results of this study it seems safe to postulate that the vastus lateralis muscle is not a representative muscle from which to obtain samples when prolonged running is performed on a relatively flat course. The same is most likely true for cross-country sking (*cf* Bergstrom, Hultman and Saltin 1973). In both the exercises the calf muscles may be more involved than the thigh muscles. Further support for such a statement comes from measurement of oxidative enzyme activities that have demonstrated that the highest values for runners are found in the gastrocnemius muscle and in cross country skiers in the gastrocnemius and del-

toideus muscles (unpublished data). In contrast in bicyclists the highest activities are found in the lateral portion of the quadriceps (Gollnick *et al.* 1972).

In an earlier study (Costill *et al.* 1971) of prolonged running (race of ≈ 2.5 h) it was found for the thigh that a depletion of glycogen occurred almost exclusively in the ST fibres. This was true except for the first part of the run when some FT fibres also demonstrated a rapid glycogen loss. Only in the early phases of the race did the runners try to maintain a high speed when running uphill. V_{O_2} approached maximal values during these brief periods. The hypothesis put forth to explain these earlier findings was that the quadriceps muscles were more involved in uphill running and that in very intense exercise the FT fibres were recruited. Both these assumptions seem to be supported by the results of this and other recent studies (Costill *et al.* 1974; Gollnick *et al.* 1973; Gollnick *et al.* 1974).

Of note is the rather marked glycogen depletion that occurred in downhill running which for the vastus lateralis was more pronounced than for running on the level. This was unexpected since negative exercise which to a large extent downhill running consists of would have been anticipated to produce only a small glycogen breakdown (Bonde Petersen, Knuttgen and Henriksson 1972). On the other hand a considerable amount of energy was required to resist the gravitational acceleration. Most of this may have been performed by the quadriceps muscles. Training seems to be important for the efficient performance of negative work (Khusen and Knuttgen 1971). As mentioned above the subject experienced some discomfort during the downhill exercise. He also had difficulty in sustaining the run for 2 h. Training for downhill running may result not only in a lower caloric expenditure but also a smaller glycogen depletion in the leg muscles.

Some of the present data are contrary to those reported earlier by Costill and associates (Costill *et al.* 1971). In contrast to the earlier finding of a 32 and 47% greater glycogen content in the soleus as compared to the gastrocnemius and vastus lateralis muscles respectively, only minor differences existed in the present study. This was true in spite of the wide variation in fibre composition of the muscles. Thus the soleus muscle containing an average of 83% ST fibres had a glycogen content only slightly less than the vastus lateralis (60% ST) and gastrocnemius (62% ST) muscles. This supports our earlier histochemical observation of no major difference in the glycogen content of the 2 major fibre types found in the muscles studied (Costill *et al.* 1974; Gollnick *et al.* 1972; Gollnick *et al.* 1973). Further support for this statement is now also available from direct determination of the glycogen content of individual human skeletal muscle fibres (Essen and Henriksson 1974).

In summary it appears that the utilization of glycogen by a muscle during exercise is related to the involvement of the particular muscle in the work. Thus in any study of local metabolic response an estimate of the relative exercise intensity of the muscle(s) in question is a necessity before any conclusions regarding whole body metabolism can be made. Moreover in studies of the local response to physical training it is of importance to sample from a muscle that has been entirely involved in the training.

This study was supported by Grants from the Swedish Medical Research Council (40\ 2903) and Research Council of the Swedish Sports Federation

■ D Gollnick was the recipient of a Visiting Professorship Swedish Medical Research Council (14\ 4014)

References

- BERGSTROM J Muscle electrolytes in man *Scand J clin Lab Invest* 1967 Suppl 68
- BERGSTROM J, E HULTMAN and B SALTIN Muscle glycogen consumption during cross country skiing *Intern Z angew Physiol* 1973 31 91-95
- BONDE PETERSEN F, H G KAUTTGEN and J H HENRIKSSON Muscle metabolites during exercise with concentric and eccentric contractions *J appl Physiol* 1972 33 792-795
- COSTILL, D L, K SPARKS, R GREGOR and C TURNER Muscle glycogen utilization during exhaustive running *J appl Physiol* 1971 31 353-356
- COSTILL D L, P D GOLLNICK, E C JAMES, B SALTIN and E M STEIN Glycogen depletion pattern in human muscle fibres during distance running *Acta physiol scand* 1973 89 374-383
- ESSEN B and J HENRIKSSON Glycogen content of individual muscle fibres in man *Acta physiol scand* 1974 90 645-647
- GOLLNICK P D, ■ B ARMSTRONG, C W SAUBERT IV, K PIEHL and B SALTIN Enzyme activity and fibre composition in skeletal muscle of trained and untrained man *J appl Physiol* 1972 33 312-319
- GOLLNICK P D, R B ARMSTRONG, W L SEMBROWICH, R E SHILPHERD and B SALTIN Glycogen depletion pattern in human skeletal muscle fibres after heavy exercise *J appl Physiol* 1973 34 615-618
- GOLLNICK P D, R B ARMSTRONG, C W SAUBERT IV, W L SEMBROWICH, R E SHILPHERD and B SALTIN Glycogen depletion patterns in human skeletal muscle fibres during prolonged work *Pflügers Arch ges Physiol* 1973 344 1-11
- KARLSSON J, B DIAMANT and B SALTIN Muscle metabolites during submaximal and maximal exercise in man *Scand J clin Lab Invest* 1971 26 385-394
- KLATSEN K and H G KAUTTGEN Effect of training on oxygen consumption in negative muscular work *Acta physiol scand* 1971 93 319-323
- PADYKULA M A and F HERMAN The specificity of the histochemical method for adenosine triphosphatase *J Histochem Cytochem* 1953 3 170-193
- FEARSE A G E *Histochemistry—Theoretical and Applied* 1961 Boston Mass Little Brown ■ 832
- SALTIN B and J KARLSSON Muscle glycogen utilization during work of different intensities In *Muscle Metabolism During Exercise* Plenum Press New York 1971
- SCHOLZ R, H SCHMITZ, T BLECHER and J O LAMPERT Die Wirkung von Nystatin auf Bakterien *Biochem Z* 1959 331 71-86

Middle Ear Muscle Effects on Cochlear Responses to Bone-conducted Sound

By

D. R. F. IRVINE¹ and A. G. WESTER

Received 11 February 1974

Abstract

IRVINE D. R. F. and WESTER A. G. Middle ear muscle effects on cochlear responses to bone conducted sound. *Acta physiol scand* 1974 91 482-496

Contractions of the stapedius and tensor tympani muscles were elicited by electrical stimulation of their motor nerves or of the muscles themselves in anesthetized cats. The effects of these contractions on cochlear microphonic responses to air- and bone-conducted sound were examined. Stapedius contractions that produced changes in air conduction similar to those observed under physiological conditions had almost identical effects on bone conduction. Tensor tympani effects on bone conduction were of similar magnitude but greater complexity than those on air and varied as a function of the location of the bone conductor on the skull. Control observations established that the effects were attributable to the middle ear muscles and not to either consequence of the experimental procedures and that they did not reflect modification of an air conduction component of the bone conduction stimulus. The functional significance of the effects is discussed in terms of protection against masking of environmental sounds by self-generated bone-conducted sound.

The effects of the middle ear muscles (MEM) on air-conducted sound are well established. Contraction of the stapedius and tensor tympani muscles alters the mobility of the ossicular chain and thereby modifies the transmission of acoustic energy to the cochlea. Under most conditions transmission is attenuated by such contractions. In animals both muscles exhibit reflex contractions to adequate acoustic stimuli (Wever and Vernon 1955, 1956; Wersall 1958) but reflex activity in man is apparently restricted to the stapedius (Klockhoff 1961; Djupesland 1967). Non-reflex contraction of both muscles have been described in association with general motor activity, particularly that involving the facial musculature (Klockhoff 1961; Carmel and Starr 1964; Salomon and Starr 1963; Djupesland 1967).

¹ Present address: Neuropsychology Laboratory, Department of Psychology, Monash University, Clayton, Victoria 3168, Australia.

Present address: Institute of Neurophysiology, University of Oslo, Karl Johans Gate 47, Oslo 1, Norway.

Despite considerable knowledge of MEM activity the function of the muscles remains unclear. The most popular theory has been that they serve to protect the cochlea against damage from intense sounds. Although there is some evidence for this view (Hilding 1960, 1961; Simmons 1963), the protection afforded by the muscles is limited by their long latency (Wersall 1958). Borg (1972 b, c) has suggested a number of other ways in which the muscles might serve to extend the dynamic range of the auditory system and has reviewed evidence indicating a possible anti masking function (Laden *et al.* 1964). None of these theories takes any account of the non reflex activity of the muscles although Simmons (1964) has proposed that such activity might provide protection against masking of environmental sound by self generated noise. This is an attractive theory but it has proved difficult to obtain clear evidence of such protection (Irvine and Webster 1972).

The failure to develop a comprehensive account of MEM function suggests that the muscles might have significant effects other than those on air conducted sound. Some evidence for such a possibility can be found in the literature concerning bone conduction hearing. Clinical and theoretical considerations have prompted numerous studies of the effects of middle ear manipulations on bone conduction. Specifically there have been a number of reports that immobilization of the ossicles results in a decrease in bone conduction responses at low and middle frequencies (Smith & R 1943; Legoux and Tarab 1959; Tonndorf and Tabor 1962; Tonndorf *et al.* 1966). The ossicular immobilization employed in these studies has at least superficial similarities to that produced by MEM contractions and these data therefore suggest that such contractions might themselves affect bone conduction. If this were the case the nature of such effects might be expected to provide some clarification of MEM function. The experiments reported here were therefore designed to examine the effects of MEM activity on cochlear microphonic (CM) responses to bone conducted acoustic signals.

Methods

Subjects and surgery

Subjects were 37 adult cats shown by otoscopic examination to be free of external and middle ear infections. Data from some of the initial subjects have been presented in a preliminary technical note (Irvine and Webster 1973). The present report is based primarily on a second series of 21 experiments in which a number of procedural refinements described below were introduced.

Each subject was anesthetized with sodium pentobarbital injected *iv* and anesthesia was maintained by supplementary injections as required. Surgery and testing were carried out in a shielded sound attenuating room and rectal temperature was maintained at 36–38°C. The bulla on the left side as exposed by a ventro-lateral approach. Under microscopic control a stainless steel spring electrode was located on the round window (RW) and cemented to the bulla. The defect in the bulla was then repaired with dental acrylic. In the first series of experiments changes in intra bullar pressure consequent on eustachian tube collapse were found to influence tensor tympani effects. Subsequently one end of a short length (1–1.5 m) of small bore (1.1 mm) polyethylene tube was sealed into the hole in the bulla at the turn of electrode implantation. The tube permitted static pressure equalization without changing the resonance characteristics of the bulla.

In the majority of the stapedius experiments and in approximately half of the tensor tympani experiments contractions of the muscles were elicited by electrical stimulation of their motor

Middle Ear Muscle Effects on Cochlear Responses to Bone conducted Sound

By

D R F IRVINE¹ and A G WESTER

Received 11 February 1974

Abstract

IRVINE D R F and WESTER A G *Middle ear muscle effects on cochlear responses to bone conducted sound* Acta physiol scand 1974 91 482-496

Contractions of the stapedius and tensor tympani muscles were elicited by electrical stimulation of their motor nerves or of the muscles themselves in anesthetized cats. The effects of these contractions on cochlear microphonic responses to air and bone conducted sound were examined. Stapedius contractions that produced changes in air conduction similar to those observed under physiological conditions had almost identical effects on bone conduction. Tensor tympani effects on bone conduction were of similar magnitude but greater complexity than those on air and varied as a function of the location of the bone conductor on the skull. Control observations established that the effects were attributable to the middle ear muscles and not to other consequences of the experimental procedures and that they did not reflect modification of an air-conduction component of the bone conduction stimulus. The functional significance of the effects is discussed in terms of protection against masking of environmental sounds by self-generated bone conducted sound.

The effects of the middle ear muscles (MEM) on air-conducted sound are well established. Contraction of the stapedius and tensor tympani muscles alters the mobility of the ossicular chain and thereby modifies the transmission of acoustic energy to the cochlea. Under most conditions transmission is attenuated by such contractions. In animals both muscles exhibit reflex contractions to adequate acoustic stimuli (Wever and Vernon 1972, 1976; Werall 1978) but reflex activity in man is apparently restricted to the stapedius (Klockhoff 1961; Djupesland 1967). Non-reflex contraction of both muscles have been described in association with general motor activity particularly that involving the sacral musculature (Klockhoff 1961; Carmel and Starr 1963; Salomon and Starr 1963; Djupesland 1967).

¹ Present address: Neuropsychology Laboratory, Department of Psychology, Monash University Clayton Victoria 3168 Australia.

² Present address: Institute of Neurophysiology, University of Oslo, Karl Johans Gate 4, Oslo 1, Norway.

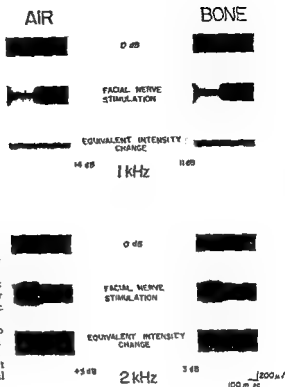


Fig 1 Envelopes of CM responses to air conduction (left column) and bone conduction (right column) acoustic stimulation. At each frequency upper trace shows response to acoustic stimulus alone (0 dB). Second trace effect of facial nerve stimulation sweep triggered at onset of stimulus train. Third trace CM response after adjustment of intensity to match effect of stapedius contraction. Extracranial branches of facial nerve sectioned.

Results

Stapedius Basic Effects

Contractions of the stapedius muscle produced similar changes in the CM responses elicited by air and bone conduction stimulation. The effects of stapedius contractions at 2 frequencies and the titration technique used to quantify these effects are illustrated in Fig 1. At 1 kHz there is a marked attenuation of both responses equivalent to a decrease in SPL of 14 dB for air and 11 dB for bone. At 2 kHz however facial nerve stimulation results in a small (3 dB) potentiation of each response.

In Fig 2 A-C frequency functions for the effects of stapedius on both modes of stimulation are shown for three individual subjects. In the majority of subjects as in Fig 2 A and B the changes in air and bone conduction CM were similar at all frequencies. In Fig 2 C an unusual case of large high-frequency effects and dissociation between the air and bone changes is illustrated. In all three subjects there is a clear potentiation of CM in the region of 1.8–2.5 kHz. Potentiation of this kind was observed in 16 of the 17 animals in which its occurrence was systematically investigated. In Fig 2 D responses in the transition zone are shown for subject B. Although the function suggests a simple transition from attenuation to potentiation it is apparent in Fig 2 D that the potentiation first manifests itself as a transient increase followed by an attenuation (e.g. at 1.8 and 2.0 kHz). In a number of cases

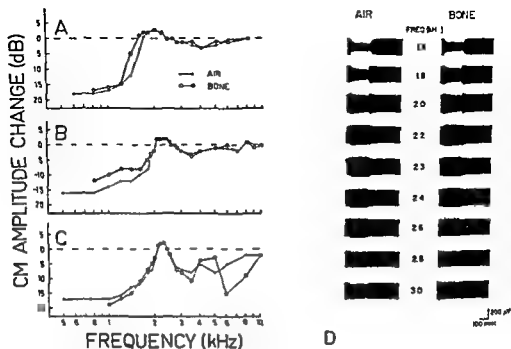


Fig. 3. A-C Frequency function for effects of stapedius contraction on air and bone-conduction CM in three animals. D CM envelopes from one animal (function B) showing changes in effect over frequency range (1.4–3.0 kHz) within a high stapedius contraction produces potentiation of CM.

the potentiation was abolished or shifted to a lower frequency when the bulla was opened. This factor was not examined systematically, but these observations suggest that the potentiation is a resonance phenomenon.

The parametric characteristics of the stapedius effects were investigated in a number of subjects. In all cases the magnitude of the effect varied monotonically with nerve stimulation intensity. In Fig. 3A intensity functions at two frequencies are shown for one animal. For both the attenuation at 1 kHz and the potentiation at 2 kHz the amplitude of the effect increased monotonically with stimulation intensity. Furthermore, the nature of the stapedius effect at a given frequency was invariant with acoustic stimulus intensity. In Fig. 3B the 2 kHz potentiation can be seen to occur over the range of CM linearity. Varying the location of the bone conductor on the skull resulted in changes in CM amplitude but had no effect on the stapedius effects. Measurements were usually made on the sustained contraction produced by 200 ms pulse trains, but in a few cases train duration was varied and twitches produced by one or two pulses were examined. For both air and bone the effect varied in a direct fashion with train duration.

Stapedius Control Observations

A number of control techniques were employed to establish that the observed ef

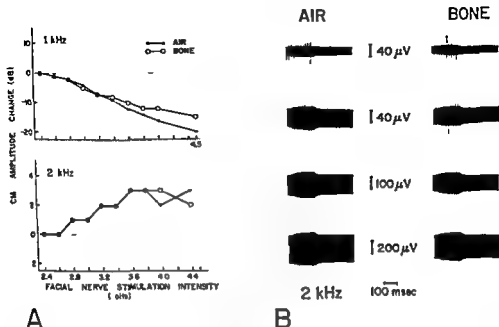


Fig 3 A Intensity functions for one subject showing effect of facial nerve stimulation intensity on magnitude of effect at two frequencies (1 kHz and 2 kHz) B CM envelopes for one subject illustrating invariance of stapedius effect with changes in acoustic stimulus intensity

fects were the result of stapedius activity and not of other peripheral manifestations of central stimulation. In most subjects the extracranial branches of the facial nerve were transected where they leave the skull at the stylomastoid foramen. This procedure resulted in complete abolition of the peripheral effects of facial nerve stimulation but produced no change in the CM effects. The frequency functions in Fig 2 and the control data shown in Fig 4 were obtained in experiments in which this procedure was employed. In another series of observations that are discussed in more detail below, it was found that the effects of facial nerve stimulation were unaltered by tenotomy of tensor tympani but were completely abolished by tenotomy of the stapedius (see Fig 4). Together these data establish unequivocally that the effects reported were the result of stapedius contractions and not of other consequences of facial nerve stimulation.

A further control requirement is indicated by the possibility that the bone conduction effects might merely reflect effects on air conducted sound associated with bone-conduction stimulation. There are two potential sources of such sound. One is the acoustic field generated by the bone-conduction transducer itself. The other is sound generated by deformation of the walls of the meatus during bone conduction stimulation (Tonndorf *et al* 1966; Tonndorf, Greenfield and Kaufman 1966a). In Fig 4 A and B the effects of blocking the meatus are shown. This procedure resulted in a large decrease in air conduction CM and a potentiation of the bone

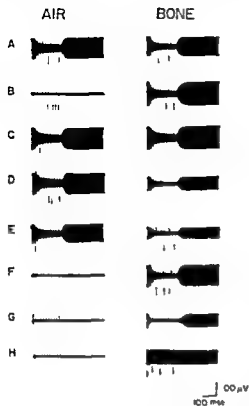


Fig. 4. Stapedius control sequence for one subject. Successive traces show effect of facial nerve stimulation on air and bone-conduction CM under following conditions: A in normal preparation; B after obturation of meatus; C after removal of plug from meatus and reorientation of animal to enable opening of bulla; D after opening bulla and septum; E after tenotomy of tensor tympani; F after laceration of tympanic membrane; G after disarticulation of incudostapedial joint; H after tenotomy of stapedius.

conduction response. The latter effect is a well established consequence of obturation of the meatus (Tonndorf *et al.* 1966a). Under these conditions the stapedius effect on bone conduction was unchanged. This result establishes that the acoustic field generated by the transducer is not a factor in the bone conduction response but is equivalent with respect to sound generated within the meatus. In Fig. 4 C–F the effects of damage to the tympanic membrane are shown. Access to the middle ear was achieved by opening the bulla and septum and this operation produced a decrease in the bone-conduction CM but no change in the air conduction response (Fig. 4 D). Tenotomy of tensor tympani had no effect on either the responses or the effects of facial nerve stimulation (Fig. 4 E). Laceration of the drum however almost completely abolished the air conduction CM but potentiated bone conduction CM and the magnitude of the stapedius effect. Survival of the bone-conduction responses in the absence of air conduction input establishes clearly that the latter made no contribution to those responses.

In three animals the control observations were extended in order to obtain information on the mechanisms of the observed effects. In Fig. 4 G–H the effects of further manipulations on the same subject are shown. Disarticulation of the incudostapedial joint eliminated the small air conduction CM that had survived drum laceration but produced only a small reduction of the bone conduction

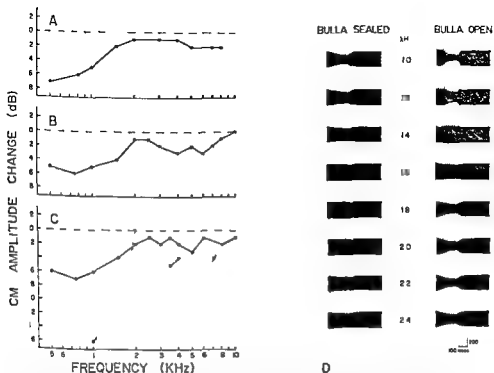


Fig 5 A—C Frequency functions for effects of tensor tympani contractions on air conduction CM for 3 subjects A and B central stimulation of trigeminal nerve (peripheral branches cut in A) C direct stimulation of tensor Dotted line in C gives frequency function at higher intensity of electrical stimulation D CM envelopes showing effects of trigeminal stimulation on air conduction transmission at frequencies of 10—24 kHz with bulla sealed (left column) and after opening bulla (right column)

response. More importantly, this procedure did not alter the magnitude of the stapedius effect on bone conduction (Fig 4 G) which was finally eliminated by tenotomy of the muscle (Fig 4 H). Survival of the stapedius effect after incudo-stapedial disarticulation was observed in all three animals in which this procedure was investigated.

Tensor tympani Basic effects

Tensor tympani effects on bone conduction CM differed in some respects from those on air conduction responses and the two sets of data will be presented separately. Typical air conduction effects are illustrated in the left (bulla sealed) column of Fig 5 D. Comparison of the effect at 1 kHz with that of the stapedius in Fig 1 reveals that the contraction and relaxation times of tensor tympani are considerably longer. Air-conduction frequency functions for tensor tympani are presented for three subjects in Fig 5 A—C. Functions were usually obtained at a stimulus intensity that produced a decrement in air conduction CM of approxi-

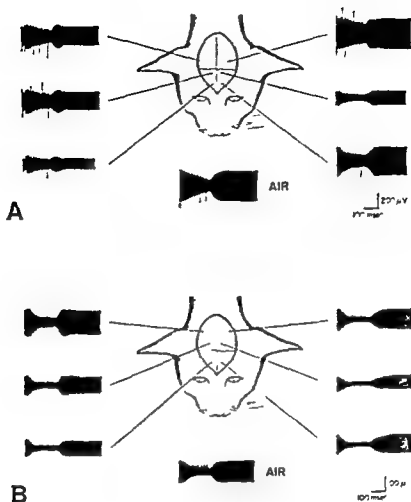


Fig. 11. Effects of bone-conductor location on nature of tensor tympani effects at 1 kHz in two animals. Contraction elicited by central stimulation in A, direct stimulation in B.

mately 11 dB at frequencies below 1 kHz. At this level some functions showed a small inflection in the region of 2 kHz (e.g. Fig. 5B) but in other cases the small magnitude of all effects above 2 kHz made the presence of such an inflection hard to discern (Fig. 5A and C). In a few animals therefore frequency functions were also obtained at a higher (and probably unphysiological) stimulation intensity. Under these conditions an inflection was clearly apparent (broken line curve in Fig. 5C). This potentiation like that produced by the stapedius appeared to be a resonance phenomenon. In Fig. 5D effects over the frequency range from 1.0 to 2.4 kHz are shown before and after a hole was drilled in the bulla and septum. As a consequence of this procedure the potentiation shifted to a lower frequency (1.4 kHz).

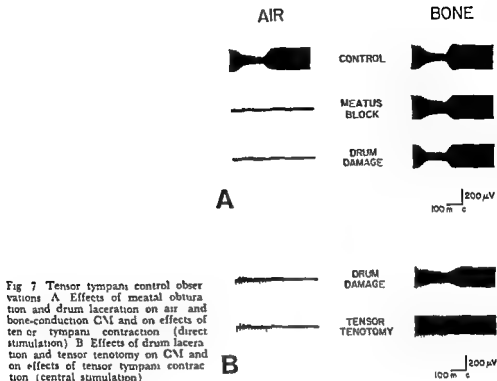


Fig 7 Tensor tympani control observations A Effects of meatal obturation and drum laceration on air and bone-conduction CM and on effects of ten or tympani contraction (direct stimulation) B Effects of drum laceration and tensor tenotomy on CM and on effects of tensor tympani contraction (central stimulation)

In the initial experiments tensor tympani effects on bone conduction CM were more complex than those on air in some cases exhibiting patterns of alternating potentiation and attenuation. These effects proved to be artifactual consequences of the ear bar effects and intra bullar pressure changes mentioned previously. When these factors were eliminated ten or effects on bone conduction were of similar magnitude to those on air-conduction (see Fig 6) although differences in the configuration of the effect were still observed. Experiments in which the position of the bone conductor was systematically varied suggested that differences in transducer location were responsible for this variability. The effects of this factor are shown for two subjects in Fig 6 A and B. In both cases contraction of tensor tympani produced a relatively simple attenuation of CM when the bone conductor was on the side (left) from which CM recordings were made. For contralateral (right) bone-conductor sites however the effect consisted of an initial potentiation followed by attenuation. Potentiation is also apparent during relaxation of the muscle on cessation of the shock train. At sites from which this pattern was obtained bone conduction intensity-functions were non monotonic exhibiting a simple potentiation at threshold and potentiation followed by a monotonically increasing attenuation at higher levels.

A laterality effect of this kind was observed in three of six animals in which this factor was systematically investigated. In the remaining animals tensor contractions

produced attenuation of bone-conduction CM for all transducer locations although the configuration of the effect varied between sites. The existence of these variations precluded detailed parametric analysis and frequency and intensity functions were therefore not obtained for tensor effects on bone conduction.

Tensor Tympani Control Observations

The effects of tensor contractions elicited by direct stimulation did not differ from those produced by central stimulation (see e.g. Fig. 5C and 6B). This observation indicates that the effects of central stimulation were not attributable to other peripheral consequences of this procedure. Unequivocal support for this conclusion is provided by the fact that the effects of central stimulation were abolished by tenotomy of tensor tympani. Tenotomy data are presented in Fig. 7B for an animal in which laceration of the drum had abolished the air-conduction response but left bone-conduction CM and the tensor attenuation unaffected. Tenotomy of the muscle completely abolished the effect of trigeminal stimulation.

The results of blocking the meatus and of damaging the drum are shown for one animal in Fig. 7A; both procedures abolished air-conduction CM but had little effect on the bone-conduction response. Although the configuration of the tensor tympani effect on bone conduction was influenced by these procedures it is clear that the effects were not attributable to modification of an air-conduction component of the bone-conduction response.

Discussion

These data provide strong support for the contention that MEM activity modifies bone-conduction responses. The control observations establish that the observed effects are attributable to the activity of the muscles and not to other consequences of the experimental procedures. Moreover, despite the coarseness of the electrical stimulation technique, a number of considerations indicate that the contractions elicited in this laboratory are similar to those occurring under physiological conditions.

One such consideration concerns the time course of the effects. Both the contraction and relaxation time of the tensor activity elicited by electrical stimulation were longer than that of the trapezius. Wersall (1958) reported similar differences in the time course of contraction in cats and others have made similar observations on the activity elicited by direct nerve or muscle stimulation (Starr 1959; Teig 1972a). These differences are in accordance with morphological and histochemical evidence that the trapezius contains almost exclusively twitch fibres while tensor tympani contain a much larger proportion of slow muscle fibres (Erulkar *et al.* 1961; Fernand and Hess 1969; Selden *et al.* 1971; Teig 1972b; Teig and Dahl 1972).

The second consideration concerns the magnitude of the effects. As stimulation intensities were routinely adjusted to give effects of physiological magnitude at frequencies below 1 kHz, this argument rests on the hope of the air-conduction

frequency functions. There is general agreement that the effects of reflex contractions in intact animals (Galambos and Rupert 1959 Simmons 1959 Price 1966) and voluntary contractions in man (Smith H D 1943 Reger *et al* 1963) are greatest for frequencies below approximately 2 kHz (see also Møller 1972). This general pattern was obtained for both muscles in the experiments reported here. However, more detailed comparison is made difficult by the limited nature of available evidence on the effects of the muscles individually.

The position is most clear with respect to the stapedius. Møller (1965) presented a frequency function for contralaterally elicited reflex contractions in anesthetized rabbits that is almost identical to those reported here and exhibits similar potentiation in the 2 kHz region. Wever and Bray (1942) reported that the effects of artificial tension on the stapedius tendon were greatest for frequencies up to approximately 3 kHz. Their curves indicate that tensions within the range of physiological effects produced potentiation from 1.5 to 2.0 kHz and Wiggers (1937) also observed potentiation from 1.3 to 1.8 kHz during spontaneous stapedius contractions. Potentiation occurred at higher frequencies in the present experiments but shifted to lower frequencies when the bulla was open, as it appears to have been in these earlier studies.

In the case of the tensor, the physiological nature of the contractions is more difficult to establish. The high intensity stimulation data presented here and the results of earlier electrical stimulation (Starr 1959 Teig 1973) and artificial tension (Wever and Bray 1937) experiments indicate that tensor tympani is capable of producing attenuation of considerable magnitude. But there is some doubt as to whether this potential is realized under physiological conditions. Although Wever and Vernon (1955) reported that contralaterally-elicited tensor contractions produced attenuation of as much as 9–10 dB, there have been a number of reports that the effects of the stapedius alone are almost identical to those observed when both muscles are intact (Galambos and Rupert 1959 Carmel and Starr 1963 Borg 1972 a, b). Moreover, the protection against trauma afforded by the muscles is attributable entirely to the stapedius (Simmons 1959 Hilding 1960, 1961). This evidence suggests that the 5–6 dB effects produced at the stimulation level employed in the present experiments might in fact exceed the normal effects of the muscle.

These considerations support the contention that the stapedius contractions elicited in the present studies were similar to those occurring under physiological conditions. The position with respect to tensor tympani is less clear, but this uncertainty is probably not critical in view of the relatively minor contribution of this muscle to normal MEM activity. It therefore seems reasonable to conclude that activity of the muscles has significant effects on bone conduction under physiological conditions. There appears to have been no previous report of such effects, although Reger *et al* (1963) reported modification of bone-conduction transmission during voluntary contraction of the muscles in man. The dependence of the changes on MEM activity was not established in their studies, however, and it is not improbable

that voluntary contraction of the muscles is associated with other changes that might affect bone conduction transmission.

Because of the impedance mismatch between air and the skull bone conduction resulting from airborne sound is not a significant factor in hearing. The functional significance of MEM effects on bone conduction is therefore most likely to be associated with internally generated sound and with the non reflex activity of the muscles. The present data suggest that MEM contractions associated with vocalization mastication and other activities of the facial musculature would provide considerable attenuation of the bone conducted sound associated with such activities. If this were so the muscles could provide protection against masking of environmental sounds by self generated bone conducted sound. This proposed function for MEM non reflex activity is an extension of that suggested by Simmons (1964). It is in accordance with the view that the construction of the middle ear is such as to enhance sensitivity to environmental sounds while reducing sensitivity to internal sounds. Biriny (1938) and Bekesy (1949) demonstrated that the structure and suspension of the ossicular chain are such as to have this consequence. It now appears probable that the MEM contribute to this selectivity.

Further evidence on a number of issues is required to clarify the nature of these effects and the extent to which they fulfill the function suggested above. The limitation of the bone-conduction transducer employed in these studies precluded examination of effects below 600–800 Hz. Self generated noise of the type considered here is predominantly of low frequency and it is these frequencies that are favoured by bone conduction (Tonndorf *et al* 1966b). The nature of the effects in this range is therefore of particular importance. Further research is also required to determine the effects on bone conduction of simultaneous contractions of the two muscle under physiological conditions.

A final issue concerns the mechanism of MEM effects on bone conduction. The present data provide no conclusive evidence on this question although the survival of bone conduction CM and the stapedius effect after incudo stapedial disarticulation is of considerable interest. This observation indicates that the effects cannot be accounted for simply in terms of a decrease in ossicular inertia (Biriny 1938, Tonndorf *et al* 1966, Tonndorf 1972). However more detailed investigation will be required to elucidate the nature of the mechanisms involved.

This work was undertaken in the laboratory of Dr R F Thomson whose support is gratefully acknowledged. It was supported in part by grants from the National Institute of Health (NS 00111) and the National Institute of Mental Health (MH 19314).
D R F Irvine is a Public Health Service International Postdoctoral Research Fellowship (TW 018) and K G Wester is supported by Grant 70-474 from Foundations Fund for Research in Vibration.

The authors are indebted to Shirley Adam and Sarah Beidler for technical assistance.

References

- BIRINY, E. A contribution to the physiology of bone conduction. *Acta oto laryng* (Stockh) 1938 Suppl. 26, 1–23.
BEKESY, G. von. The structure of the middle ear and the hearing of one's own voice by bone conduction. *J acoust Soc Am* 1949 21 217–23.

- BREVINS C E Innervation of the tensor tympani muscle of the cat *Amer J Anat* 1960 113 297-301
- BORG E On the change in the acoustic impedance of the ear as a measure of middle ear muscle reflex activity *Acta oto laryng* (Stockh) 1972 a 71 163-171
- BORG E Regulation of middle ear sound transmission in the nonanesthetized rabbit. *Acta physiol scand* 1972 b 86 175-190
- BORG E Acoustic middle ear reflexes: a sensory-control system *Acta oto laryng* (Stockh) 1972 c Suppl 304 1-34
- CAMEL P W and A STARR Acoustic and nonacoustic factors modifying middle-ear muscle activity in waking cats *J Neurophysiol* 1963 26 598-616
- DILFELAND G *Contractions of the tympanic muscles in man* Oslo Universitetsforlaget 1967 113 pp
- EMILKAR S D M L SHELANSKI B L WHITSEL and P OGLE Studies of muscle fibers of the tensor tympani of the cat *Anat Rec* 1961 149 249-298
- FERNAND V S V and A HELL The occurrence, structure and innervation of slow and twitch muscle fibres in the tensor tympani and stapedius of the cat *J Physiol* (Lond) 1969 200 347-354
- GALAMBOS R and A RUPERT Action of the middle ear muscles in normal cats *J acoust Soc Amer* 1959 31 349-353
- HOLDING D A The intratympanic muscle reflex as a protective mechanism against loud impulsive noise *Ann Otol* (St. Louis) 1960 69 51-60
- HOLDING D A The protective value of the stapedius reflex: an experimental study *Trans Amer Acad Ophthal Otolaryngol* 1961 63 297-307
- IRVINE D R F and W R WEBSTER Arousal effects on cochlear potentials: investigation of a two-factor hypothesis *Brain Res* 1972 39 109-119
- IRVINE D R F and A G WESTER Bone conduction as a means of acoustic input control: the effects of middle ear muscle contractions *Electroenceph clin Neurophysiol* 1973 34 80-89
- KARNOS G J MARTIN L KELLENYI and M BALER Constant intensity sound stimulation with a bone conductor in the freely moving cat *Electroenceph clin Neurophysiol* 1970 28 637-638
- KLOCKHOFF I Middle ear muscle reflexes in man *Acta oto laryng* (Stockh) 1961 Suppl 164 1-99
- LEGOLK J P and S TARAB Experimental study of bone conduction in ears with mechanical impairment of the ossicles *J acoust Soc Amer* 1959 31 1453-1457
- LEWIS G B NORDLUND and J E HAYKINS JR. Significance of the stapedius reflex for the understanding of speech *Acta oto laryng* (Stockh) 1964 Suppl 188 245-279
- MOLLER A R An experimental study of the acoustic impedance of the middle ear and its transmission properties *Acta oto laryng* (Stockh) 1965 60 124-149
- MOLLER A R The middle ear Pp 135-194 in Tobias J V ed *Foundations of modern audiology* Vol II New York Academic Press Inc 1972
- PRICE G R Middle ear muscle activity in the rabbit III: Supra threshold phenomena. *J and Res* 1966 6 175-180
- ROGER S N O J MEXEL W K ICHAS and S J STEINER Changes in air conduction and bone conduction sensitivity associated with voluntary contraction of middle ear musculature Pp 171-180 in Fletcher J L ed *Middle ear function seminar* U.S. Army Med Res Lab Rep No 516 1963
- SILVERMAN G and A STARR Electromyography of middle ear muscles in man during motor activities *Acta neurol scand* 1963 39 161-168
- SEMER H Slow muscle fibers in the tensor tympani muscle of the guinea pig *Amer J Anat* 1971 132 267-273
- SIMMONS F B Middle ear muscle activity at moderate sound level *Ann Otol St Louis* 1959 68 1126-1143
- SIMMONS F B Induced sound damage susceptibility: role of middle ear muscles *Ann Otol* (St. Louis) 1963 72 528-541
- SIMMONS F B Physiological theories of middle ear muscle function *Ann Otol St Louis* 1964 73 727-739
- SMITH H D Audiometric effects of voluntary contraction of the tensor tympani muscle *Arch otolaryng* 1943 38 362-370
- SMITH K R Bone conduction during experimental fixation of the stapes *J exp Psychol* 1943 33 96-107
- SUNDER R S and W T NEMER *A skeletal atlas of the cat* Chicago University of Chicago Press 1961
- STARR A Regulatory mechanisms of the auditory pathway Pp 101-114 in Locke E ed *Modern neurology* Boston Little Brown & Co 1979

- TEIG E. Force and contraction velocity of the middle ear muscles in the cat and the rabbit *Acta physiol scand* 1972 a 84 1—10
- TEIG E. Tension and contraction time of motor units of the middle ear muscles in the cat *Acta physiol scand* 1972 b 84 11—21
- TEIG E. Differential effects of graded contraction of middle ear muscles on the sound transmission of the ear *Acta physiol scand* 1973 88 382—391
- TEIG E. and H. A. DAHL. Actomyosin ATPase activity of middle ear muscles in the cat *Histochemie* 1972 29 1—7
- TOMNORF J. Bone conduction. Pp 197—237 in Tobias J. V. ed *Foundations of modern auditory theory*. Vol II. New York: Academic Press Inc 1972
- TOMNORF J. R. A. CAMPBELL I. BERNSTEIN and J. P. REYER. Quantitative evaluation of bone conduction components in cats *Acta otolaryng* (Stockh) 1966 Suppl 213 10—38
- TOMNORF J. E. C. GREENFIELD and R. S. HALTMAN. The occlusion of the external ear canal: its effect upon bone conduction in cats *Acta otolaryng* (Stockh) 1966 a Suppl 213 80—104
- TOMNORF J. E. C. GREENFIELD and R. S. HALTMAN. The relative efficiency of air and bone conduction in cats *Acta otolaryng* (Stockh) 1966 b Suppl 213 105—123
- TOMNORF J. and J. R. TABOR. Closure of the cochlear windows: its effect upon air and bone-conduction. *Ann o of St Louis* 1967 71 5—29
- WERSHALL R. The tympanic muscles and their reflexes *Acta otolaryng* (Stockh) 1958 Suppl 139 1—112
- WEYER E. G. and C. W. BRAY. The tensor tympani muscle and its relation to sound conduction *Ann otol* (St Louis) 1953 46 917—961
- WEYER E. G. and C. W. BRAY. The stapedius muscle in relation to sound conduction *J exp Psychol* 1949 31 35—43
- WEYER E. G. and J. A. VERNON. The effects of tympanic muscle reflexes upon sound transmission *Acta otolaryng* (Stockh) 1955 45 433—437
- WEYER E. G. and J. A. VERNON. The control of sound transmission by the middle ear muscles *Ann otol* St Louis 1956 65 5—14
- WIGGERS H. C. The functions of the intra-aural muscles *Ann J Physiol* 1937 170 171—780

Transcapillary Passage of Plasma Proteins in Experimental Burns

By

MARIA GANROT, STEN JACOBSSON and ULF ROTHMAN

Received 12 February 1974

Abstract

GANROT M, S JACOBSSON and U ROTHMAN. Transcapillary passage of plasma proteins in experimental burns. *Acta physiol scand* 1974 91 497-501

The "leakage" of proteins from plasma to interstitial fluid in burns was studied experimentally in dogs. The concentration of orosomucoid, α_1 -antitrypsin, albumin, haptoglobin, IgG, β_2 -globulin and α macroglobulin were determined in plasma and in lymph from the leg before and after scalding of the paw. The lymph/plasma ratio of all proteins except that of α macroglobulin increased after scalding, indicating an increased capillary permeability to proteins with molecular weights up to 300 000.

In burns the permeability of the capillaries of the skin is altered with an increased passage of proteins from plasma to the interstitial fluid as a result (Cope and Moore 1944). In humans the protein rich fluid thus formed has been studied by collecting exudate from blisters and determining the albumin and globulin fractions (Cope *et al* 1948). Lymph reflects the composition of the interstitial fluid and Roberts and Courtice (1969) studied the main electrophoretic protein fractions in lymph drained from burned paws in rabbits (Roberts and Courtice 1969a, b). They reported that the lymph/serum ratios of albumin and of γ globulin were increased 0-2 h after the burn.

The capillary membranes selectively prevent the passage of macromolecules. To elucidate the sieving characteristics of the capillary membrane in a burned area dextran of different molecular weights was used in dogs with experimental burns (Arturson 1961). But the largest molecule used was smaller than those of many plasma proteins. Therefore the experiments did not give a true picture of leakage of proteins from the plasma in thermal injury. Such a picture requires determination of specific proteins in lymph. The purpose of the present investigation was to ascertain what changes occur in the distribution between lymph and plasma of proteins of different molecular weights in dogs with burns.

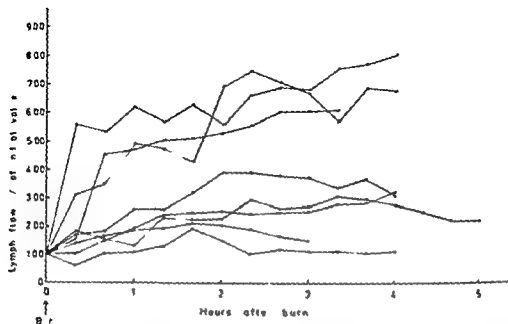


Fig. 1. Amount of lymph collected after scalding. The values are expressed as percentages of those before scalding.

Methods

Animal experiments. 8 mongrel weighing 12–25 kg were used. The hind legs were shorn the day before the experiment. The animals were anesthetized by pentobarbitone sodium (Nembutal Abbott) in a dose of 30 mg/kg bwt. When necessary small additional doses (30–60 mg) were given during the experiment. A free airway was secured by endotracheal intubation. After subcutaneous injection of 200 ml methylene blue into the paw of the hind leg a lymphatic was cannulated with a polyethylene tube (PE 50) at a point just above the ankle joint and adjacent to the saphenous vein. Lymph flow was secured by moving the paw at times every 5 min during the experiment. Lymph was collected in 20 min portions in vials filled with Na_2EDTA as an anticoagulant. Blood samples were drawn from the cannulated carotid artery. Lymph was collected for usually 1–2 h before scalding of the paw by immersing the leg about 15 cm into water of 90°C for 30 s. The lymph then was collected for 1 h after which the dog was killed.

Analytical methods. The hematocrit in arterial blood was determined in a microcapillary centrifuge.

Hemoglobin was determined as cyanmethemoglobin to estimate the amount of red blood cells which soon after appeared in the lymph after burning. The lymph was centrifugated and the clear supernatant was separated off after which the cyanid reagent was added to the sediment.

The concentration of plasma proteins in plasma and lymph were determined by electro-immunoassay (Liljell 1977). The antisera against dog plasma proteins were the same as those used previously (Ganrot 1973). Anti dog immunoglobulin G (IgG) was raised in rabbits by repeated injection of dog IgG isolated by precipitation with octanoic acid (Steinbuch and Audran 1969). A pool of plasma from healthy dogs of different breeds was used as a standard and the values obtained were expressed as percentages of those in the pool.

Results

The hematocrit increased from a mean of 37.2% immediately before the scalding to a mean of 40.8% 3 h later. The amount of red blood cells found in some of the lymph samples was always smaller than that corresponding to an admixture of

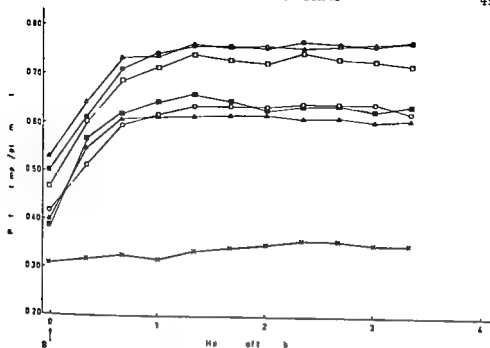


Fig 2 Mean of lymph/plasma ratios of different proteins before and after scalding in 8 dogs
 Δ—Δ orosomucoid ●—● α₁ antitrypsin □—□ albumin ○—○ haptoglobin
 ▲—▲ IgG ■—■ β_{2C} globulin ×—× α macroglobulin.

0.1 per cent of the volume of whole blood as judged from hemoglobin content of blood and lymph

In most of the dogs the lymph flow increased markedly after scalding but the inter individual variation was wide (Fig 1) 2 h after the injury the lymph flow tended to become steady in most dogs

The concentrations of different plasma proteins in the lymph before and after the experimental burning are given in Fig 2 The mean and range of lymph/plasma ratio of various proteins in 8 dogs before burn are given in Table I The ratios varied inversely with the molecular weights of the proteins

After the burn the lymph/plasma ratios of orosomucoid α₁ antitrypsin albumin haptoglobin IgG and β_{2C} globulin increased rapidly and reached a steady level within 1 h of the injury (Fig 2) The mean lymph/plasma ratios 2 h after the scalding are given in Table I The mean of the relative increase in the ratios (in the calculation of the mean log transformation was done) for the proteins mentioned was 43—61 % (Table I) The burns were not followed by any significant increase in the lymph/plasma ratio of α macroglobulin ($p > 0.1$)

Discussion

The lymph collected was only a fraction of the lymph produced because the region studied was drained by several lymph vessels Judging by the abrupt changes in some

TABLE 1. Mean and range of the lymph/plasma ratio of various proteins in 8 days before and 7 h after scalding of paw. Mean and range of the percental increase in ratio are given (mean

	orosomucoid	α_1 antitrypsin	albumin
Lymph/plasma ratio before scalding	0.53 (0.44-0.67)	0.50 (0.38-0.68)	0.4 (0.40-0.56)
Lymph/plasma ratio 2 h after scalding	0.71 (0.11-0.8)	0.76 (0.67-0.81)	0.3 (0.6-0.84)
Percental increase in ratio	43 (31-80)	48 (18-103)	57 (76-93)
Molecular weights of human proteins	44 000	45 000	69 000

of the curves the fraction obtained sometimes varied considerably. The increase observed in the lymph flow after burning therefore indicates only that the volume of lymph produced was increased but tells nothing about the actual size of this increase. But even if the fraction of lymph drained through the cannulated lymph vessel did vary, the composition of the collected lymph would nevertheless be representative of all the lymph produced in the region drained.

The burn was too small to cause any systemic changes influencing the plasma volume. The slight increase in the hematocrit during the experiment can be ascribed to mild dehydration because the animals were not given any infusion. The admixture of red blood cells in some lymph samples presumably caused by damage to the blood capillaries by the burn was so small that any possible admixture of whole blood was negligible.

The lymph/plasma ratios of the various proteins before the burn varied inversely with the molecular weights of the proteins (Table 1). The ratios found were higher than those reported by others (Ganrot, Laurell and Ohlsson 1970). As the condition of the two series of experiments such as frequency of movements of the paws which caused differences in the flow rate of the lymph or the position of the paws resulting in differences in venous pressure were not standardised the levels of the ratios are not strictly comparable.

The lymph/plasma ratios of orosomucoid, α_1 antitrypsin, albumin, haptoglobin, IgG and β_{11} globulin increased after burn to values that also varied inversely with the molecular weights of the proteins (Table 1). The mean of the relative increase of the ratios varied from 43% to 61% which did not differ significantly. It is however noteworthy that the relative increase tended to be larger the higher the molecular weights of the proteins. This means that the range of the lymph/plasma ratios of the proteins was somewhat narrower after burn which implies that the selectivity of the capillary membrane in retaining proteins with the actual molecular weights is somewhat reduced.

The lymph/plasma ratio of α_2 macroglobulin did not increase significantly indicating that the permeability of the capillary membrane to plasma proteins with a molecular weight of 820 000 was unchanged. This is incompatible with Courtois's

ritms were used in the calculations of the means) Molecular weights of the proteins in man are given for comparison

haptoglobin	IgG*	β globulin*	α macroglobulin
0.47 (0.30-0.52)	0.40 (0.33-0.47)	0.39 (0.32-0.44)	0.31 (0.24-0.39)
0.64 (0.52-0.72)	0.62 (0.57-0.67)	0.63 (0.58-0.67)	0.55 (0.28-0.44)
51 (18-97)	54 (30-83)	61 (38-98)	6 (-13-719)
100 000	160 000	300 000	870 000

* Determined in only 6 dogs

finding of increased concentrations of lipoproteins in lymph drained from burned paws of rabbits (Courtice 1959). However he determined the concentrations of the lipoproteins indirectly from the total cholesterol, phospholipid and total fatty acid levels in lymph i.e. determinations not strictly applicable to lipoproteins passing through the capillary membrane. If on the other hand the permeability of the capillary membrane to β lipoprotein (m.w. 3,200 000) really is increased in burned areas the finding of unchanged lymph/plasma ratio of α macroglobulin in this study might suggest consumption of α macroglobulin by complex formation with proteolytic enzymes in the interstitial tissue.

This investigation was supported by grants from the Swedish Medical Research Council (Project No. B74 13\ 581 10C) and the Medical Faculty University of Lund.

References

- ARTLSON G. Capillary permeability in burned and non burned areas in dogs. *Acta chir scand* 1961 Suppl. 274: 55-103.
- COPE O and F H MOORE. A study of capillary permeability in experimental burns and burn shock using radioactive dyes in blood and lymph. *J clin Invest* 1944 23: 241-257.
- COPE O, J B GRAHAM, F H MOORE and M R BALL. The nature of the shift of plasma protein to the extravascular space following thermal trauma. *Ann Surg* 1948 128: 1041-1055.
- COURTICE F C. Permeability of normal and injured skin capillaries to lipoproteins in the rabbit. *Aust J exp Biol med Sci* 1959 37: 451-464.
- GÄNROT P O, C H LAURELL and K. ÖHLSSON. Concentration of trypsin inhibitors of different molecular size and of albumin and haptoglobin in blood and in lymph of various organs in the dog. *Acta physiol scand* 1970 79: 280-286.
- GÄNROT K. Plasma protein response in experimental inflammation in the dog. *Res exp Med* 1973 161: 251-261.
- LAURELL C H. Electroimmuno assay. *Scand J clin Lab Invest* 1973 9 Suppl. 174: 21-37.
- ROBERTS J C and F C COURTICE. Measurements of protein leakage in the acute and recovery stages of a thermal injury. *Aust J exp Biol med Sci* 1969a 47: 421-433.
- ROBERTS J C and F C COURTICE. Immunoelectrophoretic analysis of proteins in lymph from the leg before and after thermal injury. *Aust J exp Biol med Sci* 1969b 47: 435-446.
- STEINBUCH M and R AUDRAN. The isolation of IgG from mammalian sera with the aid of caprylic acid. *Arch Biochem* 1969 134: 9-284.

DDT and Related Substances Effects on Permeability Properties of Myelinated *Xenopus* Nerve Fibre Potential Clamp Analysis

By

PETER ARIËN and BERNHARD FRANKENHÄUSER

Received 19 February 1974

Abstract

ARIËN P and B FRANKENHÄUSER *DDT and related substances Effects on permeability properties of myelinated *Xenopus* nerve fibre Potential clamp analysis* Acta physiol scand 1974 91 502-511

An analysis was made of the effect of DDT and related substances on the membrane currents associated with step changes of the membrane potential. The substances tested are DDT, DDD, DDE, DDM, DDA, DDC, bis (*p*-chlorophenyl) acetamide and polychlorinated biphenyls (CB, DD1, DDA and bis (*p*-chlorophenyl) acetamide). DDT and DDC had acute effects on permeability parameters of the nerve membrane. The effects of the substances differed drastically from each other. DD1 affected the turn off process of the sodium permeability mechanism after a positive potential step; the effect was large on fibres from *Rana pipiens* but negligible on fibres from *Xenopus laevis*. DDA affected the turn off process of the potassium permeability mechanism while bis (*p*-chlorophenyl) acetamide affected sodium and potassium permeability constant \bar{T}_N and \bar{T}_K . The other substances tested had no or only marginal acute effects. The main effect of DDA can be described as a specific effect on the rate constant β . The obvious differences in effect of the substances on the permeability parameters were thus related to defined numerical differences of the studied substances.

The main acute nervous effect of the insecticide DDT on vertebrates seems to be on the central nervous system (Shankland 1964; Woolley 1970). In addition some rather specific effects on myelinated nerve fibres have been described (Hille 1968; van den Bercken 1972). Hille found on fibres from *Rana pipiens* that DDT decreases the rate of decay of the sodium current after a short positive potential step. Further, the rate of sodium inactivation is decreased. The rate of turn on of the sodium current was found to be unaffected. A similar behaviour has been described for the lobster giant axon by Narahashi and Haas (1968).

The present study was undertaken to analyse the effect on myelinated nerves of *Xenopus laevis* of some substances (see Table I) which are closely related to and except for the polychlorinated biphenyl most probably metabolites of DDT (Grummit and Marsh 1949; Grummit, Berck and Richard 1950; Albont, Eglington, Evans

and Rhead 1972 Jensen Gothe and Kindstedt 1972) The substances were applied to the node in solutions with organic solvents as ethanol polyoxyethylene sorbitane mono-oleate or dimethylsulphoxide The effects of these solvents *per se* were also studied Ethanol has earlier been described to decrease the sodium and potassium permeability constants of the squid axon (Armstrong and Binstock 1964 Moore Ulbricht and Takata 1964) while polyoxyethylene sorbitane mono-oleate only has minute effects (Kishimoto and Adelman 1964) The main findings of the present investigation was that DDT DDA and bis (*p*-chlorophenyl) acetamide had strikingly different effects DDA affected mainly the potassium mechanism in a very specific manner while bis (*p*-chlorophenyl) acetamide affected both the sodium and the potassium transport mechanisms It was further found that fibres from *Xenopus laevis* and *Rana pipiens* showed a marked difference with respect to the effect of DDT The other substances tested had marginal effects only A preliminary report of the present investigation has been published (Arhem Frankenhaeuser Göthe and O Bryan 1974)

Methods

The experiments were carried out on single myelinated fibres dissected from the sciatic nerve of the clawed toad (*Xenopus laevis*) The recording cell and the electrode assembly were all held at a controlled temperature As a rule the temperature used was 12 °C The test solution surrounding the node under investigation (V_0) was changed by a peristaltic pump The nodal membrane potential was controlled by a feed back amplifier system as earlier described (Dodge and Frankenhaeuser 1958 Arhem Frankenhaeuser and Moore 1973) Most fibres were polarized to -90 or -110 mV between test pulses in order to keep sodium and potassium inactivation negligibly low i.e. $h_\infty \approx 1$ and $k_\infty \approx 1$ The peak sodium current and the steady state potassium current associated with potential steps of suitable amplitude were measured The curves relating the peak sodium permeability and the steady state potassium permeability to membrane potential were calculated by the constant field equation from the current potential measurements (Frankenhaeuser 1960 1963) The fibre was cut at the adjacent nodes V_{-1} and V_{+1} in order to minimize errors caused by an excitable membrane in the current path Current calibration was made as described by Dodge and Frankenhaeuser (1958)

Solutions The composition of the Ringers solution was NaCl 112 KCl 2.5 CaCl₂ 2.0 and tris-(hydroxymethyl) aminomethane 2.0 mM (pH = 7.2) Experiments were also made in which sodium free solutions with high potassium concentration (144.5 mM) were used

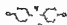
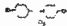






The substances of Table I were supplied to us in a purified crystallized form from the Environmental Toxicology Group at the Wallenberg Laboratory University of Stockholm and from Analytical Standards Unilab Research Corporation Berkeley Sublimated DDA and bis (*p*-chlorophenyl) acetamide were used in some experiments Unpurified commercial DDT was also tested One per cent ethanol (C₂H₅OH) was as a rule used as organic solvent Dimethylsulphoxide (CH₃)₂SO or polyoxyethylene sorbitane mono-oleate (Tween 80) was used in a few experiments The concentration of DDT DDA and bis (*p*-chlorophenyl) acetamide in the saturated Ringer ethanol solution was found to be 6.14% and 36.4% respectively Polychlorinated biphenyls (PCB) were tested partly in purified crystallized form or as commercial mixtures (Clophen A50 50 Cl or Clophen A60 60 Cl) and are similar added to the Ringer ethanol solution

Nomenclature Potentials are given as inside potential minus outside potential and outward current consequently a positive

Results

The isolated nerve fibre was mounted in the recording cell the four solution pools were connected to the appropriate electrodes and the feed back amplifiers were

TABLE 1 Acute effects of DDT related substances on permeability mechanism[†] of nerve from *Nemopus laevis*

Substance	Structure	Effect	P _K	
abbrev	purity ()	concentration (mg/100 ml)		
2,2'-Bis-(p-chlorophenyl)		1	+	—
DDT		0.2 mg/100 ml		
2,2'-Bis-(p-chlorophenyl)		—	—	—
DDE		0.2 mg/100 ml		
2,2'-Bis-(p-chlorophenyl)		—	—	—
DDD		0.2 mg/100 ml		
2,2'-Bis-(p-chlorophenyl)		—	—	—
DDVL		0.2 mg/100 ml		
Bis-(p-chlorophenyl) acetic acid		—	+	—
DDA		4 mg/100 ml		
Bis-(p-chlorophenyl) acetamide		—	—	—
DDCA		0.2 mg/100 ml		
Bis-(p-chlorophenyl) acetamide*		—	—	—
DD		1 mg/100 ml		
2,2'-Bis-(p-chlorophenyl) *				

[†] Pronounced effect only on nerve from *Rana pipiens*.

* Bis-(p-chlorophenyl) acetamide is a hydrolysis product of DDC.

** Several other polychlorinated biphenyls (PCBs) were also tested.

balanced and turned on in the way earlier described (Dodge and Frankenhauser 1958). The nodal membrane was as a rule held at a potential of -90 mV or lower in order to avoid complications by the inactivation systems (I_{Na} to maintain $h_{\infty} \approx 1$ and $k_{\infty} \approx 1$). The membrane potential was then changed from this value in rectangular steps of required amplitudes. The membrane currents associated with the potential steps were measured and analysed.

The effect on the current potential relation of the substances given in Table I were investigated. The solubility of these substances in water is very low (DDT only about 340 pM, somewhat higher for DDA and bis-(p-chlorophenyl) acetamide) while it is appreciably higher in ethanol (C₂H₅OH). The substances were therefore as a rule applied to the node in a Ringer solution with 1% (by volume) ethanol. The solutions used were as a rule saturated.

Effects of the organic solvents

The effects of 1% (by volume) ethanol on membrane current potential relation was first tested. The peak sodium current and the steady state potassium current associated with the potential step decreased less than 10%. Higher concentration decreased the peak sodium current as well as the steady state potassium current. These effects appeared within 10 s and were completely reversible at concentrations not exceeding 10%. The peak sodium permeability curve (Fig. 1) thus showed a decrease of 30–40% in 10% ethanol and a slight shift of about 5 mV along

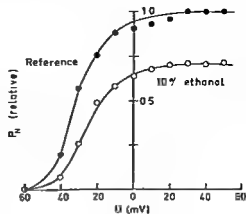


Fig. 1 Plot of peak P_A versus potential for a fibre in Ringer's solution (reference) and in solution with 10% (by volume) ethanol. Smooth curve drawn through experimental points. Temperature 12°C.

the potential axis. The steady state potassium permeability decreased 20–30%. The fibres in this investigation were polarized to about -90 mV in order to keep inactivation at a negligible level. The described effects may thus be accounted for by assuming specific effects on the permeability constants \bar{P}_A and \bar{P}_K . These findings are in agreement with the findings on squid axons by Armstrong and Binstock (1964) and Moore *et al.* (1964). Measurements of the effect-concentration relation were limited to the range below 10%. Concentrations exceeding this high concentration (about 2M) caused irreversible effects and were therefore avoided.

Dimethylsulphoxide and polyoxyethylene sorbitane mono-oleate (tween 80) were used in some experiments in order to increase the amount of DDT transported to the membrane surface. The effects caused by these substances *per se* were therefore tested. 1% dimethylsulphoxide seemed not to affect the sodium permeability change but decreased reversibly the steady state potassium current during the potential step 10–20%. The current tail at the end of a long duration step (the p tail (Frankenhaeuser 1963)) decreased reversibly about 40%. Polyoxyethylene sorbitane mono-oleate (1%) affected almost exclusively the sodium mechanism. The peak sodium permeability decreased about 90% while the steady state potassium permeability decreased less than 10%. This effect appeared within 20 s and was in sharp contrast to the minute effects of polyoxyethylene sorbitate mono-oleate on the squid giant axon (Kishimoto and Adelman 1964). The effect on the myelinated fibre was slowly reversible.

The effect of DDT. As mentioned above DDT has striking effects on the potential clamp currents of the myelinated nerve fibre. In order to check the procedures used in the present investigation especially to check the transport of DDT to the membrane the experiments with DDT were repeated on *Xenopus*. This seemed important because our intention was to investigate DDT-related substances. These experiments indicated surprisingly that DDT had a marginal effect only. This was the case independent of whether *p,p'*-DDT or *o,p'*-DDT or unpurified commercial

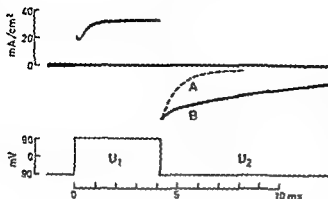


Fig. 2 Effect of DDA on membrane current associated with a potential step (U_1) to $+90$ mV followed by a step (U_2) back to holding potential -90 mV. Fibre in high $[K]$ solution. A before and B after application of DDA. A scaled from record with different time scale. Temperature 12°C .

DDT was used and also independent of whether ethanol, dimethylsulphoxide or polyoxyethylene sorbitane mono-olate (tween 80) was used as organic solvent to transport DDT to the membrane. The striking effects earlier described by Hille (1968) on *Rana* were not obtained. The discrepancy between our findings and the findings of Hille might either be explained on the basis of a difference between the two biological structures, fibres from *Xenopus* or from *Rana pipiens* respectively, or on a difference between possible contaminations of the substances used. Additional measurements were therefore also made on fibres from *Rana pipiens*. These experiments showed two main effects of DDT: (a) a decreased rate of sodium inactivation and a decreased rate of decay of the sodium current after a short positive potential step and (b) a decreased amplitude of the steady state potassium current during a potential step. The decrease of the steady state potassium current was approximately 20%. Effect (a) on the sodium current was equivalent to the findings of Hille. The effects appeared within one or two minutes and were irreversible. The consequent conclusion from the present DDT experiments is that fibres from *Xenopus* and *Rana* respond in a different manner to DDT.

The effect of DDA. DDA decreased the rate of turn off of the potassium permeability in the potential range -50 to -120 mV. The potassium current was small in this range when the external $[K]$ was low since the electro-chemical driving force is small. With the fibre in solutions of high $[K]$ the currents were however larger and the effect was more readily measured. Fig. 2 shows the membrane currents associated with a potential step (U_1) to -90 mV preceded by a step (U_2) to $+90$ mV with the fibre in high $[K]$ solution before DDA was applied and after. A very distinct change is seen in the time course of the current associated with the second potential step (U_2). The tail of potassium current decreases much slower after DDA application while no effect on the turn on the potassium permeability is seen at the beginning of the record. The potassium tail decays with a complex time course. The initial decay is too rapid for a simple exponential curve fitted to the major part of the trace. The rapid initial decay did not appear after low potential steps ($U_1 < +50$ mV). The time constant of the late exponential decay was ap

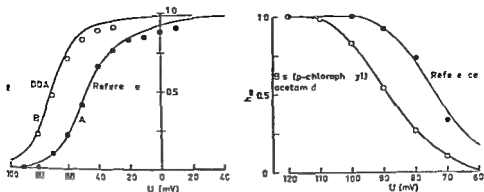


Fig 3 Effect of DDA on n_T -curve. Measurements in high $[K]$ solution. Curve A drawn through experimental points. Curve B calculated from curve A by the equation $n_{T\infty} = \frac{\alpha}{\alpha_n + \beta_n}$. Rate constant α assumed to be unchanged while rate constant β_n was calculated from tail current measurements. Temperature 12°C.

Fig 4 Effect of bis-(p-chlorophenyl) acetamide on n_T -curve. Measurements in Ringer's solution. Curves drawn through experimental points. Temperature 12°C.

approximately 10 times longer than the time constant at corresponding potential steps (U) before DDA application.

Fig 3 shows a plot of measurements of n_T (square root of steady state permeability, against membrane potential without and with DDA in the external solution. It is seen that the relation n_T to membrane potential was shifted about -20 mV due to DDA. This shift can mainly be accounted for by the effect of DDA on the rate constant β since the smooth curve A was drawn through the experimental points and curve B calculated from this with the values of β obtained from the tail measurements. However a close inspection of the time course of turn on of potassium permeability indicated that the rate constant α increased due to DDA slightly in the potential range -70 to -50 mV. The experimental resolution was not sufficient for a further quantitative treatment. In the potential range more negative than -70 mV the time constant τ is approximately inversely proportional to the rate constant β (Frankenhaeuser 1963).

The rate with which the change in tail time constant appeared during application of DDA was appreciable. The change was 90% complete within 10 s. The effect was however slowly and only partially reversible. The time for 90% recovery after washing with DDA free solution was about 15 min.

An effect by DDA on the current tail associated with repolarisations from long lasting potential steps in Ringer's solution was also noted. This tail current which is not carried by potassium has been described by Frankenhaeuser (1962, 1963). Some new details may be added to the description. The tail was not affected by tetrodotoxin. When $[Na]_o$ was increased (i.e. hypertonic solution) the size of the

tail decreased DDA decreased the rate of decay of this tail thus corresponding to a decrease of β_p . The decrease was of the same order of size as the change of β_p . An analysis of u_p from measurements with potential steps of variable duration showed no measurable DDA effect on this rate constant. The experimental resolution was however limited.

The effect of bis (*p* chlorophenyl) acetamide Bis-(*p* chlorophenyl) acetamide caused a decrease in both sodium and potassium currents without affecting their general time courses. The inactivation system was clearly affected. Fig. 4 shows the n_∞ curves for a fibre in solutions with and without bis (*p* chlorophenyl) acetamide. The shift is -15 mV. The decrease was however not caused entirely or even mainly by the change of the inactivation because it remained when the fibre was conditioned between test pulses with negative polarization which removed inactivation (i.e. $h_\infty \approx 1$ and $v_p \approx 1$ before the test pulse). The effects may therefore be described as an effect on the permeability constants (\bar{P}_{Na} and \bar{P}_K) and as an effect on the inactivation system. The decrease of \bar{P}_{Na} was about 90% and the decrease of \bar{P}_K varied between 50 and 70% for a saturated test solution containing 1% ethanol. The m_∞ -curve was not affected measurably. The described effects of bis (*p* chlorophenyl) acetamide clearly increased with an increase in ethanol concentration of the test solution. This seems to be a consequence of the solubility in water ethanol mixtures. Another problem to consider during these experiments is the decomposition of bis (*p* chlorophenyl) acetamide in water solution when stored. Solutions with bis (*p* chlorophenyl) acetamide clearly lost potency within some days even when precautions against evaporation of ethanol and water were made. The effect of bis (*p* chlorophenyl) acetamide on \bar{P}_{Na} and \bar{P}_K (40% of the final steady state) appeared within 30 s. The only partial recovery was considerably slower.

Other tested substances. The other substances of Table I (DDD, DDE, DDMU and DDCN) had no or only marginal effects on the *Xenopus* nerve within an application time of 15 min.

The experimental procedure used was the same throughout. Experiments were also made in which polychlorinated biphenyls (PCB) were applied to the *Xenopus* node. These compounds are structurally related to DDT and similarly very little water soluble but alcohol soluble. No effects on the permeability properties were observed.

Discussion

Hille (1968) and Narahashi and Haas (1968) have shown in potential clamp experiments that DDT has very specific effects on the sodium permeability mechanism. The turn off process of the sodium permeability is drastically slowed down. In order to further analyse this specificity we studied the acute effects of a number of DDT related substances including PCB. The effects of these substances have not earlier been analysed with potential clamp technique. A further cause to study these DDT

related substances was that except for PCB all of them probably are metabolites of DDT. Even PCB however has been proposed to be formed from DDT under certain conditions (Maugh 1973). All these substances except bis (*p*-chlorophenyl) acetamide have been found in nature. Bis (*p*-chlorophenyl) acetamide is however a very probable derivate of DDCN which recently has been discovered in lake sediment (Jensen, Gothe and Kindt 1972). PCB again is known to be a major and serious pollutant in the environment. All the substances used are almost insoluble in water. An organic solvent had therefore to be used in order to increase the concentration. Ethanol, dimethylsulphoxide and polyoxyethylene sorbitane monooleate (tween 80) were used for this purpose. The effect of ethanol *per se* on the myelinated fibre was found to agree with its effect on the squid axon (Armstrong and Binstock 1964; Moore *et al.* 1964). The clear and fast effect of tween 80 which is a neutral detergent on the myelinated fibre differed drastically from its almost lack of effect on the squid axon (Kishimoto and Adelman 1964). The cause of this discrepancy is not clear. DDT had much stronger and distinct effects on fibres from *Rana pipiens* than on fibres from *Xenopus laevis*. In our *Rana* experiments the DDT effects were fully consistent with the earlier mentioned findings of Hille (1968) and Narahashi and Haas (1968) while no or only marginal effects were observed on the *Xenopus* fibres even after long application times in some cases up to 40 min. The effect on the *Rana* fibres appeared within 2 min.

The fibres used in the present investigation were all large. No attempt to separate motor and sensory fibres was made. van den Bercken (1972) found in his study of the DDT effect on the action potential of the *Xenopus* nerve that motor and sensory fibres differ in their response to DDT. Only sensory fibres show DDT induced repetitive firing. In our *Rana* experiments repetitive firing was observed regularly after DDT treatment.

DDA and bis (*p*-chlorophenyl) acetamide had fast and clear effects on the myelinated nerve fibre in low concentrations (14° and 36 μ M respectively). In the pH range here used DDA is negatively charged while bis (*p*-chlorophenyl) acetamide is neutral. DDA affected the potassium permeability in a very specific manner described as mainly a decrease of the rate constant β . The mathematical description of the potassium system given by Frankenhaeuser (1963) predicts a change in the n_{∞} -curve when β is changed. This prediction was verified in the experiments described. The finding lends support for the simple idea of physically separate mechanisms for the sodium and potassium systems (see Mullins 1968 a, b; Narahashi and Moore 1968) and further for the idea of separate mechanisms for the turn on and the turn off of potassium permeability. As was mentioned the DDA modified potassium tail sometimes had a fast decaying initial phase at high potential steps. Calculations showed that this time course may be treated as the sum of the modified potassium tail with a decreased time constant β and a small fraction of unaffected tail with normal β (see Hille 1968 concerning the sodium system).

Bis (*p*-chlorophenyl) acetamide decreased the permeability constants (\bar{P}_{Na} and \bar{P}_K) and shifted the n_{∞} curve. The other substances tested (DDD, DDE, DDMU

DDCN and the chlorinated biphenyls) had no or only marginal effects on the permeability properties of *Xenopus* fibres. The experiments were all carried out with the membrane polarized to about -90 mV between test pulses in order to maintain inactivation at a negligible level. van den Bercken (1969) has proposed on the basis of measurements of the effects of DDD on the action potential that this substance might affect the inactivation system.

The main conclusion from the present investigation is that small structural differences of the used substances caused strikingly different effects on the permeability properties, some of them very specific. The only structural differences between the substances of Table I concern groups bound to the carbon atom in position 1. For example DDA has an OH group in the same position where bis (*p*-chlorophenyl) acetamide has an NH group. Preliminary experiments were performed to further analyse the importance of this OH group for the DDA effect. Thus *p,p*-dichlorobenzallic acid, which is identical to DDA except for an OH group on the carbon atom in position 2, was investigated. These experiments surprisingly showed no effect on the permeability properties.

We wish to thank the Environmental Toxicology Group, the Wallenberg Laboratory of University of Stockholm for purification and analysis of the chemical substances and for valuable discussions. This work was supported by the Swedish Medical Research Council (Project No 14\ 545) and Karolinska Institutets fondar.

References

- ALBANE, E. S., G. ELLINGTON, V. C. EVANS and M. M. RHEAP. Formation of bis (*p*-chlorophenyl) acetamide from *p,p*-DDCN from *p,p*-DDT in anaerobic sewage sludge. *Nature* (Lond.) 197, 40: 420-421.
- ARHEM, P. B., FRANKENHAELSER and L. E. MOORE. Ionic currents at resting potential in nerve fibres from *Xenopus laevis*. Potential clamp experiments. *Acta physiol. scand.* 1973, 88: 446-454.
- ARHEM, P. B., FRANKENHAELSER, R. GÖTHJE and P. O'BRYEN. DDT and related substances on myelinated nerve: effect on permeability properties. *Acta physiol. scand.* 1974, 91: 130-137.
- ARMSTRONG, C. M. and I. BINSTOCK. The effects of several alcohols on the properties of the squid giant axon. *J. gen. Physiol.* 1964, 48: 363-377.
- BERCKEN, J. VAN DEN. The effect of DDD on single Ranvier nodes of *Xenopus laevis*. *Europ. J. Pharmacol.* 1970, 14: 146-148.
- BERCKEN, J. VAN DEN. The effect of DDT and dieldrin on myelinated nerve fibres. *Europ. J. Pharmacol.* 1971, 20: 203-214.
- DODGE, F. A. and B. FRANKENHAELSER. Membrane currents in isolated frog nerve fibre under voltage clamp conditions. *J. Physiol. (Lond.)* 1958, 143: 76-90.
- FRANKENHAELSER, B. Quantitative description of sodium currents in myelinated nerve fibres of *Xenopus laevis*. *J. Physiol. (Lond.)* 1960, 121: 491-501.
- FRANKENHAELSER, B. Initial new potassium currents in myelinated nerve fibres of *Xenopus laevis*. *J. Physiol. (Lond.)* 1962, 160: 46-53.
- FRANKENHAELSER, B. A quantitative description of potassium currents in myelinated nerve fibres of *Xenopus laevis*. *J. Physiol. (Lond.)* 1963, 169: 424-430.
- GRUMMIT, O. and D. MARSH. Derivatives of Di (*p*-chlorophenyl) acetic acid. *J. Amer. chem. Soc.* 1949, 71: 4156-4157.
- GRUMMIT, O., A. BERGE and E. RICHARD. Di (*p*-chlorophenyl) acetic acid. *Org. Synth. Coll.* 1955, 3: 20-272.
- HILLE, B. Pharmacological modifications of the sodium channels of frog nerve. *J. gen. Physiol.* 1968, 51: 199-219.

- JENSEN S R, GOTHE and M O KROSTEDT Bis-(*p*-chlorophenyl) acetonitrile (DDCN) a new DDT derivative formed in anaerobic digested sewage sludge and lake sediment. *Nature* (Lond) 1972 240 421—422
- KASHIMOTO U and W J ABELMAN Effect of detergent on electrical properties of squid giant axon membrane. *J gen Physiol* 1964 47 913—936
- MALCH T M DDT an unrecognized source of polychlorinated biphenyls. *Science* 1973 180 578—579
- MOORE J W W, LEBRUCHT and M TAKATA, Effect of ethanol on the sodium and potassium conductances of the squid axon membrane. *J gen Physiol* 1964 48 279—295
- MULLINS L J A single channel or a dual channel mechanism for nerve excitation. *J gen Physiol* 1968 a, 52 550—553
- MULLINS L J Single or dual channel mechanisms. *J gen Physiol* 1968 b 52 555—556
- NARAHASHI, T and H G HAAS Interaction of DDT with the components of lobster nerve membrane conductance. *J gen Physiol* 1968 51 177—193
- NARAHASHI, T and J W MOORE A single or dual channel in nerve membranes? *J gen Physiol* 1968 52 553—555
- SHANKLAND D L Involvement of spinal cord and peripheral nerves in DDT poisoning syndrome in albino rats. *Toxicol appl Pharmacol* 1964 6 197—213
- WOOLLEY M E Effects of DDT on the nervous system of the rat. In *The Biological Impact of Pesticides in the Environment* Editor J W Gillet. Environment Sci Ser Corvallis 1970 pp 114—124

Afterhyperpolarization Conductance Time Course in Lumbar Motoneurons of the Cat

B.

F. BALDISSERA¹ and B. GUSTAFSSON

Received 19 February 1974

Abstract

BALDISSERA F and B GUSTAFSSON. Afterhyperpolarization conductance time course in lumbar motoneurons of the cat. *Acta physiol scand* 1974 91 512-527

The time and potential dependence of the conductance process(es) underlying the longlasting afterhyperpolarization (AHP) in the cat's α motoneurons were studied. The conductance changes were determined by injection of short current pulses. The conductance time course was characterized by a longlasting exponential decay interrupted by a plateau corresponding to the slower hyperpolarizing phase of the AHP. By displacing the membrane potential in the subthreshold region with the injection of longlasting current pulses it was found that the conductance was largely unaffected by membrane potential displacements. Similar characteristics were found when calculating the AHP conductance time course from the AHP voltage. It was concluded that the AHP in motoneurons is given by a potassium conductance process with this complex S shaped time course. A mathematical expression describing this time course is given.

In most central neurones the somadendritic (SD) spike is followed by a long lasting afterhyperpolarization (AHP). Thorough investigations in the cat's α motoneurons indicate the AHP to be caused by a membrane conductance increase to potassium ion. This conclusion is based on findings regarding the effect of membrane potential displacements and of iontophoreses on the AHP voltage (Coombs *et al* 1955) and on the observation of an increased membrane conductance during the AHP as measured by the voltage drop caused by injected current pulses (Ito and Ohima 1962).

The AHP has long been considered to be of particular importance as an intrinsic mechanism for repetitive firing regulation in spinal motoneurons (e.g. Eccles 1953, Eccles *et al* 1958, Kernell 1963) and there have been attempts to correlate the firing behaviour with AHP parameters such as the AHP duration and the time to peak AHP (Kernell 1963). However until a more detailed knowledge of the time

¹ Present address: Laboratorio di Biologia Spaziale del C.N.R. Via Mario Bianco 9 20131 Milano, Italia

and potential dependence of the currents underlying the AHP is acquired there is still uncertainty to which extent the firing behaviour of motoneurones can be predicted from the properties of the AHP recordable in resting conditions. This uncertainty has favoured the suggestion that other factors could be of equal importance for firing regulation (Schwindt and Calvin 1972). On the basis of an analysis of the interspike voltage trajectories (i.e. the course of membrane potential between successive spikes) during repetitive firing these authors suggested that changes in the spatial distribution of the factors regulating rhythmic firing could be of importance. For example the extent of membrane area invaded by the SD spike and thereby the amount of AHP produced could vary in a more or less continuous manner with the degree of depolarizing current which would make the firing behaviour of the motoneurones completely unpredictable from the AHP following single SD spikes. There is however evidence that the above suggestions are disputable. Recently a neurone model where the firing was regulated only by postspike conductance changes has been presented and clear similarities between the firing produced by that model and that of motoneurones were shown (Kernell and Sjöholm 1972, 1973).

In the present paper we have by studying the time and potential dependence of the mechanism underlying the AHP in the cat's motoneurones deduced a simple descriptive mathematical expression for the ionic current during the AHP. In 2 succeeding papers (Baldissera and Gustafsson 1974 a, b) we will describe the repetitive firing behaviour predicted by this expression and it will be shown that the AHP properties in fact can account for much of the firing behaviour of motoneurones. Short preliminary reports of the present findings have been published (Baldissera and Gustafsson 1970, 1971).

Methods

The experimental results presented in this and two consecutive papers (Baldissera and Gustafsson 1974 a, b) have been obtained from 25 cats. The animals were dissected and anaemically decapitated or spinalized at a low level (Th 12–Th 13) under ether anaesthesia. Afterwards the animals were given chloralose (30 mg/kg) and successive small amounts (5–10 mg/kg) of pentobarbitone (Nembutal, Abbott, up to 30–40 mg/kg) immobilized with gallamine triethiodide (Flaxedil, May and Baker Ltd) and artificially respired. Bilateral pneumothorax was always performed to reduce respiratory movements. End tidal CO_2 was monitored on a Beckman medical gas analyser and kept within 4.5–5.5%. Arterial blood pressure was monitored continuously and was always above 80 mm Hg. When necessary it was kept above that level by injection of a mixture of low and high molecular weight Dextran or by slow intravenous infusion of noradrenaline. Rectal temperature was kept within 37–39°C.

The spinal cord was exposed by laminectomy of L4 to L7 vertebrae and L5 to S1 ventral roots were cut and mounted for stimulation. The spinal cord was covered with warm paraffin oil.

Intracellular recordings from motoneurones identified by antidromic activation of the ventral roots were obtained from the L6 to S1 segments using single barrelled glass microelectrodes. The microelectrodes were filled with 2 M K-citrate or 3 M KCl solution. They had broken tips with diameters of 15–25 μm and a resistance (measured in saline) of 0–50 M Ω . Only microelectrodes showing no or slight resistance changes when tested with 0–100 nA current pulses in saline were selected for the present experiments. The recorded potentials were fed via a cathode follower to a modified Tektronix 501 oscilloscope having two pairs of beams with independent time bases and the DC membrane potential was continuously monitored on a separate oscilloscope. The membrane conductance was measured

Afterhyperpolarization Conductance Time Course in Lumbar Motoneurons of the Cat

By

F BALDISSERA¹ and H GUSTAFSSON

Received 19 February 1974

Abstract

BALDISSERA F and GUSTAFSSON H. Afterhyperpolarization conductance time course in lumbar motoneurons of the cat. *Acta physiol scand.* 1974 91 512-527

The time and potential dependence of the conductance processes underlying the long-lasting afterhyperpolarization (AHP) in the cat's α motoneurons were studied. The conductance changes were determined by injection of short current pulses. The conductance time course was characterized by a long-lasting exponential decay interrupted by a plateau corresponding to the slower hyperpolarizing phase of the AHP. By displacing the membrane potential in the subthreshold region with the injection of long-lasting current pulses it was found that the conductance was largely unaffected by membrane potential displacements. Similar characteristics were found when calculating the AHP conductance time course from the AHP voltage. It was concluded that the AHP in motoneurons is given by a potassium conductance process with this complex S-shaped time course. A mathematical expression describing this time course is given.

In most central neurones the somadendritic (SD) spike is followed by a long lasting afterhyperpolarization (AHP). Thorough investigations in the cat's α motoneurons indicate the AHP to be caused by a membrane conductance increase to potassium ions. This conclusion is based on findings regarding the effect of membrane potential displacements and of iontophoreses on the AHP voltage (Coombs *et al.* 1973) and on the observation of an increased membrane conductance during the AHP as measured by the voltage drop caused by injected current pulses (Ito and Ohshima 1962).

The AHP has long been considered to be of particular importance as an intrinsic mechanism for repetitive firing regulation in spinal motoneurons (e.g. Eccles 1933, Eccles *et al.* 1938, Kernell 1963) and there have been attempts to correlate the firing behaviour with AHP parameters such as the AHP duration and the time to peak AHP (Kernell 1963). However, until a more detailed knowledge of the time

¹ Present address: Laboratorio di Biologia Spaziale del C.N.R., Via Mario Bianco 9, 20131 Milano, Italia.

and potential dependence of the currents underlying the AHP is acquired there is still uncertainty to which extent the firing behaviour of motoneurones can be predicted from the properties of the AHP recordable in resting conditions. This uncertainty has favoured the suggestion that other factors could be of equal importance for firing regulation (Schwindt and Calvin 1972). On the basis of an analysis of the interspike voltage trajectories (*i.e.* the course of membrane potential between successive spikes) during repetitive firing these authors suggested that changes in the spatial distribution of the factors regulating rhythmic firing could be of importance. For example the extent of membrane area invaded by the SD spike and thereby the amount of AHP produced, could vary in a more or less continuous manner with the degree of depolarizing current which would make the firing behaviour of the motoneurones completely unpredictable from the AHP following single SD spikes. There is however evidence that the above suggestions are disputable. Recently a neurone model where the firing was regulated only by postspike conductance changes has been presented and clear similarities between the firing produced by that model and that of motoneurones were shown (Kernell and Sjöholm 1972, 1973).

In the present paper we have by studying the time and potential dependence of the mechanism underlying the AHP in the cat's α motoneurones deduced a simple descriptive mathematical expression for the ionic current during the AHP. In 2 succeeding papers (Baldussera and Gustafsson 1974 a, b) we will describe the repetitive firing behaviour predicted by this expression and it will be shown that the AHP properties in fact can account for much of the firing behaviour of motoneurones. Short preliminary reports of the present findings have been published (Baldussera and Gustafsson 1970, 1971).

Methods

The experimental results presented in this and two consecutive papers (Baldussera and Gustafsson 1974 a, b) have been obtained from 25 cats. The animals were dissected and anaemically decapitated or spinalized at a low level (Th 12–Th 13) under ether anaesthesia. Afterwards the animals were given chloralose (30 mg/kg) and successive small amounts (5–10 mg/kg) of pentobarbitone (Nembutal Abbott) up to 30–40 mg/kg immobilized with gallamine triethiodide (Flaxedil May and Baker Ltd) and artificially respired. Bilateral pneumothorax was always performed to reduce respiratory movements. End tidal CO₂ was monitored on a Beckman medical gas analyser and kept within 4.5–5.5%. Arterial blood pressure was monitored continuously and was always above 80 mm Hg. When necessary it was kept above that level by injection of a mixture of low and high molecular weight Dextran or by slow intravenous infusion of noradrenaline. Rectal temperature was kept within 37–39°C.

The spinal cord was exposed by laminectomy of L4 to L7 vertebrae and L5 to S1 ventral roots were cut and mounted for stimulation. The spinal cord was covered with warm paraffin oil.

Intracellular recordings from α motoneurones identified by antidromic activation of the ventral roots were obtained from the L6 to S1 segments using single barrelled glass microelectrodes. The microelectrodes were filled with 2 M K-citrate or 3 M KCl solution. They had broken tips with diameters of 1.5–2.5 μ m and a resistance (measured in saline) of 20–50 M Ω . Only microelectrodes showing no or slight resistance changes when tested with 50–100 nA current pulses in saline were selected for the present experiments. The recorded potentials were fed to a cathode follower to a modified Tektronix 50 oscillograph having two pairs of beams with independent time bases and the DC membrane potential was continuously monitored on a separate oscillograph. The membrane conductance was measured

by injecting constant current pulses through the recording microelectrode. The device used allowed compensation of the voltage drop across the microelectrode resistance (Eide 1968).

Action potentials were evoked either by stimulation of ventral roots or in neurones displaying Renshaw inhibition by direct stimulation with brief (< 1 ms) current pulses. In the computation described in section 1 the voltage and duration values were supplied to equation 1 by analog digital converters on using a Hewlett Packard divider (9864A). This procedure allowed a resolution of 0.02–0.05 mV in the AHP voltage and a time resolution of 0.1–0.4 ms. Calculations were made by a Hewlett Packard calculator 9830A and the results directly plotted by a Hewlett Packard calculator plotter 9424.

Results

Section 1. Computation of the conductance changes underlying the AHP

The AHP in cat's motoneurones lasts 40–200 ms and reaches a peak value 10–20 ms after the onset of the spike (Brock *et al.* 1952; Eccles *et al.* 1958; Huxley 1959). Usually the rapid falling phase of the spike is not immediately followed by the AHP but it is succeeded by a phase of slow repolarization (Brock *et al.* 1952; Granit *et al.* 1963; Kernell 1964) lasting for some ms, the delayed depolarization.

DD. In some motoneurones a clear depolarizing potential can be seen in this phase giving a hump-type DD.

The AHP is assumed to be caused predominantly by a potassium conductance increase (Coombs *et al.* 1955; Eccles 1957). If one accepts this interpretation a time course of the conductance underlying the AHP can be computed from the AHP voltage under some simplifying assumptions by the simple expression

$$G_K(t) = \frac{G_L \times V - C \times (dV/dt)}{V_K - V} \quad (1)$$

where G_L = potassium conductance underlying the AHP

G_L = resting membrane conductance = $1/\text{membrane resistance}$ calculated from the voltage drop caused by injection of constant current pulses

τ = membrane time constant derived from plotting the voltage transient

produced by a current pulse as $\ln \left(\frac{1}{1 - \frac{dV}{dt}} \right)$ versus time (Rall 1960)

C = membrane capacitance = $\frac{\tau}{R}$

V_K = difference (with a positive value) between the resting potential level and the E_K and thus AHP equilibrium potential estimated by extrapolation of the AHP peak voltage/membrane potential relation (Coombs *et al.* 1955)

V = difference (with a positive value) between the resting potential level and the AHP voltage.

The $G_K(t)$ computed with equation 1 would represent an expression for the AHP conductance changes under the following assumptions: 1) only potassium ions are involved in AHP production; 2) the influence of the complex geometry of the motoneurones can be neglected; 3) the motoneurone is approximated by a sphere. E.

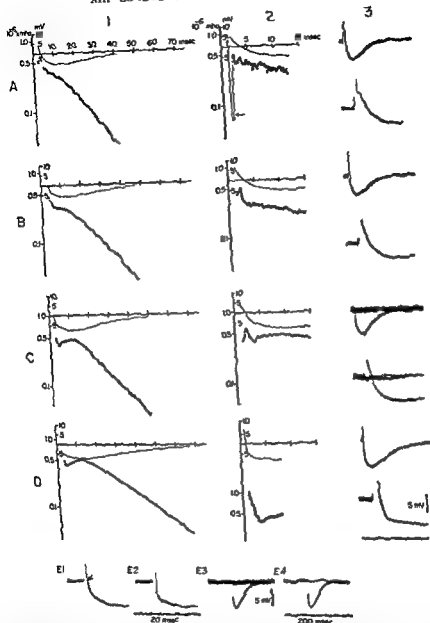


Fig 1 AHP conductance time course computed from the AHP voltage in four different lumbar motoneurons (A B C D). In A₃ to D₃ are shown the AHP records from the 4 neurones at 2 different time bases. From these records were taken the voltage values used for $G_K(t)$ computations. In the graphs A₁ to D₁ and A₂ to D₂ are plotted the computed conductance on the ordinate (logarithmic) against the interval on the abscissa with the two different time bases shown in A₁ to D₁. Above each conductance curve is drawn the time course of the respective AHP voltages on the same time scale. Antidromic spike size (mV), input resistance (M Ω), capacitance (nF) and AHP equilibrium potential (mV) of the 4 cells were A 100 1.3 4.5 18 B 83 1.4 3.3 20 C 87 1.4 2.1 20 D 85 1.1 1.2 21 respectively (see text for further details). E lumbar motoneurone spike size 11 mV. This neurone illustrates from a single cell the conversion from an AHP preceded by a slow DD (E₁) (see arrow) to an AHP lacking DD (E₂). Note the accentuation of the late hump in E₁ to E₃ concomitant with the disappearance of the DD. E₂ to E₄ same as in E₁ to E₂ but with a different time scale.

by injecting constant current pulses through the recording microelectrode. The delay and allowed compensation of the voltage drop across the microelectrode resistance (Eide 1962).

Action potentials were evoked either by stimulation of ventral roots or in neurons directly or Penfield substance by direct stimulation with brief (<1 ms) current pulses. In the experiments described in section 1 the number and duration values were applied to equal to 1 by analog digital conversion using a Hewlett-Packard converter 9254A. This procedure allowed a resolution of 0.02–0.05 mV in the AHP voltage and a time resolution of 0.1–0.5 ms. Calculations were made by a Hewlett-Packard calculator 9930A and the results directly processed by a Hewlett-Packard calculator plotter 9124.

Results

Section 1. Comparison of the conductance changes underlying the AHP

The AHP in cat motoneurons lasts 70–200 ms and reaches a peak value 10–20 mV after the onset of the spike (Brook et al. 1952; Eccles et al. 1958; Lund 1961). Usually the rapid falling phase of the spike is not immediately followed by the AHP but it is preceded by a phase of slow repolarization (Brook et al. 1952; Grant et al. 1963; Herd 1965). Later for some ms the delayed depolarization (DD). In some motoneurons a clear depolarizing potential can be seen in this phase giving a "hump-type DD".

The AHP is assumed to be caused predominantly by a postsynaptic conductance increase (Cummins et al. 1955; Eccles 1957). If one accepts this interpretation a time course of the conductance underlying the AHP can be computed from the AHP voltage under some simplifying assumptions by the simple expression

$$G_{\text{AHP}} = \frac{G_L \times (1 - C / \lambda) \times dV/dt}{V_L - V} \quad (1)$$

where G_L = resting membrane conductance underlying the AHP

G_L = resting membrane conductance = 1/membrane resistance, calculated from the voltage drop caused by injection of constant current pulses

τ = membrane time constant, derived from plotting the voltage transient produced by a current pulse as $\ln \left(\frac{1}{1 - \frac{dV}{dt}} \right)$ versus time (Rall 1959)

C = membrane capacitance = $\frac{\tau}{R}$

V_L = difference with a positive value between the resting potential level and the V_L and thus AHP equilibrium potential estimated by extrapolation of the AHP peak voltage-membrane potential relation (Cummins et al. 1955)

V = difference with a positive value between the resting potential level and the AHP voltage

The G_{AHP} computed with equation 1 would represent an expression for the AHP conductance changes under the following assumptions: 1) only postsynaptic are involved in AHP production; 2) the influence of the complex geometry of the motoneurons can be neglected; 3) the motoneuron is approximated by a sphere. Dr

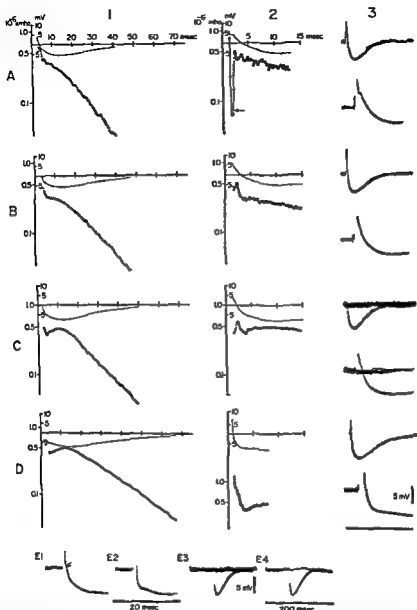


Fig. 1. AHP conductance time course computed from the AHP voltage in four different lumbar motoneurons (A, B, C, D). In A₁ to D₃ are shown the AHP records from the 4 neurons at 2 different time bases. From these records were taken the voltage values used for $G_K(t)$ computations. In the graphs A₁ to D₁ and A₂ to D₂ are plotted the computed conductance on the ordinate (logarithmic) against the interval on the abscissa with the two different time bases shown in A₃ to D₃. Above each conductance curve is drawn the time course of the respective AHP voltages on the same time scale. Antidromic spike size (mV), input resistance ($M\Omega$), capacitance (μF) and AHP equilibrium potential (mV) of the 4 cells were: A 100, 13, 4.5, 11; B 85, 14, 3.3, 20; C 87, 14, 2.1, 20; D 85, 11, 1.2, 21 respectively (see text for further details). E: lumbar motoneurone spike size 83 mV. This neurone illustrates from a single cell the conversion from an AHP preceded by a slow DD (E₁) (see arrow) to an AHP lack in DD (E₂). Note the accentuation of the late hump in E₁ to E₂ concomitant with the disappearance of the DD. E₃ to E₄ same as in E₁ to E₂ but with a different scale.

the further assumption that the potassium conductance is unaffected by the variations of the membrane potential during the AHP the $G_K(t)$ becomes a purely time dependent function as formally expressed in equation 1. The $G_K(t)$ computation has been performed for the AHPs of several motoneurons in good conditions i.e. with spike potential larger than 70 mV. The values of C , G_L , γ_K and of the AHP voltage determined for each cell were substituted in equation 1.

Typical results from these computations are illustrated in Fig. 1 in which 4 cells have been chosen as representative of the variability of the results. Besides the very early differences due to the presence and the size of the DD which will be discussed later it can be seen that in all the cells the $G_K(t)$ displays a similar S-shaped time course. The S-shape however is differently accentuated in individual neurones. In some cells like those of Fig. 1 A and B (see 1st column) the conductance decay is continuous over all the time course with a lower decaying phase during the growing phase of the AHP. In other neurones (Fig. 1 C and D 1st column) the decay is instead interrupted by a phase of conductance increase. In the curves from these last cells one can therefore distinguish a local conductance minimum which appears at about 4 ms after the spike onset and a local conductance maximum preceding the later decay. In all neurones the decay becomes approximately exponential after the peak of the AHP. The presence of the DD only modifies the very early time course of the computed $G_K(t)$ (Fig. 1 A, B, C). This modification consists in the appearance of an early dip (see arrow in A) proportional to the size of the DD and with the same latency from the spike onset and is absent in neurones apparently lacking DD (D). Such a lack of a DD was observed in 8 out of 70 neurones in good condition (cf. Kernell 1964). Since there are many indications that the process underlying the DD is probably not connected with a K^+ conductance change (Kernell 1964; Nelson and Burke 1967) we will consider as an artifact that portion of the $G_K(t)$ course which corresponds to the DD. Therefore we will accept, as a first approximation, that in all cells the $G_K(t)$ follows an early time course similar to that found in cells lacking a DD as that in Fig. 1 D.

With this approximation we conclude that the $G_K(t)$ time course as computed from the AHP potential displays a complex S-shaped decay with a plateau interposed between two phases of faster decay. The decay is continuous in some neurones in others interrupted by a phase of local conductance increase.

It is of interest that the local minimum in the $G_K(t)$ time course in the cell of Fig. 1 D is connected with a shallow hump in the AHP (D_2). In neurones with a $G_K(t)$ local maximum and a DD a similar hump is not clearly visible at resting conditions but it appears under the effect of depolarizing currents giving the impression of a DD (see Fig. 6 Baldissera and Gustafsson 1974a). As a matter of fact there are reasons to distinguish this hump from the DD: 1) it has a longer delay (4–5 ms versus 1.5–3 of the DD); 2) it is seen in cells displaying an evident DD; 3) it remains and gets more accentuated when the DD drops out. This last feature was observed in one neurone and is illustrated in Fig. 1 E. Note in E, the absence of the slow DD present in E_1 (see arrow). This “spontaneous” disappearance of the

DD is accompanied by a huge accentuation of a very shallow hump in E_1 to a clearcut hump in F 2. Observe that this change occurred without any change in the subsequent AHP size and time course (E_3-E_4). We therefore suggest that this hump is a true G_K dependent phenomenon which may have implications for the repetitive firing regulation as will be discussed in the following papers (Baldissera and Gustafsson 1974 a, b).

Section II AHP conductance measurements

A more direct approach for investigating the conductances underlying the AHP is to measure the membrane conductance change at different intervals during the AHP. This has been done by measuring the voltage drop produced by the injection of small (2–5 nA) current pulses through the cell membrane. In order to obtain a good time resolution the duration of the current pulses were kept as short as possible (2–4 ms). This procedure did not allow the potential drop to reach its final value thus giving an underestimation of the conductance change recorded during the AHP. Moreover the degree of this underestimation might vary as a function of the conductance during the course of the AHP because of the correlated changes in the membrane time constant. We have explored the degree of nonlinearity in the underestimation by utilizing the 3 time-constants model of the motoneuronal membrane proposed by Ito and Oshima (1965). In this model the voltage response of the membrane to a current step follows a time course given by the sum of 3 exponentials.

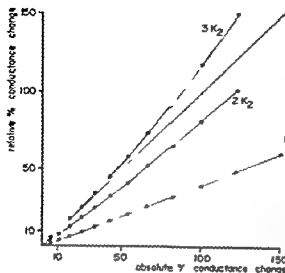


Fig. 2. Theoretical relation between the conductance change measured with current pulses of different duration and the absolute conductance change. By using the 3 time constant model of the motoneurone membrane of Ito and Oshima (1965) the conductance change derived with pulse durations of $1\times$, $2\times$ and $3\times$ the membrane time constant (k_2) was computed and plotted on the ordinate against the absolute conductance change.

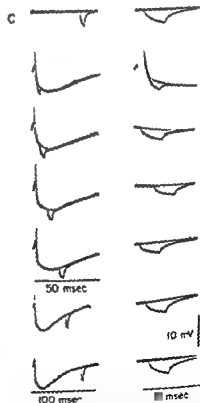
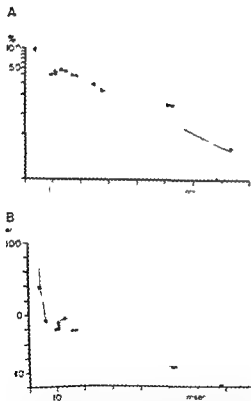


Fig. 3. Conductance time course measured with current pulses. Same neurone as in Fig. 1 D. A, conductance increase as percentage increase with respect to the conductance of the resting membrane (logarithmic ordinate), is plotted against the interval between the onset of the spike and the end of the current pulse on the abscissa (pulse duration 4 ms). B, same as in A but linear ordinate. The lines are fitted by eye. C, some of the records used for the plots in A and B with a faster time basis on the right row.

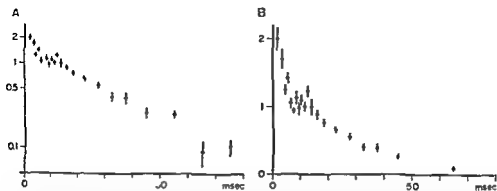


Fig. 4. Pooled conductance time course measured with current pulses. The conductance values from 12 neurones were collected and normalized, i.e. the conductance increase in the AHP peak region was put to one. The values from each cell were pooled and averaged (see text). A: the average normalized conductance change is plotted (\pm SE, logarithmic ordinate) against the interval between the spike onset and the end of the current pulse. B: same as in A, but linear ordinate.

conductance changes occurring during the entire AHP can be obtained with the use of short current pulses. However, as pointed out above, because of the presence of the third time constant, the absolute value of the membrane conductance is not easily measured with the pulse technique, whatever the pulse duration.

In Fig. 3 A and B is shown the conductance time course measured in a motoneurone with the method described above. On the ordinate (logarithmic in A, linear in B) is plotted the conductance change expressed in per cent of the resting value, and on the abscissa the interval between the onset of the spike and the end of the pulse. Observe that the time course of the conductance change displays a *local maximum* at 14 ms (corresponding to the peak of the AHP, see Fig. 3 C) followed by a decline which is roughly exponential. A *local minimum* is clearly visible at about 3 ms, interposed between the local maximum and the sharp conductance increase of the spike falling phase. The $G_K(t)$ computed from the AHP potential in this cell also displays a local minimum-maximum sequence, as illustrated in Fig. 1 D. In a preceding paper (Baldissera and Gustafsson 1971) we reported that the conductance plateau is sometimes hardly visible in those cells with a short time to peak AHP. This is true when considering single cells because of the low resolution of the measurements compared to the dimensions of the plateau (i.e. the deviation from the exponential decay). However, when pooling the conductance measurements from many neurones, a clear plateau emerges in the conductance time course. In Fig. 4 are plotted the results of such a pooling operated on 12 neurones with time to-max AHP ranging from 11–14 ms. The conductance measurements of each neurone were normalized with respect to the conductance at the peak AHP in the same neurone. After normalization, the measurements from the 12 cells falling within each ms were averaged and plotted with the standard error.

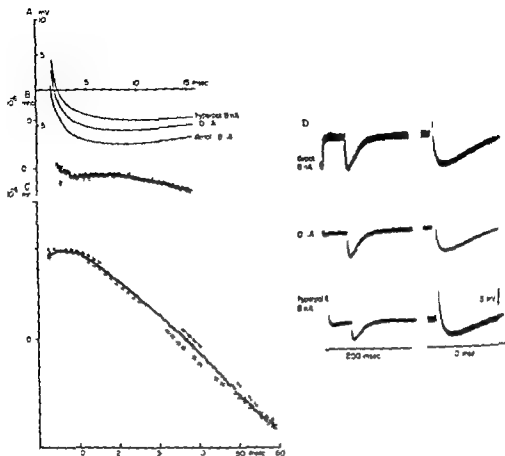


Fig. 3. Potential dependence of the conductance time course computed from the AHP voltage. Lumbar motoneurone spike size 80 mV, input resistance 0.78 M Ω , capacitance 2.3 nF, AHP equilibrium potential 23.4 mV. In D are shown the records of the AHP at different membrane potential levels from which the computations of B and C are made (faster time basis on the right row). In B and C the computed conductance time courses for 0 (filled squares), depol. 8 nA (crosses) and hyperpol. 8 nA (open squares) current are displayed on different time basis. In A the AHP voltages are drawn on the same time scale as in B.

This was made for the first part of the curve up to the time to-max, then the sample interval was raised to 20 and then to 5 ms.

The pooled curve is quite similar in its general shape to the computed curve in Fig. 1. It can be noted, however, that in the experimental conductance curves of Fig. 3 and 4 the local minimum falls at about 7–8 ms, i.e. somewhat later than seen in the time course computed from the AHP voltage. This may well be explained when considering the technique used. When the end of the current pulse where the measurements were taken was positioned at the time corresponding to the computed local minimum, most of the pulse duration fell within the high conductance period of the spike and its current shunted. It is therefore expected that the very early measurements after the falling phase are overestimating the conductance change, thus concealing the early part of the local minimum in the ex-

perimental curves. Moreover, in the pooled curve both neurones with a local minimum and a continuous decay were present, which would tend to conceal the local minimum.

During the phase preceding the local minimum the conductance measured with the pulse grows in all neurones irrespective of the presence or absence of the DD as the $G_K(t)$ computed in cells lacking a DD. Since the DD has an origin different from that of the AHP (see above) we suggest that the early phase of the $G_K(t)$ has a course like that found in all the experiments and by computation in cells without DD.

Section III Voltage dependence of the AHP conductance changes

In order to use the conductance time course derived from equation 1 for predicting the firing behaviour of motoneurones it does not suffice to demonstrate a high degree of correspondence between the computed and the experimentally determined time courses of the conductance change during the AHP. A second condition is in fact necessary, i.e. that the conductance change is time dependent but not potential dependent. During firing the absolute voltage, the shape and the amplitude of the AHP are very different than that following single spikes. Therefore if the AHP conductance was influenced by the potential level the time course determined in resting conditions would not be adequate for predicting the firing behaviour. It was assumed by Coombs *et al.* (1955) that the mechanism underlying the AHP was not appreciably affected by subthreshold membrane potential variations. This assumption was tested in the present investigation by computing the $G_K(t)$ from the AHP voltage at different membrane potential levels with the aid of equation 1 and by measuring the AHP conductance at a fixed latency from the spike after different membrane potential displacements.

In Fig. 5 is illustrated, from a motoneurone, the time course of the $G_K(t)$ computed from the AHP voltage at different potential levels. It can clearly be seen that despite the evident modification of the AHP voltage produced by the current injections the $G_K(t)$ curves are practically superimposable. Note however that the curve derived from the AHP in the hyperpolarized condition displays a somewhat longer lasting plateau than the other curves. Observe in A where the three AHPs are placed on a common baseline and in the inset records in D that the $G_K(t)$ modification is associated with a delay of the AHP peak (see also Coombs *et al.* 1955). A similar lengthening of the plateau was found in four additional neurones while in two neurones no $G_K(t)$ changes or any variation in the time to peak AHP were found over a similar range of potential displacements.

The potential dependence of the AHP conductance was also tested more directly by measuring with the pulse technique the membrane conductance at a fixed point during the descending phase of the AHP after different degrees of potential displacements. In Fig. 6 A (filled circles) and B it can be observed that the test pulse amplitude during the AHP is unaffected by the potential displacements given by current injection. Note however, that the change given by the AHP in the test

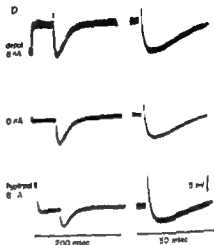
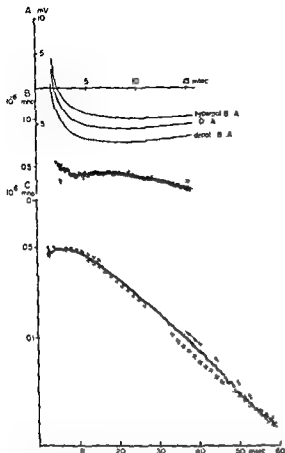


Fig. 5. Potential dependence of the conductance time course computed from the AHP voltage. Lumbar motoneurone spike size 80 mV, input resistance 678 M Ω , capacitance 93 nF. AHP equilibrium potential 23.4 mV. In D are shown the records of the AHP at different membrane potential levels from which the computations of B and C are made (faster time basis on the right row). In B and C the computed conductance time courses for 0 (filled squares), depol 8 nA (crosses) and hyperpol 8 nA (open squares) current are displayed on different time basis. In A the AHP voltages are drawn on the same time scale as in B.

This was made for the first part of the curve up to the time to-max then the sample interval was raised to 2.5 and then to 5 ms.

The pooled curve is quite similar in its general shape to the computed curve in Fig. 1. It can be noted, however, that in the experimental conductance curves of Fig. 3 and 4 the local minimum falls at about 7–8 ms, i.e. somewhat later than seen in the time course computed from the AHP voltage. This may well be explained when considering the technique used. When the end of the current pulse where the measurements were taken was positioned at the time corresponding to the computed local minimum, most of the pulse duration fell within the high conductance period of the spike and its current shunted. It is therefore expected that the very early measurements after the falling phase are overestimating the conductance change, thus concealing the early part of the local minimum in the ex-

course. We therefore sought a mathematical expression describing this complex time course and have selected the following expression

$$G_K(t) = A_1 \times \text{EXP} \left(\frac{B_1}{C_1} \right) + A_2 \times \text{EXP} \left(\frac{t}{B_2} \right) - A_2 \times t \times \text{EXP} \left(\frac{t}{C_1} \right) \times \text{EXP} \left(\frac{D_2}{E_2} \right) \quad (3)$$

(F 1) (F 2) (F 3)

which we have found to fit with good approximation to the $G_K(t)$ time course when supplied by suitable values of the parameters. Equation 3 is composed of 3 functions F 1, F 2 and F 3 which are separately represented in the graph of Fig. 7 together with the composite function F. The slow exponential F 2 has the same time constant and starting point as the line approximating (semilog plot) the long lasting decay of the $G_K(t)$ corresponding to the AHP falling phase. From this exponential is subtracted the third function F 3, thus modelling the features of the plateau. F 1 is summated for describing the fast decay of the G_K just after the spike. It has to be underlined that this expression is purely descriptive and not intended to give any suggestion about the physical processes underlying the AHP.

Discussion

The conclusion was reached that only the time course but not the absolute value of the membrane conductance could be obtained with the pulse technique. We will now discuss if the membrane conductance changes of the AHP are caused by a pure K^+ conductance.

No investigator has questioned the postulate that the repolarizing phase of the AHP is a purely K^+ driven process (Coombs *et al.* 1955; Eccles 1957). We will therefore avoid discussion on the reliability of the computation in that phase and point our attention to the phase preceding the peak of the AHP.

A chloride participation in the AHP mechanisms should be excluded because of the ineffectiveness of this ion to modify the AHP when iontophoretically injected into the cells (Coombs *et al.* 1955). But the presence of a sodium permeability which is strongly voltage dependent in the region of the AHP conductance plateau might cause a distortion of the pulse amplitude and lead to misinterpretations of the membrane conductance changes. The polarization caused by the pulse would in fact produce a change in the sodium conductance and the consequent change in the sodium current would then affect the amplitude of the voltage drop. If this hypothetical sodium conductance was increased by depolarization and decreased by hyperpolarization its presence would give rise to a conductance plateau as that found experimentally. Actually the possibility that a voltage dependent sodium conductance is active in the plateau region seems rather unlikely because of the in-

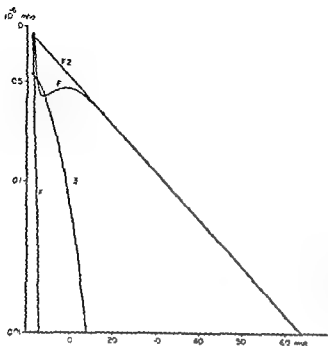


Fig. 7. Graphic representation of the mathematical expressions used to describe the AHP conductance time course. F_1 , F_2 and F_3 mark the curves of the respective expressions discussed in the text. F marks the curve representing $F_1 + F_2 - F_3$. Logarithmic ordinate.

dependence of the amplitude of a test pulse given in that region from the potential displacements (see section III of the results). In the computed curves, slight changes of $G_K(t)$ are visualized in the plateau region after potential displacements. The changes however are in the sense opposite to that expected by the existence of a strongly voltage dependent sodium permeability and are also completely lacking in some neurones.

The contribution of an increase in a sodium conductance system which is not voltage-dependent within this potential range would in itself be very small and therefore not give a conductance plateau. A contribution from other ionic conductances than the above mentioned seems unlikely on the basis of the present knowledge. In conclusion all these arguments seem to favour the view that the time course of the membrane conductance measured during the AHP expresses the changes in the permeability for potassium ions only.

The technique used in our experiments does not allow any definite conclusion about the mechanisms governing the complex conductance time course during the AHP in particular to decide if the longlasting conductance variation of the AHP and the fast G_K changes occurring during and just after the spike are different processes. However the existence in some cells of a $G_F(t)$ local minimum followed by a phase of local conductance increase seems to suggest a separation of the $G_K(t)$ variations into two kinetics: the first responsible for the falling phase of the spike and the second giving rise to the AHP. This suggestion is favoured by the recent finding in dorsal spinocerebellar tract neurones that the AHP (as in motoneurones

given by a K conductance process) can be decreased to half its control value when conditioned by a preceding AHP, without any effect on the falling phase of the spike (Gustafsson and Zangger 1974). The existence of two separate K conductance systems G_K and G_A was found in molluscan neurones (Connor and Stevens 1971) and associated with the spike and the afterhyperpolarization respectively. Although the properties of the G_A mechanism would not apply to the AHP of motoneurones the existence of such a slow G_K system at least points to the possibility that other ionic mechanisms than those described in the squid axon (Hodgkin and Huxley 1952) and in myelinated nerve fibres (Frankenhaeuser and Huxley 1964) can operate in the somadendritic membrane of central neurones. A separation of the AHP K conductance from that during the spike was also suggested for motoneurones by Eccles in 1957; it should be noted however that Eccles interpreted the presence of the delayed depolarization as a sign of this separation. More recently Kernell presented a simple neurone model of motoneurone firing in which the AHP K conductance was slowly decaying in an exponential manner from a maximal value attained during the spike (Kernell 1968). Later the same author (Kernell and Sjöholm 1972) developed a more sophisticated model where the AHP is caused by changes in a potassium (P_{K_1}) and in an unspecific partially sodium (P_p) permeability system both of which are voltage and time dependent in a way analogous to the potassium and unspecific permeabilities in the Frankenhaeuser and Huxley voltage clamp equations for the frog myelinated nerve fibre. The parameters of the equation system expressing the P_{K_1} kinetics have been chosen by Kernell to give a $G_K(t)$ time course substantially equal to that of the potassium conductance in the simple model previously mentioned. The second permeability system P_p is introduced to account for the early shape of the AHP in motoneurones.

Our results indicating a complex S shaped time course of the membrane conductance during the AHP fit better with the permeability time course intuitively proposed by Eccles than with the kinetics of Kernell's permeability systems. In Kernell's model the conductance time course during the AHP shows a rapid initial decay followed by a slower exponential decline without any interposed plateau. Despite the continuous exponential decay of the $G_K(t)$ Kernell's model is able to describe the initial shape of the motoneuronal AHP with a single mechanism giving rise to both a DD like depolarizing hump and to the gradual increase of the AHP to its peak. This result was obtained by utilizing the Frankenhaeuser's unspecific permeability system (P_p) previously mentioned. The available experimental results show that the mechanisms governing the voltage changes in the DD region are different from those acting to give the rounded shape and the long time to peak of the AHP. In real motoneurones the time to peak AHP seems unrelated to presence or absence of a DD (see Fig. 1). Moreover in some neurones a DD is followed by a shallow hump in the gradual hyperpolarizing portion of the AHP which is enhanced by injection of depolarizing currents during repetitive firing (Baldissera and Gustafsson 1974a, Fig. 6) or by drop out of the DD (see Fig. 1E). This hump which is clearly distinguishable from the DD corresponds to the $G_K(t)$ loc.

Firing Behaviour of a Neurone Model Based on the Afterhyperpolarization Conductance Time Course First Interval Firing

By

F BALDISSERA¹ and B GUSTAFSSON

Received 19 February 1974

Abstract

F BALDISSERA and B GUSTAFSSON *Firing behaviour of a neurone model based on the afterhyperpolarization conductance time course First interval firing* Acta physiol scand 1974 91 528-544

The firing behaviour of a neurone model in which the refractoriness is solely governed by a longlasting potassium conductance process with a time course similar to that underlying the afterhyperpolarization in a motoneurons (Baldissera and Gustafsson 1974a) is described. The frequency-current relation in the model is shown to display the 3 firing ranges found in real motoneurons (Kernell 1965b, Schwindt 1973). With increasing current injection the interspike voltage trajectories in the model are also undergoing the same peculiar modifications as described for real motoneurons (Schwindt and Calvin 1972, Schwindt 1973). A re-examination of the first interspike interval in real motoneurons revealed earlier not recognized firing behaviour predicted by the model. It is concluded that the model is well simulating the firing behaviour of the first interspike interval in a motoneurons.

The mechanisms regulating the repetitive firing in central nerve cells have been mainly studied by injecting constant current pulses through the cell membrane. The most extensive investigations have been performed on a motoneurons (Granit *et al* 1963, Kernell 1965a, b, c, Schwindt and Calvin 1972, Schwindt 1973).

A major line of thought has attributed the regulation of firing to the refractoriness following each action potential both in peripheral nerve terminals (Adrian and Zotterman 1926) and in central neurons (e.g. Pitts 1943, Eccles 1953, Kernell 1965c, 1968). The large and longlasting refractoriness of motoneurons is thought to be due to an increase of the membrane conductance to potassium ions (G_K) responsible for the huge afterhyperpolarization (AHP) recorded in these cells (Coombs *et al* 1952). Although the AHP has been demonstrated to be of importance for firing regulation in a motoneurons (Kernell 1965c, Baldissera and Gustafsson

¹ Present address: Laboratorio di Biologia Spaziale del C.N.R. Via Mario Bianco 11
20131 Milano, Italia

1971 b) certain features of the firing behaviour have led to suggest the participation of additional factors (Kernell 1965 b Granit *et al* 1966 Schwindt and Calvin 1972 Schwindt 1973) as discussed in the introduction in Baldissera and Gustafsson 1974 a. However these suggestions were forwarded before any comprehensive account of the time course of the processes underlying the AHP in motoneurones was presented. In the preceding paper we analysed the AHP properties in motoneurones and deduced a general expression which should fit the $G_K(t)$ time course both measured experimentally and computed from the AHP voltage. We will introduce here a model in which the repetitive firing is regulated by an AHP conductance time course described by that expression. This model accurately describes not only the changes in the duration of the first interspike interval but also the modifications of the AHP trajectories produced by increasing current steps. By postulating the summation of the AHP conductance changes after successive spikes the same model can as well account for the early adaptation of the firing as will be shown in a following report (Baldissera and Gustafsson 1974 b).

A short preliminary note of the present findings has been published (Baldissera and Gustafsson 1971 b).

Methods

The present material was collected from the same experiments fully described in a preceding paper (Baldissera and Gustafsson 1974 a). Intracellular recordings from cat hindlimb motoneurones were made with single glass micropipettes. The experimental repetitive firing reported in this and the consecutive paper (Baldissera and Gustafsson 1974 b) was performed on a total of 65 motoneurones with spike amplitudes exceeding 60 mV and displaying a stable membrane or spike potential throughout the period of measurements. In the majority of the neurones (55) the firing was evoked by long (2–5 s) constant current pulses injected through the recording microelectrode at a frequency of 7/min. For the remaining 10 neurones 6 successive pulses (500 ms) at a frequency of 0.2/s were given at each current strength. The current is expressed in nA (10^{-9} A) and the discharge frequency in impulses/second (imp/s).

Computed firing. The repetitive firing of the model was computed by a numerical solution of the differential equation 2 (see result section II) with a third order Runge-Kutta method on a Hewlett Packard calculator 9830A. The time increment was 0.1 ms.

Results

Section I The AHP conductance time course in relation to the repetitive firing

According to the hypothesis that the AHP conductance change is the major intrinsic factor in the regulation of the rhythmic activity of motoneurones the features of the curve representing the repetitive firing (frequency/current relation) should be strictly dependent on the shape of the conductance time course. Only a very approximate agreement with motoneuronal firing was found when postulating a simple exponential decay for the AHP conductance (Kernell 1968). Actually the conductance changes during the AHP of 1 motoneurones follows a more complex course with an exponential decay interrupted by a plateau corresponding to the slower hyperpolarizing phase of the AHP (Baldissera and Gustafsson 1971 b 1974 a). Accordingly it is of interest to investigate the correlation between moto-

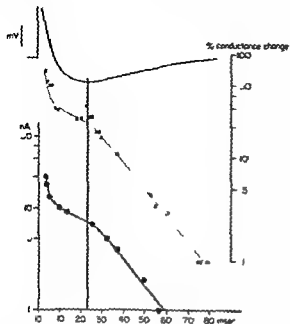


Fig. 1. Lumbar motoneurone spike amplitude 100 mV. Relation between the conductance change during the AHP and the repetitive firing evoked by steady current injection. The time course of the conductance change during the AHP after an antidromic spike is plotted (crosses) as percentage increase with respect to the conductance of the resting membrane (logarithmic ordinate on the right). The firing of the same cell is represented on the same abscissa, plotting the values of the first interspike interval (filled circles) against the log of the current exceeding the rheobase (left ordinate). In the insert is shown on the same time base the time course of the AHP of the same cell. The vertical line marks the peak of the AHP (see text). The curve fitted by eye for the interval-to-current relation is also used for the conductance time course relation with a scale factor of three.

neuronal firing and the complex time course of the AHP conductance as measured experimentally.

For a direct comparison of the AHP conductance changes with the firing characteristics of the same cell we found it convenient to represent the firing on an interval-to-current instead of that on a frequency-to-current (f/i) plot (Baldiessa and Gustafsson 1971a, b). In this way (see Fig. 1) the conductance variations recorded in a motoneurone and expressed in per cent of the resting value are plotted on the same time base as the duration of the first interval of repetitive firing produced in the same cell by different current intensities.

To simplify the description the graph has been subdivided in two parts by the vertical line passing through the peak of the AHP. In the right part the AHP conductance curve decays in an approximately exponential way and the interval-to-current relation runs parallel to it. In the left part of the graph the conductance curve shows a clear plateau situated between the high values close to the spike and the peak of the AHP. The firing curve in this phase shows a clear deviation from exponential resulting in a sudden acceleration of firing. In the earlier part of the graph both the conductance and the firing curve bend upwards and grow asymptotically. Because of the evident similarity in this motoneurone between the i/f relation and the AHP conductance time course whose complex shape is a general feature of α motoneurons we will try to compute the firing behaviour produced by such a complex conductance time course in a simplified neurone model.

Section II. A model for repetitive firing of motoneurons

The repetitive firing of α motoneurons can be simulated after some simplifying assumptions of the neurone properties by a set of equations. The assumptions are

- 1) a K conductance change is the unique mechanism underlying the AHP and giving rise to the refractoriness
- 2) the time course of the $G_K(t)$ changes can be described mathematically
- 3) the motoneurone is approximated by a sphere
- 4) the threshold voltage is constant
- 5) the K equilibrium potential and the leakage equilibrium potential and the leakage conductance (see below) are constant

A formal expression for the time course of the K conductance changes underlying the AHP has been developed (Baldissera and Gustafsson 1974a) with this general form

$$G_K(t) = A_1 \times \text{EXP}\left(-\frac{t^{B_1}}{C_1}\right) + A \times \text{EXP}\left(-\frac{t}{B}\right) - V_3 \times t^{B_3} \times \text{EXP}\left(-\frac{t}{C_3}\right) \times \text{EXP}\left(-\frac{t^{B_3}}{E_3}\right) \quad (1)$$

This equation can then be inserted under the above listed conditions in the differential equation

$$G_K(t) \times (V_K - V) - G_L \times V - C \times \frac{dV}{dt} - I = 0 \quad (2)$$

where C = cell membrane capacitance

G_L = leakage or resting membrane conductance

V_K = difference (positive value) between the threshold voltage and the AHP (K) equilibrium potential

V = difference (positive value) between the threshold voltage and the AHP voltage

I = injected current exceeding the rheobase

The model does not include any expression for the rapid falling phase of the spike. Since the rapid repolarization of the SD spike ends at a point whose voltage is largely unaffected by membrane potential displacements (Nelson and Burke 1967) that shortcoming can be compensated for by starting the computation for each value of the current injected at the same fixed voltage level below the threshold potential.

Equation 2 can then be solved numerically in V for step increase of I . The solutions are the AHP trajectories corresponding to different amounts of injected current. By measuring the time at which the AHP voltage intersects the threshold potential, i.e. the time at which a second spike would appear one can compute from the same equation the I/f_1 relation for the first interspike interval.

Section III Computed AHP trajectories

Recently it was claimed that the applicability of a model describing repetitive firing in motoneurons depends on its ability not only to account for the input/output relations in these cells but also to reproduce the features of the interspike poten-

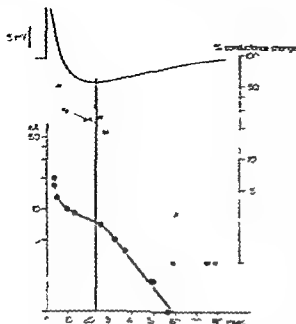


Fig. 1. Lumbar motoneuron spike amplitude 100 mV. Relation between the conductance change during the AHP and the repetitive firing evoked by steady current injection. The time course of the conductance change during the AHP after an antidromic spike is plotted (crosses) as percentage increase with respect to the conductance of the resting membrane (lower time ordinate on the right). The form of the same cell is represented on the same abscissa, plotting the values of the first interspike interval (filled circles) against the log c , the current extended to the fibre base left ordinate. In the insert is shown, on the same time base, the time course of the AHP of the same cell. The vertical line marks the peak of the AHP (see text). The curve fitted by eye to the interspike current relation is also used for the conductance time course relation with a scale factor of three.

neuron firing and the complex time course of the AHP conductance as measured experimentally.

For a direct comparison of the AHP conductance changes with the firing characteristics of the same cell, we found it convenient to represent the firing on an interval-to-current instead of that on a frequency-to-current ($f-i$) plot (Baldisera and Glatyszak 1971a, b). In this way (see Fig. 1) the conductance variations recorded in a motoneuron and expressed in per cent of the resting value are plotted on the same time base as the duration of the first interval of repetitive firing produced in the same cell by different current intensities.

To simplify the description the graph has been subdivided in two parts by the vertical line passing through the peak of the AHP. In the right part the AHP conductance curve decays in an approximate exponential way and the interval-to-current relation runs parallel to it. In the left part of the graph the conductance curve shows a clear plateau related between the high values close to the spike and the peak of the AHP. The firing curve in this phase shows a deviation from exponential resulting in a sudden acceleration of firing. In the earlier part of the graph both the conductance and the firing curve bend upwards and grow asymptotically. Because of the evident similarity in this motoneuron between the $f-i$ relation and the AHP conductance time course whose complex shape is a general feature of motoneurons we will try to compute the firing behaviour produced by such a complex conductance time course in a simplified neuron model.

Section II. A model for repetitive firing of motoneurons

The repetitive firing of a motoneuron can be simulated, after some simplifying assumptions of the neuron properties, by a set of equations. The assumptions are

- 1) a K conductance change is the unique mechanism underlying the AHP and giving rise to the refractoriness
- 2) the time course of the $G_K(t)$ changes can be described mathematically,
- 3) the motoneurone is approximated by a sphere
- 4) the threshold voltage is constant
- 5) the K equilibrium potential and the leakage equilibrium potential and the leakage conductance (see below) are constant

A formal expression for the time course of the K conductance changes underlying the AHP has been developed (Baldissera and Gustafsson 1974a) with this general form

$$G_K(t) = A_1 \times \exp\left(-\frac{t^{B_1}}{C_1}\right) + A \times \exp\left(-\frac{t}{B}\right) - A_3 \times t^{B_3} \times \exp\left(-\frac{t}{C_3}\right) \times \exp\left(-\frac{t^{D_3}}{E_3}\right) \quad (1)$$

This equation can then be inserted under the above listed conditions in the differential equation

$$G_K(t) \times (V_K - V) - G_L \times V - C \times \frac{dV}{dt} - I = 0 \quad (2)$$

where C = cell membrane capacitance

G_L = leakage or resting membrane conductance

V_K = difference (positive value) between the threshold voltage and the AHP (K) equilibrium potential

V = difference (positive value) between the threshold voltage and the AHP voltage

I = injected current exceeding the rheobase

The model does not include any expression for the rapid falling phase of the spike. Since the rapid repolarization of the SD spike ends at a point whose voltage is largely unaffected by membrane potential displacements (Nelson and Burke 1967) that shortcoming can be compensated for by starting the computation for each value of the current injected at the same fixed voltage level below the threshold potential.

Equation 2 can then be solved numerically in V for step increase of I . The solutions are the AHP trajectories corresponding to different amounts of injected current. By measuring the time at which the AHP voltage intersects the threshold potential, i.e. the time at which a second spike would appear, one can compute from the same equation the f/I relation for the first interspike interval.

Section III Computed AHP trajectories

Recently it was claimed that the applicability of a model describing repetitive firing in motoneurons depends on its ability not only to account for the input/output relations in these cells but also to reproduce the features of the interspike poten-

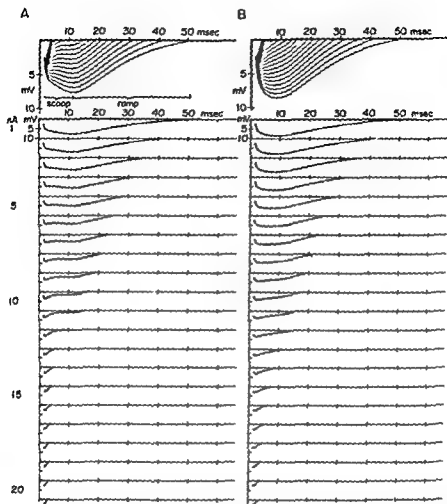
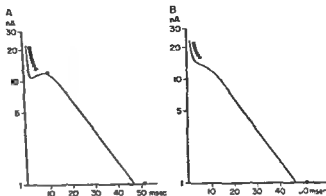


Fig 2 AHP trajectories during firing of the neurone model computed with the aid of equations 1 and 2. A Computation performed with a $G_g(t)$ time course showing a local minimum maximum sequence (see Fig 3 A). B Computation performed with a continuously decaying $G_k(t)$ (see Fig 3 B). For both model versions the AHP trajectories corresponding to 1 nA increments are displayed sequentially in the lower part and superimposed in the upper part of the graphs.

tial trajectories (Schwindt and Calvin 1972; Schwindt 1973). It seems therefore necessary to adopt temporarily the nomenclature proposed by those authors for a descriptive comparison of the model with the real motoneurone interspike trajectory. In this nomenclature the early descending and bottoming portion of the AHP trajectory is termed the scoop and the subsequent rise towards firing level, the ramp (see Fig 2 A).

In Fig 2, 3 and 4 are shown the results of two computations in which the parameters of equation 1 were chosen to account for the two general types of $G_k(t)$

Fig 3 Relation between current injected and the interspike interval in the neurone model. The value of the interspike interval (filled circles) is plotted against the current injected (logarithmic ordinate) for a $G_K(t)$ time course with local minimum maximum sequence (A) and with a continuous decay (B). The respective $G_K(t)$ time courses are shown as drawn curves. (The conductance values are multiplied by 30 ($= V_K$) and thus expressed in nA)



shape earlier described (Baldissera and Gustafsson 1974 a). In these two cases the $G_K(t)$ function has the same course except for the plateau region: here in fact the $G_K(t)$ either displays a local minimum local maximum sequence (Fig 3 A) or is continuously decaying (Fig 3 B).

The values for C, V_K, G_L fitted in equation 2 were 4 nF, 30 mV respectively. The parameters of equation 1 were $A_1 = 1.8, B_1 = 2.1, 2.2, C_1 = 20, 30, A = 0.95, 0.9, B = 1.4, 1.4, A_3 = 0.55, 0.35, B_3 = 0.08, 0.08, C_3 = 10, 10, D_3 = 2.4, 2.4, E_3 = 200, 200$ for Fig 2 A and 2 B respectively. The initial conditions for V and t were 2.5 mV and 1.5 ms in both cases.

The computed curves (Fig 2 A and B) display a behaviour which is quite similar to that of the experimental AHPs during repetitive firing (Schwindt and Calvin 1972, Schwindt 1973) except for the absence of the DD. With increasing current intensities the amplitude of the AHP at the time to peak or the scoop decreases proportionally to the strength of the injected current without much change in the course of the subsequent ramp both in A and B. As expected the differences between A and B are confined to the portion of the trajectory preceding the time to max AHP: here a clearcut hump develops in A which is matched in the trajectories of B at lower currents by a shallow upward concavity and at higher currents (> 8 nA) by a shallow upward convexity. In the model the appearance and the dimensions of the hump in A are strictly connected with the size of the local minimum concavity in the $G_K(t)$. Synthetically, the effect of the injected current on the AHP trajectory can be described as a translation of the S shape of the $G_K(t)$ into a N shape of the AHP voltage: the N first (upper) peak being the hump and the second (lower) peak the peak of the AHP. With increasing currents the AHP trajectory in the N region behaves differently in the two situations shown in A and B. When the $G_K(t)$ has a pronounced S shape the N shape of the trajectory is well marked. The reduction of the AHP amplitude with the increasing currents makes the first peak of the N to reach the threshold voltage almost simultaneously with the second peak (A: 11 nA) giving a rapid transition to a simple downward angular trajectory (A: 13 nA). When the $G_K(t)$ is

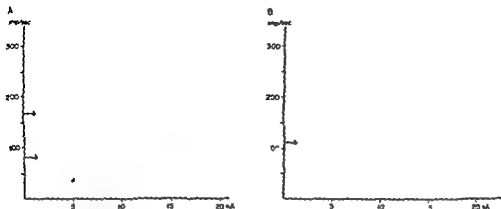


Fig. 4. Relation between the current injected and the spike frequency in the neurone model. The frequency ($1/\text{interval}$; filled circles) is plotted against the current injected for the two $G_K(t)$ configurations shown in Fig. 3 A and B. The 2 arrows in A mark the $1/\text{time to peak AHP}$ (measured at 1 nA current) and the peak of the hump respectively. The arrow in B marks the $1/\text{time to peak AHP}$ (measured at 1 nA current).

continuously decaying as in B the AHP decrease proceeds uninterrupted with the second peak of the N always at higher voltage level than the first peak. This makes the AHP trajectory disappear in a continuous manner under the effect of the current, without the discontinuity seen in the preceding situation. Note that the firing level at these high current intensities (B: 14–18 nA) is reached via an increase in the rate of rise of the trajectory in contrast to the more constant rate of rise of the ramp at lower currents (see Schwandt 1973). This trajectory behaviour is however only a continuation of the scoop rotation around the pivot point given by the end of the falling phase of the spike present also at the lower current intensities and clearly visible in the superimposed trajectories of both A and B. After the firing level has been reached by the peak of the hump (A) or by the peak of the shallow convexity (B), the trajectory assumes an angular form as earlier described for motoneurones (Schwandt 1973). Since the starting point for the computation is fixed the firing level will thereafter with increasing currents necessarily be reached mainly via an increased rate of rise of the trajectory.

Section IV. Computed i/f relation

The i/f relation for the first interval can also be constructed with the aid of equation 2. The time of firing of the second spike $i.e.$ the duration of the first interval, can in fact be measured at the intersection of the AHP trajectory with the threshold voltage.

When increasing the current intensity this firing point moves along the slow decay phase of the AHP towards its peak. Since the shape of the computed AHP in this phase is mainly generated by an exponential decay of the $G_K(t)$ the course of the i/f relation is necessarily similar to that of the $G_K(t)$ but shifted to the right due to model capacitance (see Fig. 3 A and B).

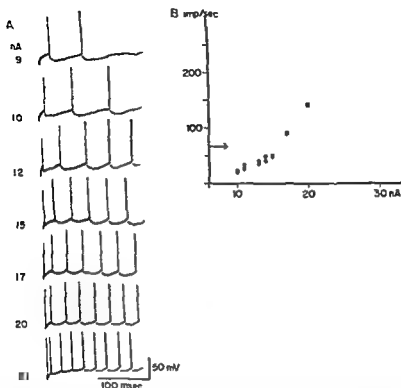


Fig. 5 Trajectory shape and frequency-current relation for the first interspike interval in a real motoneurone. Lumbar motoneurone spike size 100 mV. The frequency-current relation for the first interspike interval is shown in B. The arrow marks the $1/\text{time to peak AHP}$ measured at resting level. Inserted (A) is shown some of the records used in this plot. Note in A that the "scoop" inverts on (Schwindt and Calvin 1972) occurs between 11 and 12 nA, i.e. well within the first 1 near part in the f/I relation.

In the zone of the peak AHP the firing can follow one of two different modalities depending upon the behaviour of the λ -shaped portion of the AHP trajectory (see section III). When the $G_A(t)$ displays a well marked local minimum concavity (A) there is a well developed hump in the trajectory. With increasing current intensities this hump can reach the threshold only at slightly higher currents than the peak AHP or with a more marked minimum, before the peak AHP, i.e. when the firing point of a slightly smaller current is still on the decay phase of the AHP. This makes the firing point to pass quickly or to jump over the peak of the AHP. Correspondingly the f/I relation presents a rather flat course in the region interposed between the time-to-peak of the hump and time-to-peak AHP (compare Fig. 2 A and 3 A 11–13 nA).

On the other hand when the $G_A(t)$ is continuously decaying the upper peak of the flattened λ portion of the trajectory reaches the threshold long after the peak of the AHP and there is consequently no jump in the firing point. Under these

conditions the firing curve grows continuously but deviates from the exponential course followed before (Fig. 3B).

After the peak of the λ has reached the threshold further current increments have less and less effect in reducing the AHP duration: this is reflected in the f/i relation by the asymptotic growth of both curves of Fig. 3.

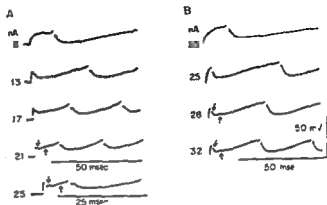
Section I. Correlation between the $G_A(t)$ time course and the f/i relation

Since most of the work on rhythmic firing has been so far analyzed in form of a f/i relation, it seems useful to discuss this type of representation in view of our model. The f/i relation in cats' motoneurons has originally been described as being composed of 2 linear relations: the primary and at higher currents the secondary range (Kernell 1965b). More recently Schwindt (1973) introduced a tertiary range, i.e. a third linear range at higher frequency levels than the secondary range. The primary range was shown by Kernell to extend maximally up to a frequency equal to $1/\text{time to peak AHP}$ (Kernell 1965c). On the other hand Schwindt put the lower limit of the tertiary range at the frequency where the AHP trajectory during firing changes to an angular shape (Schwindt 1973). In our model the two limiting frequencies which separate the three ranges should correspond to the interval durations produced when firing occurs at the 2 peaks of the λ trajectory in the AHP.

In Fig. 4 the firing of the model neurones illustrated in Fig. 2 and 3 is represented on frequency-to-current plots. On these plots the two arrows are marking the two significant frequencies separating the three portions of the curves. Note that in the first portion of the curve both the computed f/i relations deviate upward from the linearity before reaching the limiting frequency, i.e. $1/\text{time to peak AHP}$. The second portion describes the firing attained at the plateau shaped region of the $G_A(t)$ curve in λ , where the firing undergoes a jump "at the local maximum" (see the preceding section): this range is a vertical line joining the two limiting frequencies without any interposed values. In Π where there is no jump in firing the f/i curve has a certain slope whose inclination is dependent upon the slope of the $G_A(t)$ in the plateau region. The tertiary range (Schwindt 1973) corresponds in our model to the firing governed by the early fast decay of the $G_A(t)$ preceding the plateau. As far as the first interval is concerned this range is the beginning of the upward convex earlier described by Granit *et al.* (1963).

Thus both for the f/i relations and the interspike trajectories there is qualitative agreement between the model and a motoneuron. However certain qualitative features of the model behaviour both with trajectories and the f/i relations not earlier described for motoneurons. It should then be remembered that most of the experimental results on steady state firing, i.e. after adaptation, even if a gross similarity state firing and first interspike interval firing has been stated (Schwindt and Calvin 1972). It seemed then of interest to re-examine spike interval of motoneuronal firing both with regard to trajec-

Fig 3 Coexistence of delayed depolarization and a late hump **A**, Lumbar motoneurone spike size 87 mV. Note the presence of an early hump or DD (downward arrow) throughout all the records and the appearance of a later more shallow hump (upward arrow) with increasing current **B** Lumbar motoneurone spike size 73 mV. In this neuron the DD is less marked but clearly seen at 73 nA for the first interval and for all the later intervals. Note the clear late hump (upward arrow) emerging for the first interval with increasing current.



Section VI Model predictions of experimental results

a) Trajectories of first interspike interval In the descriptive analysis of motoneuronal firing (Schwindt and Calvin 1972) it was claimed that the conversion from the primary to secondary range firing was associated both for the first interval and the steady state firing with a change of the descending portion of the AHP or scoop from an upward concave to a flat or upward convex shape. As can be seen by comparing Fig 2 and Fig 4 this change in trajectory shape for the first interval is taking place well within the primary range in the model firing i.e. it is not associated with the entering into the secondary range. We therefore examined first interval trajectories in our experimental material and found a confirmation of the model behaviour in most of the neurones examined. This finding is exemplified from a typical motoneurone in Fig 5 where the first interspike f/I relation (B) and a sample of the interspike trajectories are shown (A). It is easily observed that the change in scoop shape from an upward concavity (9 nA) to an upward convexity (> 12 nA) is taking place well within the primary range for this neurone. Note also the gradual conversion of the trajectory shape to an angular form throughout the primary and secondary range f/I relation. That the trajectory behaviour is not directly connected to the different firing ranges is further illustrated by the very different trajectory form between the first interval at 12 nA and the second interval at 15 nA. These intervals which are of a similar length are both within primary range but display secondary range trajectory form (first interval) and primary range trajectory form (second interval).

Originally Kernell (1963b) described that the entrance into the secondary range was associated with a change in trajectory form characterized by a sudden reduction in the time to peak AHP indicative of a dropout of the delayed depolarization. Later Schwindt and Calvin (1972) noted instead that a hump type DD could develop in cells lacking hump type DD in primary range or at resting level.

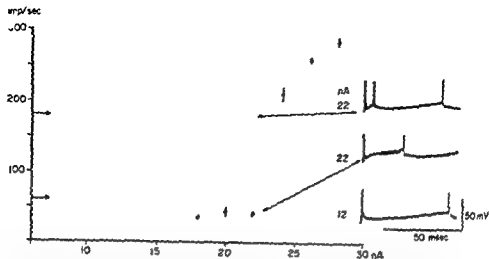


Fig. 7. AHP trajectory shape and f/i curve interruption in a real motoneurone. Single jump lumbar motoneurone spike size 83 mV. The reciprocal of the first interval is plotted on the ordinate against the current injected. The two arrows mark the frequencies corresponding to $1/\text{time to peak AHP}$ and $1/\text{time to peak of the hump}$ respectively. For each current strength (except 22 nA) is shown the average value (filled circles) \pm S.E. ($n = 4-6$). (At the lower frequencies the S.E. was within the area of the filled circles). Inserted in the graph are AHP trajectory records for 12 nA and 22 nA (before and after the jump). Observe the development of the late hump from 12 nA to 22 nA. For more details see text.

when entering secondary range while in neurones with DD at resting level the DD was remaining also in secondary range. They declared however that it was surprisingly difficult to identify the single-spike DD with the rhythmic firing DD in the same neurone. In the model firing a hump caused by the local minimum maximum concavity in the $G_K(t)$ time course clearly emerged with current injection. It should be noted that the peak of this hump is reached around 5 ms after the spike onset (i.e. much later than the delayed depolarization). A similar long latency can indeed also be found for the hump described by Schwandt and Calvin (1972). It seems therefore that this hump is connected to the $G_K(t)$ time course and thus independent (as discussed in Baldissera and Gustafsson 1974a) of the DD. The model would then predict that in cells with DD at resting level two humps should be present (i.e. one early hump given by the DD mechanism and a later one given by the $G_K(t)$ time course). Such a behaviour can indeed also be found in motoneurones and is illustrated in Fig. 6 from 2 motoneurones. Note in this figure the presence of only the early DD at threshold current (A 8 nA, B 23 nA) and the appearance of a later shallow hump with increasing currents (A 21 and 25 nA, B 28 and 32 nA).

b) f/i relation of first and spike interval. From the model behaviour it could be predicted that a local minimum maximum $G_K(t)$ course could be associated with a jump in firing giving a discontinuous f/i relation lacking secondary range, a feature previously not reported from motoneurones. Such a behaviour can,

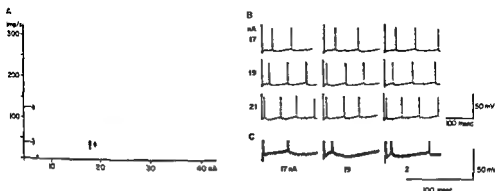


Fig 8 AHP trajectory shape and f/I curve interruption in a real motoneurone. Two stage jump Lumbar motoneurone spike size 85 mV A The reciprocal of the first interval is plotted on the ordinate against the current injected. The two arrows mark the frequencies corresponding to $1/\text{time to peak AHP}$ and $1/\text{time-to-peak of the late hump}$ respectively. The values for the lower part of the firing curve are average of 3–4 measurements. Note the deviation from linearity of the curve before reaching the lower arrow and the subsequent two stage jump between the two arrows (see text). B Records used in the plot in A. Note the stable interval value at 17 nA and at the two extreme records at 19 nA. The middle record at 19 nA shows the jump to the right part of the hump corresponding in A to the frequency value interposed between the two arrows. At 21 nA middle record the second spike is still coming at the right part of the hump while in the two extreme records the jump is completed and the remaining interspike trajectory assumes the angular or 'tertiary' range trajectory form. C Enlargement of some of the records in B. From left to right are shown the left record at 17 nA, middle record at 19 nA and the right record at 21 nA.

however be present in some motoneurones especially those with pronounced $G_h(t)$ concavity and is illustrated for the motoneurones in Fig 7 and 8. The two arrows in the graphs are marking the frequencies corresponding to the $1/\text{time to peak AHP}$ and $1/\text{time to peak of the late hump}$ respectively. Observe in Fig 7 that the firing curve is interrupted between the two arrows as in the model curve of Fig 4 because of the fluctuations of the interval duration between around $1/\text{time to-peak AHP}$ (lower arrow) and $1/\text{time to peak of the hump}$ (upper arrow). These fluctuations occurring at 22 nA correspond to the jumping of the firing point across the lower peak of the N in the AHP trajectory (as seen in the inserted records) in analogy with the model behaviour illustrated in Fig 2 A. Such a clearcut interruption in the f/I curve was not common. In other neurones as that illustrated in Fig 8 the jump in the f/I relation seems instead to proceed in 2 stages. In this cell the first interspike interval which is rather stable at 17 nA shows at 19 nA clearcut fluctuations between about 35 and 80 Hz i.e. between 30 and 12 ms. From the enlarged record of the AHP trajectory (C) it can be seen that this jump correspond to the passage of the firing point over the concavity but without overcoming the first peak of the N. At 21 nA the first interval still fluctuates between 80 and 120 Hz i.e. between 12 and 8 ms. From the corresponding record in C it appears that this fluctuation is due to the oscillation of the firing point along the rounded shape of the first peak of the N in the AHP trajectory. Out of 16 neurones in which a large

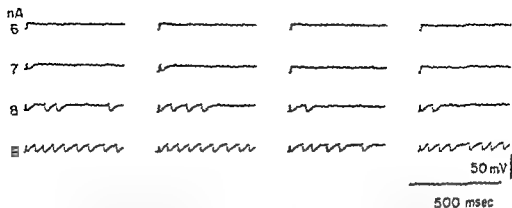


Fig. 9. Threshold current differences for the 1st, 2nd and 3rd spike with firing evoked by constant current pulses. Lumbar motoneurone spike 85 mV. In the figure are shown 4 successive sweeps at each current strength close to threshold (see text).

number of measurements of the first interspike interval was made. 2 displayed a clearcut firing interruption and 3 a double stage jumping. Of the remaining 11 neurones some, as that illustrated in Fig. 5, displayed a continuous firing curve in the secondary range associated with an uninterrupted decrease of the AHP (see section II). Other neurones, however, seemed to behave in an intermediate way with fluctuations giving partial gaps in the secondary range region.

Observe in Fig. 5B, 7 and 8A that the f/I curves for the real neurones, as previously shown for the model curves, clearly deviate from linearity before having reached the frequency corresponding to $1/\text{time to peak AHP}$. In none of the 16 neurones more closely examined did the linearity extend beyond that frequency, and in most of them the deviation definitely occurred below.

There are, however, also some direct qualitative differences between the model behaviour and that of real neurones. It has earlier been demonstrated that the threshold current for rhythmic firing is somewhat higher than that for the first spike (Kernell 1965a). Such a threshold difference is also found between the first and second spike and is illustrated from one typical neurone in Fig. 9. In this figure 4 successive sweeps with the same current step are shown in each row. The frequency in occurrence of the respective spike reveals here a threshold difference of less than 1 nA between the first and second spike and of around 1 nA between the first and third spike. In 8 neurones where the threshold difference between the first and second spike was examined, it was always less than 2 nA, usually around 1 nA. A difference of this magnitude should indeed be expected when considering the passive properties of the membrane. As earlier demonstrated in motoneurones, the voltage displacement given by a current pulse does not remain constant but decays in time due to a still unknown process (Ito and Osamura 1965; Nelson and Lux 1970). Such a decay is also clearly visible in Fig. 9, where the voltage is dropping

3 mV corresponding to 2.1 nA (input resistance 1.4 M Ω) before reaching a steady state. This would well account for the current threshold difference between the first spikes encountered in our material.

Discussion

Most of the work done on repetitive firing in nerve cells has been directed to the study of steady state firing, only little attention being paid to the first interspike interval whose analysis was omitted after having noted the gross similarity with steady state firing (Kernell 1965b; Schwindt and Calvin 1972). An analysis of the mechanism regulating the firing seems more complicated for steady state firing because of the intervention of other factors such as those underlying the adaptation. For a proper test of the hypothesis that the AHP conductance change is the main factor in firing regulation, it seems more natural to start the analysis on the first interspike interval. We were able to visualize the direct correspondence of the AHP conductance time course with the curve expressing the relation between the injected current and the duration of the first interspike interval (see section I). This evidence was the basis for starting the computations presented in this paper of a firing strictly dependent upon the K^+ conductance variations of the AHP.

The value of this model has to be judged by the extent to which it can fit to the constraints coming from facts already known and by the degree to which it can predict aspects of the behaviour not yet described. The major constraints for a model of repetitive firing in motoneurons come from the studies of the f/I relations and of the interspike voltage trajectories. The f/I relation obtained by the model displays the same characteristics as the experimental curves described in motoneurons: it displays three ranges of firing. The primary-secondary range transition occurs before the frequency corresponding to the time-to-peak AHP as described by Kernell (1965c) and the entrance into the tertiary range is associated with the change in trajectory shape to an angular form as pointed out by Schwindt (1973).

The characteristic modifications of the AHP trajectories occurring during repetitive firing have been described by Schwindt and Calvin (1972). This description concerned the steady state firing where the trajectory shapes are also influenced by the AHP summation. We therefore prefer to postpone the full discussion of the model trajectories to a following paper where the model is implemented with AHP summation (Baldissera and Gustafsson 1974b). However, when injecting current, the first interval model displays also features as scoop changes, secondary and tertiary range trajectories which according to Schwindt and Calvin (1972) and Schwindt (1973) characterize the firing and which, in their opinion, should not be envisaged by a model based on strictly postspike conductance changes.

The model was also useful in pointing out some hidden aspects of the motoneuronal firing. It was earlier stated that the trajectory modifications and their con-

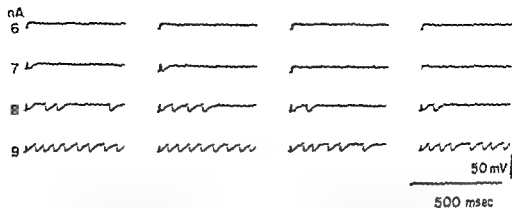


Fig. 9. Threshold current differences for the 1st, 2nd and 3rd spike with firing evoked by constant current pulses. Lumbar motoneurone spike 85 mV. In the figure are shown 4 successive sweeps at each current strength close to threshold (see text).

number of measurements of the first interspike interval was made. 2 displayed a clearcut firing interruption and 3 a double stage jumping. Of the remaining 11 neurones some, as that illustrated in Fig. 5, displayed a continuous firing curve in the secondary range associated with an uninterrupted decrease of the AHP (see section II). Other neurones however seemed to behave in an intermediate way with fluctuations giving partial gaps in the secondary range region.

Observe in Fig. 5B, 7 and 8A that the I/f curves for the real neurones as previously shown for the model curves clearly deviate from linearity before having reached the frequency corresponding to $1/\text{time to peak AHP}$. In none of the 16 neurones more closely examined did the linearity extend beyond that frequency and in most of them the deviation definitely occurred below.

There are however also some direct qualitative differences between the model behaviour and that of real neurones. It has earlier been demonstrated that the threshold current for rhythmic firing is somewhat higher than that for the first spike (Kernell 1965a). Such a threshold difference is also found between the first and second spike and is illustrated from one typical neurone in Fig. 9. In this figure 4 successive sweeps with the same current step are shown in each row. The frequency in occurrence of the respective spike reveals here a threshold difference of less than 1 nA between the first and second spike and of around 1 nA between the first and third spike. In 8 neurones where the threshold difference between the first and second spike was examined it was always less than 2 nA, usually around 1 nA. A difference of this magnitude should indeed be expected when considering the passive properties of the membrane. As earlier demonstrated in motoneurones the voltage displacement given by a current pulse does not remain constant but decays in time due to a still unknown process (Ito and Oshima 1965; Nelson and Lux 1970). Such a decay is also clearly visible in Fig. 9 where the voltage is dropping

(1964) The differences in the mechanisms underlying the refractoriness between Kernell's and our models have been earlier discussed (Baldissera and Gustafsson 1974a). These differences do not seem to substantially differentiate the behaviour of the two models as far as the f/I relation for the first interspike interval is concerned. However, even if a detailed comparison of the trajectories seems impossible because of the few examples illustrated by Kernell, it can be observed that the trajectories of that model do not undergo the same peculiar modifications described by Schwindt and Calvin (1972) for motoneurons and displayed by our model. For instance, in the Kernell model the hump produced by the P_p (the unspecific partially sodium system, Kernell and Sjöholm 1972) system is well developed at resting state and is reduced in size by the increasing current strength. On the contrary, in our model and in motoneurons the hump develops or even starts to appear with the depolarizing currents.

This work was supported by the Swedish Medical Research Council (Project No. 94) and the Medical Faculty, University of Göteborg.

References

- ADRIAN, E. D. and Y. ZOTTERMAN. The impulses produced by sensory nerve endings. Part 2. The response of a single end organ. *J. Physiol. (Lond.)* 1926 61: 151-171.
- BALDISSEIRA, F. and B. GUSTAFSSON. Supraspinal control of the α motoneurone discharge by constant current injection. *Brain Res.* 1971a 25: 642-644.
- BALDISSEIRA, F. and B. GUSTAFSSON. Regulation of repetitive firing in motoneurons by the afterhyperpolarization conductance. *Brain Res.* 1971b 30: 431-434.
- BALDISSEIRA, F. and B. GUSTAFSSON. Afterhyperpolarization conductance time course in lumbar motoneurons of the cat. *Acta physiol. scand.* 1974a 91: 512-527.
- BALDISSEIRA, F. and B. GUSTAFSSON. Firing behaviour of a neurone model based on the afterhyperpolarization conductance time course and algebraical summation. Adaptation and steady state firing. *Acta physiol. scand.* 1974b 92: 27-47.
- COOMBS, J. S., J. C. ECCLES and P. FARR. The electrical properties of the motoneurone membrane. *J. Physiol. (Lond.)* 1955 130: 291-325.
- ECCLES, J. C. *The Neurophysiological Basis of Mind. The Principles of Neurophysiology*. Clarendon Press, Oxford, 1953.
- FRANKENHAUSER, B. and A. F. HUXLEY. The action potential in the myelinated nerve fibre of *Xenopus laevis* as computed on the basis of voltage clamp data. *J. Physiol. (Lond.)* 1964 171: 302-315.
- GRANT, R. D., D. KERNELL and G. K. SHORTESS. Quantitative aspects of repetitive firing of mammalian motoneurons caused by injected currents. *J. Physiol. (Lond.)* 1963 158: 911-931.
- GRANT, R. D., D. KERNELL and Y. LAMARRE. Synaptic stimulation superimposed on motoneurons firing in the secondary range to injected current. *J. Physiol. (Lond.)* 1966 187: 401-415.
- Ito, M. and T. OSHIMA. Electrical behaviour of the motoneurone membrane during intracellularly applied current steps. *J. Physiol. (Lond.)* 1965 180: 607-635.
- KERNELL, D. The adaptation and the relation between discharge frequency and current strength of cat lumbosacral motoneurons stimulated by longlasting injected currents. *Acta physiol. scand.* 1965a 65: 65-73.
- KERNELL, D. High frequency repetitive firing of cat lumbosacral motoneurons stimulated by long lasting injected currents. *Acta physiol. scand.* 1965b 65: 74-86.
- KERNELL, D. The limits of firing frequency in cat lumbosacral motoneurons possessing different time course of afterhyperpolarization. *Acta physiol. scand.* 1965c 65: 87-100.
- KERNELL, D. Repetitive impulse discharge of a simple neurone model compared to that of spinal motoneurons. *Brain Res.* 1968 11: 685-687.
- KERNELL, D. and H. SJÖHOLM. Motoneurone models based on voltage clamp equations, peripheral nerve. *Acta physiol. scand.* 1972 86: 546-562.

- HAZELL II and H. SPONHOLM Repetitive impulse firing: Comparisons between neurone models based on "voltage clamp equations" and spinal motoneurons. *Acta physiol scand* 1973 87 40—56
- NELSON P. G. and R. E. BLAXX Delayed depolarization in cat spinal motoneurons. *Exp Neurol* 1967 17 16—26
- NELSON P. G. and H. D. LUX Some electrical measurements of motoneuron parameters. *Biophys J* 1970 10 33—33
- PITTS R. F. The basis for repetitive activity in phrenic motoneurons. *J Neurophysiol* 1943 6 439—454
- RICHTER, D. W. W. R. SCHULZ, A. H. MALKITZ and A. C. NACIMIZYTO Repetitive firing of spinal phasic motoneurons of the cat. *Pflügers Arch ges Physiol* 1972 332 Suppl 16f
- SCHWENDT P. C. Membrane potential trajectories underlying motoneuron rhythmic firing at high rates. *J Neurophysiol* 1973 36 434—449
- SCHWENDT P. C. and W. H. CALVIN Membrane potential trajectories between spikes underlying motoneuron firing rates. *J Neurophysiol* 1972 35 311—325
- WALLÖE L., J. A. S. JANSEN and A. NYGAARD A computer simulated model of a second order sensory neuron. *Kybernetik* 1969 6 130—140

Maximal Work Performance at Raised Air and Helium-Oxygen Pressures

By

LENNART FAGRAEUS

Received 27 February 1974

Abstract

FAGRAEUS L. Maximal work performance at raised air and helium oxygen pressures. Acta physiol scand 1974 91 545-556

To study the influence of increased air pressure and gas density on maximal work performance cardiorespiratory measurements were made on 8 subjects who performed maximal exercise until exhaustion on a cycle ergometer while breathing air at ambient pressures of 1.0 (control), 3.0 and 6.0 ATA and a mixture of 79% helium and 21% oxygen (He-O_2) at 3.0 ATA (same density as air at 1.0 ATA). Exposure to air at 3.0 and 6.0 ATA caused no consistent changes in maximal oxygen uptake ($\dot{V}_{O_2\text{max}}$), peak blood lactate (LA) or endurance time whereas pulmonary ventilation (\dot{V}_E) and carbon dioxide elimination (\dot{V}_{CO_2}) decreased significantly with a consequent rise of end tidal P_{CO_2} from 35 mm Hg at 1.0 ATA to 56 mm Hg at 6.0 ATA. Maximal heart rate (HR_{max}) decreased from a mean control value of 197 beats min^{-1} to 183 beats min^{-1} at 6.0 ATA. With exposure to He-O_2 at 3.0 ATA as compared to control $\dot{V}_{O_2\text{max}}$ and endurance time increased by 13 and 14% respectively whereas \dot{V}_E and HR_{max} decreased. \dot{V}_{CO_2} and LA remained unchanged and end tidal P_{CO_2} rose to 39 mm Hg. It is concluded that the beneficial effect that hyperoxia exerts on $\dot{V}_{O_2\text{max}}$ and endurance time at normal gas density is offset when the gas density is high enough to cause ventilatory impairment with concomitant CO_2 retention. The results also suggest that maximal work performance is most closely related to the LA concentration than to the P_{CO_2} or pH. Its resting with working muscle at the point of exhaustion.

Inhalation of hyperoxic gases during maximal exercise causes a significant increase of the maximal oxygen uptake ($\dot{V}_{O_2\text{max}}$) as observed under normal sea level condition (Hill, Long and Lupton 1924; Nielsen and Hansen 1937; Margaria *et al* 1961, 1972; Deroanne *et al* 1973), indicating that the maximal aerobic power may increase above normal when the arterial transport of oxygen is enhanced. $\dot{V}_{O_2\text{max}}$ has been found to increase also when hyperoxia is produced by increasing the ambient air pressure (Eagan and Plese 1969; Wyndham *et al* 1970; Fagraeus *et al* 1973b). However, Fagraeus *et al* (1973b) reported that beyond an ambient air pressure of about 1.4 ATA no further increase in $\dot{V}_{O_2\text{max}}$ takes place. On the contrary, in spite of substantial rises of the inspired O_2 pressure (P_{IO_2}), $\dot{V}_{O_2\text{max}}$ at 2.0 and 3.0 ATA showed a tendency to decrease as compared to the value at 1.4 ATA. The explanation for this inability to utilize the hyperoxia in hyperbaric air

TABLE 1 Anthropometric and functional data

Subject	Age yrs	Height cm	Weight kg	\dot{V}_{O_2} max l min ⁻¹ STPD
NP	24	175	73.0	3.66
LJ	30	189	77.0	3.87
GS	29	172	68.5	3.84
UF	26	185	75.0	4.15
KS	28	183	71.5	3.33
DL	30	172	61.0	3.12
BL	24	178	64.0	3.06
LF	33	189	81.0	3.28

not known but apparently some factor or factors related to the high pressure environment exert a retarding effect on maximal performance e.g. the increased gas density, the pressure *per se* and/or the high partial pressure of nitrogen.

The purpose of the present investigation was to study the cardiorespiratory and metabolic responses to maximal exercise within a wide range of ambient air pressures (1.0–6.0 ATA). Furthermore, in an attempt to disclose the effects of changes in the inspired gas density on the maximal performance at a given raised ambient pressure and P_{iO_2} data during air breathing at 3.0 ATA were compared with those obtained during inhalation of a mixture of oxygen and helium at the same ambient pressure.

Methods

Eight healthy male subjects performed submaximal and maximal exercise on an electrically braked cycle ergometer (Elema Schonander, Sweden). For anthropometric and functional data see Table 1. The subjects were all familiar with exhaustive exercise on a cycle ergometer and with exposure to increased ambient pressure. All experiments were performed in a dry compression chamber with the subjects breathing air at ambient pressures of (A) 1.0 ATA (control), (B) 3.0 ATA and (C) 6.0 ATA and (D) a mixture of 79% helium and 21% oxygen (He/O_2) at 3.0 ATA. The experiments at 1.0 ATA were subject to normal barometric pressure variations (mean bar 710 mm Hg, range 61–776 mm Hg) but all hyperbaric experiments were made at predetermined pressures (Table II). The various gas mixtures were humidified and supplied from Douglas bags as described elsewhere (Fagraeus *et al.* 1973b). At a flow rate of 2.0 l s⁻¹ ATP of air the pressure drop on the inspiratory side of the breathing circuit amounted to 1.2 cm H₂O at 1.0 ATA, 3.3 cm H₂O at 3.0 ATA, and 6.0 cm H₂O at 6.0 ATA. The corresponding pressure drop on the expiratory side were 2.7, 4.8 and 8.3 cm H₂O respectively. The temperature inside the chamber was kept between 21 and 23 °C during the experiments by means of an air-conditioning system.

Expired gas was collected in 300 l steel Douglas bags and the volumes were measured at atmospheric pressure by means of a balanced Tissot spirometer. The gas composition was analyzed in duplicate according to Schonander (1947). Maximal oxygen uptake was defined as the highest value obtained during the maximal work period in all cases occurring during the last two 30 s intervals. 17 double determinations of \dot{V}_{O_2} max were made at atmospheric pressure and the mean error of a single determination was found to be 2.7%. To determine end-tidal P_{CO_2} a small fraction of gas (approx. 10 l min⁻¹ ATP) was led from the mouthpiece through the chamber wall to a fast responding infrared CO_2 analyzer (Capnograph Godart). In this way end-tidal P_{CO_2} was measured continuously on a breath-by-breath basis, the values presented in Table III being time averages over the last 30 s of exhaustive exercise. Before each experiment the CO_2 analyzer was calibrated with known mixtures of CO_2 and air or CO_2 and He/O_2 . Since it is well established that during exercise end-tidal P_{CO_2} is higher than arterial P_{CO_2} (Asmussen and Nielsen 1956; Matejka 1963; Wasserman, van Heesvel and Burton 1966) the end-tidal P_{CO_2} values in the present study were reduced by 3 mm Hg when calculating the physiological dead space (V_D) according to the Enghoff modification (1938) of the Bohr equation.

TABLE II Physical characteristics of respired gases

Condition	Inspired gas mixture	Ambient pressure		Ambient temp C	Density of inspired gas mixture g l ⁻¹ BTPS	Viscosity of inspired gas mixture macropoises 3/ C	Partial pressures of inspired gases mm Hg			
		ATA	mm Hg				CO	O	N	He
A	Air	1.0	770	22.4	1.13	188	0.2	151	572	—
B	Air	3.0	2280	21.5	3.40	188	0.7	467	1765	—
C	Air	6.0	4560	21.6	6.82	188	1.4	946	3566	—
D	21.4 O ₂ in Helium	3.0	2280	21.3	1.20	203	—	479	—	1754

Values are means $n = 8$

To obtain respiratory rate (f) the cyclic pressure variations in the mouthpiece were recorded with a pressure transducer (Sanborn 270). By dividing the expired volume during the last 30 s of maximal exercise with the mean tidal volume (V_T) over the same period of time was calculated.

Post-exercise peak blood lactate concentrations were obtained from arterialized capillary samples from the finger tip 1 and 4 min after cessation of the maximal work test analyzed according to Barker and Summerson (1941) as modified by Sirom (1949). ECG was monitored continuously outside the compression chamber and heart rate was recorded with a beat-to-beat rate meter (Lindborg, Wertz and Odman 1969). Maximal heart rate (HR_{max}) was defined as the peak value at the point of exhaustion.

Rectal and chamber temperatures were measured by means of thermistor probes (Yellow Springs Instruments Inc No 401). End tidal P_{CO_2} , heart rate, pressure variations in the mouthpiece, chamber temperature and pressure and rectal temperature were recorded continuously and simultaneously on an 8-channel ink recorder (Brush Mark 700). The following variables were computed by means of standard equations: Maximal oxygen uptake ($\dot{V}_{O_{2max}}$), CO elimination (\dot{V}_{CO_2}), respiratory exchange ratio (R), end tidal CO tensions on physiological dead space ($P_{ET}CO_2$), tidal volume (V_T), ventilatory equivalents for oxygen (\dot{V}_E/\dot{V}_{O_2}) and carbon dioxide (\dot{V}_E/\dot{V}_{CO_2}) and oxygen pulse ($\dot{V}_{O_2}/\text{heart rate}$).

When used during the first minutes of acute exposure to raised ambient air pressure the Douglas bag method will yield \dot{V}_{O_2} values which are too low due to nitrogen uptake in the lungs. After 10 min exposure to air at 3 ATA the nitrogen uptake would amount to approximately 30 ml min⁻¹ STPD (cf. Hesser 1962) resulting in an underestimation of \dot{V}_{O_2} by about 8 ml min⁻¹ STPD. After the same time of exposure to air at 6.0 ATA nitrogen uptake would be about 60 ml min⁻¹ STPD leading to an underestimation of \dot{V}_{O_2} by about 15 ml min⁻¹ STPD. Breathing the present He/O₂ mixture at 3.0 ATA, on the other hand would after 10 min cause an elimination of nitrogen of about 15 ml min⁻¹ STPD and a simultaneous uptake of helium of approximately 1 ml min⁻¹ STPD. The net result in this situation could thus be an intact gas elimination of about 8 ml min⁻¹ STPD resulting in an overestimation of \dot{V}_{O_2} by about 2 ml min⁻¹ STPD. Hence the error in the \dot{V}_{O_2} determination due to intact gas exchange in the present hyperbaric experiment would be considered negligible.

Procedure

Before the hyperbaric experiments started each subject performed on separate days different maximal exercise tests in order to determine the supramaximal workload that would lead to exhaustion within 3–5 min under maximal cardiac conditions. The load was then used in all experiments throughout the maximal exercise.

All experiments were carried out according to the same general procedure except for the compression and decompression periods in the hyperbaric chamber. A typical hyperbaric experiment was performed in the following way: Upon arrival at the appropriate pressure level the subject was connected to the breathing apparatus and rested for 5 min in the sitting position on the cycle ergometer before he started standardized maximal warm-up exercise at 100 W (approx. 600 kpm min⁻¹) for 2 min immediately followed by a maximal exercise until exhaustion. Pedalling

TABLE III Measurements during last 30 s of exhaustive exercise in four different conditions (breathing air at 1.0, 3.0 and 6.0 ATA, and helium-oxygen at 3.0 ATA). Mean values and standard deviations

Variable	n = 8	Air			He O
		1.0 ATA	3.0 ATA	6.0 ATA	3.0 ATA
Pulmonary ventilation (\dot{V}_E)	M	152.5	100.2	82.0	130.6
l min ⁻¹ BTPS	SD	20.7	13.3	12.6	16.9
Tidal volume (\dot{V}_T)	M	2.96	2.93	2.55	3.19
l BTPS	SD	0.60	0.54	0.63	0.68
Respiratory rate (f)	M	52.6	34.9	33.1	49.3
breaths min ⁻¹	SD	8.3	6.1	6.2	9.0
Maximal O uptake ($\dot{V}_{O_{max}}$)	M	3.54	3.65	3.65	4.00
l min ⁻¹ STPD	SD	0.40	0.46	0.38	0.47
CO elimination (\dot{V}_{CO})	M	4.56	4.24	4.07	4.66
l min ⁻¹ STPD	SD	0.45	0.40	0.60	0.50
Respiratory exchange ratio (R)	M	1.29	1.17	1.12	1.17
	SD	0.07	0.08	0.13	0.05
End tidal P_{CO_2}	M	34.5	49.7	56.9	39.0
mm Hg	SD	2.7	4.8	4.2	4.9
Physiol. dead space (\dot{V}_D)	M	516	531	391	483
ml BTPS	SD	124	83	195	134
\dot{V}_D/\dot{V}_T ratio	M	0.17	0.18	0.16	0.15
	SD	0.03	0.01	0.09	0.04
Ventil. equivalent for O	M	43.9	27.7	22.6	32.8
(\dot{V}_E/\dot{V}_{O_2})	SD	4.4	4.0	3.3	3.3
Ventil. equivalent for CO	M	33.4	23.6	20.2	28.1
(\dot{V}_E/\dot{V}_{CO_2})	SD	2.9	2.0	1.9	2.3
Heart rate (HR)	M	191.8	184.6	182.9	187.7
beats min ⁻¹	SD	4.5	5.9	5.8	4.4
Oxygen pulse	M	18.5	19.8	20.0	21.3
ml O ₂ per heart beat	SD	2.3	2.9	2.4	3.0
Blood lactate	M	16.6	17.0	15.0	15.5
mmoles l ⁻¹	SD	2.9	4.0	2.6	1.6
Endurance time	M	3.39	3.61	3.29	3.86
min	SD	0.32	0.53	0.61	0.61

rate 60 rpm as indicated by a metronome. The work loads during the submaximal and maximal exercise tests corresponded to about 40 (range 37–45) and 140 (range 126–165) respectively of the subject's maximal aerobic power at 1.0 ATA breathing air. About 2 min after the start of maximal exercise expired gas was collected repeatedly in Douglas bags at approximately 30 s intervals until exhaustion. Decompression to normal atmospheric pressure was accomplished on air according to standard naval decompression tables. No symptoms of decompression sickness were observed. The hyperbaric experiments were rotated among the subjects each subject performing only one experiment a day.

Analysis of data. In an attempt to disclose separate and/or combined effects of changes in gas density, partial pressure of inspired gases and pressure p the data obtained in the four different experimental conditions have been compared on an intra-individual basis in the following ways.

Comparisons I, II and III. The combined effects of increased inspired P_{O_2} , P_{A_2} , gas density and pressure per se were disclosed by comparing the data obtained during air breathing at (I) 3.0 and 1.0 ATA, (II) 6.0 and 1.0 ATA, and (III) 6.0 and 3.0 ATA.

TABLE IV Differences between the four conditions of Table III Mean \pm standard error of the mean $n = 8$

Variable	Comparison I 3.0 ATA air -1.0 ATA air	Comparison II 6.0 ATA air -1.0 ATA air	Comparison III 6.0 ATA air -3.0 ATA air	Comparison IV 3.0 ATA He O -1.0 ATA air	Comparison V 3.0 ATA He O -3.0 ATA air
\dot{V}_E l min	-57.3***	-70.5***	-18.2***	-21.9**	30.4***
BTPS	± 4.1	± 3.8	± 1.7	± 4.0	± 3.4
\dot{V}_T l BTPS	-0.03	-0.41**	-0.38**	0.23	0.26*
	± 0.14	± 0.08	± 0.10	± 0.10	± 0.11
f breaths min ⁻¹	-17.7***	-19.5***	-1.8	-10.3*	7.4*
	± 3.3	± 2.1	± 1.6	± 2.4	± 2.4
$\dot{V}_{O_2\max}$ l min ⁻¹ STPD	0.11	0.11	0.00	0.46* *	0.35***
	± 0.05	± 0.07	± 0.05	± 0.06	± 0.04
\dot{V}_{CO} l min ⁻¹ STPD	-0.32**	-0.49*	-0.17	0.10	0.42*
	± 0.05	± 0.08	± 0.09	± 0.08	± 0.09
R	-0.12***	-0.17***	-0.05	-0.12***	0.00
	± 0.01	± 0.03	± 0.03	± 0.02	± 0.03
End tidal P_{CO_2} mm Hg	15.2**	21.7**	6.5**	4.5**	-10.7**
	± 1.3	± 1.8	± 1.7	± 0.8	± 1.7
\dot{V}_D ml BTPS	15	-125	-140	-33	-48
	± 50	± 70	± 66	± 50	± 60
\dot{V}_D/\dot{V}_T ratio	0.01	-0.01	-0.02	-0.02	-0.03
	± 0.02	± 0.04	± 0.03	± 0.01	± 0.02
\dot{V}_E/\dot{V}_O	-15.5*	-20.6**	-5.1***	-10.4**	5.1*
	± 0.7	± 0.7	± 0.7	± 0.9	± 0.8
\dot{V}_E/\dot{V}_{CO}	-9.8***	-13.2**	-3.4*	-5.3**	4.5* *
	± 0.6	± 0.6	± 0.6	± 0.5	± 0.5
HR beats min ⁻¹	-7.9**	-8.9***	-1.7	-4.1	3.1
	± 1.7	± 1.3	± 1.4	± 1.7	± 1.1
Oxygen pulse ml O ₂ per heart beat	1.3*	1.5*	0.2	2.8**	1.5**
	± 0.3	± 0.3	± 0.3	± 0.4	± 0.2
Blood lactate mmoles l ⁻¹	0.4	-1.1	-2.0	-1.1	-1.5
	± 1.3	± 0.9	± 1.7	± 1.4	± 2.0
Endurance time min	0.27	-0.17	-0.39	0.4	0.25
	± 0.15	± 0.22	± 0.16	± 0.17	± 0.06

p < 0.05

p < 0.01

* p < 0.001

Comparison I: The effects of increment in inspired P_{O_2} and ambient pressure with no change in gas density were estimated by comparing data from 3.0 ATA He O₂ with those from 1.0 ATA air.

Comparison II: The effects of increasing the gas density and inspired P_T at constant level of hypoxia and ambient pressure were disclosed by comparing data obtained on He O₂ and on air at 3.0 ATA.

Conventional statistical analysis was applied and the significance of intra-individual mean differences was tested with the Student *t* test.

Results

The information obtained from measurements on eight subjects during exhaustive exercise in four different conditions is presented in Table III with mean values and

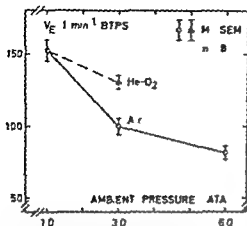


Fig. 1 Pulmonary ventilation during last 30 s of maximal work at different ambient pressures breathing air (open circles) and 21% O₂ in helium (solid triangle).

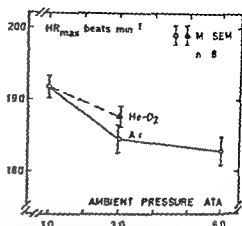


Fig. 2 Heart rate at the point of exhaustion in maximal work under same conditions as in Fig. 1. Symbols as in Fig. 1.

standard deviations. The intraindividual mean differences between the various conditions (Comparisons I—I) are shown in Table IV together with results of the statistical analyses. Values given in the tables and below refer to the last 30 s of exhaustive exercise in the control condition (air breathing at 1.0 ATA) and in the experimental conditions at 3.0 and 6.0 ATA.

Maximal oxygen uptake averaged 3.54 l min^{-1} STPD in the control condition and remained essentially unchanged when the pressure was raised to 3.0 and 6.0 ATA respectively. With He-O₂ breathing at 3.0 ATA $V_{O_{2max}}$ increased significantly by 13% to 4.01 l min^{-1} STPD.

Carbon dioxide elimination decreased from a control value of 4.56 l min^{-1} STPD to 4.24 and 4.07 l min^{-1} STPD ($p < 0.001$) with a rise in ambient pressure to 3.0 and 6.0 ATA respectively, but showed no consistent change with exposure to He-O₂ at 3.0 ATA.

Respiratory exchange ratio decreased significantly from 1.29 in the control condition to 1.17 at 3.0 ATA and 1.12 at 6.0 ATA. At 3.0 ATA exposure to He-O₂ and to air yielded similar R values.

Pulmonary ventilation (Fig. 1) averaged 153 l min^{-1} BTPS in the control condition and decreased by 34% to 100 l min^{-1} at 3.0 ATA and by 46% to 82 l min^{-1} at 6.0 ATA. With He-O₂ at 3.0 ATA V_E averaged 131 l min^{-1} BTPS and thus was 14% lower than in the control condition, but 31% larger than with air breathing at 3.0 ATA.

Ventilatory equivalents for oxygen and carbon dioxide decreased significantly as the pressure was raised to 3.0 and 6.0 ATA (Table III and IV). With He-O₂ breathing at 3.0 ATA both V_E/V_{O_2} and V_E/V_{CO_2} were significantly smaller than in the control condition but significantly larger than with air breathing at 3.0 ATA.

End tidal P_{CO_2} increased with the ambient pressure from a control value of 34.5 mm Hg to 56 mm Hg at 6.0 ATA. When He O_2 was substituted for air at 3.0 ATA end tidal P_{CO_2} was significantly decreased from 49.7 to 39.0 mm Hg.

Heart rate (Fig. 2) at the point of exhaustion decreased with increasing ambient pressure from a control value of 192 beats min^{-1} to 183 beats min^{-1} at 6.0 ATA ($p < 0.001$). With He O_2 at 3.0 ATA HR_{max} decreased to 188 beats min^{-1} ($p < 0.05$) this value being significantly higher, however, than that obtained with air breathing at the same pressure.

Blood lactate concentration after maximal exercise averaged 16.6 mmol l^{-1} at 1.0 ATA and showed no consistent differences between the various conditions.

Endurance time i.e. the time from start of maximal exercise to exhaustion averaged 3.4 min in the control condition and showed no consistent changes as the ambient pressure was raised to 3.0 and 6.0 ATA. However, when He O_2 was substituted for air at 3.0 ATA the endurance time increased significantly to 3.9 min.

Rectal temperature averaged 37.5 °C (range 37.2–37.9) in the experiments at 1.0 ATA air and showed no significant differences in the hyperbaric conditions.

The subjective experience of performing maximal work varied somewhat between the various conditions. Whereas muscular fatigue of the legs was reported to be the main reason to stop the work task when breathing air at 1.0 and 3.0 ATA, respiratory discomfort clearly contributed in the majority of subjects at 6.0 ATA. Three subjects also experienced a short lasting period of dizziness at 6.0 ATA. At 3.0 ATA He O_2 muscular fatigue was reported to be the dominant sensation but all subjects found it easier to perform the maximal work test in this condition than at 1.0 ATA air.

Discussion

In a previous study (Fagraeus *et al.* 1973b) it was shown that $\dot{V}_{O_2\text{max}}$ during air breathing increased with the ambient pressure up to 1.4 ATA but then showed a tendency to decrease as the pressure was further raised to 2.0 and 3.0 ATA. It was concluded that beyond an air pressure of 1.4 ATA the beneficial effect on $\dot{V}_{O_2\text{max}}$ of a raised P_{IO_2} (hyperoxia) was counteracted by other factors operating in the hyperbaric environment. The present experiments were designed to study the effect on $\dot{V}_{O_2\text{max}}$ of ambient air pressures up to 6.0 ATA and to evaluate the separate effects of increased P_{O_2} and P_{N_2} , gas density and pressure *per se* on $\dot{V}_{O_2\text{max}}$. This was done by studying the effects of different combinations of these factors on various cardiorespiratory functions.

Pulmonary ventilation and CO_2 elimination The present experiments confirm earlier observations (Fagraeus *et al.* 1973b) that the maximal exercise ventilation at the point of exhaustion declines considerably as the ambient air pressure is increased to 3.0 ATA. An additional decrease in \dot{V}_E occurred as the pressure was raised from 3.0 to 6.0 ATA (Table IV, Comparison III) the total reduction in \dot{V}_E amounting to no less than 46% when compared to its value at normal atmospheric pressure (Comparison II, Fig. 1). That part of this ventilatory depression was due to the

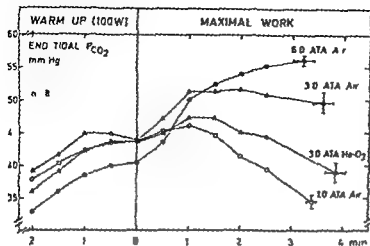


Fig. 3. Time courses of end tidal CO_2 tension during submaximal (warm up) and maximal work until exhaustion under same conditions as in Fig. 1. Mean values at 30 s intervals. Vertical and horizontal bars at the end points indicate \pm one standard error of mean.

increased P_{IO_2} is probable from the results of *Comparison II* which show that when the ambient pressure was increased to 3.0 ATA without increasing the density of the gas, the threefold increase in P_{IO_2} resulted in a 14 % reduction of the ventilation. Such O_2 dependent depression of the ventilation presumably occurred also in the 6.0 ATA air condition where P_{IO_2} was further elevated. This depression is analogous to that observed when oxygen enriched gas mixtures are administered during exhaustive exercise at normal atmospheric pressure (cf. Asmussen and Nielsen 1946, 1958, Bannister and Cunningham 1954, Derouanne *et al.* 1973), and can be ascribed mainly to withdrawal of a hypoxic ventilatory drive originating in the arterial chemoreceptors.

The extent to which factors other than increased P_{IO_2} contributed to the ventilatory depression at 3.0 and 6.0 ATA air may be judged from the results of *Comparison I* which show that at 3.0 ATA more than half of the 34 % reduction in V_E was due to the increased P_{N_2} or gas density. In the 6.0 ATA condition this non O_2 dependent ventilatory depression was presumably responsible for the dominant portion of the 46 % reduction in V_E , since the share contributed by hyperoxia is probably maximal already at 3.0 ATA air corresponding to an inspired O_2 concentration of 60 % at normal atmospheric pressure (cf. Bannister and Cunningham 1954). The non O_2 dependent depression of ventilation at 3.0 and 6.0 ATA air can be ascribed mainly to increased airway resistance caused by the increased gas density, a respiratory depressant (narcotic) effect of the increased N_2 pressure itself being unlikely in view of previous findings that high N_2 pressures exert no significant influence on neural structures involved in the control of respiration (cf. Fagraeus, Hecker and Linnarsson 1974).

As a result of the reduced ventilatory responses to exercise at 3.0 and 6.0 ATA air, mean end tidal P_{CO_2} at the point of exhaustion rose from 34.5 to 49.7 and 56.2 mm Hg respectively (Table III). Thus the relative hyperventilation with regard to metabolically produced CO_2 that is typical for exhaustive exercise under normal

conditions (Asmussen 1965) was no longer present in the 3.0 and 6.0 ATA air conditions which were instead marked by considerable degree of hypoventilation with concomitant CO_2 retention (Fig. 3) induced by the combined effects of hyperoxia and increased gas density. By contrast exposure to 3.0 ATA He-O_2 did not result in hypercapnia, although end tidal P_{CO_2} was somewhat higher than at 1.0 ATA air (Fig. 3) due to hyperoxia induced ventilatory depression. As an expression of the relative hypoventilation in the hyperbaric air conditions the ventilatory equivalents for O_2 and CO_2 decreased progressively as the ambient air pressure was raised (Table III).

Factors influencing $\dot{V}_{\text{O}_2\text{max}}$ The present results support the conclusion of Fagraeus *et al.* (1973b) that the clear cut gain in $\dot{V}_{\text{O}_2\text{max}}$ that these authors observed during air breathing at 1.4 ATA and which was ascribed to the slight hyperoxia present at this pressure is counteracted as the ambient pressure is increased to 3.0 ATA. Thus, no significant gain in $\dot{V}_{\text{O}_2\text{max}}$ was observed at 3.0 or 6.0 ATA as compared to 1.0 ATA (Table IV) in spite of the associated increases of P_{IO_2} to 467 and 946 mm Hg respectively. It is of interest to note however that exposure to 3.0 ATA He-O_2 resulted in an average increase in $\dot{V}_{\text{O}_2\text{max}}$ of no less than 0.46 l min^{-1} which indicates that hyperoxia exerts a beneficial influence on $\dot{V}_{\text{O}_2\text{max}}$ as long as the inspired gas density is not increased. This is analogous to the well known effect of hyperoxia on $\dot{V}_{\text{O}_2\text{max}}$ produced by oxygen enriched gases at sea level pressure (Hill *et al.* 1924, Nielsen and Hansen 1937, Margaria *et al.* 1961, 1972, Deroanne *et al.* 1973) and supports the concept that the working muscles are potentially capable of increasing their metabolism if excess O_2 is offered by the circulating blood.

The clue to the observation that $\dot{V}_{\text{O}_2\text{max}}$ remained unchanged in the 3.0 and 6.0 ATA air experiments despite the associated increases in P_{IO_2} should be sought in the defective CO_2 elimination at these pressures secondary to increased gas density and hypoventilation. For as shown in recent experiments at normal barometric pressure breathing through increased resistance (Cerretelli, Sihan and Farhi 1969) or addition of 15 mm Hg P_{CO_2} to the inspired air (Luft, Finkelstein and Elliott 1974) decreases the maximal O_2 uptake attainable during exercise. A similar mechanism was presumably involved in the hyperbaric air experiments where the reduced ventilatory response to exercise led to marked hypercapnia. With the data at hand however it cannot be settled whether this CO_2 effect acted by setting a limit due to respiratory distress or by interfering with the supply or utilization of oxygen in the working muscles. As to possible direct effects of high N_2 pressures on \dot{V}_{O_2} experiments have so far been carried out only on isolated tissues such as rat diaphragm and brain tissue (Stadie, Riggs and Haugaard 1945, Rodgers, Fenn and Craig 1969). The results have shown no significant change in \dot{V}_{O_2} in the presence of 4–7 ATA N_2 or He at a P_{O_2} of 1.0 ATA. However it cannot be excluded that N_2 molecules interfered with the diffusion of O_2 in the present hyperbaric experiments in which metabolic rates were greatly increased.

Cardiac function Previous reports have shown that the cardiac rate at rest and in submaximal exercise is depressed in man exposed to high pressures of air or

and/or inert gases (for review, see Fagraeus *et al* 1974). In a recent study evidence was presented that the relative bradycardia during submaximal exercise in hyperbaric air is due both to the increase in O_2 pressure and to some factor or factors related to the increase in N_2 pressure (Fagraeus *et al* 1974). In the present study it was found that acute exposure to $He O_2$ at 3.0 ATA caused a significant reduction of the heart rate also during maximal exercise (Table IV, *Comparison II*), and that a further reduction of HR_{max} occurred when air was substituted for $He O_2$ at 3.0 ATA (*Comparison V*). However, contrary to the case in submaximal exercise, these reductions of HR_{max} can probably not be explained as caused in part by the elevated O_2 pressure, since it has been shown that hyperoxia at normal ambient pressure does not reduce HR_{max} (Miller *et al* 1952, Margaria *et al* 1972, Deroanne *et al* 1973). It may be concluded, therefore, that the reduction of HR_{max} occurring in hyperbaric environment is entirely due to factors related to the increase in hydrostatic and/or inert gas pressure. The fact that HR_{max} was decreased more with air than with $He O_2$ breathing at 3.0 ATA, indicates that a given high pressure of nitrogen has a greater depressant effect on heart rate than has the same pressure of helium. Although the true nature of the factor or factors responsible for this reduction of HR_{max} has not yet been established, recent observations suggest that the non oxygen dependent reduction of the cardiac rate at high pressures is mainly due to a reduction of the adrenergic stimulation of the heart (Fagraeus and Linnarsson 1973, Fagraeus, Haggendal and Linnarsson 1973a).

Since the cardiac stroke volume during maximal exercise has been shown to be unaffected both by an increase of the inspired O_2 pressure to 0.5 ATA (Ekblom 1974) or 3.0 ATA (Kaiser 1970) and by beta receptor blockade (Epstein *et al* 1965), it seems probable that the changes of HR_{max} in the present study do reflect corresponding changes of cardiac output, i.e. reductions of cardiac output of only about 2% in the $He O_2$ experiments and 4–5% in the air experiments at 3.0 and 6.0 ATA.

Point of exhaustion. The subjects participated in several preliminary tests and were therefore familiar with the sensations experienced in exhaustive exercise both under normal conditions and at increased ambient pressures. Thus any influence of psychological factors on the point of exhaustion was minimized except possibly in the 6.0 ATA air condition where respiratory distress and dizziness were present in varying degrees. An interesting observation was that in the experiments at 3.0 ATA $He O_2$ the blood lactate concentration did not differ from control while V_{O_2max} and endurance time were increased (Table IV). These findings which are in accordance with earlier observations on the effects of hyperoxia at normal ambient pressure (Asmussen, von Döbeln and Nielsen 1948, Margaria *et al* 1972) or induced by moderately raised ambient air pressures (Fagraeus *et al* 1973b, Linnarsson *et al* 1974) indicate a lowered rate of lactate production in the $He O_2$ experiments. The observation that in all conditions irrespective of endurance times the peak blood lactate concentrations were similar whereas end tidal P_{CO_2} levels differed widely (Table IV) suggests that maximal work performance was more closely related to

lactate concentration than to the P_{CO_2} or pH levels existing in the working muscles at the point of exhaustion. If this interpretation is correct, the lowered rate of lactate accumulation in the 3.0 ATA H_2O_2 condition would seem to explain the longer endurance time in this case.

This work was supported by the Swedish Medical Research Council (Project No. 40\4-687).

References

- ASMUSEN E. Muscular exercise. In *Handbook of Physiology: Respiration*, edited by W. O. Fenn and H. Rahn. Washington D. C.: Am. Physiol. Soc. 1965, Sect. 3, Vol. II, Chapt. 36, 939-978.
- ASMUSEN E. W. VON DOBELN and M. NIELSEN. Blood lactate and oxygen debt after exhaustive work at different oxygen tensions. *Acta physiol scand* 1948 15: 57-62.
- ASMUSEN E. and M. NIELSEN. Studies on the regulation of respiration in heavy work. *Acta physiol scand* 1946 12: 171-188.
- ASMUSEN E. and M. NIELSEN. Physiological dead space and alveolar gas pressures at rest and during muscular exercise. *Acta physiol scand* 1956 38: 1-21.
- ASMUSEN E. and M. NIELSEN. Pulmonary ventilation and effect of oxygen breathing in heavy exercise. *Acta physiol scand* 1958 43: 365-378.
- BANISTER R. G. and D. J. C. CUNNINGHAM. The effects on the respiration and performance during exercise of adding oxygen to the inspired air. *J. Physiol. (Lond)* 1954 125: 118-137.
- BARBER S. B. and W. H. SUMMERSON. The colorimetric determination of lactic acid in biological material. *J. Biol. Chem.* 1941 138: 535-554.
- CERRATELLI P. R. S. SIKAND and L. E. FARHS. Effect of increased airway resistance on ventilation and gas exchange during exercise. *J. Appl. Physiol.* 1969 27: 597-600.
- DEROANNE R. J. DUJARDIN, M. LAVY, R. MARECHAL, J. M. PEYRAT and F. PIRNAY. Effect of hyperbaric oxygenation on maximum aerobic work capacity. *F. S. arsmedicin (Stockholm)* 1973 9: 352-356.
- EAGAN C. J. and L. R. PLESE. Cardiorespiratory and metabolic effects of work during hypo- and hyperbaria. *Int. J. Proc.* 1969 28: 593.
- EKLUND B. 1974. Personal communication.
- ENGSTROM H. Volumen Ineffizien. Bemerkungen zur Frage des schädlichen Raumes. *Lp. la Lek. - Fo. m. F. h.* 1938 44: 191-218.
- EFFENDY S. E. B. F. ROBINSON, R. L. KAHLER and E. BRALY. Effects of beta adrenergic blockade on the cardiac response to maximal and submaximal exercise in man. *J. Clin. Invest.* 1965 44: 1745-1753.
- FAGRAEUS L. and D. LINNARSSON. Heart rate in hyperbaric environment after autonomic blockade. *F. S. arsmedicin (Stockholm)* 1973 9: 260-264.
- FAGRAEUS L. J. HAGGEGDAL and D. LINNARSSON. Heart rate, arterial blood pressure and noradrenaline levels during exercise with hyperbaric oxygen and nitrogen. *F. S. arsmedicin (Stockholm)* 1973a 9: 205-210.
- FAGRAEUS L. C. M. HESLER and D. LINNARSSON. Cardiorespiratory responses to graded exercise at increased ambient air pressure. *Acta physiol. and* 91: 59-64.
- FAGRAEUS L. J. KARLSSON, D. LINNARSSON and B. SALTIN. Oxygen uptake during maximal work at low and at sea level ambient pressures. *Acta physiol. and* 1973b 8: 411-421.
- HESLER C. M. Breath holding under high pressure. In *Physiol. J. f. Bre. h. Hold. D. m. a. d. the Im. of J. h. m. d. d. by H. Rahn and T. Yok. am. Natl. Acad. S. - Natl. R. s. Council. Publ.* 1341 1965 16: -181.
- HILL A. V. C. N. H. LONG and H. LUTT. Muscular use of lactic acid and the supply and utilization of oxygen. *Proc. Roy. Soc. B* 1949 Part VII 155-16.
- KATJSER L. Limiting factors for aerobic muscle performance. *Acta physiol. scand* 1970 9: Suppl. 346: 1-9.
- LEDBORC B. O. WIGERTZ and Th. ÖDUM. A beat-to-beat heart rate meter with line analog output for muscular exercise studies. *Rept. Lab. 4 at Natl. Med. Fac. Inst. Stockholm* Dec. 1969 73 pp.
- LINNARSSON D. J. KARLSSON, L. FAGRAEUS and B. SALTIN. Muscle metabolism and oxygen deficit with exercise in hypo- and hyperoxia. *J. Appl. Physiol.* 1974 37: 399-407.
- LUTT U. C. S. F. NIELSEN and J. C. ELLIOTT. Respiratory gas exchange, acid base balance and electrolytes during and after maximal work breathing 15 mm Hg P_{CO_2} . In *Proceedings of a Small Symposium of the XVI International Congress of Physiology, 1971 on CO₂ and the Regulation of*. New York: Springer. In press.

- MARGARIA R E CAMPORESI P AGHEMO and G SASSI The effect of O_2 breathing on maximal aerobic power *Pflü Arch ges Physiol* 1977 336 225-235
- MARGARIA R ■ CERRETELLI S MARCHI and L ROSSI Maximum exercise in oxygen *Int J an ex Physiol* 1961 18 465-467
- MATTELL G Time-courses of changes in ventilation and arterial gas tensions in man induced by moderate exercise *Acta physiol scand* 1963 58 Suppl 206 1-53
- MILLER A T JR H L LERDUE E L TEAGUE JR and J S FEREBEE Influence of oxygen administration on cardiovascular function during exercise and recovery *J appl Physiol* 1959 5 165-168
- NIELSEN M and O HANSEN Maximale körperliche Arbeit bei Atmung O_2 -reicher Luft *Skand Arch Physiol* 1937 16 37-59
- RODGERS ■ H W O FENN and A B CRAIG JR The oxygen consumption of rat tissues in the presence of nitrogen helium or hydrogen *Respir Physiol* 1969 6 168-177
- SCHOLANDER P F Analyzer for accurate estimation of respiratory gases in one half cubic centimeter samples *J biol Chem* 1947 167 235-250
- STADIE W C ■ C RIGGS and N HALGAARD Oxygen poisoning III The effect of high oxygen pressures upon the metabolism of brain *J biol Chem* 1945 160 191-208
- STROM G The influence of anoxia on lactate utilization in man after prolonged muscular work. *Acta physiol scand* 1949 17 440-451
- WASSERMAN K A L VAN KESSEL and G G BURTON Interaction of physiological mechanisms during exercise *J appl Physiol* 1967 22 71-85
- WYNDHAM C H ■ B STRYDOM A J VAN RENSBURG and G G ROGERS Effects on maximal oxygen intake of acute changes in altitude in a deep mine *J appl Physiol* 1970 29 552-555

Transport and Oxidation of Amino Acids and Glucose in the Isolated Exocrine Mouse Pancreas Effects of Insulin and Pancreozymin

By

ÅKE DANIELSSON and JANOVE SEHLIN

Received 19 February 1974

Abstract

DANIELSSON Å and J SEHLIN *Transport and oxidation of amino acids and glucose in the isolated exocrine mouse pancreas Effects of insulin and pancreozymin* Acta physiol scand 1974 91 557—565

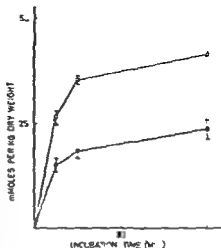
The uptake and oxidation of L-alanine and L-leucine as well as the oxidation of D-glucose were studied in pieces of microdissected exocrine mouse pancreas. The main observations and conclusions were as follows: The rate of oxidation of D-glucose was low and was only slightly enhanced by increasing its concentration in the medium from 3 to 20 mM. Even at a concentration as low as 0.1 mM both amino acids were oxidized at a higher rate than D-glucose. Thus mouse exocrine pancreas seems to prefer amino acids to D-glucose as substrate for its energy metabolism. The uptake of L-alanine and L-leucine in the exocrine cells was studied with a double label technique using ^{14}C -L-glucose as an extracellular marker. Both amino acids were rapidly taken up and accumulated in the exocrine cells. D-glucose inhibited both the uptake and oxidation of L-alanine. The decreased rate of oxidation of this amino acid might have been due to the reduction in uptake. Stimulation of secretion by cholecystokinin, pancreozymin increased the oxidation of D-glucose, L-alanine and L-leucine. However, no effect on the transport of the amino acids into the exocrine cells was observed. Therefore the effect of CCK-PZ on oxidation seems not to depend on an increased uptake of the amino acids. The presence of insulin (100 $\mu\text{g/ml}$) stimulated the oxidation of D-glucose but not that of the amino acids. Insulin had no effect on the transport of the amino acids into the exocrine cells.

Both the exocrine and endocrine parts of the pancreas are influenced by gastrointestinal hormones (Dupré *et al* 1969, Dreiling 1969). Evidence has also been presented for a functional relationship between endocrine and exocrine cells within the pancreas (*cf* Bank 1972). Thus insulin seems to inhibit the secretion of amylase from incubated mouse pancreas (Danielsson 1974b), as well as to enhance the *in vivo* incorporation of labelled amino acids into rat pancreatic amylase (Soling and Unger 1972). The latter effect of insulin could be due to direct stimulation of protein synthesis or be an indirect result of enhanced uptake of amino acid.

The exocrine cells display a low glycolytic activity which accounts for less than 10% of the energy output under normal conditions (Bauduin *et al* 1969). How

- MARGARIA P L CAMPORESI P AGHEMO and G SASSI The effect of O_2 breathing on maximal aerobic power *Pflug Arch ges Physiol* 1972 336 223-233
- MARGARIA R P CERRETELLI S MARCHI and L ROSSI Maximum exercise in oxygen *Int Z angew Physiol* 1961 18 463-467
- MATELL G Time courses of changes in ventilation and arterial gas tensions in man induced by moderate exercise *Acta physiol scand* 1963 58 Suppl 206 1-53
- MILLER A T JR H L PERDUE C L TEAGLE JR and J S FENWICK Influence of oxygen administration on cardiovascular function during exercise and recovery *J appl Physiol* 1959 5 165-168
- NIELSEN M and O HANSEN Maximale körperliche Arbeit bei Atmung O_2 reicher Luft *Skand Arch Physiol* 1937 76 37-59
- RODGERS S H W O TEAL and A B CRAIG JR The oxygen consumption of rat tissues in the presence of nitrogen helium or hydrogen *Respir Physiol* 1969 6 168-177
- SCHOLANDER P F Analyzer for accurate estimation of respiratory gases in one half cubic centimeter samples *J Biol Chem* 1947 167 235-250
- STADIE W C B C RIGGS and A HALGARD Oxygen poisoning III The effect of high oxygen pressures upon the metabolism of brain *J Biol Chem* 1943 160 191-208
- STROM G The influence of apnoea on lactate utilization in man after prolonged muscular work. *Acta physiol scand* 1949 17 440-451
- WASSERMAN K A L VAN KESSEL and G G BURTON Interaction of physiological mechanisms during exercise *J appl Physiol* 1967 22 71-85
- WYNDHAM C H A B STRYDOM A J VAN RENSBURG and G G ROGERS Effects on maximal oxygen intake of acute changes in altitude in a deep mine *J appl Physiol* 1970 29 552-559

Fig. 1 Uptake of L-glucose (■) and urea (□) in microdissected exocrine mouse pancreas with time. After preincubation for 30 min in Krebs-Ringer bicarbonate buffer supplemented with 3 mM D-glucose pieces of pancreas were incubated for different periods time in D-glucose free media supplemented with 3 mM L-[1- 14 C]glucose (10 mCi/mmol) or 3 mM [14 C]urea (20 mCi/mmol). The contents of L-glucose and urea in the tissue pieces are expressed as nmoles/kg dry weight. Each point represents mean values \pm S.E. for 4 experiments.



Materials and Methods

Chemicals D-[1- 14 C]glucose, L-[1- 14 C]glucose, [14 C]urea, L-[1- 14 C]leucine, L-[1- 14 C]alanine, L-[3- 3 H]leucine and L-[2,3- 3 H]alanine were obtained from the Radiochemical Centre, Amersham, Bucks, U.K. Unlabelled D-glucose was from British Drug Houses Ltd, Poole, Dorset, U.K., and unlabelled L-leucine, L-alanine and urea as well as bovine serum albumin (Fraction V) and cholecystokinin pancreozymin (CCK-PZ, (grade II) were supplied by Sigma Chemical Co., St. Louis, Mo., U.S.A. Crystalline ox insulin was kindly donated by Novo A/S, Copenhagen, Denmark. All other chemicals were commercially available reagents of analytical grade. Distilled and deionized water was used throughout.

Animals and general design of experiments Female mice 6—months old were obtained from a colony bred in our laboratory (Hollman 1963). This strain carries a gene *ob* which in the homozygous state gives rise to a syndrome of obesity and hyperlipemia. However, only mice of normal phenotype were used in this study. After starvation for 16—18 h the animals were decapitated and the pancreas was rapidly excised and transferred to a gassed O_2 , CO_2 and 5% CO_2 Krebs-Ringer bicarbonate buffer (KRB) (Lambert *et al.* 1964) containing 3 mg bovine serum albumin per ml and 3 mM D-glucose. About 43 small pieces of exocrine pancreas (mean dry weight about 10 mg each) were cut out under a stereomicroscope by means of micro-scalpels. It is ascertained that the pieces of exocrine pancreas did not contain any islet pancreatic islets. Measurements of insulin by radioimmunoassay of extracts of pieces of pancreas revealed a content of less than 0.1 μ g insulin per g dry weight of pancreas. Applying figures on μ -cell dry weight and insulin content (Pirani 1968) this amount of insulin would correspond to roughly 4 μ U/cell. The pieces of exocrine pancreas were transferred to incubation vessels and preincubated for 30 min at 37°C with shaking (140 strokes/min) and 30 cm amplitude in the same medium as the present experiment. The dissection KRB supplemented with 3 mg bovine serum albumin per ml was used as the basal medium in all further incubations.

Order of D-glucose and amino acids After the preincubation period the pieces of pancreas were incubated for 60 min at 37°C in basal medium supplemented with different concentrations of [14 C]labelled D-glucose, L-leucine or L-alanine as well as unlabelled test substances. The details of the incubation media are given in the appendixes to Table I and F.

The incubations were performed in liquid scintillation vials equipped with a small glass centre well (Keen *et al.* 1963; Hollman *et al.* 1963a) containing 100 μ l medium. About 5 pieces of pancreas were pooled in each vessel. B.A.s were obtained by incubating radioactivity media without pancreas. At the end of the incubation period, 100 μ l of 0.1 N HCl was injected into the centre well to arrest metabolism and to liberate [14 C]-H $_2$ O. H $_2$ O (100 μ l) was then injected onto a circular piece of filter paper placed on the bottom of the outer corner well before incubation. The liberated [14 C]- CO_2 was trapped in the same well by shaking the vessel for 1 h at room temperature. The centre well was removed and 10 ml of scintillation liquid (3 g of PPO and 50 mg of dimethyl POPOP in 1 l of toluene) was added and the radioactivity counted in a liquid scintillation spectrometer (Packard Model 3355).

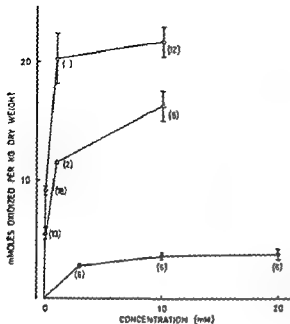


Fig 2 Concentration dependence of the rates of oxidation of D-glucose (●), L-leucine (Δ) and L-alanine (○). After preincubation as described in the legend to Fig 1 pieces of pancreas were incubated for 60 min in media supplemented with different concentrations of D-[U- ^{14}C]glucose (0.9–5.7 mCi/mmol), L-[U- ^{14}C]leucine (1.5–150 mCi/mmol) or L-[U- ^{14}C]alanine (1.5–150 mCi/mmol). Production of $^{14}\text{CO}_2$ is expressed as mmol of glucose or amino acid equivalents oxidized/kg dry weight of pancreas/h, assuming complete oxidation of each molecule. Mean values \pm SE for the number of experiments given in parenthesis.

After incubation the pieces of exocrine pancreas were placed on aluminum foil and freed of as much contaminating fluid as possible with the aid of micropipettes. After freeze-drying overnight (-40°C , 0.001 mm Hg) the tissue pieces were weighed on an electrobalance (Cahn Division, Paramount, Calif., U.S.A.).

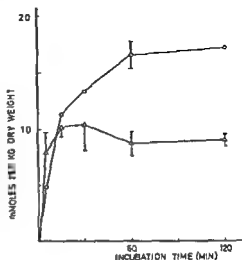
Uptake of urea, L-glucose and amino acids. Batches of 5 pancreas pieces were after the preincubation period incubated for different periods of times at 37°C in 200 μl basal medium supplemented with ^{14}C urea, ^{14}C L-glucose and/or ^3H labelled amino acids. The incubation times and the presence of other additives are specified in the legends to Fig 1 and 3 and Table II.

L-glucose is an extracellular space marker in the pancreatic islets (Hellman *et al.* 1971b). To check whether this is also the case in the exocrine pancreas, small pieces of exocrine tissue were incubated with either 5 mM ^{14}C L-glucose or 5 mM ^{14}C urea, a compound which is assumed to equilibrate in the total tissue water. Fig 1 shows that L-glucose equilibrates in a space much smaller than that of urea, which would be expected if L-glucose is restricted to the extracellular space. ^{14}C L-glucose was therefore present in the following incubations to make it possible to correct for extracellular and contaminating ^3H amino acid with out washing the tissue.

After incubation the pieces of exocrine pancreas were handled as described for the oxidation experiment. The weighed tissue pieces were placed in liquid scintillation vials and dissolved by incubation in 100 μl hyamine for 45 min at room temperature. 10 ml of scintillation liquid was then added and radioactivity was counted. When both ^3H and ^{14}C were present in the same sample the settings of the discriminators were such that less than 1% of the ^3H counts were also counted in the ^{14}C -channel. Spill-over to the ^3H -channel was 25% of the count in the ^{14}C -channel.

Evaluation of results. The radioactivity of incubated exocrine pancreas or that of $^{14}\text{CO}_2$ was standardized in relation to the incubation media. For this purpose samples (5 μl each) of the media were dissolved in 100 μl hyamine and counted in parallel with the other samples in each experiment. The results were then expressed as mmol of glucose or amino acid equivalents/kg dry weight of pancreas. Within each experiment all factors under study were tested in duplicate or triplicate incubations. The statistical probability that the effect of an additive to the incubation medium was due to chance was estimated from the mean difference between the test and control incubations in a series of identical but separate experiments.

Fig 3 Uptake of L-leucine (Δ) and L-alanine (\circ) in microdissected exocrine mouse pancreas with time. Preincubation was performed as described in the legend to Fig 1. Pieces of exocrine pancreas were incubated for different periods of time in media supplemented with 1 mM L-[2,3- ^3H]alanine (15 mCi/mmol) or 1 mM L-[G- ^3H]leucine (15 mCi/mmol). These incubation media also contained 2.5 mM L-[1- ^{14}C]glucose (30 mCi/mmol). The amounts of amino acid taken up were calculated by correction for label in the L-glucose space. The results are expressed as nmol of amino acid equivalents/kg dry weight of pancreas. Each point represents mean values \pm S.E. for 4 expts except for the 5, 15, 30 and 120 min values for L-alanine which are means of 2 observations.



Results

The concentration dependence of the oxidation of L-alanine, L-leucine and D-glucose in pancreatic exocrine tissue is shown in Fig 2. The oxidation of D-glucose was only slightly increased when its concentration in the medium was raised from 3 to 20 mM. Even at a concentration as low as 0.1 mM, both amino acids were oxidized at a higher rate than D-glucose. When the amino acid concentration was increased from 0.1 to 10 mM, the oxidation also increased markedly. The rate of oxidation of L-alanine was higher than that of L-leucine at all concentrations tested.

The effects of various test substances on the rates of oxidation of L-alanine, L-leucine and D-glucose are presented in Table I. Cholecystokinin pancreozymin (CCK-PZ) significantly increased the oxidation of all three compounds. The presence of insulin during the incubation slightly enhanced the rate of oxidation of D-glucose but did not affect the oxidation of the amino acids. The addition of D-glucose to the incubation medium tended to decrease the oxidation of L-alanine at a concentration of 10 mM and significantly inhibited that of 0.1 mM L-alanine. D-glucose had no effect on the oxidation of L-leucine.

Fig 3 shows the uptake of L-alanine and L-leucine with time. Both amino acids were rapidly transported into the exocrine pancreas, but L-alanine reached a higher steady state level than did L-leucine. The difference between the amounts of urea and L-glucose (Fig 1) in the pancreas pieces after 60 min of incubation was 17.4 nmol/kg dry weight. This corresponds to an intracellular water space of 3.5 l/kg dry weight of pancreas. At 120 min of incubation, the exocrine pancreatic cell contained radioactivity from labelled L-alanine and L-leucine corresponding to 17.1 and 9.0 nmol/kg dry weight respectively. If the intracellular water is 3.5 l/kg dry weight of pancreas, the intracellular concentration of labelled L-alanine

TABLE II After preincubation as described in the legend to Fig. 1 pieces of exocrine pancreas were incubated for 5 min in media containing 1 mM L-[2,3- ^3H] alanine (15 mCi/mmol) or 1 mM L-[G- ^3H] leucine (15 mCi/mmol). The incubation media also contained 2.5 mM L-[1- ^{14}C] glucose (30 mCi/mmol) as an extracellular space marker. The amounts of amino acid taken up were calculated by correction for label in the L glucose space. Mean values \pm S.E. for 6 expts.

Amino acid	Test substance	Amino acid uptake (nmol/kg dry weight of pancreas)		
		Control	Test	Difference
L-alanine	Insulin 100 $\mu\text{g/ml}$	7.57 \pm 0.39	6.97 \pm 0.68	-0.61 \pm 0.58
	CCK PZ 0.02 Crock U/ml	7.57 \pm 0.39	6.50 \pm 0.59	-1.07 \pm 0.58
	D glucose 20 mM	7.57 \pm 0.39	5.97 \pm 0.42	-1.65 \pm 0.79
L-leucine	Insulin 100 $\mu\text{g/ml}$	7.86 \pm 0.47	7.51 \pm 0.32	-0.36 \pm 0.49
	CCK PZ 0.02 Crock U/ml	7.86 \pm 0.47	7.88 \pm 0.40	+0.01 \pm 0.31
	D glucose 20 mM	7.86 \pm 0.47	7.98 \pm 0.09	+0.11 \pm 0.49

^a $p < 0.005$

120 min of incubation amounted to 4.9 and that of L-leucine to 2.6 mM. This indicates that both amino acids were accumulated in the exocrine pancreas.

CCK PZ and insulin, which affect the secretory function of the exocrine pancreas, were tested for effects on the transport of L-alanine and L-leucine into the exocrine pancreatic cells. As shown in Table II, neither insulin nor CCK PZ had any effect on the amino acid transport. The same result was obtained when the pieces of pancreas were preincubated with the hormones for 30 min. On the other hand, the presence of D-glucose inhibited the uptake of L-alanine but not that of L-leucine.

Discussion

The exocrine part of the pancreas differs markedly from the endocrine part with respect to metabolic pattern, although both are specialized secretory organs. In the exocrine pancreatic cells, the rate of D-glucose oxidation is low. Both L-alanine and L-leucine are oxidized at a considerably higher rate than D-glucose. In contrast, the pancreatic islets rapidly oxidize D-glucose with a maximal rate of over 50 nmol/kg dry weight (Hellman *et al.* 1973). In the islets, amino acids are oxidized at much lower rates than D-glucose.

It is notable that the exocrine pancreas, in which there is a very high rate of protein synthesis (Daly and Mirsky 1952), seems to prefer amino acids to D-glucose as substrate for its energy metabolism. Even if the amino acid uptake is rapid, as shown by our data as well as others (Begin and Scholefield 1964), the rapid de-

gradation of amino acids might theoretically lead to a competition between secretion and synthesis since both processes require an adequate supply of energy (Bauduin *et al* 1973) and the cells also require sufficient intracellular pools of amino acids for protein synthesis. If there is such competition for energy and amino acids stimulation of one process would predictably lead to inhibition of the other. In fact it has been reported that protein synthesis is inhibited during strong stimulation of enzyme secretion from the exocrine rat pancreas (Bauduin *et al* 1969 1973). However not all authors have observed such an effect (Kramer and Poort 1968 Poort and Kramer 1969 Meldolesi 1970 Morisset and Webster 1971 Reggio *et al* 1971). To explore the idea that various cellular processes compete for energy supply it was decided to investigate the rates of glucose and amino acid oxidation during stimulated secretion. CCK PZ a gastrointestinal hormone with secretagogic action on the exocrine pancreas increased the oxidation of D glucose L-alanine and L-leucine. This was probably not due to an increased uptake of amino acids since CCK PZ did not affect the transport of L-alanine or L-leucine into the exocrine pancreatic cells.

In the islets there is a striking parallelism between D glucose metabolism and insulin secretion (Ashcroft *et al* 1970 1972 1973). It has been extensively discussed whether this correlation is due to enhancement of glucose metabolism by insulin release or vice versa. The interpretation of data is complicated by the fact that D glucose is both a major metabolic substrate for the pancreatic β cells and the major physiological stimulus of insulin discharge. Recent studies on the independence of insulin release and glucose metabolism in the pancreatic β cells indicate however that insulin secretion has a positive feed back effect on D glucose metabolism in these cells (Hellman *et al* 1973). In the present study when amylase secretion from exocrine pancreas was stimulated by CCK PZ the oxidation of all substrates tested was also increased. The fact that glutamate fumarate and pyruvate *in vitro* potentiate stimulated secretion without having any effect by their own (Danielsson 1974 a) suggests that the supply of exogenous substrates may be rate limiting for the secretion. Our data therefore support the view that CCK PZ does not stimulate amylase secretion by increasing the rate of metabolism but that a stimulation of secretion leads to increased metabolic activity to meet the increased demand for energy.

The dispersal of the islets of Langerhans in the exocrine tissue suggests that there may be a functional relationship between the two parts of the pancreas. Administration of glucose to starved mice increases the amylase content of the pancreas. This enhancement is reversed by the concomitant injection of diazoxide an inhibitor of glucose induced insulin release (Danielsson 1974 c). Alloxan diabetic rats display a decrease of the level and the rate of synthesis of pancreatic amylase which is restored to normal values by daily injections of insulin (Palla *et al* 1968). The incorporation of labelled amino acids into rat pancreatic amylase (Soling and Unger 1972) and protein (Couture *et al* 1972) is stimulated by the *in vivo* injection of insulin. However it has been claimed (Couture *et al* 1972) that the insulin effect is not due

TABLE II After preincubation as described in the legend to Fig. 1 pieces of exocrine pancreas were incubated for 5 min in media containing 1 mM L-[2,3- ^3H] alanine (15 mCi/mmol) or 1 mM L-[G- ^3H] leucine (15 mCi/mmol). The incubation media also contained 2.5 mM L-[1- ^3C] glucose (30 mCi/mmol) as an extracellular space marker. The amounts of amino acid taken up were calculated by correction for label in the 1 glucose space. Mean values \pm S.E. for 6 experiments.

Amino acid	Test substance	Amino acid uptake (nmol/kg dry weight of pancreas)		
		Control	Test	Difference
L-alanine	Insulin 100 $\mu\text{g/ml}$	7.57 ± 0.39	6.97 ± 0.68	-0.61 ± 0.58
	CCK-PZ 0.02 Crock U/ml	7.57 ± 0.39	6.50 ± 0.59	-1.07 ± 0.58
	D-glucose 20 mM	7.57 ± 0.39	5.92 ± 0.42	-1.65 ± 0.29
L-leucine	Insulin 100 $\mu\text{g/ml}$	7.86 ± 0.47	7.51 ± 0.52	-0.36 ± 0.49
	CCK-PZ 0.02 Crock U/ml	7.86 ± 0.47	7.88 ± 0.40	$+0.01 \pm 0.31$
	D-glucose 20 mM	7.86 ± 0.47	7.98 ± 0.09	$+0.11 \pm 0.49$

$^*p < 0.005$

120 min of incubation amounted to 4.9 and that of L-leucine to 2.6 mM. This indicates that both amino acids were accumulated in the exocrine pancreas.

CCK-PZ and insulin, which affect the secretory function of the exocrine pancreas, were tested for effects on the transport of L-alanine and L-leucine into the exocrine pancreatic cells. As shown in Table II, neither insulin nor CCK-PZ had any effect on the amino acid transport. The same result was obtained when the pieces of pancreas were preincubated with the hormones for 30 min. On the other hand, the presence of D-glucose inhibited the uptake of L-alanine but not that of L-leucine.

Discussion

The exocrine part of the pancreas differs markedly from the endocrine part with respect to metabolic pattern, although both are specialized secretory organs. In the exocrine pancreatic cells the rate of D-glucose oxidation is low. Both L-alanine and L-leucine are oxidized at a considerably higher rate than D-glucose. In contrast, the pancreatic islets rapidly oxidize D-glucose with a maximal rate of over 50 mmol/kg dry weight (Hellman *et al.* 1973). In the islets amino acids are oxidized at much lower rates than D-glucose.

It is notable that the exocrine pancreas, in which there is a very high rate of protein synthesis (Daly and Mirsky 1952), seems to prefer amino acids to D-glucose as substrate for its energy metabolism. Even if the amino acid uptake is rapid as shown by our data as well as others (Begin and Scholefield 1964), the rapid de-

- BALDIN H M, COLIN and J E DUMONT Energy sources for protein synthesis and enzymatic secretion in rat pancreas *in vitro* *Biochim biophys Acta* (Amst) 1969 174 122-133
- BALDIN H T, TONDEUR J, VAN SANDE and D VINCENT Secretion and protein metabolism in the rat pancreas *in vitro* *Biochim biophys Acta* (Amst) 1973 304 81-97
- BEGIN N and P G SCHOLEFIELD The uptake of amino acids by mouse pancreas *in vitro* I General characteristics *Biochim biophys Acta* (Amst) 1964 90 87-89
- COUTLER Y J, DUNNIGAN and J MORISSET Stimulation of pancreatic amylase secretion and protein synthesis by insulin *Scand J Gastroent* 1972 7 257-263
- DALI M M and A E MIRSAH Formation of protein in the pancreas *J gen Physiol* 1952 36 243-254
- DANIELSSON A Techniques for measuring amylase secretion from pieces of mouse pancreas *Analyt Biochem* 1974 a 59 220-234
- DANIELSSON A Effects of glucose insulin and glucagon on amylase secretion from incubated mouse pancreas *Pflugers Arch ges Physiol* 1974 b 348 333-342
- DANIELSSON A Effects of nutritional state and of administration of glucose glibenclamide or diazoxide on the storage of amylase in mouse pancreas *Digestion* 1974 c In press
- DREILING D A Mechanisms of pancreatic exocrine secretion *Amer J Gastroent* 1969 52 17-24
- DUPRE J J, D CURTIS R H, UNGER R W, WADELL and J C BECK Effects of secretin, pancreozymin or gastrin on the response of the endocrine pancreas to administration of glucose or arginine in man *J clin Invest* 1969 46 745-757
- GUZZOTTI G G, B LUNEBURG and A F BORGHETTI Amino acid uptake in isolated chick embryo heart cells Effect of insulin *Biochem J* 1969 114 97-105
- HELLMAN B Studies in obese hyperglycemic mice *Ann N Y Acad Sci* 1965 131 541-558
- HELLMAN B J, SEHLIN and I B TALJEDAL Effects of glucose and other modifiers of insulin release on the oxidative metabolism of amino acids in microdissected pancreatic islets *Biochem J* 1971 a 123 513-521
- HELLMAN B J, SEHLIN and I B TALJEDAL Evidence for mediated transport of glucose in mammalian pancreatic β cells *Biochim biophys Acta* (Amst) 1971 b 241 147-154
- HELLMAN B J, SEHLIN and I B TALJEDAL Uptake of alanine arginine and leucine by mammalian pancreatic β cell *Endocrinology* 1971 89 1432-1439
- HELLMAN B, L A IDAN, A LERNMARK, J SEHLIN and I B TALJEDAL The pancreatic β cell recognition of insulin secretagogues Effects of calcium and sodium on glucose metabolism and insulin release *Biochem J* 1974 138 33-45
- HEEN H J, B FIELD and J H PASTAN A simple method for *in vitro* metabolic studies using small volumes of tissue and medium *Metabolism* 1963 12 143-147
- KRAMER M F and C POORT The peri-insular acin of the pancreas of the rat *Z Morphol* 1968 86 475-486
- MELDOLISI J Effect of caerulein on protein synthesis and secretion in the guinea pig pancreas *Brit J Pharmacol* 1970 40 721-731
- MORISSET J A and M D WEBSTER *In vitro* and *in vivo* effects of pancreozymin, urechole and cyclic AMP on rat pancreas *Ann r J Physiol* 1971 20 207-208
- PALLA J C, A BEN ABDELJIL and P DESVUELLES Action de l'insuline sur la biosynthèse de l'amylase et de quelques autres enzymes du pancréas de rat *Biochim biophys Acta* (Amst) 1968 158 25-35
- PETERSSON B The dry mass of the pancreatic β cells in relation to their content of secretion granules *Histochem J* 1968 1 55-58
- POORT C and M F KRAMER Effect of feeding on the protein synthesis in mammalian pancreas *Gastroenterology* 1969 57 689-696
- REGGIO H, H CHALLA DECKMANN and G MARCUS MOLREY Effect of pancreozymin on pancreatic enzyme biosynthesis *J cell Biol* 1971 50 333-343
- SOLING H D and K O UNGER The role of insulin in the regulation of protein synthesis in the rat pancreas *Europ J Clin Invest* 1972 2 199-210
- UMBERG W W, R H BLAIR and J F STAUFFER *In Vitro* Burger Publ Co Minneapolis 1964 132

Effects of Piperoxane on Sleep and Waking in the Rat Evidence for Increased Waking by Blocking Inhibitory Adrenaline Receptors on the Locus Coeruleus

By

KJELL FUXE PETER LIDBRINK TOMAS HOKFELT PER BOLME and MENA GOLDSTEIN

Recently adrenaline (A) neurons have been discovered in the rat brain (Hokfelt *et al* 1973 1974). Adrenaline terminals were *eg* found to innervate the noradrenaline (NA) cell bodies of the locus coeruleus (Dahlstrom and Fuxe 1964) which gives rise to the cortical NA innervation of the forebrain. This pathway is probably a tonic arousal system (Jones *et al* 1969 Lidbrink and Fuxe 1973 Lidbrink 1974). It is known that piperoxane can reduce the sedative and blood pressure lowering actions of clonidine (Schmitt *et al* 1971 Delburre and Schmitt 1973) and indications have recently been obtained that clonidine is mainly an A receptor stimulating agent an action which may be responsible for its effects on vasomotor and respiratory functions (Bolme *et al* 1974). On the basis of this information it seems likely that clonidine exerts its sedative action by stimulation of adrenaline receptors on the NA nerve cells of the locus coeruleus. Evidence for this view is presented in the present paper by showing that piperoxane in a dose which causes a selective increase in cortical NA turnover (Bolme *et al* 1974) can produce a significant increase in wakefulness.

Male Sprague Dawley rats (250 g bwt) were operated upon in a stereotaxic instrument under halothane oxygen anesthesia 2 weeks before the starting of the EEG recordings. 4 electrodes for cortical LFG recordings and 2 for LMG recordings were implanted as previously described (Lidbrink and Fuxe 1973 Lidbrink 1974). 4 different stages of EEG activity were distinguished (see Lidbrink 1974): waking (W) slow wave sleep (SWS) 1 SWS 2 and paradoxical sleep (PS). Each minute of the record was scored as belonging to one of these 4 stages.

The results are shown in Table I. Piperoxane in a dose of 5 mg/kg is seen to produce a significant increase in waking by about 30 per cent. The other stages of sleep are not significantly changed. It is of interest to note that after lesion of the ascending NA bundle to the cortex cerebri there occurs a reduction of waking of the same order of magnitude (Lidbrink and Fuxe 1973 Lidbrink 1974). The present results support the hypothesis mentioned in the introduction that the cortical NA

TABLE I The effect of piperoxane on sleep and waking in the rat

The EEG recording started at 9 a.m. immediately after the piperoxane (5 mg/kg i.p.) or saline injection and lasted for 6 h. Each animal was used for 4–5 days. The first day saline was used followed by drug on the second day. This schedule was then repeated. The values for sleep and waking are expressed as per cent of total time. 6 animals have been used. n = number of 6 h recordings.

Treatment	n	W*	SWS 1*	SWS 2*	PS*
Saline	12	19.5 ± 1.6	14.1 ± 1.7	50.5 ± 2.0	15.3 ± 0.7
Piperoxane	11	26.0 ± 1.6*	11.6 ± 1.7	48.5 ± 2.5	13.6 ± 0.7

For explanation of symbols see text.
p < 0.01 (Student's t test).

Arousal system is controlled by inhibitory A synapses. Clonidine may cause sedation by activation of these A receptors and piperoxane arousal by blocking these receptors. Thus it seems possible to develop a new class of psychostimulant drugs which may lack the dependence-producing actions of other psychostimulant drugs such as amphetamine which release amines from DA and NA nerve terminals in the brain (Carlsson *et al.* 1966).

This work has been supported by a grant from Nelson Research and Development Company and by a grant from the Swedish Medical Research Council (04X 15).

References

- BOLME, P., H. CORRODI, K. FLUXÉ, T. HÖKFELT and P. LIDBRINK. Possible involvement of central adrenaline neurons in vasomotor and respiratory control. Studies on clonidine and its interactions with piperoxane and yohimbine. *Europ. J. Pharmacol.* 1974. In press.
- CARLSSON, A., K. FLUXÉ, B. HAMBERGER and M. LINDQVIST. Biochemical and histochemical studies on the effects of imipramine-like drugs and (+) amphetamine on central and peripheral catecholamine neurons. *Acta physiol. scand.* 1966, 67: 481–497.
- DÄHLSTRÖM, A. and K. FLUXÉ. Evidence for the existence of monoamine-containing neurons in the central nervous system. I. Demonstration of monoamines in the cell bodies of brain stem neurons. *Acta physiol. scand.* 1964, 69: 1–55.
- DELBARRE, B. and H. SCHMITT. A further attempt to characterize sedative receptors activated by clonidine in chickens and mice. *Europ. J. Pharmacol.* 1973, 27: 355–359.
- HÖKFELT, T., K. FLUXÉ, M. GOLDSTEIN and O. JOHANSSON. Evidence for adrenaline neurons in the rat brain. *Acta physiol. scand.* 1973, 89: 286–288.
- HÖKFELT, T., K. FLUXÉ, M. GOLDSTEIN and O. JOHANSSON. Immunohistochemical evidence for the existence of adrenaline neurons in the rat brain. *Brain Res.* 1974, 66: 235–251.
- JONES, M. E., P. BOBILIER, et M. JOUVEY. Effets de la destruction des neurones contenant des catecholamines du mésencéphale sur le cycle veille-sommeil du chat. *C. R. Soc. Biol. (Paris)* 1969, 163: 176–180.
- LIDBRINK, M. The effect of lesions of ascending noradrenaline pathways on sleep and waking in the rat. *Brain Res.* 1974, 74: 19–40.
- LIDBRINK, P. and K. FLUXÉ. Effect of intracerebral injections of 6-hydroxydopamine on sleep and waking in the rat. *J. Pharm. Pharmacol.* 1973, 25: 84–87.
- SCHMITT, H., MME H. SCHMITT and S. FENARD. Evidence for an sympathomimetic component in the effects of catapresin on vasomotor centres. Antagonism by piperoxane. *Europ. J. Pharmacol.* 1971, 14: 98–100.

Myosin ATPase in Skeletal Muscle of Healthy Men

By

A W TAYLOR BIRGITTA ESSEN and B SALTIN¹

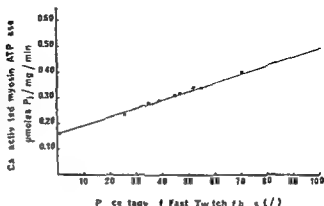
Barany (1967) has demonstrated that the intrinsic speed of muscle contraction with and without load is a characteristic property of the ATPase activity of myosin in the skeletal muscle of several mammalian species. The ATPase hydrolysis is found to have a higher maximal velocity in the fast contracting fibres (FT) as compared to the ATPase which predominates in the slow fibres (ST). The differences in the contractile properties of FT and ST muscles are considered to be due to these differences in the kinetic properties of the myosin ATPase. The myosins obtained from FT and ST muscle have been observed to possess different biochemical properties e.g. the myosin ATPase of FT muscle has a greater alkaline stability and is more sensitive to trypsin than myosin extracted from predominantly ST muscle (Samaha Guth and Albers 1970). There may be differences between the myosin ATPase activities of FT and ST fibres also in human skeletal muscle. A biochemical and histochemical approach was therefore undertaken to study myosin ATPase in mixed human skeletal muscles with different fibre composition and we were able to relate the Ca^{++} activated ATPase with the percentage of FT fibres.

11 healthy adult males served as subjects for biopsy samples from the vastus lateralis, gastrocnemius and soleus muscles. Muscle samples (3–28 mg \bar{x} = 11 mg) for biochemical determinations were quickly frozen in liquid nitrogen. Myosin was isolated by a modification of the Szent Gyorgi KI method (1951) and Ca^{++} or EDTA activated ATPase measured following the procedure described by Jablonski and Kaufman (1973). Histochemical analysis for acid and alkaline stable myosin ATPase were performed to obtain the ratio between FT and ST fibres (see Guth and Samaha 1969).

The protein content of the 3 muscles did not differ (Table I) and were within the accepted range for myosin values previously found in mammalian muscle. The Ca^{++} activated ATPase activities were found to be $0.34 \mu\text{mol Pi/mg protein/min}$ in the vastus lateralis and gastrocnemius muscles and $0.23 \mu\text{mol Pi/mg protein/min}$ in the soleus muscle. The EDTA activated myosin ATPase was on average 50–60% higher. The average percentage of FT fibres in soleus and the other 2 muscles were 23 and 48, respectively. When the Ca^{++} activated ATPase activity was correlated with the percentage of FT fibres present in the muscle sample a linear regression was

¹ Present address: Bengt Saltin, August Krogh Institute, University of Copenhagen, Universitetsparken 13, DK 2100 COPENHAGEN, Denmark.

Fig 1 Individual Ca^{++} activated myosin ATPase values in relation to percentage of FT fibres found in three leg muscles of human subjects. In addition to the data summarized in Table I values from three successful athletes with high FT fibre composition also are included (unfilled circles) ($r = 0.16 \pm 0.0039$)



attained ($r = 0.89$ Fig 1). A good correlation has been demonstrated to exist between fibre composition and fibre area in man (Gollnick *et al* 1972) but the 5–10% variation noted may account for part of the variation around the regression line in the present study.

The myosin and myosin ATPase values found in the present study of human skeletal muscle biopsy samples compare favourably with literature values for large muscle samples from rat, cat, guinea pig and rabbit. Barany (1967) found Ca^{++} ATPase activities for cat slow twitch soleus and fast twitch flexor hallucis longus (FHL) to be 0.15 and 0.36 $\mu\text{mol Pi/mg protein/min}$ respectively. The contraction times for these muscles were found to be inversely proportional to the myosin ATPase: 75 ms for soleus and 28 ms for FHL. Histological determinations of fibre composition of these muscles have been found to range from 0–18% FT for soleus and 23–49% FT for FHL (Arano, Armstrong and Edgerton 1973). If our regression line is extrapolated to represent muscle samples with 100% ST and 100% FT fibres, the Ca^{++} activated myosin ATPase values are found to be 0.16 and 0.49 $\mu\text{mol Pi/mg myosin/min}$ respectively, values which blanket the data of Barany (1967) for several other mammalian species.

Recently Buchthal, Dahl and Rosenfalck (1973) have electrically stimulated intact human muscle and found a range of contraction times of 16–68 ms in gastrocnemius and 52–120 ms in soleus muscle. Extrapolation of our data from

TABLE I Myosin content and ATPase activity (Means \pm S.E.) of skeletal muscle biopsy samples from 9 men

Muscle	Myosin (mg/g)	FT fibres (%)	ATPase activity Ca^{++} ($\mu\text{mol Pi/mg/min}$)
Vastus lateralis	21.5 ± 3.1	47	0.34 ± 0.07
Gastrocnemius	22.1 ± 4.2	48	0.34 ± 0.05
Soleus	23.8 ± 3.4	23	0.23 ± 0.03

ATPase activities would suggest that the contraction times in the present study would approximate 58 ms for soleus and 37 ms for vastus lateralis and gastrocnemius muscles. To what extent use and disuse may change the myosin ATPase activity of the fibre cannot be stated by the present study. The fact that Ca^{2+} activated myosin ATPase values from both physically inactive and active subjects were so highly correlated with fibre composition rather than fitness level may indicate that any large effect in man of training on myosin ATPase activity would not be anticipated.

This study was made possible by a grant from the Swedish Medical Research Council (14X 4155).

References

- ARIANO M. A., R. B. ARMSTRONG and V. R. EDERTON. Hindlimb muscle fiber populations of five mammals. *J. Histochem. Cytochem.* 1973, 21, 51-55.
- BARANY M. ATPase activity of myosin correlated with speed of muscle shortening. *J. gen. Physiol.* 1967, 50, 197-218.
- BUCHTHAL F., K. DAHL and P. ROSEN-FALCK. Rise time of the spike potential in fast and slowly contracting muscle of man. *Acta physiol. scand.* 1973, 87, 261-269.
- GOLLNICK P. D., R. B. ARMSTRONG, C. W. SAUBERT IV, K. FREIL and B. SALTIN. Enzyme activity and fiber composition in skeletal muscle of untrained and trained men. *J. appl. Physiol.* 1972, 33, 312-319.
- GUTH L. and F. J. SAMAHIA. Qualitative differences between actomyosin ATPase of slow and fast mammalian muscle. *Exp. Neurol.* 1969, 25, 138-152.
- JABLECKI C. and M. KAUFMAN. Myosin adenine triphosphatase activity during work induced growth of slow and fast skeletal muscle in the normal rat. *J. biol. Chem.* 1973, 248, 1056-1062.
- SAMAHIA F. J., L. GUTH and R. W. AIBERS. Differences between slow and fast muscle myosins. *J. biol. Chem.* 1970, 245, 219-224.
- SZENT-GYORGI A. G. A new method for the preparation of actin. *J. biol. Chem.* 1951, 192, 361-369.

Reinnervation of the Rat Diaphragm during Perfusion with α -Bungarotoxin

By

DAVID VAN ESSEN and JAN H. S. JANSEN

Mammalian skeletal muscle fibres are innervated by only a single axon and will not normally accept additional innervation by a foreign motor nerve. Several experimental manipulations are known to alter the muscle so that synapse formation by available nerve fibres is permitted. It is remarkable that the state of accepting or inducing synapse formation is in all known cases associated with the presence of acetylcholine receptors in the muscle fibre membrane. For example fetal muscle is sensitive to acetylcholine (ACh) before it is innervated (Diamond and Miledi 1967). After denervation poisoning with botulinum toxin or anesthetization of the nerve muscle fibres become supersensitive to ACh and will accept innervation anywhere on their surface (Axelsson and Thesleff 1959, Thesleff 1960, Lomo and Rosenthal 1972, Guth and Zalewski 1963, Fex *et al* 1966, Jansen *et al* 1973). Direct electrical stimulation of denervated muscle prevents the development of supersensitivity and also blocks foreign nerve innervation. However ACh sensitivity in the region of the original endplates is maintained during direct electrical stimulation and after foreign innervation neither of these procedures prevents reinnervation by the original nerve (Gutmann and Hanzlikova 1967, Lomo and Rosenthal 1972, Jansen *et al* 1973). Several investigators have therefore suggested that the presence of ACh receptors may be required for synapse formation in skeletal muscle (Katz and Miledi 1964, Fex *et al* 1966).

To test this hypothesis more directly we have compared the reinnervation of the diaphragm in normal rats and in rats perfused continuously with α bungarotoxin. This toxin is a protein which binds very tightly to the ACh receptor (Berg and Hall 1974) and it might therefore prevent or interfere with synapse formation.

The left hemidiaphragms of young rats (100—200 g) were denervated by crushing the phrenic nerve in the thorax just before it enters the diaphragm. Subsequently the reinnervation of the central 10 mm strip of the diaphragm was followed 1) by measuring the maximal twitch tension produced by nerve stimulation and comparing it to that caused by direct electrical stimulation of the muscle strip, 2) by recording end plate potentials and action potentials following nerve stimulation in individual muscle fibres on the surface of the diaphragm and 3) by histological examination of regenerating nerve terminals in preparation with zinc iodide-osmium (Jansen and Sandri 1968).

In control rats extensive reinnervation of the diaphragm occurred over a three day period between the third and the sixth day after a nerve crush. In 6 of 8 preparations tested 3 days after denervation there was no contraction to nerve stimulation; in the other 2 the tension produced by nerve stimulation was 2% and 13% of the maximal tension to direct stimulation. By the sixth day after denervation the average degree of reinnervation was 77% (range 64% to 95% in 9 animals). Similar results were obtained when the degree of reinnervation was assessed by microelectrode surveys of superficial muscle fibres.

Experimental animals were kept completely paralyzed during this 3 day period when most reinnervation takes place. Paralysis was produced by an initial i.a. injection of 1 mg bungarotoxin/kg b.wt. and maintained with a steady infusion of either 1 or 2 mg toxin/kg/day. The infusion mixture also contained Ringer's solution, glucose, atropine and analgesics (fentanyl plus droperidol). The rats were artificially respired and they remained in good condition as judged by their arterial blood pressure, pO_2 and pH.

In both experimental rats we found a virtually normal degree of reinnervation after 6 days of denervation and 3 days of paralysis. Immediately after removal of the diaphragm there was no contraction to nerve stimulation in either the denervated or the control hemidiaphragm. In one preparation an initial microelectrode survey was made and only one end plate potential (0.5 mV) was seen in the 30 fibres that were examined. However, after several hours of washing in oxygenated Ringer's solution small end plate potentials (0.2–6.0 mV) were recorded from 19 of 30 fibres (63%) tested in one preparation and 31 of 47 fibres (66%) tested in the other preparation. In both preparations regenerated nerve terminals were found after staining with zinc iodide osmium; their appearance was similar to the terminals seen in control rats 6 days after denervation.

We conclude from these experiments that reinnervation of the rat diaphragm proceeds normally even in the presence of enough bungarotoxin to eliminate end plate potentials throughout the period of synapse formation. Similar results have been obtained by studying the establishment of neuromuscular connections in organ cultures treated with D-tubocurarine (Crain and Peterson 1971; Cohen 1972). The normal synapse formation in the presence of bungarotoxin makes it unlikely that the ACh receptor (or at least that part of the receptor to which the toxin binds) is the membrane component which directly controls synapse formation in skeletal muscle.

We thank Drs Zach Hall and Eric Frank for their advice and Drs John Iversman and R. Brady for our initial supply of toxin. D.V.E. was supported by a postdoctoral fellowship from the Helen Hay Whitney Foundation.

References

- AKERT, K. and C. SANDRI. An electron microscopic study of zinc iodide osmium impregnation of neurons. I. Staining of synaptic vesicles at cholinergic junctions. *Brain Res.* 1968, 7: 286–295.
- AXELSSON, J. and S. THESLEFF. A study of supersensitivity in denervated mammalian skeletal muscle. *J. Physiol. (Lond.)* 1959, 147: 178–193.

- BEA, D. K. and E. W. HALL: Fate of a bungarotoxin bound to acetylcholine receptors of normal and denervated muscle. *Science* 1974 181 413-415
- COREN, M. W.: The development of neuromuscular connexions in the presence of D-tubocurarine. *Brain Res* 1977 41 457-463
- CRAIG, S. M. and E. R. PETERSON: Development of paired explants of fetal spinal cord and adult skeletal muscle during chronic exposure to curare and hemicholinium. *In Vitro* 1981 6 373
- DIAMOND, J. and R. MILEDI: A study of foetal and new born rat muscle fibres. *J Physiol (Lond)* 1967 167 393-408
- FEX, S. B. SORESSON, S. THIESLEFF and J. ZELENKA: Nerve implants in botulinum poisoned mammalian muscle. *J Physiol (Lond)* 1966 184 812-887
- GUTH, L. and A. A. ZALEWSKI: Disposition of cholinesterase following implantation of nerve into innervated and denervated muscle. *Exp Neurol* 1963 7 316-376
- GUTMAN, E. and V. HANZLIKOVÁ: Effects of accessory nerve supply to muscle achieved by implantation into muscle during regeneration of its nerve. *Physiol bohemoslo* 1961 16 244-250
- JENSEN, J. K. S., T. LOMO, K. NICOLAYSEN and R. H. WESTGAARD: Hyperinnervation of skeletal muscle fibers: Dependence on muscle activity. *Science* 1973 181 350-351
- KATZ, H. and R. MILEDI: The development of acetylcholine sensitivity in nerve-free segment of skeletal muscle. *J Physiol (Lond)* 1964 170 389-396
- LOMO, T. and J. ROSENTHAL: Control of ACh sensitivity by muscle activity in the rat. *J Physiol (Lond)* 1977 271 493-513
- THIESLEFF, S.: Supersensitivity of skeletal muscle produced by botulinum toxin. *J Physiol (Lond)* 1960 151 598-607

The Temperature Dependence of Action Potentials in Rat Skeletal Muscle Fibres

By

M. R. WARD¹ and S. THESLEFF

In experiments carried out at 29°C Redfern and Thesleff (1971a) noted that the maximum rate of rise (MRR) of direct action potentials recorded from rat extensor digitorum longus (EDL) muscles was much reduced after the muscles had been surgically denervated. After 2-7 days of denervation the MRR was some 250 V/s less than that of innervated muscles. In some experiments made at 37°C we observed that this difference between action potentials from innervated and denervated muscle fibres was less pronounced. The temperature sensitivity of skeletal muscle action potentials therefore deserved further attention.

Experiments were carried out on EDL muscles of young male Wistar rats weighing 200-250 g. The muscles were denervated and 6-8 days later were removed and mounted in a controlled temperature bath perfused with an oxygenated bathing fluid (Liles 1956).

Action potentials were generated and recorded with a double microelectrode technique as described by Redfern and Thesleff (1971a). The current passing electrode was also used for local polarization of muscle fibres to -100 mV before a 3-5 ms cathodal shock was applied to produce an action potential with 1-3 ms latency. Only one action potential was elicited in each muscle fibre.

The maximum rate of rise (MRR) and maximum rate of fall (MRF) of action potential were obtained by use of an RC derivating circuit. The duration at zero potential (i.e. the duration of the overshoot) was taken as an indication of the time course of an action potential.

Experiments were done at 23°C, 28°C, 33°C or 37°C ($\pm 0.5^\circ\text{C}$). In a few experiments muscles were maintained in bathing fluid containing tetrodotoxin (TTX, Sankyo Tokyo) at a concentration of 10^{-6} M .

In accordance with the findings of Hodgkin and Katz (1949) the MRR of action potentials in innervated and denervated muscle fibres increased with temperature over the range studied. It was noticeable however that the large difference between the MRR from innervated and denervated fibres observed at 23°C became less pronounced as temperature was increased so that at 33°C and 37°C the MRR from denervated fibres approached that from innervated fibres (Fig. 1) although it was still significantly less ($p < 5\%$). The Q_{10} of the MRR for innervated fibres was about 1.3 (Fig. 1) which is in good agreement with the Q_{10} of 1.2 for the sodium influx during an impulse in squid axons measured by tracer techniques.

¹ Present address: Muscular Dystrophy Group Laboratories, Regional Neurological Centre, Newcastle General Hospital, Newcastle upon Tyne, England.

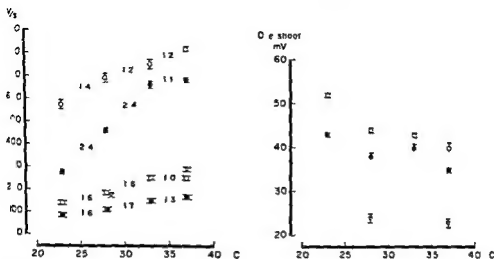


Fig 1 MRR (V/s) of innervated (O) and denervated (●) muscle fibres MRF for innervated (□) or denervated (■) fibres as a function of temperature MRR of denervated fibre in the presence of 10^{-6} M TTX is shown by (▽) Values are means \pm SE from 23–41 fibres Figures between points indicate Q_{10} between adjacent points

Fig 2 The amount by which action potentials exceeded zero membrane potential i.e. overshoot from innervated (O) and denervated (●) muscle fibres as a function of temperature The effect of 10^{-6} M TTX is shown by (▽) The values are means \pm SE from the same action potentials as those used in Fig 1

(Cohen and Landowne 1974) In contrast the Q_{10} of the MRR for denervated fibres was approximately twice that of innervated fibres (2.4) as temperature was raised from 23°C to 28°C and from 28°C to 33°C (Fig 1) Above 33°C MRR plateaued

The amplitude of the overshoot of action potentials from both innervated and denervated fibres declined with increasing temperature (Fig 2) At all temperatures studied the overshoot from denervated fibres was significantly less than that from innervated fibres

Hodgkin and Katz (1949) attributed the decline in amplitude of action potential with increasing temperature to a greater acceleration of the falling phase as compared to the rising phase of the spike This does not seem an adequate explanation for denervated muscle however Fig 1 demonstrates that although the MRR from denervated fibres was always less than that from innervated fibres the Q_{10} of the MRR was similar in both situations Furthermore the Q_{10} of MRR from denervated fibres up to 33°C (1.6) was considerably less than the Q_{10} of MRR (2.4)

After denervation the muscle action potential becomes relatively insensitive to the blocking action of 10^{-6} M TTX (Redfern and Thesleff 1971 b) It was therefore of interest to determine whether the TTX resistant action potential represented particularly temperature sensitive component of the action potential of denervated

muscle. The MRR of the TTX-resistant action potential showed a Q_{10} of 1.8 (Fig. 1).

The duration of the overshoot of action potentials from denervated fibres was always greater than that from innervated fibres at all temperatures studied. In both situations the duration was reduced to a similar extent with increasing temperature. As temperature was raised from 23°C to 37°C, overshoot duration from innervated fibres decreased from 0.8 ± 0.01 ms (mean \pm S.E.) to 0.3 ± 0.01 ms, and from denervated fibres from 1.3 ± 0.03 ms to 0.5 ± 0.01 ms.

The change in the conformation of action potentials from both innervated and denervated fibres with temperature reflects the temperature dependence of the rate constants of the permeability changes associated with the action potential, particularly α_m , β_m , α_h and β_h (Frankenhaeuser and Moore 1963). It could be that α_m becomes particularly temperature sensitive after denervation and/or that denervation alters the temporal relationship between these rate constants.

M. R. W. was supported by a Wellcome Swedish Research Fellowship. The work was supported by a grant (B74 14\ 3112) of the Swedish Medical Research Council.

References

- COHEN, L. B. and D. LANDOWNE. The temperature dependence of the movement of sodium ions associated with nerve impulses. *J. Physiol. (Lond.)* 1914 26: 95—111.
- FRANKENHAEUSER, B. and L. E. MOORE. The effect of temperature on the sodium and potassium permeability changes in myelinated nerve fibres of *Xenopus laevis*. *J. Physiol. (Lond.)* 1963 169: 431—437.
- HODGKIN, A. L. and B. KATZ. The effect of temperature on the electrical activity of the giant axon of the squid. *J. Physiol. (Lond.)* 1949 109: 240—249.
- LILEY, A. W. An investigation of spontaneous activity of the neuromuscular junction of the rat. *J. Physiol. (Lond.)* 1956 132: 650—666.
- REDFERN, P. and S. THIESLEFF. Action potential generation in denervated rat skeletal muscle. I. Quantitative aspects. *Acta physiol. scand.* 1971a 81: 557—564.
- REDFERN, P. and S. THIESLEFF. Action potential generation in denervated rat skeletal muscle. II. The action of tetrodotoxin. *Acta physiol. scand.* 1971b 82: 70—78.

